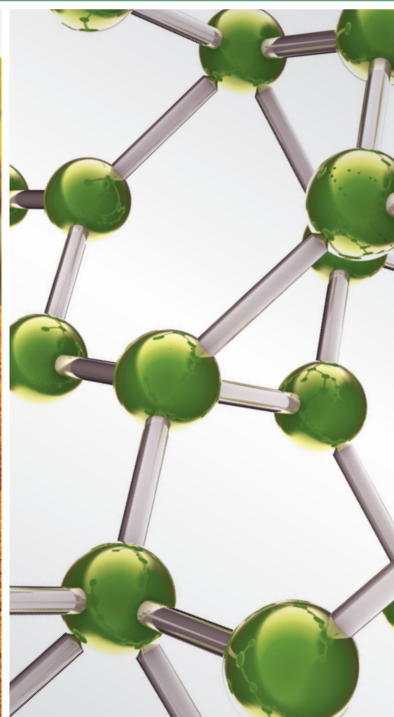


MEDICINAL PLANTS IN THE PREVENTION AND TREATMENT OF CHRONIC DISEASES

GUEST EDITORS: MOHAMED EDDOUKS, DEBPRASAD CHATTOPADHYAY, VINCENZO DE FEO,
AND WILLIAM C. CHO





Medicinal Plants in the Prevention and Treatment of Chronic Diseases

Medicinal Plants in the Prevention and Treatment of Chronic Diseases

Guest Editors: Mohamed Eddouks,
Debprasad Chattopadhyay, Vincenzo De Feo,
and William C. Cho



Copyright © 2012 Hindawi Publishing Corporation. All rights reserved.

This is a special issue published in "Evidence-Based Complementary and Alternative Medicine." All articles are open access articles distributed under the Creative Commons Attribution License, which permits unrestricted use, distribution, and reproduction in any medium, provided the original work is properly cited.

Editorial Board

- Terje Alraek, Norway
Shrikant Anant, USA
Sedigheh Asgary, Iran
Hyunsu Bae, Republic of Korea
Lijun Bai, China
Sarang Bani, India
Vassya Bankova, Bulgaria
Winfried Banzer, Germany
Vernon A. Barnes, USA
Debra L. Barton, USA
Jairo Kenupp Bastos, Brazil
David Baxter, New Zealand
André-Michael Beer, Germany
Alvin J. Beitz, USA
Paolo Bellavite, Italy
Yong C. Boo, Republic of Korea
Francesca Borrelli, Italy
Gloria Brusotti, Italy
Arndt Bssing, Germany
Subhash C. Mandal, India
Leigh F. Callahan, USA
Raffaele Capasso, Italy
Opher Caspi, Israel
Shun-Wan Chan, Hong Kong
Il-Moo Chang, Republic of Korea
Chun-Tao Che, USA
Yunfei Chen, China
Tzeng-Ji Chen, Taiwan
Kevin W. Chen, USA
Juei-Tang Cheng, Taiwan
Evan Paul Cherniack, USA
Jen-Hwey Chiu, Taiwan
Jae Y. Cho, Republic of Korea
William C. S. Cho, Hong Kong
Shuang-En Chuang, Taiwan
Edwin L. Cooper, USA
Vincenzo De Feo, Italy
Rocio De la Puerta, Spain
Alexandra Deters, Germany
Drissa Diallo, Norway
Mohamed Eddouks, Morocco
Amr E. Edris, Egypt
Nobuaki Egashira, Japan
Tobias Esch, Germany
Yibin Feng, Hong Kong
- Josue Fernandez-Carnero, Spain
Juliano Ferreira, Brazil
Peter Fisher, UK
Joel J. Gagnier, Canada
M. Nabeel Ghayur, Canada
Anwarul Hassan Gilani, Pakistan
Michael Goldstein, USA
Svein Haavik, Norway
S.-H. Hong, Republic of Korea
Markus Horneber, Germany
Ching Liang Hsieh, Taiwan
Benny Tan Kwong Huat, Singapore
Roman Huber, Germany
Alyson Huntley, UK
Angelo Antonio Izzo, Italy
Kanokwan Jarukamjorn, Thailand
Stefanie Joos, Germany
Z. Kain, USA
Osamu Kanauchi, Japan
Kenji Kawakita, Japan
Youn C. Kim, Republic of Korea
JongYeol Kim, Republic of Korea
Cheorl-Ho Kim, Republic of Korea
Yoshiyuki Kimura, Japan
Toshiaki Kogure, Japan
Ching Lan, Taiwan
Alfred Längler, Germany
Lixing Lao, USA
Charlotte Leboeuf-Yde, Denmark
Tat leang Lee, Singapore
Myeong Soo Lee, Republic of Korea
Jang-Hern Lee, Republic of Korea
Christian Lehmann, Canada
Marco Leonti, Italy
Ping-Chung Leung, Hong Kong
Shao Li, China
Xiu-Min Li, USA
Chun Guang Li, Australia
Sabina Lim, Republic of Korea
Wen Chuan Lin, China
Christopher G. Lis, USA
Gerhard Litscher, Austria
I.-Min Liu, Taiwan
Ke Liu, China
Yijun Liu, USA
- Gaofeng Liu, China
Cynthia R. Long, USA
Irène Lund, Sweden
Gail Mahady, USA
Jeanine L. Marnewick, South Africa
Francesco Marotta, Italy
Virginia S. Martino, Argentina
James H. McAuley, Australia
Andreas Michalsen, Germany
David Mischoulon, USA
Hyung-In Moon, Republic of Korea
Albert Moraska, USA
Mark Moss, UK
Mark A. Moyad, USA
Stephen Myers, Australia
MinKyun Na, Republic of Korea
Vitaly Napadow, USA
F. R. F. Nascimento, Brazil
Isabella Neri, Italy
T. Benoît Nguelefack, Cameroon
Martin Offenbacher, Germany
Ki-Wan Oh, Republic of Korea
Y. Ohta, Japan
Olumayokun A. Olajide, UK
Thomas Ostermann, Germany
Stacey A. Page, Canada
Tai-Long Pan, Taiwan
Patchareewan Pannangpetch, Thailand
Bhushan Patwardhan, India
Berit Smestad Paulsen, Norway
Andrea Pieroni, Italy
Richard Pietras, USA
Xianqin Qu, Australia
Cassandra L. Quave, USA
Roja Rahimi, Iran
Khalid Rahman, UK
Cheppail Ramachandran, USA
Cesar R. Ramos-Remus, Mexico
Ke Ren, USA
Mee-Ra Rhyu, Republic of Korea
José Luis Ríos, Spain
Paolo Roberti di Sarsina, Italy
Bashar Saad, Palestinian Authority
Andreas Sandner-Kiesling, Austria
A. Roberto Soares Santos, Brazil

G. Schmeda-Hirschmann, Chile
Andrew Scholey, Australia
Veronique Seidel, UK
Dana Seidlova-Wuttke, Germany
Senthamil R. Selvan, USA
Tuhinadri Sen, India
Ronald Sherman, USA
Karen J. Sherman, USA
Kan Shimpo, Japan
B.-C. Shin, Republic of Korea
Jian-nan Song, China
Rachid Soulimani, France
Elisabet S.-Victorin, Sweden
Mohd R. Sulaiman, Malaysia
Venil N. Sumantran, India
Toku Takahashi, USA
Takashi Takahashi, Japan
Rabih Talhouk, Lebanon
Joanna Thompson-Coon, UK

Mei Tian, China
Yao Tong, Hong Kong
K. V. Trinh, Canada
Volkan Tugcu, Turkey
Yew-Min Tzeng, Taiwan
Catherine Ulbricht, USA
Dawn M. Upchurch, USA
Alfredo Vannacci, Italy
Mani Vasudevan, Malaysia
Joseph R. Vedasiromoni, India
Carlo Ventura, Italy
Wagner Vilegas, Brazil
Pradeep Visen, Canada
Aristo Vojdani, USA
Dietlind Wahner-Roedler, USA
Chong-Zhi Wang, USA
Shu-Ming Wang, USA
Chenchen Wang, USA
Y. Wang, USA

Kenji Watanabe, Japan
Wolfgang Weidenhammer, Germany
Jenny M. Wilkinson, Australia
V. C. N. Wong, Hong Kong
Charlie Changli Xue, Australia
Haruki Yamada, Japan
Nobuo Yamaguchi, Japan
Hitoshi Yamashita, Japan
Yong Qing Yang, China
Ken Yasukawa, Japan
E. Yesilada, Turkey
M. Yoon, Republic of Korea
Hong Q. Zhang, Hong Kong
Hong Zhang, China
Ruixin Zhang, USA
Boli Zhang, China
Haibo Zhu, China

Contents

Medicinal Plants in the Prevention and Treatment of Chronic Diseases, Mohamed Eddouks, Debprasad Chattopadhyay, Vincenzo De Feo, and William C. Cho
Volume 2012, Article ID 458274, 2 pages

Ferulic Acid Modulates SOD, GSH, and Antioxidant Enzymes in Diabetic Kidney, Ahmed Amir Radwan Sayed
Volume 2012, Article ID 580104, 9 pages

Efficacy of *Boesenbergia rotunda* Treatment against Thioacetamide-Induced Liver Cirrhosis in a Rat Model, Suzy M. Salama, Mehmet Bilgen, Ahmed S. Al Rashdi, and Mahmood A. Abdulla
Volume 2012, Article ID 137083, 12 pages

***In Vitro* and *In Vivo* Toxicity of Garcinia or Hydroxycitric Acid: A Review**, Li Oon Chuah, Swee Keong Yeap, Wan Yong Ho, Boon Kee Beh, and Noorjahan Banu Alitheen
Volume 2012, Article ID 197920, 12 pages

Animal Models as Tools to Investigate Antidiabetic and Anti-Inflammatory Plants, Mohamed Eddouks, Debprasad Chattopadhyay, and Naoufel Ali Zeggwagh
Volume 2012, Article ID 142087, 14 pages

Larix laricina*, an Antidiabetic Alternative Treatment from the Cree of Northern Quebec Pharmacopoeia, Decreases Glycemia and Improves Insulin Sensitivity *In Vivo, Despina Harbilas, Diane Vallerand, Antoine Brault, Ammar Saleem, John T. Arnason, Lina Musallam, and Pierre S. Haddad
Volume 2012, Article ID 296432, 10 pages

***Brachytemma calycinum* D. Don Effectively Reduces the Locomotor Disability in Dogs with Naturally Occurring Osteoarthritis: A Randomized Placebo-Controlled Trial**, Maxim Moreau, Bertrand Lussier, Jean-Pierre Pelletier, Johanne Martel-Pelletier, Christian Bédard, Dominique Gauvin, and Eric Troncy
Volume 2012, Article ID 646191, 9 pages

Reversion of P-Glycoprotein-Mediated Multidrug Resistance in Human Leukemic Cell Line by Diallyl Trisulfide, Qing Xia, Zhi-Yong Wang, Hui-Qing Li, Yu-Tao Diao, Xiao-Li Li, Jia Cui, Xue-Liang Chen, and Hao Li
Volume 2012, Article ID 719805, 11 pages

Polyphenol-Rich Fraction of Brown Alga *Ecklonia cava* Collected from Gijang, Korea, Reduces Obesity and Glucose Levels in High-Fat Diet-Induced Obese Mice, Eun Young Park, Eung Hwi Kim, Mi Hwi Kim, Young Wan Seo, Jung Im Lee, and Hee Sook Jun
Volume 2012, Article ID 418912, 11 pages

Green Tea Polyphenols for the Protection against Renal Damage Caused by Oxidative Stress, Takako Yokozawa, Jeong Sook Noh, and Chan Hum Park
Volume 2012, Article ID 845917, 12 pages

Antiatherosclerotic Effect of *Canarium odontophyllum* Miq. Fruit Parts in Rabbits Fed High Cholesterol Diet, Faridah Hanim Shakirin, Azrina Azlan, Amin Ismail, Zulkhairi Amom, and Lau Cheng Yuon
Volume 2012, Article ID 838604, 10 pages

***Ganoderma tsugae* Induces S Phase Arrest and Apoptosis in Doxorubicin-Resistant Lung Adenocarcinoma H23/0.3 Cells via Modulation of the PI3K/Akt Signaling Pathway**, Yang-Hao Yu, Han-Peng Kuo, Hui-Hsia Hsieh, Jhy-Wei Li, Wu-Huei Hsu, Shih-Jung Chen, Muh-Hwan Su, Shwu-Huey Liu, Yung-Chi Cheng, Chih-Yi Chen, and Ming-Ching Kao
Volume 2012, Article ID 371286, 13 pages

Norcantharidin Induces HL-60 Cells Apoptosis In Vitro, You-Ming Jiang, Zhen-Zhi Meng, Guang-Xin Yue, and Jia-Xu Chen
Volume 2012, Article ID 154271, 4 pages

Caffeic Acid Phenylethyl Amide Protects against the Metabolic Consequences in Diabetes Mellitus Induced by Diet and Streptozocin, Yi-Chun Weng, Sung-Ting Chuang, Yen-Chu Lin, Cheng-Fung Chuang, Tzong-Cherng Chi, Hsi-Lin Chiu, Yueh-Hsiung Kuo, and Ming-Jai Su
Volume 2012, Article ID 984780, 12 pages

6-Gingerol Inhibits Growth of Colon Cancer Cell LoVo via Induction of G2/M Arrest, Ching-Bin Lin, Chun-Che Lin, and Gregory J. Tsay
Volume 2012, Article ID 326096, 7 pages

The Effect of *Labisia pumila* var. *alata* on Postmenopausal Women: A Pilot Study, Azidah Abdul Kadir, Nik Hazlina Nik Hussain, Wan Mohammad Wan Bebakar, Dayang Marshitah Mohd, Wan Mohd Zahiruddin Wan Mohammad, Intan Idiana Hassan, Norlela Shukor, Nor Azmi Kamaruddin, and Wan Nazaimoon Wan Mohamud
Volume 2012, Article ID 216525, 6 pages

Quercetin Protects against Cadmium-Induced Renal Uric Acid Transport System Alteration and Lipid Metabolism Disorder in Rats, Ju Wang, Ying Pan, Ye Hong, Qing-Yu Zhang, Xiao-Ning Wang, and Ling-Dong Kong
Volume 2012, Article ID 548430, 14 pages

The Crude Extract from *Puerariae* Flower Exerts Antiobesity and Antifatty Liver Effects in High-Fat Diet-Induced Obese Mice, Tomoyasu Kamiya, Mayu Sameshima-Kamiya, Rika Nagamine, Masahito Tsubata, Motoya Ikeguchi, Kinya Takagaki, Tsutomu Shimada, and Masaki Aburada
Volume 2012, Article ID 272710, 6 pages

Antimicrobial Activity of Essential Oils against *Streptococcus mutans* and their Antiproliferative Effects, Lívia Câmara de Carvalho Galvão, Vivian Fernandes Furletti, Salete Meyre Fernandes Bersan, Marcos Guilherme da Cunha, Ana Lúcia Tasca Góis Ruiz, João Ernesto de Carvalho, Adilson Sartoratto, Vera Lúcia Garcia Rehder, Glyn Mara Figueira, Marta Cristina Teixeira Duarte, Masarahu Ikegaki, Severino Matias de Alencar, and Pedro Luiz Rosalen
Volume 2012, Article ID 751435, 12 pages

Chronic Treatment with Squid Phosphatidylserine Activates Glucose Uptake and Ameliorates TMT-Induced Cognitive Deficit in Rats via Activation of Cholinergic Systems, Hyun-Jung Park, Seung Youn Lee, Hyun Soo Shim, Jin Su Kim, Kyung Soo Kim, and Insop Shim
Volume 2012, Article ID 601018, 8 pages

The Immunomodulatory Effect of You-Gui-Wan on *Dermatogoides-pteronyssinus*-Induced Asthma, Li-Jen Lin, Chin-Che Lin, Shulhn-Der Wang, Yun-Peng Chao, and Shung-Te Kao
Volume 2012, Article ID 476060, 12 pages

Analgesic and Anti-Inflammatory Activities of Methanol Extract of *Ficus pumila* L. in Mice,

Chi-Ren Liao, Chun-Pin Kao, Wen-Huang Peng, Yuan-Shiun Chang, Shang-Chih Lai, and Yu-Ling Ho
Volume 2012, Article ID 340141, 9 pages

Inhibition of NO₂, PGE₂, TNF- α , and iNOS Expression by *Shorea robusta* L.: An Ethnomedicine Used for Anti-Inflammatory and Analgesic Activity,

Chattopadhyay Debprasad, Mukherjee Hemanta, Bag Paromita, Ojha Durbadal, Konreddy Ananda Kumar, Dutta Shanta, Haldar Pallab Kumar, Chatterjee Tapan, Sharon Ashoke, and Chakraborti Sekhar
Volume 2012, Article ID 254849, 14 pages

Ethanol Extract of *Dianthus chinensis* L. Induces Apoptosis in Human Hepatocellular Carcinoma HepG2 Cells *In Vitro*,

Kyoung Jin Nho, Jin Mi Chun, and Ho Kyoung Kim
Volume 2012, Article ID 573527, 8 pages

***Ecklonia cava* Inhibits Glucose Absorption and Stimulates Insulin Secretion in Streptozotocin-Induced Diabetic Mice,**

Hye Kyung Kim
Volume 2012, Article ID 439294, 7 pages

Xanthohumol, a Prenylated Flavonoid from Hops (*Humulus lupulus*), Prevents Platelet Activation in Human Platelets,

Ye-Ming Lee, Kuo-Hsien Hsieh, Wan-Jung Lu, Hsiu-Chu Chou, Duen-Suey Chou, Li-Ming Lien, Joen-Rong Sheu, and Kuan-Hung Lin
Volume 2012, Article ID 852362, 10 pages

The Observation of Humoral Responses after Influenza Vaccination in Patients with Rheumatoid Arthritis Treated with Japanese Oriental (Kampo) Medicine: An Observational Study,

Toshiaki Kogure, Naoyuki Harada, Yuko Oku, Takeshi Tatsumi, and Atsushi Niizawa
Volume 2012, Article ID 320542, 6 pages

Antidepressant-Like Activity of the Ethanolic Extract from *Uncaria lanosa* Wallich var. *appendiculata* Ridsd in the Forced Swimming Test and in the Tail Suspension Test in Mice,

Lieh-Ching Hsu, Yu-Jen Ko, Hao-Yuan Cheng, Ching-Wen Chang, Yu-Chin Lin, Ying-Hui Cheng, Ming-Tsuen Hsieh, and Wen Huang Peng
Volume 2012, Article ID 497302, 12 pages

Mechanisms of Gastroprotective Effects of Ethanolic Leaf Extract of *Jasminum sambac* against HCl/Ethanol-Induced Gastric Mucosal Injury in Rats,

Ahmed S. AlRashdi, Suzy M. Salama, Salim S. Alkiyumi, Mahmood A. Abdulla, A. Hamid A. Hadi, Siddig I. Abdelwahab, Manal M. Taha, Jamal Hussiani, and Nur Asykin
Volume 2012, Article ID 786426, 15 pages

Biological Effect of Leaf Aqueous Extract of *Caesalpinia pyramidalis* in Goats Naturally Infected with Gastrointestinal Nematodes,

Roberto Robson Borges-dos-Santos, Jorge A. López, Luciano C. Santos, Farouk Zacharias, Jorge Maurício David, Juceni Pereira David, and Fernanda Washington de Mendonça Lima
Volume 2012, Article ID 510391, 6 pages

Chemical Composition, Toxicity and Vasodilatation Effect of the Flowers Extract of *Jasminum sambac* (L.) Ait. "G. Duke of Tuscany",

Phanukit Kunhachan, Chuleratana Banchonglikitkul, Tanwarat Kajsongkram, Amonrat Khayungarnnawee, and Wichet Leelamanit
Volume 2012, Article ID 471312, 7 pages

Editorial

Medicinal Plants in the Prevention and Treatment of Chronic Diseases

Mohamed Eddouks,¹ Debprasad Chattopadhyay,² Vincenzo De Feo,³ and William C. Cho⁴

¹ *Moulay Ismail University, BP 21, Errachidia 52000, Morocco*

² *ICMR Virus Unit, Division of Ethnomedicine, ID & BG Hospital, General Block 4, 57 Dr. Suresh C Banerjee Road, Kolkata 700 010, India*

³ *Dipartimento di Scienze Farmaceutiche e Biomediche, Università degli Studi di Salerno, Via Ponte don Melillo, 84084 Fisciano, Italy*

⁴ *Department of Clinical Oncology, Queen Elizabeth Hospital, Kowloon, Hong Kong*

Correspondence should be addressed to Mohamed Eddouks, mohamed.eddouks@laposte.net

Received 25 June 2012; Accepted 25 June 2012

Copyright © 2012 Mohamed Eddouks et al. This is an open access article distributed under the Creative Commons Attribution License, which permits unrestricted use, distribution, and reproduction in any medium, provided the original work is properly cited.

Since the dawn of human civilization, human beings have found remedies within their habitat and have adopted different therapeutic strategies depending upon climatic, phytogeographic, sociocultural, floral, and faunal characteristics. Traditional systems thus contain beliefs and practices in order to avoid, prevent, or avert ailments, which constitute traditional preventive medicine. The use of medicinal herbs and herbal medicine is an age-old tradition and the recent progress in modern therapeutics has stimulated the use of natural product worldwide for diverse ailments and diseases. The educated public and health care professionals have enormous interests in the medicinal uses of herbs, but there is a great deal of confusion about their identification, effectiveness, therapeutic dosage, toxicity, standardization, and regulation. According to WHO, traditional medicine is popular in all regions of the world and its use is rapidly expanding even in developed countries. For example, in China, traditional herbal preparations account for 30–50% of the total medicinal consumption and now the annual global market for herbal medicine is over 60 billion USD. Thus, Western trained physicians should not ignore the impact of traditional medicine on their patients.

This special issue on medicinal plants in the prevention and treatment of chronic diseases is an attempt to summarize the current knowledge of promising traditional medicines and their phytochemicals to compounds tested against diverse chronic diseases. The therapeutic properties and structure activity relationship of some important and potentially useful phytoformulations are addressed with a focus on how

these age-old wisdom can lead to the development of useful therapeutics lead for preclinical or clinical evaluation. Manuscripts in this special issue covered several aspects of recent developments in the fields of (1) natural substances as lead compounds in chronic and degenerative diseases research, (2) natural products involved in the prevention of chronic diseases, (3) herbal pharmacotherapy and phytochemical studies, (4) role of functional foods and nutraceuticals in chronic diseases, and (5) studies involving toxicology and pharmacological and toxicological mechanisms of action of medicinal plants used in the treatment and prevention of chronic diseases. In-depth information prepared by experts from diverse fields provide the use of diverse medicinal herbs and their active components as antioxidants, antidiabetic, antihypertensive, antiatherosclerosis, gastroprotective, analgesic, anticancer, antidepressant, antiasthma, antiobesity, antiatherosclerosis, antimicrobial, anti-inflammatory agents and as immunomodulators, along with their safety issues and toxic effects.

In the coming days, more issues of eCAM will be released to offer researchers working on diverse aspects of medicinal plants with a complete coverage of ethnology, pharmacology, toxicology, and medicinal properties. This special issue will provide essential materials to those who are working in the fields of traditional systems of medicine and drug industry. It is the outcome of our research involvement for the last two decades with the subject and consultations among biomedical scientists and clinicians. Our group of four coeditors active in phytotherapy research in three continents

has been very pleased to receive a substantial feedback of 59 submissions to this special issue.

Acknowledgments

We are immensely grateful to those colleagues for their support in developing the concept. Our special thanks and gratitude go to the Editorial Board of eCAM for not only inviting us to edit this special issue, but for their constant help, suggestions and guidance. With great pleasure and respect, we extend our sincerest thanks and indebtedness to all the contributors for their timely responses, excellent updated contributions, and consistent cooperation as well as patience. We would like to express our deep gratitude to all the scientific colleagues who help immensely by providing their valuable time to review these manuscripts. All the credit to develop this issue goes to all its contributors and the editorial team.

*Mohamed Eddouks
Debprasad Chattopadhyay
Vincenzo De Feo
William C. Cho*

Research Article

Ferulsinaic Acid Modulates SOD, GSH, and Antioxidant Enzymes in Diabetic Kidney

Ahmed Amir Radwan Sayed^{1,2}

¹ Biochemistry Department, Faculty of Science, King Abdulaziz University, P.O. Box 80203, Jeddah 21589, Saudi Arabia

² Chemistry Department, Faculty of Science, Minia University, El-Minia 61519, Egypt

Correspondence should be addressed to Ahmed Amir Radwan Sayed, sayedaar1@yahoo.com

Received 28 January 2012; Revised 9 May 2012; Accepted 10 May 2012

Academic Editor: Debprasad Chattopadhyay

Copyright © 2012 Ahmed Amir Radwan Sayed. This is an open access article distributed under the Creative Commons Attribution License, which permits unrestricted use, distribution, and reproduction in any medium, provided the original work is properly cited.

The efficacy of Ferulsinaic acid (FA) to modulate the antioxidant enzymes and to reduce oxidative stress induced-diabetic nephropathy (DN) was studied. Rats were fed diets enriched with sucrose (50%, wt/wt), lard (30%, wt/wt), and cholesterol (2.5%, wt/wt) for 8 weeks to induce insulin resistance. After a DN model was induced by streptozotocin; 5, 50 and 500 mg/kg of FA were administrated by oral intragastric intubation for 12 weeks. In FA-treated diabetic rats, glucose, kidney/body weight ratio, creatinine, BUN, albuminuria, and creatinine clearance were significantly decreased compared with non treated diabetic rats. Diabetic rats showed decreased activities of SOD and GSH; increased concentrations of malondialdehyde and IL-6 in the serum and kidney, and increased levels of 8-hydroxy-2'-deoxyguanosine in urine and renal cortex. FA-treatment restored the altered parameters in a dose-dependent manner. The ultra morphologic abnormalities in the kidney of diabetic rats were markedly ameliorated by FA treatment. Furthermore, FA acid was found to attenuate chronic inflammation induced by both Carrageenan and dextran in rats. We conclude that FA confers protection against injuries in the kidneys of diabetic rats by increasing activities of antioxidant enzymes and inhibiting accumulation of oxidized DNA in the kidney, suggesting a potential drug for the prevention and therapy of DN.

1. Introduction

Diabetes mellitus (DM) is a life-threatening metabolic disorder and the disease is becoming a serious social problem. Hyperglycemia is the major cause of diabetic complications, such as retinopathy, nephropathy, and neuropathy [1, 2].

Diabetic nephropathy (DN) is characterized by structural abnormalities including hypertrophy of both glomerular and tubular elements, increase in the thickness of glomerular basement membranes, and progressive accumulation of extracellular matrix components [3]. It also results in functional alterations including the early increase in the glomerular filtration rate with intraglomerular hypertension, subsequent proteinuria, systemic hypertension, and eventual loss of renal function [3]. The development of irreversible renal change in diabetes mellitus such as glomerulosclerosis and tubulointerstitial fibrosis results ultimately in end stage renal disease [1]. Although adequate control of blood glucose levels may prevent the development of complications, it is

difficult to achieve strict blood glucose control, leading to a year-by-year increase in the number of patients with diabetes [4].

Although the mechanism of DN has not yet been clarified because of the complexity of the pathophysiology of DM, numerous factors have been reported to be involved, including the activation of the renin—angiotensin system [5], activation of protein kinase C β [6], activation of nuclear factor kappa B (NF- κ B) [7], enhanced formation of advanced glycation end products (AGEs) [8], and acceleration of oxidative stress [9]. Many experimental evidences suggest the involvement of free radicals in the pathogenesis of diabetes [10] and more importantly in the development of diabetic complications [11]. Free radicals are capable of damaging cellular molecules, DNA, proteins, and lipids leading to altered cellular functions. Many recent studies reveal that antioxidants capable of neutralizing free radicals are effective in preventing experimentally induced diabetes in animal models [12, 13] as well as reducing the severity

of diabetic complications [11]. Ferulic acid, an antioxidant of plant cell wall, was reported to prevent functional and pathological abnormalities in the kidney of diabetic rats reducing oxidative stress and inflammation [14, 15].

Many plants synthesize an array of chemical compounds that are not involved in their primary metabolism. These “secondary compounds” instead of serving a variety of ecological functions, they ultimately enhance the plant’s survival during stress. In addition, these compounds may be responsible for the beneficial effects of fruits, vegetables, and many plants on an array of health-related measures. Traditional herbal medicines have been employed for thousands of years and have contributed greatly to the prevention and treatment of various diseases, including diabetes. They are still valuable for human health and have received much attention as potential sources of new therapeutic agents due to their varied biological activity and low toxicity [16]. *Ferula sinaica* L. (Apiaceae) has some 130 species distributed throughout the Mediterranean area and central Asia. These plants are used in Egypt as spices and in the preparation of local drugs. The resins are reported to be used for stomach disorders such as a febrifuge and carminative agent and in the treatment of skin infections and hysteria [17]. Previous work showed that the main constituents of this genus are sesquiterpenes and sesquiterpene coumarins [18]. Ferulsinaic acid (FA) is the first member of a new rearranged class of sesquiterpene coumarins from the genus *Ferula*. It was isolated from *F. sinaica* L. The molecular formula of FA is found to be $C_{24}H_{30}O_5$. The structure of FA was established in a previous work of our research group [19] as indicated below in Scheme 1.

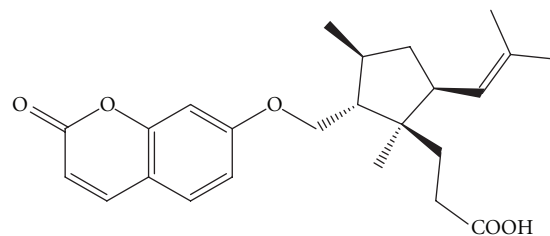
Extracts of *F. sinaica* was found to inhibit the spontaneous movements of rabbit jejunum and guinea pig ileum and acetylcholine induced contractions. Extracts also inhibited the contractions of rabbit tracheal smooth muscle induced by acetylcholine stimulation and the contractions of guinea pig tracheal smooth muscle induced by histamine stimulation. In addition, the extract inhibited the contractions of rabbit aorta induced by norepinephrine stimulation [20]. Furthermore, extracts of *F. sinaica* inhibited the spontaneous movements of rat and guinea pig uterine smooth muscle and also the contractions induced by oxytocin stimulation and have some antioxytotic potential [21].

FA was found to extend life span of wildtype *Caenorhabditis elegans* (*C. elegans*) under standard condition. Moreover, resistance to both heat stress and induced chemical stress of *C. elegans* were improved. Furthermore, FA was found to attenuate the formation reactive oxygen species (ROS) and advanced glycation end products (AGEs) in *C. elegans* [22].

In the present study, the antioxidant power as well as the anti-inflammatory effect of FA were examined to evaluate its efficacy to attenuate ROS production, inflammation, and to modulate the antioxidant enzymes of diabetic kidney in rats.

2. Materials and Methods

2.1. Animals. Adult male Albino rats weighing 180 to 200 g were used throughout this study. The animals were housed in



SCHEME 1

cages and received normal rat chow and tap water *ad libitum* in a constant environment (room temperature $28 \pm 2^\circ\text{C}$, room humidity $60 \pm 5\%$) with a 12 h light and 12 h dark cycle. The animals were kept under observation for one week prior to the start of the experiments.

2.2. Isolation and Purification of FA. Air-dried roots of *F. sinaica* were collected from North Sinai Peninsula, El-Arish, Egypt. 15 kg of *F. sinaica* were ground and extracted with CH_2Cl_2 at room temperature. The extract was concentrated to obtain a residue of 1100 g. The residue was fractionated by silica gel CC (6 · 120 cm) eluted with hexane, followed by gradient elution with hexane- CH_2Cl_2 up to 100% CH_2Cl_2 and finally with CH_2Cl_2 -MeOH (85 : 15). The hexane- CH_2Cl_2 extract (1 : 3, 140 g) was purified by HPLC (MeOH- H_2O , 73 : 27) to afford FA (100 mg) [19].

2.3. Induction of DN Model and Study Design. Seventy rats were used in this experiment. Rats were fed diets enriched with sucrose (50%, wt/wt), lard (30%, wt/wt), and cholesterol (2.5%, wt/wt) for 8 weeks to induce insulin resistance. Ten rats were used as control group (group 1, $n = 10$), which received a single tail vein injection of 0.1 mol/L citrate buffer only. A group of 60 rats were intravenously injected with STZ (65 mg/kg body weight), which was freshly prepared in a 0.1 mol/L citrate buffer (pH 4.5), after fasting for 12 hours. Only rats with blood glucose higher than 200 mg/dL after 5 days will be considered as being diabetic in the fasting state, by using One Touch *select* analyzer (Life Scan, Inc., UK). Rats with blood glucose lower than 200 mg/dL were excluded from the study. All studies were carried out one week after STZ had been injected. Fifty diabetic rats were randomly divided into 5 groups: DN, diabetic and treated with metformin-HCl (MF) ($125 \text{ mg kg}^{-1} \text{ d}^{-1}$; DN + MF) [23], diabetic and treated with a low dose ($5 \text{ ng kg}^{-1} \text{ d}^{-1}$) of FA (DN + FA1), diabetic and treated with a medium dose ($50 \text{ ng kg}^{-1} \text{ d}^{-1}$) of FA (DN+FA2), and diabetic and treated with a high dose ($500 \text{ ng kg}^{-1} \text{ d}^{-1}$) of FA (DN + FA3). The LD_{50} of FA was found to be $2 \mu\text{g/kg}$. The MF and FA were administered with distilled water via intragastric intubation. Treatments were continued for 12 weeks. Body weight and blood glucose levels were measured regularly. At the end of the experiment, animals were sacrificed using ether anaesthesia. Kidneys were dissected and rinsed with cold PBS and then weighed. An index of renal hypertrophy was estimated by comparing the wet weight of the left kidney to the body weight.

2.4. Kidney Homogenate Preparation. Every kidney tissue was cut into small pieces and washed by phosphate-buffered saline. Furthermore, it was grinded in a homogenization buffer {0.05 M Tris-HCl pH 7.9, 25% glycerol, 0.1 mM EDTA, and 0.32 M $(\text{NH}_4)_2\text{SO}_4$ } containing a protease inhibitor tablet (Roche, Germany). The lysates were homogenized on ice using a Polytron homogenizer. The solution has been sonicated in an ice bath to prevent overheating for 15 seconds followed by centrifugation at 12000 rpm, 4°C for 5 minutes. The supernatant was aliquoted and stored at -80°C and assayed for protein concentration using BCA kit (Pierce, Rockford, USA) using albumin diluted in a lysis buffer as a standard. The homogenate was used for the determination of reduced glutathione (GSH), level of lipid peroxidation (MDA), concentration of *Nε*-carboxymethyl lysine (CML), activity of superoxide dismutase (SOD), and level of IL-6. The other kidneys from each group were used for histopathological examination, determination of the level of AGEs, and for isolation of renal DNA.

2.5. Blood Sampling and Analysis. Blood samples of rats were centrifuged at 2,000 g for 10 minutes at 4°C, and aliquoted for the respective analytical determinations. The diagnostic kits for determinations for plasma levels of glucose, creatinine (Cr), blood urea nitrogen (BUN), sodium, and potassium were purchased from BioSystem (Barcelona, Spain). All analyses were performed in accordance with the manuals provided by the manufacturer.

2.6. Analysis of Urine Parameters. Urine samples were collected by placing the rats in individual metabolic cages for 24 h before diabetes had been induced and the day before the end of treatment. The urine albumin concentration was determined with an ELISA kit (Nephrot II, Exocell, Philadelphia, PA, USA) and the concentration of Cr in pooled urine samples was determined by the commercial assay kit. All analyses were performed in accordance with the manuals provided by the manufacturers. The 24 h urinary albumin excretion rate (UAER) was calculated as $\text{UAER } (\mu\text{g } 24\text{ h}^{-1}) = \text{urinary albumin } (\mu\text{g mL}^{-1}) \times 24\text{ h urine volume (mL)}$. Cr clearance (Ccr) was calculated using the following equation: $\text{Ccr (mL min}^{-1}\text{ kg}^{-1}) = (\text{urinary Cr (mg dL}^{-1}) \times \text{urinary volume (mL)/serum Cr (mg dL}^{-1})) \times (1000/\text{body weight (g)}) \times (1/1440\text{ (min)})$ [24].

2.7. Determining Enzymatic Activities. The activities of total SOD (EC: 1.15.1.1) as well as the concentrations of MDA and GSH in the kidney homogenate were determined using commercially available kits from BioVision Research Products (Linda Vista Avenue, USA) according to the methods described by Nishikimi et al., and Sayed [25, 26]; Ohkawa et al. and Mekheimer et al. [27, 28], and Moron et al. [29], respectively.

2.8. Determination of IL-6. IL-6 concentration in the serum and in the kidney homogenate was determined by an ELISA kit. The ELISA for determination of IL-6 was performed using a commercially available kit from R&D (Mannheim, Germany) according to the instructions of the manufacturer.

2.9. Measurement of Urinary and Renal 8-Hydroxy-2'-deoxyguanosine. Urinary 8-hydroxy-2'-deoxyguanosine (8-OHdG) levels were determined using an enzyme-linked immunosorbent assay kit from Genox Corporation (Baltimore, MD, USA) according to the method of Matsubasa et al. [30] and corrected by using individual urine creatinine concentrations. Extraction of renal DNA was performed using a DNA extraction kit (Promega, Germany) following the manufacturer's protocol. The genomic DNA samples from kidney tissue were also used for the determination of 8-OHdG using the competitive ELISA kit.

2.10. Renal AGEs Level. The renal AGE level was determined according to a previous method with slight modifications [31, 32]. Minced kidney tissue was delipidated with chloroform and methanol (2:1, v/v) overnight. After washing, the tissue was homogenized in 0.1N NaOH, followed by centrifugation at 8,000 g for 15 min at 4°C. The amounts of AGEs in these alkali-soluble samples were determined by measuring the fluorescence at an emission wavelength of 440 nm and an excitation wavelength of 370 nm using a fluorescence spectrophotometer (Hitachi, Japan). A native bovine serum albumin (BSA) preparation (1 mg mL^{-1} of 0.1N NaOH) was used as a standard. The fluorescence values of samples were measured at a protein concentration of 1 mg mL^{-1} and expressed in AU compared with a native BSA preparation.

2.11. Assessment of Renal CML. The supernatant of the kidney homogenate was tested for CML using the anti-CML rat autoantibody ELISA kit which employs the semiquantitative enzyme immunoassay technique. The absorbance of the resulting yellow product is measured at 450 nm [33].

2.12. Histopathological Examination. Renal tissues were collected after animal sacrifice, fixed in 10% formalin, processed routinely, and embedded in paraffin. 5- μm thick sections were prepared and stained with periodic acid Schiff (PAS). Glomerular histopathological changes and mesangial lesions were scored in term of the glomerular mesangial expansion (increase in the mesangial matrix) [34].

In order to evaluate the anti-inflammatory activity of FA on the acute inflammation, carrageenan-induced rat paw edema and dextran-induced rat paw edema were estimated as described by Arunachalam et al. [35] with slight modification.

2.13. Carrageenan-Induced Rat Paw Edema. Thirty rats were divided into 5 groups, each 6 rats. FA at 5, 50, and 500 ng/kg and indomethacin at 10 mg/kg body weight in olive oil were given to rats orally 30 min before carrageenan injection. The same volume of the vehicle was given to control group. The left rear plantar region of the rats was injected with 0.1 mL of carrageenan (1% in saline). The edema produced was determined by measuring the difference of the paw diameter using an analogic pakimeter (vernier) before carrageenan injection and at 0, 3, and 5 h after carrageenan injection.

2.14. Dextran-Induced Rat Paw Edema. The paw edema was induced in the right hind paw by subplantar injection of 0.1 mL of freshly prepared 1% dextran solution. Paw thickness was measured at 0, 45, and 90 min after dextran injection. The rats were treated as above. The percentage of inhibition was calculated.

2.15. Statistical Analysis. All group values are expressed as the mean \pm SD. Data was evaluated using the Sigma Stat (version 13.0) statistical analysis program (by using SPSS 11.09 for windows). An analysis of variance test was performed initially to test differences in the treatment. After the analyses of variance, a Tukey post-hoc test was performed to examine whether there were any significant differences between different treatment groups, the level of significance was set at $P < 0.05$.

3. Results

3.1. Effects of FA Treatment on Blood Glucose and Kidney/Body Weight Ratio. Data in Table 1 showed that the STZ injection resulted in a nearly 5-fold increase of the fasting blood glucose levels in the Albino rats. At the end of the 12-week period, the final kidney/body weight ratios of untreated diabetic animals were significantly higher than those of control animals ($P < 0.05$). FA-treated diabetic animals showed a significant reduction of this kidney/body weight ratio, which approached the levels of the MF group compared with the diabetic animals ($P < 0.05$). Moreover, there was also a significant correlation ($P < 0.05$) between the dosage groups.

3.2. Effects of FA Treatment on Renal Function. Table 1 shows that the BUN, creatinine, 24-hour Upro, sodium, potassium, and Ccr levels were significantly higher in the DN group than in the normal control group ($P < 0.05$). The low dose of FA markedly reduced Upro, potassium, and Ccr in the DN group but did not reduce serum BUN and Scr. The medium and high doses of FA significantly reduced all previously listed renal functional parameters in the DN rats ($P < 0.05$).

3.3. Effects of FA Treatment on Activities of Antioxidant Enzymes and Oxidative Stress Markers. The activity of SOD and concentration of GSH were lower, whereas concentration of MDA was higher in the kidney homogenate of the DN group than the control group ($P < 0.05$), suggesting that these rats suffered from oxidative stress (Table 2). Treatment with medium and high doses of FA significantly decreased the concentrations of MDA and significantly increased SOD activity and GSH concentrations ($P < 0.05$). These results indicate that FA ameliorates oxidative stress in DN rats. Metformin HCl significantly increased the antioxidant enzymes activities ($P < 0.05$).

3.4. Effects of FA Treatment on Serum and Renal IL-6. Diabetes significantly increases the degree of inflammation and the release of IL-6 in DN group compared with the normal control group ($P < 0.05$). Treatment of animals with FA and metformin appreciably attenuated this inflammation

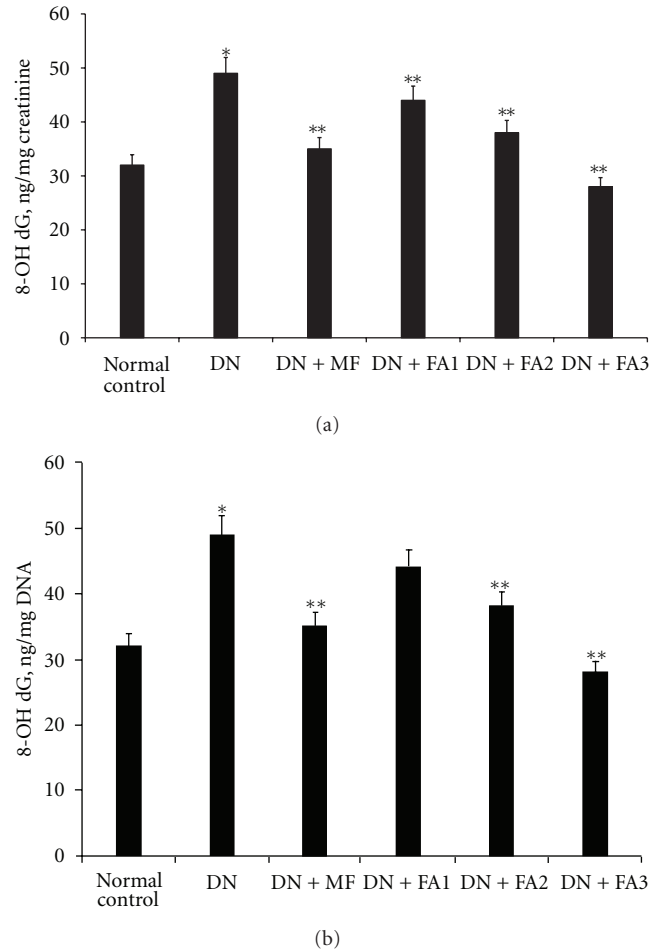


FIGURE 1: 8-Hydroxy-2'-deoxyguanosine levels in the urine (a) and renal cortex (b) of rats. Urinary and renal cortex 8-OHdG levels in diabetic rats were significantly attenuated in a dose-dependent manner after FA administration. Data are expressed as the means \pm SD. DN indicates diabetes untreated group; FA1, FA2, and FA3, diabetic rats treated with low dose (5 ng/kg) of FA (DN + FA1), middle dose (50 ng/kg) of FA (DN + FA2), and high dose (500 ng/kg) of FA (DN + FA3), respectively. * $P < 0.05$ versus normal control group, ** $P < 0.05$ versus diabetes untreated group.

and IL-6 production in all treated groups compared with DN group ($P < 0.05$), Tables 1 and 2.

3.5. Effects of FA on the Renal AGEs and CML. As a result of diabetes the renal levels of AGEs and CML were significantly elevated in the STZ-diabetic rats. These elevated levels were effectively lowered in a dose-dependent manner by FA treatment for 12 weeks (Table 2).

3.6. Effects of FA Treatment on Urinary and Renal 8-OHdG. The total amounts of urinary 8-OHdG excretion were significantly greater in STZ-induced diabetic rats than in control rats at 12 weeks after the onset of diabetes ($P < 0.05$). Administration of FA suppressed the increase in urinary excretion of 8-OHdG in the diabetic rats to the same extent as MF ($P < 0.05$). In parallel with the urine results, the

TABLE 1: Physiological, biochemical, and renal functional parameters of the rats.

	Normal control	DN	DN + MF	DN + FA1	DN + FA2	DN + FA3
Initial body weight, g	190.3 ± 9.5	192.4 ± 8	191.5 ± 7.4	190.9 ± 7	193 ± 9.2	191.3 ± 6.9
Final body weight, g	265.5 ± 8.1	163.9 ± 9.2 ^a	206.3 ± 8.5 ^{a,b}	201.3 ± 17.5 ^{a,b}	211.2 ± 8.9 ^{a,b}	212 ± 11.3 ^{a,b}
Glucose, mmol/L	4.98 ± 0.48	16.15 ± 1.55 ^a	6.2 ± 1.59 ^{a,b,d}	8.2 ± 1.5 ^{a,b,d}	7.81 ± 1.3	7.31 ± 0.59 ^{a,b,c}
Kidney/body weight, g/g, ×10 ⁻³	6.29 ± 0.35	11.2 ± 1.52 ^a	8.1 ± 1.2 ^{a,b}	8.5 ± 1.31 ^{a,b,d}	7.9 ± 1.39 ^{a,b}	7.5 ± 1.5 ^{a,b,c}
BUN, mmol/L	6.81 ± 1.3	12.35 ± 3.1 ^a	9.59 ± 1.65 ^{a,b}	11.34 ± 1.35 ^{a,d}	9.2 ± 1.1 ^{a,b,c}	8.55 ± 1.29 ^{a,b,c}
Serum creatinine, mmol/L	50.6 ± 7.1	65.12 ± 8.7 ^a	57.9 ± 6.5 ^a	62.1 ± 5.9 ^{a,d}	54.3 ± 3.4 ^{a,b,c}	52.16 ± 6.8 ^{a,b,c}
Ccr mL min ⁻¹ kg ⁻¹	3.39 ± 0.4	6.39 ± 0.6 ^a	4.52 ± 0.35 ^{a,b}	4.45 ± 0.41 ^{a,b}	3.98 ± 0.51 ^b	3.75 ± 0.46 ^b
U prot, mg/24 h	8 ± 1.1	23.6 ± 2.5 ^a	16.8 ± 2.5 ^{a,b}	18.9 ± 2.1 ^{a,b,d}	16.2 ± 2.9 ^{a,b}	15.5 ± 2.25 ^{a,b,c}
Serum sodium, mmol/L	145.1 ± 5.3	191 ± 10.5 ^a	153.5 ± 13.7 ^{a,b}	167.5 ± 8.9 ^{a,b,d}	155.3 ± 9.3 ^{a,b,c}	148.3 ± 2.3 ^{b,c,d}
Serum potassium, mmol/L	4.77 ± 0.54	7.24 ± 0.98 ^a	5.45 ± 0.5 ^b	6.8 ± 0.51 ^{a,d}	5.65 ± 0.66 ^{a,b,c}	5.15 ± 0.54 ^{b,c}
Serum IL-6, g/mL	81.2 ± 0.44	672.2 ± 15.6 ^a	256.5 ± 13.2 ^{a,b}	454.1 ± 1233 ^{a,b,d}	344.8 ± 14.7 ^{a,b,c}	261.2 ± 12.34 ^{a,b,c,d}

Data are expressed as the means ± SD. DN: diabetes group; FA1, FA2, FA3, and MF: diabetic rats treated with low dose (5 mg/kg) of FA (DN + FA1), middle dose (50 mg/kg) of FA (DN + FA2), high dose (500 mg/kg) of FA (DN + FA3), and (125 mg/kg) of metformin (DN + MF), respectively. Each group consisted of 10 animals.

^a $P < 0.05$ versus normal control group; ^b $P < 0.05$ versus DN group; ^c $P < 0.05$ versus DN + FA1 group; ^d $P < 0.05$ versus DN + FA2 group.

TABLE 2: Oxidant/antioxidant parameters as well as concentration of AGEs, CML, and IL-6 of rat kidney.

	Normal control	DN	DN + MF	DN + FA1	DN + FA2	DN + FA3
SOD, U/mg protein	21.3 ± 3.12	8.9 ± 2.1 ^a	18.25 ± 1.55 ^{a,b,d}	15.5 ± 1.8 ^{a,b,d}	19.93 ± 1.4 ^{b,c}	20.5 ± 1.55 ^{b,c}
GSH, nmol/mg protein	25.6 ± 2.12	17.41 ± 2.13 ^a	20.4 ± 2.2 ^{a,b}	19.85 ± 2.19 ^{a,b}	20.29 ± 2.17 ^{a,b}	23.78 ± 1.33 ^{b,c,d}
MDA, nmol/g protein	3.32 ± 0.2	7.1 ± 0.7 ^a	5.1 ± 0.35 ^{a,b,c}	6.2 ± 0.21 ^{a,b,d}	5.05 ± 0.5	4.07 ± 0.13 ^{b,c,d}
AGEs, AU	3.4 ± 0.2	7.1 ± 0.4 ^a	4.2 ± 0.3 ^{b,c}	6.2 ± 0.35 ^{a,b,d}	4.85 ± 0.55 ^{a,b,c}	3.9 ± 0.6 ^{b,c}
CML, ng/mg protein	22.2 ± 5.5	48.16 ± 6.1 ^a	30.5 ± 3.5 ^{a,b,c}	40.8 ± 5.4 ^{a,b,d}	32.3 ± 4.8 ^{a,b,c}	29.5 ± 4.1 ^{a,b,c,d}
IL-6, ng/mg protein	115 ± 2.5	1350 ± 45 ^a	560 ± 24 ^{a,b,c,d}	850 ± 35 ^{a,b,d}	628 ± 31 ^{a,b,c}	490 ± 28 ^{a,b,c,d}

Data are expressed as the means ± SD. DN: diabetes group; FA1, FA2, FA3, and MF: diabetic rats treated with low dose (5 mg/kg) of FA (DN + FA1), middle dose (50 mg/kg) of FA (DN + FA2), high dose (500 mg/kg) of FA (DN + FA3), and (125 mg/kg) of metformin (DN + MF), respectively. Each group consisted of 10 animals.

^a $P < 0.05$ versus normal control group, ^b $P < 0.05$ versus DN group, ^c $P < 0.05$ versus DN + FA1 group, ^d $P < 0.05$ versus DN + FA2 group.

levels of 8-OHdG in the DNA were markedly increased in the kidney of diabetic rats, and those increases were reversed by FA treatment ($P < 0.05$). In addition, the magnitude of these increases was reduced by FA treatment in a dose-dependent manner ($P < 0.05$; Figures 1(a) and 1(b)).

3.7. Histopathological Findings. A significant enlargement of the glomeruli, thickening of capsular basement membranes (CBMs), glomerular basement membranes (GBMs), and tubular basement membranes (TBMs), increased amounts of mesangial matrix, and tubular dilatation were observed in diabetic untreated rats (Figure 2(b)). The renal histology in untreated diabetic rats showed accelerated mesangial expansion, thickening of CBMs, GBMs, and TBMs, characterized by an increase in PAS-positive area as compared with control animals (Figures 2(a) and 2(b)). The treatment of rats with FA and MF reduced the glomerular size, thickening of CBMs, GBMs, and TBMs, increased amounts of mesangial matrix, and tubular dilatation as compared with diabetic untreated rats (Figures 2(c)–2(f)).

3.8. Effect of FA on the Acute Inflammation. In carrageenan-induced inflammatory rat models, FA at concentrations 5, 50 and 500 ng/kg inhibited the edema formation in the third

hour by 38% ($P < 0.05$), 42%, and 57% ($P < 0.005$) in a dose dependent manner, respectively. This effect also extended and significantly increased up to the fifth hour ($P < 0.005$). In addition, in dextran-induced inflammatory model, FA at 45 min inhibited the paw edema by 42%, 49%, and 57% ($P < 0.005$) of inhibition at the concentrations of 5, 50 and 500 ng/kg, respectively. At 90 min, there was an increase in the percentage of inhibition by 47%, 53% and 62%, respectively as shown in Tables 3(a) and 3(b)

4. Discussion

DN is one of the major microvascular complications of diabetes mellitus. Hyperglycemia can lead to both a rise in reactive oxygen species (ROS) production and the attenuation of free radical scavenging compounds [36]. In the present study, the development of DN was confirmed by significant elevations of kidney/body weight ratio, Scr, sodium, potassium, and BUN as well as Upro in diabetic rats, as earlier reported by other groups [14, 15, 23, 28, 37]. Oxidative stress can also affect nucleic acids resulting in modified DNA bases. 8-Hydroxy-2'-deoxyguanosine is a major product of DNA damage, and the measurement of its serum or urinary level provides information on various

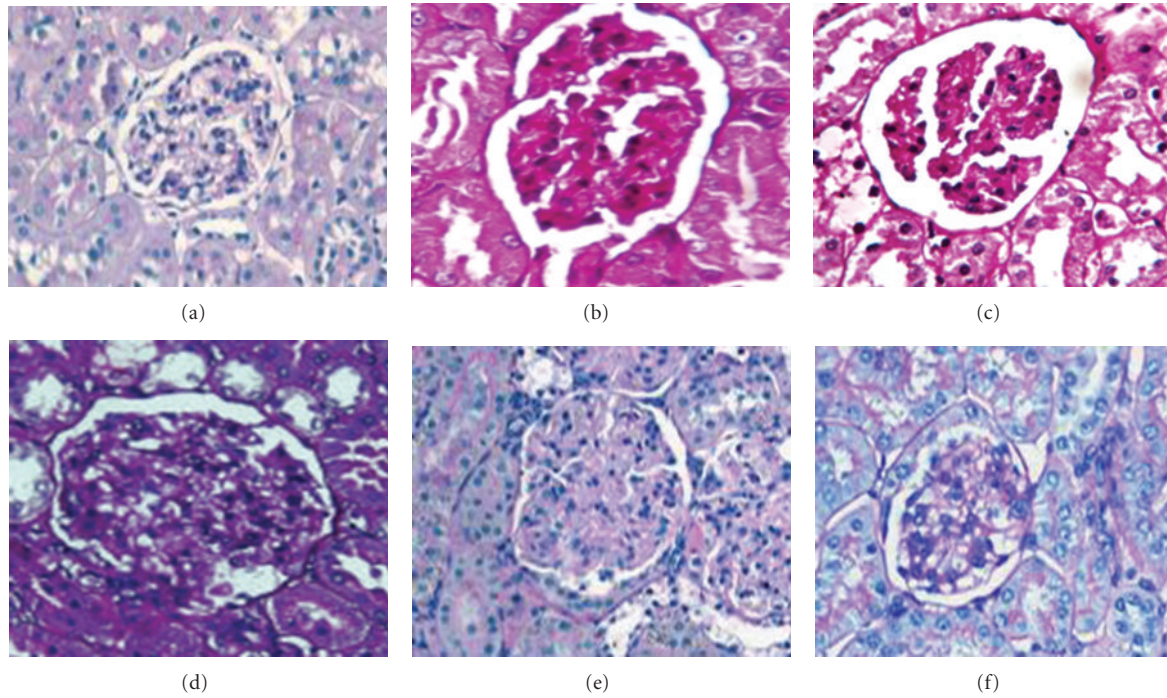


FIGURE 2: Figure (2): PAS staining of kidney sections of normal control rats (a), DN rats (b), DN treated with MF (c), FA1 (d), FA2 (e), and FA3 (f), respectively. Increased mesangial matrix, thickened CBMs, TBMs, and GBMs are present in the glomerulus of diabetic untreated rats as compared with the control and diabetic treated rats.

TABLE 3

(a) Effect of FA on carrageenan-induced rat paw edema

Treatment	Thickness of the injected foot, mm	
	3 h	5 h
Olive oil	5.1 ± 0.12	5.03 ± 0.14
Indomethacin 10 mg/kg	1.68 ± 0.15 (62%)**	1.51 ± 0.10 (70%)**
FA, 5 ng/kg	3.16 ± 0.21 (38%)*	3.05 ± 0.09 (39%)*
FA, 50 ng/kg	2.95 ± 0.13 (42%)**	2.81 ± 0.17 (44%)**
FA, 500 ng/kg	2.18 ± 0.21 (57%)**	2.05 ± 0.15 (59%)**

(b) Effect of FA on dextran-induced rat paw edema

Treatment	Thickness of the injected foot, mm	
	45 min	90 min
Olive oil	6.10 ± 0.17	5.90 ± 0.17
Indomethacin, 10 mg/kg	1.95 ± 0.15 (68%)**	1.66 ± 0.10 (72%)**
FA, 5 ng/kg	3.52 ± 0.16 (42%)*	3.1 ± 0.09 (47%)*
FA, 50 ng/kg	3.1 ± 0.21 (49%)**	2.75 ± 0.17 (53%)**
FA, 500 ng/kg	2.65 ± 0.12 (57%)**	2.25 ± 0.15 (62%)**

Values are mean ± SE, $n = 6$, * $P < 0.05$, ** $P < 0.001$ compared with control, post-hoc test. Values given in parentheses represent percentage of inhibition.

degrees of oxidative stress at the DNA level [38]. Urinary 8-OHdG excretion was significantly increased 12 weeks after the onset of diabetes. In addition, the renal cortex showed a markedly high expression of 8-OHdG in DNA. Moreover, we found for the first time that this oxidative damage is attenuated by FA treatment in a dose-dependent manner.

Furthermore, based on the obtained data, urinary and renal 8-OHdG were significantly higher in the DN group than in the control group, which suggests that the observed renal injuries were attributed to high 8-OHdG levels in the diabetic kidney. However, FA administration prevented all the above functional and morphologic changes and maintained them

near normal. The obtained data indicate that FA exerts its protective effects on the renal injury of diabetic rats via inhibiting the accumulation of oxidized DNA in the kidney.

Oxidative stress influences the pathogenesis of DN and is not only through overproduction of ROS but also through the reduction of antioxidant enzyme activities, the formation of lipid peroxides, and nonenzymatic protein glycosylation. Antioxidant enzymes are induced to protect against cellular and tissue injury. An imbalance between the production of ROS and antioxidants is believed to be involved in diabetes-induced renal failure [38]. Induction of diabetes in the present study caused a significant elevation of MDA and a reduction of both SOD activity and GSH concentration in the kidneys, as compared with the control group. Treatment with FA for 12 weeks reversed these oxidant/antioxidant parameters. The reversal of the oxidative damage due to FA is shown as a measure of antioxidant enzymes and indicates that it has possible antioxidant properties, which plays a crucial role in the defense against oxygen free radicals. The obtained data are in line with previous work [14, 15, 39].

The hyperglycemia condition results in irreversible tissue damage by the protein glycation reaction, which leads to the formations of glycosylated proteins and AGEs [40]. AGEs accumulation in the kidney have been regarded as an index of progressive renal damage in DN. CML is formed during the metal-catalyzed oxidation of polyunsaturated fatty acids in the presence of protein [41]. Therefore, CML could serve as a general biomarker of oxidative stress resulting from carbohydrate and lipid oxidation reactions. AGEs have the ability to activate NF- κ B signaling pathway which regulate the expression of many inflammatory genes like IL-6 [8, 42]. To test this hypothesis, we measured AGEs, CML, and IL-6 in the different groups. Actually, not only the overexpression of AGEs but also the higher levels of IL-6 in kidney of diabetic untreated rats were alleviated by 12 weeks of FA treatment. It seems that FA influenced not only the AGE-RAGE signaling but also the NF- κ B-IL-6-dependent pathway to some extent, thus leading to attenuate renal damage caused by the protein glycation reaction.

To test the direct anti-inflammatory action of FA, we measured its effect on the acute inflammation induced by carrageenan and dextran on rats. FA was found to exert anti-inflammatory effect which supports data obtained from the measurement of IL-6 in diabetic rats.

Controlling hyperglycemia in diabetic patients with insulin or other hypoglycemic agents and the reduction of oxidative stress, ROS production and inflammation result in the attenuation of diabetic complications especially DN. All of these findings support our hypothesis that FA has a renal protective role against oxidative damage, which may be due to its antioxidant/anti-inflammatory potential. Therefore, we accepted our hypothesis. In addition, metformin was selected as a positive control in the present study because of its well-known hypoglycemia effect. Table 1 shows that the hypoglycemic effect of all doses of FA was still lower than that of the positive drug MF. However, the high dose of FA reversed all of the renal lesions, inflammation, and oxidant/antioxidant status to almost the levels of the MF

group. Therefore, our results might provide further insight into therapeutic strategies for diabetic kidney disease.

Acknowledgments

This paper was funded by the Deanship of Scientific Research (DSR), King Abdulaziz University, Jeddah, under Grant no. (34-130-D1432). The author, therefore, acknowledges with thanks DSR technical and financial support. The author wishes to acknowledge Dr. Michael Morcos, Department of Internal Medicine I (Endocrinology, Metabolism and Clinical Chemistry) Faculty of Medicine, Lüprecht-Karls University, Heidelberg, Germany, who provided ELISA kits and some fine chemicals and for his kind and continuous advice. Deep thanks go to Dr. Wafae Goma, Pathology Department, Faculty of Medicine, King Abdulaziz University, KSA who did the histopathological examinations.

References

- [1] D. Mahmood, B. K. Singh, and M. Akhtar, "Diabetic neuropathy: therapies on the horizon," *Journal of Pharmacy and Pharmacology*, vol. 61, no. 9, pp. 1137–1145, 2009.
- [2] S. Shelbaya, H. Amer, S. Seddik et al., "Study of the role of interleukin-6 and highly sensitive C-reactive protein in diabetic nephropathy in type 1 diabetic patients," *European Review for Medical and Pharmacological Sciences*, vol. 16, no. 2, pp. 176–182, 2012.
- [3] Y. S. Kanwar, J. Wada, L. Sun et al., "Diabetic nephropathy: mechanisms of renal disease progression," *Experimental Biology and Medicine*, vol. 233, no. 1, pp. 4–11, 2008.
- [4] I.-M. Liu, T.-F. Tzeng, S.-S. Liou, and C. J. Chang, "Beneficial effect of traditional chinese medicinal formula Danggui-Shaoyao-San on advanced glycation end-product-mediated renal injury in streptozotocin-diabetic rats," *Evidence-based Complementary and Alternative Medicine*, vol. 2012, Article ID 140103, 2012.
- [5] G. Giacchetti, L. A. Sechi, S. Rilli, and R. M. Carey, "The renin-angiotensin-aldosterone system, glucose metabolism and diabetes," *Trends in Endocrinology and Metabolism*, vol. 16, no. 3, pp. 120–126, 2005.
- [6] M. Kitada, D. Koya, T. Sugimoto et al., "Translocation of glomerular p47phox and p67phox by protein kinase C- β activation is required for oxidative stress in diabetic nephropathy," *Diabetes*, vol. 52, no. 10, pp. 2603–2614, 2003.
- [7] A. A. R. Sayed and M. Morcos, "Thymoquinone decreases AGE-induced NF- κ B activation in proximal tubular epithelial cells," *Phytotherapy Research*, vol. 21, no. 9, pp. 898–899, 2007.
- [8] M. Morcos, A. A. R. Sayed, A. Bierhaus et al., "Activation of tubular epithelial cells in diabetic nephropathy," *Diabetes*, vol. 51, no. 12, pp. 3532–3544, 2002.
- [9] S. Bhatia, R. Shukla, S. V. Madhu, J. K. Gambhir, and K. M. Prabhu, "Antioxidant status, lipid peroxidation and nitric oxide end products in patients of type 2 diabetes mellitus with nephropathy," *Clinical Biochemistry*, vol. 36, no. 7, pp. 557–562, 2003.
- [10] G. G. Wang, X. H. Lu, W. Li, X. Zhao, and C. Zhang, "Protective effects of luteolin on diabetic nephropathy in STZ-induced diabetic rats," *Evidence-based Complementary and*

- Alternative Medicine*, vol. 2011, Article ID 323171, 7 pages, 2011.
- [11] B. Lipinski, "Pathophysiology of oxidative stress in diabetes mellitus," *Journal of Diabetes and its Complications*, vol. 15, no. 4, pp. 203–210, 2001.
 - [12] M. Naziroğlu and M. Çay, "Protective role of intraperitoneally administered vitamin E and selenium on the antioxidative defense mechanisms in rats with diabetes induced by streptozotocin," *Biological Trace Element Research*, vol. 79, no. 2, pp. 149–159, 2001.
 - [13] J. J. Bhaskar, M. S. Shobha, K. Sambaiah, and P. V. Salimath, "Beneficial effects of banana (*Musa sp. var. elakki bale*) flower and pseudostem on hyperglycemia and advanced glycation end-products (AGEs) in streptozotocin-induced diabetic rats," *Journal of Physiology and Biochemistry*, vol. 67, no. 3, pp. 415–425, 2011.
 - [14] R. Choi, B. H. Kim, J. Naowaboot et al., "Effects of ferulic acid on diabetic nephropathy in a rat model of type 2 diabetes," *Experimental and Molecular Medicine*, vol. 43, no. 12, pp. 676–683, 2011.
 - [15] A. Fujita, H. Sasaki, A. Doi et al., "Ferulic acid prevents pathological and functional abnormalities of the kidney in Otsuka Long-Evans Tokushima Fatty diabetic rats," *Diabetes Research and Clinical Practice*, vol. 79, no. 1, pp. 11–17, 2008.
 - [16] T. Nakagawa, T. Yokozawa, K. Terasawa, and K. Nakanishi, "Therapeutic usefulness of Keishi-bukuryo-gan for diabetic nephropathy," *Journal of Pharmacy and Pharmacology*, vol. 55, no. 2, pp. 219–227, 2003.
 - [17] G. Appendino, P. Spagliardi, G. Cravotto, V. Pocock, and S. Milligan, "Daucane phytoestrogens: a structure-activity study," *Journal of Natural Products*, vol. 65, no. 11, pp. 1612–1615, 2002.
 - [18] M. H. Abd El-Razek, S. Ohta, and T. Hirata, "Terpenoid coumarins of the genus *Ferula*," *Heterocycles*, vol. 60, no. 3, pp. 689–716, 2003.
 - [19] A. A. Ahmed, M. E. F. Hegazy, A. Zellagui et al., "Ferulsinaic acid, a sesquiterpene coumarin with a rare carbon skeleton from *Ferula* species," *Phytochemistry*, vol. 68, no. 5, pp. 680–686, 2007.
 - [20] M. B. Aqel, S. Al-Khalil, F. Afifi, and D. Al-Eisawi, "Relaxant effects of *Ferula sinaica* root extract on rabbit and guinea pig smooth muscle," *Journal of Ethnopharmacology*, vol. 31, no. 3, pp. 373–381, 1991.
 - [21] M. B. Aqel, S. Al-Khalil, and F. Afifi, "Effects of a *Ferula sinaica* root extract on the uterine smooth muscle of rat and guinea pig," *Journal of Ethnopharmacology*, vol. 31, no. 3, pp. 291–297, 1991.
 - [22] A. A. R. Sayed, "Ferulsinaic acid attenuation of advanced glycation end products extends the lifespan of *Caenorhabditis elegans*," *Journal of Pharmacy and Pharmacology*, vol. 63, no. 3, pp. 423–428, 2011.
 - [23] W. Xue, J. Lei, X. Li, and R. Zhang, "*Trigonella foenum graecum* seed extract protects kidney function and morphology in diabetic rats via its antioxidant activity," *Nutrition Research*, vol. 31, no. 7, pp. 555–562, 2011.
 - [24] A. Troudi, I. Ben Amara, N. Soudani, A. M. Samet, and N. Zeghal, "Oxidative stress induced by gibberellic acid on kidney tissue of female rats and their progeny: biochemical and histopathological studies," *Journal of Physiology and Biochemistry*, vol. 67, no. 3, pp. 307–316, 2011.
 - [25] M. Nishikimi, N. Appaji Rao, and K. Yagi, "The occurrence of superoxide anion in the reaction of reduced phenazine methosulfate and molecular oxygen," *Biochemical and Biophysical Research Communications*, vol. 46, no. 2, pp. 849–854, 1972.
 - [26] A. A. Sayed, "Thymoquinone and proanthocyanidin attenuation of diabetic nephropathy in rats," *European Reviews for Medical and Pharmacological Science*, vol. 16, no. 6, pp. 808–815, 2012.
 - [27] H. Ohkawa, N. Ohishi, and K. Yagi, "Assay for lipid peroxides in animal tissues by thiobarbituric acid reaction," *Analytical Biochemistry*, vol. 95, no. 2, pp. 351–358, 1979.
 - [28] R. A. Mekheimer, A. A. Sayed, and E. A. Ahmed, "Novel 1,2,4-triazolo[1,5-a]pyridines and their fused ring systems attenuate oxidative stress and prolong lifespan of *Caenorhabditis elegans*," *Journal of Medicinal Chemistry*, vol. 55, no. 9, pp. 4169–4177, 2012.
 - [29] M. S. Moron, J. W. Depierre, and B. Mannervik, "Levels of glutathione, glutathione reductase and glutathione S-transferase activities in rat lung and liver," *Biochimica et Biophysica Acta*, vol. 582, no. 1, pp. 67–78, 1979.
 - [30] T. Matsubasa, T. Uchino, S. Karashima, M. Tanimura, and F. Endo, "Oxidative stress in very low birth weight infants as measured by urinary 8-OHdG," *Free Radical Research*, vol. 36, no. 2, pp. 189–193, 2002.
 - [31] H. Nakayama, T. Mitsushashi, S. Kuwajima et al., "Immunochemical detection of advanced glycation end products in lens crystallins from streptozotocin-induced diabetic rat," *Diabetes*, vol. 42, no. 2, pp. 345–350, 1993.
 - [32] A. A. Sayed, K. El-Shaieb, and A. Mourad, "Life span extension of *Caenorhabditis elegans* by Novel pyrido perimidine derivative," *Archives of Pharmacal Research*, vol. 35, no. 1, pp. 69–76, 2012.
 - [33] A. Schlotterer, G. Kukudov, F. Bozorgmehr et al., "C. elegans as model for the study of high glucose-mediated life span reduction," *Diabetes*, vol. 58, no. 11, pp. 2450–2456, 2009.
 - [34] S. Fukuzawa, Y. Watanabe, D. Inaguma, and N. Hotta, "Evaluation of glomerular lesion and abnormal urinary findings in OLETF rats resulting from a long-term diabetic state," *Journal of Laboratory and Clinical Medicine*, vol. 128, no. 6, pp. 568–578, 1996.
 - [35] G. Arunachalam, D. Chattopadhyay, S. Chatterjee, A. B. Mandal, T. K. Sur, and S. C. Mandal, "Evaluation of anti-inflammatory activity of *Alstonia macrophylla* Wall ex A. DC. leaf extract," *Phytomedicine*, vol. 9, no. 7, pp. 632–635, 2002.
 - [36] J. W. Baynes, "Role of oxidative stress in development of complications in diabetes," *Diabetes*, vol. 40, no. 4, pp. 405–412, 1991.
 - [37] D. Koya, K. Hayashi, M. Kitada, A. Kashiwagi, R. Kikkawa, and M. Haneda, "Effects of antioxidants in diabetes-induced oxidative stress in the glomeruli of diabetic rats," *Journal of the American Society of Nephrology*, vol. 14, no. 3, pp. S250–S253, 2003.
 - [38] K. E. Knoll, J. L. Pietrusz, and M. Liang, "Tissue-specific transcriptome responses in rats with early streptozotocin-induced diabetes," *Physiological Genomics*, vol. 21, pp. 222–229, 2005.
 - [39] A. A. Sayed, M. Khalifa, and F. F. Abdelatif, "Fenugreek attenuation of diabetic nephropathy in alloxan-diabetic rats," *Journal of Physiology and Biochemistry*, vol. 68, no. 2, pp. 263–269, 2012.
 - [40] M. Morcos, A. Schlotterer, A. A. Sayed et al., "Rosiglitazone reduces angiotensin II and advanced glycation end product-dependent sustained nuclear factor-kappaB activation in cultured human proximal tubular epithelial cells," *Hormone and Metabolic Research*, vol. 40, no. 11, pp. 752–759, 2008.

- [41] M.-X. Fu, J. R. Requena, A. J. Jenkins, T. J. Lyons, J. W. Baynes, and S. R. Thorpe, "The advanced glycation end product, N ϵ -(carboxymethyl)lysine, is a product of both lipid peroxidation and glycoxidation reactions," *The Journal of Biological Chemistry*, vol. 271, no. 17, pp. 9982–9986, 1996.
- [42] A. A. R. Saved, "Thymoquinone protects renal tubular cells against tubular injury," *Cell Biochemistry and Function*, vol. 26, no. 3, pp. 374–380, 2008.

Research Article

Efficacy of *Boesenbergia rotunda* Treatment against Thioacetamide-Induced Liver Cirrhosis in a Rat Model

Suzy M. Salama,¹ Mehmet Bilgen,² Ahmed S. Al Rashdi,¹ and Mahmood A. Abdulla¹

¹Department of Molecular Medicine, Faculty of Medicine, University Malaya, 50603 Kuala Lumpur, Malaysia

²Radiology Department, Faculty of Medicine, Erciyes University, Kayseri 38039, Turkey

Correspondence should be addressed to Mahmood A. Abdulla, mahmood955@yahoo.com

Received 30 January 2012; Accepted 13 July 2012

Academic Editor: Vincenzo De Feo

Copyright © 2012 Suzy M. Salama et al. This is an open access article distributed under the Creative Commons Attribution License, which permits unrestricted use, distribution, and reproduction in any medium, provided the original work is properly cited.

Background. Experimental research in hepatology has focused on developing traditional medicines into potential pharmacological solutions aimed at protecting liver from cirrhosis. Along the same line, this study investigated the effects of ethanol-based extract from a traditional medicine plant *Boesenbergia rotunda* (BR) on liver cirrhosis. **Methodology/Results.** The BR extract was tested for toxicity on 3 groups of rats subjected to vehicle (10% Tween 20, 5 mL/kg) and 2g/kg and 5g/kg doses of the extract, respectively. Next, experiments were conducted on a rat model of cirrhosis induced by thioacetamide injection. The rats were divided into five groups and, respectively, administered orally with 10% Tween-20 (5 mL/kg) (normal control group), 10% Tween-20 (5 mL/kg) (cirrhosis control group), 50 mg/kg of silymarin (reference control group), and 250 mg/kg and 500 mg/kg of BR extract (experimental groups) daily for 8 weeks. The rats in normal group were intraperitoneally injected with sterile distilled water (1 mL/kg) 3 times/week, and those in the remaining groups were injected intraperitoneally with thioacetamide (200 mg/kg) thrice weekly. At the end of the 8 weeks, the animals were sacrificed and samples were collected for comprehensive histopathological, coagulation profile and biochemical evaluations. Also, the antioxidant activity of the BR extract was determined and compared with that of silymarin. Data from the acute toxicity tests showed that the extract was safe to use. Histological analysis of the livers of the rats in cirrhosis control group revealed uniform coarse granules on their surfaces, hepatocytic necrosis, and lymphocytes infiltration. But, the surfaces morphologically looked much smoother and the cell damage was much lesser in those livers from the normal control, silymarin and BR-treated groups. In the high-dose BR treatment group, the livers of the rats exhibited nearly normal looking lobular architecture, minimal inflammation, and minimal hepatocyte damage, the levels of the serum biomarkers and liver enzymes read nearly normal, and these results were all comparable to those observed or quantified from the normal and silymarin-treated groups. The BR extract had the antioxidant activity about half of what was recorded for silymarin. **Conclusion.** The progression of the liver cirrhosis can be intervened using the ethanol-based BR extract, and the liver's status quo of property, structure, and function can be preserved. This capability of the extract warrants further studies exploring the significance of its pharmacologic potential in successfully treating the liver cirrhosis in humans.

1. Introduction

Pharmaceutical compounds with formulations based on interferon, colchicines, penicillamine, and corticosteroids are currently available for treating common liver diseases of cirrhosis, fatty liver, and chronic hepatitis, but with either inconsistent efficacies or high incidences of side effects [1]. A number of natural compounds extracted from plants offer alternative treatment options that are safe and effective [2]. Extracts from newly discovered or already known plant

species are constantly being tested on animal model systems mimicking human diseases and injuries [3]. Presently, many natural extracts are used for treating human disorders in organs, but other than the liver [4]. Therefore, the potential roles and effectiveness of these extracts in liver diseases are yet to be studied. An extract obtained from the perennial herb *Boesenbergia rotunda* (BR) is one of those in this category and waiting for exploration of its role in liver pathologies.

The plant BR belongs to the family Zingiberaceae and is traditionally called *temu kunci*. With unique finger-like

rhizomes, it is commonly used as a folk medicine in Southeast Asia for treating several diseases including aphthous, dry mouth, stomach discomfort, leucorrhea, and dysentery. Scientific investigations in the past have reported that the extracts isolated from the BR plant using various solutions (such as methanol, hexane, or chloroform) have neuroprotective [5], antibacterial [6], anticancer [7], antifeedant [8], and antiviral [9] effects. The methanol-based extract was shown to contain chemical compounds Quercetin and Kaempferol, which are known to play critical role in antioxidant and anti-inflammatory cascades or processes [10]. When the hexane or chloroform is used in the isolation process, the resulting extract contains other important antioxidants: three flavanones (pinostrobin, pinocembrin, and alpinetin) and two chalcones (cardamonin and boesenbergin) [11].

Our laboratory has been investigating the therapeutic values of various plant-based extracts in prevention and protection of liver against toxins [12]. As a continuation of our efforts, in this study, for the first time, we evaluated the previously demonstrated anti-oxidant property of the ethanol-based BR extract in progressive liver damage. In particular, we tested the efficacy of the extract as a therapeutic agent on a rat model of liver cirrhosis induced chemically by thioacetamide (TAA) administration. We have been working with this experimental model because it closely mimics the etiology and pathology of the disease seen in humans.

To objectively evaluate the therapeutic value of the BR extract on the liver cirrhosis, we also employed another herbal substance silymarin—a hepatoprotectant with a well-established record [13]. Silymarin is a purified extract obtained from the seeds of the plant *Silybum marianum* and used widely as a supportive therapy for liver disorders such as cirrhosis, hepatitis, and fatty acid infiltration due to alcohol and toxic chemicals [14]. We compared the positive effects achieved with the BR extract on the cirrhotic liver against the benchmark protection provided by silymarin. In the following, we describe each of the processes and procedures employed in our experiments for assessing the anti-oxidant power, toxicity, and effectiveness of the BR extract. We present extensive data showing pathological and biochemical changes obtained with and without the extract treatment in groups of experiments and discuss our findings in detail regarding the merit of the BR extract as a potential agent for protecting the liver from cirrhosis.

2. Materials and Methods

2.1. Experimental Animals. Animal protocols governing the experiments were approved by the Ethics Committee for Animal Experimentation, Faculty of Medicine, University of Malaya, Malaysia and the Ethic number PM/07/05/2010/MMA (a) (R) and PM/28/08/2010/MAA (R). Sprague Dawley rats of 6–8 weeks old and weighed between 180 and 200 g were obtained from the institutional animal facility. Throughout the study, the rats were cared humanely and maintained for their normal circadian rhythms by following the guidelines provided in the “Guide

for the Care and Use of laboratory Animals” which was prepared by the National Academy of Sciences and published by the National Institute of Health, Malaysia. The rats were given standard pellet diet and tap water, kept in wire-bottomed cages at $25 \pm 2^\circ\text{C}$, exposed to 12 hours light and dark cycle, and housed in an animal room with 50–60% humidity range.

The study was performed in three phases. The first phase involved removing the extract from the BR plant rhizomes and measuring its anti-oxidative property. In the second phase, the toxicity of the extract was examined on 36 (18 males and 18 females) healthy *Sprague Dawley* rats. In the third phase, the efficacy of the extract on inhibiting the development of liver cirrhosis was evaluated using 30 healthy adult male *Sprague Dawley* rats weighing 200–240 g. This experimental phase required chemically inducing cirrhosis by TAA injection to the rats and also using another plant extract silymarin for a reference comparison.

2.2. Extract Removal from the Plant BR. Fresh rhizomes of the plant BR were purchased from a commercial company (Ethno Resources Sdn Bhd, Selangor, Malaysia), and identified by comparing it with the voucher specimen deposited at the Herbarium of Rimba Ilmu, Institute of Science Biology, University of Malaya, Kuala Lumpur, Malaysia. After washing with tap water first and then distilled water later, the rhizomes were sliced and left in a shade for a duration of 10 days to dry out. The dried samples were then grounded finely, and 100 g of the resulting powder was mixed in 1000 mL solution of 95% ethanol for 7 days at room temperature. The ethanol extract was distilled under a reduced pressure in Eyela Rotary Evaporator (Sigma-Aldrich, USA), and dried at 40°C in an incubator for 3 days giving a gummy yield of 9.49% (w/w). For the oral administration to the rats, the final product was further dissolved in Tween 20 (10% w/v) and the desired dose for the administration was expressed as concentration in mg/mL per body weight in kg.

2.3. Antioxidant Power of the BR Extract. The anti-oxidant power of the BR extract was determined using a test sensitive to its scavenging ability towards reactive oxygen species or reagents containing iron. In this regard, the ferric reducing anti-oxidant power (FRAP) of the BR extract was determined using an assay by following the method described in [15], but with a slight modification. The FRAP reagent was prepared by mixing 300 mM acetate buffer (3.1 mg sodium acetate/mL, pH 3.6), 10 mM 2,4,6-tripyridyl-S-triazine (TPTZ) (Merck, Darmstadt Germany) solution and 20 mM $\text{FeCl}_3 \cdot \text{H}_2\text{O}$ (5.4 mg/mL). The BR extract and the following standards: Gallic acid, Quercetin, Ascorbic acid, Rutin, Trolox, and 2,6-di-tert-butyl-4-methyl phenol (BHT), were sampled in amounts of $10 \mu\text{L}$ of 1 mg/mL and $10 \mu\text{L}$ each along with $10 \mu\text{L}$ of 0.1 mg/mL silymarin. To each sample separately, $290 \mu\text{L}$ of the reagent TPTZ were added. The absorbencies of the resulting mixtures were read repetitively at every 4 min for up to 2 hr using ELISA reader (Shimadzu, The Netherlands) at 593 nm wavelength. We note that the dynamic range of the instrument was limited to read the

dose amounts of 500 mg/kg for the BR extract and 50 mg/kg dose for silymarin administered to the rats daily, as described below. To compensate this deficiency, we performed the measurements in equivalent amounts obtained by scaling the administered doses up by 20 times, respectively. The readings from the mixtures containing the BR extract and silymarin were compared against the following standards: Gallic acid, Quercetin, Ascorbic acid, Rutin, Trolox, and BHT (2,6-di-tert-butyl-4-methyl phenol) [14].

2.4. Toxicity of the BR Extract. The toxicity of the BR extract was evaluated in normal healthy rats by subjecting them significantly to high doses of the extract. Rats were assigned equally into 3 groups, each with 6 males and 6 females, labeled as vehicle (10% Tween-20, 5 mL/kg) and 2 g/kg and 5 g/kg of rhizome extract preparation, respectively. The rats were deprived of food but not water prior to the dosing. Food was withheld for another 3-4 hours after the dosing. The animals were observed at 30 min and 2, 4, 8, 24, and 48 hours after the oral administration to detect the onset of clinical or toxicological symptoms. The animals were sacrificed on day 15. Through the jugular vein, blood was collected directly at the time of the sacrifice. Histological Prothrombin time and serum biochemical parameters were determined following the standard methods [16].

2.5. Treatment Groups and Experiments. A set of experiments were carried out to test the therapeutic effects of the BR extract on liver cirrhosis. For this purpose, thirty male rats were acquired and randomly divided into 5 groups where each consisted of 6 rats. The experiments lasted for 8 weeks, and all of the rats were kept alive during this timeframe. Classifications of the groups were as follows.

Group 1 served as the normal control group. The rats in this group were administered orally with 10% Tween-20 (5 mL/kg) daily and injected intraperitoneally (IP) with sterile distilled water (1 mL/kg) thrice weekly.

The rats in the remaining *Groups 2–5* were exposed to Thioacetamide (TAA) toxicity to induce cirrhosis in their livers. Constant exposure with this amount of TAA induces changes in liver pathology from both biological and morphological aspects comparable to the etiology of cirrhosis seen in humans [17] and therefore used very often as a preferred model in experimental studies of liver cirrhosis. Highest grade of TAA was purchased in crystal form from Chemolab Supplies, (Sigma-Aldrich, USA). The crystals were diluted in sterile distilled water and stirred well until all fully dissolved to prepare a stock solution of 5 g/L. TAA was injected IP three times a week at a dose of (200 mg/kg/mL in distilled water) [18].

Group 2 served as the cirrhosis control group with cirrhotic rats injected IP with TAA three times a week at a dose of (200 mg/kg/mL in distilled water) and oral delivery of 10% Tween 20 (5 mL/kg) daily.

Group 3 was the silymarin-treated group. The cirrhotic rats in this group were administered orally with silymarin (50 mg/kg) daily. Silymarin (International Laboratory, USA) is a standard drug and was prepared by dissolving in 10% Tween 20 [19].

Groups 4 and 5 were the treatment groups, where the cirrhotic rats were administered orally with the BR extract at respectively 250 mg/kg and 500 mg/kg doses daily.

We rationalized that the above protocol of applying treatment with silymarin or the BR extract in parallel after inducing cirrhosis using TAA injection was clinically equivalent to instituting the therapy as soon as the onset of the cirrhosis was diagnosed. In this regard, the treatment is preventive since it slows down the progression of the cirrhosis and protective since the liver is protected from further deterioration.

After 8 weeks, each rat was made to fast for 24 hours after the last treatment and then perfused under Ketamine (30 mg/kg, 100 mg/mL) and Xylazil (3 mg/kg, 100 mg/mL) anesthesia [20]. Through the jugular vein, blood was withdrawn and collected for prothrombin time and biochemical examinations. After the perfusion, the liver was excised and washed in ice-cold normal saline, blotted in filter paper, weighed and carefully inspected for the presence of any gross pathology. The liver tissues were further assessed as described below.

2.6. Postmortem Liver Tissue Analysis. For the histopathological analysis, the liver specimens were fixed in 10% buffered formaldehyde, processed by automated tissue processing machine, and then embedded in paraffin wax. Sections were prepared in 5 μ m thicknesses, stained with hematoxylin-eosin (H&E), and examined under the light microscope.

For determining the normality of the hepatocytes, the number of normal cells was counted at the center of the cirrhotic area as well as the normal areas adjacent to both sides of the cirrhotic area using a light microscope with an oil immersion objective ($\times 40$) covering 0.15 mm² [21]. Percentage of the normal cells was calculated by using the formula: %Normal cells = [(Normal cells/(Normal + apoptotic cells) \times 100].

2.7. Evaluation of Cellular Damage. Malondialdehyde (MDA) is a natural product of lipid peroxidation after cellular injury, and used as an indicator of cellular oxidative stress [22]. Superoxide dismutase enzyme (SOD) plays crucial role in defense mechanisms governing the antioxidant activities and hence in prevention of diseases linked to oxidative stress [23]. To examine the actions of the BR extract on the levels of MDA and SOD in the livers of the rats in all experimental Groups 1–5, the liver tissues were extracted, washed in saline, homogenized (10% w/v) in 50 mM cold potassium phosphate buffer (pH 7.4) by using teflon homogenizer (Polytron, Heidolph RZR 1, Germany), and processed at 3500 rpm for 10 minutes at 4°C in a centrifuge (Heraeus, Germany). The MDA level was measured from the supernatant using thiobarbituric acid as the lipid peroxidation marker [24]. Similarly, the SOD activity was assessed based on a method described in [25].

2.8. Biochemical Analysis. On sacrifice, blood samples of the rats were collected through the jugular vein into tubes with sodium citrate for determining prothrombin time or

into gel-activated tubes for the assessment of lipid profile and biochemical markers such as alkaline phosphatase (AP), alanine aminotransferase (ALT), aspartate aminotransferase (AST), lactate dehydrogenase (LDH), total protein, albumen, and bilirubin. The gel-activated tubes were allowed to clot, centrifuged at 3000 rpm for 10 minutes at 4°C. The serum samples were used for measuring the liver biochemicals. The markers were spectrophotometrically assayed by standard-automated techniques using the equipment at the Central Diagnostic Laboratory of the Medical Centre of University Malaya.

2.9. Statistical Analysis. The measurements from the experimental Groups 1–5 were evaluated statistically, and the statistical differences between the groups were determined using one-way ANOVA followed by Tukey Post-Hoc test analysis using SPSS program (version 18, SPSS Inc., Chicago, IL, USA). A value of $P < 0.05$ was considered as an indicative of statistically significant difference between the measurements of the two compared groups. All readings and calculated values were reported as Mean \pm SEM.

3. Results

3.1. Anti-Oxidant Property of the BR Extract. As shown in Figure 1, the ferric reducing antioxidant power (FRAP) of 1 mg/mL of BR extract was measured as 288.9 ± 0.002 mmol/1 mg while the calibration curve equation was $y = 0.0006 + 0.065x$, $R^2 = 0.9976$. The measured value was relatively lower than those of the standards Gallic acid, Quercetin, Ascorbic acid, Rutin, Trolox, and BHT, but comparable to the reference drug silymarin, which read 600.6 ± 0.003 mmol/0.1 mg. Silymarin contains several antioxidant compounds that play hepatoprotective roles. The BR extract may be playing similar role as it has free radical scavenging property and hence help the liver maintain its status quo.

3.2. Acute Toxicity Test. All the rats in the acute toxicity test remained alive and did not manifest mortality or any visible signs of toxicity throughout the 15-days-long study at the high doses of the BR extract 2 g/kg and 5 g/kg that they were subjected to. The physical observations indicated no signs of changes in their skins and furs, eyes and mucus membranes, behavior patterns, tremors, salivations, diarrhea occurrences, and sleeps. The body weight of the treated male and female rats increased gradually but were not significantly different as compared to those of the control rats. Gross necropsy findings did not reveal visible changes in any of the organs. The clinical observations were that serum biochemical measurements reflected the functional status of normal kidney and liver, and the histopathological evaluations of the kidney and the liver tissues all together revealed that there were no significant differences between the control and test groups, as shown by the quantitative data in Tables 1 and 2, and qualitative data in Figure 2.

3.3. Effects of the BR Extract on Liver Cirrhosis

3.3.1. Body Weight and Liver Index. The total body of each rat was weighted prior to the sacrifice. Similarly, the liver was weighted after being excised (Table 3). The control rats in Groups 1 followed natural growth pattern and attained normal weight gains from about 200 g to 347 g in 8 weeks. The injection of TAA made the rats hepatotoxic (Group 2) and suffer growth retardation as they weighted significantly less (mean = 217 g) than those measured from the other groups. When the body weights were factored in, the cirrhotic rats in Group 2 had the highest liver index (mean = 5.27). The rats in the silymarin and high dose (500 mg/kg) BR treatments in Groups 3 and 5, respectively, attained weights as equivalent as the normal rats in Group 1. The rats in the low-dose (250 mg/kg) BR treatment Group 4 had better weight gain than those in Group 2, but not as much as those attained in Groups 3 and 5.

These findings implied that the outcome of the treatment was susceptible to the administered dose amount, but the BR extract at this high-dose appeared to be optimal since it was as effective as silymarin in counteracting the progression of cirrhosis. In light of this, we suggest administering the 500 mg/kg dose of the BR extract in strategizing any treatment plan targeting to offset cirrhosis in the future experimental studies with translational focus.

3.3.2. Gross Anatomy and Histopathology. Figures 3 and 4, respectively, depict the gross appearances and the H&E-stained sections of the example liver samples from the experimental Groups 1–5. Grossly, the livers from the control rats in Group 1 (Figure 3(a)) appeared in reddish color, had smooth surfaces, and did not show any sign of nodules. The histological examination (Figure 4(a)) showed normal liver architecture with normal plates of hepatocytes separated by sinusoidal capillaries and central vein. In cirrhotic Group 2, the liver appeared congested with numerous micro- and macronodules (Figure 3(b)), lost its normal architecture by the presence of regenerating nodules that were separated by fibrous septae extending from the central vein to portal triad (Figure 4(b)). In addition, the fibrous septae were accompanied by severe proliferation of bile duct and heavy invasion of inflammatory cells. The cirrhotic nodules showed thick purple-colored bundles of collagen fibers. The livers of the reference control silymarin Group 3 (Figures 3(c) and 4(c)) and the high doses of BR extract (Figures 3(e) and 4(e)) showed a relatively minor micronodules, a lesser amount of fibrous septae development and expansion and an increase in the extension of normal hepatic parenchyma compared to those from the reference Group 3. In contrast, the livers of the low-dose BR Group 4 were occupied by lesser macronodules and lesser fibrotic nodules than those of the reference Group 3, but the improvements were not as much as those seen in Groups 3 or 5. These results based on the visual evaluations provided further independent confirmation that the applied BR extract was effectively protecting the liver against the progression of cirrhosis.

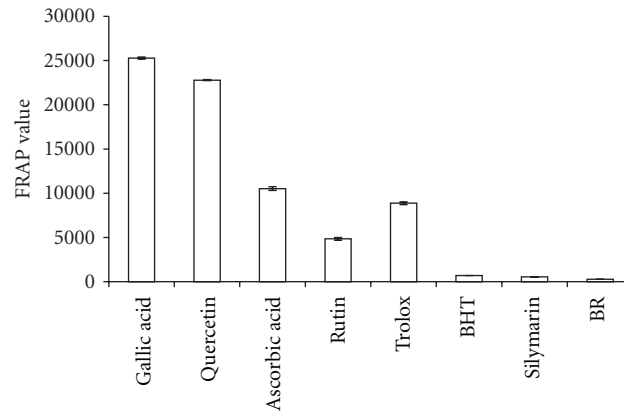


FIGURE 1: Antioxidant activity of the BR extract compared with the following standards: Gallic acid, Quercetin, Ascorbic acid, Rutin, Trolox, BHT as well as the standard drug Silymarin. Values were expressed as Mean \pm SEM. Significant value was at $P < 0.001$.

TABLE 1: Renal function measured from the acute toxicity test of the BR extract on rats.

Dose	Sodium (mmol/L)	Potassium (mmol/L)	Chloride (mmol/L)	Urea (mmol/L)	Creatinine (μ mol/L)
Vehicle (5 mL/kg)	138.25 \pm 0.45	5.03 \pm 0.19	104.03 \pm 0.15	5.63 \pm 0.41	50.18 \pm 1.34
LD (2 g/kg)	137.65 \pm 0.43	5.21 \pm 0.16	102.61 \pm 1.22	4.96 \pm 0.43	48.97 \pm 0.81
HD (5 g/kg)	137.21 \pm 0.51	4.89 \pm 0.15	102.67 \pm 0.76	5.93 \pm 0.39	48.60 \pm 1.80

The values were expressed as mean \pm S.E.M. There were no significant differences between the three groups. Significant value was at $P < 0.05$.

TABLE 2: Liver function measured from the acute toxicity test of the BR extract on rats.

Dose	Total protein (g/L)	Albumin (g/L)	TB (μ mol/L)	AP (IU/L)	ALT (IU/L)	AST (IU/L)	GGT (IU/L)
Vehicle (5 mL/kg)	71.37 \pm 1.44	11.36 \pm 0.53	1.91 \pm 0.17	134.78 \pm 9.57	53.05 \pm 3.27	153.65 \pm 9.35	4.91 \pm 0.93
LD (2 g/kg)	71.47 \pm 0.52	11.61 \pm 0.34	2.18 \pm 0.16	133.37 \pm 8.63	51.90 \pm 1.33	156.07 \pm 3.56	5.00 \pm 1.23
HD (5 g/kg)	71.81 \pm 1.03	11.72 \pm 0.16	1.88 \pm 0.21	135.13 \pm 6.52	52.27 \pm 3.25	155.00 \pm 5.35	5.32 \pm 1.07

TB: total bilirubin; AP: alkaline phosphatase; ALT: alanine aminotransferase; AST: aspartate aminotransferase; GGT: gamma-glutamyl transferase. The values were expressed as mean \pm S.E.M. There were no significant differences between the three groups. Significant value was at $P < 0.05$.

TABLE 3: Liver index measurements from the rats at the end of the 8-week study.

Treatment	Body weight (gm)	Liver weight (gm)	Liver index (LW/BW %)
Group 1 (normal rats)	347 \pm 5.04	9.70 \pm 0.16	2.79 \pm 0.21
Group 2 (rats with cirrhosis)	183 \pm 2.32	9.44 \pm 0.60	5.18 \pm 0.06**
Group 3 (silymarin-treated rats)	347 \pm 3.58	10.28 \pm 0.66	2.97 \pm 0.35*
Group 4 (treatment with the BR extract at 250 mg/kg dose)	255 \pm 2.91	10.03 \pm 0.46	3.93 \pm 0.44*
Group 5 (treatment with the BR extract at 500 mg/kg dose)	376 \pm 5.67	9.71 \pm 0.71	2.59 \pm 0.36*

Data were expressed as Mean \pm SEM. Means between the silymarin-treated Group 3, low-dose BR-treated Group 4, and high-dose BR-treated Group 5 had significant differences when compared with the cirrhosis control Group 2 with * $P < 0.001$ and compared with the normal control Group 1 with ** $P < 0.001$.

TABLE 4: Effect of BR ethanol extract on plasma levels of specific liver enzymes at the end of the 8-week study.

Treatment	AP IU/L	ALT IU/L	AST IU/L	LDH IU/L
Group 1 (normal rats)	79.28 \pm 0.58	30.57 \pm 1.51	70.35 \pm 0.21	490.97 \pm 3.90
Group 2 (rats with cirrhosis)	270.50 \pm 4.88**	150.42 \pm 2.60**	250.88 \pm 2.99**	991.72 \pm 5.01**
Group 3 (silymarin-treated rats)	83.85 \pm 1.06	31.62 \pm 0.63	70.35 \pm 0.43	546.33 \pm 10.46
Group 4 (treatment with the BR extract at 250 mg/kg dose)	110.22 \pm 0.49*	91.02 \pm 1.61*	106.00 \pm 2.59*	792.00 \pm 3.51*
Group 5 (treatment with the BR extract at 500 mg/kg dose)	86.13 \pm 0.56*	33.42 \pm 0.56*	71.10 \pm 0.78*	574.00 \pm 5.34*

AP: alkaline phosphatase; ALT: alanine transferase; AST: aspartate transferase; LDH lactate dehydrogenase. Means between the silymarin-treated Group 3, low-dose BR-treated Group 4, and high-dose BR-treated Group 5 had significant differences when compared with the cirrhosis control Group 2 with * $P < 0.001$ and compared with the normal control Group 1 with ** $P < 0.001$.

TABLE 5: Effect of Br ethanol extract on serum protein, albumen, and globulin levels and prothrombin time ratio at the end of the 8-week study.

Treatment	Protein g/L	Albumen g/L	Bilirubin umol/L	Prothrombin time ratio
Group 1 (normal rats)	76.58 ± 0.70	31.93 ± 0.64	1.20 ± 0.06	1.02 ± 0.006
Group 2 (rats with cirrhosis)	59.92 ± 1.14**	11.22 ± 0.33**	4.98 ± 0.12**	1.38 ± 0.024**
Group 3 (silymarin-treated rats)	75.82 ± 0.70	32.38 ± 0.88	1.28 ± 0.07	1.02 ± 0.005
Group 4 (treatment with the BR extract at 250 mg/kg dose)	63.37 ± 1.20	20.20 ± 0.20*	2.85 ± 0.10*	1.28 ± 0.009*
Group 5 (treatment with the BR extract at 500 mg/kg dose)	75.10 ± 1.07*	29.38 ± 0.28*	1.68 ± 0.05*	1.03 ± 0.002*

Means between the silymarin-treated Group 3, low-dose BR-treated Group 4, and high-dose BR-treated Group 5 had significant differences when compared with the cirrhosis control Group 2 with * $P < 0.001$ and compared with the normal control Group 1 with ** $P < 0.001$.

TABLE 6: Effect of BR ethanol extract on serum lipid profiles at the end of the 8-week study.

Treatment	Cholesterol mmol/L	HDL mmol/L	LDL mmol/L	Triglycerides mmol/L
Group 1 (normal rats)	1.42 ± 0.05	1.13 ± 0.04	0.13 ± 0.02	1.27 ± 0.03
Group 2 (rats with cirrhosis)	3.22 ± 0.06**	0.53 ± 0.04**	2.50 ± 0.10**	2.83 ± 0.07**
Group 3 (Silymarin-treated rats)	1.80 ± 0.04	1.32 ± 0.04	0.33 ± 0.03	1.45 ± 0.04
Group 4 (treatment with the BR extract at 250 mg/kg dose)	2.00 ± 0.06*	0.62 ± 0.07	1.22 ± 0.07*	1.78 ± 0.03*
Group 5 (treatment with the BR extract at 500 mg/kg dose)	1.57 ± 0.05*	1.17 ± 0.05*	0.23 ± 0.02*	1.42 ± 0.05*

Means between the silymarin-treated Group 3, low-dose BR-treated Group 4, and high-dose BR-treated Group 5 had significant differences when compared with the cirrhosis control Group 2 with * $P < 0.001$ and compared with the normal control Group 1 with ** $P < 0.001$.

3.3.3. Cell Loss and Survival. The results concerning the normality of the hepatocytes were illustrated in Figure 5 for the rats in Groups 1–5. According to the data, the administration of TAA has observed to significantly decrease the number of normal liver cells from about 94% measured from the livers of the normal rats in Group 1 to about 11% measured from the livers of the cirrhotic rats in Group 2. Hepatocytic fatty degeneration was also present. In the low dose BR (250 mg/kg) treatment Group 4, the population of the normal cells was higher, about 71%. But, the treatment with the high dose BR maintained much higher number of normal cells, about 93%, which was nearly equal to those obtained from the silymarin-treated rats in Group 3 and comparable in the same manner to the normal rats in Group 1.

The loss of hepatocytes in the livers of the cirrhotic rats was probed indirectly via lipid peroxidation with MDA and anti-oxidant enzymatic activity with SOD, and the results were plotted in Figures 6 and 7. The MDA level reads relatively high value of 3.87 ± 0.08 nmol/mg protein in the cirrhosis control group when compared with the reading from the normal group 1.22 ± 0.08 nmol/mg protein. The SOD readings followed this trend but inversely, meaning that the cirrhotic rats in Group 2 had lower value of 9.80 ± 0.13 u/mg protein than 14.89 ± 0.28 u/mg protein from the normals in Group 1. These results indicated the presence of severely damaged cells in the cirrhotic livers. Treating the cirrhotic rats with the BR extract has significantly helped the survival of the hepatocytes as indicated by the reduced MDA and increased SOD levels in both the low- and high-dose groups, but the effect was more pronounced in the latter group. In the low- and high-dose groups, the MDA reads 2.08 ± 0.04 nmol/mg protein versus 1.60 ± 0.03 nmol/mg protein, and SOD reads 12.03 ± 0.06 u/mg protein versus

14.17 ± 0.19 u/mg protein, respectively. The MDA and SOD readings from the normal group were 1.22 ± 0.08 nmol/mg protein and 14.89 ± 0.28 u/mg protein, respectively and the corresponding values for the silymarin treated-group were 1.86 ± 0.03 nmol/mg protein and 14.03 ± 0.18 u/mg protein, respectively. These results collectively suggested that the BR treatment provided a host environment favorable for both preventing and protecting the hepatocytes from further damage.

3.3.4. Liver Markers and Lipid Profiles. Liver function of each rat was measured by determining the plasma levels of specific liver enzymes and lipid profile, and the results were presented in Tables 4, 5, and 6. According to the data in Tables 4 and 5, the TAA-induced liver damage significantly elevated the levels of specific liver enzymes AP, ALT, AST, LDH, bilirubin and prothrombin time ratio ($P < 0.001$) and significantly declined the protein and albumin levels in the cirrhotic rats of Group 2 as compared with those measured from all the other groups. Similarly, the lipid profiles in the cirrhotic rats altered significantly such that the cholesterol, LDL, and triglycerides levels were higher, and the HDL level was lower (Table 6). The high-dose BR (500 mg/kg) treatment Group 5 resulted in the readings on the biochemical markers that were comparable to those of the control Group 1 and the silymarin-treated (50 mg/kg) Group 3, and better than the readings obtained from the treatment with the low-dose BR (250 mg/kg) Group 4. These data further supported the qualitative gross anatomical, histopathological findings, the quantitative cell counts, presented above, and demonstrated that the effects of the toxicity induced by TAA on the liver function can effectively be counterbalanced by the positive effects of the BR extract treatment, but in a dose-dependent manner.

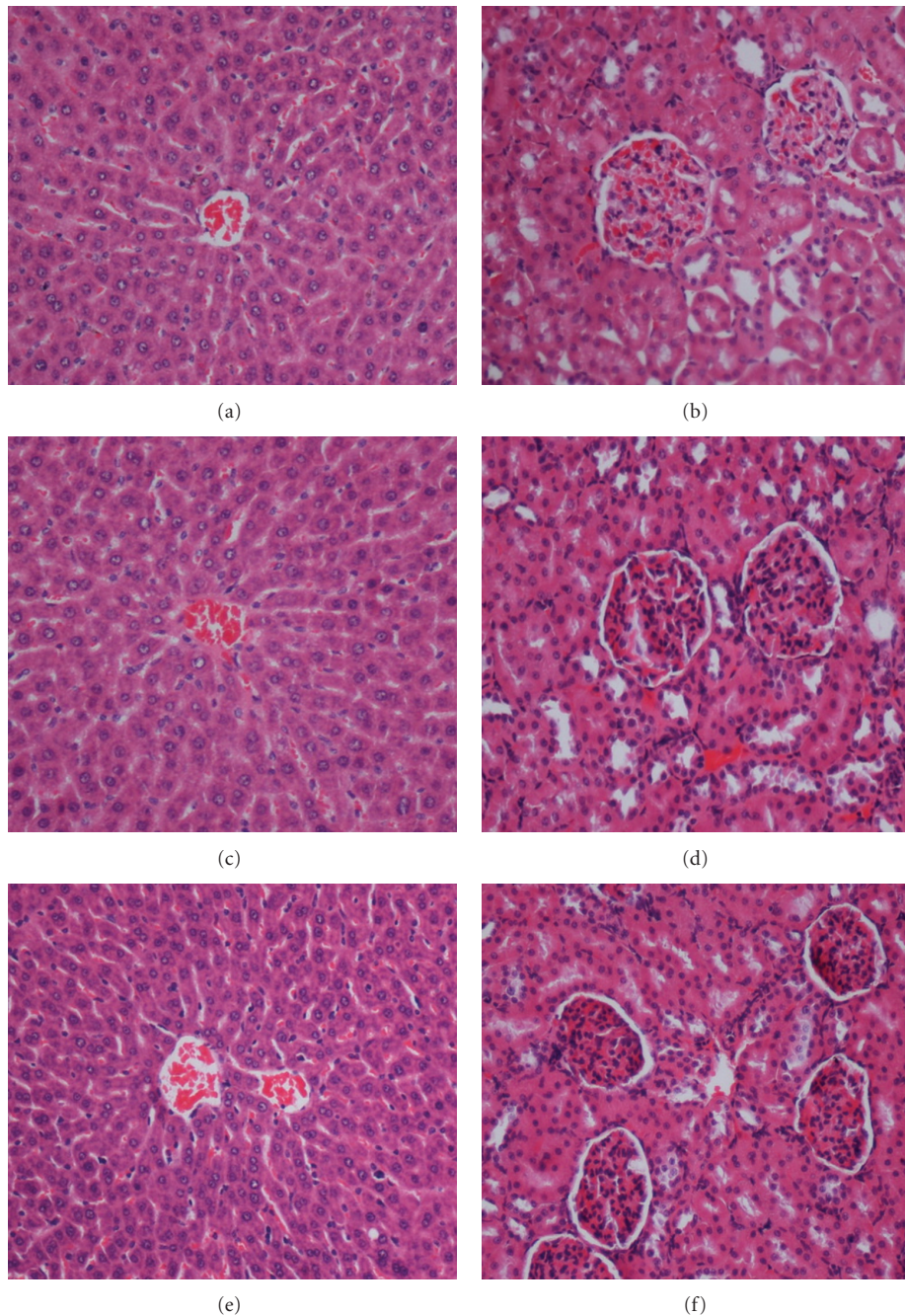


FIGURE 2: Examples of H&E-stained histological sections of livers (left column) and kidneys (right column) obtained from the rats in the acute toxicity test. Rat with the liver and kidney shown in (a) and (b) was treated with 5 mL/kg vehicle (10% Tween 20). Rat with the liver and kidney shown in (c) and (d) was treated with 2 g/kg (5 mL/kg) dose of the BR extract. Rat with the liver and kidney shown in (e) and (f) was treated with 5 g/kg (5 mL/kg) dose of the BR extract. There was no significant difference in the structures of the liver and kidney between the treatment and control groups.

4. Discussion

Liver cirrhosis has become a serious public health problem because of the broader use of prescription drugs with side effects in modern life or the substance abuse. Consequently, the current research has focused on understanding the

underlying metabolisms and subsequently finding new therapeutic solutions to interrupt the signaling pathways and minimize the damages inflicted on the liver [26]. Beyond the strategies with synthetic pharmacology, the search also pursues alternative approaches that rely on natural products. Especially, it targets those plants in the folk medicine with

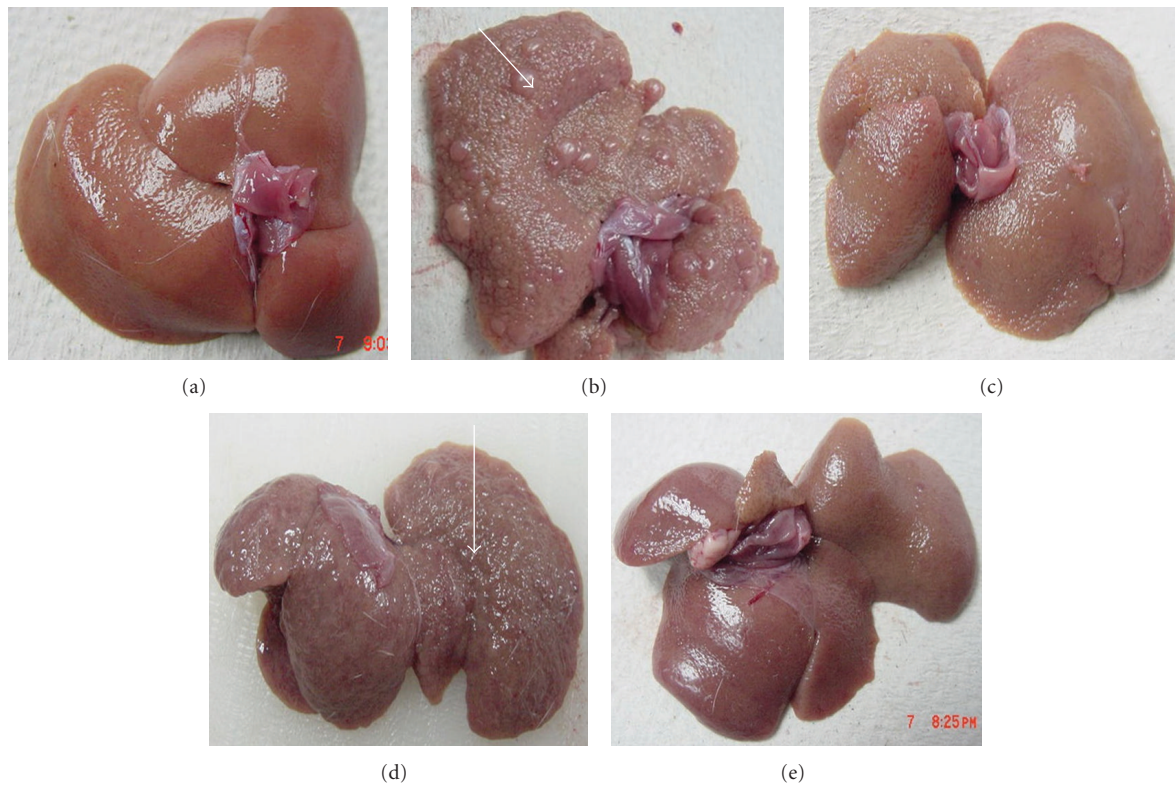


FIGURE 3: Example images showing macroscopic appearances of the livers sampled from rats in different experimental groups. (a) The liver of a control rat exhibiting regular smooth surface. (b) The liver of a hepatotoxic rat depicting numerous irregular whitish micro- and macronodular on its surface and a large area of ductular cholangiocellular proliferation (arrow) embedded within fibrosis. (c) The liver of a hepatoprotective rat treated with silymarin showing normal smooth surface. (d) The liver of a rat treated with 250 mg/kg of the BR extract illustrating nearly smooth surface with fewer granules (arrow head). (e) The liver of a rat treated with 500 mg/kg of the BR extract having normal smooth surface.

known history or demonstrated potential of positive effects against the diseases of the liver or other organs [27]. To aid these efforts, in this study, we examined the potential of ethanol-based extract from the plant BR as a promising therapeutic agent for treating liver cirrhosis.

In phase 2 of our study, we tested the toxicity of the BR extract. Our data in Figure 2 and Tables 1 and 2 showed that the extract at high doses caused no significant pathological abnormalities in the liver and kidney, and the clinical biochemistry readings remained within the normal range. These results were in agreement with the previous reports on the safety of consuming the BR extract [28].

In the next set of experiments, we examined the influence of the BR extract on the course of the cirrhosis development. The cirrhotic condition was induced by a prolonged exposure to TAA. Manipulating the amount of TAA dose produces different grades of liver damage that may range from the parenchymal cell necrosis and liver cell proliferation to the production of pseudolobules and nodular cirrhosis, [29]. In this study, we have chosen 200 mg/kg dose-administered IP for 2 months because this protocol was reported to yield etiology similar to the human cirrhosis in terms of anatomical, structural, functional, and architectural tissue characteristics as well as the readings on the common

biochemical markers [30]. The same was again reconfirmed collectively by the qualitative *ex vivo* visualization of the nodules in Figures 3 and 4, the quantitative data on the lower body weights of the cirrhotic rats in Table 3, the biochemical imbalances in the liver markers in Tables 4 and 5, and altered lipid profiles in Table 6. Therefore, our experimental rat model of cirrhosis was suitable for testing the efficacy of any applied preclinical therapy with a clinical translation in focus.

The TAA action in the development of cirrhosis was suggested to be multifaceted and to involve multiple mechanisms [19]. For example, TAA interferes with the RNA transference from nucleus to cytoplasm via its metabolite thioacetamide-S-oxide (TASO₂). Concerning the hepatocytes, a compromise in the RNA transfer leads to hepatic cell death via the processes of apoptosis and necrosis [31]. Quantitative histopathological analysis indicated the presence of severe hepatocellular loss since the percentage of the viable cells were substantially lower 11% in the cirrhotic rats in Group2 than 94% in normals in Group 1 (Figure 5). Lipid peroxidation is also a common event in a toxic phenomenon and causes cell death due to the degradation of membrane lipids [32]. Through another pathway, the TAA toxicity contributes to the liver damage by stimulating

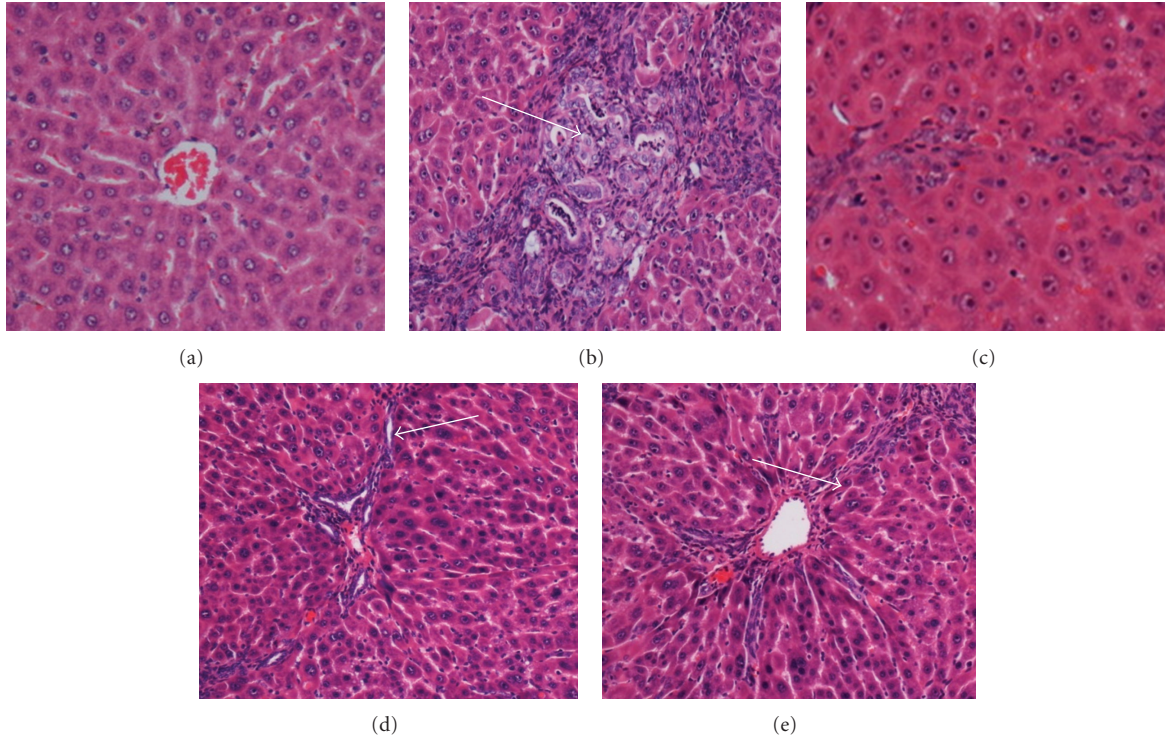


FIGURE 4: Example histopathological sections of livers sampled from rats in different experimental groups. (a) Normal histological structure and architecture were seen in livers of the control rats. (b) Severe structural damage, formation of pseudolobules with thick fibrotic septa and necrotic areas were present in the liver of the hepatotoxic rat. (c) Mild inflammation but no fibrotic septa was depicted in the liver of the hepatoprotective rat treated with silymarin. (d) Partially preserved hepatocyte and architecture with small area of necrosis and fibrotic septa existed in the liver of the rat treated with 250 mg/kg of the BR extract. (e) Partially preserved hepatocyte and architecture with small areas of mild necrosis were observed in the liver of the rat treated with 500 mg/kg of the BR extract. (H&E stain original magnification 20x).

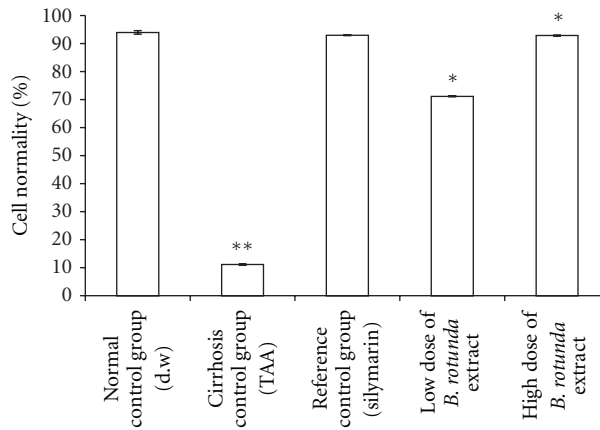


FIGURE 5: Effect of BR ethanol extract on % cell normality. Data are expressed as mean \pm SEM. Means among groups ($n = 6$ rats/group) show significant difference, * $P < 0.001$ compared to cirrhosis control group and ** $P < 0.001$ compared to normal control group.

the production of excessive reactive oxygen species [33]. This effect was recorded in Figures 6 and 7. The data indicated that the hepatocytes were under oxidative stress, lipid peroxidation was prevalent as reflected by the larger MDA readings, and the anti-oxidant defense mechanism was failed as hinted by the attenuated SOD readings.

The cirrhotic livers responded favorably to the treatment with the BR extract at both doses (250 mg/kg and

500 mg/kg) and the reference extract silymarin at the daily dose of 50 mg/kg. Each of the treatment regimens unequivocally produced significant improvements in the anatomical, structural, functional, and architectural signatures of the otherwise cirrhotic livers. The efficacy in protecting the liver was however marginally better with the higher BR dose, and encouragingly very close to that of silymarin. Nearly identical responses between the high-dose BR and silymarin

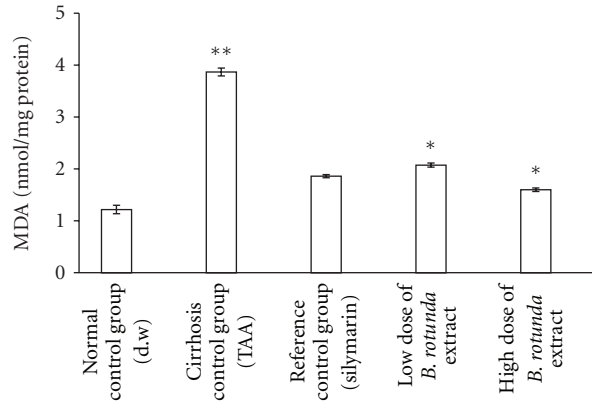


FIGURE 6: Effect of the BR extract on the level of MDA in the liver tissue. Data were expressed as Mean \pm SEM. Means between the silymarin treated Group 3, low-dose BR-treated Group 4, and high-dose BR-treated Group 5 had significant differences when compared with the cirrhosis control Group 2 with $*P < 0.001$ and compared with the normal control Group 1 with $**P < 0.001$.

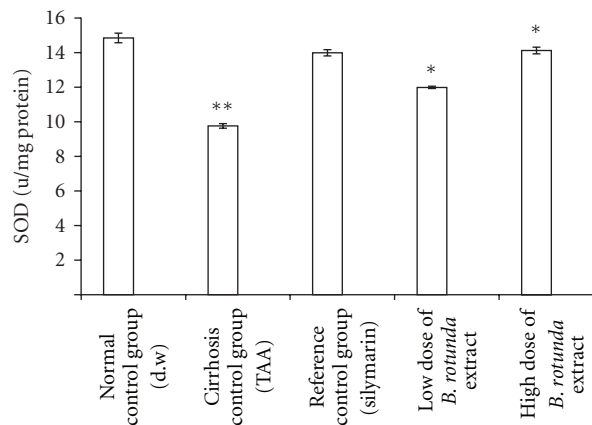


FIGURE 7: Effect of BR ethanol group on SOD level in the liver tissue. Data are expressed as mean \pm SEM. Means among groups ($n = 6$ rats/group) show significant difference, $*P < 0.001$ compared to cirrhosis control group, and $**P < 0.001$ compared to normal control group.

treatments can be explained by the anti-oxidant powers of the two extracts, as asserted by the FRAP measurements in Figure 1.

In the treated rats, the rise of the serum levels of ALT, AST, AP, LDH, and bilirubin and the decline in the levels of albumin and total protein were prevented. The trends in restoring the balance in serum chemicals may be attributed to the capacity of the BR extract to regulate the hepatic antioxidant status or to directly participate in the radical scavenging process [34]. In the TAA metabolism, anti-oxidants work against oxidative stress by scavenging the byproduct TASSO₂ and, thereby, reducing the magnitude of the impact on the liver. Phenol compounds are very effective anti-oxidants with strong free radical-scavenging abilities [35]. Flavonoids are polyphenols and used in treating many diseases including liver cirrhosis. Flavonoids (Kaempferol and Quercetin) are present in the plant BR and therefore likely be responsible for the membrane stabilizing activities demonstrated by the observed reductions in the serum levels of the liver enzymes. The lowered bilirubin levels meant the presence of more stable erythrocyte plasma membranes.

This consequently implied that the BR extract stabilized the hepatocyte membranes and hence interrupted the release of the liver enzymes into the blood [36]. The inhibitory effect of BR extract on the lipid peroxidation of the macromolecules in the membrane can again be credited to the scavenging effect of the flavonoid content of the plant [37].

5. Conclusions

The progression of the liver cirrhosis induced by TAA in rats can be inhibited using ethanol-based BR extract. Specifically, this natural extract has the power to protect the liver by preventing the cascade of harmful events in liver cirrhosis. The effects are comparable to those of silymarin (50 mg/kg) when the corresponding daily dose was 500 mg/kg. The capability of the BR extract to preserve the liver status quo of property, structure, and function against toxic exposure is encouraging and warrants further studies. The significance of its pharmacologic potential in successfully treating liver cirrhosis can be explored by mapping the molecular pathways of its action in the future.

Acknowledgments

This paper was funded by University of Malaya research Grant PV042-2011A and High Impact Research Grant (HIR-F000009-21001).

References

- [1] C. L. Raison, M. Demetrashvili, L. Capuron, and A. H. Miller, "Neuropsychiatric adverse effects of interferon- α : recognition and management," *CNS Drugs*, vol. 19, no. 2, pp. 105–123, 2005.
- [2] H. Yang, S. H. Sung, and Y. C. Kim, "Two new hepatoprotective stilbene glycosides from *Acer* mono leaves," *Journal of Natural Products*, vol. 68, no. 1, pp. 101–103, 2005.
- [3] N. Wang, P. Li, Y. Wang et al., "Hepatoprotective effect of *Hypericum japonicum* extract and its fractions," *Journal of Ethnopharmacology*, vol. 116, no. 1, pp. 1–6, 2008.
- [4] H. S. El-Abhar, L. N. A. Hammad, and H. S. A. Gawad, "Modulating effect of ginger extract on rats with ulcerative colitis," *Journal of Ethnopharmacology*, vol. 118, no. 3, pp. 367–372, 2008.
- [5] K. Shindo, M. Kato, A. Kinoshita, A. Kobayashi, and Y. Koike, "Analysis of antioxidant activities contained in the *Boesenbergia pandurata* Schult. rhizome," *Bioscience, Biotechnology and Biochemistry*, vol. 70, no. 9, pp. 2281–2284, 2006.
- [6] S. P. Voravuthikunchai, S. Phongpaichit, and S. Subhadhirasakul, "Evaluation of antibacterial activities of medicinal plants widely used among AIDS patients in Thailand," *Pharmaceutical Biology*, vol. 43, no. 8, pp. 701–706, 2005.
- [7] C. Kirana, G. P. Jones, I. R. Record, and G. H. McIntosh, "Anticancer properties of panduratin A isolated from *Boesenbergia pandurata* (Zingiberaceae)," *Journal of Natural Medicines*, vol. 61, no. 2, pp. 131–137, 2007.
- [8] P. C. Stevenson, N. C. Veitch, and M. S. J. Simmonds, "Polyoxygenated cyclohexane derivatives and other constituents from *Kaempferia rotunda* L.," *Phytochemistry*, vol. 68, no. 11, pp. 1579–1586, 2007.
- [9] R. Othman, T. S. Kiat, N. Khalid et al., "Docking of noncompetitive inhibitors into dengue virus type 2 protease: understanding the interactions with allosteric binding sites," *Journal of Chemical Information and Modeling*, vol. 48, no. 8, pp. 1582–1591, 2008.
- [10] H. S. Rho, A. K. Ghimeray, D. S. Yoo et al., "Kaempferol and kaempferol rhamnosides with depigmenting and anti-inflammatory properties," *Molecules*, vol. 16, no. 4, pp. 3338–3344, 2011.
- [11] A. Y. L. Ching, S. W. Tang, M. A. Sukari, G. E. C. Lian, M. Rahmani, and K. Khalid, "Characterization of flavonoid derivatives from *Boesenbergia rotunda* (L.)," *The Malaysian Journal of Analytical Sciences*, vol. 11, no. 1, pp. 154–159, 2007.
- [12] M. A. Alshawsh, M. A. Abdulla, S. Ismail, and Z. A. Amin, "Hepatoprotective effects of *Orthosiphon stamineus* extract on thioacetamide-induced liver cirrhosis in rats," *Evidence-Based Complementary and Alternative Medicine*, vol. 2011, Article ID 103039, 6 pages, 2011.
- [13] S. C. Pradhan and C. Girish, "Hepatoprotective herbal drug, silymarin from experimental pharmacology to clinical medicine," *The Indian Journal of Medical Research*, vol. 124, no. 5, pp. 491–504, 2006.
- [14] Pliny the Elder, "Historia Naturalis 77 A.D."
- [15] L. J. Jing, M. Mohamed, A. Rahmat, and M. F. A. Bakar, "Phytochemicals, antioxidant properties and anticancer investigations of the different parts of several gingers species (*Boesenbergia rotunda*, *Boesenbergia pulchella* var *attenuata* and *Boesenbergia armeniaca*)," *Journal of Medicinal Plant Research*, vol. 4, no. 1, pp. 27–32, 2010.
- [16] A. A. Mahmood, A. A. Mariod, S. I. Abdelwahab, S. Ismail, and F. Al-Bayaty, "Potential activity of ethanolic extract of *Boesenbergia rotunda* (L.) rhizomes extract in accelerating wound healing in rats," *Journal of Medicinal Plants Research*, vol. 4, no. 15, pp. 1570–1576, 2010.
- [17] G. Beale, D. Chattopadhyay, J. Gray et al., "AFP, PIVKAI1, GP3, SCCA-1 and follistatin as surveillance biomarkers for hepatocellular cancer in non-alcoholic and alcoholic fatty liver disease," *BMC Cancer*, vol. 8, no. 1, article 200, 2008.
- [18] A. F. Aydin, Z. Küskü-Kiraz, S. Doğru-Abbasoğlu, M. Güllüoğlu, M. Uysal, and N. Koçak-Toker, "Effect of carnosine against thioacetamide-induced liver cirrhosis in rat," *Peptides*, vol. 31, no. 1, pp. 67–71, 2010.
- [19] A. Ahmad, K. K. Pillai, A. K. Najmi, S. J. Ahmad, S. N. Pal, and D. K. Balani, "Evaluation of hepatoprotective potential of jigrine post-treatment against thioacetamide induced hepatic damage," *Journal of Ethnopharmacology*, vol. 79, no. 1, pp. 35–41, 2002.
- [20] F. Fatemi, A. Allameh, H. Khalafi, and J. Ashrafihelan, "Hepatoprotective effects of γ -irradiated caraway essential oils in experimental sepsis," *Applied Radiation and Isotopes*, vol. 68, no. 2, pp. 280–285, 2010.
- [21] F. Al Bayaty, M. Abdulla, M. I. Abu Hassan, and M. I. Masud, "Wound healing potential by hyaluronate gel in streptozotocin-induced diabetic rats," *Scientific Research and Essays*, vol. 5, no. 18, pp. 2756–2760, 2010.
- [22] D. K. Dash, V. C. Yeligar, S. S. Nayak et al., "Evaluation of hepatoprotective and antioxidant activity of *Ichnocarpus frutescens* (Linn.) R. Br. on paracetamol-induced hepatotoxicity in rats," *Tropical Journal of Pharmaceutical Research*, vol. 6, no. 3, pp. 755–765, 2007.
- [23] L. L. Ji, "Modulation of skeletal muscle antioxidant defense by exercise: role of redox signaling," *Free Radical Biology and Medicine*, vol. 44, no. 2, pp. 142–152, 2008.
- [24] H. Wang, W. Wei, N. P. Wang et al., "Melatonin ameliorates carbon tetrachloride-induced hepatic fibrogenesis in rats via inhibition of oxidative stress," *Life Sciences*, vol. 77, no. 15, pp. 1902–1915, 2005.
- [25] W. Guo, T. Adachi, R. Matsui et al., "Quantitative assessment of tyrosine nitration of manganese superoxide dismutase in angiotensin II-infused rat kidney," *American Journal of Physiology*, vol. 285, no. 4, pp. H1396–H1403, 2003.
- [26] A. K. Daly, P. T. Donaldson, P. Bhatnagar et al., "HLA-B5701 genotype is a major determinant of drug-induced liver injury due to flucloxacillin," *Nature Genetics*, vol. 41, no. 7, pp. 816–819, 2009.
- [27] D. Khanna, G. Sethi, K. S. Ahn et al., "Natural products as a gold mine for arthritis treatment," *Current Opinion in Pharmacology*, vol. 7, no. 3, pp. 344–351, 2007.
- [28] A. A. Mahmood, A. A. Mariod, S. I. Abdelwahab, S. Ismail, and F. Al-Bayaty, "Potential activity of ethanolic extract of *Boesenbergia rotunda* (L.) rhizomes extract in accelerating wound healing in rats," *Journal of Medicinal Plants Research*, vol. 4, no. 15, pp. 1570–1576, 2010.
- [29] S. Sadasivan, P. G. Latha, J. M. Sasikumar, S. Rajashekar, S. Shyamal, and V. J. Shine, "Hepatoprotective studies on *Hedyotis corymbosa* (L.) Lam.," *Journal of Ethnopharmacology*, vol. 106, no. 2, pp. 245–249, 2006.
- [30] D. Plonné, H. P. Schulze, U. Kahlert et al., "Postnatal development of hepatocellular apolipoprotein B assembly and

- secretion in the rat,” *Journal of Lipid Research*, vol. 42, no. 11, pp. 1865–1878, 2001.
- [31] L. H. Chen, C. Y. Hsu, and C. F. Weng, “Involvement of P53 and Bax/Bad triggering apoptosis in thioacetamide-induced hepatic epithelial cells,” *World Journal of Gastroenterology*, vol. 12, no. 32, pp. 5175–5181, 2006.
- [32] Y. Yang, R. Sharma, A. Sharma, S. Awasthi, and Y. C. Awasthi, “Lipid peroxidation and cell cycle signaling: 4-Hydroxynonenal, a key molecule in stress mediated signaling,” *Acta Biochimica Polonica*, vol. 50, no. 2, pp. 319–336, 2003.
- [33] K. Sarkar and P. C. Sil, “A 43 kDa protein from the herb *Cajanus indicus* L. protects thioacetamide induced cytotoxicity in hepatocytes,” *Toxicology in Vitro*, vol. 20, no. 5, pp. 634–640, 2006.
- [34] T. A. Ajith, U. Hema, and M. S. Aswathy, “*Zingiber officinale* Roscoe prevents acetaminophen-induced acute hepatotoxicity by enhancing hepatic antioxidant status,” *Food and Chemical Toxicology*, vol. 45, no. 11, pp. 2267–2272, 2007.
- [35] I. C. W. Arts and P. C. H. Hollman, “Polyphenols and disease risk in epidemiologic studies,” *The American Journal of Clinical Nutrition*, vol. 81, no. 1, supplement, pp. 317S–325S, 2005.
- [36] X. Tang, J. Gao, Y. Wang et al., “Effective protection of *Terminalia catappa* L. leaves from damage induced by carbon tetrachloride in liver mitochondria,” *The Journal of Nutritional Biochemistry*, vol. 17, no. 3, pp. 177–182, 2006.
- [37] J. Prince Vijeya Singh, K. Selvendiran, S. Mumtaz Banu, R. Padmavathi, and D. Sakthisekaran, “Protective role of Apigenin on the status of lipid peroxidation and antioxidant defense against hepatocarcinogenesis in Wistar albino rats,” *Phytomedicine*, vol. 11, no. 4, pp. 309–314, 2004.

Review Article

In Vitro and In Vivo Toxicity of *Garcinia* or Hydroxycitric Acid: A Review

Li Oon Chuah,¹ Swee Keong Yeap,² Wan Yong Ho,³ Boon Kee Beh,⁴ and Noorjahan Banu Alitheen^{2,3}

¹ School of Industrial Technology, University Science Malaysia, 11800 Penang, Malaysia

² Institute of Bioscience, University Putra Malaysia, 43400 Serdang, Selangor, Malaysia

³ Department of Cell and Molecular Biology, Faculty of Biotechnology and Biomolecular Sciences, Universiti Putra Malaysia, 43400 Serdang, Selangor, Malaysia

⁴ Department of Bioprocess Technology, Faculty of Biotechnology and Biomolecular Sciences, University Putra Malaysia, 43400 Serdang, Selangor, Malaysia

Correspondence should be addressed to Noorjahan Banu Alitheen, noorjahan@biotech.upm.edu.my

Received 8 March 2012; Revised 11 June 2012; Accepted 25 June 2012

Academic Editor: Debprasad Chattopadhyay

Copyright © 2012 Li Oon Chuah et al. This is an open access article distributed under the Creative Commons Attribution License, which permits unrestricted use, distribution, and reproduction in any medium, provided the original work is properly cited.

Obesity is one of the pandemic chronic diseases commonly associated with health disorders such as heart attack, high blood pressure, diabetes or even cancer. Among the current natural products for obesity and weight control, *Garcinia* or more specifically hydroxycitric acid (HCA) extracted from *Garcinia* has been widely used. The evaluation of the potential toxicity of weight control supplement is of the utmost importance as it requires long term continuous consumption in order to maintain its effects. Majority of reports demonstrated the efficacy of *Garcinia*/HCA without any toxicity found. However, a few clinical toxicity reports on weight-loss diet supplements of which some were combinations that included *Garcinia*/HCA as an active ingredient showed potential toxicity towards spermatogenesis. Nonetheless, it cannot be concluded that *Garcinia*/HCA is unsafe. Those products which have been reported to possess adverse effects are either polyherbal or multi-component in nature. To date, there is no case study or report showing the direct adverse effect of HCA. The structure, mechanism of action, long history of the use of *Garcinia*/HCA and comprehensive scientific evidence had shown “no observed adverse effect level (NOAEL)” at levels up to 2800 mg/day, suggesting its safety for use.

1. Introduction

Focus on disease prevention by complementary supplementation of nutraceutical products to medication has heralded the growing demand for healthy food. In addition, rising healthcare costs have greatly boosted the growth of the nutraceutical industry [1]. Nonetheless, scientific evidence confirming the effects claimed by the nutraceutical products is scanty at best. Scientific investigation on potential health promoting effects of herbal preparations as diet supplement is essential for new discoveries of alternative therapies. The consistency, safety, and bioavailability of the active herbal supplements are of utmost importance [2]. Taking these into considerations, the 103rd US Congress passed the Dietary Supplement Health and Education Act (DSHEA) in

1994 [3, 4]. In the “findings” section of the Act, the US Congress noted that “consumers should be empowered to make choices about preventive health care programs based on data from scientific studies of health benefits related to particular dietary supplements” [5]. Phenomenal growth in consumer acceptance of dietary supplements was evidenced by the 10 million daily users and an estimated annual market of \$12 billion, in the 4.5 years after the passage of the DSHEA [6]. Currently, the dietary supplement industry in the USA is fully regulated under DSHEA, Food and Drug Administration (FDA) Modernization Acts of 1997 and 2011, Dietary Supplement and Nonprescription Drug Consumer Protection Act (DSNDCPA) of 2006 and other acts of US Congress, which provides the US FDA with statutory authority on regulation of the industry [4].

Garcinia has been used for centuries in Asian countries for culinary purposes as a condiment and flavoring agent in place of tamarind or lemon, and to make meals more filling. *Garcinia* or more specifically *G. cambogia*, *G. atroviridis*, and *G. indica* have been found to contain large amounts of hydroxycitric acid (HCA) [7]. It has been widely used as an antiobesity herbal supplement for decades around the world. This is because HCA is able to inhibit lipogenesis, a process in which carbohydrate is converted to fat in the body, via the inhibition of ATP citrate lyase (EC 4.1.3.8) in cells [8, 9]. Prevention of carbohydrate conversion to fat by HCA thus induces the body to oxidize the excess carbohydrates, promoting glycogen storage, which in turn may play a part in suppressing the appetite [10]. Furthermore, HCA suppressed the feeling of hunger by increasing the release/availability of serotonin, a neurotransmitter that regulates eating behavior and appetite control [11, 12]. It had also been reported that HCA decreased serum leptin in mice [13] and human [14], as well as expression level of abdominal fat leptin in rats [15]. Despite many publications on *Garcinia*/HCA exerting antiobesity effects, the results on the effects of HCA on appetite, body weight and energy expenditure (EE), and its potential contribution as a weight loss agent in humans were controversial [16–19]. Although some mild adverse effects such as headache, and upper respiratory tract and gastrointestinal symptoms have been reported in overweight subjects, the nonsignificant difference in the occurrence of the adverse effects between treatment groups [20] did not justify the definitive risk of HCA consumption. In the studies published thus far, the safety and efficacy of HCA have been the subject of debate. The aim of this review was to critically assess the evidence from the *in vitro*, *in vivo*, and clinical trials on the safety of *Garcinia*/HCA as a dietary supplement for treating obesity.

2. In Vitro and In Vivo Toxicology Studies

2.1. Cytotoxicity. Varalakshmi et al. [21] evaluated the *in vitro* antiproliferative effects of the aqueous extracts of dried fruit rind of *G. indica* (0, 50, 100, 200 $\mu\text{g}/\text{mL}$) on Balb/c 3T3 mouse fibroblasts and human peripheral lymphocytes. The results showed that *G. indica* extracts inhibited lymphocytes and 3T3 fibroblast cell survival. Thus, the authors concluded that *G. indica* extracts exhibited pronounced cytotoxic effects. However, there was a flaw in their methodology, since the authors also reported that *Azadirachta indica* and *Coleus aromaticus* exhibited cytotoxic effects on lymphocytes despite the low cell viability in the control group (only 50–55% of viable lymphocytes). In the case of *G. indica*, percentage of viability in lymphocytes was not even mentioned. Thus, definitive conclusion of *G. indica* induced cytotoxicity could not be drawn due to the poorly-described methodology of their study.

2.2. Genotoxicity. K. H. H. HHLee and B. M. Lee [22] conducted a study to evaluate the genotoxicity of Super Citri-Max (HCA-SX) containing 60% HCA using bacterial reverse mutation assay (Ames test), *in vitro* chromosomal aberration

(CA) test, and *in vivo* micronucleus (MN) test. For the Ames test (plate incorporation method), five *Salmonella typhimurium* strains (TA98, TA100, TA102, TA1535, and TA1537) were used and six different doses of HCA-SX (0, 20, 100, 500, 2500, 12500 $\mu\text{M}/\text{plate}$) were tested. No significant increase ($P < 0.05$) in the number of revertants was observed, indicating that HCA-SX did not induce mutagenic activity in any of the five bacterial strains tested, under any of the activation conditions examined. In the CA test, HCA-SX-treated Chinese hamster ovary cells were fixed on glass slides and stained with Giemsa staining solution. The stained cells were viewed under an optical microscope, where at least 100 metaphases were counted at a resolution of 1000x. No significant mutagenic potency was detected by the CA tests. In the MN test, suspensions containing HCA-SX were administered to 7-to-8-week-old old ICR mice via intraperitoneal (ip) injection as follows: group 1, negative control (vehicle alone); group 2, positive control (Mitomycin C, 2 mg/kg); groups 3, 4, 5, 6, and 7, HCA-SX-treated (at dose levels of 20, 100, 500, 2500, or 12,500 $\mu\text{mol}/\text{kg}$, resp.). The bone marrow cells were fixed, stained, and viewed using an optical microscope. HCA tended to increase the number of micronucleated polychromatic erythrocytes (MNPCEs/1000 polychromatic erythrocytes) and the polychromatic erythrocytes/normochromatic erythrocytes PCE/(PCE + NCE) ratios, and they reached significance level at a dose of 12,500 $\mu\text{mol}/\text{kg}$. Taken all together, the authors suggested that HCA-SX possessed no genotoxic effect by bacterial or by chromosome aberration testing, but preferentially induced micronuclei.

However, Lau et al. [23] refuted the authors' conclusion in the abstract section that the "results suggest that HCA preferentially induces micronuclei" [22]. Considering that DMSO may react with HCA-SX to induce adverse effects, they suggested that the highest dose used in the study (12,500 $\mu\text{mol}/\text{kg}$) may have been too high and exceeded the maximum tolerated dose. Besides, Lau and colleagues pointed out several limitations in the experimental design and the interpretation of the results, as follows: (1) selection of ip delivery of HCA-SX rather than the recommended oral administration for this supplement, (2) selection of DMSO as a vehicle, which was not recommended for the *in vivo* rodent erythrocyte micronucleus assay, (3) five different HCA-SX doses were selected in the absence of a prior ip LD50 determination, (4) the range of doses (increased by a factor of 5) chosen in the study deviated from that of the conventional dose levels used in toxicological studies, (5) no significant difference ($P < 0.05$) in the values of percent MNPCE between 500 $\mu\text{mol}/\text{kg}$ and 12,500 $\mu\text{mol}/\text{kg}$, suggesting the use of the highest dose was probably unnecessary, and (7) poor statistical analysis.

2.3. Acute and Short-Term Toxicological Studies. Acute safety studies of HCA-SX (containing 60% HCA) as demonstrated in acute oral and dermal toxicity studies were conducted [11, 12]. In the acute oral toxicological study, the acute oral median lethal dose (LD_{50}) was determined to evaluate the potential systemic toxicity of HCA-SX when administered as

a single dose to male and female Albino rats. HCA-SX at a single dose of 5000 mg/kg was administered orally via gastric intubation in a dose volume of 10 mL/kg. Toxicological studies revealed no death, remarkable body weight changes or gross necropsy findings in Albino rats following a single oral dose of 5000 mg/kg, equivalent to 350 g or 233 times the maximum dose of 1.5 g/day of HCA in humans. Clinical findings were limited to soft stool and rales for one male and two female rats, respectively. Taken all together, the authors suggested that the oral LD₅₀ of HCA-SX in rats (administered once orally via gastric intubation to fasted male and female Albino rats) was more than 5000 mg/kg [12].

2.4. Subchronic and Chronic Toxicological Studies. However, a long-term study on the safety and efficacy of HCA-SX or any of the HCA products still remained to be conducted. Hence, Shara et al. [24, 25] extended their study and conducted a 90-day chronic safety study in both male and female rats, where HCA-SX was dissolved in water and administered by gavage at dose levels of 0.2, 2.0, and 5.0% of feed intake (equivalent to approximately 100, 1000, and 2500 mg/kg/day, resp.). The gavage dose volume was 5 mL/kg body weight. HCA-SX was administered by gavage rather than through feed as gavage administration most simulates the method of intake in humans, consumed over a relatively short period of time. The 0.2% HCA-SX supplementation is equivalent to the daily recommended dosage in humans, while 2.0 and 5.0% represent 10 and 25 times higher doses, respectively. Dose- and time-dependent effects of HCA-SX on body weight, hepatic and testicular lipid peroxidation and DNA fragmentation of mice over a period of 90 days were evaluated. HCA-SX of three doses significantly ($P < 0.05$) reduced body weight and feed intake in both male and female rats, but not water intake and lipid peroxidation. Moreover, no significant effects on liver and testis weight, hepatic and testicular DNA fragmentation morphology were observed in HCA-SX treated rats [24].

Further evaluation on the safety of HCA-SX was conducted by Shara et al. [25] where vital organ weights (including adrenal glands, brain, heart, kidneys, liver, prostate and seminal vesicles, spleen, testes and thymus in male rats, and adrenal glands, brain, heart, kidneys, liver, ovaries, spleen, thymus, and uterus in female rats) were assessed and correlated as a % of body weight and brain weight at 90 days of the treatment. No significant difference was detected between treatment groups. Besides, dose- and time-dependent effects of HCA-SX on hematology parameters (including WBC, RBC, hemoglobin, hematocrit and platelet count, and total serum protein and albumin) in male and female rats were examined. No significant difference was detected between treatment groups. Similarly, clinical chemistry analysis (alkaline phosphatase, blood urea nitrogen, creatinine, aspartate aminotransferase, alanine aminotransferase, cholesterol, total bilirubin, glucose, calcium, chloride, phosphorus, sodium, potassium, iron, total iron binding capacity, and iron/total iron bonding capacity) revealed no significant difference between treatment groups. Histopathology of different organs including adrenal glands,

brain, epididymes, esophagus, eyes, heart, intestine, kidney, liver, lymph nodes, lungs, mammary glands, ovary (females only), pancreas, pituitary, prostate, salivary glands, seminal vesicles, skin, spleen, stomach, testes (males only), thymus gland, thyroid gland, trachea, and urinary bladder of all treatment groups were assessed after 90 days of treatment. HCA-SX supplementation caused no significant morphological changes in the organs tested. Scattered minimal or mild histologic lesions observed in a number of organs were all randomly distributed in all groups and considered to be incidental findings commonly seen in rats. Besides, hemorrhage noted in brain appeared to be agonal or necropsy artifacts. The inflammatory lesions noted were in agreement with mild subclinical infections caused by *Mycoplasma* sp. The minimal hepatocyte vacuolation noted in HCA-SX groups were limited and not considered significant/treatment-related as one control animal had a similar lesion. Another change noted was within the glandular stomach where the mucosa of the glandular stomach of one animal was severely atrophied and mineralized. Besides, scattered minimal or mild foci of gastric gland dilation were also noted. No necrosis or inflammation was seen. These changes were noted in animals supplemented with HCA-SX as well as the untreated control group. The results obtained did not indicate the change being either more severe or more numerous in any particular dose group. In any case, the morphological changes noted appeared to be minimal and not significant, thus indicating the safety and efficacy of HCA-SX in weight management [25].

Another study performed by Roy et al. [15] showed that none of the animals in their study exhibited early removal criteria such as self-mutilation, guarding, vocalization, hunched posture, inactivity, lethargy, rough hair coat, lack of righting reflex, weight loss of more than 20%, lesions, bleeding, and anorexia for >24 h. In addition, DNA microarray analysis showed that HCA supplementation did not affect vital genes associated with transcription of mitochondrial/nuclear protein and those essential for fundamental support of tissue. Taken together, dietary HCA-SX supplementation at a dose of 10 mg per kg body weight which corresponds to a 500 mg daily dose for an average person weighing 50 kg was safe.

2.5. Skin Irritation Studies. In another study, the potential systemic toxicity and local irritative potential of HCA-SX were evaluated using Albino rabbits. HCA-SX administration at a single dose of 500 mg/site was directly applied to shaved intact skin to assess the local dermal irritative potential. Each animal received a single, 4 h semioccluded exposure and application sites were evaluated at approximately 30–60 min and 24, 48, and 72 h after patch removal. Minimal irritation was noted in this study. Very slight erythema on a single animal was noted at the beginning of observation, but completely subsided by the end of day 1. All dose sites were stained yellow. No gross toxicological pathology (except for reddened application sites and accessory spleen for two rabbits each, and single occurrence of pale kidneys, mottled lungs, and hair loss for one rabbit each) was found

on autopsy. HCA-SX was classified as nonirritating, as the primary irritation index was calculated to be 0 [12].

2.6. Eye Irritation Studies. HCA-SX was administered by direct conjunctival instillation, a standard administration route for local ocular irritative potential assessment. HCA-SX at a dose of 54 mg/right eye was applied directly into the cupped lower conjunctival sac of the right (test) eye of six New Zealand white Albino rabbits. In this study, no death or significant changes in body weights ($P < 0.05$) was noted. Ocular observation revealed that a small area of inflammatory exudate with enlarged blood vessels was present at the apex of the lower conjunctival sac for three rabbits on day 7. The inflammation completely subsided by the end of study for two animals, but not the other one. Positive iridal and conjunctival reactions were induced in all animals, but subsided within 48 h. The maximum average score of 15 (out of 110) was obtained, indicating HCA-SX possessed mild irritation on eye [12].

2.7. Reproduction and Developmental Studies. *G. cambogia*/HCA has been safely used in cooking and as weight-loss herbal supplements for many decades, but not without precedent that adverse effects had been reported. Saito et al. [26] investigated the dose-dependent ability of *G. cambogia* extract (containing 41.2 wt% of (-)-HCA, the ratio of free to lactone form was 36.6 to 63.4) in suppression of body fat accumulation and the safety of its high doses. Diets containing different levels of *G. cambogia* (equivalent to 0, 10, 51, 102, and 154 mmol HCA/kg diet) were fed to 6-week-old male Zucker obese rats for 92 or 93 days. Significant increases ($P < 0.05$) in ATP-citrate lyase activity and concentrations of liver glycogen, and reduction ($P < 0.05$) in plasma nonesterified fatty acid were detected in rats fed with 154 mmol HCA/kg diet. A dietary HCA level over 3.0 wt% (154 mmol HCA/kg diet) caused severe diarrhea in rat models. HCA administration reduced the testis weights by half in male Zucker obese rats. Histopathological examinations revealed marked testicular atrophy and impairment of spermatogenesis in the highest and second highest HCA groups. However, no significant differences in all the parameters in this study were observed in rats fed with 0, 10, and 51 mmol HCA/kg diet. Taken all together, the authors suggested that high dose of *G. cambogia* effectively suppresses fat accumulation in developing male Zucker obese rats, but was highly toxic to the testis.

In a continuation to the study conducted by Saito et al. [26], Kiyose et al. [27] investigated the cause of impaired spermatogenesis due to ingestion of *G. cambogia* powder (containing 41.2 wt% of (-)-HCA, the ratio of free to lactone form was 36.6 to 63.4) at 102 mmol/kg diet in young Fischer 344 male rats. By considering that 4,4-dimethyl-5 α -cholesta-8,24-diene-3 β -ol, a testis meiosis-activating sterole (T-MAS), was a specific intermediate product of cholesterol biosynthesis in testicular germ cells, the authors elucidated the relationship between impaired spermatogenesis and MAS production in rats testis, postingestion of *G. cambogia*.

Histopathology examinations of rat testis showed that spermatogenesis was immature in all rats of both treatment and control group after 2 weeks of *G. cambogia* administration (six-week-old, sexually immature). After 4 weeks (eight-week-old, sexually mature), normal spermatogenesis was observed in control group, with abundance of elongation and elongated spermatids in all seminiferous tubules. On the contrary, there was a complete absence of spermatid elongation in the *G. cambogia* group, with some round spermatids being released in clusters instead. The concentrations of testosterone, luteinizing hormone (LH), follicle-stimulating hormone (FSH), and inhibin-B, the four hormones related to spermatogenesis, were measured. No significant difference ($P < 0.05$) in testosterone and LH concentrations were detected between groups. However, a significant reduction of inhibin-B concentration was detected in the *G. cambogia*-treated group, concurrently with an increase in FSH concentration, compared to the control group after 2 weeks of feeding. Similar results were obtained after 4 weeks of feeding, when the rats reached sexual maturation. Inhibin-B is an important marker of the function of Sertoli cells and spermatogenesis. The concomitant decrease in inhibin-B and increase in FSH concentrations indicated impaired spermatogenesis [28–30]. Therefore, the authors revealed that severe impairment of spermatogenesis occurred in rats administered (-)-HCA-containing *G. cambogia*, probably associated with a blockade of MAS substances accumulation.

With regards to the study conducted by Saito et al. [26], Burdock et al. [31] had raised several questions, such as toxicity associate with the form of (-)-HCA and the use of Zucker rats as a model in testicular toxicity evaluation. They suggested the possibility that the use of the atypical form of HCA containing 63% lactone resulted in toxicity. In addition, they indicated that Zucker rat may not be an appropriate model to evaluate testicular toxicity as obese male Zucker rat has a defect in testicular testosterone production [32]. The same question of whether the toxicity was possibly due to the atypical form of HCA containing 63% lactone could be applied on the study conducted by Kiyose et al. [27]. Therefore, the claim of HCA in affecting the functionality of testis is yet to be concluded.

Nevertheless, it would be more convincing to evaluate the effect of HCA consumption in fertility of both male and female models rather than only the testicular function to justify the effect of HCA on reproductive capacity. Pragmatic maternal observations indicated that maternal toxicity might occur due to reduced weight gain during pregnancy. Decrease in body weight of about 20% had been reported to possess adverse effects on fertility and reproduction in rats and mice [33]. In this regard, *G. cambogia*/HCA has been used by women for weight loss after delivery. However, Shara et al. [24, 25] reported that decrease in body weight in the range of 10–15% did not adversely affect weight and histopathology of both male and female reproductive organs of Sprague-Dawley rats. In their 90-day study, administration of HCA-SX at a dose of 5% of dietary intake resulted in 10–15% of weight loss in both male and female rats. Observations from human studies also demonstrated weight loss of approximately 10% following

consumption of HCA-SX for a period of 4–12 weeks [14, 34, 35]. Hence, HCA is expected to cause no adverse effect on fertility and reproduction on the basis of weight loss.

A two-generation reproduction toxicity study was also conducted to evaluate the effects of HCA-SX on the reproductive systems of male and female rats, postnatal maturation and reproductive capacity of their offsprings, and possible cumulative effects through multiple generations. Rats were fed with diet containing 0, 1000, 3000, or 10,000 ppm of HCA-SX for a period of 10 weeks prior to mating, during mating, and across two generations, until their termination. No treatment-related adverse effects on reproductive performance in terms of fertility and mating, gestation, parturition, litter properties, lactation, sexual maturity, and development of offspring were observed during HCA-SX exposure of male and female rats from F₀ and F₁ generations. These results suggested that the “no observed adverse effect level (NOAEL)” of HCA-SX in both parental and offspring exceeded 10,000 ppm (equivalent to 1018 and 1524 mg/kg/day, in male and female rats, resp.) [36].

Several mechanism of action studies showed that HCA did not affect fatty acid synthesis in the fetus [37–39]. Jones and Ashton (1976) reported that HCA did not inhibit lipid synthesis in slices of fetal liver from guinea pigs, despite changes in fat synthesis and storage [37]. Besides, HCA did not affect fatty acid synthesis in explants of 18-day fetal lung tissue stimulated by the hormone dexamethasone, a drug known to stimulate the synthesis of fatty acids [38]. Another study conducted by Greenwood et al. [39] showed that HCA supplementation decreased feed intake and body weight of Zucker obese female rats, without affecting the percent of body fat and the fat cell size of these rats, as compared to the controls. These results suggested that HCA will not affect fatty acid synthesis in either the maternal animals or their offspring. In a continuation of the two-generation reproductive toxicity study, Deshmukh et al. [40] conducted a developmental toxicity study to evaluate the teratogenic potential of HCA-SX in Sprague-Dawley rats. In their teratology study, the rats were selected randomly postweaning from each F₂ litter of the F₁ generation from the two-generation reproductive toxicity study and allowed to grow up to 10 to 12 weeks of age before mating. Dietary exposure levels of 1000, 3000, and 10,000 ppm (equivalent to the dose levels of 103, 352, or 1240 mg/kg/day, resp.) were subjected indirectly to the male and female rats in HCA-SX treatment groups during lactation, and directly postweaning (4 weeks old) till they were terminated (including growth phase, mating period, and gestation). Maternal toxicity and effects on the developing embryo were evaluated throughout the gestation period until the 20th day of gestation. Apart from a slight (13%) lowering of maternal body weight gain in the group administered 10,000 ppm HCA-SX, no evidence of maternal toxicity, adverse effects on the parameters evaluated for the gravid uteri, external abnormalities in the fetuses, soft tissue abnormalities in the fetuses, or skeletal abnormalities in the fetuses was noted. The results suggested that HCA-SX (up to dose level of 1240 mg/kg/day) was not teratogenic to Sprague-Dawley rats. Considering the comprehensive

reproductive and developmental studies reported on safety profile of HCA [24, 25, 36–40], it was strongly suggested that HCA consumption possessed no reproductive and developmental toxicity.

3. Clinical Toxicity

A total of 17 clinical studies with approximately 873 subjects were summarized to assess the effects of HCA and HCA-SX intake on human body weight and its safety for human consumption. Out of these studies, only 1 subject was reported itching around the mouth and 2 with headache and nausea. Taken all together, these studies provided sufficient qualitative and quantitative scientific evidence to report “no observed adverse effect level (NOAEL)” at levels up to 2800 mg/day, suggesting its safety in-use [41, 42]. In this section, we have analyzed the symptoms of adverse reactions reported in 15 clinical trials carried out in human subjects after the administration of *G. cambogia* extract (Table 1). There are 12 parallel, randomized, double-blind, placebo-controlled studies, involving 745 subjects [43–54], one parallel, randomized, single-blind, placebo-controlled study [55], three cross-over, randomized, double-blind, placebo-controlled trials [56–58], one cross-over, randomized, single-blind, placebo-controlled study [59], and one reexamination [50] of the data from two previous parallel, randomized, double-blind, placebo-controlled clinical trials [34, 60]. Out of 16, only nine of the clinical studies were performed with *G. cambogia* extract/HCA alone.

A number of hepatotoxicity cases associated with the consumption of hydroxycut had led to the assumption that HCA is the primary causative agents to the hepatotoxicity [61–65]. Those products having adverse reactions were either polyherbal or multicomponent in nature. Furthermore, polyherbal dietary supplements reported with adverse effects either contain HCA in negligible amounts or no HCA at all. These polyherbal products contain up to 20 different ingredients, with only 8 out of the 14 marketed hydroxycut products contain HCA [66, 67], and in only two acute liver injuries associated with use of hydroxycut was HCA shown to be present in the product [61]. However, a single case report on adverse effects in *G. cambogia* extract/HCA-containing dietary supplement does not justify definitive attribution of causality in most cases. It is impossible to tell with certainty which ingredient(s) is responsible for the adverse effects reported in the various case reports. The majority of the case reports were insufficiently documented to make an informed judgment about a relationship between the use of *G. cambogia* extract/HCA or *G. cambogia* extract/HCA-containing dietary supplements and the adverse event in question. Mozersky et al. [68] also suggested in the Health Hazard Report on hydroxycut that the board did not know which type of ingredient(s) present in hydroxycut was the causative agent(s) of hepatotoxicity. In addition, there were no preclinical animal studies and clinical studies showing HCA consumption had direct adverse effects. The results obtained from various reports suggested a dosage of

TABLE 1: Summary of clinical studies conducted to date on the results and safety record of HCA. Only the subjects who manage to complete the trial is counted in the table below.

Duration	Mode of trial	Formulation	Results	Safety	Conclusion	Reference
8 weeks	Parallel, randomized, double-blind, placebo control, 39 subjects	1500 mg <i>G. cambogia</i> + 300 µg chromium picolinate/day	No significant effect between groups	Itching around mouth in both treatment and placebo groups.	None toxic	[43]
8 weeks	Parallel, randomized, double-blind, placebo control, 35 subjects	1500 mg <i>G. cambogia</i> before meal/day	No changes in blood glutamic oxaloacetic transaminase (SGOT), glutamic pyruvic transaminase (SGPT) and glucose.	Headaches and nausea in both treatment (2) and placebo (1) groups	None toxic	[44]
4 weeks	Parallel, randomized, double-blind, placebo control, 144 subjects	55 mg <i>G. cambogia</i> + 19 mg chromium + 240 mg chitosan/day	Treated group possessed significant weight loss, lower TC, LDL and higher HDL as compared to placebo	Headaches and nausea in both treatment (2) and placebo (1) groups	None toxic	[45]
12 weeks	Parallel, randomized, double blind, placebo control, 84 subjects	3000 mg <i>G. cambogia</i> (50% HCA)/day	No significant effect between groups	Intestinal disorders, headache, or upper airway symptoms in both treatment and placebo groups	None toxic	[46]
6 weeks	Parallel, randomized, double blind, placebo control, 18 subjects	750 mg <i>G. cambogia</i> + 750 mg calcium + 750 mg guggulsterone + 750 mg L-tyrosine/day	No significant effect between groups	Not reported	—	[47]
12 weeks	Parallel, randomized, double blind, placebo control, 33 subjects	300 mg <i>G. cambogia</i> + 1200 mg <i>Phaseolus vulgaris</i> + 1200 mg inulin/day	Better weight loss in treated group	Not reported	—	[48]
12 weeks	Parallel, randomized, double blind, placebo control, 89 subjects	2400 mg <i>G. cambogia</i> /day	Better weight loss in treated group	Not reported	—	[49]
8 weeks	Parallel, randomized, double-blind, placebo-control, 82 moderate obese subjects	2800 mg HCA; 4667 mg of HCA-SX in combination with niacin-bound chromium and standardized <i>Gymnema sylvestre</i> extract/day	Significant weight loss, reduction in BMI, increased fat oxidation, favorable lipid profile, reduction in circulating plasma leptin levels, increase in serum serotonin levels, and decreased appetite as determined by reductions in food intake were detected in HCA-SX treatment group, and to a greater extent the combination of the 3 ingredients	No serious adverse effects were detected, except several minor adverse effects such as leg cramps, heartburn, diarrhea, gas, increased appetite, headaches, stomach burn, and menstrual disorders	None toxic	[50]
12 weeks	Parallel, randomized, double blind, placebo control, 98 subjects	<i>G. cambogia</i> + kidney bean pods + chromium yeast	Better weight loss in treated group	More gastrointestinal symptoms in treated group.	None toxic	[51]
12 weeks	Parallel, randomized, double blind, placebo control, 44 subjects	1,667.3 mg of <i>G. cambogia</i> extract/day (1,000 mg HCA/day)	No significant effect on TG between treatment and placebo group. Answer to the concept of potential spermatogenesis impair [27]	No significant reproductive toxicity on serum testosterone, estrone, and estradiol levels, hematology, serum triacylglycerol, and serum clinical pathology parameters	None toxic	[52]
12 weeks	Parallel, randomized, double blind, placebo control, 58 subjects	2400 mg <i>G. cambogia</i> + 1500 mg <i>Amorphophallus konjac</i> /day	No significant effect between groups	No significant difference between treatment and placebo groups	None toxic	[53]
2 weeks × 3 times	Parallel, randomized, double blind, placebo control, 21 subjects	500 mg HCA + 300 medium chain TG/day	No significant effect between groups	Not reported	—	[54]

TABLE 1: Continued.

Duration	Mode of trial	Formulation	Results	Safety	Conclusion	Reference
8 weeks	Parallel, randomized, single blind, placebo control, 40 subjects	1000 mg of HCA/day	Reduction of visceral fat area and visceral fat area/subcutaneous fat area	No significant difference in hematological parameters (white blood cells, red blood cells, hemoglobin, hematocrit and platelets) and clinical chemistry parameters (SGPT, SGOT, c glutamyl transpeptidase, lactate dehydrogenase, blood urea nitrogen, creatinine, glucose, insulin, acetoacetic acid, 3-hydroxybutyric acid, and total ketone bodies) between groups	None toxic	[55]
10 days	Cross-over, randomized, placebo control, 44 subjects	1000, 2000, 3000 and 4000 mg G. <i>cambogia</i> /day		No significant different in hematology and clinical chemistry analysis before and after treatment no unusual electrocardiographic effects.	NOAEL > 4 g HCA	[56]
5 hours	Cross-over, randomized, double blind, placebo control, 20 subjects	extracts of, <i>G. cambogia</i> , green tea, caffeine, and yerba mate		No unusual electrocardiographic effects.		[57]
??	Cross-over, randomized, double blind, placebo control	5600 mg HC/A/day	??	Yet to be published	??	[58]
2 weeks	Cross-over, randomized, single blind, placebo control, 24 subjects	900 mg HCA/day	Decreased energy intake	No adverse effect	None toxic	[59]

TABLE 2: Summary on the advantages, disadvantages, benefits, and pitfall of up-to-date *in vitro*, *in vivo* and clinical toxicology studies on *Garcinia/HCA*.

Methodology	Study target	Summary	Advantages	Disadvantages	Benefits	Pitfall of experiment
<i>In vitro</i> cytotoxicity	3T3 fibroblast [21]	<i>G. indica</i> was cytotoxic on 3T3	Rapid test	Not fully representative compared to animal/human subject.	First line screening	Poor methodology, only Balb/c 3T3 was screened.
<i>In vitro</i> genotoxicity ~Ames test ~Chromosomal aberration test	~ <i>Salmonella typhimurium</i> , ~Chinese hamster ovarian cell [22]	HCA-SX did not induced mutagenic activity	Rapid test	Not fully representative compared to animal/human subject.	First line screening	
<i>In vivo</i> genotoxicity Micronucleus test	8 weeks old ICR mice [22]	Micronucleated polychromatic erythrocytes in bone marrow cell	Better representation than <i>in vitro</i> cell line study	Variation among animal.	Preclinical screening	i.p. injection with DMSO as vehicle not suitable; no prior i.p. LD_{50} predetermination; 12,500 μ mol/kg exceed the highest dose, poor statistic analysis [23]. Only LD_{50} , gross necropsy and body weight were recorded. No blood biochemical profiling and full blood count.
<i>In vivo</i> acute toxicity	Albino rat [12]	HCA SX $LD_{50} > 5$ g/kg body weight	High dosage (233X higher than maximum dose of 1.5 g/day in human)	Single administration.	Understand acute toxic effect at high concentration	
<i>In vivo</i> subchronic	Rat [24, 25]	HCA-SX reduced body weight, feed intake but no effect on other parameters.	Experiment was design to represent actual recommended dosage.	—	Good reference to support the entry of clinical studies.	—
<i>In vivo</i> skin irritation	Albino rabbit [12]	HCA-SX was none irritating with primary irritation index = 0.	More representative than <i>in vitro</i> test.	Single exposure.		This study only tested the irritative potential with single exposure.
<i>In vivo</i> eye irritation	Albino rabbit [12]	HCA-SX was mild irritant on eye.	More representative than <i>in vitro</i> test.	—	HCA-SX is an oral supplement. Results for <i>in vivo</i> skin and eye irritation can help to strengthen the MSDS.	—
<i>In vivo</i> reproduction toxicity	Rat [36, 40]	HCA-SX did not affect the postnatal maturation, reproductive capacity.	“No observed adverse effect level” of HCA-SX higher than 1.5 mg/kg/day was determined in both parental, offspring generation and HCA-SX was not teratogenic.	—	Good reference to support that HCA was none toxic effect against reproductive system.	—

TABLE 2: Continued.

Methodology	Study target	Summary	Advantages	Disadvantages	Benefits	Pitfall of experiment
<i>In vivo</i> reproduction toxicity	Zucker obese rats [26, 27]	<i>G. cambogia</i> powder (containing 41.2 wt% of (-)-HCA, the ratio of free to lactone form is 36.6 to 63.4) impaired spermatogenesis	—	—	—	Zucker rat is not suitable in this study since it has a defect in testicular testosterone production. HCA used in this experiment contains high lactone that may contributed to it the impairment of spermatogenesis [31]
Clinical studies (as stated in Table 1)	873 subjects	<i>Garcinia/HCA</i> is generally none toxic with NOAEL > 4 g HCA	<i>Garcinia/HCA</i> was recorded as none toxic up to 12 weeks consumption.	None of the studies recorded the use of <i>Garcinia/HCA</i> for more than 12 weeks.	<i>Garcinia/HCA</i> is generally safe to consume up to 3 months.	Continue monitoring on the consumers who take <i>Garcinia/HCA</i> for more than 3 months can strengthen the knowledge of long term safety assessment of <i>Garcinia/HCA</i> .

G. cambogia extract in clinical trials ranging from 1,500 to 4,667 mg/day (25 to 78 mg/kg/day), whereby their equivalent HCA dose ranging from 900 to 2,800 mg/day (15 to 47 mg/kg/day) is safe for human consumption [41, 69]. *G. cambogia* is available in capsule or tablet form with a maximum dose of 1,500 mg/day. A study conducted by Deshmukh et al. [40] determined the dietary dose levels of 1240 mg/kg/day as the NOAEL of HCA-SX.

4. Summary

Based on the results obtained in an array of toxicological and safety studies, a comprehensive safety profile on *G. cambogia* extract/HCA as dietary supplements for treating obesity has been established [41, 42, 66, 70] (Table 2). Cytotoxicity study [21], genotoxicity study [22, 23], acute toxicity studies (such as acute oral, acute dermal, primary dermal irritation, and primary eye irritation toxicity studies) [11, 12], sub-chronic 90-day safety study [15, 24, 25], two-generation reproductive and teratogenicity studies [24, 25, 36–40], and clinical studies on *G. cambogia* extract/HCA [43–58] support its safety demonstrating a wide margin of safety for human consumption. Recent animal and clinical toxicology studies have shown that *G. cambogia*/HCA is generally safe and is classified as NOAEL up to 1240 mg/kg/day [40]. In experimental animal studies at up to 233x the human equivalency dose of HCA (1500 mg/day of HCA), toxicological studies revealed no death, remarkable body weight changes, or gross necropsy findings in Albino rats [12]. Furthermore, the fact that *G. cambogia* extract has been widely used as an antiobesity herbal supplement for decades around the world without a birth defect or reproductive problem suggests that HCA is unlikely to cause reproductive or developmental toxicity. However, most randomized control trials (RCTs) have been conducted on small samples and mainly over a short term. None of them have shown whether the efficacy and safety of *G. cambogia* extract/HCA consumption persist beyond 12 weeks of intervention. Thus, more long term clinical trials or followups could be conducted, especially on consumers who have been taking HCA for a long period of time to add value to the NOAEL for long-term consumption.

Acknowledgment

The authors would like to thank Prof S. G. Tan for the proof-reading of this paper.

References

- [1] D. Jeremiah and C. Low, "Spurt in brain-related disorders trigger growth in the Asia Pacific Cognitive Health Ingredients Markets," Frost and Sullivan, 2011, <http://www.frost.com/prod/servlet/press-release.pag?Src=RSS&docid=239300577>.
- [2] B. H. Sindler, "Herbal therapy for management of obesity: observations from a clinical endocrinology practice," *Endocrine Practice*, vol. 7, no. 6, pp. 443–447, 2001.
- [3] "Dietary Supplement Health and Education Act of 1994," Public Law 103-417: 103rd Congress. October 25, 1994, <http://dshea.com/DSHEA.Legal/dshea.html>.
- [4] R. W. Soller, H. J. Bayne, and C. Shaheen, "The regulated dietary supplement industry: myths of an unregulated industry dispelled," *HerbalGram*, vol. 93, pp. 42–57, 2012.
- [5] R. W. Soller, "Regulation in the herb market: the myth of the 'unregulated industry,'" *HerbalGram*, vol. 49, pp. 64–67, 2000.
- [6] J. Henney, "Implementation of the Dietary Supplement Health Education Act," Testimony before the house committee on government reform, FDA speech archives, March 25, 1999, www.fda.gov/NewsEvents/Testimony/ucm115082.htm.
- [7] W. Sergio, "A natural food, the Malabar Tamnarind, may be effective in the treatment of obesity," *Medical Hypotheses*, vol. 27, no. 1, pp. 39–40, 1988.
- [8] A. C. Sullivan, M. Singh, P. A. Srere, and J. P. Glusker, "Reactivity and inhibitor potential of hydroxycitrate isomers with citrate synthase, citrate lyase, and ATP citrate lyase," *Journal of Biological Chemistry*, vol. 252, no. 21, pp. 7583–7590, 1977.
- [9] J. Triscari and A. C. Sullivan, "Comparative effects of (–)-hydroxycitrate and (+)-allo hydroxycitrate on acetyl CoA carboxylase and fatty acid and cholesterol synthesis in vivo," *Lipids*, vol. 12, no. 4, pp. 357–363, 1977.
- [10] A. C. Sullivan, J. Triscari, J. G. Hamilton, and O. N. Miller, "Effect of (–)-hydroxycitrate upon the accumulation of lipid in the rat: II. Appetite," *Lipids*, vol. 9, no. 2, pp. 129–134, 1974.
- [11] S. E. Ohia, S. O. Awe, A. M. LeDay, C. A. Opere, and D. Bagchi, "Effect of hydroxycitric acid on serotonin release from isolated rat brain cortex," *Research Communications in Molecular Pathology and Pharmacology*, vol. 109, no. 3-4, pp. 210–216, 2001.
- [12] S. E. Ohia, C. A. Opere, A. M. LeDay, M. Bagchi, D. Bagchi, and S. J. Stohs, "Safety and mechanism of appetite suppression by a novel hydroxycitric acid extract (HCA-SX)," *Molecular and Cellular Biochemistry*, vol. 238, no. 1-2, pp. 89–103, 2002.
- [13] K. Hayamizu, H. Hirakawa, D. Oikawa et al., "Effect of *Garcinia cambogia* extract on serum leptin and insulin in mice," *Fitoterapia*, vol. 74, no. 3, pp. 267–273, 2003.
- [14] H. G. Preuss, D. Bagchi, M. Bagchi, C. V. S. Rao, D. K. Dey, and S. Satyanarayana, "Effects of a natural extract of (–)-hydroxycitric acid (HCA-SX) and a combination of HCA-SX plus niacin-bound chromium and *Gymnema sylvestre* extract on weight loss," *Diabetes, Obesity and Metabolism*, vol. 6, no. 3, pp. 171–180, 2004.
- [15] S. Roy, C. Rink, S. Khanna et al., "Body weight and abdominal fat gene expression profile in response to a novel hydroxycitric acid-based dietary supplement," *Gene Expression*, vol. 11, no. 5-6, pp. 251–262, 2004.
- [16] V. Badmaev, M. Majeed, and A. A. Conte, "*Garcinia cambogia* for weight loss," *The Journal of the American Medical Association*, vol. 282, no. 3, pp. 233–235, 1999.
- [17] L. Firenzuoli and L. Gori, "*Garcinia cambogia* for weight loss," *The Journal of the American Medical Association*, vol. 282, no. 3, pp. 234–235, 1999.
- [18] S. B. Heymsfield, D. B. Allison, J. R. Vasselli, A. Pietrobello, D. Greenfield, and C. Nunez, "*Garcinia cambogia* for weight loss," *The Journal of the American Medical Association*, vol. 282, no. 3, pp. 233–235, 1999.
- [19] J. L. Schaller, "*Garcinia cambogia* for weight loss," *The Journal of the American Medical Association*, vol. 282, no. 3, pp. 234–235, 1999.
- [20] S. B. Heymsfield, D. B. Allison, J. R. Vasselli, A. Pietrobello, D. Greenfield, and C. Nunez, "*Garcinia cambogia* (hydroxycitric acid) as a potential antiobesity agent: a randomized controlled trial," *Journal of the American Medical Association*, vol. 280, no. 18, pp. 1596–1600, 1998.

- [21] K. N. Varalakshmi, C. G. Sangeetha, U. S. Samee, G. Irum, H. Lakshmi, and S. P. Prachi, "In vitro safety assessment of the effect of five medicinal plants on human peripheral lymphocytes," *Tropical Journal of Pharmaceutical Research*, vol. 10, no. 1, pp. 33–40, 2011.
- [22] K. H. Lee and B. M. Lee, "Evaluation of the genotoxicity of (–)-hydroxycitric acid (HCA-SX) isolated from *Garcinia cambogia*," *Journal of Toxicology and Environmental Health*, vol. 70, no. 5, pp. 388–392, 2007.
- [23] F. C. Lau, M. Bagchi, and D. Bagchi, "Evaluation of the genotoxicity of (–)-hydroxycitric acid (HCA-SX) isolated from *Garcinia cambogia*," *Journal of Toxicology and Environmental Health*, vol. 71, no. 5, pp. 348–349, 2008.
- [24] M. Shara, S. E. Ohia, T. Yasmin et al., "Dose- and time-dependent effects of a novel (–)-hydroxycitric acid extract on body weight, hepatic and testicular lipid peroxidation, DNA fragmentation and histopathological data over a period of 90 days," *Molecular and Cellular Biochemistry*, vol. 254, no. 1-2, pp. 339–346, 2003.
- [25] M. Shara, S. E. Ohia, R. E. Schmidt et al., "Physico-chemical properties of a novel (–)-hydroxycitric acid extract and its effect on body weight, selected organ weights, hepatic lipid peroxidation and DNA fragmentation, hematology and clinical chemistry, and histopathological changes over a period of 90 days," *Molecular and Cellular Biochemistry*, vol. 260, no. 1, pp. 171–186, 2004.
- [26] M. Saito, M. Ueno, S. Ogino, K. Kubo, J. Nagata, and M. Takeuchi, "High dose of *Garcinia cambogia* is effective in suppressing fat accumulation in developing male Zucker obese rats, but highly toxic to the testis," *Food and Chemical Toxicology*, vol. 43, no. 3, pp. 411–419, 2005.
- [27] C. Kiyose, K. Kubo, and M. Saito, "Effect of *Garcinia cambogia* administration on female reproductive organs in rats," *Journal of Clinical Biochemistry and Nutrition*, vol. 38, no. 3, pp. 188–194, 2006.
- [28] F. H. Pierik, J. T. M. Vreeburg, T. Stijnen, F. H. de Jong, and R. F. A. Weber, "Serum inhibin B as a marker of spermatogenesis," *Journal of Clinical Endocrinology and Metabolism*, vol. 83, no. 9, pp. 3110–3114, 1998.
- [29] A. S. Sheikh, A. Ameena, F. M. Alvi, G. Jaffery, M. Tayyab, and N. A. Chaudhary, "A correlation of serum inhibin with sperm count and sperm motility in fertile and infertile males," *Biomedica*, vol. 20, pp. 10–15, 2004.
- [30] X. R. Plazas, J. P. B. Gasi6n, M. O. Moragues, and P. P. Reus, "Utility of inhibin B in the management of male infertility," *Actas Urol6gicas Espa6olas*, vol. 34, no. 9, pp. 781–787, 2010.
- [31] G. Burdock, M. Bagchi, D. Bagchi, and M. Saito, "*Garcinia cambogia* toxicity is misleading," *Food and Chemical Toxicology*, vol. 43, no. 11, pp. 1683–1684, 2005.
- [32] R. A. Young, R. Frink, and C. Longcope, "Serum testosterone and gonadotropins in the genetically obese male Zucker rat," *Endocrinology*, vol. 111, no. 3, pp. 977–981, 1982.
- [33] C. J. Henry, "Impact of dietary restriction on bioassay and recommendations for future research: panel discussion," in *Biological Effects of Dietary Restriction*, L. Fishbein, Ed., pp. 321–336, Springer, New York, NY, USA.
- [34] H. G. Preuss, D. Bagchi, M. Bagchi, C. V. S. Rao, S. Satyanarayana, and D. K. Dey, "Efficacy of a novel, natural extract of (–)-hydroxycitric acid (HCA-SX) and a combination of HCA-SX, niacin-bound chromium and *Gymnema sylvestre* extract in weight management in human volunteers: a pilot study," *Nutrition Research*, vol. 24, no. 1, pp. 45–58, 2004.
- [35] H. G. Preuss, C. V. S. Rao, R. Garis et al., "An overview of the safety and efficacy of a novel, natural (–)-hydroxycitric acid extract (HCA-SX) for weight management," *Journal of Medicine*, vol. 35, no. 1–6, pp. 33–48, 2004.
- [36] N. S. Deshmukh, M. Bagchi, T. Yasmin, and D. Bagchi, "Safety of a novel calcium/potassium salt of hydroxycitric acid (HCA-SX): I. Two-generation reproduction toxicity study," *Toxicology Mechanisms and Methods*, vol. 18, no. 5, pp. 433–442, 2008.
- [37] C. T. Jones and I. K. Ashton, "Lipid biosynthesis in liver slices of the foetal guinea pig," *Biochemical Journal*, vol. 154, no. 1, pp. 149–158, 1976.
- [38] Z. X. Xu, D. A. Smart, and S. A. Rooney, "Glucocorticoid induction of fatty-acid synthase mediates the stimulatory effect of the hormone on choline-phosphate cytidyltransferase activity in fetal rat lung," *Biochimica et Biophysica Acta*, vol. 1044, no. 1, pp. 70–76, 1990.
- [39] M. R. C. Greenwood, M. P. Cleary, and R. Gruen, "Effect of (–)-hydroxycitrate on development of obesity in the Zucker obese rat," *American Journal of Physiology*, vol. 3, no. 1, pp. E72–E78, 1981.
- [40] N. S. Deshmukh, M. Bagchi, T. Yasmin, and D. Bagchi, "Safety of a novel calcium/potassium salt of (–)-hydroxycitric acid (HCA-SX): II. Developmental toxicity study in rats," *Toxicology Mechanisms and Methods*, vol. 18, no. 5, pp. 443–451, 2008.
- [41] M. G. Soni, G. A. Burdock, H. G. Preuss, S. J. Stohs, S. E. Ohia, and D. Bagchi, "Safety assessment of (–)-hydroxycitric acid and Super CitriMax, a novel calcium/potassium salt," *Food and Chemical Toxicology*, vol. 42, no. 9, pp. 1513–1529, 2004.
- [42] B. W. Downs, M. Bagchi, G. V. Subbaraju, M. A. Shara, H. G. Preuss, and D. Bagchi, "Bioefficacy of a novel calcium-potassium salt of (–)-hydroxycitric acid," *Mutation Research*, vol. 579, no. 1-2, pp. 149–162, 2005.
- [43] A. A. Conte, "A non-prescription alternative in weight reduction therapy," *American Journal of Bariatric Medicine*, pp. 17–19, Summer 1993.
- [44] R. R. Ramos, J. L. Saenz, and C. F. Aguilar, "Extract of *Garcinia cambogia* in the control of obesity," *Investigacion Medica Internacional*, vol. 22, pp. 97–100, 1995.
- [45] M. Girola, M. de Bernardi, and S. Contos, "Dose effect in lipid lowering activity of a new dietary integrator (Chitosan, *Garcinia cambogia* extract, and Chrome)," *Acta Toxicologica et Therapeutica*, vol. 17, pp. 25–40, 1996.
- [46] S. B. Heymsfield, D. B. Allison, J. R. Vasselli, A. Pietrobello, D. Greenfield, and C. Nunez, "*Garcinia cambogia* (hydroxycitric acid) as a potential antiobesity agent: a randomized controlled trial," *Journal of the American Medical Association*, vol. 280, no. 18, pp. 1596–1600, 1998.
- [47] J. Antonio, C. M. Colker, G. C. Torina, Q. Shi, W. Brink, and D. Kalman, "Effects of a standardized guggulsterone phosphate supplement on body composition in overweight adults: a pilot study," *Current Therapeutic Research*, vol. 60, no. 4, pp. 220–227, 1999.
- [48] E. Thom, "A randomized, double-blind, placebo-controlled trial of a new weight-reducing agent of natural origin," *Journal of International Medical Research*, vol. 28, no. 5, pp. 229–233, 2000.
- [49] R. D. Mattes and L. Bormann, "Effects of (–)-hydroxycitric acid on appetite variables," *Physiology & Behavior*, vol. 71, no. 1-2, pp. 87–94, 2000.
- [50] H. G. Preuss, R. I. Garis, J. D. Bramble et al., "Efficacy of a novel calcium/potassium salt of (–)-hydroxycitric acid in weight control," *International Journal of Clinical Pharmacology Research*, vol. 25, no. 3, pp. 133–144, 2005.

- [51] T. Opala, P. Rzymyski, I. Pischel, M. Wilczak, and J. Woźniak, "Efficacy of 12 weeks supplementation of a botanical extract-based weight loss formula on body weight, body composition and blood chemistry in healthy, overweight subjects—a randomised double-blind placebo-controlled clinical trial," *European Journal of Medical Research*, vol. 11, no. 8, pp. 343–350, 2006.
- [52] K. Hayamizu, H. Tomi, I. Kaneko, M. Shen, M. G. Soni, and G. Yoshino, "Effects of *Garcinia cambogia* extract on serum sex hormones in overweight subjects," *Fitoterapia*, vol. 79, no. 4, pp. 255–261, 2008.
- [53] C. A. R. Vasques, S. Rossetto, G. Halmenschlager et al., "Evaluation of the pharmacotherapeutic efficacy of *Garcinia cambogia* plus smorphophallus konjac for the treatment of obesity," *Phytotherapy Research*, vol. 22, no. 9, pp. 1135–1140, 2008.
- [54] E. M. R. Kovacs, M. S. Westerterp-Plantenga, M. de Vries, F. Brouns, and W. H. M. Saris, "Effects of 2-week ingestion of (–)-hydroxycitrate and (–)-hydroxycitrate combined with medium-chain triglycerides on satiety and food intake," *Physiology & Behavior*, vol. 74, no. 4-5, pp. 543–549, 2001.
- [55] K. Hayamizu, Y. Ishii, I. Kaneko et al., "Effects of long-term administration of *Garcinia cambogia* extract on visceral fat accumulation in humans: a placebo controlled double blind trial," *Journal of Oleo Science*, vol. 50, no. 10, pp. 805–812, 2001.
- [56] K. Hayamizu, Y. Ishii, I. Kaneko et al., "No-Observed-Adverse-Effect Level (NOAEL) and sequential-high-dose administration study on *Garcinia cambogia* extract in humans," *Journal of Oleo Science*, vol. 51, no. 5, pp. 365–369, 2002.
- [57] B. Min, B. F. McBride, M. J. Kardas et al., "Electrocardiographic effects of an ephedra-free, multicomponent weight-loss supplement in healthy volunteers," *Pharmacotherapy*, vol. 25, no. 5, pp. 654–659, 2005.
- [58] S. D. Anton, J. Shuster, and C. Leeuwenburgh, "Investigations of botanicals on food intake, satiety, weight loss and oxidative stress: Study protocol of a double-blind, placebo-controlled, crossover study," *Journal of Chinese Integrative Medicine*, vol. 9, no. 11, pp. 1190–1198, 2011.
- [59] M. S. Westerterp-Plantenga and E. M. R. Kovacs, "The effect of (–)-hydroxycitrate on energy intake and satiety in overweight humans," *International Journal of Obesity*, vol. 26, no. 6, pp. 870–872, 2002.
- [60] H. G. Preuss, D. Bagchi, M. Bagchi, C. V. S. Rao, D. K. Dey, and S. Satyanarayana, "Effects of a natural extract of (–)-hydroxycitric acid (HCA-SX) and a combination of HCA-SX plus niacin-bound chromium and *Gymnema sylvestre* extract on weight loss," *Diabetes, Obesity & Metabolism*, vol. 6, no. 3, pp. 171–180, 2004.
- [61] T. Stevens, A. Qadri, and N. N. Zein, "Two patients with acute liver injury associated with use of the herbal weight-loss supplement hydroxycut," *Annals of Internal Medicine*, vol. 142, no. 6, pp. 477–478, 2005.
- [62] L. Dara, J. Hewett, and J. K. Lim, "Hydroxycut hepatotoxicity: a case series and review of liver toxicity from herbal weight loss supplements," *World Journal of Gastroenterology*, vol. 14, no. 45, pp. 6999–7004, 2008.
- [63] M. Shim and S. Saab, "Severe hepatotoxicity due to hydroxycut: a case report," *Digestive Diseases and Sciences*, vol. 54, no. 2, pp. 406–408, 2009.
- [64] G. C. Chen, V. S. Ramanathan, D. Law et al., "Acute liver injury induced by weight-loss herbal supplements," *World Journal of Gastroenterology*, vol. 2, no. 11, pp. 410–415, 2010.
- [65] T. Sharma, L. Wong, N. Tsai, and R. D. Wong, "Hydroxycut (herbal weight loss supplement) induced hepatotoxicity: a case report and review of literature," *Hawaii Medical Journal*, vol. 69, no. 8, pp. 188–190, 2010.
- [66] S. J. Stohs, H. G. Preuss, S. E. Ohia et al., "No evidence demonstrating hepatotoxicity associated with hydroxycitric acid," *World Journal of Gastroenterology*, vol. 15, no. 32, pp. 4087–4089, 2009.
- [67] S. J. Stohs, H. G. Preuss, S. E. Ohia et al., "Safety and efficacy of hydroxycitric acid derived from *Garcinia cambogia*—a literature review," *HerbalGram*, vol. 85, pp. 58–63, 2010.
- [68] D. O. Mozersky, K. Klonz, and L. M. Katz, "The Problem: Liver toxicity following consumption of dietary supplement, Hydroxycut," Health Hazard Review Board Food and Drug Administration, 2009, <http://www.fda.gov/downloads/NewsEvents/PublicHealthFocus/UCM160672.pdf>.
- [69] S. J. Stohs, F. C. Lau, D. Kim, S. U. Kim, M. Bagchi, and D. Bagchi, "Safety assessment of a calcium-potassium salt of (–)-hydroxycitric acid," *Toxicology Mechanisms and Methods*, vol. 20, no. 9, pp. 515–525, 2010.
- [70] F. Márquez, N. Babio, M. Bulló, and J. Salas-Salvadó, "Evaluation of the safety and efficacy of hydroxycitric acid or *Garcinia cambogia* extracts in humans," *Critical Reviews in Food Science and Nutrition*, vol. 52, no. 7, pp. 585–594, 2012.

Review Article

Animal Models as Tools to Investigate Antidiabetic and Anti-Inflammatory Plants

Mohamed Eddouks,¹ Debprasad Chattopadhyay,² and Naoufel Ali Zeggwagh¹

¹ Moulay Ismail University, BP 21, Errachidia 52000, Morocco

² ICMR Virus Unit, ID & BG Hospital, General Block 4, 57 Dr. Suresh C. Banerjee Road, Kolkata 700010, India

Correspondence should be addressed to Mohamed Eddouks, mohamed.eddouks@laposte.net

Received 17 April 2012; Accepted 30 May 2012

Academic Editor: Vincenzo De Feo

Copyright © 2012 Mohamed Eddouks et al. This is an open access article distributed under the Creative Commons Attribution License, which permits unrestricted use, distribution, and reproduction in any medium, provided the original work is properly cited.

Plants have been historically used for diabetes treatment and related anti-inflammatory activity throughout the world; few of them have been validated by scientific criteria. Recently, a large diversity of animal models has been developed for better understanding the pathogenesis of diabetes mellitus and its underlying inflammatory mechanism and new drugs have been introduced in the market to treat this disease. The aim of this work is to review the available animal models of diabetes and anti-inflammatory activity along with some *in vitro* models which have been used as tools to investigate the mechanism of action of drugs with potential antidiabetic properties and related anti-inflammatory mechanism. At present, the rigorous procedures for evaluation of conventional antidiabetic medicines have rarely been applied to test raw plant materials used as traditional treatments for diabetes; and natural products, mainly derived from plants, have been tested in chemically induced diabetes model. This paper contributes to design new strategies for the development of novel antidiabetic drugs and its related inflammatory activity in order to treat this serious condition which represents a global public health problem.

1. Introduction

More than 1000 plants have been described as efficacious in the treatment of diabetes mellitus. However, many of these descriptions are anecdotal accounts of traditional usage, and fewer than half of these plants or plant extracts have received a thorough medical or scientific evaluation of their purported benefits. This paper reviews the preclinical *in vivo* methods and clinical procedures used to investigate the antidiabetic activity of plants and plant-derived extracts, including a consideration of the ethical issues affecting use of traditional plant treatments for diabetes [1, 2].

Animal models have been used extensively to investigate the *in vivo* efficacy, mode of action and side effects of antidiabetic plants and their active principles. Due to the heterogeneity of diabetic conditions in man, no single animal model is entirely representative of a particular type of human diabetes. Thus, many different animal models have been used, each displaying a different selection of features

seen in human diabetic states [3–5]. Normal nondiabetic animals and animals with impaired glucose tolerance and insulin resistance (but not overt diabetes) have been used to demonstrate hypoglycemic activity and to investigate the mode of action of antidiabetic plant materials. It is noteworthy that agents that show a blood-glucose-lowering effect in animals are not necessarily effective in man and vice-versa. This may be due at least in part to differences in hepatic metabolism, where the metabolites are the active compounds [6–8]. Considerable variations in sensitivity to the same agent can also occur between species due to different rates of absorption, metabolism, and elimination [2, 9–11]. The most widely used animal models are small rodents, which are less expensive to maintain than larger animals and generally show a more rapid onset of their diabetic condition consistent with their short lifespan. Moreover, a greater variety of mutations leading to diabetes observed in rodents have been characterized in more detail than those in other animal groups [12–15].

TABLE 1: Classification of type 2 diabetes models in animals.

Model category	Type 2 diabetic models	
	Obese	Nonobese
(I) Spontaneous or genetically derived diabetic animals	<i>ob/ob</i> mouse, <i>db/db</i> mouse KK mouse, KK/ A_y mouse NZO mouse NONcNZO10 mouse TSOD mouse, M16 mouse Zucker fatty rat, ZDF rat SHR/N-cp rat, JCR/LA-cp rat OLETF rat Obese rhesus monkey	Cohen diabetic rat, GK rat Torri rat Nonobese C57BL/6 (Akita) mutant mouse, ALS/Lt mouse
(II) Diet/nutrition induced diabetic animals	Sand rat C57/BL 6J mouse, Spiny mouse	—
(III) Chemically induced diabetic animals	GTG-treated obese mice	Low-dose ALX or STZ adult rats, mice, and so forth; Neonatal STZ rat
(IV) Surgical diabetic animals	VMH lesioned dietary obese diabetic rat	Partial pancreatectomized animals, for example, dog, primate, pig, and rat
(V) Transgenic/knock-out diabetic animals	β_3 receptor knockout mouse Uncoupling protein (UCP1) knock-out mouse	Transgenic or knockout mice involving genes of insulin, insulin receptor, and its components of downstream Insulin signaling, for example, IRS-1, IRS-2, GLUT-4, PTP-1B, and others PPAR-g tissue-specific knockout mouse Glucokinase or GLUT 2 knockout mice Human islet amyloid polypeptide (HIP) over expressed rat

KK: Kuo Kondo; KK/ A_y : yellow KK obese; VMH: ventromedial hypothalamus; ZDF: Zucker diabetic fatty; NZO: New Zealand obese; TSOD: Tsumara Suzuki obese diabetes; SHR/N-cp: spontaneously hypertensive rat/NIH-corpulent; JCR: James C Russel; OLETF: Otuska Long Evans Tokushima fatty; GTG: gold thioglucose; ALX: alloxan; STZ: streptozotocin; GLUT: glucose transporter; IRS: insulin receptor substrate; GK: Goto-Kakizaki; PPAR: peroxisome proliferator activated receptor; PTP: phosphotyrosine phosphatase; ALS: alloxan sensitive.

2. In Vivo Animal Models of Diabetes Mellitus

2.1. Pharmacological Induction. Diabetes can be induced by pharmacologic, surgical, or genetic manipulations in several animal species. Most experiments in diabetes are carried out on rodents, although some studies are still performed in larger animals [16–18]. The classical model employed by Banting and Best was pancreatectomy in dogs [19–22]. It is also described prone strains to diabetes mellitus that have been employed in several researches [23–26]. Currently, the murine model is one of the most used due to the availability of over 200 well-characterized inbred strains and the ability to delete or overexpress specific genes through knockout and transgenic technologies [26–29].

Actually, till date there is neither any evidence nor any validation that a natural plant material can serve as a complete substitute for insulin. Though, several plant products have been reported to mimic the effects of insulin partially or enhance the effects of very low endogenous insulin concentrations, but none has sustained life in the total absence of insulin [19, 21, 30]. Nevertheless, animal models of insulin-dependent diabetes provide a valuable insight into the efficacy of potential adjuncts to insulin therapy in

severely hypoinsulinemia states. The classifications of type 2 diabetes animal models are presented in Table 1. The main insulin-dependent models are as follows:

- (i) spontaneous syndromes (e.g., BB rat, NOD mouse, LEW.1AR1/Ztm-iddm rat),
- (ii) experimentally induced (e.g., chemically, with alloxan or streptozotocin or surgically by near-total pancreatectomy).

These incur extensive or complete loss of pancreatic β -cells and the consequent lack of insulin thereby cause extreme hyperglycemia with glycosuria, polyuria, polydipsia, hyperphagia, and weight loss [31–33].

If untreated, these forms of diabetes culminate in fatal hyperosmolar ketoacidosis. The majority of studies published in the field of ethnopharmacology between 1996 and 2006 employed these models. Streptozotocin (STZ, 69%) and alloxan (31%) are by far the most frequently used drugs, and this model has been useful for the study of multiple aspects of the disease. Both drugs exert their diabetogenic action when they are administered parenterally: intravenously, intraperitoneally, or subcutaneously [34–36].

TABLE 2: Advantages and disadvantages of different categories of type 2 diabetic animal models*.

Model category	Advantages	Disadvantages
(I) Spontaneous diabetic animals	Development of type 2 diabetes is of spontaneous origin involving genetic factors, and the features resemble human type 2 diabetes	Highly inbred, homogenous and mostly monogenic. Inheritance and development is genetically determined, unlike heterogeneity of humans
	Most inbred animal models are homogeneous and environmentally controlled, that allows easy genetic dissection	Limited availability and expensive. Mortality due to ketosis is high in animals with brittle pancreas (db/db, ZDF rat <i>P. obesus</i> , etc.), and it requires insulin in later stage for survival
	Variability of results is minimum and require small sample size	Require sophisticated maintenance
(II) Diet/nutrition induced diabetics	Develop diabetes with obesity due to over nutrition like diabetes syndrome of human	Mostly require long dietary treatment
	Toxicity of chemicals on other vital organs can be avoided	No frank hyperglycaemia develops upon dietary treatment in normal animals and hence unsuitable for screening antidiabetic agents on circulating glucose parameters
(III) Chemical induced diabetic animals	Selective loss of pancreatic beta cells (alloxan/STZ) leaving alpha and delta cells intact	Hyperglycaemia develops by cytotoxic action on the beta cells, leads to insulin deficiency rather than insulin resistance
	Residual insulin secretion help animals to live long without insulin treatment	Diabetes induced by chemicals is less stable and is reversible due to spontaneous regeneration of beta cells. Thus, care is required to assess beta cell function in long-term experiments
	Ketosis and mortality is relatively less	Chemically induced toxicity on other organs along with its cytotoxic action on beta cells
(IV) Surgical diabetic animals	Comparatively cheaper, easier to develop and maintain	Variability of results on development of hyperglycaemia is high
	Avoids cytotoxic effects of chemical diabetogenes on other organs	Involvement of cumbersome technical and post operative procedures
	Resembles human type 2 diabetes due to reduced islet beta cell mass	Occurrence of some digestive problems, due to excision of exocrine portion leads to the deficiency of amylase
(V) Transgenic/knock out diabetic animals	<i>In vivo</i> effect of single gene or mutation on diabetes can be investigated	Dissection of alpha cells (secreting glucagon) along with beta cells leads to the counter regulatory response to hypoglycaemia
	Dissection of complex genetics of type 2 diabetes is easier	Mortality is comparatively higher
		Highly sophisticated and costly for production and maintenance
		Expensive for regular screening experiments

* After [40].

The required dose of these agents for inducing diabetes depends on the animal species, route of administration, and nutritional status. According to the administered dose of these agents, syndromes similar to either type 1, type 2 diabetes, mellitus or glucose intolerance can be induced. Protocols are available anywhere, being critical the pH and type of buffer employed as well as the preparation of the solution of either alloxan or streptozotocin in the day of the experiments [37–39]. The advantages and disadvantages of different categories of type 2 diabetic models are depicted in Table 2.

The cytotoxic action of these diabetogenic agents is mediated by reactive oxygen species (ROS), but both drugs

differ in their mechanism of action. Alloxan and the product of its reduction, dialuric acid, establish a redox cycle with the formation of superoxide radicals. These radicals undergo dismutation to hydrogen peroxide with a simultaneous massive increase in cytosolic calcium concentration, which causes rapid destruction of pancreatic β -cells. The range of the diabetogenic dose of alloxan is quite narrow and even light overdosing may be generally toxic and may cause the loss of many animals [41–43]. This loss is likely to stem from tubular cell necrotic toxicity in kidney, in particular when too high doses of alloxan are administered. The most frequently used intravenous dose of alloxan in rats is 65 mg/kg, but when it is administered intraperitoneally

(i.p.) or subcutaneously its effective dose must be higher. For instance, an intraperitoneal dose below 150 mg/kg may be insufficient for inducing diabetes in this animal species. In mice, doses vary among 100–200 mg/kg by intravenous (i.v.) route [16, 44–46].

Streptozotocin enters the pancreatic β -cell via a glucose transporter-GLUT2 and causes alkylation of DNA [38, 47, 48]. Furthermore, STZ induces activation of polyadenosine diphosphate ribosylation and nitric oxide (NO) release. As a result of STZ action, pancreatic β -cells are destroyed by necrosis. In adult rats, 60 mg/kg is the most common dose of STZ to induce insulin-dependent diabetes, but higher doses are also used. STZ is also efficacious after intraperitoneal administration of a similar or higher dose, but single doses below 40 mg/kg may be ineffective. In general, rats are considered diabetic if tail blood glucose concentrations in fed animals are greater than 200–300 mg/dL, 2 days after STZ injection [23, 49–51]. A model of type 2 diabetes can be induced in rats by either i.v. (tail vein) or i.p. treatment with STZ in the first days of life. At 8–10 weeks of age and thereafter, rats neonatally treated with STZ manifest mild basal hyperglycemia, an impaired response to the glucose tolerance test, and a loss of pancreatic β -cell sensitivity to glucose. It has been observed that STZ at first abolished the pancreatic β -cell response to glucose, but a temporary return of responsiveness appears which is followed by its permanent loss. In adult mice, STZ given in multiple low doses (40 mg/kg, i.v. for 5 days) induces insulin-dependent diabetes that is quite similar to the autoimmune forms (islet inflammation and β -cell death) of type 1 diabetes [26, 27, 52–54]. On the other hand, a single dose between 60 and 100 mg/kg of STZ, administered systemically, can also cause insulin-dependent diabetes, but it lacks the autoimmune profile [20, 55].

The potential problem with STZ due to its toxic effects is not restricted to pancreatic β -cells since it may cause renal injury, oxidative stress, inflammation, and endothelial dysfunction [34–36, 56]. The doses of alloxan and streptozotocin used in both intravenous (i.v.) and intraperitoneal (i.p.) route in different animal species are presented in Table 3.

The destruction of pancreatic β -cells by both drugs is associated with a huge release of insulin which makes animals more susceptible to severe hypoglycemia which may be lethal. Thus, following treatment with either STZ or alloxan, animals are fed with glucose solution (5%) for 12–24 h. Afterwards, an increase of glucose levels is observed in comparison to control animals due to insulin deficiency. It is also reported that fasted animals are more susceptible to alloxan effects and increased blood glucose in fed animals provides partial protection. In general, experimental protocols recommend that administration of either STZ or alloxan must be done in the fasting period (8–12 h) followed by addition of glucose solution to avoid hypoglycemia [43, 48, 57–59]. Besides rats, dogs, and mice, other animal species such as rabbits and monkeys have been employed to induce diabetes by these protocols, but rabbits and pigs are more resistant to STZ [16, 60–62].

TABLE 3: The doses of two chemical diabetogenes in different species.

Chemicals	Species	Dose (s) in mg/kg
Alloxan	Rat	40–200 (i.v./i.p.)
	Mice	50–200 (i.v./i.p.)
	Rabbit	100–150 (i.v.)
	Dog	50–75 (i.v.)
Streptozotocin	Rat	35–65 (i.v./i.p.)
	Mice	100–200 (i.v./i.p.)
	Hamster	50 (i.p.)
	Dog	20–30 (i.v.)
	Pig	100–150 (i.v.)
	Primates	50–150 (i.v.)

i.v.: intravenous; i.p.: intraperitoneal.

After [40].

In general, by using these models of diabetes induced by chemical drugs, the majority of published studies report the amount of reduction of blood glucose which is always evaluated after a period of fasting following acute or chronic treatment with a specific natural product [63–67]. Comparative studies are carried out with nondiabetic and/or diabetic animal groups treated with known antidiabetic drugs, but results do not permit to further explore the mechanism of action of the studied natural product. Glucose is measured by standard glucose oxidase or dehydrogenase assays, mainly by means of commercial meters available everywhere. Insulin determination is available in experimental animals by different methodologies (radioimmunoassay (RIA) or immunometric assays) [68–71].

It is necessary to reemphasize that natural products display several effects besides lowering blood glucose in these experimental models. In view of the lack of parallel studies of their toxicity, these models of diabetes induced by either alloxan or STZ are considered a screening step in the search for drugs for the treatment of diabetes [2, 11–13, 72].

Considering the diversity of active principles found in the crude plant extracts, some studies also include further analysis of lipids (cholesterol and triglycerides) as well as additional evaluation of the antioxidant properties of the product. This can be exemplified with studies using the fruit-pulp, seeds, and leaves extracted from *Eugenia jambolona*, a plant used in folk medicine with recognized antidiabetic properties in several countries. Despite of lack of dose standardization, plant environment selection, and toxicological studies, different other studies have confirmed that the ethanolic extracts of either the fruit-pulp or seeds of this plant have hypoglycemic, hypolipidemic, and antioxidant properties [6, 73–75]. These results suggest that numerous active principles may be present in the raw extract of the plant and highlight the need to further advance in their characterization. In line with this hypothesis, several compounds with antihyperglycemic properties have been isolated from plants. The identification of these products explains, in part, why these compounds present antioxidant, antihyperglycemic, antilipidemic properties and even

enhance the process of wound healing in diabetic and nondiabetic animals. Due to the nonspecific action of compounds isolated from extracts of natural products, some studies have aggregated additional *in vitro* protocols to the *in vivo* studies, such as liver perfusion, to evaluate glucose influx inhibition, gastrointestinal absorption methodologies, and antioxidant enzyme systems, as well as liver glycogen level, among others [9, 71, 76, 77]. These protocols contribute to extend the analysis of the antidiabetic effects of certain natural products. In this context, liver perfusion methodologies with the simultaneous measurement of glucose influx help to elucidate if the natural product exerts extrapancreatic effects like metformin and glitazones. On the other hand, other studies suggest that inhibition of carbohydrate absorption may be linked to the antidiabetic properties of the natural product [10, 12]. Thus, inclusion of at least two different routes of treatment, for instance, i.p. and oral route (p.o.) can help in the analysis of the possible site of action of a studied natural product [10, 12, 69, 71, 78].

2.2. Surgical Models of Diabetes. Another technique used to induce diabetes is the complete removal of the pancreas. Few researchers have employed this model recently to explore effects of natural products with animal species such as rats, pigs, dogs, and primates [3, 7, 73, 79]. Limitations to this technique include high level of technical expertise and adequate surgical room environment, major surgery, high risk of animal infection, adequate postoperative analgesia and antibiotic administration, supplementation with pancreatic enzymes to prevent malabsorption, and loss of pancreatic counter regulatory response to hypoglycemia. More recently, partial pancreatectomy has been employed, but large resection (more than 80% in rats) is required to obtain mild-to-moderate hyperglycemia. In this case, small additional resection can result in significant hypoinsulinemia [9, 78, 80].

3. Spontaneous and Transgenic Animal Models

These models permit the evaluation of the effect of a natural product in an animal without the interference of side effects induced by chemical drugs like alloxan and STZ reported above. Several recent publications summarized the major advances in this state similar to the human condition. In some of these models, insulin resistance predominates in association with obesity, dyslipidemia, and hypertension, which provides valuable insights to study some events that are observed in human type 2 diabetes mellitus. Conversely, some strains like Ob/Ob mouse may maintain euglycemia due to a robust and persistent compensatory pancreatic β -cell response, matching the insulin resistance with hyperinsulinemia [4, 8, 13, 72, 75]. On the other hand, the db/db mouse rapidly develops hyperglycemia since their pancreatic β -cells are unable to maintain the high levels of insulin secretion required throughout life. Thus, food intake is important in determining the severity of the diabetic phenotype, and restriction of energy intake reduces both the obesity and hyperglycemia seen in this strain of mice. Another example is the spontaneously diabetic Goto-Kakizaki rat which is

a genetic lean model of type 2 diabetes originating from selective breeding over many generations of glucose-intolerant nondiabetic Wistar rats. Regarding type 1 diabetes models, the NOD mouse typically presents hyperglycemia between 12 and 30 weeks of age, whereas in BB rats it occurs around 12 weeks of age. One great advantage of these models is that they can also be employed as model of atherosclerosis which represents the long-term complication of diabetes mellitus and tested against several natural products [70, 76, 78, 80–82].

Another valuable spontaneous syndrome occurs in the sand rat (*Psammomys obesus*). In the wild, these animals actively forage for a meager diet. Constrained under laboratory conditions with free access to an energy-rich diet, they become hyperphagic, obese, and hyperinsulinemic and develop insulin resistance and hyperglycemia. In later life, some of these animals incur β -cell failure with severe hyperglycemia. Rhesus monkeys (*Macaca mulatta*) maintained in captivity with limited space and unrestricted availability to an energy-rich diet are also prone to become obese and develop diabetes [46, 64, 83, 84]. Although this closely reflects human type 2 diabetes, primate models have received very limited use due to expense and the relatively long time period of diabetes development [36, 42, 58, 85]. The Ob/Ob mouse lacks biologically active leptin due to a mutation in the leptin gene. This model develops severe insulin resistance and marked hyperinsulinemia with gross obesity, extensive β -cell hyperplasia, and mild-to-moderate hyperglycemia [18, 65, 66, 84]. Thus, ob/ob mouse provides an especially challenging test for any potential treatment against insulin resistance. The Zucker fatty (fa/fa) rat, which results from a mutation in the leptin receptor, is also used as a model of insulin resistance [69, 76, 86, 87]. However, the fa/fa rat seems to exhibit more impaired glucose tolerance than overt diabetes. Cross-breeding of rats carrying the fa mutation has produced other insulin-resistant models which develop overt diabetes, such as the Zucker diabetic fatty (ZDF) rat and the Wistar Kyoto (WKY) fatty rat [9, 10, 14, 73, 88].

4. Right Model for Right Plant

The guidelines that apply to preclinical testing of a new chemical entity (NCE) do not necessarily apply to a traditional plant treatment. For example, the plant may have normal dietary ingredients traditionally taken as a raw or cooked part of the whole plant (e.g., leaf or root) or as an unrefined extract (e.g., simple decoction or infusion).

The heterogeneity of human types of diabetes and the lack of exact replicas among nonprimate animals often require efficacious studies in more than one model, especially to investigate the mode of action. Accounts of the traditional use of an antidiabetic plant in type 1 or type 2 diabetic patients provide an indication of the type of model (e.g., insulin dependent or noninsulin dependent) that might be suitable for initial investigation of hypoglycemic activity [1, 3, 78, 79, 88]. As it was noted previously, experimentally induced models of insulin-dependent diabetes are often not completely devoid of endogenous insulin. This is an important consideration when claims of an insulin substitute

are being investigated. To test the efficacy of antidiabetic plants using STZ-induced or alloxan-induced diabetes in rodents, a convenient procedure is to commence plant therapy within a few days of STZ/alloxan administration before hyperglycemia becomes severe [6, 7]. Efficacy can then be judged by a slower progression and less severe hyperglycemia. If the study is continued until a parallel placebo (untreated) group develops ketoacidosis and requires insulin, this suggests that antidiabetic activity in an insulin-dependent state. However, it is possible that the therapeutic intervention has prevented complete β -cell destruction [6, 7]. This can be seen if insulin concentrations are measured and animals survive when the intervention is discontinued. Because some natural regeneration of islets can occur from islet remnants, long-term survival cannot be exclusively attributed to the therapeutic intervention. An alternative protocol to test efficacy in an insulin-dependent state is to introduce plant therapy to spontaneously or experimentally induced models which have already developed severe hyperglycemia and are controlled by exogenous insulin injections [71, 78, 82, 87]. When plant treatment is introduced and the dosage titrated up, evidence of reduced hyperglycemia or a reduction of insulin dosage without deterioration of glycemic control can be used as indices of efficacy [15, 73].

The selection of noninsulin-dependent models to assess efficacy of antidiabetic plants can also provide important information about mechanism of action [23, 49]. Human type 2 diabetes arises through the combined impact of insulin resistance and β -cell dysfunction, and it is advantageous if a model designed to test efficacy exhibits both of these pathogenic features. Therapies that ameliorate obesity and dyslipidemia offer secondary benefits to improve glycemic control; therefore, models that incorporate these features can often yield additional relevant information [29, 53]. Thus, the diabetic db/db mouse and male ZDF rat provide very useful models. It is noteworthy that a plant treatment may have no efficacy if the model in which it is tested lacks the particular pathogenic feature (e.g., insulin resistance, β -cell dysfunction, obesity, dyslipidemia) against which the treatment exerts its main effect. Consequently, it may be necessary to conduct studies in several animal models to establish efficacy as well as to determine mode of action [27, 30, 53, 55].

At present no drug is able to arrest the progressive loss of pancreatic β -cells which occurs in type 2 diabetes mellitus. According to the United Kingdom Prospective Diabetes Study (UKPDS) results, at the time of type 2 diabetes mellitus diagnoses, 50% of pancreatic β -cell function had already been lost [38, 42, 47, 57]. Thus, the efficacy and side effect of marketed oral antidiabetic drugs still need to be optimized. The recent introduction in the market of incretin analogs opened a new field to evaluate drugs with putative properties that may cause both proliferation and maturation of human pancreatic β -cells [16, 17, 83, 84]. Currently, a standard model of experimental diabetes to study effects of drugs, which could help in preventing the progressive loss of pancreatic islet function, remains to be established [76, 86, 89].

5. Models for Evaluation of Anti-Inflammatory Activity

Inflammation is protective and defense mechanism of the body and thus, during inflammation various pathological changes take place. The production of active inflammatory mediators is triggered by microbial products or by host proteins, such as proteins of the complement, kinins, and coagulation systems that are activated by damaged tissues. In preclinical studies, these changes can be induced by administration of the agents causing inflammation. For purpose of evaluation of anti-inflammatory activity, we will discuss some *in vivo* animal models commonly used in laboratory practice. Numerous reports have been demonstrated in increased incidence of inflammatory condition in lifestyle diseases like diabetes, as inflammation is one of the most important natural defence mechanisms. Its main purpose is to destroy the injurious agent and/or minimize its effects. Though inflammation is normally protective but, if untreated, it can go for chronic condition leading to serious complications. Inflammation is the dynamic pathological process consisting of a series of interdependent changes. Inflammation is body's response to disturbed homeostasis caused by infection, injury, trauma, and several other reasons resulting in systemic and local effects. The Roman writer Celsus in 1st century AD identified the four Cardinal Signs of inflammation as redness (Rubor), swelling or edema (Tumor), heat (Calor), and pain (Dolor) [90]. Inflammation constitutes the body's response to injury and is characterized by a series of events including the inflammatory reaction, a sensory response perceived as pain, and a repair process. The main causes of inflammatory reaction are infection (invasion and multiplication within tissues by bacteria, fungi, viruses, protozoa causing damage to the host cells), trauma penetrating injury, blunt trauma, thermal injury, chemical injury, and immunologically mediated injury (humoral or cellular), and as a result of the loss of blood supply (ischemia) [91].

Inflammation may be acute and chronic, where inflammatory response occurs in three distinct phases. The first phase is caused by an increase in vascular permeability resulting in exudation of fluids from the blood into the interstitial space, the second phase involves the infiltrations of leukocytes from the blood into the tissue and in third phase granuloma formation and tissue repair. Mediators of inflammation originate either from plasma (e.g., complement proteins, Kinins) or from cells (e.g., histamine, prostaglandins, cytokines). The production of active mediators is triggered by microbial products or host proteins, such as proteins of the complement, kinins, and coagulation systems that can cause tissue damage. Generally the mediators of inflammation are histamine, prostaglandins (PGs), leukotrienes (LTB₄), nitric oxide (NO), platelet-activation factor (PAF), bradykinin, serotonin, lipoxins, cytokines, growth factors. Here, we will address the commonly used animal models for the evaluation of anti-inflammatory activity in laboratory along with the principle and procedure of using animal model.

6. Acute Inflammation

6.1. Carrageenan-Induced Paw Edema in Rats [92]. This model is based on the principle of release of various inflammatory mediators by carrageenan. Edema formation due to carrageenan in the rat paw is biphasic, where in the initial phase the release of histamine and serotonin takes place. The second phase is due to the release of prostaglandins, protease and lysosome [93, 94]. Subcutaneous injection of carrageenan into the rat paw produces inflammation resulting from plasma extravasation, increased tissue water and plasma protein exudation, along with neutrophil extravasation, due to the metabolism of arachidonic acid [95]. The first phase begins immediately after injection of carrageenan and diminishes in two hours, while the second phase begins at the end of first phase and remains through three to five hours. *Procedure.* Animals are divided into three groups ($n = 6$) starved overnight with water *ad libitum* prior to the experiment. The control group receives vehicle orally, while test group receives test drug and standard drug, respectively. Left paw is marked with ink at the level of lateral malleolus; basal paw volume is measured plethysmographically by volume displacement method using plethysmometer by immersing the paw till the level of lateral malleolus. The animals are given drug treatment. One hour after dosing, the rats are challenged by a subcutaneous injection of 0.1 mL of 1% solution of carrageenan into the subplantar side of the left hind paw. The paw volume is measured again at 1, 2, 3, 4, and 5 hours after challenge. The increase in paw volume is calculated as percentage compared with the basal volume. The difference of average values between treated animals and control group is calculated for each time interval and evaluated statistically. The percent inhibition is calculated using the formula as follows: % edema inhibition = $[1 - (V_t/V_c)] \times 100$ (V_t and V_c are edema volume in the drug treated and control groups, resp.).

6.2. Histamine-Induced Paw Edema in Rats [96]. Histamine-induced paw edema occur in earlier stage in mounting of vascular reaction in the chemically induced inflammation. Here, swelling occurs primarily due to action of histamine. Generally, histamine is released following the mast cell degranulation by a number of inflammatory mediators including interleukin-1 (IL-1). This is likely to evoke the release of neuropeptides as well as release of prostaglandins and monohydroxy eicosatetraenoic acid from endothelial cell leading to hyperalgesia and other proinflammatory effects [96]. *Procedure:* The procedure is same as that of carrageenan-induced paw edema, only instead of carrageenan the rats are challenged by a subcutaneous injection of 0.1 mL of 1% solution of histamine into the subplantar side of the left hind paw. The paw volume is measured and the percent inhibition of inflammation is calculated and compared with control group with the formula: % Inhibition = $V_c - V_t \times 100$ (V_t and V_c are the edema volume in the drug treated and control groups, resp.).

6.3. Acetic-Acid-Induced Vascular Permeability [97]. The test is used to evaluate the inhibitory activity of drugs against

increased vascular permeability induced by acetic acid as it can release inflammatory mediators [98]. Mediators such as histamine, prostaglandins, and leukotrienes are released following stimulation of mast cells, leading to a dilation of arterioles and venules thereby increase the vascular permeability. As a consequence, fluid and plasma protein are extravasated and edemas are formed. *Procedure.* Animals are divided into three groups ($n = 6$). The control group received vehicle orally, while other groups received test drug and standard drug, respectively, followed by the injection of 0.25 mL of 0.6% solution of acetic acid intraperitoneally. Immediately after administration, 10 mg/kg of 10% (w/v) Evan's blue is injected intravenously through the tail vein. Thirty minutes after Evan's blue injection, the animals are held by a flap of abdominal wall and the viscera irrigated with distilled water over a Petri dish. The exudate is then filtered and makes the volume up to 10 mL. The dyes leaking out into the peritoneal cavity measured spectrophotometrically using visible spectra at 10 nm and compared with the control group.

6.4. Xylene-Induced Ear Edema Thickness and Weight [99]. In xylene-induced ear edema model, the application of xylene induces neurogenous edema, which is partially associated with the substance P, an undecapeptide of central and peripheral nervous system, and acts as a neurotransmitter or neuromodulator in several physiological processes. Substance P is released from the neurons in the midbrain in response to stress, where it facilitates dopaminergic neurotransmission from sensory neurons in the spinal cord against noxious stimuli and excites dorsal neurons. In the periphery, release of substance P from sensory neurons causes vasodilatation and plasma extravasations suggesting its role in neurogenous inflammation. Thus, it can cause the swelling of ear in the mice. *Xylene-Induced Ear Edema (Thickness).* The animals (mice) can be divided into five groups ($n = 6$), fasted overnight and allowed free access to water. The animals are administered with drugs to respective groups. One hour later, each animal received 30 mL of xylene using micropipette on anterior and posterior surfaces of the right ear. The left ear is considered as control. Again after one hour later, the thickness of the ear is determined using Digimatic Caliper. The percentage of ear edema is calculated based on the left ear without xylene. *Xylene-Induced Ear Edema (weight).* The animals (mice) were divided into five groups ($n = 6$), fasted overnight and allowed free access to water. The animals are administered with drugs to respective groups. One hour later, each animal received 30 mL of xylene using micropipette on anterior and posterior surfaces of the right ear lobe. The left ear is considered as control. After one hour, the animals were sacrificed by ether anesthesia and both the ears are removed. Circular sections are taken, using a cork borer (7 mm dia), and weighed. The percentage of ear edema is calculated based on the left ear without xylene [99].

6.5. Arachidonic-Acid-Induced Ear Edema [100]. This model is based on the principle of metabolism of arachidonic acid by cyclooxygenase (COX) leading to the generation of PGs and thromboxanes that mediate pain and edema associated with inflammation. Inhibition of these mediators by test

drug is evaluated. *Procedure.* Inflammation is induced by topical application of arachidonic acid (2 mg in 20 μ L of acetone) of both surfaces of the right ear of each mouse. Rest procedure is same as that like of xylene induced ear edema (thickness and weight parameter).

6.6. Phorbol Myristate Acetate-Induced Ear Edema in Mice [101]. Phorbol myristate acetate (PMA) is a protein kinase C (PKC) promoter, which induces the formation of free radicals *in vivo*. It has been demonstrated that pretreatment of mouse skin by antagonists of PKC suppresses inflammation and ROS (reactive oxygen species), that involved in the synthesis of mediators and regulated the production of TNF α . TNF- α in turn stimulate PLA₂ activity, which releases arachidonic acid from phospholipids and stimulate the activity of COX and Lipoxygenase (LOX), involved in release of different inflammatory mediators. *Procedure.* PMA (4 μ g per ear) in 20 μ L of acetone is applied to the both ear of each mouse. The left ear (control) receives the vehicle. Test drug is administered 1 h before PMA application. Two control groups are used, a group with application of PMA on the right ear and a positive control group that receive standard drug. Six hours after PMA application, the mice are killed by cervical dislocation and a 6 mm diameter disc from each ear is removed with a metal punch and weigh. Ear edema is calculated by subtracting the weight of the left ear (vehicle) from the right ear (treatment) and is expressed as a reduction in weight with respect to the control group.

6.7. Myeloperoxidase (MPO) Assay [102]. MPO is present in neutrophil and in monocytes and macrophages (less amount). It is known that the level of MPO activity is directly proportional to the neutrophil concentration on the inflamed tissue. Inhibition of MPO activity by the drug preventing the generation of oxidants such as hypochlorous acid. *Procedure.* Tissue samples of each ear, from the PMA model, are assessed biochemically with neutrophil marker enzyme MPO. The ear tissue is homogenized in 50 mM K₂PO₄ (pH 6) containing 0.5% hexadecyl trimethylammonium bromide (HTAB) using a homogenizer. After freeze-thawing thrice, the samples are centrifuged at 2500 rpm for 30 min at 4°C and the resulting supernatant is assayed spectrophotometrically for MPO determination. In brief, 40 μ L sample is mixed with 960 μ L of 50 mM phosphate buffer (pH 6), containing 0.167 mg/mL O-dianisidine dihydrochloride and 0.0005% hydrogen peroxide. The change in absorbance at 460 nm is measured with spectrophotometer. MPO activity data is presented as units per mg of tissue. One unit of MPO activity is defined as that degrading 1.0 μ mol of peroxide per minute at 25°C.

6.8. Oxazolone-Induced Ear Edema in Mice [103]. The oxazolone-induced ear edema in mice is a model of delayed contact hypersensitivity that permits the quantitative evaluation of the topical and systemic anti-inflammatory activity of a compound following topical administration. *Procedure.* Mice are divided into various groups ($n = 6$), and a fresh 2% solution of oxazolone (4-ethoxymethylene-2-phenyl-2-oxazolin-5-one) in acetone is prepared. The mice are

sensitized by application of halothane anesthesia (0.1 mL on the shaved abdominal skin or 0.01 mL the inside of both ears). The mice were challenged with 0.01 mL 2% oxazolone solution 8 days later, under anesthesia, inside the right ear (control) or 0.01 mL of oxazolone solution in which the test compound or standard drug is dissolved. Groups of 10 to 15 animals are treated with the irritant alone or with the solution of the test compound. The left ear remains untreated. The maximum inflammation occurs 24 h later, when the animals are sacrificed under anesthesia and a disc of 8 mm diameter is punched from both sides. The discs are immediately weighed on a balance and the weight difference is an indicator of the inflammatory edema.

7. Subacute Model

7.1. Carrageenan-Induced Granuloma Pouch Model [104]. Carrageenan-induced granuloma pouch model is an excellent subacute inflammatory model in which fluid extravasations, leukocyte migration, and various biochemical exudates involved in inflammatory response can be detected readily. The air pouch has the advantage of supplying a suitable space for the induction of inflammatory responses. The injection of irritants such as carrageenan into subcutaneous air pouch on the dorsal surface of rats initiates an inflammatory process. *Procedure.* The animals used in this method are rats divided into five groups ($n = 6$), fasted overnight, and allowed free access to water. The animals are administered with vehicle, standard drug, and test drug. One hour after dosing, the back of the animal is shaved and disinfected. With a very thin needle, subcutaneous dorsal granuloma pouch is made in ether anaesthetized rats by injecting 6 mL of air, followed by injection of 4 mL of 2% carrageenan in normal saline to avoid any leakage of air and the treatment continued for seven consecutive days. On day 8, the pouch is opened under anesthesia and the amount of exudates was collected with a syringe. The average volume of exudates, total WBC count, and weights of granuloma is determined.

7.2. Formalin-Induced Paw Edema [105]. This model is based upon the ability of test drug to inhibit the edema produced in the hind paw of the mice after injection of formalin. The nociceptive effect of formalin is biphasic, an early neurogenic component followed by a later tissue-mediated response. In the first phase, there is release of histamine, 5-HT, and kinin, while the second phase is related to the release of prostaglandins. *Procedure.* The animals are divided into three groups ($n = 6$), and inflammation is produced by subplantar injection of 20 μ L of freshly prepared 2% formalin in the right hind paw. The paw thickness is measured by Plethysmometrically 1 h before and after formalin injection. The drug treatment is continued for 6 consecutive days. The increase in paw thickness and percentage inhibition are calculated and compared with control group.

8. Chronic Model

8.1. Cotton Pellet-Induced Granuloma in Rats [106]. This model is based on the foreign body granuloma that can

provoke by subcutaneous implantation of pellets of compressed cotton in rats. After several days, giant cells and undifferentiated connective tissue can be observed beside the fluid infiltration. The amount of newly formed connective tissue can be measured by weighing the dried pellets after removal. More intensive granuloma formation has been observed if the cotton pellets have been impregnated with carrageenan. *Procedure.* The rats are divided into five groups ($n = 6$), fasted overnight, and allowed free access to water. The animals are administered with vehicle, standard drug and test drugs. One hour after the first dosing, the animals are anesthetized with anesthetic ether and 20 mg of the sterile cotton pellet is inserted one in each axilla and groin of rats by making small subcutaneous incision. The incisions are sutured by sterile catgut [106] and the animals are sacrificed by excess anesthesia on 8th day and cotton pellets are removed surgically. Pellets are separated from extraneous tissue and dried at 60°C until weight become constant. The net dry weight, that is after subtracting the initial weight of the cotton pellet will be determined. The average weight of the pellet of the control group as well as of the test groups is calculated. The percent change of the granuloma weight relatively with vehicle control is determined and statistically evaluated, using the formula: % inhibition = $(W_c - W_d)/W_c \times 100$. W_d = difference in pellet weight of the drug treated group; W_c = difference in pellet weight of the control group.

8.2. *The Glass Rod Granuloma [107].* The glass rod granuloma, described by Vogel, reflects the chronic proliferative inflammation. Of the newly formed connective tissue not only wet and dry weight, but also chemical composition and mechanical properties can be measured. *Procedure.* Glass rods (6 mm dia, 40 mm length) with rounded ends can be made in flame. Rods are sterilized before implantation. Male Sprague-Dawley rats (130 g) are anaesthetized, the back skin shaved and disinfected. From an incision in the caudal region, a subcutaneous tunnel is formed in cranial direction with a closed blunted forceps. One glass rod is introduced into this tunnel finally lying on the back of the animal. The incision wound is closed by sutures. The animals are kept in separate cages. The rods remain in situ for 20 or 40 days. Treatment with drugs is either during the whole period or only during the last 10 or 2 days. At the end, the animals are sacrificed under CO₂ anesthesia. The glass rods are prepared together with the surrounding connective tissue which forms a tube around the glass rod. By incision at one end, the glass rod is extracted and the granuloma sac inverted forming a plain piece of pure connective tissue. Wet weight of the granuloma tissue is recorded and the specimens are kept in a humid chamber until further analysis. Finally, the granuloma tissue is dried and the dry weight is recorded.

9. Estimation of Proinflammatory Mediators and Cytokines *In Vitro*

9.1. *Lipopolysaccharide Stimulation of THP-1 Cells.* The human monocytic leukemia cell line THP-1 was used for studying antiinflammatory potential of natural products or pharmaceuticals as it is a highly differentiated monocytic

cell line with phagocytic properties and has Fc as well as C3b receptors. Indeed, it is the most commonly used model to study the biology of foam cell formation because it can be easily induced to a macrophage phenotype after phorbol ester treatment [108]. Furthermore, these cells have been reported to produce proinflammatory cytokines (IL-1, IL-6, and TNF) and chemokines (IL-8 and MCP-1) in response to lipopolysaccharide (LPS) stimulation [109, 110]. The THP-1 cell line, rather than human monocytes, was used as *in vitro* model system to minimize variability and to allow for high throughput. Using the THP-1 cells, one can demonstrate that, under hyperglycemic conditions, superoxide anion and IL-6 release are increased, as observed in diabetic monocytes, and can elucidated the molecular mechanisms that mediate the increased superoxide anion and cytokine release from diabetic monocytes [111–113]. Thus, the THP-1 cell line is the best *in vitro* model system to understand monocyte/macrophage biology as it relates to human disease.

The cells will be grown in 75 mm² flasks in RPMI supplemented with fetal bovine serum until they attained 70% confluency. On reaching confluency, the cells will be plated in 12-well tissue culture plates (5×10^5 cells/mL) in serum-free medium at 37°C in 5% CO₂. The cells will be challenged with different concentrations (0–1000 µg/L) of LPS for different times (4, 12, and 24 h). The supernatants will be harvested after each time point and stored frozen at –20°C until analysis. IL-1β, TNF-α, and IL-6 will be quantified in all supernatants. The cells were lysed in 0.1 mol/L NaOH and the results for release of each cytokine will be reported as per milligram of protein. The intra- and interassay CVs for the cytokine assays will be <10%, and the specific time points at which maximum cytokine stimulation achieved will be noted.

9.2. *Testing the Antiinflammatory Activity of Various Compounds.* The various compounds including dietary supplements and pharmacologic agents can be tested on this model system. The TNF-α was the cytokine released at the earliest time point (4 h as opposed to 24 h for IL-1β and IL-6) and also at the lowest LPS concentration (half maximum 50 µg/L). Therefore, testing the antiinflammatory effects of such compounds, THP-1 cells will be incubated with LPS (50 µg/L) for a duration of 4 h and TNF-α concentrations will be assayed in supernatants. THP-1 cells will be pretreated with different concentrations of various compounds at biologically relevant concentrations. After 1 h of pretreatment with these compounds, the cells will be challenged with LPS (50 µg/L) for 4 h. The supernatants will be used for measurement of TNF-α, at the range of calibrators of 0–1000 ng/L.

9.3. *Cell Viability Assay (MTT Assay).* Cytotoxicity studies can be performed in 96-well plates. The mechanically scraped THP-1 cells will be plated at 1×10^5 /well in 96-well plates containing 100 µL of DMEM with 10% heat-inactivated FBS and incubated for overnight. Test samples will be dissolved in DMSO (at 0.1% concentrations). After overnight incubation, the test material will be added, and the plates will be incubated for 24 h. Cells will be washed once

and added with 50 μL of FBS-free medium containing MTT (5 mg/mL). After 4 h of incubation at 37°C, the medium will be discarded and the formazan blue that formed in the cells will be dissolved in DMSO (100 μL), and the optical density will be measured at 540 nm.

9.4. Assay of Proinflammatory Mediators and Cytokines. Nitrite Assay. Nitrite (NO) accumulation can be estimated as a measure of NO production, using the Griess reaction. Briefly, 100 μL of cell culture medium will be mixed with 100 μL of Griess reagent (equal volumes of 1% (w/v) sulfanilamide in 5% (v/v) phosphoric acid and 0.1% (w/v) naphthylethylenediamine-HCl), incubated at room temperature for 10 min. Absorbance at 550 nm will be measured by a microplate reader, using fresh culture medium as a blank for all experiments. The amount of nitrite in samples will be measured by standard curve prepared by using sodium nitrite solutions. *PGE2*, *TNF- α* , *Interleukine (IL-2, IL-6, etc.) Assay.* Prostaglandin E2 (PGE2), tumor necrosis factor α (TNF- α) interleukine levels in macrophage culture medium will be quantified by commercially available enzyme immunoassay (EIA) kits according to the manufacture's instructions.

9.5. Western Blot Assay of Cellular Proteins. Cellular proteins extracted from control and drug treated THP-1 cells can also be measured. The washed cell pellets will be resuspended in extraction lysis buffer (50 mM HEPES pH 7.0, 250 mM NaCl, 5 mM EDTA, 0.1% Nonidet P-40, 1 mM phenylmethylsulfonyl fluoride, 0.5 mM dithiothreitol, 5 mM NaF, and 0.5 mM Na orthovanadate) containing 5 $\mu\text{g}/\text{mL}$ each of leupeptin and aprotinin and incubated with 15 min at 4°C. After removal of cell debris by microcentrifugation, supernatants can quickly freeze. Protein concentration will be determined by protein assay reagent according to the manufacture's instruction. 40–50 μg of cellular proteins from treated and untreated cell extracts will be electroblotted onto nitrocellulose membrane following separation on a 10% sodium dodecyl sulfate (SDS)-polyacrylamide gel electrophoresis. The immunoblot will be incubated overnight with blocking solution (5% skim milk) at 4°C, followed by incubation for 4 h with a 1 : 500 dilution of monoclonal anti-iNOS and COX-2 antibody (Santacruz, CA, USA). Blots will be washed twice with PBS and incubated with a 1 : 1000 dilution of horseradish peroxidase-conjugated goat anti-mouse IgG secondary antibody (Santacruz, CA, USA) for 1 h at room temperature. Blots will be re washed thrice in Tween 20/Tris buffered saline (TTBS) and then developed by enhanced chemiluminescence (Amersham Life Science, Arlington Heights, IL, USA).

10. Conclusion

The above models have broad spectrum for evaluation of antidiabetic and related anti-inflammatory activity. In spite of the worldwide use of herbs and medicinal plants, the effective treatment of diabetes with phytochemicals has not been validated with scientific criteria which may support their substitution for the current therapy. Although some studies

have been published with raw natural products, they have not shed light on the mechanisms of action of these products. This implies that several models are necessary to demonstrate that a putative natural product exerts antihyperglycemic activity. Thus, by focusing on other targets of pancreatic islet cell dysfunction, new models may help to elucidate effects of medicinal plants employed in the treatment of diabetes mellitus.

In different models, the inflammation has produced by different inducers by releasing inflammatory mediators. Each is having different mechanism of action for producing inflammation either by increased in vascular permeability, infiltrations of leukocytes or granuloma formation and tissue repair. Among these methods, the most commonly employed techniques is based upon the ability of such agents to inhibit the edema produced in the hind paw of rat after injection of a phlogistic agent (irritant) like brewer's yeast, formaldehyde, dextran, egg albumin, kaolin, aerosil, sulfated polysaccharides (carrageenan or naphthoylheparamine), as well as histamine, xylene, arachidonic acid, phorbol myristate acetate, oxazolone, croton oil, and formalin. For evaluating the most effective and widely used model for inflammation is carrageenan-induced paw edema, carrageenan is polysaccharides of sulfated galactose units and is derived from Irish Sea moss *Chondrus crispus*, which initially releases histamine and serotonin followed by prostaglandins, protease, and lysosomes. In Histamine-induced paw edema, histamine causes vasodilation and increases in vascular permeability followed by edema. Xylene releases substance P from sensory neurons cause's vasodilatation and plasma extravasations. While arachidonic acid administration produces metabolism of arachidonic acid by cyclooxygenase leading to the generation of PGs and thromboxanes, that mediate pain and edema. Phorbol myristate acetate synthesizes mediators and regulates the production of TNF α which in turn stimulate PLA₂ activity. In acetic acid induced vascular permeability, acetic acid causes dilation of arterioles and venules and increased vascular permeability by releasing histamine, prostaglandins, and leukotrienes following stimulation of mast cells and myeloperoxidase in neutrophils indicates intensity of inflammation. In air pouch model formation of exudates with migration of leukocytes and interleukins takes place, due to angiogenesis, nitric oxide synthesis, and Kinin release. Angiogenesis in a chronic inflammatory state, which facilitates migration of inflammatory cells to the inflammatory site and supplies nutrients and oxygen to granulation tissue. Thus, the suppression of angiogenesis in granulation tissue is important to suppress the development of chronic granulation tissue [114]. Nitric oxide synthesis (NO), by inducible nitric oxide synthase (iNOS), increases in inflammation and leads to cellular injury; while kinins cause vasodilatation, increase vascular permeability and WBC migration in the early stages of the inflammation, and are also responsible for, collagen formation in the later stage. It may also be responsible for the vascular flushing that occurs in the carcinoid syndrome and also implicated in the endotoxin shock, hereditary angioneurotic edema, anaphylaxis, arthritis, and in acute pancreatitis. Kinins degranulate mast cells to release histamine and other mediators and plasma extravasation by

contraction of vascular endothelial cells. Kinins are potent algogenic substances, which induce pain by directly stimulating nociceptors in skin joint, and muscles [96]. In cotton-pellet-induced or glass rod granuloma, the foreign (cotton or glass rod) implanted in the skin is producing undifferentiated connective tissue indicating inflammation. The amount of newly formed connective tissue is measured by weighing the dried pellet after removal as an index of the extended severity of inflammation and thus, which indicates the proliferative phase of the inflammation of macrophages, neutrophils, fibroblasts and collagen formation. Therefore, a decrease in the granuloma formation indicates the suppression of the proliferative phase [115].

References

- [1] A. Serafin, J. Molin, M. Márquez et al., "Diabetic neuropathy: electrophysiological and morphological study of peripheral nerve degeneration and regeneration in transgenic mice that express IFN β in β cells," *Muscle and Nerve*, vol. 41, no. 5, pp. 630–641, 2010.
- [2] H. Shevalye, R. Stavniichuk, W. Xu et al., "Poly(ADP-ribose) polymerase (PARP) inhibition counteracts multiple manifestations of kidney disease in long-term streptozotocin-diabetic rat model," *Biochemical Pharmacology*, vol. 79, no. 7, pp. 1007–1014, 2010.
- [3] A. Van den Bergh, P. Vangheluwe, A. Vanderper et al., "Food-restriction in obese dyslipidaemic diabetic mice partially restores basal contractility but not contractile reserve," *European Journal of Heart Failure*, vol. 11, no. 12, pp. 1118–1125, 2009.
- [4] L. Vedtofte, T. B. Bodvarsdottir, C. F. Gotfredsen, A. E. Karlsen, L. B. Knudsen, and R. S. Heller, "Liraglutide, but not vildagliptin, restores normoglycaemia and insulin content in the animal model of type 2 diabetes, *Psammomys obesus*," *Regulatory Peptides*, vol. 160, no. 1–3, pp. 106–114, 2010.
- [5] J. Xiao, Y. Lv, S. Lin et al., "Cardiac protection by basic fibroblast growth factor from ischemia/reperfusion-induced injury in diabetic rats," *Biological and Pharmaceutical Bulletin*, vol. 33, no. 3, pp. 444–449, 2010.
- [6] Y. J. Wang, G. S. Fu, F. M. Chen, and H. Wang, "The effect of valsartan and fluvastatin on the connective tissue growth factor expression in experimental diabetic cardiomyopathy," *Zhonghua Nei Ke Za Zhi*, vol. 48, no. 8, pp. 660–665, 2009.
- [7] D. Wei, J. Li, M. Shen et al., "Cellular production of n-3 PUFAs and reduction of n-6-to-n-3 ratios in the pancreatic β -cells and islets enhance insulin secretion and confer protection against cytokine-induced cell death," *Diabetes*, vol. 59, no. 2, pp. 471–478, 2010.
- [8] G. Z. Wu, G. Hong, W. P. Zhang, and H. B. Zhang, "Effect of 1-[4-[2-(4-bromobenzenesulfonamino)ethyl]phenylsulfonyl]-3-(trans-4-methylcyclohexyl)urea (14), a new synthetic sulfonylurea compound, on glucose metabolism in vivo and in vitro," *Arzneimittel-Forschung*, vol. 59, no. 11, pp. 550–556, 2009.
- [9] S. Ro, C. Park, J. Jin et al., "A model to study the phenotypic changes of interstitial cells of Cajal in gastrointestinal diseases," *Gastroenterology*, vol. 138, no. 3, pp. 1068–1078.e2, 2010.
- [10] E. Seo, E. J. Park, Y. Joe et al., "Overexpression of AMPK α 1 ameliorates fatty liver in hyperlipidemic diabetic rats," *Korean Journal of Physiology and Pharmacology*, vol. 13, no. 6, pp. 449–454, 2009.
- [11] D. V. Serreze, M. Niens, J. Kulik, and T. P. Di Lorenzo, "Bridging mice to men: using HLA transgenic mice to enhance the future prediction and prevention of autoimmune type 1 diabetes in humans," *Methods in Molecular Biology*, vol. 602, pp. 119–134, 2010.
- [12] V. Sordi, R. Melzi, A. Mercalli et al., "Mesenchymal cells appearing in pancreatic tissue culture are bone marrow-derived stem cells with the capacity to improve transplanted islet function," *Stem Cells*, vol. 28, no. 1, pp. 140–151, 2010.
- [13] A. M. Stranahan, T. V. Arumugam, K. Lee, and M. P. Mattson, "Mineralocorticoid receptor activation restores medial perforant path LTP in diabetic rats," *Synapse*, vol. 64, no. 7, pp. 528–532, 2010.
- [14] S. Sugii, P. Olson, D. D. Sears et al., "PPAR γ activation in adipocytes is sufficient for systemic insulin sensitization," *Proceedings of the National Academy of Sciences of the United States of America*, vol. 106, no. 52, pp. 22504–22509, 2009.
- [15] M. L. Sugrue, K. R. Vella, C. Morales, M. E. Lopez, and A. N. Hollenberg, "The thyrotropin-releasing hormone gene is regulated by thyroid hormone at the level of transcription in vivo," *Endocrinology*, vol. 151, no. 2, pp. 793–801, 2010.
- [16] Y. Luzardo and C. E. Mathews, "Attacking the source: Anti-PDX-1 responses in type 1 diabetes," *Laboratory Investigation*, vol. 90, no. 1, pp. 6–8, 2010.
- [17] H. Matsui-Inohara, H. Uematsu, T. Narita et al., "E2F-1-deficient NOD/SCID mice developed showing decreased saliva production," *Experimental Biology and Medicine*, vol. 234, no. 12, pp. 1525–1536, 2009.
- [18] Y. Matsumoto, K. Torimoto, H. Matsuyoshi et al., "Long-term effects of diabetes mellitus on voiding function in a new model of type 2 diabetes mellitus, the Spontaneously Diabetic Torii (SDT) rat," *Biomedical Research*, vol. 30, no. 6, pp. 331–335, 2009.
- [19] E. Fernández-Millán, M. N. Gangnerau, L. De Miguel-Santos et al., "Undernutrition of the GK rat during gestation improves pancreatic IGF-2 and beta-cell mass in the fetuses," *Growth Factors*, vol. 27, no. 6, pp. 409–418, 2009.
- [20] N. Gagliani, T. Jofra, A. Stabilini et al., "Antigen-specific dependence of Tr1-cell therapy in preclinical models of islet transplant," *Diabetes*, vol. 59, no. 2, pp. 433–439, 2010.
- [21] N. F. Gonzalez-Cadavid and J. Rajfer, "Treatment of Peyronie's disease with PDE5 inhibitors: an antifibrotic strategy," *Nature Reviews Urology*, vol. 7, no. 4, pp. 215–221, 2010.
- [22] K. D. Hall, "Mathematical modelling of energy expenditure during tissue deposition," *British Journal of Nutrition*, vol. 104, no. 1, pp. 4–7, 2010.
- [23] L. Alhonen, A. Uimari, M. Pietilä, M. T. Hyvönen, E. Pirinen, and T. A. Keinänen, "Transgenic animals modelling polyamine metabolism-related diseases," *Essays in biochemistry*, vol. 46, pp. 125–144, 2009.
- [24] U. Ariz, J. M. Mato, S. C. Lu, and M. L. Martínez Chantar, "Nonalcoholic steatohepatitis, animal models, and biomarkers: what is new?" *Methods in Molecular Biology*, vol. 593, pp. 109–136, 2010.
- [25] H. Baribault, "Mouse models of type II diabetes mellitus in drug discovery," *Methods in Molecular Biology*, vol. 602, pp. 135–155, 2010.
- [26] E. Bolotin, H. Liao, T. C. Ta et al., "Integrated approach for the identification of human hepatocyte nuclear factor 4 α target genes using protein binding microarrays," *Hepatology*, vol. 51, no. 2, pp. 642–653, 2010.
- [27] J. V. Busik, M. Tikhonenko, A. Bhatwadekar et al., "Diabetic retinopathy is associated with bone marrow neuropathy

- and a depressed peripheral clock," *Journal of Experimental Medicine*, vol. 206, no. 13, pp. 2897–2906, 2009.
- [28] J. H. Chen, E. C. Cottrell, and S. E. Ozanne, "Early growth and ageing," *Nestle Nutrition Workshop Series: Pediatric Program*, vol. 65, pp. 41–54, 2010.
- [29] J. Crisóstomo, L. Rodrigues, P. Matafome et al., "Beneficial effects of dietary restriction in type 2 diabetic rats: the role of adipokines on inflammation and insulin resistance," *British Journal of Nutrition*, vol. 104, no. 1, pp. 76–82, 2010.
- [30] K. S. Foo, H. Brauner, C. G. Östenson, and C. Broberger, "Nucleobindin-2/nesfatin in the endocrine pancreas: distribution and relationship to glycaemic state," *Journal of Endocrinology*, vol. 204, no. 3, pp. 255–263, 2010.
- [31] B. Halter, J. L. Gonzalez de Aguilar, F. Rene et al., "Oxidative stress in skeletal muscle stimulates early expression of Rad in a mouse model of amyotrophic lateral sclerosis," *Free Radical Biology and Medicine*, vol. 48, no. 7, pp. 915–923, 2010.
- [32] J. Han and Y. Q. Liu, "Reduction of islet pyruvate carboxylase activity might be related to the development of type 2 diabetes mellitus in Agouti-K mice," *Journal of Endocrinology*, vol. 204, no. 2, pp. 143–152, 2010.
- [33] A. Higuchi, K. Ohashi, R. Shibata, S. Sono-Romanelli, K. Walsh, and N. Ouchi, "Thiazolidinediones reduce pathological neovascularization in ischemic retina via an adiponectin-dependent mechanism," *Arteriosclerosis, Thrombosis, and Vascular Biology*, vol. 30, no. 1, pp. 46–53, 2010.
- [34] H. Hotta, T. Miura, T. Miki et al., "Short communication: angiotensin II type 1 receptor-mediated upregulation of calcineurin activity underlies impairment of cardioprotective signaling in diabetic hearts," *Circulation Research*, vol. 106, no. 1, pp. 129–132, 2010.
- [35] A. Hussain, H. Mahmood, and S. EL-Hasani, "Can Roux-en-Y gastric bypass provide a lifelong solution for diabetes mellitus?" *Canadian Journal of Surgery*, vol. 52, no. 6, pp. E269–E275, 2009.
- [36] E. Hyun, R. Ramachandran, N. Cenac et al., "Insulin modulates protease-activated receptor 2 signaling: implications for the innate immune response," *Journal of Immunology*, vol. 184, no. 5, pp. 2702–2709, 2010.
- [37] I. Jarchum and T. P. DiLorenzo, "Ins2 deficiency augments spontaneous HLA-A*0201-restricted T Cell responses to insulin," *Journal of Immunology*, vol. 184, no. 2, pp. 658–665, 2010.
- [38] J. H. Jeong, S. H. Kim, M. Lee et al., "Non-viral systemic delivery of Fas siRNA suppresses cyclophosphamide-induced diabetes in NOD mice," *Journal of Controlled Release*, vol. 143, no. 1, pp. 88–94, 2010.
- [39] T. Jiang, Z. Huang, Y. Lin, Z. Zhang, D. Fang, and D. D. Zhang, "The protective role of Nrf2 in streptozotocin-induced diabetic nephropathy," *Diabetes*, vol. 59, no. 4, pp. 850–860, 2010.
- [40] K. Srinivasan and P. Ramarao, "Animal models in type 2 diabetes research: an overview," *Indian Journal of Medical Research*, vol. 125, no. 3, pp. 451–472, 2007.
- [41] N. P. Kumar, A. R. Annamalai, and R. S. Thakur, "Antinociceptive property of emblica officinalis gaertn (Amla) in high fat dietfed/low dose streptozotocin induced diabetic neuropathy in rats," *Indian Journal of Experimental Biology*, vol. 47, no. 9, pp. 737–742, 2009.
- [42] M. Labieniec, O. Ulicna, O. Vancova, J. Kucharska, T. Gabryelak, and C. Watala, "Effect of poly(amido)amine (PAMAM) G4 dendrimer on heart and liver mitochondria in an animal model of diabetes," *Cell Biology International*, vol. 34, no. 1, pp. 89–97, 2010.
- [43] Y. M. Lee, O. C. Gweon, Y. J. Seo et al., "Antioxidant effect of garlic and aged black garlic in animal model of type 2 diabetes mellitus," *Nutrition Research and Practice*, vol. 3, no. 2, pp. 156–161, 2009.
- [44] C. Liang, K. DeCourcy, and M. R. Prater, "High-saturated-fat diet induces gestational diabetes and placental vasculopathy in C57BL/6 mice," *Metabolism*, vol. 59, no. 7, pp. 943–950, 2010.
- [45] C. L. Lin, J. Y. Wang, J. Y. Ko, Y. T. Huang, Y. H. Kuo, and F. S. Wang, "Dickkopf-1 promotes hyperglycemia-induced accumulation of mesangial matrix and renal dysfunction," *Journal of the American Society of Nephrology*, vol. 21, no. 1, pp. 124–135, 2010.
- [46] T. Märker, J. Kriebel, U. Wohlrab, and C. Habich, "Heat shock protein 60 and adipocytes: characterization of a ligand-receptor interaction," *Biochemical and Biophysical Research Communications*, vol. 391, no. 4, pp. 1634–1640, 2010.
- [47] N. Ishizaka, M. Hongo, G. Matsuzaki et al., "Effects of the AT1 receptor blocker losartan and the calcium channel blocker benidipine on the accumulation of lipids in the kidney of a rat model of metabolic syndrome," *Hypertension Research*, vol. 33, no. 3, pp. 263–268, 2010.
- [48] H. Y. Jin, W. J. Liu, J. H. Park, H. S. Baek, and T. S. Park, "Effect of dipeptidyl peptidase-IV (DPP-IV) inhibitor (Vildagliptin) on peripheral nerves in streptozotocin-induced diabetic rats," *Archives of Medical Research*, vol. 40, no. 7, pp. 536–544, 2009.
- [49] T. Archer and R. M. Kostrzewa, "Staging neurological disorders: expressions of cognitive and motor disorder," *Neurotoxicity Research*, vol. 18, no. 2, pp. 107–111, 2010.
- [50] A. Aydemir-Koksoy, A. Bilginoglu, M. Sariahmetoglu, R. Schulz, and B. Turan, "Antioxidant treatment protects diabetic rats from cardiac dysfunction by preserving contractile protein targets of oxidative stress," *Journal of Nutritional Biochemistry*, vol. 21, no. 9, pp. 827–833, 2010.
- [51] N. M. Bazhan and E. N. Makarova, "The effect of the "yellow" mutation at the mouse agouti locus on the hormonal profile of pregnancy and lactation," *Rossiiskii Fiziologicheskii Zhurnal Imeni I.M. Sechenova*, vol. 95, no. 11, pp. 1254–1257, 2009.
- [52] T. L. Broderick and P. Wong, "Influence of the estrous cycle on hypoxic failure in the female rat heart," *Gender Medicine*, vol. 6, no. 4, pp. 596–603, 2009.
- [53] Y. B. Chen, J. Li, Y. Qi et al., "The effects of electromagnetic pulses (EMP) on the bioactivity of insulin and a preliminary study of mechanism," *International Journal of Radiation Biology*, vol. 86, no. 1, pp. 22–26, 2010.
- [54] M. Falasca, D. Chiozzotto, H. Y. Godage et al., "A novel inhibitor of the PI3K/Akt pathway based on the structure of inositol 1,3,4,5,6-pentakisphosphate," *British Journal of Cancer*, vol. 102, no. 1, pp. 104–114, 2010.
- [55] L. Gaohua and H. Kimura, "A mathematical model of brain glucose homeostasis," *Theoretical Biology and Medical Modelling*, vol. 6, no. 1, article 26, 2009.
- [56] M. Hiroi, Y. Morishita, M. Hayashi et al., "Activation of vasopressin neurons leads to phenotype progression in a mouse model for familial neurohypophysial diabetes insipidus," *American Journal of Physiology*, vol. 298, no. 2, pp. R486–R493, 2010.
- [57] M. E. Khamseh, B. Safarnejad, and H. R. Baradaran, "The effect of captopril on progression of retinopathy in type 2 diabetes," *Diabetes Technology and Therapeutics*, vol. 11, no. 11, pp. 711–715, 2009.

- [58] Z. Lan, R. Zassoko, W. Liu et al., "Development of techniques for gastrojejunal bypass surgery in obese mice," *Microsurgery*, vol. 30, no. 4, pp. 289–295, 2010.
- [59] C. J. Li, Q. M. Zhang, M. Z. Li, J. Y. Zhang, P. Yu, and D. M. Yu, "Attenuation of myocardial apoptosis by alpha-lipoic acid through suppression of mitochondrial oxidative stress to reduce diabetic cardiomyopathy," *Chinese Medical Journal*, vol. 122, no. 21, pp. 2580–2586, 2009.
- [60] H. V. Lin, L. Plum, H. Ono et al., "Divergent regulation of energy expenditure and hepatic glucose production by insulin receptor in agouti-related protein and POMC neurons," *Diabetes*, vol. 59, no. 2, pp. 337–346, 2010.
- [61] J. Liu, H. Tang, L. Niu, and Y. Xu, "Upregulation of Tanis mRNA expression in the liver is associated with insulin resistance in rats," *Tohoku Journal of Experimental Medicine*, vol. 219, no. 4, pp. 307–310, 2009.
- [62] T. Matsumoto, Y. Ozawa, K. Taguchi, T. Kobayashi, and K. Kamata, "Chronic treatment with losartan (angiotensin II type 1 receptor antagonist) normalizes enhanced acetylcholine-induced coronary vasoconstriction in isolated perfused hearts of type 2 diabetic OLETF rats," *Journal of Smooth Muscle Research*, vol. 45, no. 5, pp. 197–208, 2009.
- [63] C. M. Mayer and D. D. Belsham, "Palmitate attenuates insulin signaling and induces endoplasmic reticulum stress and apoptosis in hypothalamic neurons: rescue of resistance and apoptosis through adenosine 5' monophosphate-activated protein kinase activation," *Endocrinology*, vol. 151, no. 2, pp. 576–585, 2010.
- [64] Z. Ming, D. J. Legare, and W. W. Lutt, "Obesity, syndrome X, and diabetes: the role of HISS-dependent insulin resistance altered by sucrose, an antioxidant cocktail, and age," *Canadian Journal of Physiology and Pharmacology*, vol. 87, no. 10, pp. 873–882, 2009.
- [65] A. B. Motta, "Dehydroepiandrosterone to induce murine models for the study of polycystic ovary syndrome," *Journal of Steroid Biochemistry and Molecular Biology*, vol. 119, no. 3–5, pp. 105–111, 2010.
- [66] J. F. Ndisang, N. Lane, N. Syed, and A. Jadhav, "Up-regulating the heme oxygenase system with hemin improves insulin sensitivity and glucose metabolism in adult spontaneously hypertensive rats," *Endocrinology*, vol. 151, no. 2, pp. 549–560, 2010.
- [67] S. J. Noh, S. H. Miller, Y. T. Lee et al., "Let-7 microRNAs are developmentally regulated in circulating human erythroid cells," *Journal of Translational Medicine*, vol. 7, article 98, 2009.
- [68] K. N. Phoenix, F. Vumbaca, M. M. Fox, R. Evans, and K. P. Claffey, "Dietary energy availability affects primary and metastatic breast cancer and metformin efficacy," *Breast Cancer Research and Treatment*, vol. 123, no. 2, pp. 333–344, 2010.
- [69] L. H. Pojoga, J. R. Romero, T. M. Yao et al., "Caveolin-1 ablation reduces the adverse cardiovascular effects of N- ω -Nitro-L-Arginine methyl ester and angiotensin II," *Endocrinology*, vol. 151, no. 3, pp. 1236–1246, 2010.
- [70] M. Pravenec, "Use of rat genomics for investigating the metabolic syndrome," *Methods in Molecular Biology*, vol. 597, pp. 415–426, 2010.
- [71] M. J. Prior, V. C. Foletta, J. B. Jowett et al., "The characterization of Abelson helper integration site-1 in skeletal muscle and its links to the metabolic syndrome," *Metabolism*, vol. 59, no. 7, pp. 1057–1064, 2010.
- [72] A. A. Spasov, A. F. Kucheriavenko, and O. A. Salaznikova, "Effect of hypoglycemic drugs on hemorheological parameters," *Ekspierimental'naia i Klinicheskaia Farmakologija*, vol. 72, no. 5, pp. 31–34, 2009.
- [73] C. Tan, A. Salehi, S. Svensson, B. Olde, and D. Erlinge, "ADP receptor P2Y₁₃ induce apoptosis in pancreatic β -cells," *Cellular and Molecular Life Sciences*, vol. 67, no. 3, pp. 445–453, 2010.
- [74] K. M. Utzschneider and K. V. Kowdley, "Hereditary hemochromatosis and diabetes mellitus: implications for clinical practice," *Nature Reviews Endocrinology*, vol. 6, no. 1, pp. 26–33, 2010.
- [75] R. Venkataraman, L. Belardinelli, B. Blackburn, J. Heo, and A. E. Iskandrian, "A study of the effects of ranolazine using automated quantitative analysis of serial myocardial perfusion images," *JACC: Cardiovascular Imaging*, vol. 2, no. 11, pp. 1301–1309, 2009.
- [76] S. Parajes, L. Loidi, N. Reisch et al., "Functional consequences of seven novel mutations in the CYP11B1 gene: four mutations associated with nonclassic and three mutations causing classic 11 β -hydroxylase deficiency," *Journal of Clinical Endocrinology and Metabolism*, vol. 95, no. 2, pp. 779–788, 2010.
- [77] J. M. Park, H. Y. Bong, H. I. Jeong, Y. K. Kim, J. Y. Kim, and O. Kwon, "Postprandial hypoglycemic effect of mulberry leaf in Goto-Kakizaki rats and counterpart control Wistar rats," *Nutrition Research and Practice*, vol. 3, no. 4, pp. 272–278, 2009.
- [78] P. H. Reddy, "Role of mitochondria in neurodegenerative diseases: mitochondria as a therapeutic target in Alzheimer's disease," *CNS Spectrums*, vol. 14, no. 8, pp. 8–13, 2009.
- [79] S. Tracy, K. M. Drescher, J. D. Jackson, K. Kim, and K. Kono, "Enteroviruses, type 1 diabetes and hygiene: a complex relationship," *Reviews in Medical Virology*, vol. 20, no. 2, pp. 106–116, 2010.
- [80] S. Renner, C. Fehlings, N. Herbach et al., "Glucose intolerance and reduced proliferation of pancreatic β -cells in transgenic pigs with impaired glucose-dependent insulinotropic polypeptide function," *Diabetes*, vol. 59, no. 5, pp. 1228–1238, 2010.
- [81] S. S. Scherer, G. Pietramaggiore, J. C. Mathews, and D. P. Orgill, "Short periodic applications of the vacuum-assisted closure device cause an extended tissue response in the diabetic mouse model," *Plastic and Reconstructive Surgery*, vol. 124, no. 5, pp. 1458–1465, 2009.
- [82] K. Schroder, R. Zhou, and J. Tschopp, "The NLRP3 inflammasome: a sensor for metabolic danger?" *Science*, vol. 327, no. 5963, pp. 296–300, 2010.
- [83] S. R. Mayack, J. L. Shadrach, F. S. Kim, and A. J. Wagers, "Systemic signals regulate ageing and rejuvenation of blood stem cell niches," *Nature*, vol. 463, no. 7280, pp. 495–500, 2010.
- [84] B. A. McGivney, S. S. Eivers, D. E. MacHugh et al., "Transcriptional adaptations following exercise in thoroughbred horse skeletal muscle highlights molecular mechanisms that lead to muscle hypertrophy," *BMC Genomics*, vol. 10, article 638, 2009.
- [85] S. E. Lee, W. Ma, E. M. Rattigan et al., "Ultrastructural features of retinal capillary basement membrane thickening in diabetic swine," *Ultrastructural Pathology*, vol. 34, no. 1, pp. 35–41, 2010.
- [86] K. Oishi and N. Ohkura, "Strain- and tissue-dependent induction of plasminogen activator inhibitor-1 gene expression in fasted mice," *Biological and Pharmaceutical Bulletin*, vol. 33, no. 3, pp. 530–531, 2010.

- [87] C. J. Ramnanan, D. S. Edgerton, N. Rivera et al., "Molecular characterization of insulin-mediated suppression of hepatic glucose production in vivo," *Diabetes*, vol. 59, no. 6, pp. 1302–1311, 2010.
- [88] Y. Shimoshige, R. Enomoto, T. Aoki, N. Matsuoka, and S. Kaneko, "The involvement of aldose reductase in alterations to neurotrophin receptors and neuronal cytoskeletal protein mRNA levels in the dorsal root ganglion of streptozotocin-induced diabetic rats," *Biological and Pharmaceutical Bulletin*, vol. 33, no. 1, pp. 67–71, 2010.
- [89] E. J. Pawson, B. Duran-Jimenez, R. Suroskyheather et al., "Engineered zinc finger protein-mediated VEGF-A activation restores deficient VEGF-A in sensory neurons in experimental diabetes," *Diabetes*, vol. 59, no. 2, pp. 509–518, 2010.
- [90] M. Harsh, *Inflammation and Healing*, Jaypee Publication, 2002.
- [91] Robbins and Cortran, *Acute and Chronic inflammation. Pathologic Basis of Disease*, Elsevier, San Diego, Calif, USA, 7 edition, 2004.
- [92] C. A. Winter, E. Risley, and G. Nuss, "Carrageenan-induced edema in hind paw of the rat as an assay for anti-inflammatory drugs," *Proceedings of the Society for Experimental Biology and Medicine*, vol. 111, pp. 544–547, 1962.
- [93] R. Vinegar, W. Schreiber, and R. Hugo, "Biphasic development of carrageenin edema in rats," *Journal of Pharmacology and Experimental Therapeutics*, vol. 166, no. 1, pp. 96–103, 1969.
- [94] I. Posadas, M. Bucci, F. Roviezzo et al., "Carrageenan-induced mouse paw oedema is biphasic, age-weight dependent and displays differential nitric oxide cyclooxygenase-2 expression," *British Journal of Pharmacology*, vol. 142, no. 2, pp. 331–338, 2004.
- [95] V. A. Chatpalliwar, A. A. Joharapurkar, M. M. Wanjari, R. R. Chakraborty, and V. T. Kharkar, "Anti-inflammatory activity of *Martynia diandra glox*," *Indian Drugs*, vol. 39, no. 10, pp. 543–545, 2002.
- [96] A. Dray, "Inflammatory mediators of pain," *British Journal of Anaesthesia*, vol. 75, no. 2, pp. 125–131, 1995.
- [97] B. A. Whittle, "The use of changes in capillary permeability in mice to distinguish between narcotic and non-narcotic analgesic," *British Journal of Pharmacology and Chemotherapy*, vol. 22, no. 2, pp. 24–253, 1964.
- [98] A. Miles and E. Miles, "Vascular reactions to histamine, histamine-liberator and leukotaxine in the skin of guinea-pigs," *Journal of Physiology*, vol. 118, no. 2, pp. 228–257, 1992.
- [99] J. Kou, Y. Ni, N. Li, J. Wang, L. Liu, and Z. H. Jiang, "Analgesic and anti-inflammatory activities of total extract and individual fractions of Chinese medicinal ants *Polyrhachis lamellidens*," *Biological and Pharmaceutical Bulletin*, vol. 28, no. 1, pp. 176–180, 2005.
- [100] C. Romay, N. Ledón, and R. González, "Further studies on anti-inflammatory activity of phycocyanin in some animal models of inflammation," *Inflammation Research*, vol. 47, no. 8, pp. 334–338, 1998.
- [101] D. E. Griswold, L. D. Martin, A. M. Badger, J. Breton, and M. Chabot-Fletcher, "Evaluation of the cutaneous anti-inflammatory activity of azaspiranes," *Inflammation Research*, vol. 47, no. 2, pp. 56–61, 1998.
- [102] P. P. Bradley, D. A. Priebat, R. D. Christensen, and G. Rothstein, "Measurement of cutaneous inflammation: estimation of neutrophil content with an enzyme marker," *Journal of Investigative Dermatology*, vol. 78, no. 3, pp. 206–209, 1982.
- [103] D. P. Evans, M. Hossack, and D. S. Thomson, "Inhibition of contact sensitivity in the mouse by topical application of corticosteroids," *British Journal of Pharmacology*, vol. 43, no. 2, pp. 403–408, 1971.
- [104] H. Selye, "An experimental study with the granuloma pouch technique," *The Journal of the American Medical Association*, vol. 152, no. 13, pp. 1207–1213, 1953.
- [105] R. Turner, *Screening Method in Pharmacology. Anti-Inflammatory Agent*, vol. 13, Academic Press, New York, NY, USA, 1965.
- [106] P. Crunkhorn and S. C. Meacock, "Mediators of the inflammation induced in the rat paw by carrageenin," *British Journal of Pharmacology*, vol. 42, no. 3, pp. 392–402, 1971.
- [107] S. Goldstein, L. Shemano, R. Daweo, and J. Betler, "Cotton pellet granuloma pouch method for evaluation of anti-inflammatory activity," *Archives Internationales de Pharmacodynamie et de Thérapie*, vol. 165, pp. 294–301, 1976.
- [108] C. L. Banka, A. S. Black, C. A. Dyer, and L. K. Curtiss, "THP-1 cells form foam cells in response to coculture with lipoproteins but not platelets," *Journal of Lipid Research*, vol. 32, no. 1, pp. 35–43, 1991.
- [109] B. Wong, W. C. Lumma, A. M. Smith, J. T. Sisko, S. D. Wright, and T. Q. Cai, "Statins suppress THP-1 cell migration and secretion of matrix metalloproteinase 9 by inhibiting geranylgeranylation," *Journal of Leukocyte Biology*, vol. 69, no. 6, pp. 959–962, 2001.
- [110] L. Håversen, B. G. Ohlsson, M. Hahn-Zoric, L. Å. Hanson, and I. Mattsby-Baltzer, "Lactoferrin down-regulates the LPS-induced cytokine production in monocytic cells via NF- κ B," *Cellular Immunology*, vol. 220, no. 2, pp. 83–95, 2002.
- [111] S. Devaraj and I. Jialal, "Low-density lipoprotein postsecretory modification, monocyte function, and circulating adhesion molecules in type 2 diabetic patients with and without macrovascular complications: the effect of α -tocopherol supplementation," *Circulation*, vol. 102, no. 2, pp. 191–196, 2000.
- [112] S. K. Venugopal, S. Devaraj, T. Yang, and I. Jialal, " α -Tocopherol decreases superoxide anion release in human monocytes under hyperglycemic conditions via inhibition of protein kinase C- α ," *Diabetes*, vol. 51, no. 10, pp. 3049–3054, 2002.
- [113] S. Devaraj, S. K. Venugopal, U. Singh, and I. Jialal, "Hyperglycemia induces monocytic release of interleukin-6 via induction of protein kinase C- α and - β ," *Diabetes*, vol. 54, no. 1, pp. 85–91, 2005.
- [114] A. K. Ghosh, N. Hirasawa, H. Niki, and K. Ohuchi, "Cyclooxygenase-2-mediated angiogenesis in carrageenin-induced granulation tissue in rats," *Journal of Pharmacology and Experimental Therapeutics*, vol. 295, no. 2, pp. 802–809, 2000.
- [115] S. Kavimani, R. Ilango, C. Loganathan, S. Karpagam, G. Krishnamoorthy, and B. Jaykar, "Antiinflammatory activity of benidipine hydrochloride," *Indian Drugs*, vol. 36, no. 2, pp. 147–149, 1999.

Research Article

Larix laricina*, an Antidiabetic Alternative Treatment from the Cree of Northern Quebec Pharmacopoeia, Decreases Glycemia and Improves Insulin Sensitivity *In Vivo

Despina Harbilas,^{1,2,3,4} Diane Vallerand,^{1,2,3,4} Antoine Brault,^{1,2,3,4} Ammar Saleem,^{1,4,5} John T. Arnason,^{1,4,5} Lina Musallam,^{1,2,3,4} and Pierre S. Haddad^{1,2,3,4}

¹ Canadian Institutes of Health Research Team in Aboriginal Antidiabetic Medicines, Department of Pharmacology, University of Montreal, P.O. Box 6128, Downtown Station, Montreal, QC, Canada H3C 3J7

² Natural Health Products and Metabolic Diseases Laboratory, Department of Pharmacology, University of Montreal, Montreal, QC, Canada H3C 3J7

³ Institute of Nutraceuticals and Functional Foods, Laval University, Quebec City, QC, Canada G1V 0A6

⁴ Montreal Diabetes Research Center, University of Montreal Hospital Center, Montreal, QC, Canada H1W 4A4

⁵ Department of Biology and Center for Research in Biopharmaceuticals and Biotechnology, University of Ottawa, Ottawa, ON, Canada K1N 6N5

Correspondence should be addressed to Lina Musallam, l.musallam@gmail.com and Pierre S. Haddad, pierre.haddad@umontreal.ca

Received 10 March 2012; Accepted 7 May 2012

Academic Editor: Vincenzo De Feo

Copyright © 2012 Despina Harbilas et al. This is an open access article distributed under the Creative Commons Attribution License, which permits unrestricted use, distribution, and reproduction in any medium, provided the original work is properly cited.

Larix laricina K. Koch is a medicinal plant belonging to traditional pharmacopoeia of the Cree of Eeyou Istchee (Eastern James Bay area of Canada). *In vitro* screening studies revealed that, like metformin and rosiglitazone, it increases glucose uptake and adipogenesis, activates AMPK, and uncouples mitochondrial function. The objective of this study was to evaluate the antidiabetic and antiobesity potential of *L. laricina* in diet-induced obese (DIO) C57BL/6 mice. Mice were subjected for eight or sixteen weeks to a high fat diet (HFD) or HFD to which *L. laricina* was incorporated at 125 and 250 mg/kg either at onset (prevention study) or in the last 8 of the 16 weeks of administration of the HFD (treatment study). *L. laricina* effectively decreased glycemia levels, improved insulin resistance, and slightly decreased abdominal fat pad and body weights. This occurred in conjunction with increased energy expenditure as demonstrated by elevated skin temperature in the prevention study and improved mitochondrial function and ATP synthesis in the treatment protocol. *L. laricina* is thus a promising alternative and complementary therapeutic approach for the treatment and care of obesity and diabetes among the Cree.

1. Introduction

The prevalence of obesity and type 2 diabetes (T2D) has reached epidemic proportions worldwide. In Canada alone, obesity and T2D affect 25% [1–3] and roughly 6% [4] of the population, respectively. The incidence of these diseases is worsened among the aboriginal population of Canada. The Cree of Eeyou Istchee (CEI) of the Northern James Bay Area of Quebec are particularly affected where 21% of adults over the age of 20 are diagnosed as diabetic and 38% as obese [5–10]. This increased prevalence might

be caused by their adoption of more westernized way of living: sedentary lifestyle and nontraditional diet (with increased consumption of carbohydrates and saturated fats) in addition to a low-compliance to modern T2D therapies [11–13]. The implementation of educational programs on lifestyle intervention (diet and exercise) has come to no avail, wherefrom the importance to identify alternative and culturally adapted treatments or solutions for obesity and T2D [6, 9–11, 13, 14].

Currently, around 70–95% of the population in the world relies on alternative and complementary medicine

in order to respond to their primary healthcare needs. Since the CEI possess a rich traditional pharmacopoeia, we conducted an ethnobotanical survey to identify plant species with potential to treat symptoms related to T2D [15]. These plant species were screened for their antidiabetic potential in extensive *in vitro* studies [16–24]. Of the 17 plants identified, *Larix laricina* K. Koch, belonging to the Pinaceae family, demonstrated antidiabetic potential by increasing glucose uptake and phosphorylation levels of AMPK and ACC in C2C12 myotubes to levels almost comparable to those of metformin [20, 24]. It also potentiated adipogenesis in 3T3-L1 adipocytes, thus acting like the commonly used thiazolidinedione (TZD), rosiglitazone [24]. In addition, we showed that *L. laricina* was one of the strongest uncouplers by severely disrupting mitochondrial function and decreasing ATP production [20]. Uncouplers increase metabolic rate and therefore fuel consumption in order to compensate for decreased ATP, which makes them potential antiobesity agents [20]. Obesity contributes to 55% of all cases of T2D, therefore affecting one or the other might have therapeutic potential for both diseases [25].

There are a variety of medications available on the market, which help in the management of T2D. Some of them, such as the antidiabetic medications metformin (biguanide) and exenatide (GLP-1 analogue), have been reported to produce a minimal amount of weight loss, albeit not strong enough to be considered as an antiobesity agent [26, 27]. The diet-induced obese (DIO) mice are an excellent model to study the well-documented relation of losing weight and improving insulin resistance. It relies on high-calorie diet and inactivity (no genetic involvement) to induce significant weight gain, hyperglycemia, and hyperinsulinemia, thus reflecting the establishment of the metabolic syndrome and a prediabetic state. Therefore, we wanted to study the antidiabetic and antiobesity potential of *L. laricina* in the DIO mouse model using two different administration regimens. Animals either received the plant concomitantly with high fat diet (prevention study) or received the plant after becoming obese and pre-diabetic (treatment study).

2. Materials and Methods

2.1. Plant Extracts. Specimens of the plant species used in this study, *L. laricina* K. Koch, of the Pinaceae family, were collected in 2004 from the territories of the CEI of Northern Quebec, Canada. Dr. Alain Cuerrier, taxonomist at the Montreal Botanical Garden, confirmed the botanical identity of the plant species. Voucher specimens of the plant species were deposited in the Marie-Victorin Herbarium of the Montreal Botanical Garden in Montreal, QC, Canada (Whap04-11, Mis03-12, Mis03-47). Crude 80% ethanolic extract of *L. laricina* was prepared as previously described [24].

2.2. Animals. Four-week-old male nondiabetic C57BL/6 mice were purchased from Charles River Laboratories (Saint-Constant, QC, Canada). All mice had *ad libitum* access to food and water. They were housed in individual cages and

maintained on a 12 h light-dark cycle in a temperature-controlled animal room. All experimental protocols were approved by the animal experimentation ethics committee of the Université de Montréal and were carried out in full respect of the guidelines from the Canadian Council for the Care and Protection of Animals.

2.3. Prevention Protocol. Following acclimatization, the four-week-old male nondiabetic C57BL/6 mice were divided into four groups of approximately 12 mice each, where they were monitored for 8 weeks. The control groups consisted in administering to one group (Chow) a standard diet purchased from Charles River (18% protein content, 4.5% crude fat, Charles River Animal rodent diet) and to another group (DIO) a high-fat diet (HFD) acquired from Bio-Serv (Bio-Serv Diet no. F3282, Frenchtown, NJ), 60% fat by energy). The remaining groups received the HFD to which was incorporated the dried 80% crude ethanolic plant extract of *L. laricina* at levels adjusted to deliver 125 or 250 mg/kg body weight.

2.4. Treatment Protocol. Following acclimatization, the four-week-old male nondiabetic C57BL/6 mice were divided into four groups of approximately 12 mice each. Chow controls received a standard diet (18% protein content, 4.5% crude fat; Charles River Animal rodent diet) for 16 weeks. Other groups were fed a HFD (Bio-Serv Diet no. F3282; 60% energy from fat) for 8 weeks. *L. laricina* at 125 or 250 mg/kg was incorporated in the HFD and treatments continued for an additional 8 weeks, with DIO controls receiving only HFD. Based on published observations and criteria, the animals fed a HFD were segregated into low responders (LRs) and high responders (HRs) (roughly 50/50) according to the data just prior to plant administration (at 8 weeks). Indeed, it has been reported that pooling animals with a more normal metabolic profile even when fed with HFD (such as low weight gain, weak IR, and near-normal glycemia; LR) with animals displaying overt obesity and insulin-resistant state when fed HFD (such as high weight gain, frank IR, and hyperglycemia; HR) can yield misleading results [28]. For simplicity reasons, LR fed with the HFD in the presence or absence of the plant extract will not be depicted since they portrayed an almost normal metabolic profile.

The data representing the effect of a HFD on C57BL/6 mice as compared to their CHOW-fed congeners will not be discussed since the DIO mouse model is well established. However, our model (in both the prevention and treatment studies) follows the expected and published data. In addition, the CHOW group was used as a nonobese control to insure that the model is functional, and therefore the results of this group are not presented. Therefore, the effects of the plant extract, *L. laricina*, will be compared to their respective HFD controls for all the stated parameters, for both the prevention and treatment protocols.

2.5. Continuous Physiological and Morphological Parameters. In both protocols body weight, food, and water intake, as well as glycemia, were measured 3 times/week during the course

of the study, consistently at the same time, day, in the same order by the same person, throughout the entire duration of the protocols. In order to assess blood glucose levels, blood was collected from puncturing the tail vein and measured using a commercial glucometer (Accu-Check Roche, Montreal, QC, Canada). The area under the curve (AUC) was calculated for these parameters, and the total AUC was then separated into two parts: fraction 1 (F1), representing AUC between weeks 0 and 4 and fraction 2 (F2) corresponding to the AUC between weeks 4 and 8 of plant extract administration. This segregation served to determine the temporal course of action of *L. laricina* in both the prevention and treatment protocols, that is, whether it was effective early in onset (first 4 weeks), later (last 4 weeks), or throughout the study.

2.6. Surgical Procedure. At the end of each experimental protocol, the mice were anesthetized using 50 mg/kg pentobarbital intraperitoneally and then sacrificed by exsanguination via the inferior vena cava. During the sacrifice, various organs were removed, collected, and weighed, notably, liver, muscle, white adipose tissue (WAT; epididymal and retroperitoneal fat pads), and subscapular brown fat (BAT). All were placed in liquid nitrogen and then stored at -80°C until further use. As for the livers, they were flushed with a physiological saline solution, weighed, and the median lobes were then dissected, immediately placed in liquid nitrogen, and then stored at -80°C until further use.

2.7. Blood Parameters. In order to ensure uninterrupted delivery of plant extract and to avoid the complications of interrupting the dietary plant treatment (for example, drop in food intake and body weight caused by fasting the animals), glycemia, insulin, and adipokines correspond to non-fasting measurements. Plasma insulin, adiponectin, and leptin were assessed by radioimmunoassay (RIA: Linco Research, St. Charles, MO, USA) according to manufacturer's instructions.

2.8. Tissue Triglyceride Measurement. Tissue triglyceride content was measured by grinding up into powder, under liquid nitrogen, around 100 mg of each of the collected liver and muscle samples, and then using Folch's chloroform/methanol (2:1) extraction method [29]. Triglyceride content was then quantified using a commercial kit (Randox Laboratories Ltd., UK).

2.9. Skin Temperature. In the prevention protocol, after 4 and 8 weeks of treatment, the temperature of the animals was read and recorded with a digital thermometer (Cole-Parmer Instrument Company, USA) by placing a probe on the external intercostal region of the animal for 2 minutes. This procedure is noninvasive and the least stressful for the animals [30].

2.10. Isolation of Mitochondria and Measurement of Respiration. Following anesthetization, the livers of mice from the treatment protocol were flushed with the Krebs-Henseleit

buffer (pH 7.4, 22°C). Mitochondria were then isolated following the method of Johnson and Lardy, as previously described [31–33].

2.11. Statistical Analysis. Data were analyzed by one-way analysis of variance (ANOVA), followed by post hoc analysis (Bonferroni-Dunn test or Holm-Sidak) as appropriate using Sigma Stat software (Jandel Scientific, San Rafael, CA, USA). Areas under the curve (AUC) were calculated by using PRISM software (GraphPad, San Diego, CA, USA). Data are expressed as mean \pm SEM of the indicated number of determinations. Statistical significance was set at $P < 0.05$.

3. Results

3.1. *L. laricina* Significantly Improved Glycemia in the Treatment Protocol. Glycemia levels, which increased with HFD as compared to CHOW (by 19%; data not shown), were not significantly altered when *L. laricina* was added concomitantly with the HFD (prevention study; NS; Figures 1(a)–1(c)). However, HFD-induced hyperglycemia (32% as compared to CHOW congeners; data not shown) significantly decreased in the group receiving the plant as treatment (following 8 weeks on HFD; Figures 1(a)–1(c)). Indeed, blood glucose levels, as measured by the area under the curve (AUC) of glycemia versus time, decreased in a dose-dependent manner by 10% and 12% with 125 mg/kg and 250 mg/kg doses, respectively (AUC_T ; $P < 0.05$; Figure 1(a)). In order to determine the temporal aspect of this antihyperglycemic effect, we fractionated the AUC between the first month of treatment (weeks 0–4; AUC_{F1} ; Figure 1(b)) and second month (weeks 4–8; AUC_{F2} ; Figure 1(c)). Our findings show that *L. laricina* lowered glycemia levels from the onset of the treatment (by 11–13%; $P < 0.05$; Figure 1(b)), and this was maintained throughout the treatment, albeit remained significant with highest dose only (13% at 250 mg/kg; $P < 0.05$; Figure 1(c)).

3.2. *L. laricina* Significantly Decreased Insulin Levels in the Treatment Protocol Only, While Decreasing Leptin/Adiponectin Ratio in Both Protocols. Administration of either dose of *L. laricina* tended to lower insulin levels by 25% to 35% in the prevention study, but failed to reach statistical significance (NS; Table 1). In the treatment protocol, however, *L. laricina*-induced decrease of insulinemia levels reached 72% with the 250 mg/kg dose ($P < 0.05$; Table 1), suggesting improvement of insulin resistance state and coinciding with the plant's highest effect on glycemia as mentioned above.

Other indicators were measured to confirm the re-establishment of insulin sensitivity. Adipose tissue is considered an endocrine organ, releasing into circulation adipokines, such as leptin and adiponectin, involved in the development of insulin resistance. A decrease of leptin/adiponectin ratio is thus considered as a marker of improved insulin sensitivity. In both prevention and treatment protocols, *L. laricina* tended to increase adiponectin levels by 16–26%, however, reaching statistical significance with the 125 mg/kg dose in the prevention protocol only ($P < 0.05$; Table 1). In parallel, leptin levels were reduced with

TABLE 1: Effects of HFD and *L. laricina* administration on systemic parameters at sacrifice.

	Prevention protocol			Treatment protocol		
	DIO	<i>L. laricina</i> 125 mg/kg	<i>L. laricina</i> 250 mg/kg	DIO	<i>L. laricina</i> 125 mg/kg	<i>L. laricina</i> 250 mg/kg
Insulin (ng/mL)	9.2 ± 1.8	6.9 ± 1.1	6.0 ± 0.9	39.9 ± 5.8	29.4 ± 9.1	11.0 ± 1.9*
Leptin (ng/mL)	39.3 ± 3.5	37.7 ± 3.2	33.1 ± 2.0	39.0 ± 3.0	27.1 ± 5.4	30.9 ± 2.1
Adiponectin (µg/mL)	8.8 ± 0.7	11.1 ± 0.8*	10.8 ± 0.4	11.1 ± 0.6	10.9 ± 0.7	12.8 ± 0.6
Leptin/adiponectin ratio	4.9 ± 0.6	3.7 ± 0.5	3.1 ± 0.2*	3.5 ± 0.2	2.5 ± 0.5*	2.4 ± 0.2*

Measurements were obtained after 8 weeks (prevention) or 16 weeks (treatment) of administration with either HFD (DIO) or *L. laricina* at 125 or 250 mg/kg, which was incorporated in the HFD for 8 weeks in the prevention protocol and for the last 8 of 16 weeks in the treatment protocol. All values represent the mean ± SEM (prevention protocol DIO = 11; *L. laricina* 125 = 13; *L. laricina* 250 = 13, and for the treatment protocol DIO = 7; *L. laricina* 125 = 5; *L. laricina* 250 = 8). * denotes that treated groups are significantly different as compared to DIO (one-way ANOVA; post hoc analysis Holm-Sidak or Bonferroni-Dunn test; $P < 0.05$).

L. laricina administration by 4–16% in the prevention study and by 21–30% in the treatment study, without, however, being statistically significant (NS; Table 1). Overall, these changes in adipokines levels resulted in significant decrease of the leptin/adiponectin ratio. Indeed, administration of *L. laricina* significantly lowered this ratio by 37% at 250 mg/kg in the prevention study ($P < 0.05$; Table 1) and by 29–31% with both doses in the treatment study ($P < 0.05$; Table 1). Therefore, *L. laricina* seems to decrease systemic insulin resistance.

Furthermore, since accumulation of lipids in the liver and skeletal muscle have been implicated in insulin resistance, we measured hepatic and muscular triglyceride (TG) levels. Despite *L. laricina* decreasing systemic insulin resistance, as suggested by improvement in the aforementioned parameters, hepatic or muscular triglyceride levels were not significantly altered (NS, Table 2).

3.3. *L. laricina* Diminished Body Weight Gain in Both the Prevention and Treatment Protocols, While Decreasing Fat Pad Weight in the Prevention Protocol Only. Continuous measurements of cumulative change in body weight (CCBW), represented as the area under the curve (AUC), revealed that while the effect of *L. laricina* on body weight gain was immediate in the prevention protocol for both doses (10% for AUC_{F1}; NS; Figure 2(b)), it only reached significant proportions in the second half of the protocol (AUC_{F2}) with the highest dose, decreasing it by 14% as compared to DIO controls (AUC_{F2}; $P < 0.05$; Figure 2(c)). In contrast, in the treatment protocol, *L. laricina* produced its strongest and most significant effect in the first half of administration lowering AUC_{F1}-CCBW by 10% at 250 mg/kg as compared to DIO congeners (AUC_{F1}; $P < 0.05$; Figure 2(b)). However, its antiobesity effect was not maintained; *L. laricina* reduced AUC_{F2} by only 4% at 250 mg/kg (NS; Figure 2(c)).

Consistent with the observed decrease in body weight gain, *L. laricina* significantly lowered retroperitoneal/abdominal fat pad weight in the prevention study by 15% at 250 mg/kg ($P < 0.05$; Table 3) as compared to DIO controls. As for the treatment, it corresponded to a slight decrease with both doses (5%–11%; NS; Table 3).

It is interesting to note that, in both protocols, mice administered *L. laricina* maintained similar food intake to

their DIO controls (NS; Figures 2(d)–2(f)), while being less prone to gaining weight. Finally, *L. laricina* exhibited no toxicity as demonstrated by unaltered blood biochemical parameters and tissue histological examination (data not shown).

3.4. *L. laricina* Improved Mitochondrial Function. Regulation of body temperature requires regulating both heat production and heat loss. Mitochondria metabolism is an important source of heat production. For the most part, variations in the rate of electron transport are directly related to the demand by the cells for ATP. However, exogenous substances, which uncouple mitochondria, can lead to the disruption of oxidative phosphorylation, decreasing ATP synthesis and increasing heat production. Previous screening studies have shown that *L. laricina* uncoupled mitochondrial function in isolated Wistar rat hepatocytes [20]. Therefore, we used skin temperature as an indirect measure of energy expenditure and possible mitochondrial uncoupling in the prevention study. After 4 and 8 weeks of treatment, we observed a gradual and dose-dependent increase in skin temperature with *L. laricina* administration ($P < 0.05$; Figures 3(a) and 3(b)).

Having perfected the isolation of mitochondria in mice, we opted to directly evaluate mitochondrial function in the treatment study in plant-treated mice compared to DIO controls. As expected DIO mice, which have increased fatty acid deposition in the liver, exhibited a lower respiratory control ratio (RCR) accompanied by decreased ATP production, in comparison to CHOW animals, although data variability precluded statistical significance (Table 4). Despite a small sample, animals treated with 250 mg/kg of *L. laricina* seemed to restore mitochondrial function and capacity to the level of chow values, as observed by an increase in RCR and ATP synthesis (Table 4).

4. Discussion

According to the International Diabetes Federation latest figures, the number of people living with diabetes will rise from 366 million in 2011 to 552 millions by 2030 [34]. The magnitude and impact of this disease dictate the urgent need for action. Although several drugs exist on the market to treat diabetes, the need to discover novel therapeutic options is warranted, especially in aboriginal context, such as the CEI [6, 9–11, 13, 14]. Indeed, recent lifestyle changes and

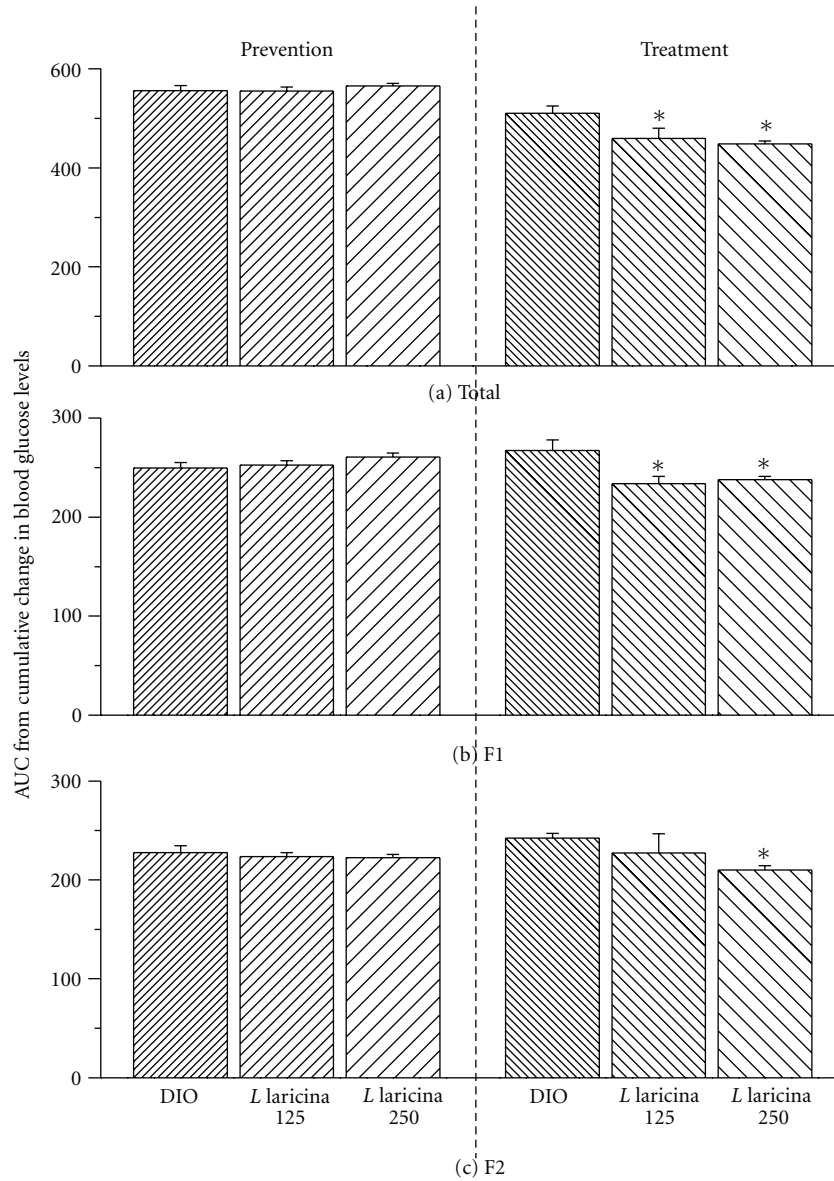


FIGURE 1: Area under the curve (AUC) of nonfasting glycemia levels, in C57BL/6 mice treated with either HFD (DIO) or *L. laricina* at 125 or 250 mg/kg, which was incorporated in the HFD for 8 weeks in the prevention protocol and for the last 8 of 16 weeks in the treatment protocol. Total AUC for blood glucose levels versus time (a) was calculated and then fractionated into the first and second half of the feeding period corresponding to weeks 0–4 (AUC_{F1}; b) and weeks 4–8 (AUC_{F2}; c), respectively. All values are mean ± SEM. Number of animals/group for prevention protocol DIO = 11; *L. laricina* 125 = 13; *L. laricina* 250 = 13, and for the treatment protocol DIO = 7; *L. laricina* 125 = 5; *L. laricina* 250 = 8). *denotes significantly different as compared to DIO group (one-way ANOVA; post hoc analysis Holm-Sidak or Bonferroni-Dunn test; $P < 0.05$).

TABLE 2: Effects of HFD and *L. laricina* administration on hepatic and muscular triglyceride accumulation.

	Prevention protocol			Treatment protocol		
	DIO	<i>L. laricina</i> 125 mg/kg	<i>L. laricina</i> 250 mg/kg	DIO	<i>L. laricina</i> 125 mg/kg	<i>L. laricina</i> 250 mg/kg
Liver TG levels (mg/g total liver)	331 ± 54	407 ± 47	374 ± 52	1041 ± 173	919 ± 240	1138 ± 118
Muscle TG levels (µg/mg)	84 ± 12	60 ± 6	65 ± 8	212 ± 29	224 ± 80	255 ± 33

The colorimetric dosage of TG levels in both the liver and muscle was determined using a commercial kit (as described in detail in Section 2.8). Measurements were obtained after 8 (prevention) or 16 (treatment) weeks of administration with either HFD (DIO) or *L. laricina* at 125 or 250 mg/kg, which was incorporated in the HFD for 8 weeks in the prevention protocol and for the last 8 of 16 weeks in the treatment protocol. All values represent the mean ± SEM (prevention protocol DIO = 11; *L. laricina* 125 = 13; *L. laricina* 250 = 13, and for the treatment protocol DIO = 7; *L. laricina* 125 = 5; *L. laricina* 250 = 8).

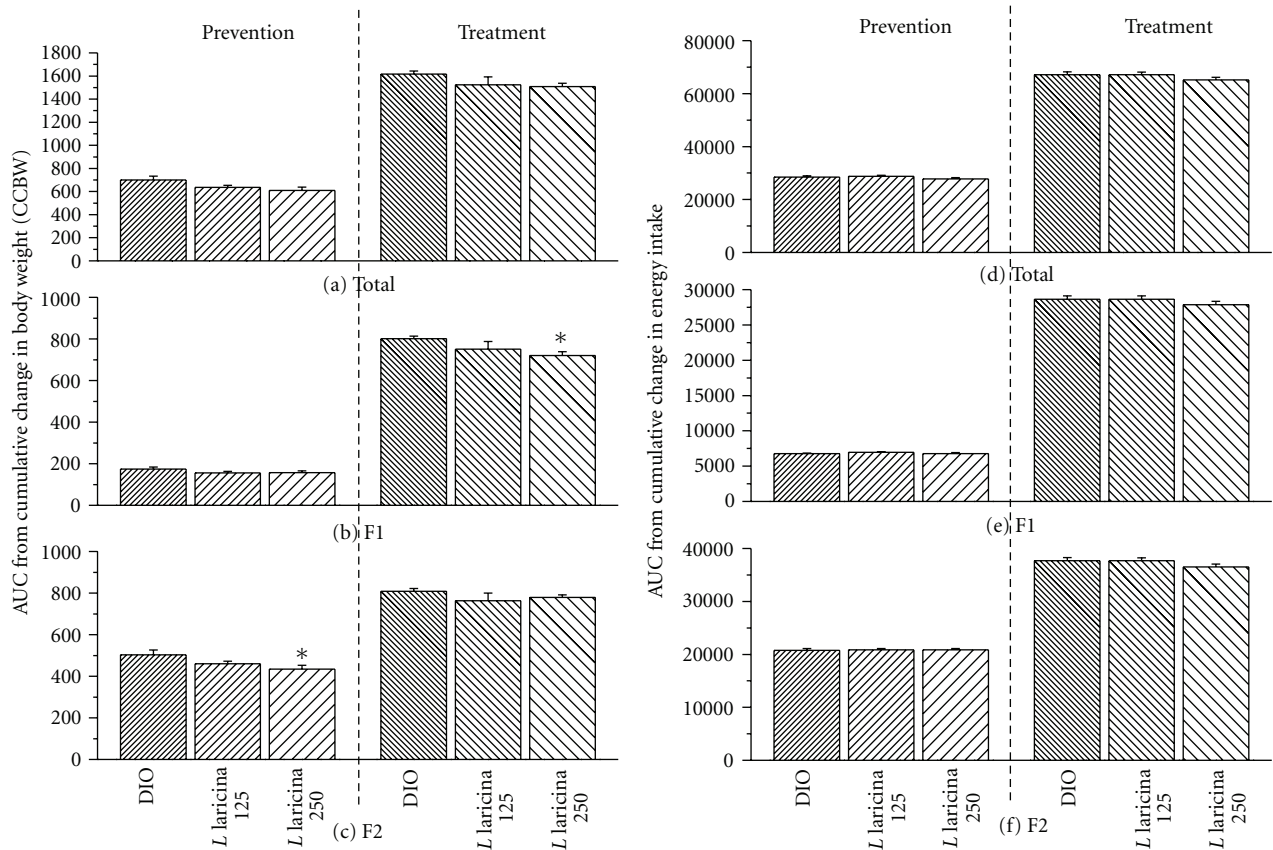


FIGURE 2: Area under the curve (AUC) of cumulative change in body weight (CCBW; a–c) and cumulative change in energy intake (CCEI; d–f) in C57BL/6 mice treated with either HFD (DIO), or *L. laricina* at 125 or 250 mg/kg, which was incorporated in the HFD for 8 weeks in the prevention protocol and for the last 8 of 16 weeks in the treatment protocol. Total AUC for CCBW-versus-time (a) or CCEI-versus-time (d) was calculated and then fractionated into the first and second half of the feeding period corresponding to weeks 0–4 (AUC_{F1}; b or e) and weeks 4–8 (AUC_{F2}; c or f), respectively. All values are mean \pm SEM. Number of animals/group for prevention protocol DIO = 11; *L. laricina* 125 = 13; *L. laricina* 250 = 13, and for the treatment protocol DIO = 7; *L. laricina* 125 = 5; *L. laricina* 250 = 8. * denotes significantly different as compared to DIO group (one way ANOVA; post-hoc analysis Holm-Sidak or Bonferroni-Dunn test; $P < 0.05$).

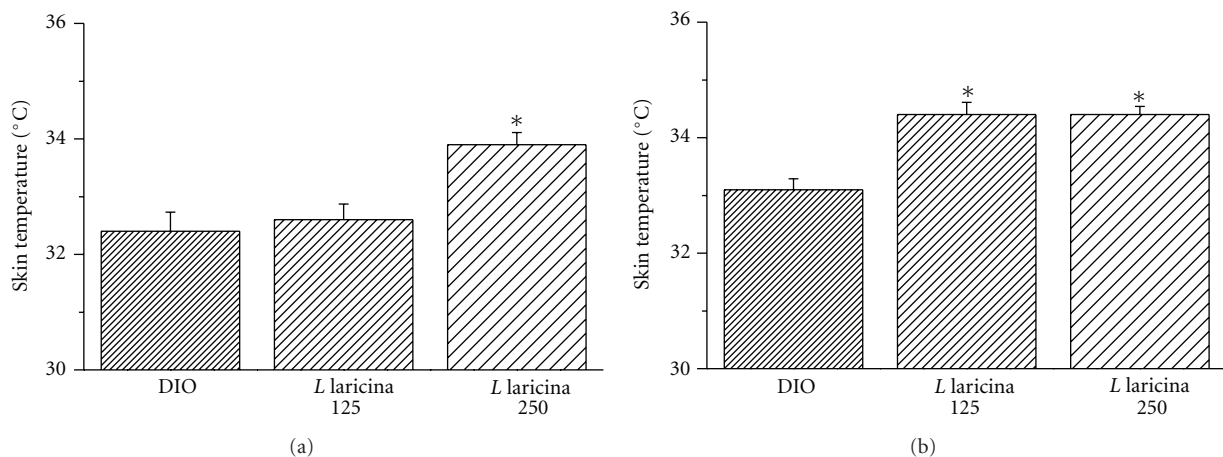


FIGURE 3: Skin temperature was measured in the prevention study after 4 weeks (a) and after 8 weeks (b) of treatment, from mice treated with either HFD (DIO) or *L. laricina* at 125 or 250 mg/kg, which was incorporated in the HFD for 8 weeks. All values are mean \pm SEM. Number of animals/group for prevention protocol DIO = 11; *L. laricina* 125 = 13; *L. laricina* 250 = 13. * denotes significantly different as compared to DIO group (one-way ANOVA; post hoc analysis Holm-Sidak or Bonferroni-Dunn test; $P < 0.05$).

TABLE 3: Effects of HFD and *L. laricina* administration on organ weights at sacrifice.

	Prevention protocol			Treatment protocol		
	DIO	<i>L. laricina</i> 125 mg/kg	<i>L. laricina</i> 250 mg/kg	DIO	<i>L. laricina</i> 125 mg/kg	<i>L. laricina</i> 250 mg/kg
Retroperitoneal fat pad (g)	1.34 ± 0.05	1.26 ± 0.04	1.14 ± 0.05*	1.51 ± 0.08	1.35 ± 0.24	1.44 ± 0.04
Epididymal fat pad (g)	2.40 ± 1.00	2.56 ± 0.08	2.56 ± 0.07	1.21 ± 0.03	1.32 ± 0.18	1.85 ± 0.12*
Brown fat pad (g)	0.30 ± 0.03	0.33 ± 0.01	0.28 ± 0.02	0.44 ± 0.01	0.37 ± 0.06	0.42 ± 0.02
Liver weight (g)	1.77 ± 0.09	1.85 ± 0.05	1.80 ± 0.07	2.62 ± 0.15	2.44 ± 0.38	2.57 ± 0.12
Liver index	410 ± 2	429 ± 1	437 ± 1	551 ± 3	539 ± 5	555 ± 2

Measurements were obtained after 8 weeks (prevention) or 16 weeks (treatment) of administration with either HFD (DIO) or *L. laricina* at 125 or 250 mg/kg, which was incorporated in the HFD for 8 weeks in the prevention protocol and for the last 8 of 16 weeks in the treatment protocol. The liver index corresponds to liver weight (mg)/body weight (mg). All values represent the mean ± SEM (prevention protocol DIO = 11; *L. laricina* 125 = 13; *L. laricina* 250 = 13, and for the treatment protocol DIO = 7; *L. laricina* 125 = 5; *L. laricina* 250 = 8). * denotes that treated groups are significantly different as compared to DIO (one-way ANOVA; post hoc analysis Holm-Sidak or Bonferroni-Dunn test; $P < 0.05$).

noncompliance with western medicines could account for the staggering diabetes prevalence of 29% in adults over 20 years old in this community [5, 6, 11–13].

In our quest to discover a culturally adapted diabetes treatment, we identified *L. laricina* from the CEI pharmacopoeia as potential antidiabetic medicinal plant. Initial *in vitro* screening showed that this plant stimulated glucose uptake, potentiated adipogenesis [24], activated AMPK, and acted as mitochondrial uncoupler/inhibitor (on normal isolated mitochondria) [20]. These effects are reminiscent of the action of Metformin, which partially mediates its action through inhibition of mitochondrial respiration, activation of AMPK, and upregulation of glucose uptake as well [20, 35–39]. It was therefore interesting to test the antidiabetic effect of *L. laricina* in a mouse model mimicking type 2 diabetes as a consequence of obesity by subjecting C57BL/6 mice to HFD (diet-induced-obesity model; DIO). We tested the plant in two different regiments: (1) *L. laricina* was administered concomitantly with HFD for 8 weeks in order to confirm its capacity to attenuate the development of obesity, diabetes, and the associated insulin-resistance (prevention study); (2) *L. laricina* was administered to obese and insulin resistant C57BL/6 mice (already on HFD for 8 weeks) for 8 weeks to test its ability to reverse the establishment of both of these states (treatment study).

Typically, the DIO model is characterized by increased body weight gain, hyperglycemia, and establishment of insulin-resistant state (hyperinsulinemia, increase of the leptin/adiponectin ratio, ectopic fat storage in the liver and muscle) [40, 41]. We therefore examined these parameters to determine the effect of *L. laricina in vivo*.

The results of the present studies confirm that *L. laricina* holds great promise as an antidiabetic medicinal plant. Although this plant had no effect of glycemia when administered concomitantly with HFD (prevention study), on the contrary, it significantly and dose-dependently decreased glycemia in the treatment study. These findings correlate well with our *in vitro* data where this plant extract increased glucose uptake in skeletal muscle cells and adipocytes [24], which accounts for 85% of postprandial glucose disposal, [42] and increased AMPK activity in C2C12 muscle cells

[20]. It is worthy to note that glycemia levels of animals receiving HFD in the treatment study are higher than those in the prevention study (32% versus 19%, respectively, compared to CHOW). One could suggest that *L. laricina* exerts its antihyperglycemic effect better when disease processes are more pronounced, thus explaining the observed difference in the plant's effect between the prevention and the treatment study.

Insulin resistance parameters were also modulated with administration of *L. laricina* in both treatment regiments. While strong tendencies are apparent in the prevention study, insulinemia and leptin/adiponectin ratio were significantly decreased in the treatment study (especially with the highest dose of *L. laricina*), suggesting improvement of systemic insulin resistance. Intriguingly, *L. laricina* failed to decrease hepatic and muscle triglycerides in both studies. Several lines of evidence suggest that hepatic triglyceride accumulation leads to insulin-defective signaling in the liver with increased hepatic glucose output. However, Buettner et al. have shown that TG accumulation in the liver is not always sufficient to impair insulin signaling [43, 44]. In fact, they argue that systemic factors (such as adipokines, free fatty acids, pro-inflammatory cytokines) may play an important role in the regulation of hepatic glucose output and insulin sensitivity *in vivo* [43, 44]. Hence, our data on the lack of depletion in intrahepatic and intramuscular triglyceride levels needs to be evaluated in further detail. Indeed, continued administration of HFD alongside *L. laricina* could make elimination of steatosis difficult. Another possibility could be that since oxidation pathways are saturated with fatty acids being mobilized from the adipose tissue (decrease in adipose tissue weight due to probable hormone-sensitive lipase activity), this could consequently hinder any decrease in tissue triglyceride stores [45]. In all cases, since adiponectin levels tended to increase and leptin/adiponectin ratio (an indicator of insulin resistance) [46–50] significantly decreased with ingestion of *L. laricina*, proinsulin-resistant systemic factors seem to be decreased and insulin sensitivity improved. Interestingly, we have shown that treatment of hepatic cells *in vitro* by *L. laricina* inhibits the activity of enzymes implicated in hepatic gluconeogenesis, such as glucose-6-phosphatase

TABLE 4: Effects of obesity as well as *L. laricina* administration on hepatic mitochondrial function.

	Treatment protocol			
	Chow	DIO	<i>L. laricina</i> 125 mg/kg	<i>L. laricina</i> 250 mg/kg
State 3	62.90 ± 4.50	59.81 ± 8.34	51.41 ± 6.91	62.91 ± 3.34
State 4	18.23 ± 1.05	17.43 ± 0.89	16.20 ± 1.04	16.29 ± 0.85
RCR	3.45 ± 0.08	3.37 ± 0.32	3.18 ± 0.35	3.87 ± 0.14
ATP synthesis	3.53 ± 0.53	3.20 ± 0.52	2.73 ± 0.40	3.52 ± 0.25

Mitochondrial function was measured as described in detail in Section 2.10, after 16 weeks of administration with either standard diet (CHOW), HFD (DIO), or *L. laricina* at 125 or 250 mg/kg, which was incorporated in the last 8 of 16 weeks in the treatment protocol. State 3 represents the rate of oxygen consumed during oxidative phosphorylation; state 4 represents the rate of oxygen consumption obtained after oxidative phosphorylation; RCR (respiratory control ratio) represents the ratio between state 3 and state 4. All values represent the mean ± SEM (for the treatment protocol CHOW = 4; DIO = 5; *L. laricina* 125 = 4; *L. laricina* 250 = 4).

and activates those promoting glycogen formation, such as glycogen synthase (GS), thus directly modulating hepatic glucose output [51].

This plant showed slight decrease of body weight with both studies, which was significant if continuous measurements were taken into account for the first and second month of administration. These changes occurred while the animals were on a continuous hypercaloric/fat-laden diet and without any observed change in energy intake. This could represent an indirect modulation of body weight as a consequence of *L. laricina* antidiabetic activity, which in some cases is similar to Metformin.

L. laricina administration also decreased retroperitoneal fat pad weight significantly in the prevention study and showed a tendency to do so in the treatment study. This represents an important action in the fight against insulin resistance since visceral adipose tissue has been implicated in the detrimental effects of obesity and insulin resistance [52]. Hence, modulation of this tissue would influence adipokine secretion and contribute to the improvement of insulin sensitivity, as can be seen in our plant-treated mice.

On the molecular level, we have shown that *L. laricina* activates AMPK in C2C12 myotubes [20] and H4IIE hepatic cell line [51]. This activation may be secondary to a variety of factors, including adiponectin or metabolic stress induced by the disruption of mitochondrial energy transduction [53–56]. In the literature, it has been reported that animals (mice or rat) fed a high-fat diet exhibit a decreased mitochondrial respiratory capacity (state 3/state 4), as was observed in this treatment protocol in mice administered a HFD [57]. Increased consumption of dietary fat may lead to alterations in mitochondrial membrane composition and increased ROS production and peroxidation of fatty acids, which could damage mitochondrial structures, all affecting mitochondrial function [57]. Uncoupling agents are beneficial in alleviating the mitochondrial stress induced by a HFD, by increasing fatty acid oxidation and decreasing ROS production [58]. In the treatment study, *L. laricina* at 250 mg/kg improved mitochondrial capacity and ATP production to levels comparable to those observed in animals fed a standard Chow diet. As demonstrated in previous *in vitro* screening studies, the uncoupling effect of *L. laricina* is short-lived and is followed by a prolonged activation of AMPK

and an overshoot phenomenon occurring to restore energy homeostasis, where ATP production is greatly increased, through raised carbohydrate and lipid oxidation [20]. Other benefits of increased AMPK activity include protecting cells from further damage by potentiating mitochondrial biogenesis [20, 59, 60]. Therefore, it seems that in the current animal treatment protocol, the long-term effect of *L. laricina* improved mitochondrial capacity and most probably through AMPK activation regulated glucose homeostasis. Of note, uncoupling agents usually lead to increased heat production due to increased energy expenditure. *L. laricina*-treated animals in the prevention study exhibited elevated skin temperature, thus confirming its uncoupling activity *in vivo*.

In conclusion, this study confirms the antidiabetic activity of *L. laricina* in the context of diet-induced obesity in a mouse model. The results clearly show that *L. laricina* decreased hyperglycemia and insulin resistance and improved mitochondrial function in the treatment study, while partially modulating parameters involved in insulin sensitivity in the prevention one. It also had a slight effect on body weight gain in both studies. The exact mechanisms of action of *L. laricina* remain to be identified, but results point toward possible activation of AMPK and its downstream effectors. In view of the soaring increase in both obesity and diabetes among aboriginal populations and in particular the CEI, *L. laricina* represents a valuable alternative, and culturally adapted treatment for both these diseases.

Conflict of Interests

The authors declare no conflict of interests.

Acknowledgments

A Team Grant from the Canadian Institutes of Health Research (CTP-79855) to P. S. Haddad, L. Musallam, and J. T. Arnason funded these studies. Very special thanks are due to S. Petawabano, L. Petawabano, C. Coon, S. Coon, M. Gunner, A. Mark, K. Mark, E. C. Come, H. Matoush, S. Matoush, R. Coon, and E. C. Come from the Cree Nation of Mistissini and A. Mamianskum, A. Kawapit, A. Natachequan, A. Sandy, E. G. Mamianskum, E. Kawapit,

J. Kawapit, J. Masty, J. Petagumskum Sr., L. Rupert, M. Natachequan, and M. Natachequan from Whapmagoostui First nation, as well as to 41 other Cree Elders of both nations who kindly agreed to be interviewed. They made this paper possible by allowing the authors to use, for the purposes of this research, their knowledge relating to medicinal plants transmitted to them by their elders. Their trust has also enabled a useful exchange between indigenous knowledge and Western science.

References

- [1] PHAC, *Obesity in Canada-Snapshot*, 2009.
- [2] PHAC, *Obesity in Canada: A Joint Report from the Public Health Agency of Canada and the Canadian Institute for Health Information*, 2011.
- [3] PHAC, "Diabetes among first Nations, inuit, and Métis populations," in *Diabetes in Canada: Facts and Figures from a Public Health Perspective*, chapter 6, 2011.
- [4] Statcan, "Diabetes," in *Statistics Canada*, 2010.
- [5] D. Dannenbaum, E. Kuzmina, P. Lejeune, J. Torrie, and M. Gangbe, "Prevalence of diabetes and diabetes-related complications in first nations communities in Northern Quebec (Eeyou Istchee), Canada," *Canadian Journal of Diabetes*, vol. 32, no. 1, pp. 46–52, 2008.
- [6] E. Kuzmina, P. Lejeune, D. Dannenbaum, and J. E. Torrie, "Cree diabetes information system (CDIS)," in *Annual Report*, J. E. Torrie, Ed., 2009.
- [7] P. Brassard, E. Robinson, and C. Lavallee, "Prevalence of diabetes mellitus among the James Bay Cree of northern Quebec," *Canadian Medical Association Journal*, vol. 149, no. 3, pp. 303–307, 1993.
- [8] E. Kuzmina and D. Dannenbaum, "Cree diabetes information system (CDIS)," in *Annual Report*, 2004.
- [9] G. Légaré, *Projet de Surveillance du Diabète Chez les Cris d'Eeyou Istchee*, Institut National de Santé Publique du Québec et Conseil Cri de la Santé et des Services Sociaux de la Baie-James, Quebec, Canada, 2004.
- [10] G. Légaré, D. Dannenbaum, J. Torrie, E. Kuzmina, and P. Linton, *Effects of Diabetes on the Health of the Cree of Eeyou Istchee: What Can be Learned from Linking the Cree Diabetes Information System (CDIS) with the Quebec Diabetes Surveillance System (QDSS)*, Public Health Occasional, 2004, Edited by Bay IndspdQaCBoHaSSoJ.
- [11] P. Boston, S. Jordan, E. MacNamara et al., "Using participatory action research to understand the meanings aboriginal canadians attribute to the rising incidence of diabetes," *Chronic Diseases in Canada*, vol. 18, no. 1, pp. 5–12, 1997.
- [12] R. A. Hegele, "Genes and environment in type 2 diabetes and atherosclerosis in aboriginal Canadians," *Current atherosclerosis reports*, vol. 3, no. 3, pp. 216–221, 2001.
- [13] T. K. Young, J. Reading, B. Elias, and J. D. O'Neil, "Type 2 diabetes mellitus in Canada's first nations: status of an epidemic in progress," *Canadian Medical Association Journal*, vol. 163, no. 9, pp. 561–566, 2000.
- [14] K. Gray-Donald, E. Robinson, A. Collier, K. David, L. Renaud, and S. Rodrigues, "Intervening to reduce weight gain in pregnancy and gestational diabetes mellitus in Cree communities: an evaluation," *Canadian Medical Association Journal*, vol. 163, no. 10, pp. 1247–1251, 2000.
- [15] C. Leduc, J. Coonishish, P. Haddad, and A. Cuerrier, "Plants used by the cree nation of eeyou istchee (Quebec, Canada) for the treatment of diabetes: a novel approach in quantitative ethnobotany," *Journal of Ethnopharmacology*, vol. 105, no. 1–2, pp. 55–63, 2006.
- [16] H. M. Eid, L. C. Martineau, A. Saleem et al., "Stimulation of AMP-activated protein kinase and enhancement of basal glucose uptake in muscle cells by quercetin and quercetin glycosides, active principles of the antidiabetic medicinal plant *vaccinium vitis-idaea*," *Molecular Nutrition and Food Research*, vol. 54, no. 7, pp. 991–1003, 2010.
- [17] H. M. Eid, D. Vallerand, A. Muhammad, T. Durst, P. S. Haddad, and L. C. Martineau, "Structural constraints and the importance of lipophilicity for the mitochondrial uncoupling activity of naturally occurring caffeic acid esters with potential for the treatment of insulin resistance," *Biochemical Pharmacology*, vol. 79, no. 3, pp. 444–454, 2010.
- [18] M. H. Fraser, A. Cuerrier, P. S. Haddad, J. T. Arnason, P. L. Owen, and T. Johns, "Medicinal plants of Cree communities (Québec, Canada): antioxidant activity of plants used to treat type 2 diabetes symptoms," *Canadian Journal of Physiology and Pharmacology*, vol. 85, no. 11, pp. 1200–1214, 2007.
- [19] D. Harbilas, L. C. Martineau, C. S. Harris et al., "Evaluation of the antidiabetic potential of selected medicinal plant extracts from the Canadian boreal forest used to treat symptoms of diabetes: part II," *Canadian Journal of Physiology and Pharmacology*, vol. 87, no. 6, pp. 479–492, 2009.
- [20] L. C. Martineau, D. C. A. Adeyiwola-Spoor, D. Vallerand, A. Afshar, J. T. Arnason, and P. S. Haddad, "Enhancement of muscle cell glucose uptake by medicinal plant species of Canada's native populations is mediated by a common, Metformin-like mechanism," *Journal of Ethnopharmacology*, vol. 127, no. 2, pp. 396–406, 2010.
- [21] L. C. Martineau, J. Hervé, A. Muhamad et al., "Anti-adipogenic activities of *Alnus incana* and *Populus balsamifera* bark extracts, part I: sites and mechanisms of action," *Planta Medica*, vol. 76, no. 13, pp. 1439–1446, 2010.
- [22] L. C. Martineau, A. Muhammad, A. Saleem et al., "Anti-adipogenic activities of *alnus incana* and *populus balsamifera* bark extracts, part II: bioassay-guided identification of actives salicortin and oregonin," *Planta Medica*, vol. 76, no. 14, pp. 1519–1524, 2010.
- [23] L. A. Nistor Baldea, L. C. Martineau, A. Benhaddou-Andaloussi, J. T. Arnason, E. Levy, and P. S. Haddad, "Inhibition of intestinal glucose absorption by anti-diabetic medicinal plants derived from the James Bay Cree traditional pharmacopeia," *Journal of Ethnopharmacology*, vol. 132, no. 2, pp. 473–482, 2010.
- [24] D. C. A. Spoor, L. C. Martineau, C. Leduc et al., "Selected plant species from the Cree pharmacopoeia of northern Quebec possess anti-diabetic potential," *Canadian Journal of Physiology and Pharmacology*, vol. 84, no. 8–9, pp. 847–858, 2006.
- [25] M. S. Eberhardt, C. Ogden, M. Engelgau, B. Cadwell, A. A. Hedley, and S. H. Saydah, *Prevalence of Overweight and Obesity Among Adults with Diagnosed Diabetes*, CDC, and Department of Health and Human Services, 2004.
- [26] A. R. Desilets, S. Dhakal-Karki, and K. C. Dunican, "Role of metformin for weight management in patients without type 2 diabetes," *The Annals of Pharmacotherapy*, vol. 42, no. 6, pp. 817–826, 2008.
- [27] S. M. Grundy, "Drug therapy of the metabolic syndrome: minimizing the emerging crisis in polypharmacy," *Nature Reviews Drug Discovery*, vol. 5, no. 4, pp. 295–309, 2006.
- [28] M. L. Peyot, E. Pepin, J. Lamontagne et al., " β -cell failure in diet-induced obese mice stratified according to body weight gain: secretory dysfunction and altered islet lipid metabolism

- without steatosis or reduced β -cell mass," *Diabetes*, vol. 59, no. 9, pp. 2178–2187, 2010.
- [29] J. Folch, M. Lees, and G. H. Sloane Stanley, "A simple method for the isolation and purification of total lipides from animal tissues," *The Journal of Biological Chemistry*, vol. 226, no. 1, pp. 497–509, 1957.
- [30] R. Dallmann, S. Steinlechner, S. von Horsten, and T. Karl, "Stress-induced hyperthermia in the rat: comparison of classical and novel recording methods," *Laboratory Animals*, vol. 40, no. 2, pp. 186–193, 2006.
- [31] A. Benhaddou-Andaloussi, L. C. Martineau, D. Vallerand et al., "Multiple molecular targets underlie the antidiabetic effect of *Nigella sativa* seed extract in skeletal muscle, adipocyte and liver cells," *Diabetes, Obesity and Metabolism*, vol. 12, no. 2, pp. 148–157, 2009.
- [32] D. Johnson and H. Lardy, "Isolation of liver or kidney mitochondria," *Methods in Enzymology*, vol. 10, pp. 94–96, 1967.
- [33] H. Ligeret, A. Brault, D. Vallerand, Y. Haddad, and P. S. Haddad, "Antioxidant and mitochondrial protective effects of silibinin in cold preservation-warm reperfusion liver injury," *Journal of Ethnopharmacology*, vol. 115, no. 3, pp. 507–514, 2008.
- [34] IDF, *One Adult in Ten has Diabetes in North America, 51.2 Million People in North America and the Caribbean will be Living with the Disease by 2030*, International Diabetes Federation, Brussels, Belgium, 2011, Edited by Federation I. D., World Diabetes Day.
- [35] B. Brunmair, K. Staniek, F. Gras et al., "Thiazolidinediones, like metformin, inhibit respiratory complex I: a common mechanism contributing to their antidiabetic actions?" *Diabetes*, vol. 53, no. 4, pp. 1052–1059, 2004.
- [36] E. Elia, V. Sander, C. G. Luchetti et al., "The mechanisms involved in the action of metformin in regulating ovarian function in hyperandrogenized mice," *Molecular Human Reproduction*, vol. 12, no. 8, pp. 475–481, 2006.
- [37] Y. D. Kim, K. G. Park, Y. S. Lee et al., "Metformin inhibits hepatic gluconeogenesis through AMP-activated protein kinase-dependent regulation of the orphan nuclear receptor SHP," *Diabetes*, vol. 57, no. 2, pp. 306–314, 2008.
- [38] J. M. Lee, W. Y. Seo, K. H. Song et al., "AMPK-dependent repression of hepatic gluconeogenesis via disruption of CREB/CRTC2 complex by orphan nuclear receptor small heterodimer partner," *The Journal of Biological Chemistry*, vol. 285, no. 42, pp. 32182–32191, 2010.
- [39] B. Viollet, F. Andreelli, S. B. Jorgensen et al., "Physiological role of AMP-activated protein kinase (AMPK): insights from knockout mouse models," *Biochemical Society Transactions*, vol. 31, no. 1, pp. 216–219, 2003.
- [40] W. T. Cefalu, "Animal models of type 2 diabetes: clinical presentation and pathophysiological relevance to the human condition," *ILAR News*, vol. 47, no. 3, pp. 186–198, 2006.
- [41] T. Jiang, Z. Wang, G. Proctor et al., "Diet-induced obesity in C57BL/6j mice causes increased renal lipid accumulation and glomerulosclerosis via a sterol regulatory element-binding protein-1c-dependent pathway," *The Journal of Biological Chemistry*, vol. 280, no. 37, pp. 32317–32325, 2005.
- [42] R. A. DeFronzo, "Pathogenesis of type 2 diabetes mellitus," *The Medical Clinics of North America*, vol. 88, no. 4, pp. 787–835, 2004.
- [43] R. Buettner, I. Ottinger, J. Scholmerich, and L. C. Bollheimer, "Preserved direct hepatic insulin action in rats with diet-induced hepatic steatosis," *American Journal of Physiology. Endocrinology and Metabolism*, vol. 286, no. 5, pp. E828–E833, 2004.
- [44] R. Buettner, J. Schölmerich, and L. C. Bollheimer, "High-fat diets: modeling the metabolic disorders of human obesity in rodents," *Obesity*, vol. 15, no. 4, pp. 798–808, 2007.
- [45] R. Crescenzo, F. Bianco, I. Falcone et al., "Hepatic mitochondrial energetics during catch-up fat with high-fat diets rich in lard or safflower oil," *Obesity*. In press.
- [46] F. Abbasi, J. W. Chu, C. Lamendola et al., "Discrimination between obesity and insulin resistance in the relationship with adiponectin," *Diabetes*, vol. 53, no. 3, pp. 585–590, 2004.
- [47] F. M. Finucane, J. Luan, N. J. Wareham et al., "Correlation of the leptin: adiponectin ratio with measures of insulin resistance in non-diabetic individuals," *Diabetologia*, vol. 52, no. 11, pp. 2345–2349, 2009.
- [48] O. Tschritter, A. Fritsche, C. Thamer et al., "Plasma adiponectin concentrations predict insulin sensitivity of both glucose and lipid metabolism," *Diabetes*, vol. 52, no. 2, pp. 239–243, 2003.
- [49] C. Weyer, T. Funahashi, S. Tanaka et al., "Hypoadiponectinemia in obesity and type 2 diabetes: close association with insulin resistance and hyperinsulinemia," *Journal of Clinical Endocrinology and Metabolism*, vol. 86, no. 5, pp. 1930–1935, 2001.
- [50] Y. Yamamoto, H. Hirose, I. Saito et al., "Correlation of the adipocyte-derived protein adiponectin with insulin resistance index and serum high-density lipoprotein-cholesterol, independent of body mass index, in the Japanese population," *Clinical Science*, vol. 103, no. 2, pp. 137–142, 2002.
- [51] A. Nachar, A. Saleem, D. Vallerand et al., "Beneficial effects in the liver of antidiabetic plants used in traditional medicine by the Cree of Bay James in Canada," in *Proceedings of the 10th Annual Oxford International Conference on the Science of Botanicals*, Planta Medica, Mississippi, Miss, USA, 2011.
- [52] E. S. Freedland, "Role of a critical visceral adipose tissue threshold (CVATT) in metabolic syndrome: Implications for controlling dietary carbohydrates: a review," *Nutrition and Metabolism*, vol. 1, no. 1, article 12, 2004.
- [53] Z. P. Chen, K. I. Mitchelhill, B. J. Michell et al., "AMP-activated protein kinase phosphorylation of endothelial NO synthase," *FEBS Letters*, vol. 443, no. 3, pp. 285–289, 1999.
- [54] N. Fujii, N. Jessen, L. J. Goodyear et al., "AMP-activated protein kinase and the regulation of glucose transport," *American Journal of Physiology. Endocrinology and Metabolism*, vol. 291, no. 5, pp. E867–E877, 2006.
- [55] N. Ruderman and M. Prentki, "AMP kinase and malonyl-CoA: targets for therapy of the metabolic syndrome," *Nature Reviews. Drug Discovery*, vol. 3, no. 4, pp. 340–351, 2004.
- [56] W. W. Winder and D. G. Hardie, "AMP-activated protein kinase, a metabolic master switch: possible roles in type 2 diabetes," *The American Journal of Physiology*, vol. 277, no. 1, part 1, pp. E1–E10, 1999.
- [57] C. Raffaella, B. Francesca, F. Italia, P. Marina, L. Giovanna, and I. Susanna, "Alterations in hepatic mitochondrial compartment in a model of obesity and insulin resistance," *Obesity*, vol. 16, no. 5, pp. 958–964, 2008.
- [58] M. K. C. Hesselink, M. Mensink, and P. Schrauwen, "Lipotoxicity and mitochondrial dysfunction in type 2 diabetes," *Immunology, Endocrine & Metabolic Agents in Medicinal Chemistry*, vol. 7, pp. 3–17, 2007.
- [59] R. M. Reznick and G. I. Shulman, "The role of AMP-activated protein kinase in mitochondrial biogenesis," *The Journal of Physiology*, vol. 574, part 1, pp. 33–39, 2006.
- [60] W. W. Winder, "Energy-sensing and signaling by AMP-activated protein kinase in skeletal muscle," *Journal of Applied Physiology*, vol. 91, no. 3, pp. 1017–1028, 2001.

Research Article

BrachySTEMMA calycinum D. Don Effectively Reduces the Locomotor Disability in Dogs with Naturally Occurring Osteoarthritis: A Randomized Placebo-Controlled Trial

Maxim Moreau,^{1,2} Bertrand Lussier,^{2,3} Jean-Pierre Pelletier,² Johanne Martel-Pelletier,² Christian Bédard,⁴ Dominique Gauvin,^{1,2} and Eric Troncy^{1,2}

¹ Research Group in Animal Pharmacology of Quebec (GREPAQ), Faculty of Veterinary Medicine, Université de Montréal, C.P. 5000, Saint-Hyacinthe, QC, Canada J2S 7C6

² Osteoarthritis Research Unit, Centre Hospitalier de l'Université de Montréal (CRCHUM), Notre-Dame Hospital, 1560 Sherbrooke Street East, Montreal, QC, Canada H2L 4M1

³ Department of Clinical Sciences, Faculty of Veterinary Medicine, Université de Montréal, C.P. 5000, Saint-Hyacinthe, QC, Canada J2S 7C6

⁴ Department of Pathology and Microbiology, Faculty of Veterinary Medicine, Université de Montréal, C.P. 5000, Saint-Hyacinthe, QC, Canada J2S 7C6

Correspondence should be addressed to Eric Troncy, eric.troncy@umontreal.ca

Received 7 April 2012; Accepted 30 May 2012

Academic Editor: Vincenzo De Feo

Copyright © 2012 Maxim Moreau et al. This is an open access article distributed under the Creative Commons Attribution License, which permits unrestricted use, distribution, and reproduction in any medium, provided the original work is properly cited.

Objective. The aim of this randomized placebo-controlled trial was to evaluate the beneficial effect of a whole plant extract of *BrachySTEMMA calycinum* D. Don (BCD) in naturally occurring osteoarthritis (OA) in dogs. **Methods.** Dogs had stifle/hip OA and poor limb loading based on the peak of the vertically oriented ground reaction force (PVF) measured using a force platform. At baseline, PVF and case-specific outcome measure of disability (CSOM) were recorded. Dogs (16 per group) were then assigned to receive BCD (200 mg/kg/day) or a placebo. The PVF was measured at week (W) 3 and W6. Locomotor activity was recorded throughout the study duration using collar-mounted accelerometer, and CSOM was assessed biweekly by the owner. **Results.** BCD-treated dogs had higher PVF at W3 and W6 when compared to Baseline ($P < 0.001$) and at W6 when compared to placebo-treated dogs ($P = 0.040$). Higher daily duration ($P = 0.024$) and intensity ($P = 0.012$) of locomotor activity were observed in BCD-treated dogs compared to baseline. No significant change was observed in either group for CSOM. **Conclusions.** Treatment with BCD improved the limb impairment and enhanced the locomotor activity in dogs afflicted by naturally-occurring OA. Those preclinical findings provide interesting and new information about the potential of BCD as an OA therapeutic.

1. Introduction

A group of experts recently emphasized the uses of companion animals suffering from naturally occurring diseases to accelerate the development of human therapeutics [1]. Hence to fulfill preclinical data, undertaking a trial in companion animals may represent an interesting way to provide additional evidence on the therapeutic potential of a new drug in development.

Naturally occurring osteoarthritis (OA) is common in companion animals, particularly in dogs. One study estimated that 20 per cent of dogs over one year of age are

afflicted by the condition [2]. Traumatic insults to the cranial cruciate ligament (CCL) and hip dysplasia are among the arthropathies considered to be etiopathogenic of OA in this specie [3, 4]. Biological and biomechanical factors merge to induce and perpetuate OA, generating pain, lameness, and limb dysfunction [5, 6].

As for human, the therapeutics modalities to manage canine OA remains largely palliative, from which nonsteroidal anti-inflammatory drugs (NSAIDs) take place as the first line of treatment [7]. Only the alleviation of pain-related clinical sign(s) is claimed by actual modalities; structural benefits cannot be expected from current evidences and

still represent a clinical challenge [8]. Therefore, there is an unmet need for OA therapeutics that combines disease modifying properties and the capacity to improve the locomotor disability.

Surgical transection of the CCL in dogs impairs the limb function and creates lesions that mimic those encountered in human [9, 10]. In this model, the extract of *Brachytemma calycinum* D. Don (BCD), an indigenous plant of southwestern China (the Himalayas) has shown promising disease modifying potential against the development of OA lesions and limb impairment [11]. It was reported that the decrease in the levels of protease-activated receptor 2 (PAR 2), inducible nitric oxide synthase (iNOS), and matrix metalloproteinase 13 (MMP-13) were the key factors tributary of the effect of BCD. However, whether BCD is effective against the locomotor impairment that prevails in dogs naturally afflicted with OA could be informative on its curative potential and need to be scrutinized.

With the idea of providing preclinical data to enhance the development of human therapeutics, the objective of this trial was to determine whether BCD can improve the locomotor disability seen in naturally occurring OA in dogs.

2. Materials and Methods

2.1. Design and Subject Selection. This study was a randomized, double-blind, parallel-group, placebo-controlled trial lasting 6 weeks. The trial was conducted under the approbation of the Institutional Animal Care and Use Committee (#Rech 1434) in accordance with the guidelines of the Canadian Council on Animal Care. All owners provided written informed consent.

Adult dogs weighed more than 20 kg and had radiographic evidence of OA exclusively at the hip or stifle joints. Radiographs (hips, stifles, and elbows) were obtained under sedation as described [12]. Hind limb lameness in association with the presence of OA was confirmed by a certified veterinary surgeon (B. Lussier). At the time of screening, all dogs were free of any compound purported to relieve the clinical signs of OA according to washout periods ranging between 4 to 12 weeks. Hence, a 4-week washout period was respected for oral NSAIDs and a 6-week period for natural health products including fatty acid supplement, OA therapeutic diets, or treats. Dogs having received injectable pentosan polysulfate sodium or corticosteroid one year before the screening visit were not eligible. A 12-week period was requested for injectable polysulfated glycosaminoglycan, and hyaluronan, and for oral or topical corticosteroid. During the study, dogs were free of any type of medication except those prescribed for exo- and endoparasite control. Additional exclusion criteria were as follows: dogs with surgical repair of the CCL within 1 year prior to study initiation, dogs suffering from neurologic or other musculoskeletal lesions, dogs that underwent orthopaedic surgery within the past year, and dogs with CCL disease having gross instability (positive drawer motion upon orthopaedic exam).

2.2. Complete Blood Count and Biochemistry Panel. Each dog underwent routine blood hematology and biochemistry analyses (C. Bédard) in order to evaluate health status at study entrance and to ensure that physiologic disturbance did not occur following treatment administration (W6).

2.3. Randomization, Blinding, and Therapy Regimen. Thirty-two privately owned dogs were randomized. The restricted randomisation process was defined as a random permuted blocks randomisation, which included a block size of four, with two treatments (A and B) distributed in one-to-one ratio. In blocks of four, there are six possible block allocation sequences: (1) AABB; (2) ABAB; (3) ABBA; (4) BBAA; (5) BABA; (6) BAAB. The treatment allocation sequence was defined using a list of true random integers from 10 to 99 (<http://www.random.org/>). The block allocation sequence was defined using the first eight single digit of the true random numbers list, omitting numbers outside the range 1 to 6. Among the eight designated blocks of four, a true random integer from 1 to 8 served to define which block was excluded from the balanced attribution of locomotor activity recording. In each of the seven remaining blocks, a true random integer from 1 to 2 served to allocate motor activity recording to treatment A (i.e., when a 1 was generated, motor activity recording was allocated to the first treatment A for a given block). The same procedure was repeated to allocate locomotor activity recording to treatment B, leading to the randomized attribution of seven dogs in each treatment group for monitoring locomotor activity. The 32 treatment allocations (with or without locomotor activity recording) were transcript on individual cards in sequentially numbered, sealed, opaque envelopes to ensure concealment. The person responsible of the randomization process (D. Gauvin) and the treatment preparation was not involved in the enrolment and followup. The test agent or the placebo were blinded to treatment A or B by a third party (E. Troncy). At trial site, both treatments were labelled exclusively as treatment A or treatment B and were encapsulated identically. The trialists (B. Lussier, M. Moreau), the veterinary technicians, and all dog owners were blinded to which treatment (A or B) was given to each randomized subject. The key code revealing what referred to treatment A and B (BCD or placebo) was kept confidential by the third party and was revealed only after study completion and preliminary analyses.

The test agent (BCD extract) was obtained as previously described [11]. The test agent or the placebo (corn starch) was given at a dosage of 200 mg/kg/day (minimum 197 mg/kg/day, maximum 240 mg/kg/day) using a combination of capsules (Torpac Inc., NJ, USA) that contains between 1 to 5 g/capsule. Initially, some dogs ($n = 14$) received a 5-day placebo treatment to establish baseline values, particularly of locomotor activity (see 2.5 below). Treatments were given in the morning, before or after meal. Treatments were encapsulated in the same fashion. The dose of BCD was the one used previously in experimental CCL-sectioned dogs and was based on the dose administered in humans (120 mg/kg) according to the following formula:

human dose $\times [k_{m\text{human}}/k_{m\text{animal}}]$, where k_m is the surface area to weight ratio.

2.4. Force Platform Measurement. Peak of the vertically oriented ground reaction force (PVF) was measured at baseline (day 0), W3 (day 21), and W6 (day 42) at the trot gait (1.9–2.2 m/s) using a force platform, as previously described [12]. The PVF was reported and defined as the primary outcome of interest. Normalized PVF in percentage of body weight (% BW) from the first five valid trials was used for statistical purposes. To be eligible, dogs must have hind limb PVF value less than 66% BW which is consistent to minus one SD of the value measured in normal dogs [13]. When bilateral lameness was observed, the hind limb having the lowest PVF, in accordance with orthopaedic exam findings, determined which one was selected for evaluation, otherwise the dog was excluded. The change in PVF was the mean difference between a given week value versus baseline.

2.5. Locomotor Activity Recording. Accelerometer-based motor activity recording was done using Actical system (Bio-Lynx Scientific Equipment Inc., Canada) as described [14]. According to the balanced attribution of motor activity recording, collar-mounted accelerometers were worn by seven dogs per group for the entire treatment duration (42 days, 24 hour/day). In addition, collar-mounted accelerometers were worn during a short period (5 days) that preceded real treatment initiation. This period was used to establish baseline level of locomotor activity recording before treatment administration. During this period, the entire 14 dogs were attributed to receive a placebo treatment managed by the person responsible of the randomization process (D. Gauvin). The duration and intensity of motion were continuously monitored and expressed as counts every 2 minutes, giving 720 counts per day. Daily duration of active period (DDAP) referred to the time spent (expressed in hour) when the count exceeded 30 in term of intensity. This cut-off value was based on intern data and was used to discern active from inactive period [14, 15]. Daily averaged total intensity (DATI) referred to the mean of all counts per day (unitless). Among the 47 days of continuous recording, three periods of 120 hours were predefined: baseline (day –5 to day 0), first period (day 17 to day 21), and the second period (day 38 to day 42). Owners of dogs were requested to come at day –5 and back at day 0 to the investigation site to acquire other baseline data.

2.6. Case-Specific Outcome Measure of Disability. Assessment of at-home functional disability was done using CSOM as previously described [14]. Owners assessed the ability of their dogs to perform between two to five activities using a 5-point scale for each activity that ranged from no problem (0) to incapacity (4). Each activity was selected by the owner according to his/her own perception of what characterise(s) the disability of the dog. Assessments were done twice weekly using a specific form that was kept at home by the owner. For each dog, medians of the activity scores were determined at each assessment (13 assessments) and were then used for

statistical purposes. Among the 13 assessments, three periods were predefined: baseline (1st assessment done at day 0), first period (day 3 to day 21), and the second period (day 24 to day 42).

2.7. Statistical Analysis. All statistical tests were two tailed with significance determined by reference to the 5% threshold. Equality of efficacy was the null hypothesis based on the primary endpoint (PVF). Pre trial log-transformed PVF data were analyzed with a repeated measures general linear mixed model that includes two fixed factors (time and group) and their interaction (time \times group interaction), with trials and dogs nested in treatment group as random effects. The compound symmetry covariance structure was used for this analysis. *Post hoc* analyses were done with appropriate Bonferroni adjustments. Log-transformed DATI and DDAP were analyzed similarly to PVF (time (period) and group as fixed factors) and their interaction (time \times group interaction) with days and dogs nested in treatment group as random effects. A repeated measures generalized linear model was used to analyze median CSOM data under poisson distribution function using independent working matrix. Fixed factors were time (period) and group and their interaction (time \times group interaction) with assessments and dogs nested in treatment group as random effects. Scale factor was estimated by Pearson's chi-square. The last recording was carried forward in the event of missing data. Data are presented as mean (standard deviation).

2.8. Sample Size Calculation. According to previous works done in similar conditions [15], a sample size of 16 dogs/treatment group ensured that a difference of 4.2% BW in the primary endpoint (PVF) between BCD and control (placebo) dogs could be detected assuming 75% power, an SD of 4.5 and a 5% significance threshold.

3. Results

3.1. Animal Description. No clinically relevant changes were observed on physical examination, observation, haematological, and biochemical analyses in the entire study cohort. Baseline characteristics of the dogs stratified per group are presented in Table 1. Groups were well balanced according to the outcomes of interest as significant difference was not observed for the levels of PVF ($P = 0.452$), locomotor activity recording when expressed as DDAP ($P = 0.751$) and DATI ($P = 0.869$), and also for CSOM ($P = 0.194$).

3.2. Study Withdrawal. The numbers of dogs who were screened, randomly assigned, and analysed in each group are detailed in Figure 1. Last data (PVF and CSOM) were carried forward when incomplete data set were encountered.

3.3. Peak Vertical Force Measurement. The PVF (primary endpoint) generated by the disabled hind limb during the stance phase of the stride was increased in the overall study cohort (time effect; $P < 0.001$), without significant group effect ($P = 0.129$). Increment in PVF was mostly

TABLE 1: Baseline characteristics of the dogs stratified per group.

Characteristics	Groups	
	Placebo	<i>Brachyostemma calycinum</i> D. Don
Age (year)	5.9 (1.9)	5.6 (2.5)
Sex (male/female)	6/10	8/8
Body weight (kg)	42.5 (7.5)	40.3 (11.4)
Peak vertical force (% BW)	56.3 (6.4)	58.2 (6.7)
Locomotor activity recording (over 5-day)		
Daily duration of active period (h)	6.7 (1.8)	6.5 (1.5)
Daily averaged total intensity (unitless)	191 (66)	194 (79)
Case-specific outcome measure of disability	1.9 (0.6)	1.6 (0.5)
Osteoarthritis-afflicted joint		
Hip (count)	10	11
Stifle (count)	13	12
Hip and Stifle (count)	7	7

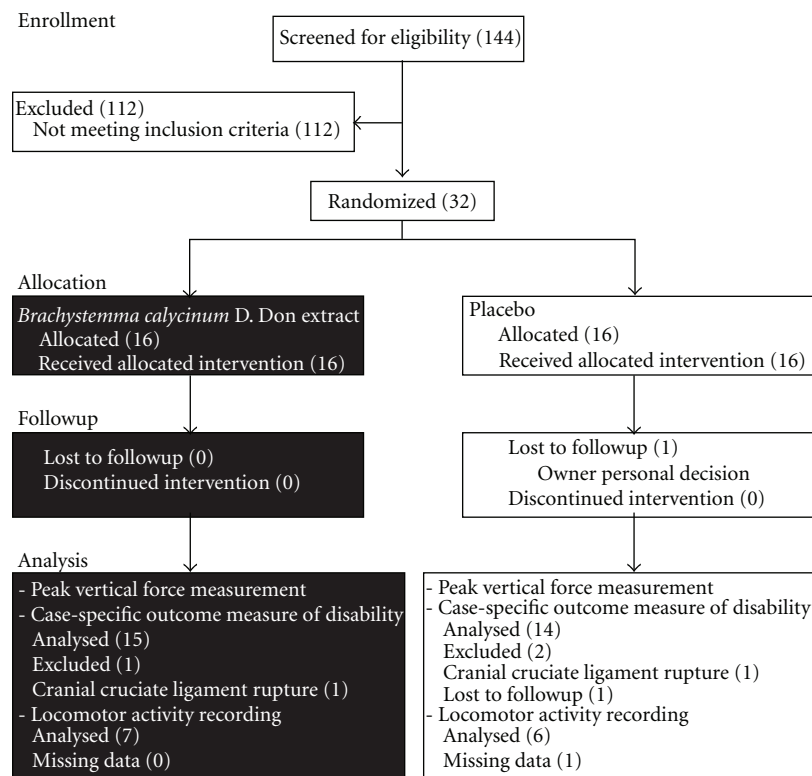


FIGURE 1: Flow chart of the study enrolment, randomization, followup, and analysis.

attributed to the changes observed in BCD-treated dogs. Hence, a significant time \times group interaction ($P < 0.001$) was observed which means that groups evolved distinctively from baseline to the end of the study. More specifically, analyses revealed that the PVF of the BCD-treated dogs was significantly increased at W3 ($P = 0.001$) and at W6 ($P < 0.001$), when compared to baseline (Figure 2). At the opposite, neither W3 nor W6 value was significantly different than baseline in placebo-treated dogs. Analyses revealed that the change in PVF in BCD-treated dogs showed a tendency to be higher than placebo at W3 ($P = 0.099$), reaching

significant level at W6 ($P = 0.040$). Figure 3 presents the respective individual changes in PVF recorded at W6 as well as the mean change denoted in each group after 6 weeks of treatment.

3.4. Sensitivity Analyses. Sensitivity analyses were done using alternative forms of imputation to confirm the robustness of the results analysed with the last-observation-carried-forward method. Data management conducted with the exclusion of dog having incomplete data set provided an increase in PVF of 3.7 (5.6)% BW at W6 (*post hoc*

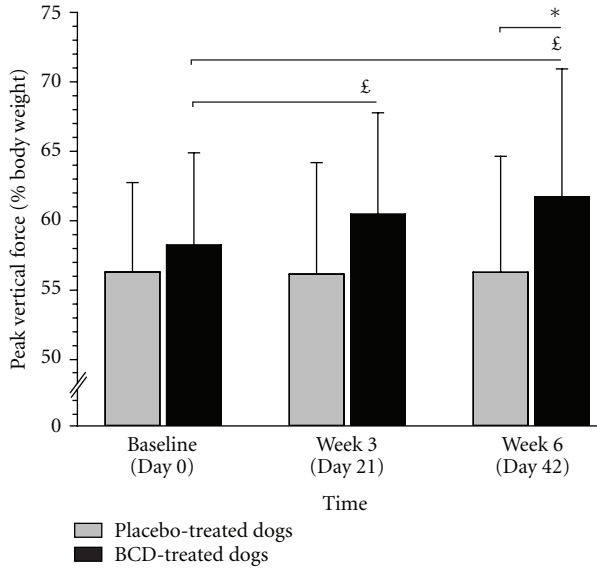


FIGURE 2: Mean (standard deviation) peak vertical force recorded in dogs having received either *Brachystemma calycinum* D. Don (BCD) or a placebo. Values are expressed as percentage of body weight. *Significantly different compared to placebo-treated dogs. £Significantly different compared to baseline.

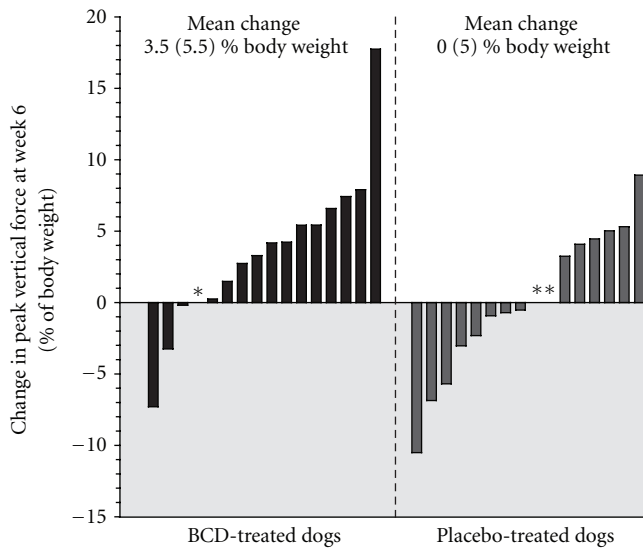


FIGURE 3: Individual changes in peak vertical force after 6 weeks of treatment with *Brachystemma calycinum* D. Don (BCD) or a placebo. Changes were the difference between Week 6 versus baseline. *Incomplete data were managed using last data carried forward method. Grey zone represent negative change (i.e., worsening).

comparison between groups at W6; $P = 0.045$). When positive data (+3.5% BW) were used to replace missing data, results were consistent with an increase in PVF of 3.7 (5.5)% BW at W6 (*post hoc* comparison between groups at W6; $P = 0.040$). When negative results (-3.5% BW) were used to replace missing data, results supported an increase in PVF of

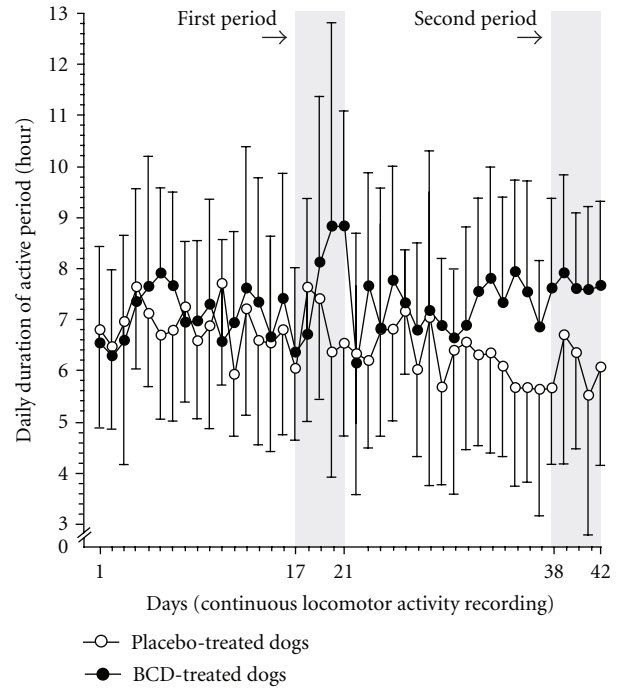


FIGURE 4: Temporal evolution of the locomotor activity recording over a 6-week period (42 days) in dogs receiving either treatment with *Brachystemma calycinum* D. Don (BCD) or a placebo. Data are the daily duration of active period and are expressed as mean (standard deviation). Periods were baseline (day -5 to day 0, not shown), first period (day 17 to day 21), and the second period (day 38 to day 42). At the second period, BCD-treated dogs had significantly higher daily duration of active period ($P = 0.024$) when compared to baseline.

3.3 (5.7)% BW at W6 (*post hoc* comparison between groups at W6; $P = 0.043$).

3.5. Locomotor Activity Recording. The accelerometer recorded the motion of the dogs over the entire daily duration. The continuous recording was successful in 7 BCD- and 6 placebo-treated dogs. For DDAP, statistical findings were as follows: time effect ($P = 0.032$), group effect ($P = 0.575$), and time \times group interaction ($P < 0.001$). Analyses revealed a tendency for higher DDAP in BCD-treated dogs during the first period (7.3 (1.7) h, $P = 0.068$), reaching a significant level at the second period (7.4 (1.3) h, $P = 0.024$) when compared to baseline (Table 1, Figure 4). Placebo-treated dogs had DDAP values at the first [6.8 (1.4) h] and the second period [6.2 (1.7) h] that did not differ from baseline (Table 1, Figure 4).

According to DATI, statistical findings were as follows: period effect ($P = 0.103$), group effect ($P = 0.722$), and period \times group interaction ($P = 0.006$). In BCD-treated dogs, analyses revealed significantly higher DATI during the first period (233 (98), $P = 0.042$) and the second period (229 (85), $P = 0.012$) when compared to baseline (see Table 1). Placebo-treated dogs had DATI values at the first (199 (66)) and the second period (185 (75)) that did not differ from

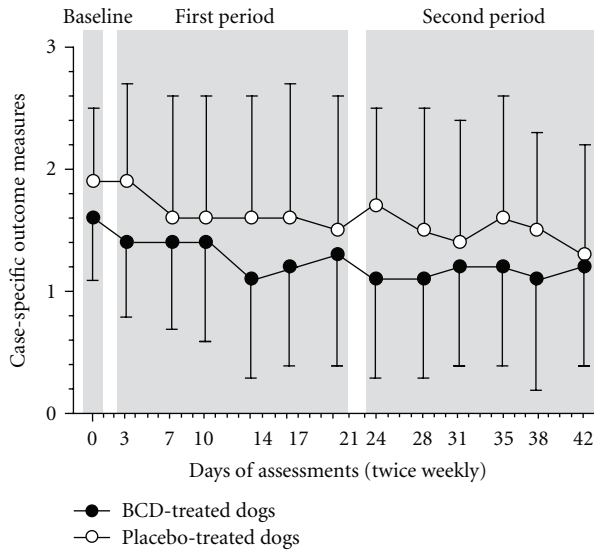


FIGURE 5: Temporal evolution of the case-specific outcome measures of disability (CSOM) over a 6-week period in dogs receiving either treatment with *Brachytemma calycinum* D. Don (BCD) or a placebo. Data are expressed as mean (standard deviation). Periods were baseline (day 0), first period (day 3 to day 21), and the second period (day 24 to day 42).

baseline (see Table 1). Neither DDAP nor DATI denoted any significant difference between groups at baseline, as well as during the first and second period.

3.6. Case-Specific Outcome Measure. The CSOM assessed the severity of daily life disability in accordance with specific activities reported to be problematic, altered, and/or painful. Statistical findings were as follows: time effect ($P = 0.003$), group effect ($P = 0.149$), and time \times group interaction, ($P = 0.732$). Figure 5 presents the evolution of the CSOM recorded twice weekly over a 6-week period. Over time, no significant change in either group was observed. Placebo-treated dogs had mean CSOM of 1.6 (1.0) and 1.5 (0.9) at the first and second period, respectively. Mean values for BCD-treated dogs were 1.3 (0.8) and 1.1 (0.8) at the first and second period, respectively.

4. Discussion

In the experimental dog CCL model of OA, it was previously demonstrated that BCD treatment helps to reduce cartilage loss and improve functional disability [11]. According to those findings, hypothesis was then raised about the therapeutic potential of BCD in dogs naturally afflicted by the OA disease under curative conditions. Therefore, a randomized, double-blind, placebo-controlled trial was undertaken with the idea to fulfill preclinical evidences and to promote clinical trial in human OA. Based upon the measurement of the PVF defined as the primary endpoint, BCD improved the limb disuse in dogs afflicted by hind limb OA. When given once daily, improvements were seen as early as 3 weeks and reached further gain by a 6-week period. The magnitude of

the therapeutic benefits was moderate in accordance with an effect size of 0.7 (95% confidence interval, 0.0–1.4).

Force platform is a recording instrument that measures the forces (such as vertical force) generated by the musculoskeletal system in close relationship with acceleration and mass of the body. Such platform has been considered as an objective measure of gait disability in OA patient [16–19]. In dogs with OA, pain-related limb disuse is discriminated by abnormally low PVF. An improvement is translated when an increment over initial condition occurs, as denoted following current therapies (Table 2). With respect to those clinical findings, the change in PVF provided by BCD (+3.7 (5.6)% BW at W6) was within the expected level of improvement provided by nonsteroidal anti-inflammatory drugs [20–22], COX-LOX inhibitor [15], complementary and alternative medicine [21, 23], and veterinary therapeutic diets [24–26]. The improvement demonstrated herein was translated into a willingness to load an average of ± 1.4 kg on the painful afflicted limb.

The outcome measurements of the present study were in agreement with the pain, physical function, and patient global assessment included in the OMERACT-OARSI responder criteria [27]. There are actually no such criteria for OA clinical trials in dogs. Development of such an approach would be most useful to monitor the beneficial effects in a randomized clinical trial such as ours. In the absence of such consensus, an increment in PVF was instinctively considered as a positive response. According to Figure 3, 66% of the overall responders were BCD-treated dogs. At the opposite, 73% of dogs having worsened their condition probably due to natural fluctuations in disease severity (maturation effect) were placebo treated.

The monitoring of ambulatory activities using accelerometers is a reliable technique, providing continuous, unsupervised, objective monitoring of mobility [28]. In the field of OA, it is well known that afflicted patients suffer limitations in their walking ability as monitored using accelerometer [29–31]. In dogs, this device was deemed adequate for at-home activity monitoring [32] while being a valid tool to document the therapeutic outcome of an OA management [33].

In the present trial, we denoted that BCD-treated dogs had higher locomotor activity (intensity and duration) at the end of the treatment duration. While placebo dogs had similar intensity and duration of active period, BCD-treated dogs reached higher levels, gaining an hour of activity per day. Aerobic and strengthening exercises are beneficial in reducing pain caused by OA [34–36]. Therefore, the effect of BCD could have been translated into more active dog that rehabilitated the painful and disused limb toward better muscular strength, allowing animal to load more weight on the afflicted limb. Such association was previously demonstrated in OA dogs by our group [37]. Hence, higher levels of daily motion have been mirrored by an improvement in limb loading, which supports the benefits of physical rehabilitation [38].

The way both groups evolved according to the objective measures of function was not replicated by the assessment of daily life activity performance. Rather, the study cohort

TABLE 2: Selected studies that reported statistically significant changes (i.e., improvement) in peak vertical force following different therapeutic approaches in dogs naturally afflicted by osteoarthritis.

Therapeutic approaches	Authors	Changes in peak vertical force (% BW)	Trial duration (sample size)
Nonsteroidal anti-inflammatory drugs			
Etodolac	Budsberg et al. [20]	2.3 (0.4)	8 days (34)
Carprofen	Moreau et al. [22]	2.4 [−3.4 to 17.0]	60 days (16)
Meloxicam	Moreau et al. [22]	4.7 [−4.9 to 92.2]	60 days (16)
Licofelone	Moreau et al. [15]	2.9 ± 1.7	28 days (13)
Carprofen	Hielm-Bjorkman et al. [21]	3.2 [−8.2 to 11.8]	56 days (15)
Complementary and alternative medicine			
Elk velvet antler	Moreau et al. [23]	2.4 ± 0.7	60 days (25)
Multitherbal preparation	E. Troncy (internal data)	2.6 (2.1)	56 days (13)
Homeopathic preparation	Hielm-Bjorkman et al. [21]	2.3 [−3.4 to 10.2]	56 days (14)
Veterinary therapeutic diets			
Omega-3 fatty acids	Roush et al. [26]	3.9 ± 1.3	90 days (22)
Green lipped mussel	Rialland et al. [24]	2.5 (4.2)	60 days (23)
Omega-3 fatty acids	Moreau et al. [25]	3.5 (6.8)	90 days (14)

% BW stands for percentage of body weight. Mean (standard deviation). Median (minimum to maximum). Mean ± standard error of the mean.

demonstrated an overall decrease in CSOM, without specific changes in the condition of BCD- and placebo-treated dogs. Longer treatment administration may preclude to a full monitoring of treatment efficacy for such level of PVF improvement, as previously denoted following 3 months of feeding a therapeutic diet in OA dogs [39]. Of note, CSOM was defined as complementary to PVF measurement, providing insights on different clinical aspects of the OA disease [14].

Whether BCD-treated dogs were improved through the preservation of joint structure, the relief of pain, or via a combination of these main aspects of the OA disease cannot be answered with regards to the present trial. However, from the previous study CCL model of OA [11], it was shown that action on key inflammatory mediators, such as iNOS and PAR 2, was tributary of the therapeutic potential of BCD. Under BCD treatment, lower levels of these mediators were encountered consistently with a protection against cartilaginous changes and better limb remission in CCL-deficient dogs.

Evidences indicate that PAR 2 participates in the development of experimental OA [40, 41]. Furthermore, PAR 2 activation has been shown to sensitize peripheral nociceptive receptors such as vanilloid, ATP-gated ion channels, and glutamate types [42–45]. Such sensitization contributes to the mechanical hypersensitivity and pain-related dysfunction that is pathognomonic of OA [46, 47]. When integrated, those findings support the putative therapeutic target of PAR 2 to limit the functional disability as well as the structural changes of OA.

A number of important limitations need to be considered: (1) the short duration of the study (6 weeks) for a chronic disease such as OA; (2) the absence of pharmacokinetic data on this plant extract may have precluded to suboptimal dosage; (3) the imputation method for missing data was the last-observation-carried-forward method. This

approach preserved the sample size, assuming that the response remains constant at the last observed and that missing data were at random. Underestimation or overestimation of the treatment effect may have occurred. Noteworthy, data managed using different imputation methods provided similar results, supporting the robustness of the primary endpoint results.

5. Conclusion

This study provided clinical evidences of the beneficial effect of BCD extract through its improvement to the locomotor disability associated with naturally occurring OA in dogs. Using objective measure of spontaneous mechanical allodynia and discomfort, the daily administration of 200 mg/kg/day of BCD extract was efficient, enough to improve the limb disuse, and to enhance the locomotor activity. These preclinical findings hopefully may eventually prove to have relevance for the treatment of OA in man.

Acknowledgments

The authors would like to acknowledge Katherine Bernier and Anne-André Mignault for their technical support. This study was funded in part by a grant from Vita Green Pharmaceutical (HK) Limited, ArthroLab Inc., an ongoing New Opportunities Fund Grant (E. Troncy) from the Canada Foundation for Innovation (no. 9483) for the pain/function equipment, and by the Osteoarthritis Chair of the University of Montreal Hospital Centre, Université de Montréal. Vita Green Pharmaceutical (HK) Limited participated in the decision to submit the paper for publication but was not involved in the study design, acquisition, analysis and interpretation of data, or the writing of the paper. M. Moreau received a Doctoral Scholarship from the Canadian Institutes of Health Research—Strategic Training Program (MENTOR).

References

- [1] R. Poole, S. Blake, M. Buschmann et al., "Recommendations for the use of preclinical models in the study and treatment of osteoarthritis," *Osteoarthritis and Cartilage*, vol. 18, supplement 3, pp. S10–S16, 2010.
- [2] S. A. Johnston and S. C. Budsberg, "Nonsteroidal anti-inflammatory drugs and corticosteroids for the management of canine osteoarthritis," *Veterinary Clinics of North America. Small Animal Practice*, vol. 27, no. 4, pp. 841–862, 1997.
- [3] R. M. McLaughlin, "Hind limb lameness in the young patient," *Veterinary Clinics of North America. Small Animal Practice*, vol. 31, no. 1, pp. 101–123, 2001.
- [4] J. K. Roush, "Hind limb lameness in the mature dog," *Veterinary Clinics of North America. Small Animal Practice*, vol. 31, no. 1, pp. 125–141, 2001.
- [5] J. L. Cook, "Cranial cruciate ligament disease in dogs: biology versus biomechanics," *Veterinary Surgery*, vol. 39, no. 3, pp. 270–277, 2010.
- [6] J. S. Madsen and E. Svalastoga, "Inclination and anteversion of collum femoris in hip dysplasia and coxarthrosis," *Acta Veterinaria Scandinavica*, vol. 35, no. 2, pp. 115–119, 1994.
- [7] C. L. Aragon, E. H. Hofmeister, and S. C. Budsberg, "Systematic review of clinical trials of treatments for osteoarthritis in dogs," *Journal of the American Veterinary Medical Association*, vol. 230, no. 4, pp. 514–521, 2007.
- [8] J. P. Pelletier and J. Martel-Pelletier, "DMOAD developments: present and future," *Bulletin of the NYU Hospital for Joint Diseases*, vol. 65, no. 3, pp. 242–248, 2007.
- [9] G. N. Smith, S. L. Myers, K. D. Brandt, E. A. Mickler, and M. E. Albrecht, "Effect of intraarticular hyaluronan injection on vertical ground reaction force and progression of osteoarthritis after anterior cruciate ligament transection," *Journal of Rheumatology*, vol. 32, no. 2, pp. 325–334, 2005.
- [10] J. P. Pelletier, C. Boileau, R. D. Altman, J. Martel-Pelletier et al., "Animal models of osteoarthritis," in *Rheumatology*, M. C. Hochberg et al., Ed., pp. 1731–1739, Mosby, Elsevier, 5th edition, 2010.
- [11] C. Boileau, J. Martel-Pelletier, J. Caron et al., "Oral treatment with a *BrachySTEMMA calycinum* D don plant extract reduces disease symptoms and the development of cartilage lesions in experimental dog osteoarthritis: inhibition of protease-activated receptor 2," *Annals of the Rheumatic Diseases*, vol. 69, no. 6, pp. 1179–1184, 2010.
- [12] M. Moreau, É. Troncy, S. Bichot, and B. Lussier, "Influence of changes in body weight on peak vertical force in osteoarthritic dogs: a possible bias in study outcome," *Veterinary Surgery*, vol. 39, no. 1, pp. 43–47, 2010.
- [13] E. Madore, L. Huneault, M. Moreau, and J. Dupuis, "Comparison of trot kinetics between dogs with stifle or hip arthrosis," *Veterinary and Comparative Orthopaedics and Traumatology*, vol. 20, no. 2, pp. 102–107, 2007.
- [14] P. Rialland, S. Bichot, M. Moreau et al., "Validation of clinical pain assessment methods with canine osteoarthritis," *Osteoarthritis and Cartilage*, vol. 17, pp. S254–S255, 2009.
- [15] M. Moreau, B. Lussier, M. Doucet, G. Vincent, J. Martel-Pelletier, and J. P. Pelletier, "Efficacy of licofelone in dogs with clinical osteoarthritis," *Veterinary Record*, vol. 160, no. 17, pp. 584–588, 2007.
- [16] C. Detrembleur, J. De Nayer, and A. van den Hecke, "Celecoxib improves the efficiency of the locomotor mechanism in patients with knee osteoarthritis. A randomised, placebo, double-blind and cross-over trial," *Osteoarthritis and Cartilage*, vol. 13, no. 3, pp. 206–210, 2005.
- [17] H. Gök, S. Ergin, and G. Yavuzer, "Kinetic and kinematic characteristics of gait in patients with medial knee arthrosis," *Acta Orthopaedica Scandinavica*, vol. 73, no. 6, pp. 647–652, 2002.
- [18] S. P. Messier, R. F. Loeser, J. L. Hoover, E. L. Semble, and C. M. Wise, "Osteoarthritis of the knee: effects on gait, strength, and flexibility," *Archives of Physical Medicine and Rehabilitation*, vol. 73, no. 1, pp. 29–36, 1992.
- [19] T. J. Schnitzer, J. M. Popovich, G. B. J. Andersson, and T. P. Andriacchi, "Effect of piroxicam on gait in patients with osteoarthritis of the knee," *Arthritis and Rheumatism*, vol. 36, no. 9, pp. 1207–1213, 1993.
- [20] S. C. Budsberg, S. A. Johnston, P. D. Schwarz, C. E. DeCamp, and R. Claxton, "Efficacy of etodolac for the treatment of osteoarthritis of the hip joints in dogs," *Journal of the American Veterinary Medical Association*, vol. 214, no. 2, pp. 206–210, 1999.
- [21] A. Hielm-Bjorkman, R. M. Tulamo, H. Salonen, and M. Raekallio, "Evaluating complementary therapies for canine osteoarthritis—part II: a homeopathic combination preparation (Zeel)," *Evidence-Based Complementary and Alternative Medicine*, vol. 6(2009), no. 4, pp. 465–471, 2009.
- [22] M. Moreau, J. Dupuis, N. H. Bonneau, and M. Desnoyers, "Clinical evaluation of a nutraceutical, carprofen and meloxicam for the treatment of dogs with osteoarthritis," *Veterinary Record*, vol. 152, no. 11, pp. 323–329, 2003.
- [23] M. Moreau, J. Dupuis, N. H. Bonneau, and M. Lécuyer, "Clinical evaluation of a powder of quality elk velvet antler for the treatment of osteoarthritis in dogs," *Canadian Veterinary Journal*, vol. 45, no. 2, pp. 133–139, 2004.
- [24] P. Rialland, S. Bichot, B. Lussier et al., "Effect of a green-lipped mussel-enriched diet on pain behaviours and functioning in dogs with clinical osteoarthritis," *Canadian Journal of Veterinary Research*. In press.
- [25] M. Moreau, E. Troncy, J. RE del Castillo, C. Bedard, D. Gauvin, and B. Lussier, "Effects of feeding a high omega-3 fatty acids diet in dogs with naturally occurring osteoarthritis," *Journal of Animal Physiology and Animal Nutrition*. In press.
- [26] J. K. Roush, A. R. Cross, W. C. Renberg et al., "Evaluation of the effects of dietary supplementation with fish oil omega-3 fatty acids on weight bearing in dogs with osteoarthritis," *Journal of the American Veterinary Medical Association*, vol. 236, no. 1, pp. 67–73, 2010.
- [27] T. Pham, D. van der Heijde, R. D. Altman et al., "OMERACT-OARSI initiative: osteoarthritis research society international set of responder criteria for osteoarthritis clinical trials revisited," *Osteoarthritis and Cartilage*, vol. 12, no. 5, pp. 389–399, 2004.
- [28] J. B. J. Bussmann, J. H. M. Tulen, E. C. G. Van Herel, and H. J. Stam, "Quantification of physical activities by means of ambulatory accelerometry: a validation study," *Psychophysiology*, vol. 35, no. 5, pp. 488–496, 1998.
- [29] D. D. Dunlop, J. Song, P. A. Semanik, L. Sharma, and R. W. Chang, "Physical activity levels and functional performance in the osteoarthritis initiative: a graded relationship," *Arthritis and Rheumatism*, vol. 63, no. 1, pp. 127–136, 2011.
- [30] J. N. Farr, S. B. Going, T. G. Lohman et al., "Physical activity levels in patients with early knee osteoarthritis measured by accelerometry," *Arthritis and Rheumatism*, vol. 59, no. 9, pp. 1229–1236, 2008.
- [31] C. C. Winter, M. Brandes, C. Müller et al., "Walking ability during daily life in patients with osteoarthritis of the knee or the hip and lumbar spinal stenosis: a cross sectional study," *BMC Musculoskeletal Disorders*, vol. 11, article 233, 2010.

- [32] B. D. Hansen, D. X. Lascelles, B. W. Keene, A. K. Adams, and A. E. Thomson, "Evaluation of an accelerometer for at-home monitoring of spontaneous activity in dogs," *American Journal of Veterinary Research*, vol. 68, no. 5, pp. 468–475, 2007.
- [33] D. C. Brown, R. C. Boston, and J. T. Farrar, "Use of an activity monitor to detect response to treatment in dogs with osteoarthritis," *Journal of the American Veterinary Medical Association*, vol. 237, no. 1, pp. 66–70, 2010.
- [34] K. L. Bennell and R. S. Hinman, "A review of the clinical evidence for exercise in osteoarthritis of the hip and knee," *Journal of Science and Medicine in Sport*, vol. 14, no. 1, pp. 4–9, 2011.
- [35] E. Mlacnik, B. A. Bockstahler, M. Müller, M. A. Tetrick, R. C. Nap, and J. Zentek, "Effects of caloric restriction and a moderate or intense physiotherapy program for treatment of lameness in overweight dogs with osteoarthritis," *Journal of the American Veterinary Medical Association*, vol. 229, no. 11, pp. 1756–1760, 2006.
- [36] J. K. Rychel, "Diagnosis and treatment of osteoarthritis," *Topics in Companion Animal Medicine*, vol. 25, no. 1, pp. 20–25, 2010.
- [37] M. Moreau, B. Lussier, S. Bichot et al., "Functional outcomes in dogs with naturally occurring osteoarthritis: force platform gait analysis and locomotor activity recording," *Osteoarthritis and Cartilage*, vol. 17, article S83, 2009.
- [38] K. L. Bennell, M. A. Hunt, T. V. Wrigley, B. W. Lim, and R. S. Hinman, "Role of muscle in the genesis and management of knee osteoarthritis," *Rheumatic Disease Clinics of North America*, vol. 34, no. 3, pp. 731–754, 2008.
- [39] M. Moreau, É. Troncy, D. Gauvin, and B. Lussier, "Effects of feeding a high omega-3 fatty acid diet on the pain-related disability in dogs with naturally occurring osteoarthritis," *Osteoarthritis and Cartilage*, vol. 18, article S23, 2010.
- [40] N. Amiable, J. Martel-Pelletier, B. Lussier, S. K. Tat, J. P. Pelletier, and C. Boileau, "Proteinase-activated receptor-2 gene disruption limits the effect of osteoarthritis on cartilage in mice: a novel target in joint degradation," *Journal of Rheumatology*, vol. 38, no. 5, pp. 911–920, 2011.
- [41] N. Amiable, S. K. Tat, D. Lajeunesse et al., "Proteinase-activated receptor (PAR)-2 activation impacts bone resorptive properties of human osteoarthritic subchondral bone osteoblasts," *Bone*, vol. 44, no. 6, pp. 1143–1150, 2009.
- [42] S. Amadesi, G. S. Cottrell, L. Divino et al., "Protease-activated receptor 2 sensitizes TRPV1 by protein kinase C ϵ - and A-dependent mechanisms in rats and mice," *Journal of Physiology*, vol. 575, part 2, pp. 555–571, 2006.
- [43] A. D. Grant, G. S. Cottrell, S. Amadesi et al., "Protease-activated receptor 2 sensitizes the transient receptor potential vanilloid 4 ion channel to cause mechanical hyperalgesia in mice," *Journal of Physiology*, vol. 578, part 3, pp. 715–733, 2007.
- [44] A. Kawabata, N. Kawao, H. Itoh et al., "Role of N-methyl-D-aspartate receptors and the nitric oxide pathway in nociception/hyperalgesia elicited by protease-activated receptor-2 activation in mice and rats," *Neuroscience Letters*, vol. 329, no. 3, pp. 349–353, 2002.
- [45] W. J. Zhu, Y. Dai, T. Fukuoka et al., "Agonist of proteinase-activated receptor 2 increases painful behavior produced by alpha, beta-methylene adenosine 5'-triphosphate," *NeuroReport*, vol. 17, no. 12, pp. 1257–1261, 2006.
- [46] M. Imamura, S. T. Imamura, H. H. S. Kaziyama et al., "Impact of nervous system hyperalgesia on pain, disability, and quality of life in patients with knee osteoarthritis: a controlled analysis," *Arthritis Care and Research*, vol. 59, no. 10, pp. 1424–1431, 2008.
- [47] X. Li, J. S. Kim, A. J. van Wijnen, and H. J. Im, "Osteoarthritic tissues modulate functional properties of sensory neurons associated with symptomatic OA pain," *Molecular Biology Reports*, vol. 38, no. 8, pp. 5335–5339, 2011.

Research Article

Reversion of P-Glycoprotein-Mediated Multidrug Resistance in Human Leukemic Cell Line by Diallyl Trisulfide

Qing Xia,¹ Zhi-Yong Wang,² Hui-Qing Li,³ Yu-Tao Diao,³ Xiao-Li Li,⁴ Jia Cui,⁵
Xue-Liang Chen,¹ and Hao Li¹

¹ Department of Hematology, Qilu Hospital, Shandong University, Shandong, Jinan 250012, China

² Department of Emergency, Qilu Hospital, Shandong University, Shandong, Jinan 250012, China

³ Institute of Basic Medicine, Shandong Academy of Medical Sciences, Shandong, Jinan 250062, China

⁴ Soochow University and Department of Hematology, Branch Guangci of First Affiliated Hospital, Jiangsu, Suzhou 215128, China

⁵ Shouguang Centre for Disease Control and Prevention, Shouguang 262700, China

Correspondence should be addressed to Xue-Liang Chen, xlchen1999@163.com and Hao Li, haoli611@yahoo.com.cn

Received 15 February 2012; Accepted 16 May 2012

Academic Editor: Vincenzo De Feo

Copyright © 2012 Qing Xia et al. This is an open access article distributed under the Creative Commons Attribution License, which permits unrestricted use, distribution, and reproduction in any medium, provided the original work is properly cited.

Multidrug resistance (MDR) is the major obstacle in chemotherapy, which involves multiple signaling pathways. Diallyl trisulfide (DATS) is the main sulfuric compound in garlic. In the present study, we aimed to explore whether DATS could overcome P-glycoprotein-(P-gp)-mediated MDR in K562/A02 cells, and to investigate whether NF- κ B suppression is involved in DATS-induced reversal of MDR. MTT assay revealed that cotreatment with DATS increased the response of K562/A02 cells to adriamycin (the resistance reversal fold was 3.79) without toxic side effects. DATS could enhance the intracellular concentration of adriamycin by inhibiting the function and expression of P-gp, as shown by flow cytometry, RT-PCR, and western blot. In addition, DATS resulted in more K562/A02 cell apoptosis, accompanied by increased expression of caspase-3. The expression of NF- κ B/p65 (downregulation) was significantly linked to the drug-resistance mechanism of DATS, whereas the expression of I κ B α was not affected by DATS. Our findings demonstrated that DATS can serve as a novel, nontoxic modulator of MDR, and can reverse the MDR of K562/A02 cells in vitro by increasing intracellular adriamycin concentration and inducing apoptosis. More importantly, we proved for the first time that the suppression of NF- κ B possibly involves the molecular mechanism in the course of reversion by DATS.

1. Introduction

The multidrug resistance (MDR) of leukemic cells to chemotherapy remains the most significant cause of treatment failure in acute leukemia [1]. A number of studies have shown that the major contributor to MDR is increased drug efflux mediated by P-glycoprotein (P-gp), a product of the *mdr-1* gene [2, 3]. Enormous efforts have been exerted to find reversal agents of the drug-efflux pump to overcome MDR [4]. Although hundreds of compounds have been found to reverse MDR, their clinical application is limited due to unacceptable side effects or toxicity at the doses required for effectiveness [5, 6]. Therefore, searching for reversal agents with low toxicity and high reversal activity has become an important research task.

Many plant-derived drugs or herbal formulations have been proven to have antitumor potential in vitro and in vivo [7–9]. Many of them, such as carnosic acid, puerarin, and ampelopsin, may reverse P-gp-mediated MDR via a decrease in the expression of *mdr-1* in K562/A02 cells, which is an adriamycin-selective, Pgp-overexpressing subline [10–12]. However, there have been several reports which claimed that some of the plant-derived drugs could increase the P-GP function [13].

Diallyl trisulfide (DATS) is the main sulfuric compound in garlic. Garlic compounds have been shown to have antiviral, antibacterial, antioxidant, anti-inflammatory, antiproliferative, and antiangiogenic activities [14–19]. In vitro and in vivo preclinical studies have implicated DATS as an important mediator of cyclins and cell cycle arrest, apoptosis,

cell adhesion, and angiogenesis [20–27]. Engdal proposed that garlic compounds could inhibit P-gp expression in vitro and in vivo [28]. DATS may have the ability to reverse drug resistance, but its molecular mechanism is still not fully understood.

We evaluated the P-gp-modulating potential of DATS in MDR K562/A02 cells to prove the effect of DATS as a reversal agent for human leukemic cells in vitro. In our previous study, the IC₁₀ of DATS to K562/A02 cells was 2 μmol/L, a noncytotoxic concentration dose also used in the present study. A verapamil-treated (4 μg/mL) group was used as positive control. Our goal was to ascertain whether transcription nuclear factor B (NF-κB) activation is involved in the reversal mechanism of DATS.

2. Materials and Methods

2.1. Drugs and Reagents. The following compounds were purchased: DATS (Shandong Lukang Xin Chen Pharmaceutical Co., Ltd., Shandong, China), verapamil (Shanghai Harvest Pharmaceutical Co., Ltd., Shanghai, China), adriamycin (ADM, Sigma Chemical Co., MO, USA), annexin V-FITC/PI (JingMei Bioengineering Co., Ltd., China), mouse antihuman P-gp monoclonal (BD Pharmingen Co., Ltd., USA), mouse antihuman mdr-1 antibody (Chemicon Co., Ltd., USA), rabbit anti-NF-κB (P65) antibody and mouse antihuman IκBα antibody (Cell Signaling Co., Ltd., USA), and caspase-3 rabbit antihuman monoclonal antibody (Beijing Biosynthesis Biotechnology Co., Ltd., Beijing, China). The primers were synthesized by Shanghai Boshang Biotechnology Co., Ltd. (Shanghai, China).

2.2. Cell Lines and Cell Culture. Human leukemia cell line K562 and its adriamycin-selective, Pgp-overexpressing subline K562/A02 were obtained from the Institute of Basic Medicine, Shandong Academy of Medical Sciences, China. Both cell lines were cultured in RPMI1640 medium (Gibco, Los Angeles, CA, USA) supplemented with 10% (v/v) heat-inactivated newborn calf serum (HangZhou Sijiqing Biological Engineering Materials Co., Ltd., China), 100 U/mL penicillin, and 100 μg/mL streptomycin. Furthermore, both cell lines were grown in a humidified incubator at 37°C and 5% CO₂. In particular, the K562/A02 cell line was maintained in 1 μg/mL adriamycin-containing medium and incubated in adriamycin-free medium for 2 weeks before the experiments.

2.3. Assay of In Vitro Drug Sensitivity. 3-(4,5-Dimethylthiazol-2-yl)-2,5-diphenyltetrazoliumbromide (MTT) assay was used to compare the MDR of the K562 and K562/A02 cells to adriamycin. K562 and K562/A02 cells were grown in a 96-well plate at 1 × 10⁵ cells/mL in a complete RPMI 1640 medium. Adriamycin was then added at various drug concentrations. K562 and K562/A02 cells without drugs in the medium were used as the blank controls. After the treatments were incubated for 44 h at 37°C, 20 μL MTT was added into each well, and incubation continued for another 4 h. The medium was then removed, and 150 μL dimethyl sulfoxide was added to each well to dissolve the

formazan crystals. The absorbance value was measured with a spectrophotometer at the wavelength of 570 nm. IC₅₀ of the drugs was calculated based on the MTT assay

Inhibition of cell viability

$$= 1 - \frac{\text{average A value of experimental group}}{\text{average A value of blank control group}} \times 100\%,$$

$$\text{Drug resistance fold} = \frac{\text{IC}_{50} \text{ of drug-resistant group}}{\text{IC}_{50} \text{ of sensitive group}}. \quad (1)$$

K562/A02 cells were seeded into 96-well culture plates at a density of 1 × 10⁵ cells/mL to determine whether DATS can sensitize MDR cells to the cytotoxicity of adriamycin. Adriamycin was then added with varying concentrations. The experimental group was treated with DATS at a concentration of 2 μmol/L. Verapamil (4 mg/L) treatment served as positive control. The cells were analyzed using the MTT method

$$\text{Reverse fold} = \frac{\text{IC}_{50} \text{ before reversal}}{\text{IC}_{50} \text{ after reversal}}. \quad (2)$$

2.4. Detection of Intracellular Adriamycin Concentration by FCM. The adriamycin concentration in K562/A02 cells was measured by flow cytometry (FCM). The K562 cells and K562/A02 cells without treatment were used as negative control. K562/A02 cells were treated with 2 μmol/L DATS or 4 mg/L verapamil and incubated for 48 h [29]. Adriamycin was then added to each sample to a final concentration of 5 mg/L. After incubating further for 2 h [30], the cells were harvested by centrifugation, washed twice with ice-cold phosphate buffered solution (PBS), and then resuspended in PBS. Adriamycin was excited effectively at a single wavelength (488 nm), and the emitted light was collected in the fluorescence-3 (FL3) channel. Events were gated on an FSC versus SCC dot plot to exclude the influences of cell debris and aggregates. A total of 10000 gated cells were detected for each sample, which were analyzed by Modfit LT software.

2.5. Detection of P-gp Expression by FCM. P-gp expression on the surface membrane of K562/A02 cells was determined by a direct immunofluorescence staining technique. K562/A02 cells were cocultured with 2 μmol/L DATS or 4 mg/L verapamil for 48 h. They were washed twice and suspended in PBS. The cell suspension was incubated with phycoerythrin-conjugated UIC2, mouse antihuman P-gp monoclonal antibody (P-gp-PE), and the homotype control IgG2a-PE. The mixture was reacted at room temperature and away from light for 30 min, washed twice, and then detected by FCM. The specific P-gp antibody UIC2 was detected in the FL-2 channel; thus, P-gp expression can be assessed on the cell surface. Protein expression was analyzed using Cell Quest software.

2.6. Observation of Morphological Changes by Light Microscopy. The morphological changes of apoptotic cells with

hematoxylin-eosin (HE) staining were observed by light microscopy. K562/A02 cells were grown at 1×10^5 cells/mL in a complete RPMI 1640 medium on a 24-well plate with a coverslip set at the bottom. After treatment with $2 \mu\text{mol/L}$ DATS combined with a final concentration of 1 mg/L adriamycin for 24 h to 72 h, (treatment with adriamycin alone as control), the coverslip was removed in each experimental group. Using 95% ethanol, the coverslip contents were fixed for 20 min. A series of washings were then performed as follows: carefully washed with PBS two times, hematoxylin for 2 min to 3 min, water to wash away hematoxylin for 1 s to 3 s, 1% hydrochloric acid and ethanol for 2 s to 3 s to reduce the cytoplasmic stain, lightly washed for 10 s, ammonia for 10 s to 20 s, and running water for 10 s. Eosin staining was performed for 1 min, then the stain was removed by washing with water for 1 s to 2 s, 80% ethanol 1 s to 2 s, 95% ethanol for 3 min to 5 min, ethanol for 5 min to 10 min, xylene (I) for 3 min to 5 min, and xylene (II) for 2 min to 5 min. The coverslip was then air-dried and mounted with neutral gum. Finally, the specimen was observed by light microscopy.

2.7. Apoptosis Assay by Statistical FCM. The apoptosis rates were measured using flow cytometric assay. Cell labeling was performed using annexin V conjugated to FITC, which binds to phosphatidylserine exposed on the surface membrane of cells undergoing apoptosis. After incubation in the medium containing different drugs ($2 \mu\text{mol/L}$ DATS or 4 mg/L verapamil) at 37°C for 48 h, the cell suspensions were washed twice with PBS and centrifuged at $550 \times g$ for 5 min. The cells were suspended in $500 \mu\text{L}$ binding buffer, $5 \mu\text{L}$ annexin V-FITC, and $10 \mu\text{L}$ ($20 \mu\text{g/mL}$) PI solution incubated at room temperature for 15 min in the dark. The samples were measured using a flow cytometer with FACS software.

2.8. Semiquantitative RT-PCR Assay. After treatment with the drugs ($2 \mu\text{mol/L}$ DATS or 4 mg/L verapamil), in vitro total mRNA was extracted from the cells with trizol reagent (Invitrogen Co., CA, USA) according to the manufacturer's instructions. Single-stranded cDNA was synthesized by reverse transcription from $1 \mu\text{g}$ of the total RNA using reverse transcriptase RNase M-MLV (Invitrogen Co., CA, USA) and oligo-dT. The amplification was performed in a final volume of $50 \mu\text{L}$, containing $5 \mu\text{L}$ cDNA, $0.5 \mu\text{L}$ of each oligonucleotide primer, $1 \mu\text{L}$ of each dNTP, and 1 unit of Taq DNA polymerase. Amplification was carried out in a thermal cycler. The PCR primers and expected product size were as follows: mdr-1 (167 bp) were 5'-0-3' (forward) and 5'-GTTCAAACCTTCTGCTCCTCA-3' (reverse); β -actin (540 bp) were 5'-GTGGGGCGCCCCAGGCACCA-3' (forward) and 5'-CTCCTTAATGTCACGCACGATTTTC-3' (reverse); NF- κ B/p65 (293 bp) were 5'-TGACCTAGCTGCCAAAGAAGGA-3' (forward) and 5'-TCTGCTCCTGCTGCTTTGAGAA-3' (reverse); I κ B α (634 bp) were 5'-GCAGAGGATTACGAGCAGAT-3' (forward) and 5'-CCTGGTAGGTTACTCTGTTG-3' (reverse); Caspase-3 (358 bp) were 5'-CCCATTTCTCCATACGCACT-3' (forward) and 5'-TGACAGCCAGTGAGACTTGG-3' (reverse). The

circulating conditions were as follows: 94°C for 1 min, 58°C for 1 min, and 72°C for 1 min for 26 cycles, and then extended for 7 min at 72°C . The products were identified by electrophoresis using 1.5% agarose gel. Using β -actin as internal reference, the products were further analyzed using Alpha gel image analysis system.

2.9. Western Blot Analysis of Protein Expression. After treatment with the drugs ($2 \mu\text{mol/L}$ DATS or 4 mg/L verapamil), total protein was isolated and subjected to sodium dodecyl sulfate PAGE analysis and transferred to a polyvinylidene difluoride membrane. The blots were stained with primary antibodies (1:1000–1200, mouse anti-human mdr-1 antibody, rabbit anti-human NF- κ B (P65) antibody, mouse anti-human I κ B α antibody, and rabbit anti-human caspase-3 monoclonal antibody) overnight at 4°C , and then with horseradish peroxidase-conjugated goat antirabbit IgG (1:5000) for 1 h at room temperature. The signal was detected with an ECL Western blot detection kit (ZhongShan Co., Beijing, China). After normalization by the corresponding β -actin expression, protein expression level was determined by densitometry scans and measured with Quantity One software.

2.10. Analyses. Statistical calculations were carried out with SPSS 17.0 for Windows software package. The results were expressed as mean \pm standard deviation of three independent experiments. Student's *t*-test was used for the statistical analyses, and *P* values < 0.05 were considered significant. The synergetic effect of the two drugs was analyzed using factorial analysis.

3. Results

3.1. Drug Sensitivity. MTT assay was used to study the cytotoxicity of adriamycin. The ability of DATS at $2 \mu\text{mol/L}$ to enhance the cytotoxicity of adriamycin in K562/A02 was examined. The MTT assay results are summarized in Table 1. The IC₅₀ value of adriamycin for K562/A02 decreased after treatment with DATS ($P < 0.01$). The time- and concentration-dependent reversal effects of DATS on the K562/A02 cells were observed for 24, 48, and 72 h. The data of the three experiments are shown in Figure 1. The higher the concentration of DATS used, the better the inhibitive effect.

3.2. Detection of Intracellular Adriamycin Concentration. The effect of DATS on the intracellular accumulation of adriamycin was examined by FCM. The autofluorescence intensity of the K562 and K562/A02 cells was very low (Figures 2(a) and 2(b)). The fluorescence intensity of adriamycin in K562 cells was 4.24 ± 0.15 , whereas it was 2.49 ± 0.27 in K562/A02 cells (Figures 2(c) and 2(d), $P < 0.01$). After treatment with DATS, adriamycin fluorescence intensity in K562/A02 cells increased to 4.38 ± 1.08 (Figure 2(e)), showing a significant difference compared with that without DATS treatment cells ($P < 0.01$). These results showed that DATS can enhance the intracellular concentration of adriamycin.

TABLE 1: IC₅₀ of adriamycin in K562 and K562/A02 cells.

Cell line	IC ₅₀ (ADM $\mu\text{g/mL}$)	Drug resistance fold	Reverse fold
K562	0.11 \pm 0.037		
K562/A02	6.79 \pm 0.58	61.73 ^{▲▲}	
K562/A02 + DATS	1.80 \pm 0.348		3.79 ^{**}
K562/A02 + verapamil	0.56 \pm 0.045		12.31 ^{**}

^{▲▲} $P < 0.01$ versus K562, ^{**} $P < 0.01$ versus K562/A02.

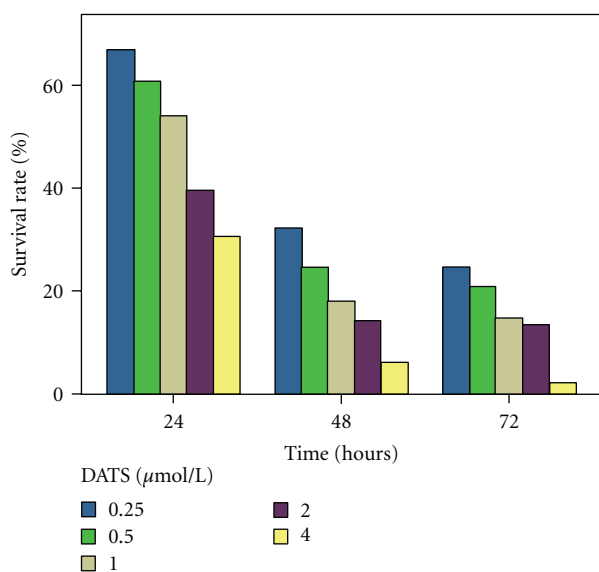


FIGURE 1: The time- and concentration-dependent reversal effects of DATS on the K562/A02 cells. K562/A02 cells were treated with adriamycin (5 $\mu\text{g/mL}$) for varying time intervals (24 h, 48 h, and 72 h) in the presence of 0.25–4 $\mu\text{mol/L}$ DATS.

3.3. Alteration of P-gp Expression. DATS-treated K562/A02 cells were incubated with phycoerythrin-conjugated UIC2, and then detected by FCM. The expression of P-gp in K562 was lower than that in K562/A02 ($P < 0.01$). After treatment with DATS in K562/A02 cells, P-gp expression decreased. A significant difference was observed between untreated K562/A02 cells and treated K562/A02 cells ($P < 0.01$) (Figure 3).

3.4. Apoptosis Observed by Light Microscopy. Adriamycin (1 $\mu\text{g/mL}$) alone did not inhibit the proliferation of K562/A02 cells significantly (Figures 4(a) and 4(b)). After simultaneous treatment of adriamycin (1 $\mu\text{g/mL}$) with DATS (2 $\mu\text{mol/L}$) for 24 h, the proliferation of K562/A02 cells slowed down (Figure 4(c)). After 48 h, the K562/A02 cells showed cell shrinkage, chromatin condensation, margination, nuclear fragmentation, apoptotic bodies, and typical apoptotic cytomorphological features (Figure 4(d)). After 72 h, more apoptotic cells and less surviving K562/A02 cells were detected (Figure 4(e)).

3.5. Apoptosis Statistical FCM Assay. Apoptosis of K562/A02 cells was induced by DATS or verapamil. After incubation with either DATS (2 $\mu\text{mol/L}$) or verapamil (4 $\mu\text{g/mL}$) for

48 h, apoptotic percentages of K562/A02 cells were $12.15 \pm 0.78\%$ and $11.55 \pm 1.91\%$, respectively. Evident differences were found compared with the control ($0.9 \pm 0.17\%$, $P = 0.000$) (Figure 5).

3.6. Detection of Gene Expression. As demonstrated by semiquantitative RT-PCR, overexpression of *mdr1* mRNA was detected better in the K562/A02 cells compared with the K562 cells ($P < 0.05$). The K562/A02 cells expressed high-levels of NF- κ B/p65, but expressed low-levels of I κ B α and caspase-3. DATS could downregulate the expression of *mdr1* and NF- κ B/p65 ($P < 0.05$) and upregulate the expression of caspase-3 ($P < 0.05$). However, DATS cannot evidently increase the expression level of I κ B α ($P > 0.05$) (Figure 6).

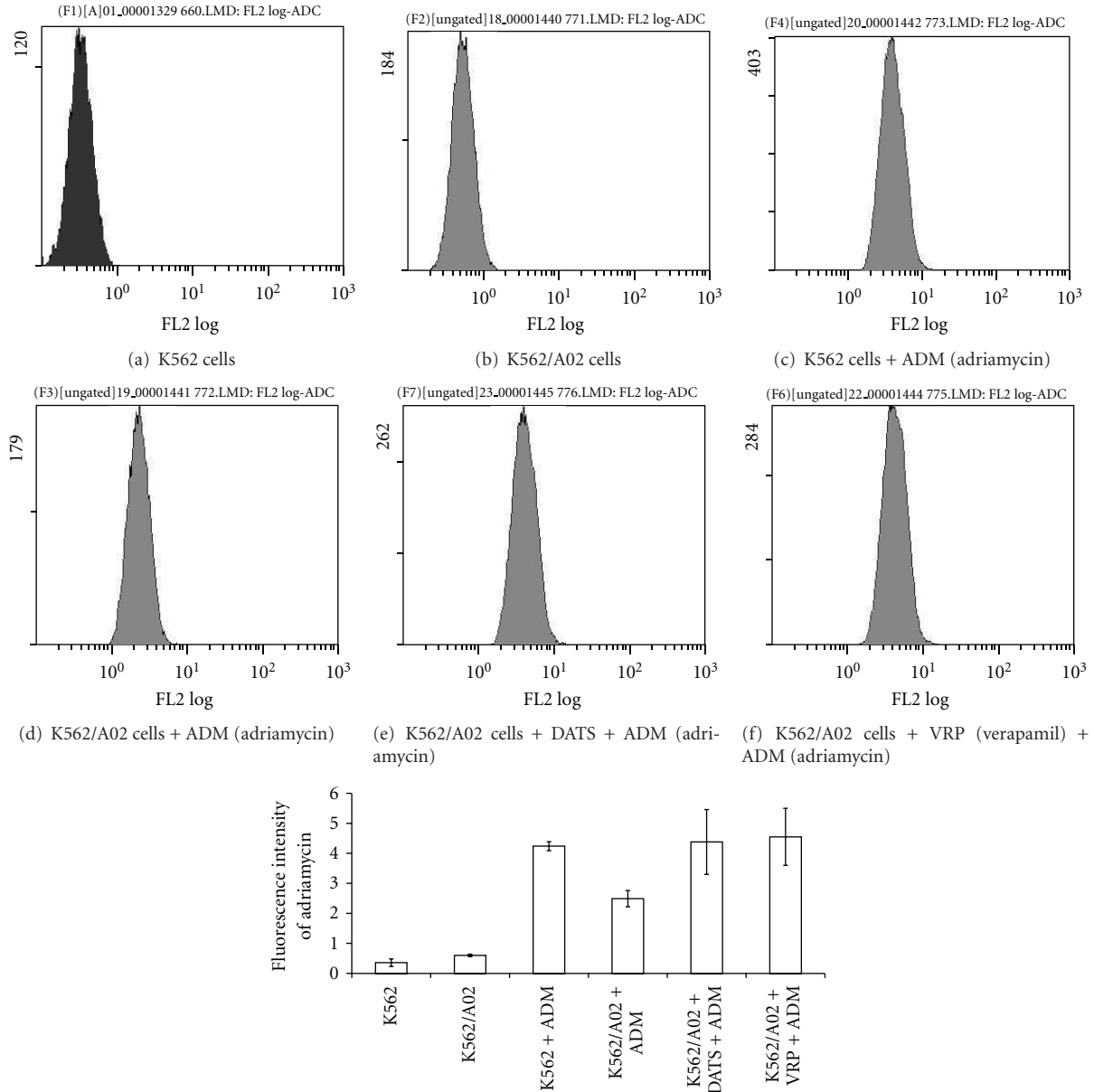
3.7. Western Blot Analysis of Protein Expression. The Western blot report revealed that the expression of *mdr1* protein and NF- κ B/p65 protein were much higher in K562/A02 cells compared with those in K562 cells ($P < 0.05$). The expression level of I κ B α protein and caspase-3 protein in K562/A02 cells was much lower than that in K562 cells ($P < 0.05$). DATS could downregulate the expression of *mdr1* and NF- κ B/p65 ($P < 0.05$) and upregulate the expression of caspase-3 ($P < 0.05$). However, DATS cannot evidently increase the expression level of I κ B α ($P > 0.05$) (Figure 7).

4. Discussion

In the present study, we have shown that DATS can significantly reverse the MDR of K562/A02 cells in vitro by increasing intracellular adriamycin concentration through downregulating the overexpression of P-gp and inducing apoptosis via increased caspase-3 expression. More importantly, we have proved that the NF- κ B signaling pathway is involved in the reversal mechanism of DATS.

The active efflux of xenobiotics is a major mechanism of cell adaptation to environmental stress. The ATP-dependent transmembrane transporter P-gp confers long-term cell survival in the presence of different toxins, including anticancer drugs.

P-gp, a product of the *mdr-1* gene, is a 170 kDa ATP-dependent transmembrane transporter that acts as a drug efflux pump, decreasing intracellular drug accumulation and therefore reducing intracellular drug efficacy [2, 3]. A high P-gp expression level is usually observed in MDR cell lines. However, in sensitive cells, P-gp is usually not detected. The drug intake capacity of cells with high *mdr-1* gene expression



(g) K562/A02 cells were treated with DATS (2 μ mol/L) or verapamil (4 mg/L) for 48 h, then adriamycin (5 mg/L) was added and cocubated for a further 2 h

FIGURE 2: Concentration of adriamycin in K562 or K562/A02 cells.

levels have no difference compared with sensitive cells, but drug efflux capacity is significantly increased [31, 32].

MDR is one of the major causes of failure in leukemic chemotherapy and is associated with the overexpression of P-gp in leukemic cell membranes. Studies have shown that in acute myeloid leukemia patients, the clinical remission (CR) rate of original leukemia cells with P-gp expression is 50%, whereas the CR rate of P-gp-negative cells is 81%. The P-gp expression in recrudescing leukemia group is significantly higher than in the first treatment group.

Enormous efforts have been exerted to find reversal agents of the drug efflux pump and overcome MDR. Various compounds, such as verapamil, cyclosporin, quinidine,

tamoxifen, progesterone, reserpine, and others, have been reported to overcome MDR in vitro by decreasing mdr-1 expression [4]. However, their clinical application is limited due to their unacceptable side effects or toxicity at the doses required for effectiveness.

Plant-derived drugs or herbal formulations have multi-target functions and have low toxicity. Recently, traditional Chinese medicine and its extracts have been shown to have high reversal activity on MDR. Yu et al. proved that carnosic acid (CA) can reverse the MDR of K562/A02 cells in vitro by increasing intracellular adriamycin concentration, downregulating the expression of mdr1, and inhibiting the function of P-gp [10]. Chen et al. found that puerarin can reverse

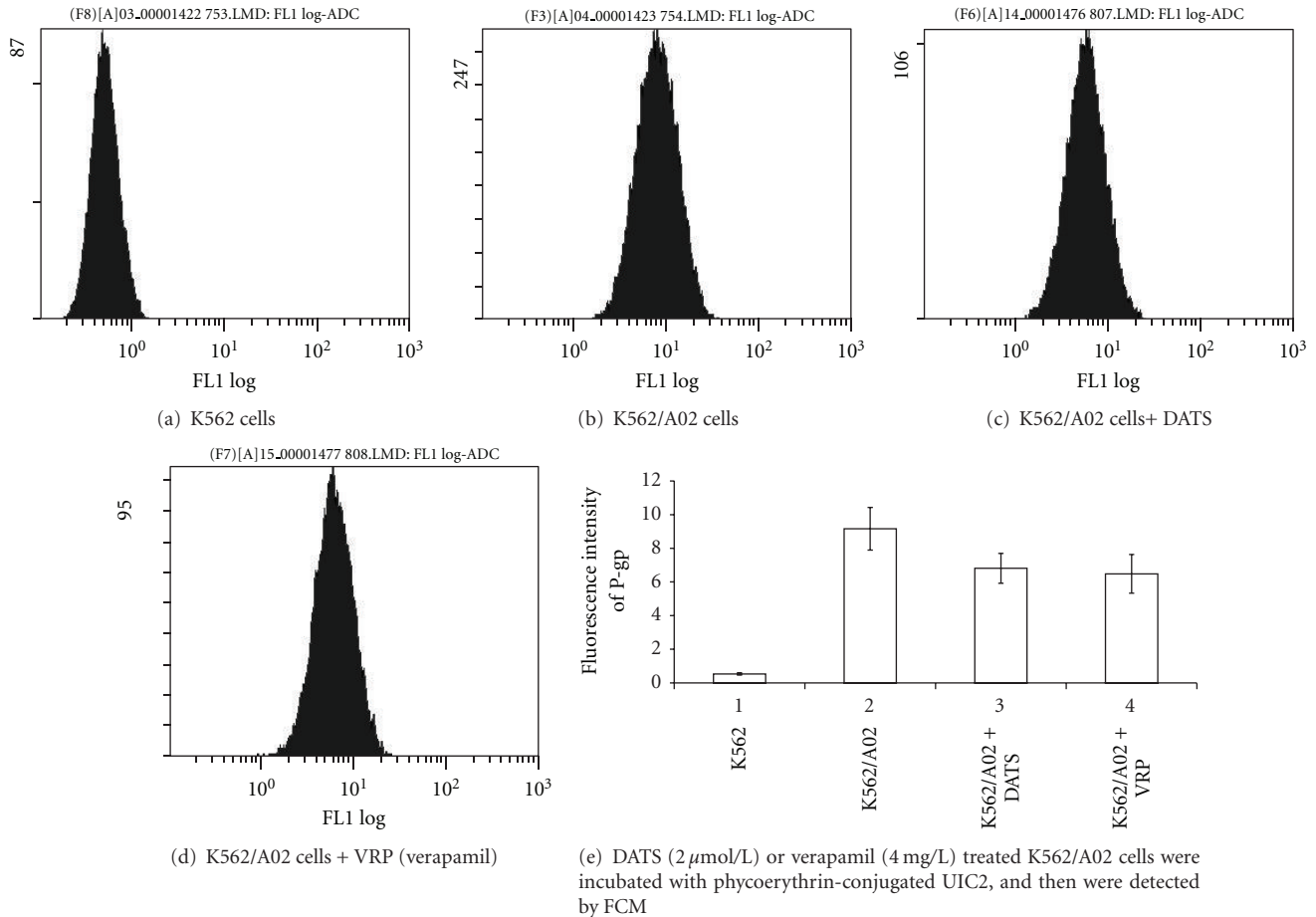


FIGURE 3: The expression of P-gp on the membrane surface of K562 or K562/A02 cells.

the multidrug resistance of K562/A02 to ADR by inhibiting the expression of p-gp and survivin [11]. Ye discovered that ampelopsin (AMP) could increase the cytotoxicity and intracellular accumulation of chemotherapeutic drugs in MDR-associated tumor cells by inhibiting the efflux of drugs by P-gp [12].

DATS is the main sulfuric compound of garlic, and garlic has been confirmed to be beneficial to human health via multiple mechanisms. Arora et al. discovered that nontoxic concentration of DATS enhances the cytotoxic effects of VBL and VCR in VBL-resistant human leukemia (K562/R) cells in a time-dependent manner by decreasing the expression levels of P-gp [33]. However, Lai et al. proved that DAS, DADS, and DATS promote expression of *mdr1* genes in colo 205 human colon cancer cells [34]. Therefore, the reversal effect of DATS to multidrug resistance is still controversial.

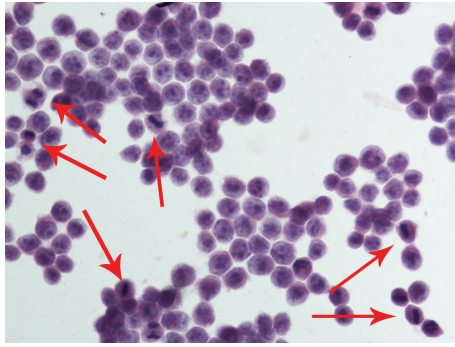
In the current study, we showed through MTT assays that DATS enhances the toxicity of adriamycin in K562/A02. The MDR leukemia cell line K562/A02 was established through in vitro selection of K562 cells with an increasing concentration of adriamycin [35] overexpressing the *mdr1* gene and P-gp. DATS could decrease the IC₅₀ of adriamycin against K562/A02 cells, as well as increase its chemosensitivity, which means DATS could reverse MDR. The fluorescence intensity

value of adriamycin measured via FCM reinforced the finding that DATS could increase the toxicity of adriamycin by increasing intracellular adriamycin concentration.

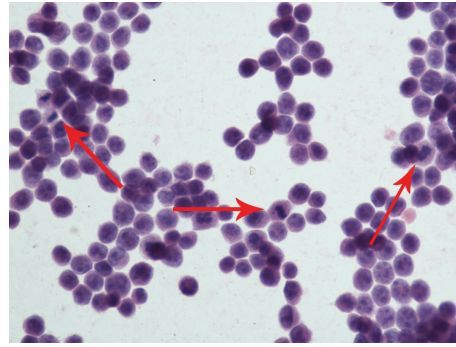
We used FCM to detect P-gp protein expression on the K562/A02 cell surface, which determined whether DATS could reduce P-gp expression. After treatment with DATS, P-gp expression decreased significantly, which demonstrated that DATS could reverse MDR by inhibiting P-gp overexpression. The decreased expression of P-gp was consistent with the downregulation of the *mdr1* gene and protein, as demonstrated by RT-PCR and Western blot. The result was similar to the report of Arora. But its molecular mechanism is still not fully understood.

We found that the intracellular adriamycin concentration in DATS-treated K562/A02 cells was 1.76-fold that in untreated K562/A02 cells. The extent of drug resistance reversal to adriamycin of DATS-treated K562/A02 cells was 3.79-fold that of untreated K562/A02 cells. Thus, other factors probably play important roles in the MDR mechanism, besides the reduction of intracellular drug accumulation.

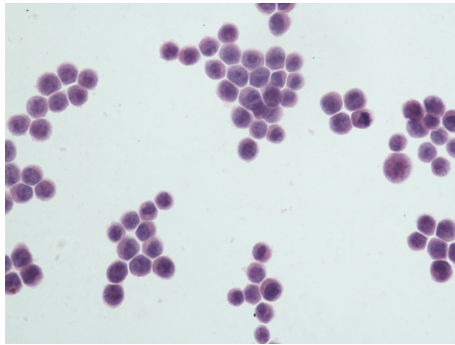
In recent years, studies have shown that apoptosis is closely related to MDR. Many anticancer drugs with different structures and different targets can induce apoptosis in tumor cells. The mechanism of apoptosis may be involved in



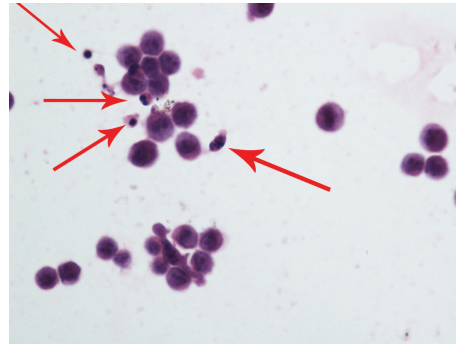
(a) K562/A02 cells grown 48 hours without drugs (400 magnification). Cells proliferated actively, mitotic easy to see (shown with †)



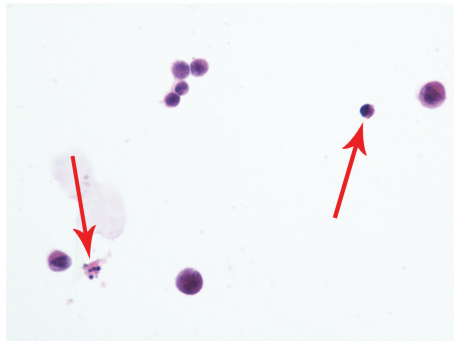
(b) K562/A02 cells grown 48 hours with adriamycin (1 µg/mL) (400 magnification). Cells proliferated actively, mitotic easy to see (shown with †)



(c) K562/A02 cells grown 24 hours with adriamycin and DATS (2 µmol/L) (400 magnification). Proliferation of K562/A02 cells slowed down, mitotic rarely to see



(d) K562/A02 cells grown 48 hours with adriamycin and DATS (400 magnification). K562/A02 cells showed cell shrinkage, chromatin condensation, margination, nuclear fragmentation, apoptotic bodies easy to see (shown with †)



(e) K562/A02 cells grown 72 hours with adriamycin and DATS (400 magnification). Survival rate of K562/A02 cells reduced, apoptotic bodies easy to see (shown with †)

FIGURE 4: Morphology observed by light microscopy.

the mechanism of MDS. Apoptosis is the common pathway of many different drugs. Due to the inhibition of apoptosis, the tumor cells are not only resistant to a certain drug, but are resistant to other drugs at the same time. This phenomenon leads to MDR.

We compared the morphological changes of cells with HE staining by light microscopy. As shown in Figure 4, the effect of DATS combined with a small dose of chemotherapeutic agent on K562/A02 cells resulted in strikingly increased apoptosis. At the same time, the apoptosis rate of

K562/A02 cells induced by DATS was measured using flow cytometric assay. The proapoptotic mechanism played an important role in the process of reversal of MDR by DATS, as revealed by evidence.

The caspase family, a large class of proteases, plays a very important role in the activation and execution of apoptosis. Thus, some researchers have named them the effectors of apoptosis. In the caspase family, caspase-3 is the key element of implementation because it participates in many apoptotic signaling pathways. The weakened expression of caspase-3

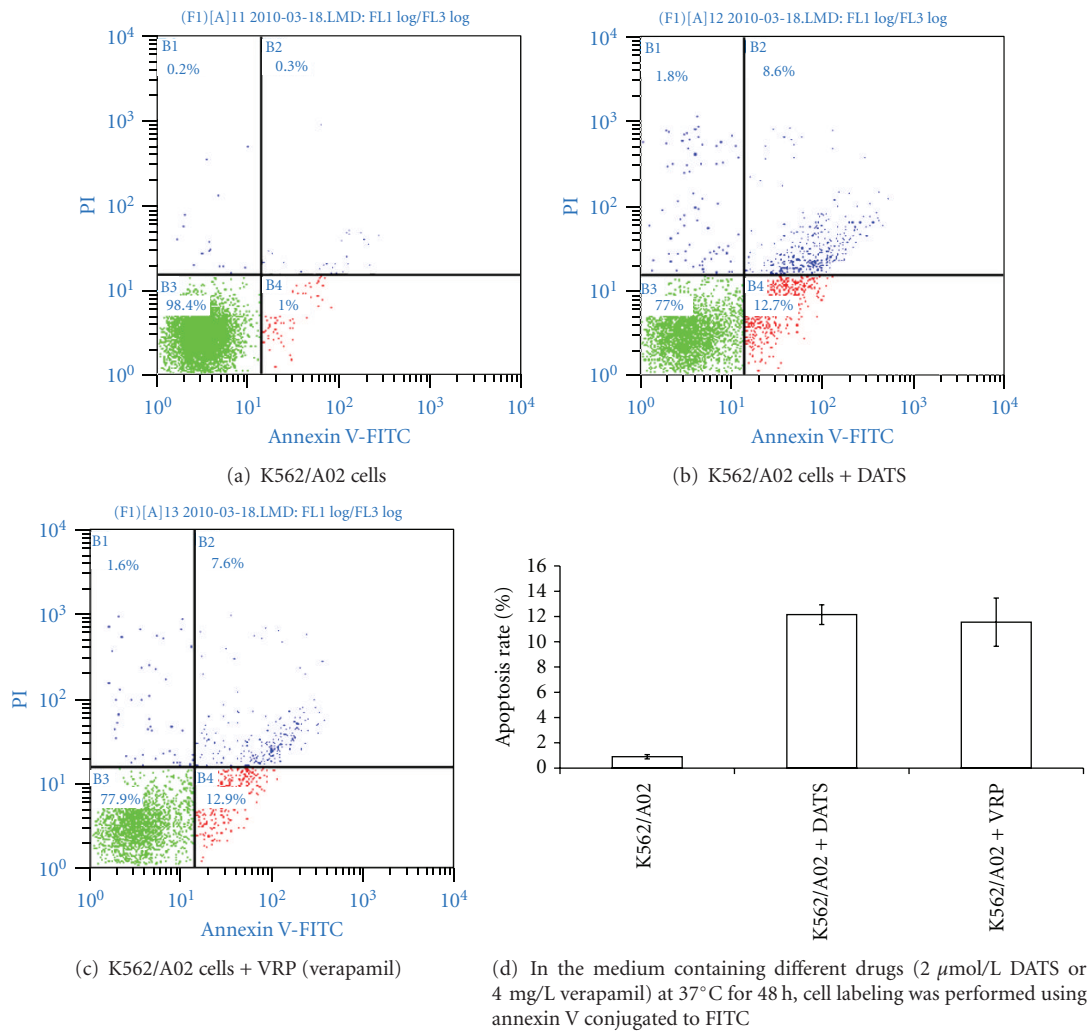


FIGURE 5: Apoptosis of K562/A02 cells induced by DATS or verapamil.

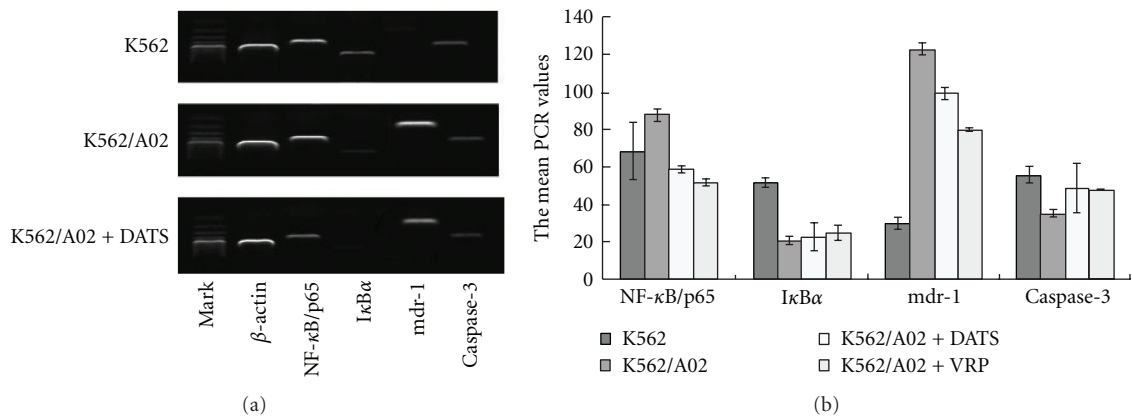


FIGURE 6: The mean PCR values of the ratio relative to the β -actin gene DATS (2 μ mol/L) or verapamil (4 mg/L) treated K562 cells and K562/A02 cells.

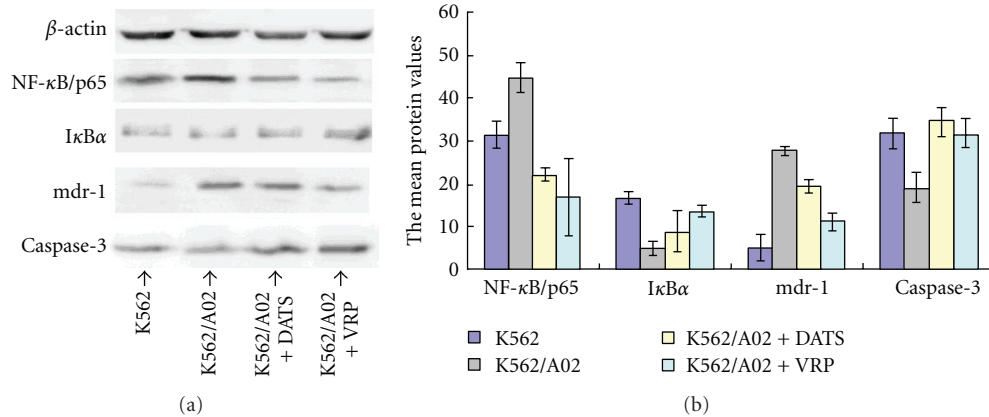


FIGURE 7: The mean protein values of the ratio relative to the β -actin DATS (2 μ mol/L) or verapamil (4 mg/L) treated K562 cells and K562/A02 cells.

has been associated with drug resistance and apoptotic inhibition in hematologic malignancies [36, 37]. The induced cell death in K562-Vinc cells was associated with activation of caspase-3 [38]. Several studies have documented that garlic can increase the activation of caspase-3 [39–41]. The current study arrived at the same conclusion. The ratio of caspase-3 expression in drug-resistant strains was significantly lower than in the sensitive strains. DATS could upregulate caspase-3 protein significantly in K562/A02 cells, which means DATS can promote apoptosis by adjusting caspase-3 expression.

As revealed in the current experiment, DATS can reverse the MDR of K562/A02 cells by increasing intracellular adriamycin concentration via downregulating the overexpression of P-gp and inducing apoptosis by activating increased caspase-3 expression. However, no research has yet indicated the signaling pathway through which DATS can adjust these genes.

The importance of NF- κ B in the process of cancerization has been mentioned in previous research. NF- κ B proteins are a small group of related and evolutionarily conserved proteins, in which mammals consists of five members, namely, Rel (c-Rel), RelA/p65, RelB, p50, and p52. In resting cells, NF- κ B is sequestered in the cytoplasm through the inhibitory molecule, termed inhibitor of NF- κ B (I κ B), such as I κ B α , which masks the nuclear localization sequence of NF- κ B. The stimulation of cells with various stimuli, including the stimulation of the TCR signaling pathway, leads to the activation of the I κ B kinase (IKK). NF- κ B signaling can be dichotomized into a “classical” pathway in which I κ B kinase (IKK β) phosphorylates I κ B α . An “alternative” NF- κ B pathway exists, in which IKK α phosphorylates the p100 precursor of the NF- κ B p52 subunit. The activated IKK phosphorylates I κ B, triggering rapid ubiquitination and degradation of I κ B by the 26S proteasome complex, which unmask the nuclear localization sequence of NF- κ B. Therefore, NF- κ B can be rapidly translocated into the nucleus to initiate the transcription of its target genes. The result of these signaling events is the accumulation of the heterodimeric NF- κ B transcription factors in the nucleus, with the classical pathway regulating mainly p50/p65 and

p50/c-Rel dimers, and the alternative pathway regulating p52/relB dimers [42].

NF- κ B can intervene in oncogenesis by regulating the expression of a large number of genes that regulate apoptosis, cell proliferation and differentiation, as well as inflammation, angiogenesis, and tumor migration [43]. Therefore, the inhibition of NF- κ B has been proposed as an adjuvant therapy for cancer. Many Phase I and II clinical studies involving different inhibitors are underway. Previous studies have proven that some Chinese medicines, such as Guan-Jen-Huang, can induced apoptosis by inhibiting NF- κ B activation [44].

A constitutive NF- κ B activity has been observed in several hematological malignancies, and this is associated with its antiapoptotic role [45, 46]. NF- κ B could participate in the chemoresistance of tumor cells mediated by the expression of the MDR protein. As previously confirmed, NF- κ B can increase the MDR gene expression in tumor cells. A purified NF- κ B binding sequence (5'2 CCTTTCGGG23') was found in the first exon of the mdr-1 promoter region, which confirmed that there are binding sites of NF- κ B in the mdr-1 gene. Mdr-1 may thus be NF- κ B downstream genes [47]. Furthermore, previous literature has confirmed that anticancer drugs, such as adriamycin and other chemicals, can damage tumor cell DNA, which can lead to the activation of NF- κ B. Activated NF- κ B promotes the transcription of mdr-1 via NF- κ B binding sites. Therefore, if the expression of NF- κ B can be inhibited, the sensitivity of chemotherapy can be increased [11, 48–50].

We have proved that K562/A02 cells display higher levels of NF- κ B/p65 protein expression than K562 cells. DATS can regulate the expression of NF- κ B/p65. In K562/A02 cells, the expression of P-gp and mdr-1 are positively correlated with NF- κ B/p65. Therefore, one of the mechanisms of NF- κ B antiapoptotic regulation in K562/A02 cells is correlated with mdr-1 and P-gp expression. Inhibition of NF- κ B activation may be involved in the reversal of MDR in K562/A02 cells by DATS.

Although the molecular mechanism of NF- κ B activation in leukemic stem cells or AML blasts remains elusive at present, NF- κ B and its unique role in the apoptotic and proli-

feration pathways and in drug resistance could represent an attractive target of selective drugs. NF- κ B inhibition has been proposed as an adjuvant therapy for cancer [47].

In conclusion, the present study has demonstrated that DATS can serve as a novel, nontoxic modulator of MDR and can reverse the MDR of K562/A02 cells *in vitro* by increasing intracellular adriamycin concentration, downregulating *mdr-1* expression, and inducing apoptosis by activating increased caspase-3 expression. We therefore conclude for the first time that DATS can block NF- κ B activation, which produces the downstream inhibitory effects on chemotherapy sensitivity and apoptosis of K562/A02 cells. DATS could be a highly feasible candidate for the development of a new MDR reversal agent.

Authors' Contribution

Q. Xai and Z.-Y. Wang contributed equally to this work.

Acknowledgment

This work was supported by the National Nature Science Foundation of China (no. 30600258).

References

- [1] M. M. Gottesman, T. Fojo, and S. E. Bates, "Multidrug resistance in cancer: role of ATP-dependent transporters," *Nature Reviews Cancer*, vol. 2, no. 1, pp. 48–58, 2002.
- [2] J. P. Gillet, T. Efferth, and J. Remacle, "Chemotherapy-induced resistance by ATP-binding cassette transporter genes," *Biochimica et Biophysica Acta*, vol. 1775, no. 2, pp. 237–262, 2007.
- [3] M. Mimeault, R. Hauke, and S. K. Batra, "Recent advances on the molecular mechanisms involved in the drug resistance of cancer cells and novel targeting therapies," *Clinical Pharmacology and Therapeutics*, vol. 83, no. 5, pp. 673–691, 2008.
- [4] M. Inaba, R. Fujikura, S. Tsukagoshi, and Y. Sakurai, "Restored *in vitro* sensitivity of adriamycin- and vincristine-resistant P388 leukemia with reserpine," *Biochemical Pharmacology*, vol. 30, no. 15, pp. 2191–2194, 1981.
- [5] J. M. Ford and W. N. Hait, "Pharmacology of drugs that alter multidrug resistance in cancer," *Pharmacological Reviews*, vol. 42, no. 3, pp. 155–199, 1990.
- [6] A. F. List, K. J. Kopecky, C. L. Willman et al., "Benefit of cyclosporine modulation of drug resistance in patients with poor-risk acute myeloid leukemia: a Southwest Oncology Group study," *Blood*, vol. 98, no. 12, pp. 3212–3220, 2001.
- [7] C. Y. Chang, H. L. Chan, H. Y. Lin et al., "Rhein induces apoptosis in human breast cancer cells," *Evidence-Based Complementary and Alternative Medicine*, vol. 2012, Article ID 952504, 8 pages, 2012.
- [8] H. W. Lai, S. Y. Chien, S. J. Kuo et al., "The potential utility of curcumin in the treatment of HER-2-overexpressed breast cancer: an *in vitro* and *in vivo* comparison study with herceptin," *Evidence-Based Complementary and Alternative Medicine*, vol. 2012, Article ID 486568, 12 pages, 2012.
- [9] P. N. Chen, M. L. Ho, Y. S. Hsieh et al., "Antimetastatic potentials of *Dioscorea nipponica* on melanoma *in vitro* and *in vivo*," *Evidence-Based Complementary and Alternative Medicine*, vol. 2011, Article ID 507920, 13 pages, 2011.
- [10] X. N. Yu, X. L. Chen, H. Li, X. X. Li, H. Q. Li, and W. R. Jin, "Reversion of P-glycoprotein-mediated multidrug resistance in human leukemic cell line by carnosic acid," *The Chinese journal of physiology*, vol. 51, no. 6, pp. 348–356, 2008.
- [11] J. W. Chen, S. Tao, R. Luo, G. S. Zhang, and Y. X. Xu, "Molecular mechanism of reversing multi-drug resistance of K562/A02 by puerarin," *Zhong Nan Da Xue Xue Bao Yi Xue Ban*, vol. 33, no. 3, pp. 216–221, 2008.
- [12] J. Ye, Y. Zheng, and D. Liu, "Reversal effect and its mechanism of ampelopsin on multidrug resistance in K562/ADR cells," *Zhongguo Zhongyao Zazhi*, vol. 34, no. 6, pp. 761–765, 2009.
- [13] P. D. L. Chao, S. P. Lin, P. P. Wu et al., "Different influences on tacrolimus pharmacokinetics by coadministrations of Zhi Ke and Zhi Shi in rats," *Evidence-based Complementary and Alternative Medicine*, vol. 2011, Article ID 751671, 6 pages, 2011.
- [14] G. W. Chen, J. G. Chung, H. C. Ho et al., "Effects of garlic compounds disllyl sulphide and diallyl disulphide on arylamine N-acetyltransferase activity in *Klebsiella pneumoniae*," *Journal of Applied Toxicology*, vol. 19, no. 2, pp. 75–81, 1999.
- [15] S. Ankri and D. Mirelman, "Antimicrobial properties of allicin from garlic," *Microbes and Infection*, vol. 1, no. 2, pp. 125–129, 1999.
- [16] R. T. Ackermann, C. D. Mulrow, G. Ramirez, C. D. Gardner, L. Morbidoni, and V. A. Lawrence, "Garlic shows promise for improving some cardiovascular risk factors," *Archives of Internal Medicine*, vol. 161, no. 6, pp. 813–824, 2001.
- [17] L. Y. Chung, "The antioxidant properties of garlic compounds: alyl cysteine, alliin, allicin, and allyl disulfide," *Journal of Medicinal Food*, vol. 9, no. 2, pp. 205–213, 2006.
- [18] Y. H. Siddique and M. Afzal, "Antigenotoxic effect of allicin against SCEs induced by methyl methanesulphonate in cultured mammalian cells," *Indian Journal of Experimental Biology*, vol. 42, no. 4, pp. 437–438, 2004.
- [19] O. C. Ohaeri and G. I. Adoga, "Anticoagulant modulation of blood cells and platelet reactivity by garlic oil in experimental diabetes mellitus," *Bioscience Reports*, vol. 26, no. 1, pp. 1–6, 2006.
- [20] D. Xiao, A. Herman-Antosiewicz, J. Antosiewicz et al., "Diallyl trisulfide-induced G2-M phase cell cycle arrest in human prostate cancer cells is caused by reactive oxygen species-dependent destruction and hyperphosphorylation of Cdc25C," *Oncogene*, vol. 24, no. 41, pp. 6256–6268, 2005.
- [21] A. Herman-Antosiewicz and S. V. Singh, "Checkpoint kinase 1 regulates diallyl trisulfide-induced mitotic arrest in human prostate cancer cells," *Journal of Biological Chemistry*, vol. 280, no. 31, pp. 28519–28528, 2005.
- [22] N. Li, R. Guo, W. Li et al., "A proteomic investigation into a human gastric cancer cell line BGC823 treated with diallyl trisulfide," *Carcinogenesis*, vol. 27, no. 6, pp. 1222–1231, 2006.
- [23] A. Das, N. L. Banik, and S. K. Ray, "Garlic compounds generate reactive oxygen species leading to activation of stress kinases and cysteine proteases for apoptosis in human glioblastoma T98G and U87MG cells," *Cancer*, vol. 110, no. 5, pp. 1083–1095, 2007.
- [24] D. Xiao, Y. Zeng, E. R. Hahm, Y. A. Kim, S. Ramalingam, and S. V. Singh, "Diallyl trisulfide selectively causes bax- and bak-mediated apoptosis in human lung cancer cells," *Environmental and Molecular Mutagenesis*, vol. 50, no. 3, pp. 201–212, 2009.
- [25] X. J. Wu, Y. Hu, E. Lamy, and V. Mersch-Sundermann, "Apoptosis induction in human lung adenocarcinoma cells by

- oil-soluble allyl sulfides: triggers pathways and modulators," *Environmental and Molecular Mutagenesis*, vol. 50, no. 3, pp. 266–275, 2009.
- [26] D. Xiao, M. Li, A. Herman-Antosiewicz et al., "Diallyl trisulfide inhibits angiogenic features of human umbilical vein endothelial cells by causing Akt inactivation and down-regulation of VEGF and VEGF-R2," *Nutrition and Cancer*, vol. 55, no. 1, pp. 94–107, 2006.
- [27] S. Shankar, Q. Chen, S. Ganapathy, K. P. Singh, and R. K. Srivastava, "Diallyl trisulfide increases the effectiveness of TRAIL and inhibits prostate cancer growth in an orthotopic model: molecular mechanisms," *Molecular Cancer Therapeutics*, vol. 7, no. 8, pp. 2328–2338, 2008.
- [28] S. Engdal, O. Klepp, and O. G. Nilsen, "Identification and exploration of herb-drug combinations used by cancer patients," *Integrative Cancer Therapies*, vol. 8, no. 1, pp. 29–36, 2009.
- [29] Y. P. Gong, T. Liu, Y. Q. Jia, L. Qin, C. Q. Deng, and R. Y. O. Yang, "Comparison of Pgp- and MRP-mediated multidrug resistance in leukemia cell lines," *International Journal of Hematology*, vol. 75, no. 2, pp. 154–160, 2002.
- [30] L. Chen, X. P. Xu, J. M. Wang et al., "Reversal of multidrug resistance in leukemia cell line by cyclosporin a combining with tamoxifen and interferon- α ," *Journal of Leukemia & Lymphoma*, vol. 12, no. 3, pp. 135–138, 2003.
- [31] J. L. Biedler and H. Riehm, "Cellular resistance to actinomycin D in Chinese hamster cells in vitro: cross-resistance, radioautographic, and cytogenetic studies," *Cancer Research*, vol. 30, no. 4, pp. 1174–1184, 1970.
- [32] R. L. Juliano and V. Ling, "A surface glycoprotein modulating drug permeability in Chinese hamster ovary cell mutants," *Biochimica et Biophysica Acta*, vol. 455, no. 1, pp. 152–162, 1976.
- [33] A. Arora, K. Seth, and Y. Shukla, "Reversal of P-glycoprotein-mediated multidrug resistance by diallyl sulfide in K562 leukemic cells and in mouse liver," *Carcinogenesis*, vol. 25, no. 6, pp. 941–949, 2004.
- [34] K.-C. Lai, C.-L. Kuo, H.-C. Ho et al., "Diallyl sulfide, diallyl disulfide and diallyl trisulfide affect drug resistant gene expression in colo 205 human colon cancer cells in vitro and in vivo," *Phytomedicine*, vol. 19, no. 7, pp. 625–630, 2012.
- [35] L. Feng-Jun, "Establishment of the multidrug-resistant cell line K562/A02 and its drug-resistant properties," *Zhonghua Zhong Liu Za Zhi*, vol. 15, no. 2, pp. 101–103, 1993.
- [36] N. Voorzanger-Rousselot, L. Alberti, and J. Y. Blay, "CD40L induces multidrug resistance to apoptosis in breast carcinoma and lymphoma cells through caspase independent and dependent pathways," *BMC Cancer*, vol. 6, article no. 75, 2006.
- [37] J. J. Mezhir, K. D. Smith, M. C. Posner et al., "Ionizing radiation: a genetic switch for cancer therapy," *Cancer Gene Therapy*, vol. 13, no. 1, pp. 1–6, 2006.
- [38] Y. Assef, F. Rubio, G. Coló, S. del Mónaco, M. A. Costas, and B. A. Kotsias, "Imatinib resistance in multidrug-resistant K562 human leukemic cells," *Leukemia Research*, vol. 33, no. 5, pp. 710–716, 2009.
- [39] H. F. Lu, C. C. Sue, C. S. Yu, S. C. Chen, G. W. Chen, and J. G. Chung, "Diallyl disulfide (DADS) induced apoptosis undergo caspase-3 activity in human bladder cancer T24 cells," *Food and Chemical Toxicology*, vol. 42, no. 10, pp. 1543–1552, 2004.
- [40] K. B. Kwon, S. J. Yoo, D. G. Ryu et al., "Induction of apoptosis by diallyl disulfide through activation of caspase-3 in human leukemia HL-60 cells," *Biochemical Pharmacology*, vol. 63, no. 1, pp. 41–47, 2002.
- [41] S. Oommen, R. J. Anto, G. Srinivas, and D. Karunakaran, "Allicin (from garlic) induces caspase-mediated apoptosis in cancer cells," *European Journal of Pharmacology*, vol. 485, no. 1–3, pp. 97–103, 2004.
- [42] C. Y. Wang, M. W. Mayo, R. G. Korneluk, D. V. Goeddel, and A. S. Baldwin, "NF- κ B antiapoptosis: induction of TRAF1 and TRAF2 and c-IAP1 and c-IAP2 to suppress caspase-8 activation," *Science*, vol. 281, no. 5383, pp. 1680–1683, 1998.
- [43] B. B. Aggarwal, "Nuclear factor- κ B: the enemy within," *Cancer Cell*, vol. 6, no. 3, pp. 203–208, 2004.
- [44] Y. H. Liu, M. L. Li, M. Y. Hsu et al., "Effects of a chinese herbal medicine, Guan-Jen-Huang (*Aeginetia indica* Linn.), on renal cancer cell growth and metastasis," *Evidence-based Complementary and Alternative Medicine*, vol. 2012, Article ID 935860, 10 pages, 2012.
- [45] M. Karin, Y. Cao, F. R. Greten, and Z. W. Li, "NF- κ B in cancer: from innocent bystander to major culprit," *Nature Reviews Cancer*, vol. 2, no. 4, pp. 301–310, 2002.
- [46] L. Bemal-Mizrachi, C. M. Lovly, and L. Ratner, "The role of NF- κ B-1 and NF- κ B-2-mediated resistance to apoptosis in lymphomas," *Proceedings of the National Academy of Sciences*, vol. 103, no. 24, pp. 9220–9222, 2006.
- [47] M. Bentires-Alj, V. Barbu, M. Fillet et al., "NF- κ B transcription factor induces drug resistance through MDR1 expression in cancer cells," *Oncogene*, vol. 22, no. 1, pp. 90–97, 2003.
- [48] S. Kokura, N. Yoshida, N. Sakamoto et al., "The radical scavenger edaravone enhances the anti-tumor effects of CPT-11 in murine colon cancer by increasing apoptosis via inhibition of NF- κ B," *Cancer Letters*, vol. 229, no. 2, pp. 223–233, 2005.
- [49] J. H. Um, C. D. Kang, B. G. Lee, D. W. Kim, B. S. Chung, and S. H. Kim, "Increased and correlated nuclear factor-kappa B and Ku autoantigen activities are associated with development of multidrug resistance," *Oncogene*, vol. 20, no. 42, pp. 6048–6056, 2001.
- [50] Y. G. Lin, A. B. Kunnumakkara, A. Nair et al., "Curcumin inhibits tumor growth and angiogenesis in ovarian carcinoma by targeting the nuclear factor- κ B pathway," *Clinical Cancer Research*, vol. 13, no. 11, pp. 3423–3430, 2007.

Research Article

Polyphenol-Rich Fraction of Brown Alga *Ecklonia cava* Collected from Gijang, Korea, Reduces Obesity and Glucose Levels in High-Fat Diet-Induced Obese Mice

Eun Young Park,^{1,2} Eung Hwi Kim,^{1,2} Mi Hwi Kim,^{1,2} Young Wan Seo,³
Jung Im Lee,³ and Hee Sook Jun^{1,2}

¹ College of Pharmacy, Gachon University, Incheon 406-840, Republic of Korea

² Lee Gil Ya Cancer and Diabetes Institute, Gachon University, Incheon 406-840, Republic of Korea

³ Division of Marine Environment and Bioscience, Korea Maritime University, Busan 606-791, Republic of Korea

Correspondence should be addressed to Hee Sook Jun, hsjun@gachon.ac.kr

Received 27 March 2012; Accepted 16 May 2012

Academic Editor: Vincenzo De Feo

Copyright © 2012 Eun Young Park et al. This is an open access article distributed under the Creative Commons Attribution License, which permits unrestricted use, distribution, and reproduction in any medium, provided the original work is properly cited.

Ecklonia cava (*E. cava*) is a brown alga that has beneficial effects in models of type 1 and type 2 diabetes. However, the effects of *E. cava* extracts on diet-induced obesity and type 2 diabetes have not been specifically examined. We investigated the effects of *E. cava* on body weight, fat content, and hyperglycemia in high-fat diet- (HFD) induced obese mice and sought the mechanisms involved. C57BL/6 male mice were fed a HFD (60% fat) diet or normal chow. After 3 weeks, the HFD diet group was given extracts (200 mg/kg) of *E. cava* harvested from Jeju (CA) or Gijang (G-CA), Korea or PBS by oral intubation for 8 weeks. Body weights were measured weekly. Blood glucose and glucose tolerance were measured at 7 weeks, and fat pad content and mRNA expression of adipogenic genes and inflammatory cytokines were measured after 8 weeks of treatment. G-CA was effective in reducing body weight gain, body fat, and hyperglycemia and improving glucose tolerance as compared with PBS-HFD mice. The mRNA expression of adipogenic genes was increased, and mRNA expression of inflammatory cytokines and macrophage marker gene was decreased in G-CA-treated obese mice. We suggest that G-CA reduces obesity and glucose levels by anti-inflammatory actions and improvement of lipid metabolism.

1. Introduction

The incidence of obesity has increased at an epidemic rate in the world [1, 2]. Obesity is a state of energy imbalance resulting from excessive food intake and lack of exercise [3, 4] and contributes to the development of metabolic syndrome, diabetes, cardiovascular disease, atherosclerosis, osteoarthritis, and nonalcoholic fatty liver disease [4–6]. Although exercise and dietary control are effective ways of treating obesity, pharmacological treatment is also an important strategy. Currently available therapeutic agents include sibutramine, orlistat, phentermine, and diethylpropion [7]. However, because of the adverse effects of these agents such as abuse, cardiovascular disease, and overstimulation, dietary

supplements and herbal products are being recognized as an alternative therapy.

Many types of brown algae are widely eaten in Korea and Japan. Brown algae contain various minerals and dietary fiber and are used as natural health foods. *Ecklonia cava* is a species of brown alga found abundantly in the neritic regions of Korea and Japan [8]. This alga has received attention due to the medicinal effects of its carotenoids, fucoidans, and phlorotannins [9–13], including anti-inflammatory, antioxidative and antidiabetic effects [14, 15]. With regard to its antidiabetic effects, *Ecklonia cava* extract reduces blood glucose levels and increases insulin levels in streptozotocin-induced diabetic mice, a model of type 1 diabetes [14], and the dieckol-rich extract of *Ecklonia cava* improves glucose

and lipid metabolism in C57BL/KsJ-db/db (db/db) mice, a model of type 2 diabetes [16]. However, the effects of *Ecklonia cava* on diet-induced obesity have not been specifically examined. In this study, we investigated the effects of *Ecklonia cava* on body weight, fat content, and hyperglycemia in mice fed a high-fat diet (HFD) and sought the antiobesity mechanisms. In addition, we compared the efficacy of *Ecklonia cava* from different areas (produced in Jeju or Gijang, Korea) on our HFD-induced obese mouse model.

2. Materials and Methods

2.1. Preparation of EtOAc Fraction of EC Crude Extract. The collected samples of *Ecklonia cava* were air-dried on the shade and ground into powder. The powder was extracted repeatedly with MeOH for 3 hours under reflux condition. The crude extract was partitioned between CH₂Cl₂ and H₂O. The organic layer was evaporated and repartitioned between *n*-hexane and 85% aq. MeOH. The aqueous layer was repartitioned between *n*-BuOH and H₂O, and then the *n*-BuOH layer was fractionated with EtOAc and H₂O. The EtOAc fraction was used for HFD-induced obese mouse model experiment.

2.2. Determination of Total Polyphenolic Content. The total phenol content was determined using the Folin-Ciocalteu method [17]. An aliquot (20 μ L) of each sample or standard solution was mixed with 250 μ L of dd H₂O and 250 μ L of Folin-Ciocalteu's phenol reagent. Then, 500 μ L of 35% Na₂CO₃ solution was added to the mixture followed by incubating at ambient temperature in the dark for 20 min. The absorbance against a blank was measured at 750 nm. The results were expressed as mg tannic acid equivalent (TAE)/g extract (dw).

2.3. HPLC Analysis. A portion of EtOAc fraction was subjected to silica gel column chromatography with gradient mixtures of chloroform and methanol. Each of chromatographic fractions was analyzed using an HPLC system (Dionex P580 model) equipped with Varian RI detector and a YMC ODS-A (250 \times 4.6 mm) fractionation column with a flow rate of 1 mL/min (eluting solvents, 30% and 40% aq. methanol). Identification and quantification of phlorotannins were carried out by comparing the retention times and the peak areas, respectively, with those of phlorotannin standards. Sample aliquots were filtered through C18 SPE Maxi Clean Cartridge filter prior to injection. The authentic samples of standard phlorotannins (phloroglucinol, triphloretol A, eckol, eckstolonol, phlorofucofuroeckol A, dieckol, 6,6'-bieckol, 8,8'-bieckol, fucofuroeckol A) were directly isolated from *Ecklonia cava*, and their chemical structures were confirmed by comparing with data reported in the literature.

2.4. Animals. C57BL/6 mice were obtained from the Korea Research Institute of Bioscience and Biotechnology (Daejeon, South Korea). Mice were maintained under specific pathogen-free conditions in a temperature-controlled room (23 \pm 1°C) in a 12 h light/dark cycle with *ad libitum* access to

food and water at the Animal Care Center, Lee Gil Ya Cancer and Diabetes Institute, Gachon University of Medicine and Science, South Korea. All animal experiments were approved by the Institutional Animal Care and Use Committee of the Lee Gil Ya Cancer and Diabetes Institute.

2.5. Induction of Obesity and Treatment with EtOAc Fraction of *Ecklonia cava* Extract. At 6 weeks of age, male mice were provided with either a HFD (60% fat) or normal chow (5.4% fat). After 3 weeks, mice were randomly divided into four groups ($n = 5-8$ in each group): the normal chow group (NC), the phosphate-buffered saline- (PBS-) treated HFD group (PBS-HFD), the Jeju-*Ecklonia cava*- (CA-) treated HFD group (CA-HFD), and the Gijang-*Ecklonia cava*- (G-CA-) treated HFD group (G-CA-HFD). CA or G-CA (200 mg/kg in PBS) was given by oral intubation daily for 8 weeks. The PBS-HFD group was given the same volume of PBS by oral intubation. Body weight and food consumption were measured weekly. At the end of 8 weeks of treatment, animals were killed and tissues were removed for various biochemical measurements.

2.6. Measurement of Fat Mass. Fat mass was determined using ¹H mini-spec system (Bruker, Karlsruhe, Germany) at 8 weeks of treatment. This equipment allowed us to analyze body fat weight without sedating the mice. After 8 weeks of CA and G-CA treatment, fat pads (subcutaneous, epididymal, perirenal, and mesenteric) were collected, and the weights were measured.

2.7. Plasma Analysis. After 8 weeks of CA and G-CA treatment, blood samples were collected from the orbital sinus under anesthesia after 3 hours of food deprivation. Blood samples were centrifuged at 3000 g for 20 min, and serum levels of alanine aminotransferase (ALT), aspartate aminotransferase (AST), cholesterol, triglycerides, low-density lipoprotein (LDL)-cholesterol and high-density lipoprotein (HDL)-cholesterol were measured using Beckman Coulter AU 480.

2.8. Measurement of Blood Glucose Levels. After 7 weeks of CA and G-CA treatment, mice were not fed for 14 h, and then glucose levels were measured in the tail vein blood with a glucometer.

2.9. Intraperitoneal Glucose Tolerance Test. At 7 weeks of treatment, mice were fasted for 14 h and then a glucose solution (2 g/kg body weight in PBS) was administered intraperitoneally. Blood glucose levels were measured at 0, 30, 60, 90, and 120 minutes after glucose injection.

2.10. Analysis of mRNA by Quantitative Real-Time PCR. Total RNA was isolated from the adipose and liver tissue, and cDNA was synthesized using a PrimeScript 1st strand cDNA synthesis kit (Takara). Quantitative real-time PCR was performed using the Power SYBR Green Master Mix (Applied-Biosystems) and Applied Biosystem Prism 7900HT sequence detection system. PCR was carried out and stopped

TABLE 1: Primer sequences of mouse mRNA.

Target	Forward primer	Reverse primer
PPAR γ 2	CACCAGTGTGAATTACAGCAAATC	ACAGGAGAATCTCCCAGAGTTTC
C/EBP α	GCGCAAGAGCCGAGATAAAG	CGGTTCATTGTCACTGGTCAACT
SREBP1c	GGAGCCATGGATTGCACATT	GGCCCCGGAAGTCACTGT
FAS	GCTGCGGAAACTTCAGGAAAT	AGAGACGTGTCACTCCTGGACTT
TNF α	CCAACGGCATGGATCTCAAAGACA	AGATAGCAAATCGGCTGACGGTGT
IL-1 β	CTACAGGCTCCGAGATGAACAAC	TCCATTGAGGTGGAGAGCTTTC
F4/80	TCATCAGCCATGTGGGTACAG	CACAGCAGGAAGGTGGCTATG
ACC1	ACGCTCAGGTCACAAAAAGAAT	GTAGGGTCCCAGCCACAT

at 40 cycles (2 minutes at 50°, 10 minutes at 95°, and 40 cycles of 10 seconds at 95° and 1 minute at 60°). The primer sequences used are shown in Table 1. Relative copy number was calculated using the threshold crossing point (C_t) as calculated by the $\Delta\Delta C_t$ calculations.

2.11. Immunoblot Analysis. Samples were prepared from lysates of liver tissue in 50 mM Tris-HCl (pH 7.5), 1% SDS, 150 mM sodium chloride, 10% glycerol, 1 mM EDTA, 1 mM sodium orthovanadate, 1 mM sodium pyrophosphate, 1 mM phenylmethylsulfonyl fluoride, and protease inhibitor cocktail. The protein samples were centrifuged at 10,000 g for 10 min to remove debris and stored at -70°C until use. Protein samples were separated by 10% SDS-polyacrylamide gel electrophoresis. For immunoblots, proteins were electrotransferred to a polyvinylidene fluoride membrane (Schleicher & Schuell), and nonspecific binding was blocked with 2.5% nonfat milk in Tris-buffered saline. The membrane was immunoblotted with anti-AMP-activated protein kinase (AMPK) antibody or anti-phospho-AMPK (Cell Signaling, 1:1000). The primary antibodies were detected using horseradish peroxidase-conjugated anti-rabbit IgG (Santa Cruz). Specific binding was detected using the Super Signal West Dura Extended Duration Substrate (Pierce) and exposure to RAS-4000 system (Fuji film). The band density was quantified by the software Multigaue version 3.1 (Fuji film).

2.12. Oil Red O Staining. Liver pieces were embedded in optimal cutting temperature compound. Frozen liver sections were cut at 10 μm thickness and stained with Oil Red O and Mayer's hematoxylin solution for microscopy.

2.13. Quantification of Liver Triglyceride Content. Liver tissue (50 mg) was homogenized with ethanolic KOH (2 parts EtOH: 1 part 30% KOH) for overnight, and then KOH and distilled water were added to the homogenate. After centrifugation (1000 g, for 5 min), supernatant was transferred into a new microtube and mixed with 1 M MgCl_2 . The sample was incubated for 10 min on ice and then centrifuged at 1000 g for 5 min. Triglycerides content was measured in the upper phase solution using a Cleantech TG-S kit (Asan Pharmaceutical Company).

TABLE 2: Polyphenol content in CA and G-CA extracts as determined by HPLC.

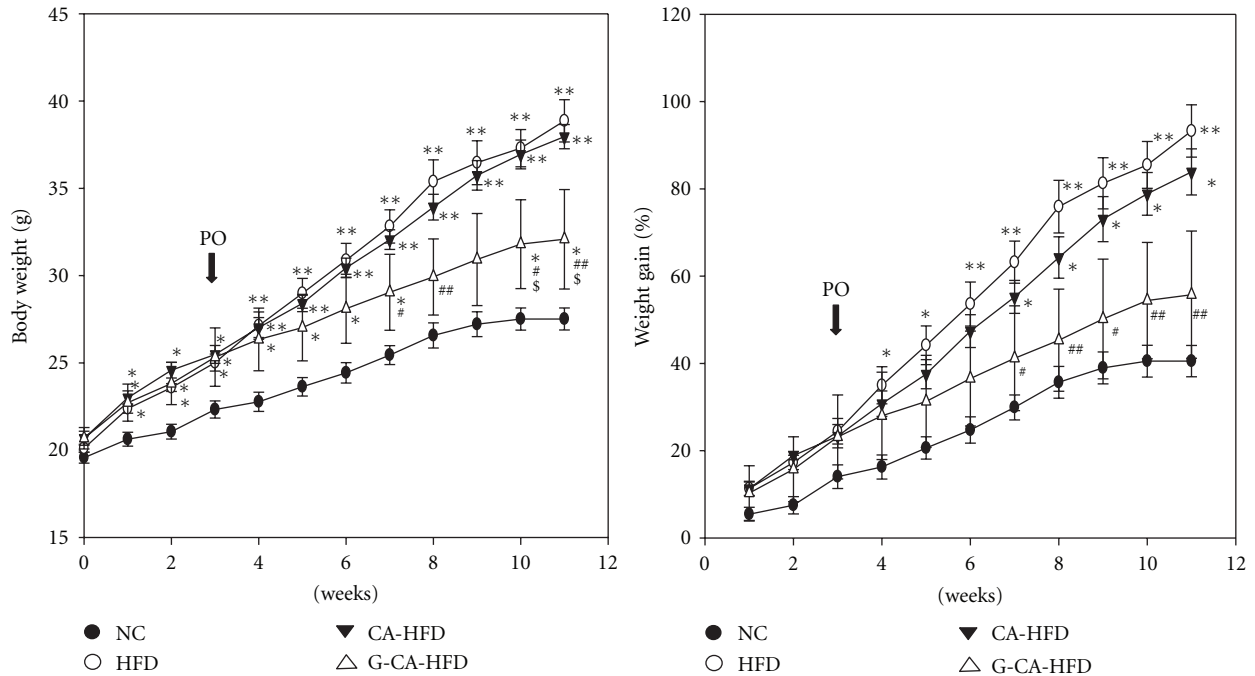
Polyphenolic component	CA	G-CA
	mg/g extract	mg/g extract
Phloroglucinol	0.80	3.17
Triphlorethol A	1.29	0.23
Eckol	12.98	4.72
Eckstolonol	12.78	0.13
Phlorofucofuroeckol A	11.04	2.57
Dieckol	16.56	1.12
6,6'-Bieckol	1.01	0.83
8,8'-Bieckol	0.00	1.79
Fucofuroeckol A	1.21	0.00
Others	42.33	85.44

2.14. Statistical Analysis. Data are presented as mean \pm SE. The significance of differences was analyzed with the 1-way ANOVA with the Duncan procedure using SPSS ver. 10.0 (SPSS Inc.) The value of statistical significance was set at $P < 0.05$.

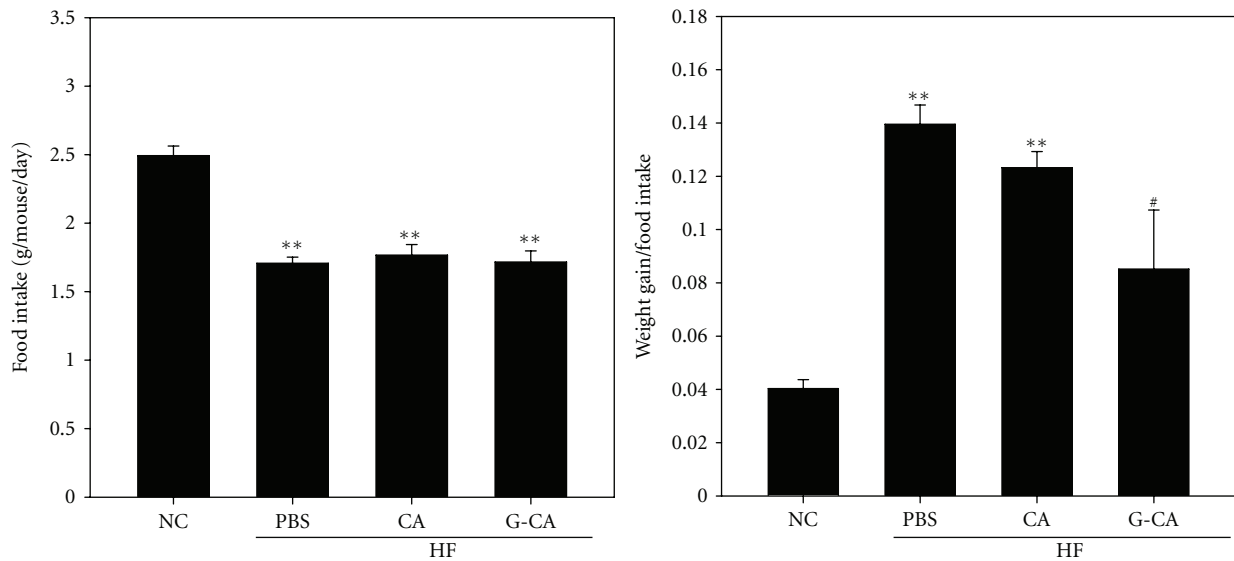
3. Results

3.1. Identification of Phlorotannins in CA and G-CA Extracts. Total polyphenolic contents of the EtOAc fraction of CA and G-CA was 68.78 and 79.70 mg/g, respectively. Phlorotannin composition was determined by HPLC analysis (Table 2). Eckol was abundant polyphenol in both G-CA and CA. Phloroglucinol content in G-CA was higher than that in CA, while triphlorethol A, eckol, eckstolonol, phlorofucofuroeckol A, and dieckol contents in CA were much higher than those in G-CA. 8,8'-bieckol and fucofuroeckol A were found only in G-CA and CA, respectively.

3.2. Reduction of Body Weight in G-CA-HFD Mice. To examine whether treatment with CA or G-CA affects body weight gain in HFD-induced obese mice, we measured the body weight in CA- or G-CA-treated mice. G-CA-HFD mice had significantly lower body weights and significantly less weight gain (40% decrease) as compared with the PBS-HFD group, whereas the CA-HFD group was not different from



(a)



(b)

FIGURE 1: Effect of CA or G-CA extracts on body weight and food intake. Three weeks after beginning a high-fat diet, C57BL6 mice were orally administered CA or G-CA extract (200 mg/kg body weight) or PBS daily for 8 weeks. (a) Body weights were monitored weekly. (b) Food intake was measured weekly. Values are the average weight of food consumed/mouse/day. NC: untreated, normal chow diet, $n = 7$; PBS: PBS-treated, high-fat diet (HFD), $n = 6$; CA: CA-treated, HFD, $n = 5$; and G-CA: G-CA-treated, HFD, $n = 5$. Values are mean \pm SE. * $P < 0.05$, ** $P < 0.01$ versus NC group; # $P < 0.05$, ## $P < 0.01$ versus PBS-HFD group; $^{\$}P < 0.05$ versus CA-HFD. PO is an abbreviation of per oral.

the PBS-HFD group (Figure 1(a)). Mice fed a HFD ate significantly less chow than mice fed a normal diet, and the amount of food consumed per day over the 8-week period was not significantly different among the PBS-HFD, CA-HFD, or G-CA-HFD groups (Figure 1(b) left). The food efficiency ratio of the G-CA-HFD mice was significantly lower than that of the PBS-HFD mice (Figure 1(b) right).

3.3. Reduction of Adiposity, ALT, and Cholesterol in G-CA-HFD Mice. Nuclear magnetic resonance measurements were conducted to evaluate body composition. At the end of the treatment, the total body fat content (Figure 2(a)) and the subcutaneous, epididymal, perirenal, and mesenteric fat pad weights (Figures 2(b)–2(e)) of G-CA-HFD mice were significantly reduced as compared with the PBS-HFD

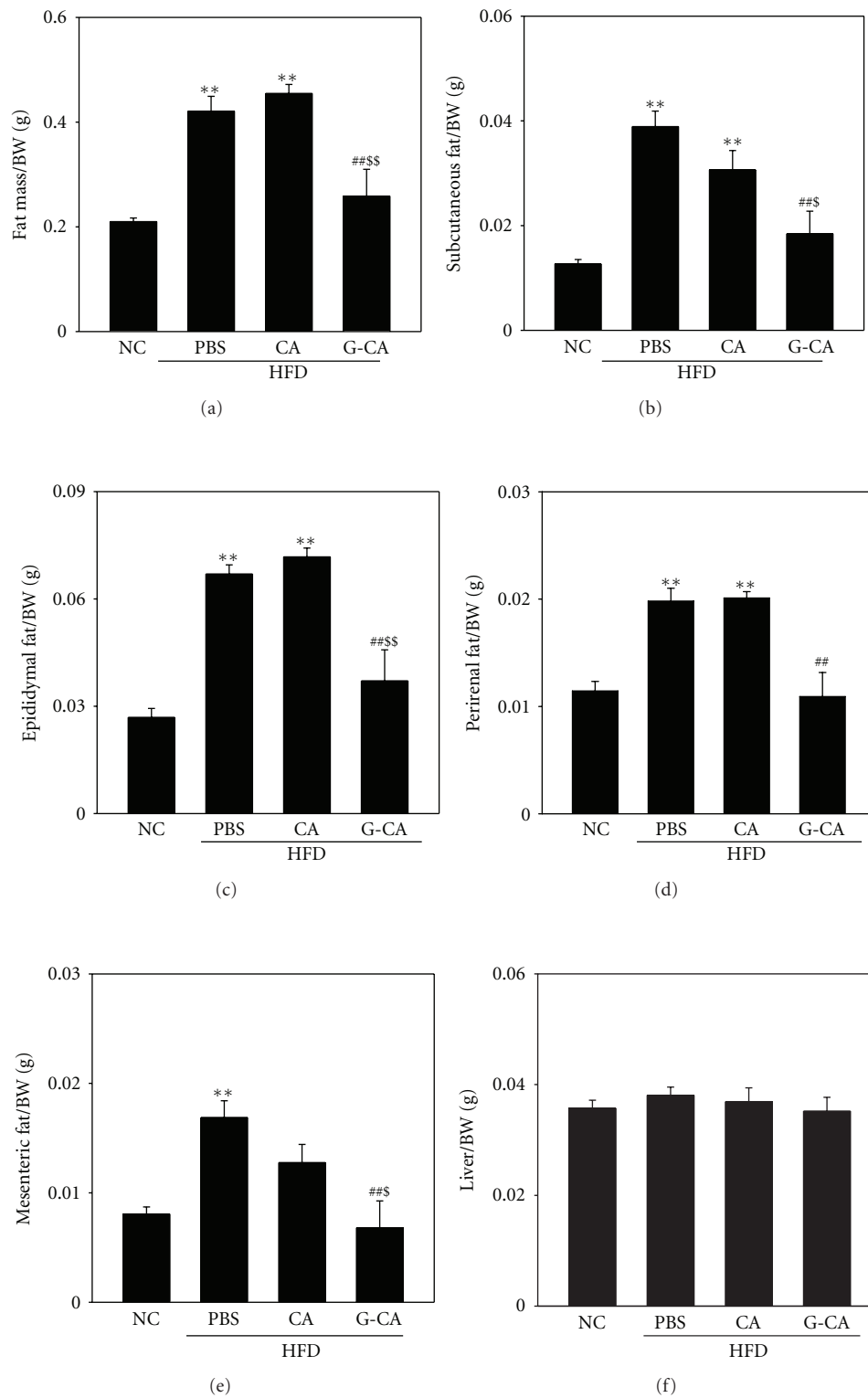


FIGURE 2: Effect of CA or G-CA extracts on total fat mass and fat tissue weight. Three weeks after beginning a high-fat diet, C57BL6 mice were orally administered CA or G-CA extract (200 mg/kg body weight) or PBS daily. (a) After 8 weeks of CA and G-CA treatment, total fat mass was measured by mini-spec. After 8 weeks of CA and G-CA treatment, ((b)–(e)) fat pads and (f) liver tissue were collected and weighed. Values are the average tissue weight as a proportion of body weight. NC: untreated, normal chow diet; PBS: PBS-treated, high-fat diet (HFD); CA: CA-treated, HFD; G-CA: G-CA-treated, HFD; $n = 5/\text{group}$. Values are mean \pm SE. ** $P < 0.01$ versus NC group; ## $P < 0.01$ versus PBS-HFD group; \$ $P < 0.05$, \$\$ $P < 0.01$ versus CA-HFD.

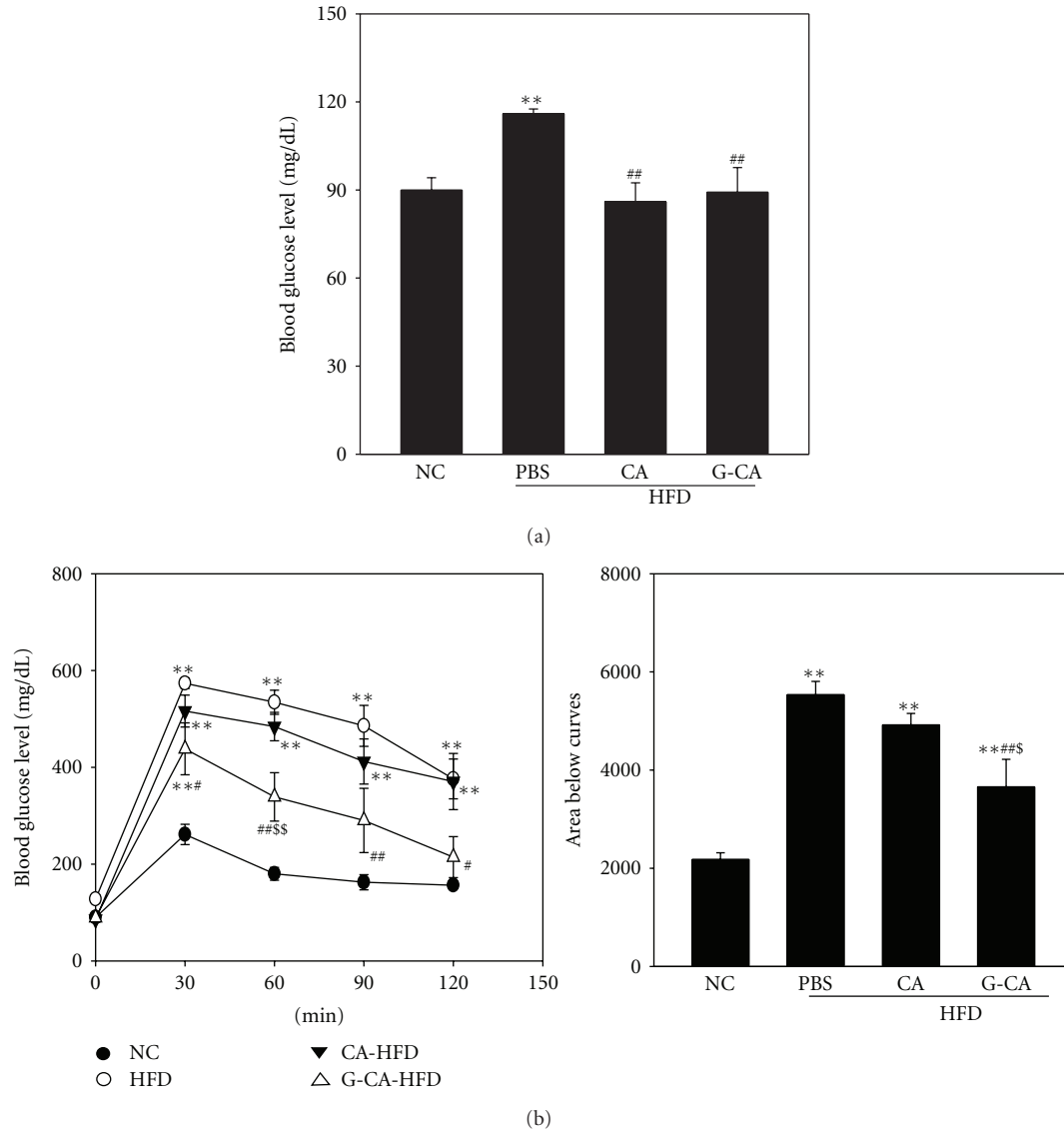


FIGURE 3: Effect of CA or G-CA extracts on blood glucose levels and glucose tolerance. Three weeks after beginning a high-fat diet, C57BL6 mice were orally administered CA or G-CA extract (200 mg/kg body weight) or PBS daily. At 7 weeks of treatment, (a) blood glucose levels were measured in mice fasted overnight ($n = 6-8$) and (b) intraperitoneal glucose tolerance tests were performed (200 mg/kg glucose body weight, $n = 5$). Values are mean \pm SE. NC: untreated, normal chow diet; PBS: PBS-treated, high-fat diet (HFD); CA: CA-treated, HFD; G-CA: G-CA-treated, HFD. Values are mean \pm SE. * $P < 0.05$, ** $P < 0.01$ versus NC group; # $P < 0.05$, ## $P < 0.01$ versus PBS-HFD group; \$ $P < 0.05$, \$\$ $P < 0.01$ versus CA-HFD.

group. The liver weights were not different among groups (Figure 2(f)). Plasma analysis showed that ALT, AST, total cholesterol, HDL-cholesterol, and LDL-cholesterol levels were significantly increased in PBS-HFD mice as compared with NC mice. Plasma ALT and cholesterol levels were significantly reduced in G-CA-HFD mice as compared with PBS-HFD mice. G-CA treatment did not affect plasma AST, triglycerides, HDL-cholesterol, or LDL-cholesterol levels compared with PBS-HFD mice (Table 3).

3.4. Reduction of Blood Glucose Levels in G-CA-HFD Mice. We measured blood glucose levels, because HFD-induced obese mice are a model for insulin resistance [18]. Plasma

blood glucose levels were significantly decreased in CA-HFD and G-CA-HFD mice compared with PBS-HFD mice at 7 weeks of treatment (Figure 3(a)). We also performed intraperitoneal glucose tolerance tests at 7 weeks. Blood glucose levels in the G-CA-HFD group were significantly lower at all time points following glucose injection compared with the PBS-HFD group (Figure 3(b), left). Area under the curve of the G-CA-HFD group was decreased 25.2% compared with the PBS-HFD group (Figure 3(b), right).

3.5. Increase in mRNA Expression of Adipogenesis-Related Genes in Adipose Tissue of G-CA-HFD Mice. In order to investigate whether CA or G-CA treatment changes

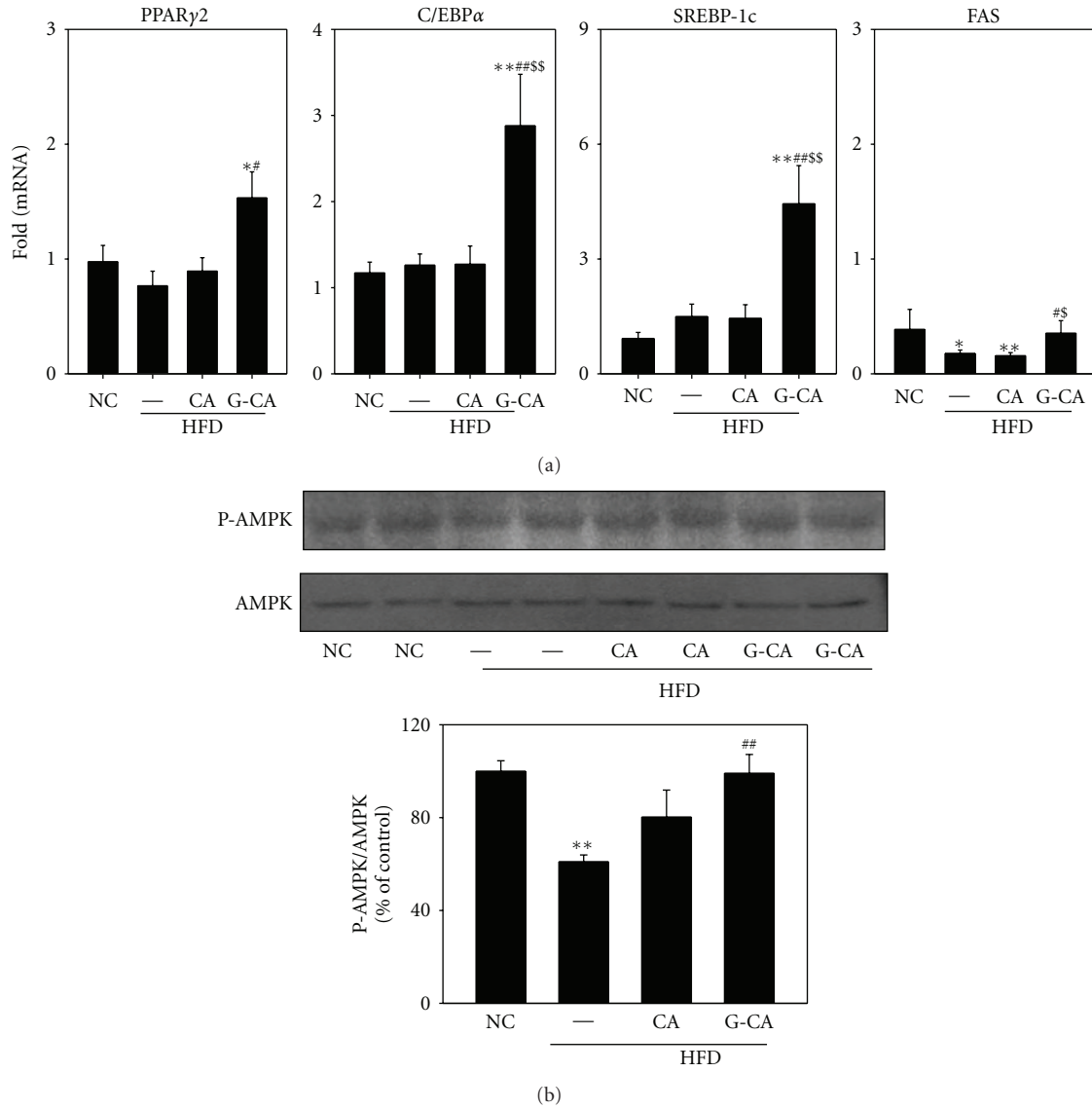


FIGURE 4: Effect of CA or G-CA extracts on adipogenic gene expression and AMPK phosphorylation. Three weeks after beginning a high-fat diet, C57BL6 mice were orally administered CA or G-CA extract (200 mg/kg body weight) or PBS daily for 8 weeks. (a) PPAR γ 2, C/EBP α , SREBP-1c, and Fas mRNA levels were measured in epididymal fat pads by quantitative real-time PCR. Values are expressed as fold change compared with the NC group. (b) Phospho (P)-AMPK and AMPK protein expression in epididymal fat pads was analyzed by western blot (upper panel) and quantified (lower panel). Values are mean \pm SE. NC: untreated, normal chow diet; PBS: PBS-treated, high-fat diet (HFD); CA: CA-treated, HFD; G-CA: G-CA-treated, HFD. * $P < 0.05$, ** $P < 0.01$ versus NC group; # $P < 0.05$, ## $P < 0.01$ versus PBS-HFD group; $^{\S}P < 0.05$, $^{\S\S}P < 0.01$ versus CA-HFD.

adipogenesis-related gene expression, we analyzed the expression of peroxisome proliferator-activated receptor (PPAR) γ 2, CCAAT-enhancer-binding protein (C/EBP) α , sterol regulatory element-binding protein (SREBP)-1c, and FAS mRNA in epididymal adipose tissue after 8 weeks of CA and G-CA treatment. mRNA levels for the adipogenic related transcription factors, PPAR γ 2, C/EBP α , and SREBP-1c, were not changed by HFD. The mRNA expression of these genes was significantly increased in G-CA-HFD mice compared with PBS-HFD mice, but not changed in CA-HFD mice (Figure 4(a)). FAS mRNA levels were significantly decreased in PBS-HFD mice and CA-HFD mice as compared with the

NC group and the G-CA-HFD group had significantly higher FAS mRNA levels as compared with PBS-HFD mice and CA-HFD mice (Figure 4(a)). Next we performed western blots to determine whether CA or G-CA treatment altered the phosphorylated protein levels of AMPK, which is involved in fatty acid oxidation. Phosphorylated AMPK levels of mice fed a HFD were decreased as compared with the NC group and whereas those of G-CA-HFD mice group were significantly increased (Figure 4(b)).

3.6. Decrease in mRNA Expression of Inflammatory Genes in G-CA-HFD Mice. Because obesity and type 2 diabetes

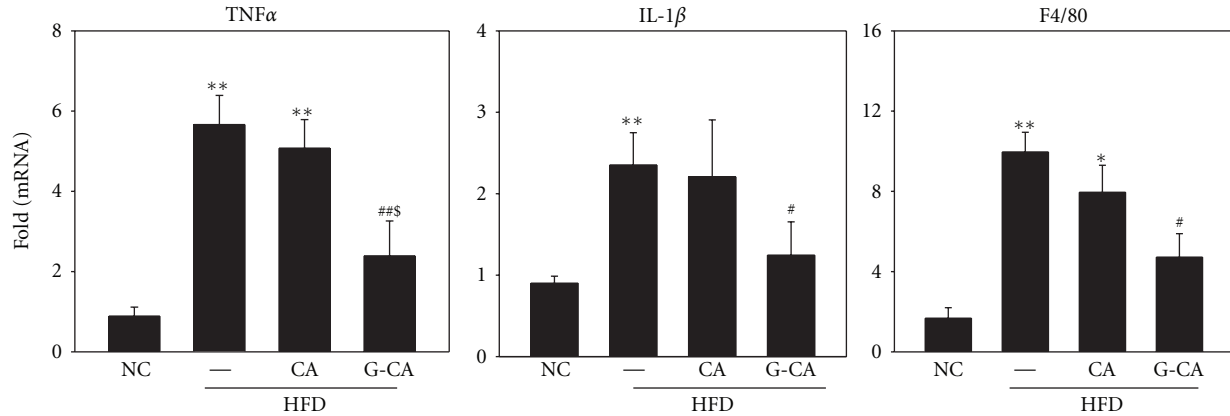


FIGURE 5: Effect of CA and G-CA extracts on inflammatory gene expression. Three weeks after beginning a high-fat diet, C57BL/6 mice were orally administered CA or G-CA extract (200 mg/kg body weight) or PBS daily for 8 weeks. TNF α , IL-1 β , and F4/80 mRNA levels were measured in epididymal fat pads. Values are expressed as fold change compared with the NC group. Values are mean \pm SE. NC: untreated, normal chow diet; PBS: PBS-treated, high-fat diet (HFD); CA: CA-treated, HFD; and G-CA: G-CA-treated, HFD. * $P < 0.05$, ** $P < 0.01$ versus NC group; # $P < 0.05$, ## $P < 0.01$ versus PBS-HFD group; \$ $P < 0.05$ versus CA-HFD.

TABLE 3: Plasma biochemical parameters.

	NC	PBS-HFD	CA-HFD	G-CA-HFD
ALT (U/L)	41.97 \pm 1.20	60.25 \pm 3.00**	46.83 \pm 4.76#	32.45 \pm 4.92##\$
AST (U/L)	77.77 \pm 20.26	147.23 \pm 14.73*	151.13 \pm 17.25*	138.48 \pm 20.24*
Cholesterol (mg/dL)	64.63 \pm 3.98	174.45 \pm 14.07**	163.25 \pm 8.16**	125.90 \pm 5.86***\$
Triglycerides (mg/dL)	61.13 \pm 5.90	76.18 \pm 5.27	87.85 \pm 14.36	66.03 \pm 9.09
HDL-cholesterol (mg/dL)	108.90 \pm 4.38	203.93 \pm 11.56**	189.28 \pm 3.42**	175.98 \pm 11.39**
LDL-cholesterol (mg/dL)	33.23 \pm 1.85	54.75 \pm 4.31*	58.58 \pm 9.38*	45.05 \pm 3.82

NC: untreated, normal chow diet, PBS-HFD: PBS-treated, high-fat diet, CA-HFD: CA-treated, high-fat diet, and G-CA-HFD: G-CA-treated, high-fat diet. * $P < 0.05$, ** $P < 0.01$ versus NC group; # $P < 0.05$, ## $P < 0.01$ versus PBS-HFD group; \$ $P < 0.05$ versus CA-HFD.

are accompanied by chronic inflammation, inflammatory cytokine levels are increased in HFD-induced obese mice [19]. Therefore, we analyzed whether CA or G-CA treatment can attenuate inflammatory signaling in the epididymal adipose tissue of HFD-induced obese mice. mRNA levels of the cytokines, tumor necrosis factor (TNF)- α , interleukin (IL)-1 β and the macrophage marker F4/80 were significantly increased in PBS-HFD mice as compared with NC mice. G-CA-HFD mice had significantly reduced TNF- α , IL-1 β , and F4/80 mRNA levels compared with PBS-HFD mice (Figure 5).

3.7. Reduced Intrahepatic Lipid Accumulation and Hepatic Lipogenic Gene mRNA Expression in G-CA-HFD Mice. Because the elevation of hepatic lipid during a HFD causes nonalcoholic fatty liver [20], we assessed the lipid content in frozen sections of liver. Lipid droplet accumulation was obviously increased in PBS-HFD mice, whereas lipid droplets were reduced in CA-HFD and G-CA-HFD mice compared with PBS-HFD (Figure 6(a)). Hepatic triglyceride levels were significantly increased in PBS-HFD mice as compared with NC mice. However, the hepatic triglyceride content in CA-HFD and G-CA-HFD mice was significantly reduced as compared with PBS-HFD mice, 19% and 32%, respectively (Figure 6(b)). When we examined the mRNA expression of

genes that control lipid metabolism in the liver, we found that ACC1, FAS, and SREBP-1c mRNA levels were significantly increased in PBS-HFD mice as compared with NC mice. The expression of these genes was significantly decreased in G-CA-HFD mice as compared with PBS-HFD mice, and FAS levels were also significantly decreased in CA-HFD mice (Figure 6(c)).

4. Discussion

In the present study, we investigated the antiobesity and glucose-lowering effects of extracts from the brown alga, *Ecklonia cava* in HFD-induced obese mice and compared the activity of algae from different areas: Jeju (CA) and Gijang (G-CA). After 8 weeks of treatment, we observed a significant antiobesity effect of G-CA extract in HFD-induced obese mice, evidenced by decrease of body weight gain relative to PBS-HFD mice, without any change in food intake. Total fat mass and peripheral fat weight were also decreased in G-CA-treated mice. In contrast, CA treatment did not result in significant reductions in either body weight or fat mass, suggesting that G-CA has a more potent antiobesity effect than CA. Both extracts significantly reduced fasting blood glucose; however G-CA had a more potent glucose-lowering effect than CA as determined by glucose tolerance tests.

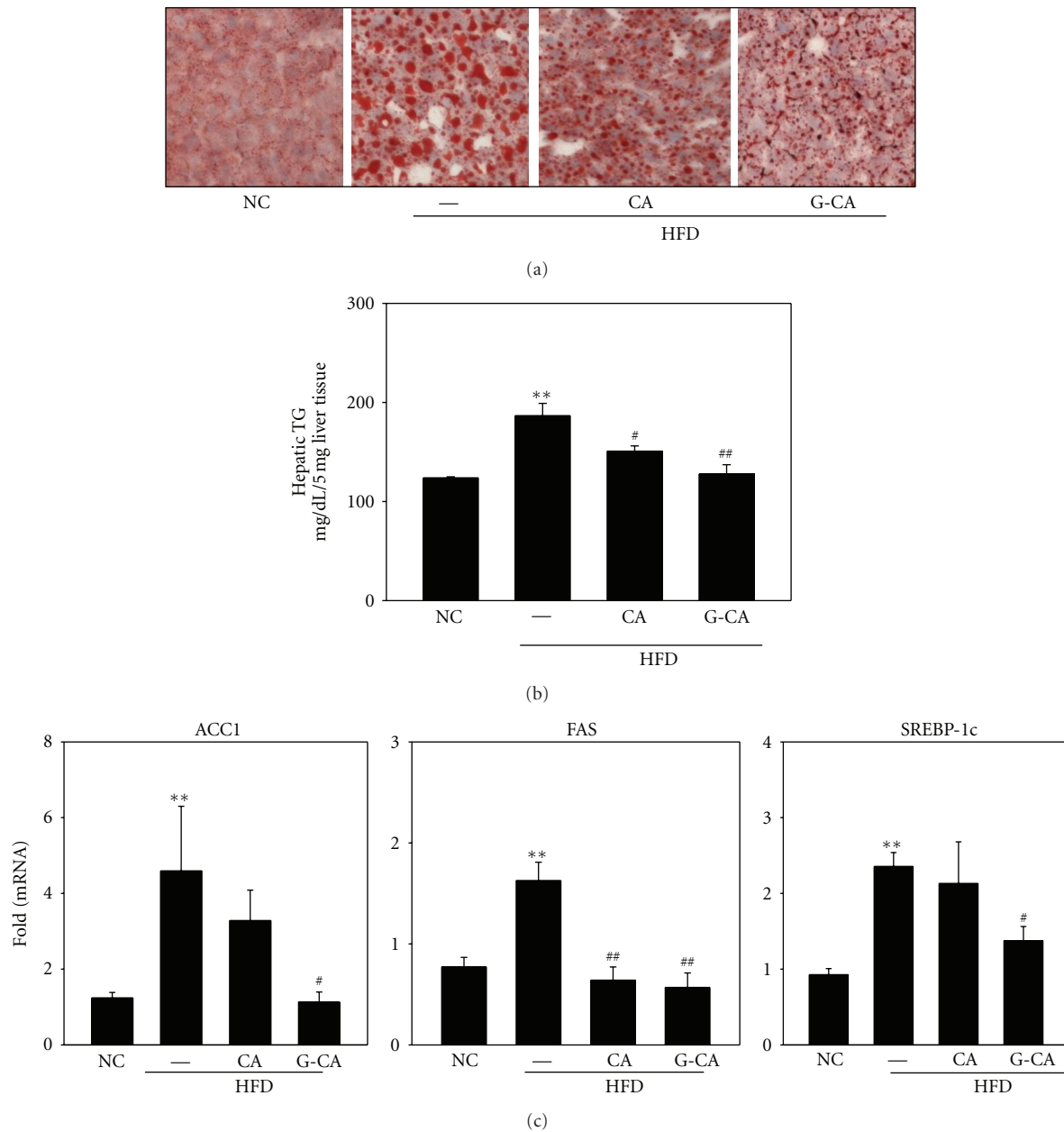


FIGURE 6: Effects of CA and G-CA extracts on hepatic steatosis. Three weeks after beginning a high-fat diet, C57BL6 mice were orally administered CA or G-CA extract (200 mg/kg body weight) or PBS daily for 8 weeks. (a) Oil red O staining was performed on frozen liver sections. (b) Hepatic triglyceride (TG) content was measured in liver tissue. (c) ACC1, Fas, and SREBP1c mRNA levels were analyzed in liver tissue. Values are expressed as fold change compared with the NC group. Values are mean \pm SE. NC: untreated, normal chow diet; PBS: PBS-treated, high-fat diet (HFD); CA: CA-treated, HFD; and G-CA: G-CA-treated, HFD. ** $P < 0.01$ compared with NC group. # $P < 0.05$, ## $P < 0.01$ compared with PBS-HFD group.

The adipose tissue plays an important role in whole-body energy homeostasis, and thus, its functional disorder has relevance for metabolic syndrome and diabetes. The transcription factors PPAR γ and C/EBP α are key regulators of adipocyte differentiation and promotion of lipid storage. SREBP1 regulates lipogenesis-related gene expression such as FAS and activates PPAR γ gene expression [21]. In our study, the mRNA expression of adipogenesis-related genes such as PPAR γ , C/EBP α , SREBP-1c and FAS did not increase,

but rather slightly decreased in epididymal fat pads as a result of the HFD. This may be part of an adaptive response to limit further fat deposition during a prolonged HFD [22], and others have also found that PPAR γ , C/EBP α and SREBP mRNA levels were decreased in the adipose tissue of a different obese mouse model [23, 24]. Furthermore, mRNA levels of SREBP-1c in obese patients were lower than those in normal weight subjects, but mRNA levels increased along with weight loss [25, 26]. The reduction of SREBP-1c

expression has relevance to lowered action or concentration of insulin, modifiable along with weight reduction [25]. We found that G-CA treatment increased the mRNA expression levels of PPAR γ , C/EBP α , SREBP-1c, and FAS in epididymal fat pads of HFD-fed mice. As well, G-CA treatment increased the phosphorylation of AMPK, a key regulator of fatty acid oxidation. These results suggest that G-CA treatment improved intracellular fatty acid metabolism by improving adipogenic gene expression and fatty acid oxidation.

Inflammation and macrophage infiltration in adipose tissue is associated with obesity and insulin resistance [27–29]. Cytokines produced from infiltrated macrophages and adipocytes regulate adipose tissue metabolism [30]. The inflammatory cytokine, TNF- α , decreases SREBP1 expression levels in adipose tissue, thus disturbing adipogenic gene expression and adipogenesis regulation [31]. As cytokines released from adipose tissue lead to insulin resistance and β -cell failure [32, 33], increase of TNF- α and IL-1 β expression is important in the pathogenesis of type 2 diabetes. We found that mRNA expression levels of TNF- α , IL-1 β and the macrophage maker, F4/80, were increased in HFD-fed mice but were decreased in G-CA-treated mice. The anti-inflammatory effect of G-CA may contribute to the reduction of obesity and improvement of glucose tolerance.

Nonalcoholic fatty liver disease is associated with metabolic syndrome. Excessive triglyceride accumulation in hepatocytes changes lipid metabolism in the liver [34]. In our study, the HFD increased fat and triglyceride accumulation and lipogenic gene expression; however, both CA and G-CA treatment lowered these measures, with G-CA being more effective than CA. Serum ALT levels, a marker of liver injury, were also significantly increased in HFD-fed mice, but decreased in G-CA-treated mice. These results indicate that G-CA and CA have an ameliorating effect on fatty liver through the impaired hepatic dyslipidemia and G-CA is more effective than CA.

Ecklonia cava has beneficial bioactive components including phlorotannins and polysaccharides such as alginic acid, fucoidans, pyropheophytin, tripeptides, and oxylipin. Of these, phlorotannins including phloroglucinol, phloroglucinol tetramer, eckol, phlorofucofuroeckol A, dieckol, 8,8'-bieckol, and dioxinodehydroeckol have been studied for their pharmacological activity. In our study, G-CA was consistently more effective than CA in reducing obesity, glucose levels, and related biochemical parameters in HFD-fed mice. The content of active components in some plants depends on environmental conditions, weather, geographic location, and soil conditions. According to our HPLC analysis, CA and G-CA contain phloroglucinol, eckol, phlorofucofuroeckol A, and dieckol in common as major components. However, triphlorethol A and eckstolonol were found as major components in CA while they were minor components in G-CA. In addition, 8,8'-bieckol was found as major components in G-CA. Total polyphenol concentration of G-CA was higher than that of CA. Whether these differences in content and kinds of active components contribute to different pharmacological effects between CA and G-CA remains to be tested in the future.

5. Conclusion

This study showed that G-CA improved obesity and glucose levels by anti-inflammatory actions and improvement of lipid metabolism. Therefore, G-CA have the potential to be developed as functional food and antiobesity therapeutic agent.

Acknowledgments

This research was financially supported by a Grant (no. 70008305) from the Ministry of Knowledge Economy (MKE) and Korea Institute for Advancement of Technology (KIAT) through the Research and Development for Regional Industry and a Grant (no. 20100293) from the Technology Development Program for Fisheries, Ministry for Food, Agriculture, Forestry and Fisheries. The authors thank Dr. Ann Kyle for editorial assistance.

References

- [1] T. H. Jafar, N. Chaturvedi, and G. Pappas, "Prevalence of overweight and obesity and their association with hypertension and diabetes mellitus in an Indo-Asian population," *CMAJ*, vol. 175, no. 9, pp. 1071–1077, 2006.
- [2] K. M. Flegal, M. D. Carroll, C. L. Ogden, and L. R. Curtin, "Prevalence and trends in obesity among US adults, 1999–2008," *JAMA*, vol. 303, no. 3, pp. 235–241, 2010.
- [3] S. Obici and L. Rossetti, "Minireview: nutrient sensing and the regulation of insulin action and energy balance," *Endocrinology*, vol. 144, no. 12, pp. 5172–5178, 2003.
- [4] T. Gurevich-Panigrahi, S. Panigrahi, E. Wiechec, and M. Los, "Obesity: pathophysiology and clinical management," *Current Medicinal Chemistry*, vol. 16, no. 4, pp. 506–521, 2009.
- [5] N. Vazzana, F. Santilli, S. Sestili, C. Cuccurullo, and G. Davi, "Determinants of increased cardiovascular disease in obesity and metabolic syndrome," *Current Medicinal Chemistry*, vol. 18, no. 34, pp. 5267–5280, 2011.
- [6] W. I. Youssef and A. J. McCullough, "Steatohepatitis in obese individuals," *Bailliere's Best Practice and Research in Clinical Gastroenterology*, vol. 16, no. 5, pp. 733–747, 2002.
- [7] K. C. Hofbauer and J. R. Nicholson, "Pharmacotherapy of obesity," *Experimental and Clinical Endocrinology and Diabetes*, vol. 114, no. 9, pp. 475–484, 2006.
- [8] W. A. J. P. Wijesinghe and Y.-J. Jeon, "Exploiting biological activities of brown seaweed *Ecklonia cava* for potential industrial applications: a review," *International Journal of Food Sciences and Nutrition*, vol. 63, no. 2, pp. 225–235, 2012.
- [9] K. A. Kang, K. H. Lee, S. Chae et al., "Triphlorethol-A from *Ecklonia cava* protects V79-4 lung fibroblast against hydrogen peroxide induced cell damage," *Free Radical Research*, vol. 39, no. 8, pp. 883–892, 2005.
- [10] K. A. Kang, K. H. Lee, S. Chae et al., "Eckol isolated from *Ecklonia cava* attenuates oxidative stress induced cell damage in lung fibroblast cells," *FEBS Letters*, vol. 579, no. 28, pp. 6295–6304, 2005.
- [11] K. Kang, J. H. Hye, H. H. Dong et al., "Antioxidant and antiinflammatory activities of ventol, a phlorotannin-rich natural agent derived from *Ecklonia cava*, and its effect on proteoglycan degradation in cartilage explant culture," *Research Communications in Molecular Pathology and Pharmacology*, vol. 115–116, pp. 77–95, 2004.

- [12] S. J. Park, G. Ahn, N. H. Lee, J. W. Park, Y. J. Jeon, and Y. Jee, "Phloroglucinol (PG) purified from *Ecklonia cava* attenuates radiation-induced apoptosis in blood lymphocytes and splenocytes," *Food and Chemical Toxicology*, vol. 49, no. 9, pp. 2236–2242, 2011.
- [13] I. Wijesekara, N. Y. Yoon, and S. K. Kim, "Phlorotannins from *Ecklonia cava* (Phaeophyceae): biological activities and potential health benefits," *BioFactors*, vol. 36, no. 6, pp. 408–414, 2010.
- [14] C. Kang, Y. B. Jin, H. Lee et al., "Brown alga *Ecklonia cava* attenuates type 1 diabetes by activating AMPK and Akt signaling pathways," *Food and Chemical Toxicology*, vol. 48, no. 2, pp. 509–516, 2010.
- [15] S. H. Lee, J. S. Han, S. J. Heo, J. Y. Hwang, and Y. J. Jeon, "Protective effects of dieckol isolated from *Ecklonia cava* against high glucose-induced oxidative stress in human umbilical vein endothelial cells," *Toxicology in Vitro*, vol. 24, no. 2, pp. 375–381, 2010.
- [16] S.-H. Lee, K.-H. Min, J.-S. Han et al., "Effects of brown alga, *Ecklonia cava* on glucose and lipid metabolism in C57BL/KsJ-db/db mice, a model of type 2 diabetes mellitus," *Food and Chemical Toxicology*, vol. 50, no. 3-4, pp. 575–582, 2012.
- [17] P. Sanoner, S. Guyot, N. Marnet, D. Molle, and J. F. Drilleau, "Polyphenol profiles of French cider apple varieties (*Malus domestica* sp.)," *Journal of Agricultural and Food Chemistry*, vol. 47, no. 12, pp. 4847–4853, 1999.
- [18] W. Huang, R. Bansode, M. Mehta, and K. D. Mehta, "Loss of protein kinase C β function protects mice against diet-induced obesity and development of hepatic steatosis and insulin resistance," *Hepatology*, vol. 49, no. 5, pp. 1525–1536, 2009.
- [19] S. E. Shoelson, L. Herrero, and A. Naaz, "Obesity, inflammation, and insulin resistance," *Gastroenterology*, vol. 132, no. 6, pp. 2169–2180, 2007.
- [20] A. A. Toyé, M. E. Dumas, C. Blancher et al., "Subtle metabolic and liver gene transcriptional changes underlie diet-induced fatty liver susceptibility in insulin-resistant mice," *Diabetologia*, vol. 50, no. 9, pp. 1867–1879, 2007.
- [21] B. M. Spiegelman and J. S. Flier, "Adipogenesis and obesity: rounding out the big picture," *Cell*, vol. 87, no. 3, pp. 377–389, 1996.
- [22] S. J. Kim, J. Y. Jung, H. W. Kim, and T. Park, "Anti-obesity effects of *Juniperus chinensis* extract are associated with increased AMP-activated protein kinase expression and phosphorylation in the visceral adipose tissue of rats," *Biological and Pharmaceutical Bulletin*, vol. 31, no. 7, pp. 1415–1421, 2008.
- [23] S. T. Nadler, J. P. Stoehr, K. L. Schueler, G. Tanimoto, B. S. Yandell, and A. D. Attie, "The expression of adipogenic genes is decreased in obesity and diabetes mellitus," *Proceedings of the National Academy of Sciences of the United States of America*, vol. 97, no. 21, pp. 11371–11376, 2000.
- [24] A. Soukas, P. Cohen, N. D. Soccia, and J. M. Friedman, "Leptin-specific patterns of gene expression in white adipose tissue," *Genes and Development*, vol. 14, no. 8, pp. 963–980, 2000.
- [25] M. Kolehmainen, H. Vidal, E. Alhava, and M. I. J. Uusitupa, "Sterol regulatory element binding protein 1c (SREBP-1c) expression in human obesity," *Obesity Research*, vol. 9, no. 11, pp. 706–712, 2001.
- [26] F. Diraison, E. Dusserre, H. Vidal, M. Sothier, and M. Beylot, "Increased hepatic lipogenesis but decreased expression of lipogenic gene in adipose tissue in human obesity," *American Journal of Physiology*, vol. 282, no. 1, pp. E46–E51, 2002.
- [27] C. Pang, Z. Gao, J. Yin, J. Zhang, W. Jia, and J. Ye, "Macrophage infiltration into adipose tissue may promote angiogenesis for adipose tissue remodeling in obesity," *American Journal of Physiology*, vol. 295, no. 2, pp. E313–E322, 2008.
- [28] K. Sun, C. M. Kusminski, and P. E. Scherer, "Adipose tissue remodeling and obesity," *The Journal of Clinical Investigation*, vol. 121, no. 6, pp. 2094–2101, 2011.
- [29] S. P. Weisberg, D. McCann, M. Desai, M. Rosenbaum, R. L. Leibel, and A. W. Ferrante Jr., "Obesity is associated with macrophage accumulation in adipose tissue," *The Journal of Clinical Investigation*, vol. 112, no. 12, pp. 1796–1808, 2003.
- [30] D. Lacasa, S. Taleb, M. Keophiphath, A. Miranville, and K. Clement, "Macrophage-secreted factors impair human adipogenesis: involvement of proinflammatory state in preadipocytes," *Endocrinology*, vol. 148, no. 2, pp. 868–877, 2007.
- [31] C. Sewter, D. Berger, R. V. Considine et al., "Human obesity and type 2 diabetes are associated with alterations in SREBP1 isoform expression that are reproduced ex vivo by tumor necrosis factor- α ," *Diabetes*, vol. 51, no. 4, pp. 1035–1041, 2002.
- [32] P. Sartipy and D. J. Loskutoff, "Monocyte chemoattractant protein 1 in obesity and insulin resistance," *Proceedings of the National Academy of Sciences of the United States of America*, vol. 100, no. 12, pp. 7265–7270, 2003.
- [33] Y. F. Zhao, D. D. Feng, and C. Chen, "Contribution of adipocyte-derived factors to beta-cell dysfunction in diabetes," *International Journal of Biochemistry and Cell Biology*, vol. 38, no. 5-6, pp. 804–819, 2006.
- [34] Y. Imai, G. M. Varela, M. B. Jackson, M. J. Graham, R. M. Crooke, and R. S. Ahima, "Reduction of hepatosteatosis and lipid levels by an adipose differentiation-related protein antisense oligonucleotide," *Gastroenterology*, vol. 132, no. 5, pp. 1947–1954, 2007.

Review Article

Green Tea Polyphenols for the Protection against Renal Damage Caused by Oxidative Stress

Takako Yokozawa,^{1,2} Jeong Sook Noh,¹ and Chan Hum Park¹

¹Institute of Natural Medicine, University of Toyama, Toyama 930-0194, Japan

²Organization for Promotion of Regional Collaboration, University of Toyama, Toyama 930-8555, Japan

Correspondence should be addressed to Takako Yokozawa, yokozawa@inm.u-toyama.ac.jp

Received 24 February 2012; Accepted 17 April 2012

Academic Editor: William C. S. Cho

Copyright © 2012 Takako Yokozawa et al. This is an open access article distributed under the Creative Commons Attribution License, which permits unrestricted use, distribution, and reproduction in any medium, provided the original work is properly cited.

Green tea, prepared from the leaves of *Camellia sinensis* L., is a beverage that is popular worldwide. Polyphenols in green tea have been receiving much attention as potential compounds for the maintenance of human health due to their varied biological activity and low toxicity. In particular, the contribution of antioxidant activity to the prevention of diseases caused by oxidative stress has been focused upon. Therefore, in this study, we investigated the effects of (–)-epigallocatechin 3-*O*-gallate and (–)-epigallocatechin 3-*O*-gallate, which account for a large fraction of the components of green tea polyphenol, on oxidative stress-related renal disease. Our observations suggest that green tea polyphenols have a beneficial effect on pathological states related to oxidative stress of the kidney.

1. Background

Clinical and experimental studies have resulted in extensive discussions of the link between renal disease and oxidative stress, which is directly or indirectly derived from various pathological conditions such as hyperglycemia, free radical-generating toxic substances, and inflammation. The free radicals are highly reactive and harmful to lipids, proteins, and nucleic acids, resulting in structural and functional impairment. Increased levels of endproducts mediated by the reactions between biomolecules and free radicals, such as malondialdehyde, 3-nitrotyrosine, and 8-hydroxy-2'-deoxyguanosine, were observed with various pathological phenomena, such as acute renal failure and hemodialysis [1–4]. Inhibitors of free radicals and antioxidants have also been shown to protect against renal damage in a number of studies [5].

Green tea polyphenols have been shown to act as metal chelators, preventing the metal-catalyzed formation of radical species, antioxidant enzyme modulators, and scavengers of free radicals, including the hydroxyl radical ($\bullet\text{OH}$), superoxide anion (O_2^-), nitric oxide (NO), and peroxynitrite (ONOO^-) [6–12]. These antioxidant activities

are considered to be closely related to their protective effects against various diseases, including renal disease, arteriosclerosis, cancer, and inflammation caused by lipid peroxidation and excessive free radical production [13]. The polyphenolic compounds of green tea mainly comprise (–)-epigallocatechin 3-*O*-gallate, (–)-epicatechin 3-*O*-gallate, (–)-epigallocatechin, and (–)-epicatechin, which are classified as the flavan-3-ol class of flavonoids. This paper gives a review of our recent findings [14–16], with emphasis on the therapeutic potential of the polyphenols of green tea in a useful experimental model of renal damage.

2. (–)-Epicatechin 3-*O*-gallate and ONOO^- -Mediated Renal Damage

Evidence for the role of reactive oxygen and nitrogen metabolites in the pathogenesis of renal diseases has accumulated, and ONOO^- formed in vivo from O_2^- and NO has been suggested to be an important causative agent in the pathogenesis of cellular damage and renal dysfunction [17, 18]. The pathological effects of ONOO^- and its decomposition product, $\bullet\text{OH}$, contribute to the antioxidant

TABLE 1: Effect of (–)-epicatechin 3-O-gallate and free radical inhibitors on plasma NO and O₂[–] radicals in rats.

Group	NO (μM)	O ₂ [–] (O.D.)
Sham operation	1.71 ± 0.18	0.315 ± 0.013
LPS plus ischemia-reperfusion		
Control	15.33 ± 0.72 ^b	0.371 ± 0.011 ^a
(–)-Epicatechin 3-O-gallate (10 mg/kg B.W.)	15.02 ± 1.15 ^b	0.377 ± 0.019 ^b
(–)-Epicatechin 3-O-gallate (20 mg/kg B.W.)	14.24 ± 0.33 ^b	0.401 ± 0.008 ^b
Ebselen (5 mg/kg B.W.)	15.98 ± 1.35 ^b	0.345 ± 0.007
Uric acid (62.5 mg/kg B.W.)	15.08 ± 1.15 ^b	0.360 ± 0.026 ^a
SOD (10,000 U/kg B.W.)	19.04 ± 1.72 ^{b,d}	0.336 ± 0.016 ^c
L-N ⁶ -(1-iminoethyl)lysine hydrochloride (3 mg/kg B.W.)	3.39 ± 0.25 ^e	0.363 ± 0.022 ^a

Significance: ^a*P* < 0.01, ^b*P* < 0.001 versus sham operation values; ^c*P* < 0.05, ^d*P* < 0.01, ^e*P* < 0.001 versus LPS plus ischemia-reperfused control values.

depletion, alterations of the protein structure and function by tyrosine nitration, and oxidative damage observed in human diseases and animal models of diseases [19–23].

The protective effect of (–)-epicatechin 3-O-gallate against ONOO[–]-mediated damage was examined using an animal model and cell culture system. This study was also carried out to elucidate whether the effect of (–)-epicatechin 3-O-gallate is distinct from that of several well-known free radical inhibitors, the ONOO[–] inhibitors ebselen and uric acid, O₂[–] scavenger copper zinc superoxide dismutase (CuZnSOD), and the selective inducible NO synthase (iNOS) inhibitor L-N⁶-(1-iminoethyl)lysine hydrochloride. To generate ONOO[–], male Wistar rats (10-week-old, male) were subjected to ischemia-reperfusion (occlusion of the renal artery and vein with clamps) together with lipopolysaccharide (LPS) injection.

In this study, the significant stimulation of NO and O₂[–] generation in response to the LPS injection plus ischemia-reperfusion process declined markedly after treatment with L-N⁶-(1-iminoethyl)lysine hydrochloride and CuZnSOD, respectively (Table 1). (–)-Epicatechin 3-O-gallate, however, did not reverse the elevations in the plasma NO and O₂[–] levels resulting from LPS plus ischemia-reperfusion. This suggests that (–)-epicatechin 3-O-gallate does not act as a scavenger of the ONOO[–] precursors NO and O₂[–]. In light of these results, we hypothesized that the protective activity of (–)-epicatechin 3-O-gallate against ONOO[–] could be attributed to the direct scavenging of ONOO[–], and so we evaluated the levels of 3-nitrotyrosine and myeloperoxidase (MPO) activity as indicators of ONOO[–] formation.

The LPS plus ischemia-reperfusion process led to elevation of the plasma 3-nitrotyrosine level in rats, suggesting that oxidative damage due to the formation of ONOO[–] had occurred (Figure 1) and the cellular formation of ONOO[–] increased by 3-morpholinonydnonimine (SIN-1) treatment (Figure 2). However, (–)-epicatechin 3-O-gallate reduced nitrotyrosine formation markedly in a dose-dependent manner compared with ebselen and CuZnSOD. The activity of (–)-epicatechin 3-O-gallate was comparable with that of L-N⁶-(1-iminoethyl)lysine hydrochloride, although (–)-epicatechin 3-O-gallate did not scavenge NO (Figure 1 and Table 1). The magnitudes of the significant elevations of ONOO[–] production in the cellular system were decreased

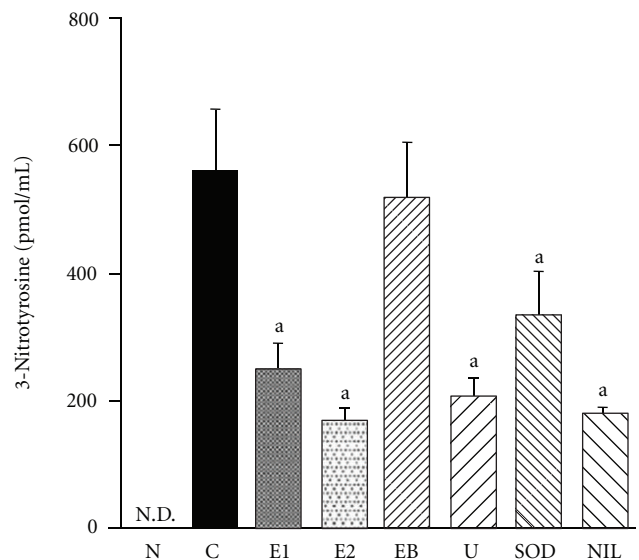


FIGURE 1: Effect of (–)-epicatechin 3-O-gallate and free radical inhibitors on plasma 3-nitrotyrosine level in rats. N, sham operation; C, LPS plus ischemia-reperfusion; E1, LPS plus ischemia-reperfusion after (–)-epicatechin 3-O-gallate (10 mg/kg body weight); E2, LPS plus ischemia-reperfusion after (–)-epicatechin 3-O-gallate (20 mg/kg body weight); EB, LPS plus ischemia-reperfusion after ebselen (5 mg/kg body weight); U, LPS plus ischemia-reperfusion after uric acid (62.5 mg/kg body weight); SOD, LPS plus ischemia-reperfusion after CuZnSOD (10,000 U/kg body weight); NIL, LPS plus ischemia-reperfusion after L-N⁶-(1-iminoethyl)lysine hydrochloride (3 mg/kg body weight). N.D., not detectable. Significance: ^a*P* < 0.001 versus LPS plus ischemia-reperfused control values.

by (–)-epicatechin 3-O-gallate treatment (Figure 2). Taken together, these findings indicate that (–)-epicatechin 3-O-gallate scavenges ONOO[–] directly but not its precursors NO and O₂[–]. In addition, the elevation of MPO activity was reversed by the administration of (–)-epicatechin 3-O-gallate, uric acid, and SOD but not by that of L-N⁶-(1-iminoethyl)lysine hydrochloride (Figure 3). We consider that the reduction of MPO activity by (–)-epicatechin 3-O-gallate ameliorated ONOO[–]-induced oxidative damage by inhibiting protein nitration and lipid peroxidation through a

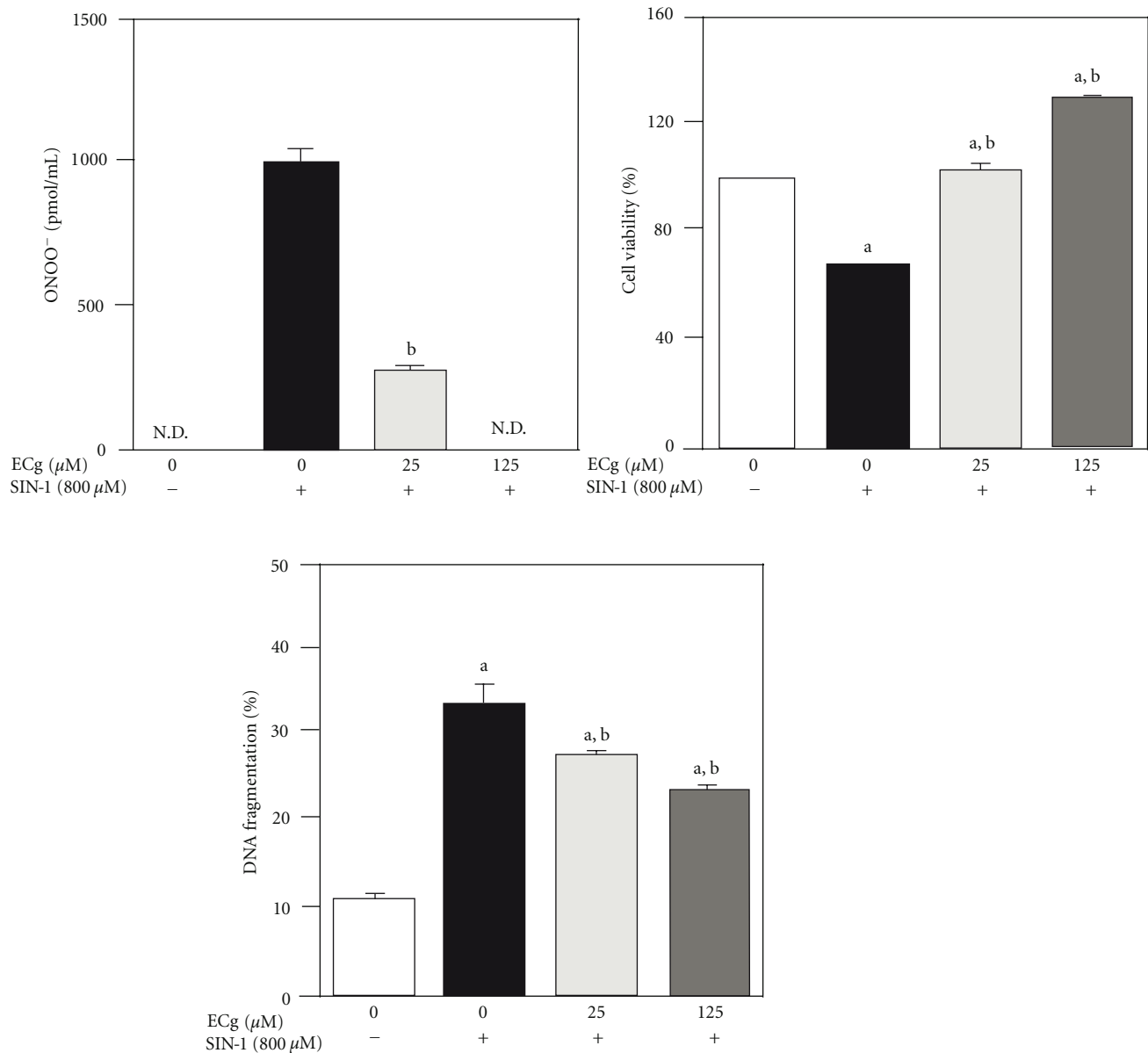


FIGURE 2: Effect of (–)-epicatechin 3-O-gallate on SIN-1-induced ONOO⁻ formation, viability, and DNA fragmentation in renal epithelial cells, LLC-PK₁. N.D., not detectable. Significance: ^a*P* < 0.001 versus no treatment values; ^b*P* < 0.001 versus SIN-1 treatment values.

mechanism distinct from that of L-N⁶-(1-iminoethyl)lysine hydrochloride, which actually increased MPO activity. In addition, uric acid acted in a similar way to (–)-epicatechin 3-O-gallate as a direct scavenger of ONOO⁻ through the inhibition of 3-nitrotyrosine and MPO activity, and not as a scavenger of ONOO⁻ precursors (Figures 1 and 3).

The antioxidative defense system was significantly suppressed by the excessive increase of ONOO⁻ resulting from the LPS plus ischemia-reperfusion process. The administration of (–)-epicatechin 3-O-gallate resulted in concentration-dependent elevations of the activities of the antioxidative enzymes, SOD, catalase, and glutathione peroxidase (GSH-Px), and the cellular antioxidant reduced glutathione (GSH) (Tables 2 and 3). Furthermore, the excessive

ONOO⁻ increased lipid peroxidation of renal mitochondria (Table 3), and we confirmed the mitochondrial oxidative damage caused by ONOO⁻. In contrast, the administration of (–)-epicatechin 3-O-gallate reduced the magnitude of the lipid peroxidation level elevation caused by the experimental process (Table 3).

Since ONOO⁻ decomposes to form a strong and reactive oxidant, •OH, the effects of free radical scavengers and (–)-epicatechin 3-O-gallate on •OH also have to be evaluated to compare their protective actions against ONOO⁻. In this study, we used the spin-trap method to determine the level of •OH in rat renal tissue formed by the Fenton reaction, and found that the magnitude of the increase in the height of the DMPO-OH peak of rats that underwent

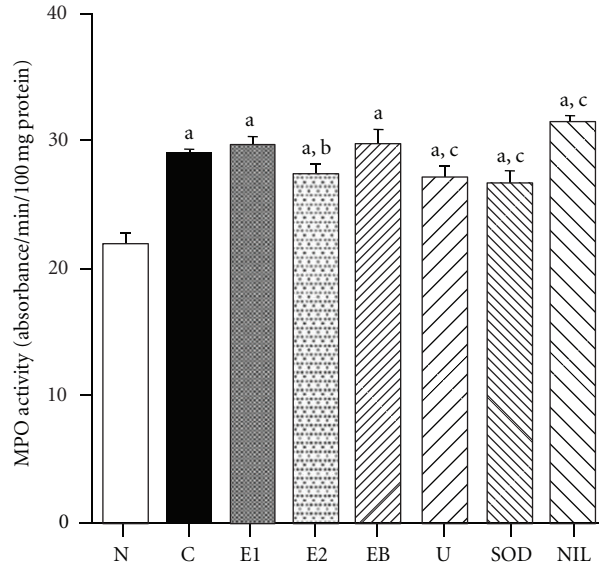


FIGURE 3: Effect of (–)-epicatechin 3-*O*-gallate and free radical inhibitors on renal MPO activity in rats. N, sham operation; C, LPS plus ischemia-reperfusion; E1, LPS plus ischemia-reperfusion after (–)-epicatechin 3-*O*-gallate (10 mg/kg body weight); E2, LPS plus ischemia-reperfusion after (–)-epicatechin 3-*O*-gallate (20 mg/kg body weight); EB, LPS plus ischemia-reperfusion after ebselen (5 mg/kg body weight); U, LPS plus ischemia-reperfusion after uric acid (62.5 mg/kg body weight); SOD, LPS plus ischemia-reperfusion after CuZnSOD (10,000 U/kg body weight); NIL, LPS plus ischemia-reperfusion after L-*N*⁶-(1-iminoethyl)lysine hydrochloride (3 mg/kg body weight). Significance: ^a*P* < 0.001 versus sham operation values; ^b*P* < 0.01, ^c*P* < 0.001 versus LPS plus ischemia-reperfusion control values.

TABLE 2: Effect of (–)-epicatechin 3-*O*-gallate on oxygen species-scavenging enzymes in renal tissue.

Group	SOD (U/mg protein)	Catalase (U/mg protein)	GSH-Px (U/mg protein)
Sham operation	31.82 ± 2.29	255.3 ± 35.0	138.7 ± 10.3
LPS plus ischemia-reperfusion			
Control	16.67 ± 2.52 ^c	146.8 ± 19.3 ^c	79.5 ± 7.2 ^c
(–)-Epicatechin 3- <i>O</i> -gallate (10 μmoles/kg B.W./day)	18.18 ± 1.70 ^c	176.0 ± 15.3 ^c	105.7 ± 8.0 ^{c,e}
(–)-Epicatechin 3- <i>O</i> -gallate (20 μmoles/kg B.W./day)	21.45 ± 3.67 ^{c,d}	194.4 ± 22.6 ^{b,d}	118.7 ± 11.0 ^{a,f}

Significance: ^a*P* < 0.05, ^b*P* < 0.01, ^c*P* < 0.001 versus sham operation values; ^d*P* < 0.05, ^e*P* < 0.01, ^f*P* < 0.001 versus LPS plus ischemia-reperfusion control values.

TABLE 3: Effect of (–)-epicatechin 3-*O*-gallate on the oxidative damage of renal mitochondria.

Group	GSH (nmol/mg protein)	TBA-reactive substance (nmol/mg protein)
Sham operation	4.42 ± 0.09	0.121 ± 0.001
LPS plus ischemia-reperfusion		
Control	2.75 ± 0.14 ^a	0.165 ± 0.007 ^a
(–)-Epicatechin 3- <i>O</i> -gallate (10 μmoles/kg B.W./day)	3.72 ± 0.18 ^{a,b}	0.147 ± 0.003 ^{a,b}
(–)-Epicatechin 3- <i>O</i> -gallate (20 μmoles/kg B.W./day)	3.77 ± 0.21 ^{a,b}	0.144 ± 0.007 ^{a,b}

Significance: ^a*P* < 0.001 versus sham operation values; ^b*P* < 0.001 versus LPS plus ischemia-reperfusion control values.

LPS plus ischemia-reperfusion was reduced by treatment with (–)-epicatechin 3-*O*-gallate, CuZnSOD, and L-*N*⁶-(1-iminoethyl)lysine hydrochloride (Table 4). These findings indicate that the effect of (–)-epicatechin 3-*O*-gallate on the highly reactive radical •OH plays a crucial role in its protective action against ONOO[–]-induced oxidative damage. Furthermore, the effects of (–)-epicatechin 3-*O*-gallate on

ONOO[–] and •OH were stronger than those of the other well-known free radical inhibitors tested, which can also be regarded as a mechanism distinct from that of the others.

The LPS plus ischemia-reperfusion process resulted in a significant elevation of the uric acid level, indicating that a pathological condition in the kidney had developed (Table 5). However, the administration of (–)-epicatechin

TABLE 4: Effect of (–)-epicatechin 3-O-gallate and free radical inhibitors on renal hydroxyl radical in rats.

Group	Hydroxyl radical (DMPO-OH)
Sham operation	0.29 ± 0.07
LPS plus ischemia-reperfusion	
Control	1.15 ± 0.15 ^a
(–)-Epicatechin 3-O-gallate (10 mg/kg B.W.)	0.18 ± 0.01 ^b
(–)-Epicatechin 3-O-gallate (20 mg/kg B.W.)	0.17 ± 0.01 ^b
Ebselen (5 mg/kg B.W.)	1.10 ± 0.18 ^a
Uric acid (62.5 mg/kg B.W.)	1.06 ± 0.07 ^a
SOD (10,000 U/kg B.W.)	0.22 ± 0.01 ^b
L-N ⁶ -(1-iminoethyl)lysine hydrochloride (3 mg/kg B.W.)	0.20 ± 0.03 ^b

Significance: ^a*P* < 0.001 versus sham operation values; ^b*P* < 0.001 versus LPS plus ischemia-reperfusion control values.

TABLE 5: Effect of (–)-epicatechin 3-O-gallate and free radical inhibitors on plasma uric acid level in rats.

Group	Uric acid (mg/dL)
Sham operation	1.53 ± 0.18
LPS plus ischemia-reperfusion	
Control	1.95 ± 0.03 ^a
(–)-Epicatechin 3-O-gallate (10 mg/kg B.W.)	1.64 ± 0.24
(–)-Epicatechin 3-O-gallate (20 mg/kg B.W.)	1.12 ± 0.11 ^c
Ebselen (5 mg/kg B.W.)	2.15 ± 0.37 ^b
Uric acid (62.5 mg/kg B.W.)	1.96 ± 0.35
SOD (10,000 U/kg B.W.)	2.09 ± 0.09 ^a
L-N ⁶ -(1-iminoethyl)lysine hydrochloride (3 mg/kg B.W.)	1.57 ± 0.25

Significance: ^a*P* < 0.05, ^b*P* < 0.01 versus sham operation values; ^c*P* < 0.001 versus LPS plus ischemia-reperfusion control values.

3-O-gallate reduced the uric acid level, while the other free radical inhibitors did not (Table 5). This effect of (–)-epicatechin 3-O-gallate on excessive uric acid levels is also considered to be a property distinct from the other free radical scavengers. The renal function parameters of serum urea nitrogen and creatinine (Cr) levels were elevated markedly by LPS plus ischemia-reperfusion, while the administration of (–)-epicatechin 3-O-gallate reduced these levels significantly, indicating the amelioration of renal dysfunction by (–)-epicatechin 3-O-gallate. In addition, uric acid and L-N⁶-(1-iminoethyl)lysine hydrochloride protected against renal dysfunction induced by this process, although their activity was relatively low compared with (–)-epicatechin 3-O-gallate.

Our results in rats showed that the LPS plus ischemia-reperfusion process led to proteinuria, demonstrated by the sodium dodecyl sulfate-polyacrylamide gel electrophoresis (SDS-PAGE) pattern with an abundance of low- and high-molecular-weight proteins relative to the marker albumin (76 kDa) (Figure 4). The administration of (–)-epicatechin 3-O-gallate and L-N⁶-(1-iminoethyl)lysine hydrochloride reduced the intensity of the low- and high-molecular-weight protein bands to a greater extent than the other radical inhibitors, which suggests that (–)-epicatechin 3-O-gallate would ameliorate proteinuria due to renal failure caused by ONOO⁻-induced oxidative damage.

In the LPS plus ischemia-reperfusion rat model, (–)-epicatechin 3-O-gallate, L-N⁶-(1-iminoethyl)lysine hydrochloride, and uric acid showed a strong protective effect

against ONOO⁻-induced oxidative damage, while CuZn-SOD and ebselen exerted relatively low activity. In light of the results of this study, we suggest that the activity of (–)-epicatechin 3-O-gallate is distinct from that of the other free radical inhibitors, especially L-N⁶-(1-iminoethyl)lysine hydrochloride and uric acid. (–)-Epicatechin 3-O-gallate scavenged ONOO⁻ directly, but it did not scavenge its precursors O₂⁻ and NO. Furthermore, (–)-epicatechin 3-O-gallate indirectly inhibits the generation of ONOO⁻ through the enhancement of antioxidant enzyme activities. In addition, the inhibition of MPO activity by (–)-epicatechin 3-O-gallate would contribute to the effective inhibition of protein nitration and lipid peroxidation. (–)-Epicatechin 3-O-gallate was also a stronger scavenger of the ONOO⁻ decomposition product •OH than any of the other free radical inhibitors tested. The improvement by (–)-epicatechin 3-O-gallate of the renal dysfunction caused by ONOO⁻-related oxidative damage was marked and distinct from that induced by any of the other free radical inhibitors.

3. (–)-Epigallocatechin 3-O-Gallate and Adenine-Induced Renal Failure

Methylguanidine (MG) is widely recognized as a strong uremic toxin [24]. The •OH radical specifically plays an important role in the pathway of MG production from Cr [25]. In this study, we investigated whether the oral administration of (–)-epigallocatechin 3-O-gallate suppresses MG production

TABLE 6: Serum constituents at 50 days of administration.

Items	Normal	Control	(-)-Epigallocatechin 3-O-gallate		
			25 mg/kg B.W./day	50 mg/kg B.W./day	100 mg/kg B.W./day
Glucose (mg/dL)	193 ± 9	592 ± 38 ^c	497 ± 22 ^{c,e}	487 ± 22 ^{c,e}	460 ± 19 ^{c,e}
Total protein (g/dL)	4.75 ± 0.11	4.21 ± 0.08 ^c	4.20 ± 0.10 ^c	4.37 ± 0.07 ^{c,d}	4.44 ± 0.06 ^{c,e}
Albumin (g/dL)	2.88 ± 0.04	2.38 ± 0.08 ^c	2.43 ± 0.06 ^c	2.56 ± 0.06 ^{c,e}	2.62 ± 0.05 ^{c,e}
Total cholesterol (mg/dL)	46.4 ± 2.4	113.6 ± 12.7 ^c	102.3 ± 6.0 ^c	83.3 ± 6.4 ^{c,e}	77.7 ± 6.8 ^{c,e}
Triglycerides (mg/dL)	63.7 ± 6.3	143.1 ± 31.4 ^c	126.6 ± 15.7 ^a	120.9 ± 27.3 ^a	116.6 ± 26.3 ^a
TBA-reactive substance (nmol/mL)	1.56 ± 0.08	3.70 ± 0.39 ^c	2.48 ± 0.18 ^{b,e}	2.50 ± 0.34 ^{b,e}	2.16 ± 0.24 ^e

Significance: ^a $P < 0.05$, ^b $P < 0.01$, ^c $P < 0.001$ versus normal values; ^d $P < 0.05$, ^e $P < 0.001$ versus diabetic nephropathy control values.

TABLE 7: Renal functional parameters at 50 days of administration.

Items	Normal	Control	(-)-Epigallocatechin 3-O-gallate		
			25 mg/kg B.W./day	50 mg/kg B.W./day	100 mg/kg B.W./day
Serum urea nitrogen (mg/dL)	16.8 ± 0.5	44.5 ± 3.1 ^b	37.9 ± 1.8 ^{b,d}	38.0 ± 2.6 ^{b,d}	28.8 ± 1.4 ^{b,d}
Serum Cr (mg/dL)	0.38 ± 0.01	0.94 ± 0.09 ^b	0.90 ± 0.08 ^b	0.82 ± 0.06 ^b	0.66 ± 0.05 ^{b,d}
Ccr (ml/kg B.W./min)	7.20 ± 0.26	3.35 ± 0.43 ^b	3.41 ± 0.32 ^b	3.65 ± 0.37 ^b	4.09 ± 0.35 ^{b,c}
Urinary protein (mg/day)	19.1 ± 0.7	82.3 ± 13.3 ^b	64.0 ± 11.9 ^b	47.9 ± 14.6 ^{a,d}	40.6 ± 6.4 ^d

Significance: ^a $P < 0.05$, ^b $P < 0.001$ versus normal values; ^c $P < 0.05$, ^d $P < 0.001$ versus diabetic nephropathy control values.

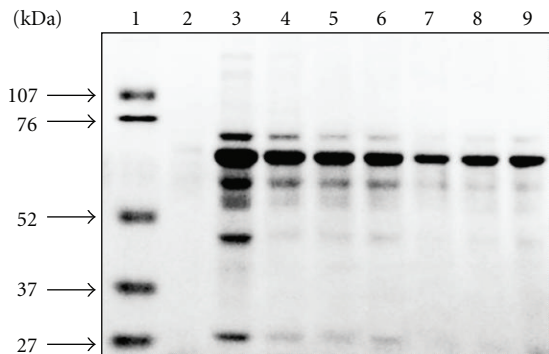


FIGURE 4: Effect of (-)-epicatechin 3-O-gallate and free radical inhibitors on SDS-PAGE pattern of proteinuria in rats. 1, marker; 2, sham operation; 3, LPS plus ischemia-reperfusion; 4, LPS plus ischemia-reperfusion after ebselen (5 mg/kg body weight); 5, LPS plus ischemia-reperfusion after uric acid (62.5 mg/kg body weight); 6, LPS plus ischemia-reperfusion after CuZnSOD (10,000 U/kg body weight); 7, LPS plus ischemia-reperfusion after L-N⁶-(1-iminoethyl)lysine hydrochloride (3 mg/kg body weight); 8, LPS plus ischemia-reperfusion after (-)-epicatechin 3-O-gallate (20 mg/kg body weight); 9, LPS plus ischemia-reperfusion after (-)-epicatechin 3-O-gallate (10 mg/kg body weight). Markers (kDa): 107, phosphorylase B; 76, bovine serum albumin; 52, ovalbumin; 37, carbonic anhydrase; 27, soybean trypsin inhibitor.

in rats with chronic renal failure after intraperitoneal Cr injection.

In 10-week-old male normal rats, Cr was rapidly excreted into the urine after Cr loading, whereas, in age-matched rats with renal failure, urinary Cr excretion was low, and high levels of Cr were present in the serum, muscle, kidney, and liver, suggesting that the body was susceptible to

oxidative alterations (Figure 5). After Cr loading, the MG levels in the serum, urine, muscle, liver, and kidney of rats with renal failure were higher than those of normal rats, confirming that MG production from Cr was increased in rats with renal failure (Figure 6). The oral administration of (-)-epigallocatechin 3-O-gallate dose-dependently reduced the serum MG levels, showing that (-)-epigallocatechin 3-O-gallate effectively inhibited increased MG production in which oxidative reactions markedly participate. (-)-Epigallocatechin 3-O-gallate (20 mg/kg body weight) reduced the urinary and kidney MG levels, which were reduced further and significantly in the 100 and 500 mg treated groups. In the muscle and liver, a significant reduction was only observed in the high dose-treated group (500 mg) (Figure 6).

We have already demonstrated that green tea polyphenols (daily dose, 400 mg) administered for 6 months to 50 patients on dialysis decreased the blood levels of MG [26], and that concomitant treatment with green tea polyphenols during 25-day adenine-feeding periods produced a dose-dependent decrease in the serum MG level [27]. Furthermore, we reported that concomitant treatment with green tea polyphenols had protective effects against the increased serum Cr and urinary protein levels and the decreased creatinine clearance (Ccr) [7, 28], indicating that green tea polyphenols can delay deterioration of the renal function. Taking the evidence from previous and present studies into consideration, we propose that green tea polyphenols exert an MG-lowering effect in dialysis patients and rats with adenine-induced renal failure through, at least in part, two actions: the improvement of renal dysfunction, and inhibition of MG production from Cr due to their ability to scavenge •OH.

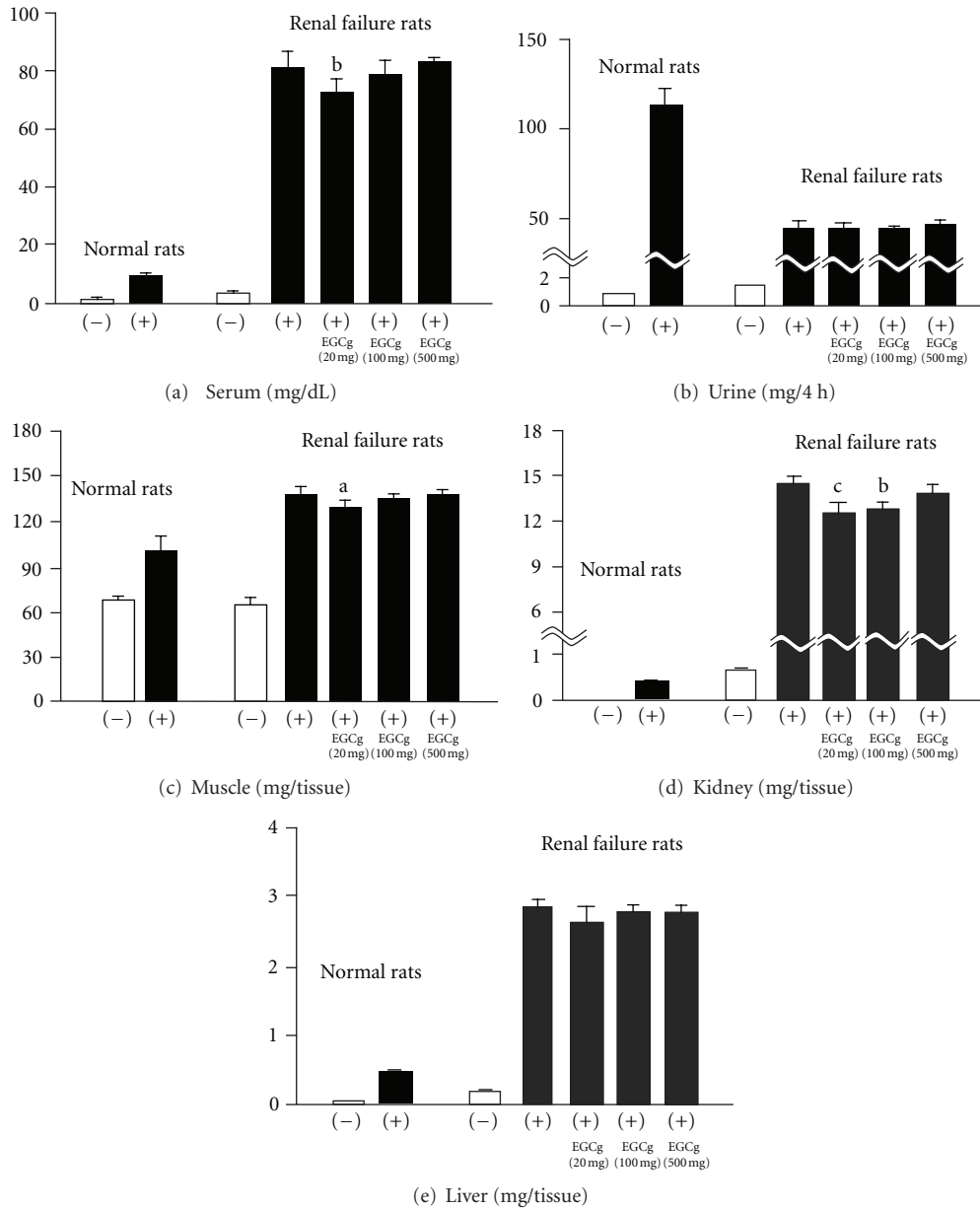


FIGURE 5: Cr levels in serum (a), urine (b), muscle (c), kidney (d), and liver (e). (-), without Cr loading; (+), with Cr loading. Significance: ^a $P < 0.05$, ^b $P < 0.01$, ^c $P < 0.001$ versus renal failure control rats with Cr loading.

4. (-)-Epigallocatechin 3-O-gallate and Diabetic Nephropathy

The pathogenesis of diabetic nephropathy has been extensively discussed for many years, and it has been accepted that oxidative stress is closely involved as a causative factor stemming from persistent hyperglycemia [29, 30]. Within the diabetic kidney, glucose-dependent pathways such as increasing oxidative stress, polyol formation, and advanced glycation endproduct (AGE) accumulation, are activated.

To evaluate the effect of (-)-epigallocatechin 3-O-gallate as a representative polyphenol on diabetic nephropathy, rats (10-week-old, male) with subtotal nephrectomy

plus streptozotocin injection were orally administered (-)-epigallocatechin 3-O-gallate at doses of 25, 50, and 100 mg/kg body weight/day for 50 days.

Hyperglycemia is the principle factor responsible for structural alterations at the renal level, and The Diabetes Control and Complications Trial Research Group [31] has elucidated that hyperglycemia is directly linked to diabetic microvascular complications, particularly in the kidney; therefore, glycemic control remains the main target of therapy. In this study, the glucose level of diabetic nephropathy rats showed a significant approximately 3-fold increase; however, (-)-epigallocatechin 3-O-gallate inhibited this increase dose-dependently (Table 6). In addition, the typical patterns

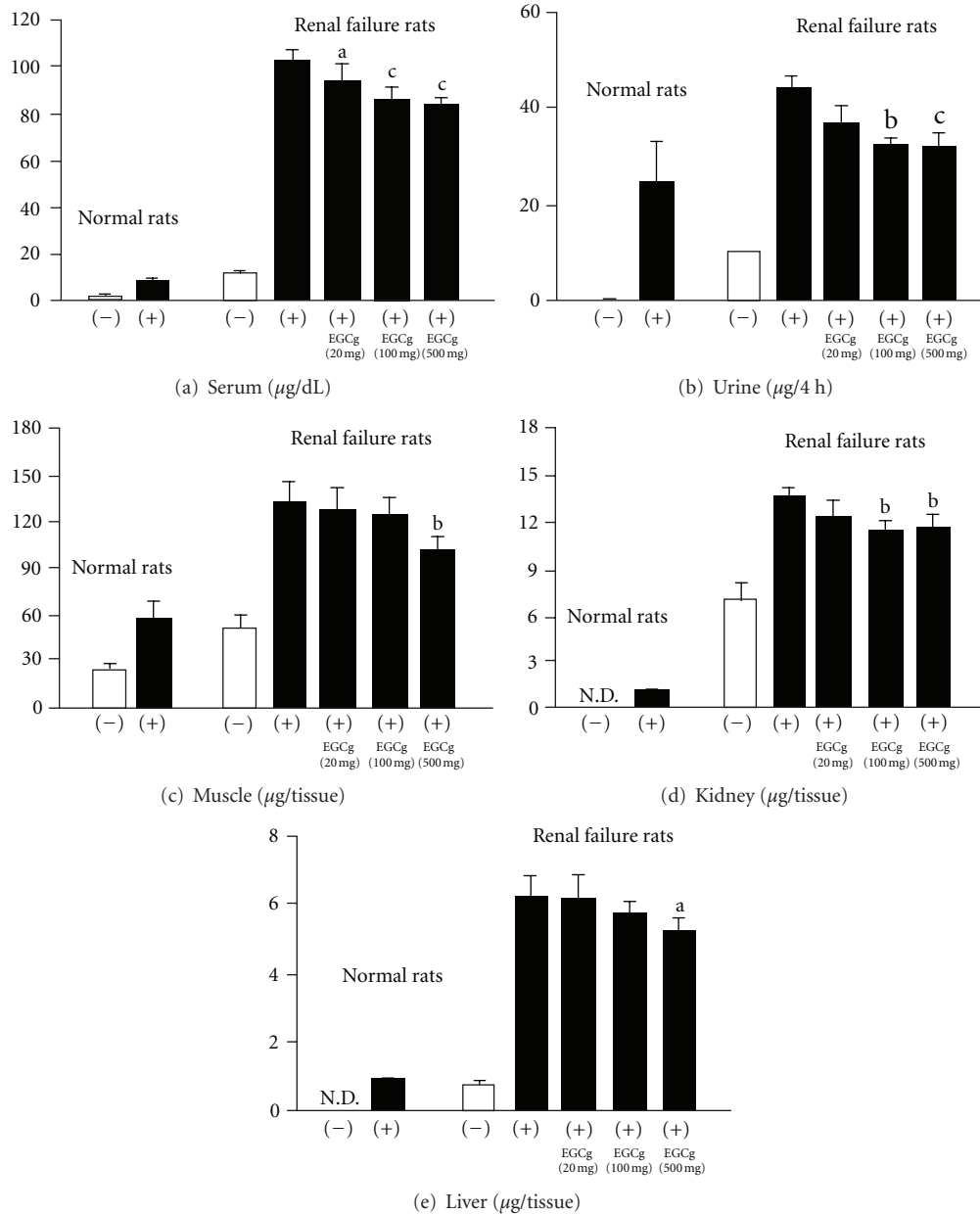


FIGURE 6: MG levels in serum (a), urine (b), muscle (c), kidney (d), and liver (e). (-), without Cr loading; (+), with Cr loading. Significance: ^a $P < 0.05$, ^b $P < 0.01$, ^c $P < 0.001$ versus renal failure control rats with Cr loading.

of serum constituents, that is, a decrease in total protein and albumin due to their excessive excretion via urine, and also an increase in lipids, for example, total cholesterol and triglycerides, whose abnormal metabolism has been proven to play a role in the pathogenesis of diabetic nephropathy [32] and to enhance lipid peroxidation, were all improved by the administration of (-)-epigallocatechin 3-O-gallate (Table 6). Therefore, we suggest that (-)-epigallocatechin 3-O-gallate had a positive effect on serum glucose and lipid metabolic abnormalities.

The results of the study presented here demonstrate that diabetic nephropathy rats showed significant increases in the serum urea nitrogen, Cr, and urinary protein excretion rate, whereas the Ccr level showed a significant decrease

compared with normal rats, representing a decline in the renal function (Table 7). However, the (-)-epigallocatechin 3-O-gallate treatment positively affected these parameters, especially in the group given 100 mg (Table 7). For further investigation, we performed pattern analysis of proteinuria using SDS-PAGE, and the (-)-epigallocatechin 3-O-gallate treatment led to a clear decrease at all parts of the molecule (Figure 7). These data suggest that not only the improvement of proteinuria, but also its individual fractions, may, at least in part, ameliorate the development of glomerular and tubulointerstitial injury.

In the state of diabetic nephropathy, there is increased glomerular basement membrane thickening and mesangial extracellular matrix (ECM) deposition, followed by

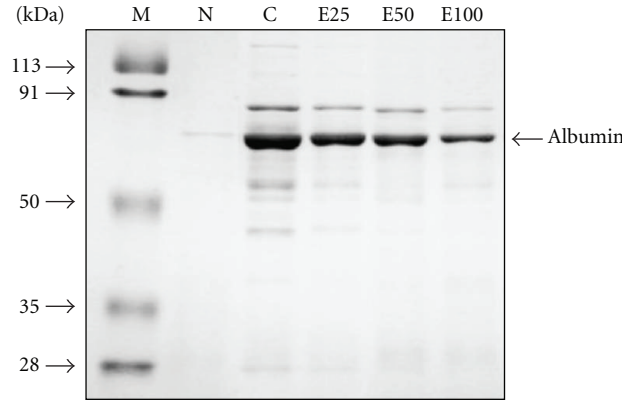


FIGURE 7: SDS-PAGE pattern of proteinuria in normal rats (N) and diabetic nephrectomized rats treated with (-)-epigallocatechin 3-O-gallate at 25 mg/kg body weight/day (E25), 50 mg/kg body weight/day (E50), 100 mg/kg body weight/day (E100), or water (control, C) for 50 days. Lane M shows the molecular weight marker.

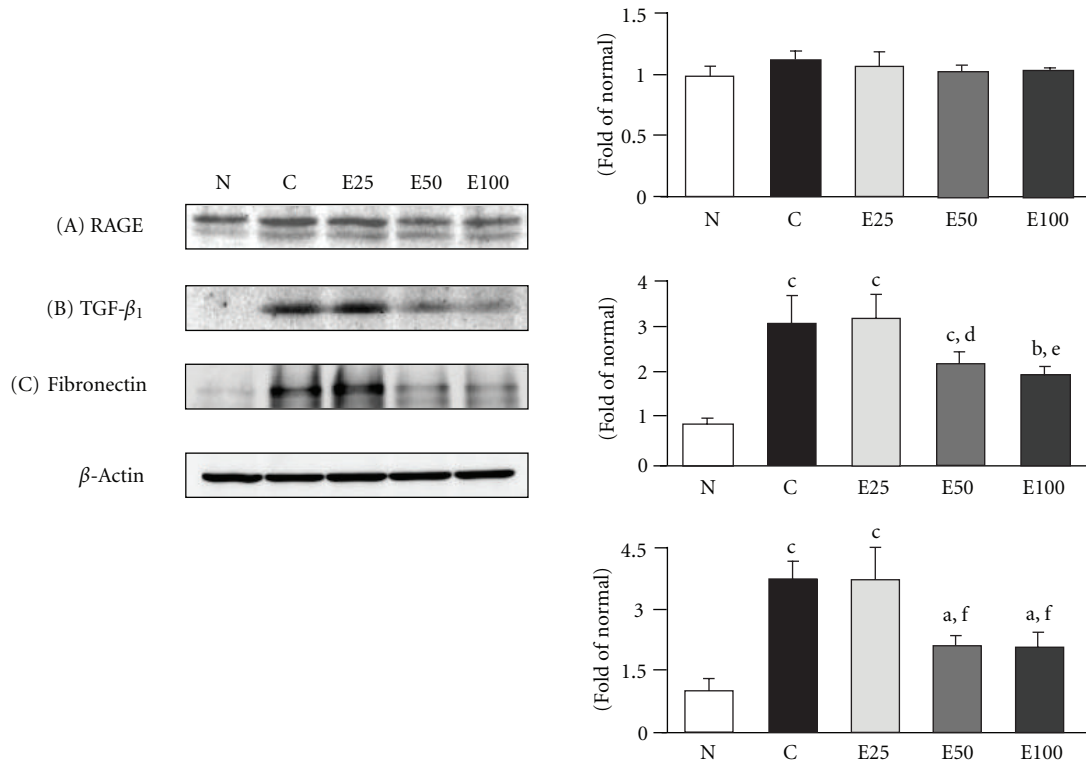


FIGURE 8: Western blot analyses of RAGE (A), TGF-β₁ (B), and fibronectin (C) protein expression in the renal cortex of normal rats (N) and diabetic nephrectomized rats treated with (-)-epigallocatechin 3-O-gallate at 25 mg/kg body weight/day (E25), 50 mg/kg body weight/day (E50), 100 mg/kg body weight/day (E100), or water (control, C) for 50 days. Significance: ^a*P* < 0.05, ^b*P* < 0.01, ^c*P* < 0.001 versus normal values; ^d*P* < 0.05, ^e*P* < 0.01, ^f*P* < 0.001 versus diabetic nephropathy control values.

mesangial hypertrophy and diffuse and nodular glomerular sclerosis, and these structural changes may be directly influenced by AGEs through excessive cross-linking of the matrix molecules in a receptor-independent way [33, 34]. In this study, we demonstrated that renal AGE accumulation observed in diabetic nephropathy rats was decreased by (-)-epigallocatechin 3-O-gallate administration, although (-)-epigallocatechin 3-O-gallate showed only a slight tendency to reduce renal receptor for advanced glycation endproduct

(RAGE) expression in diabetic nephropathy rats (Figure 8). However, a marked antioxidative activity of renal tissue was shown in the level of lipid peroxidation at 50 and 100 mg doses of (-)-epigallocatechin 3-O-gallate, resembling the results of iNOS, cyclooxygenase (COX)-2, nuclear factor-κB (NF-κB), and phosphorylated inhibitor binding protein κB-α (IκB-α) (Figure 9), and the fibrogenic cytokine transforming growth factor (TGF)-β₁ and fibronectin protein expression in the renal cortex (Figure 8).

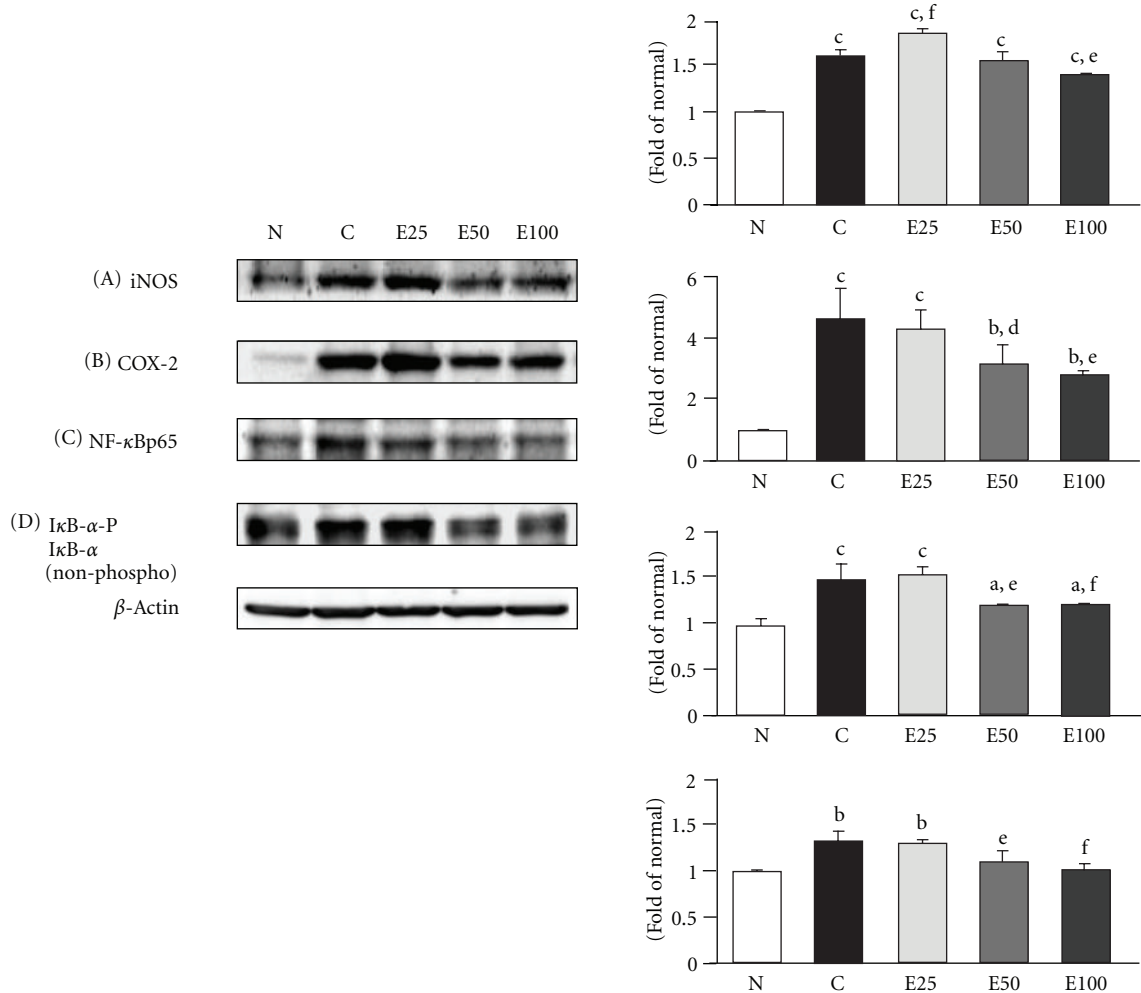


FIGURE 9: Western blot analyses of iNOS (A), COX-2 (B), NF-κBp65 (C), and IκB-α (phosphorylated and nonphosphorylated) (D) protein expression in the renal cortex of normal rats (N) and diabetic nephrectomized rats treated with (-)-epigallocatechin 3-O-gallate at 25 mg/kg body weight/day (E25), 50 mg/kg body weight/day (E50), 100 mg/kg body weight/day (E100), or water (control, C) for 50 days. Significance: ^a $P < 0.05$, ^b $P < 0.01$, ^c $P < 0.001$ versus normal values; ^d $P < 0.05$, ^e $P < 0.01$, ^f $P < 0.001$ versus diabetic nephropathy control values.

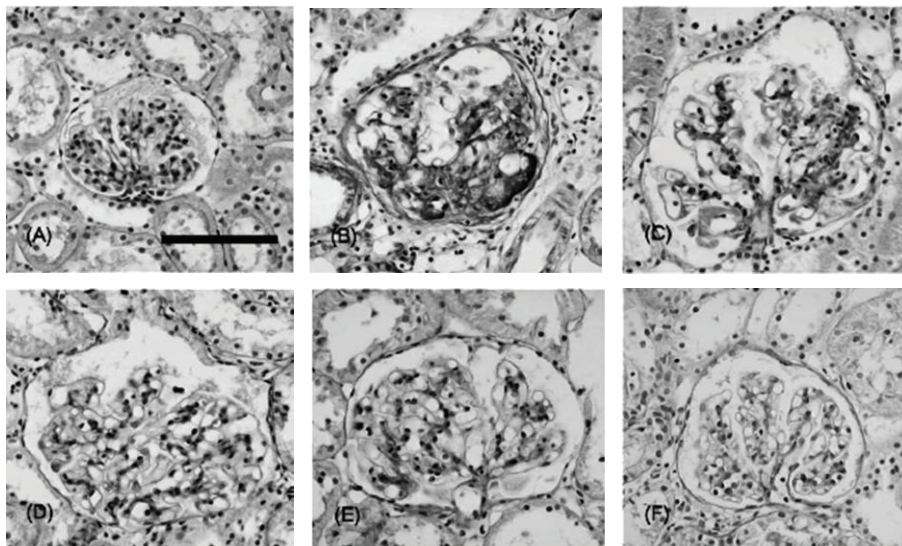


FIGURE 10: Photomicrographs of the glomeruli in normal rats (A) and diabetic nephrectomized rats treated with (-)-epigallocatechin 3-O-gallate at 25 mg/kg body weight/day (D), 50 mg/kg body weight/day (E), 100 mg/kg body weight/day (F), or water (control, B and C) for 50 days. Scale bar, 100 μm.

Moreover, diabetic nephropathy rats used in the present study showed significant glomerular hypertrophy and diffuse and exudative lesions. Longitudinal hyperfiltration is associated with renal enlargement such as an increase in the glomerular size, and diffuse lesion development is dependent on increased mesangial matrix and glomerular basement membrane thickening, because both are composed of ECM molecules, as in the case of the TGF- β system, and they also correlate with proteinuria. The other phenomenon, the exudative lesion called the capsular drop and fibrin cap, is suggested to consist of plasma components such as IgM, fibrinogen, and AGEs. According to the results of histopathological evaluation, although diabetic nephropathy rats showed a 2.2-fold increase in the glomerular area, mild but significant increases in diffuse and exudative lesions, and a slight increase in the mesangial matrix, (-)-epigallocatechin 3-O-gallate could affect glomerular hypertrophy and these lesions at 50 and 100 mg doses, reflecting the effects of AGEs, TGF- β_1 , and fibronectin levels (Figures 8 and 10). Hence, we may hypothesize that (-)-epigallocatechin 3-O-gallate could be advantageous against diabetic kidney damage, which correlates with AGEs with or without a receptor-dependent pathway and their related inflammatory responses, and then (-)-epigallocatechin 3-O-gallate subsequently suppresses the induction of mesangial hypertrophy and fibronectin synthesis in diabetic nephropathy.

Our observations presented here suggest that (-)-epigallocatechin 3-O-gallate has a beneficial effect on diabetic nephropathy via suppressing hyperglycemia, AGEs, their related oxidative stress and cytokine activations, and also pathological states due to its synergistic effect. This study may provide original and strong supporting evidence for the efficacy of (-)-epigallocatechin 3-O-gallate in the early stage of diabetic nephropathy, suggesting that it would be a superior aid for the management of patients with diabetic nephropathy.

5. Conclusion and Future Prospects

Much attention regarding green tea's benefits has been focused on the role of antioxidant activity in relation to the aging process and degenerative diseases like cancer, cardiovascular disease, and diabetes. This paper shows that, based on antioxidant activity, green tea polyphenols and their constituents exert protective effects on renal damage caused by various toxic situations such as an excessive arginine supply, strong oxidative radicals, renal toxin, diabetic nephropathy, and type 2 diabetes. Therefore, we expect that green tea polyphenols have the potential to prevent organ failure and, in particular, provide a promising therapeutic approach to renal disorders. As green tea is already one of the most popular beverages worldwide, its role should be understandably elucidated in the direct and indirect prevention of chronic diseases. In order to explain the potential mechanisms of green tea polyphenols for protection against organ damage concomitant with chronic disease, additional research is needed on the pharmacokinetics of tea constituents as well as exploration at the cellular level. Furthermore, well-designed

observational epidemiological studies and intervention trials will generate clear and safe conclusions concerning the protective effects of tea.

References

- [1] C. Fiorillo, C. Oliviero, G. Rizzuti, C. Nediani, A. Pacini, and P. Nassi, "Oxidative stress and antioxidant defenses in renal patients receiving regular haemodialysis," *Clinical Chemistry and Laboratory Medicine*, vol. 36, no. 3, pp. 149–153, 1998.
- [2] G. J. Handelman, M. F. Walter, R. Adhikarla et al., "Elevated plasma F2-isoprostanes in patients on long-term hemodialysis," *Kidney International*, vol. 59, no. 5, pp. 1960–1966, 2001.
- [3] M. Kakimoto, T. Inoguchi, T. Sonta et al., "Accumulation of 8-hydroxy-2'-deoxyguanosine and mitochondrial DNA deletion in kidney of diabetic rats," *Diabetes*, vol. 51, no. 5, pp. 1588–1595, 2002.
- [4] T. Yokozawa, C. P. Chen, D. Y. Rhyu, T. Tanaka, J. C. Park, and K. Kitani, "Potential of sanguin H-6 against oxidative damage in renal mitochondria and apoptosis mediated by peroxynitrite in vivo," *Nephron*, vol. 92, no. 1, pp. 133–141, 2002.
- [5] S. Hahn, R. J. Krieg, S. Hisano et al., "Vitamin E suppresses oxidative stress and glomerulosclerosis in rat remnant kidney," *Pediatric Nephrology*, vol. 13, no. 3, pp. 195–198, 1999.
- [6] H. Y. Chung, T. Yokozawa, D. Y. Soung, I. S. Kye, J. K. No, and B. S. Baek, "Peroxynitrite-scavenging activity of green tea tannin," *Journal of Agricultural and Food Chemistry*, vol. 46, no. 11, pp. 4484–4486, 1998.
- [7] T. Yokozawa, E. Dong, T. Nakagawa et al., "In vitro and in vivo studies on the radical-scavenging activity of tea," *Journal of Agricultural and Food Chemistry*, vol. 46, no. 6, pp. 2143–2150, 1998.
- [8] T. Yokozawa, E. J. Cho, T. Nakagawa, K. Terasawa, and S. Takeuchi, "Inhibitory effect of green tea tannin on free radical-induced injury to the renal epithelial cell line, LLC-PK₁," *Pharmacy and Pharmacology Communications*, vol. 6, no. 12, pp. 521–526, 2000.
- [9] T. Nakagawa and T. Yokozawa, "Direct scavenging of nitric oxide and superoxide by green tea," *Food and Chemical Toxicology*, vol. 40, no. 12, pp. 1745–1750, 2002.
- [10] D. K. Rah, D. W. Han, H. S. Baek, S. H. Hyon, B. Y. Park, and J. C. Park, "Protection of rabbit kidney from ischemia/reperfusion injury by green tea polyphenol pretreatment," *Archives of Pharmacological Research*, vol. 30, no. 11, pp. 1447–1454, 2007.
- [11] S. A. Khan, S. Priyamvada, N. Farooq, S. Khan, M. W. Khan, and A. N. K. Yusufi, "Protective effect of green tea extract on gentamicin-induced nephrotoxicity and oxidative damage in rat kidney," *Pharmacological Research*, vol. 59, no. 4, pp. 254–262, 2009.
- [12] A. Peng, T. Ye, D. Rakheja et al., "The green tea polyphenol (-)-epigallocatechin-3-gallate ameliorates experimental immune-mediated glomerulonephritis," *Kidney International*, vol. 80, no. 6, pp. 601–611, 2011.
- [13] B. Halliwell and J. M. C. Gutteridge, "Role of free radicals and catalytic metal ions in human disease: An overview," *Methods in Enzymology*, vol. 186, pp. 1–85, 1990.
- [14] T. Yokozawa, D. Y. Rhyu, and E. J. Cho, "(-)-Epicatechin 3-O-gallate ameliorates the damages related to peroxynitrite production by mechanisms distinct from those of other free radical inhibitors," *Journal of Pharmacy and Pharmacology*, vol. 56, no. 2, pp. 231–239, 2004.

- [15] T. Nakagawa, T. Yokozawa, M. Sano, S. Takeuchi, M. Kim, and S. Minamoto, "Activity of (-)-epigallocatechin 3-O-gallate against oxidative stress in rats with adenine-induced renal failure," *Journal of Agricultural and Food Chemistry*, vol. 52, no. 7, pp. 2103–2107, 2004.
- [16] N. Yamabe, T. Yokozawa, T. Oya, and M. Kim, "Therapeutic potential of (-)-epigallocatechin 3-O-gallate on renal damage in diabetic nephropathy model rats," *The Journal of Pharmacology and Experimental Therapeutics*, vol. 319, no. 1, pp. 228–236, 2006.
- [17] R. Radi, J. S. Beckman, K. M. Bush, and B. A. Freeman, "Peroxynitrite-induced membrane lipid peroxidation: The cytotoxic potential of superoxide and nitric oxide," *Archives of Biochemistry and Biophysics*, vol. 288, no. 2, pp. 481–487, 1991.
- [18] T. Douki, J. Cadet, and B. N. Ames, "An adduct between peroxynitrite and 2'-deoxyguanosine: 4,5-dihydro-5-hydroxy-4-(nitrosooxy)-2'-deoxyguanosine," *Chemical Research in Toxicology*, vol. 9, no. 1, pp. 3–7, 1996.
- [19] N. Fukuyama, Y. Takebayashi, M. Hida, H. Ishida, K. Ichimori, and H. Nakazawa, "Clinical evidence of peroxynitrite formation in chronic renal failure patients with septic shock," *Free Radical Biology and Medicine*, vol. 22, no. 5, pp. 771–774, 1997.
- [20] H. Ischiropoulos, "Biological tyrosine nitration: a pathophysiological function of nitric oxide and reactive oxygen species," *Archives of Biochemistry and Biophysics*, vol. 356, no. 1, pp. 1–11, 1998.
- [21] H. Nakazawa, N. Fukuyama, S. Takizawa, C. Tsuji, M. Yoshitake, and H. Ishida, "Nitrotyrosine formation and its role in various pathological conditions," *Free Radical Research*, vol. 33, no. 6, pp. 771–784, 2000.
- [22] A. Ceriello, F. Mercuri, L. Quagliaro et al., "Detection of nitrotyrosine in the diabetic plasma: evidence of oxidative stress," *Diabetologia*, vol. 44, no. 7, pp. 834–838, 2001.
- [23] S. Cuzzocrea and R. J. Reiter, "Pharmacological action of melatonin in shock, inflammation and ischemia/reperfusion injury," *European Journal of Pharmacology*, vol. 426, no. 1-2, pp. 1–10, 2001.
- [24] S. Giovannetti, P. L. Balestri, and G. Barsotti, "Methylguanidine in uremia," *Archives of Internal Medicine*, vol. 131, no. 5, pp. 709–713, 1973.
- [25] K. Ienaga and T. Yokozawa, "Creatinine and HMH (5-hydroxy-1-methylhydantoin, NZ-419) as intrinsic hydroxyl radical scavengers," *Drug Discoveries & Therapeutics*, vol. 5, no. 4, pp. 162–175, 2011.
- [26] T. Yokozawa, H. Oura, T. Shibata et al., "Effects of green tea tannin in dialysis patients," *Journal of Traditional Medicines*, vol. 13, no. 2, pp. 124–131, 1996.
- [27] T. Yokozawa, E. Dong, and H. Oura, "Proof that green tea tannin suppresses the increase in the blood methylguanidine level associated with renal failure," *Experimental and Toxicologic Pathology*, vol. 49, no. 1-2, pp. 117–122, 1997.
- [28] T. Yokozawa, H. Y. Chung, L. Q. He, and H. Oura, "Effectiveness of green tea tannin on rats with chronic renal failure," *Bioscience, Biotechnology and Biochemistry*, vol. 60, no. 6, pp. 1000–1005, 1996.
- [29] J. W. Baynes and S. R. Thorpe, "Role of oxidative stress in diabetic complications: a new perspective on an old paradigm," *Diabetes*, vol. 48, no. 1, pp. 1–9, 1999.
- [30] H. Ha and K. H. Kim, "Pathogenesis of diabetic nephropathy: the role of oxidative stress and protein kinase C," *Diabetes Research and Clinical Practice*, vol. 45, no. 2-3, pp. 147–151, 1999.
- [31] The Diabetes Control and Complications Trial Research Group, "The effect of intensive treatment of diabetes on the development and progression of long-term complications in insulin-dependent diabetes mellitus," *The New England Journal of Medicine*, vol. 329, no. 14, pp. 977–986, 1993.
- [32] L. Sun, N. Halaihel, W. Zhang, T. Rogers, and M. Levi, "Role of sterol regulatory element-binding protein 1 in regulation of renal lipid metabolism and glomerulosclerosis in diabetes mellitus," *The Journal of Biological Chemistry*, vol. 277, no. 21, pp. 18919–18927, 2002.
- [33] H. Vlassara, H. Fuh, Z. Makita, S. Krungkrai, A. Cerami, and R. Bucala, "Exogenous advanced glycosylation end products induce complex vascular dysfunction in normal animals: a model for diabetic and aging complications," *Proceedings of the National Academy of Sciences of the United States of America*, vol. 89, no. 24, pp. 12043–12047, 1992.
- [34] H. Vlassara, L. J. Striker, S. Teichberg, H. Fuh, Y. M. Li, and M. Steffes, "Advanced glycation end products induce glomerular sclerosis and albuminuria in normal rats," *Proceedings of the National Academy of Sciences of the United States of America*, vol. 91, no. 24, pp. 11704–11708, 1994.

Research Article

Antiatherosclerotic Effect of *Canarium odontophyllum* Miq. Fruit Parts in Rabbits Fed High Cholesterol Diet

Faridah Hanim Shakirin,^{1,2} Azrina Azlan,^{2,3} Amin Ismail,^{2,3}
Zulkhairi Amom,⁴ and Lau Cheng Yuon⁵

¹ Department of Biochemistry, Faculty of Biotechnology and Biomolecular Sciences, Universiti Putra Malaysia, Selangor, 43400 Serdang, Malaysia

² Department of Nutrition and Dietetics, Faculty of Medicine and Health Sciences, Universiti Putra Malaysia, Selangor, 43400 Serdang, Malaysia

³ Laboratory of Halal Science Research, Halal Products Research Institute, Universiti Putra Malaysia, Selangor, 43400 Serdang, Malaysia

⁴ Department of Basic Sciences, Faculty of Health Sciences, Universiti Teknologi Mara, Kampus Puncak Alam, 42300 Selangor, Malaysia

⁵ Department of Agriculture, Agriculture Research Centre, Semongok, Sarawak, 93720 Kuching, Malaysia

Correspondence should be addressed to Azrina Azlan, azrina@medic.upm.edu.my

Received 20 January 2012; Revised 9 May 2012; Accepted 9 May 2012

Academic Editor: Vincenzo De Feo

Copyright © 2012 Faridah Hanim Shakirin et al. This is an open access article distributed under the Creative Commons Attribution License, which permits unrestricted use, distribution, and reproduction in any medium, provided the original work is properly cited.

The effect of *C. odontophyllum* (CO) fruit parts was investigated in hypercholesterolemic rabbits. Forty-nine rabbits, which were randomly divided into seven groups of seven animals ($n = 7$), received a diet containing different parts of CO fruit parts for 8 weeks. The groups were as follows: (1) normal diet: NC group and (2) hypercholesterolemic diet: PC, HS (10 mg/kg/day simvastatin), HPO (20 g kg⁻¹ oil extracted from the pulp of CO), HKO (20 g kg⁻¹ oil extracted from the kernel of CO), HF (50 g kg⁻¹ fullfat pulp of CO), and HD (50 g kg⁻¹ defatted pulp of CO). Among these groups, rabbits receiving defatted pulp of CO showed the greatest cholesterol lowering effect as it had reduced plasma LDL-C, TC, and thiobarbiturate reactive substance (TBARS) levels as well as atherosclerotic plaques. The presence of high dietary fiber and antioxidants activity are potential factors contributing to the cholesterol lowering effect. Consequently, these results indicate the potential use of CO defatted pulp as a cholesterol lowering and antioxidant agent.

1. Introduction

Hypercholesterolemia is a condition that caused by overproduction of oxygen free radicals (OFR) and leads to oxidative stress [1]. Oxidative stress is defined as an imbalance between oxidants and antioxidants in favor of oxidants, thus potentially leading to damage to biological system [2]. OFRs have been implicated in the progression of atherosclerosis.

Increased in plasma LDL has been correlated with susceptibility to developing atherosclerosis. A high concentration of LDL can be attributed to the development of oxidized LDL (oxLDL) in hypercholesterolemia. It has been demonstrated that higher level of circulating oxLDL is found in patients with coronary heart disease (CHD) [3]. HDLs,

however, have been shown to exhibit direct antiatherogenic properties in a wide array of animal studies [4, 5]. The counteract effect of HDL is due to reverse cholesterol transport that removes cholesterol from peripheral tissues [6].

Hypercholesterolemic atherosclerosis is always correlated with an increase in the lipid peroxidation product, malondialdehyde (MDA), which indicates high OFRs level, and a decrease in the antioxidant reserve [1]. Higher plasma levels of MDA have been found in atherosclerotic patients [7]. A reduction in atherosclerosis by antioxidants has been associated with a decrease in MDA [8] and an increase in the antioxidant reserve [9]. Thus, the search for compounds from nutraceuticals sources to reduce serum cholesterol and hypercholesterolemic atherosclerosis is crucial.

Canarium odontophyllum Miq. (CO) or dabai is a fruit belongs to Burseraceae family which consists of 100 species well distributed throughout tropical Africa, Asia, and the Pacific island [10, 11]. The fruit is oval in shape [12], rich source of protein, fat, carbohydrates, and minerals (sodium, calcium, and iron) [13]. The fat content is similar to that of olive and avocado fruits [14, 15]. The matured CO fruit is dark purplish. In Malaysia, CO has been classified as under-utilized fruit and is listed as a plant genetic resources for food and agriculture in Sabah [11]. Since 1985, the Department of Agriculture (DOA) has performed number of studies on the collection, documentation, conservation, and improvement of this fruit [10]. Physicochemical characteristics showed that the fruit has high respiration production rate due to a short shelf life. Hence, the fruit must be handled properly and avoid noncold chain handling practice [12].

Considerable research has been performed worldwide on various fruits and fruit extracts for the prevention of coronary heart disease (CHD). Dietary antioxidants appear to play a protective role against the development of cardiovascular disease (CVD). The high antioxidant activity in CO fruit is a major aspect of this study. CO fruit has high antioxidant activity, determined *in vitro* using the DPPH scavenger activity, FRAP, and beta carotene bleaching assays [16, 17]. A study by Chew et al. [18] showed that CO fruit contains appreciable levels of phenolic compounds such as catechin, epigallocatechin gallate, and epicatechin.

The aim of this study was to investigate the effects of different parts of CO (fullfat pulp, defatted pulp, pulp oil, and kernel oil) in high-cholesterol diet fed rabbits on plasma lipids and plasma MDA. Histomorphometric intimal lesion analysis of the aorta was also investigated. The atherogenic index (TC to HDL-C ratio) was also calculated to determine the relative risk of CVD.

2. Materials and Methods

2.1. Sample and Preparation of Powders. Fresh fruits of CO were obtained from the Agriculture Research Centre, Semon-gok, Sarawak, Malaysia. The fruits were packed in an ice box (-4°C), transported to Peninsular Malaysia by air plane, and immediately delivered to Universiti Putra Malaysia. On arrival, the fruits without any physical damage were selected. The pulp was separated by peeling it off from pit (the inner part of fruit). The kernel was obtained by crushing the pit. Then, the pulp and kernel were freeze-dried (Virtis 5L, New York USA). After freeze-drying, the dried samples were ground using a dry grinder (Braun Multiquick ZK100 Germany) and sieved to obtain homogenized particles before undergoing oil extraction. The fatty acid composition of pulp and kernel oils obtained from the extraction was determined. Meanwhile, the proximate composition of full fat and defatted pulp was also determined.

2.2. Reagent. Chloroform, methanol, absolute alcohol, and 10% formalin were purchased from Merck (Germany), Cholesterol and Sudan IV were purchased from Sigma Chemical Co. (USA) and simvastatin was purchased from Pharmacia Logistic (Malaysia), and total cholesterol (TC), low

TABLE 1: A proximate composition of fullfat and defatted powder of *C. odontophyllum* Miq.

Constituent	Percentage (g kg^{-1})	
	Fullfat pulp powder ¹	Defatted pulp powder ²
Moisture ^a	73.4 ± 0.93	85.2 ± 0.06
Fat ^a	454.3 ± 0.15	ND
Protein ^a	67.1 ± 0.09	124.0 ± 0.07
Carbohydrate ^a	180.2 ± 0.08	140.6 ± 0.45
Ash ^a	37.0 ± 0.04	63.0 ± 0.05
TDF ^b	297.8 ± 2.00	545.6 ± 2.08
SDF ^b	79.6 ± 3.26	145.9 ± 3.61
IDF ^b	218.1 ± 0.04	399.7 ± 0.56

^a Values are based on triplicate determinations.

^b Values are based on duplicate determinations.

^{1,2,3} Values are based on 100 g of fullfat and defatted pulp of *C. odontophyllum* fruit respectively.

TDF: total dietary fiber.

IDF: insoluble dietary fiber.

SDF: soluble dietary fiber.

ND: not detected.

density lipoprotein (LDL), high density lipoprotein (HDL), and triglycerides (TG) kits were from Roche Diagnostic (Germany).

2.3. Animals and Diets. Forty-nine male New Zealand white rabbits weighing 1.5–1.7 kg 8–10 weeks old were purchased from the East Asia Company, Malaysia. The animals were placed in individual cages at 25°C under a 12 h light/dark cycle. Water was provided *ad libitum*. Food intake was measured daily. Body weight was measured at baseline, at week 4 and at week 8. After two weeks of acclimatization, the rabbits were divided into seven groups of seven rabbits each ($n = 7$). Rabbits in group 1 were assigned as the negative control and consumed a normal diet (NC); group 2 was the positive control which consumed a 0.5% cholesterol-enriched diet (PC); groups 3 (HS), 4 (HPO), 5 (HKO), 6 (HF), and 7 (HD) were the supplemented groups which consumed cholesterol supplemented with simvastatin (10 mg/kg/day), pulp oil (20 g kg^{-1}), kernel oil (20 g kg^{-1}), fullfat pulp powder (50 g kg^{-1}), or defatted pulp powder (50 g kg^{-1} of CO fruit), respectively (Table 1). All groups received experimental diet prepared within three days before feeding.

2.4. Experimental Protocol. Simvastatin, pulp, and kernel oils were orally given in groups 3 (HS), 4 (HPO), and 5 (HKO), respectively. The simvastatin was diluted in 2 mL of distilled water. Meanwhile, the fullfat pulp and defatted powder received by groups 6 (HF) and 7 (HD) were included in the food pellet.

3. Methods

3.1. Sample Preparation. Pulp and kernel oils of CO were obtained by means of solvent extraction. Dried, homogenized, and ground pulp powder was soaked in chloroform-methanol (2:1 v/v) at ratio of 1:5 (w/v). A mixture of the sample and the solvent was kept overnight at room

TABLE 2: Formulation of experimental diets (g kg^{-1}).

Ingredients	Experimental diets (g kg^{-1})						
	NC	PC	HS	HPO	HKO	HF	HD
Soybean meal	150	150	150	150	150	150	150
Corn	300	300	300	300	300	300	300
Palm kernel	360	360	360	360	360	330	310
Starch	100	100	100	100	100	100	100
Molasses	20	20	20	20	20	20	20
Corn oil	20	20	20	—	—	—	20
Vitamin mixture ^a	3	3	3	3	3	3	3
Mineral mixture ^b	35	35	35	35	35	35	35
DL-methionine	2	2	2	2	2	2	2
CaCO ₃	5	5	5	5	5	5	5
CaHPO ₄	5	5	5	5	5	5	5
Cholesterol	—	5	5	5	5	5	5
Pulp oil of CO	—	—	—	20	20	—	—
Kernel oil of CO	—	—	—	—	—	—	—
Fullfat of CO pulp	—	—	—	—	—	50	—
Defatted CO pulp	—	—	—	—	—	—	50
Total	1000	1005	1005	1005	1005	1005	1005

High cholesterol diet group; HS: treated with simvastatin, HP: treated with pulp oil of *C. odontophyllum*, HK: treated with kernel oil of *C. odontophyllum*, HF: treated with fullfat pulp of *C. odontophyllum*, HD: treated with defatted pulp of *C. odontophyllum*. ^aVitamin mixture: Vit A: 50000 i.u., Vit D3: 8000 i.u., Vit E: 8 mg. ^bMineral mixture: manganese: 320 mg, zinc: 200 mg, magnesium 1400 mg, iron: 300 mg, copper: 50 mg, cobalt: 10 mg, iodate: 20 mg, phosphorus: 10000 mg, sodium chloride: 5500 mg, and calcium: 1300 mg.

temperature and filtered the next day. The organic solvent was completely evaporated using a rotary evaporator (Buchi Rotorvapor R-200, Berlin, Germany) at 40°C. The residue was resoaked with fresh solvent twice to ensure complete extraction of the oil. The extracted oil was combined, weighed, and stored at -20°C until further analysis. The residues from the pulp were dried in an oven (Memmert, Schwabach, Germany) at 40°C to obtain defatted pulp. The contents of dried kernels were prepared in the same manner to obtain kernel oil.

3.2. Determination of Fatty Acid Composition. The fatty acid composition of the oil which was extracted using a chloroform-methanol mixture was determined by gas chromatography (Hewlett-Packard, HP1100, USA Agilent Technology). Fatty acid methyl esters (FAMES) were prepared by weighing out 100 mg of the sample in a 20 mL test tube (with a screw cap). Then, the sample was dissolved in 10 mL of hexane. Next, 100 μL of 2N potassium hydroxide in methanol was added. After vortexing (BOECO, Germany) for 30 seconds, the mixture was centrifuged. Next, 2 mL of the clear supernatant was transferred to a sample vial for fatty acid composition analysis.

3.3. Gas Chromatography (GC) Analysis. The fatty acid composition of the oil samples was analyzed using an Agilent 6890 GC (USA Agilent Technology) equipped with split-splitless injector, a detector, and a Hewlett-Packard EL-980 flame ionization detection (FID) system to separate and quantify each FAME component. FAMES were separated using a DB-23 column (60 m \times 0.25 mm I.D., 0.15 μm

polyethylene glycol film). Chromatography data were recorded and integrated using Chemstations software (Version 6.0). The oven temperature was held at 50°C for 1 min, then increased to 175°C at 4°C/min and lastly finally increased to 230°C, holding for 5 min at 230°C. The temperatures for the injector and detector were set at 250°C and 280°C, respectively. One microliter of the sample volume was injected with a split ratio of 1:50 at a column temperature the 110°C. Carrier gases that were used in the system were helium gas, 1.0 mL/min controlled at 103.4 kPa, the hydrogen and air used for FID were held at 275.6 kPa.

3.4. Preparation of Diets. The experimental diets, as shown in Table 2, were prepared based on the NC diet, which is a normal basal diet. The normal basal diet contains soybean (150 g kg^{-1}), corn (30 g kg^{-1}), starch (100 g kg^{-1}), molasses (20 g kg^{-1}), corn oil (20 g kg^{-1}), a vitamin mixture (3 g kg^{-1}), a mineral mixture (3.5 g kg^{-1}), DL-methionine (2 g kg^{-1}), calcium carbonate (5 g kg^{-1}), and calcium hydrogen phosphate (5 g kg^{-1}).

The basal diet for the NC group was prepared as follows: soybean, corn, and palm kernel cake were ground using an electric grinder, weighed and mixed manually. Later, the minerals and vitamin mixtures (minerals mixture, vitamins mixture, CaCO₃, CaHPO₄, and DL-methionine) were added. Next, oil and molasses were mixed. Starch (100 g kg^{-1}) was added to the mixture, mixed well, and placed carefully on a dish covered with aluminum foil. Then, the dough was cut into small pieces and dried in an oven (Memmert, Schwabach, Germany) at 45–50°C overnight. The prepared pellets were stored in air-tight containers at room

temperature. For the hypercholesterolemic diets (HS, HPO, HKO, HF, and HD), cholesterol (5 g kg^{-1}) was added.

Similarly, the hypercholesterolemic diets were prepared using the same method as described for the NC diet with the addition of other food ingredients in the particular diet. In the HS group, a hypercholesterol diet was given, with simvastatin (10 mg/kg per day) given orally by force-feeding. The simvastatin was prepared by dissolving simvastatin with distilled water. For the HPO and HKO diets, 20 g kg^{-1} of pulp (PO) and kernel oils (KO) extracted from the pulp and kernel of CO were added, respectively, which replaced the total fat required for the rabbits. Meanwhile, for the HF diet, 50 g kg^{-1} of fullfat pulp was added to represent the replacement of total fat and 80 g kg^{-1} of carbohydrate required. For the HD diet, 50 g kg^{-1} of CO defatted pulp was added. Defatted pulp is a rich source of dietary fiber, thus representing 14% replacement of the daily requirement of dietary fiber in the HD diet. Previous studies have shown that giving $100\text{--}150 \text{ g kg}^{-1}$ of dietary fiber from fruit such as defatted roselle [19] and defatted cocoa [20] has cholesterol-lowering effects in a hypercholesterolemic model. Thus, 50 g kg^{-1} of defatted pulp may potentially provide a similar effect.

3.5. Blood Sampling. Blood was drawn from marginal ears of the rabbits at weeks 0 (baseline), 4, and 8 from all groups. The blood was collected into an EDTA tube. All experimental protocols were approved by the Animal Care and Use Committee (ACUC) of the Faculty of Medicine and Health Sciences, Universiti Putra Malaysia (UPM), Serdang, Selangor. Plasma was obtained by centrifugation at 3000 rpm for 10 minutes at 25°C . Plasma was used for determination of TC, LDL-C, HDL-C, TG, and MDA levels.

3.6. Body Weight and Food Intake. Individual body weight and food intake of rabbits were recorded at week 0 and 8.

3.7. Biochemical Analysis. Plasma lipids were estimated spectrophotometrically using an automatic chemistry analyzer (Hitachi, UK) with standard test kits (Roche Diagnostics, UK). The plasma TBARS level was measured using the thiobarbituric acid (TBA) assay described by Buege and Aust [21].

3.8. Determination of Atheroma Plaques in the Aorta. At the end of week 8, the rabbits were sacrificed. The aorta between its origin and bifurcation into the iliac arteries was dissected, opened longitudinally, and prepared for accurate detection and estimation of lipid deposits in the intima by the macroscopic method as described by Holman et al. [22]. The aortas were washed out with normal saline and used for Sudan IV staining.

After aortas were dissected and properly cleaned of fat residue on the outer surface, sectioned longitudinally, and stretched onto a piece of board followed by fixation in 10% formalin for 24 hours. Subsequently, they were rinsed off with 70% alcohol to remove the formalin residue. Then, the aortas were immersed in Herxheimers solution (Sudan IV in

ethanol and acetate) for 2-3 minutes at room temperature. Sudan IV stain is lipophilic, so it will stain the lipid components on the surface of the tissue. After 15 min, aortas were consecutively washed in running tap water for 1 hour. Water flow was not too heavy to avoid damage to the tissues. This staining allows for a clear illustration of plaques due to their deep red color.

Images of the aortas were captured using a digital camera (EOS Canon, Japan). The total atherosclerotic areas of the intimal surface of the aorta were measured in mm^2 using graph paper. The extent of atherosclerosis was expressed as the percentage of the luminal surface covered by atherosclerotic changes. The lesion area was estimated using the following formula described by Bocan et al. [23]:

$$\text{Lesion area} = \frac{\text{lesion area on intimal surface of the aorta}}{\text{whole area of the aorta}} \quad (1)$$

3.9. Statistical Analysis. The data are presented as group means \pm SEM. Analysis of variance (ANOVA) using Statistical Package Social Sciences (SPSS) version 16.0 was used for data analysis. Statistical differences between the treatment and control groups were determined using one-way ANOVA. The Turkey post-hoc test was used for multiple group comparisons. The significance value was set at $P < 0.05$.

4. Results and Discussion

4.1. Nutrient Composition of Fullfat and Defatted Pulp of CO Fruit. Table 1 shows the nutrient composition of fullfat and defatted pulp of CO. The fruits are a rich source of fat, dietary fiber, and carbohydrates. This finding is in accordance with a study by Hoe [13], who reported that CO is rich in fat and carbohydrates. However, the dietary fiber was lower compared to the present study which could be due to the different determination method used. The fat content in this study was slightly higher than the level reported by Hoe (260 g kg^{-1}) [13]. The fat content of CO is lower compared to other species of *Canarium* [24]. The moisture, fat, and protein levels reported by Chew et al. [25] are higher than present finding because the values were based on fresh weight of fruit sample.

To our knowledge, this is the first time the value of total dietary fiber (TDF) of CO fruit has been reported. The TDF level in the fullfat pulp was two-times higher than in the defatted pulp. The insoluble dietary fiber (IDF) was higher than the soluble dietary fiber (SDF) in fullfat and defatted pulp powder. Besides, the dietary fiber of CO pulp was also higher than olive [26] but lower than other fruits such as persimmon [27], carob [28], and apple [29].

4.2. Fatty Acid Composition of Pulp and Kernel Oils of CO Fruit. Table 3 shows the fatty acid composition of pulp and kernel oils extracted from CO fruit. The fatty acids that were found abundantly in the studied oils were oleic acid (18:1), palmitic acid (16:0), and linoleic acid (18:2n6cis). Pulp oil share similar fatty acid composition with palm oil, in which equal SFAs and MUFAs content are found in these oils.

TABLE 3: Fatty acid composition of pulp and kernel oils of *C. odontophyllum* fruits.

Fatty acids	Percentage (%)	
	Pulp oil	Kernel oil
Saturated fatty acid	43.42 ± 0.05	56.2 ± 0.04
14:0	0.31 ± 0.04	0.1 ± 0.01
16:0	40.31 ± 0.01	50.22 ± 0.74
18:0	2.19 ± 1.04	5.88 ± 0.76
20:0	0.61 ± 0.07	ND
Monounsaturated fatty acid	42.53 ± 0.06	39.84 ± 0.04
16:01	0.63 ± 0.08	0.28 ± 0.05
18:01	41.9 ± 0.02	39.56 ± 0.48
Polyunsaturated fatty acid	14.05 ± 0.09	3.96 ± 0.04
18:2n6cis	14.05 ± 1.96	3.73 ± 0.41
18:3n3	ND	0.23 ± 0.04

Meanwhile slightly higher SFAs compared to UFAs were found in kernel oil. Similar fatty acid compositions of pulp oil have been reported by previous investigators [30] but with slightly higher PUFA (14.05% versus 12.76%). Furthermore, a similar fatty acid composition in pulp oil was reported by Azrina et al. [17].

4.3. Food Intake and Body Weight. The food intake and body weight in all groups were increased throughout the experimental period (Table 4). At the end of study, the highest body weight was found in the PC group. The increment might have been due to greater lipid deposition in the body tissue of this animal [31] in accordance with a previous study by Lee et al. [32]. Among the treated groups, the highest body weight was found in HD, followed by higher food intake. Higher food intake in the CO-treated group could have been due to high satiety. Thus, it can be suggested that this fruit is best consumed by humans. However, the lowest food intake in HS could have been due to low satiety and distaste for simvastatin [33].

4.4. Lipid Profile. Hyperlipidemia, especially hypercholesterolemia, is a major risk factor for coronary artery disease, and reducing plasma cholesterol levels in particular LDL cholesterol may reduce the risk of this disease. Globally, the morbidity of cardiovascular disease has increased slightly, making hyperlipidemia the leading cause of mortality. Meanwhile, epidemiologic studies have found that increased serum cholesterol predict the risk of CHD in various human and animal studies [34, 35]. Therefore, dietary strategies known to reduce cholesterol levels, such as a reduction in total and saturated fat intake as well as increased intake of dietary fiber [36], are meaningful steps to minimize the risk.

Based on data in Table 5, at baseline, the plasma TC, LDL-C, and HDL-C levels were not significantly different from each other in all groups as we had standardized the animals' condition, in terms of the room environment and fasting period [35]. For changes in lipid indices, the high cholesterol diet fed rabbits (PC) showed significantly ($P < 0.05$) increased in TC, LDL-C, HDL-C, and TG levels compared to

normal animals (NC). The TC was increased 12-fold in the first four weeks, and continued to increase a further 1.8 times by week 8. This showed that hypercholesterolemia had been successfully established in the rabbits by means of feeding 5 g kg^{-1} cholesterol in the diet over four weeks. HDL exhibits antiatherogenic effects, but the level was higher in PC. This could be due to the cholesterol load on plasma lipids, which increases the work load of plasma lipoproteins especially HDL. In the present study, simvastatin was used because it is a potent hypolipidemic drug known to exert its action by inhibiting HMG-Coa reductase, the rate-limiting step in cholesterol biosynthesis. In humans, the statin family has been well accepted as cholesterol-lowering drugs [37]. Thus, the HS group was used to compare the effectiveness of the fruit parts in reducing plasma cholesterol levels. Based on the present data, the simvastatin treated group had significantly reduced ($P < 0.05$) TC, LDL-C, and TG levels, which are all in accordance with previous studies [37–39].

Among the treatment groups, rabbits fed with the defatted pulp of CO (HD) showed the greatest reduction in plasma TC, thus indicating a positive hypocholesterolemic effect (markedly reduced TC and LDL-C, $P < 0.05$) of the defatted pulp in the context of exposure to a high cholesterol diet. The superior effect of the HD diet could have been due to the 70 mg of polyphenolic compounds found in the defatted pulp as shown by a previous investigator [40]. A possible mechanism involved in its *in vivo* antioxidant effect may be mediated by radical scavenging activity [16]. The other possible mechanisms could be the effect of bile acid binding by polyphenols which in turn increase fecal loss [28]. The hypocholesterolemic effect of defatted pulp could also be due to the presence of carotenoid content especially *trans*- β -carotene, 15-*cis*- β -carotene, 9-*cis*- β -carotene, and 13-*cis*- β -carotenes. The peel fraction which represents about 30% from the defatted pulp exhibits good inhibitory effect against hydrogen peroxide-induced haemoglobin oxidation, ranging from 45.3 to 59.7% [41].

Defatted pulp of CO consists 50% dietary fiber enriched with 70 mg of polyphenol compounds and exhibited a cholesterol lowering effect. It is well known that dietary fiber in the presence of antioxidant compounds plays an important role in reducing plasma cholesterol levels. Many animal and human studies have shown that consumption of food rich in dietary fiber with the presence of antioxidant compounds has positive effects on different parameters associated with CVD such as endothelial function, platelet activation, and biomarkers of lipid peroxidation [20, 42, 43]. It is well known that dietary fiber plays an important role in reducing plasma cholesterol levels. Previous studies have revealed that fiber-rich food such as oat bran, beans, grains, and legumes have significant effects on serum cholesterol [42, 44, 45]. Various actions of dietary fiber have been shown to lower serum cholesterol, such as hindering digestion and absorption of dietary fat, modifying bile acid absorption and the metabolism and formation of short chain fatty acids [20, 46]. Moreover, numerous studies have demonstrated that the reduction of plasma cholesterol level is likely attributed to bile acid and dietary fat binding to the fiber compound [20, 47, 48]. Therefore, it can be proposed that the cholesterol

TABLE 4: Food intake and body weight of rabbits fed experimental diets in week 0 and 8.

Group	Animal weight (kg/rabbit)		Daily food intake (g/rabbit)	
	Week		Week	
	0	8	0	8
NC	1.87 ± 0.03	2.09 ± 0.06 ^{ab}	79.80 ± 61.58	93.75 ± 2.05 ^{abc}
PC	1.82 ± 0.09	2.34 ± 0.04 ^b	80.00 ± 5.44	90.33 ± 2.69 ^{ab}
HS	1.86 ± 0.02	2.22 ± 0.09 ^{ab}	76.71 ± 2.57	82.79 ± 1.52 ^a
HPO	1.74 ± 0.02	2.19 ± 0.10 ^{ab}	74.93 ± 0.47	107.50 ± 5.75 ^c
HKO	1.74 ± 0.04	2.13 ± 0.07 ^{ab}	81.92 ± 1.39	103.37 ± 4.29 ^{bc}
HF	1.84 ± 0.08	2.02 ± 0.01 ^a	75.47 ± 0.27	102.76 ± 5.92 ^{bc}
HD	1.75 ± 0.00	2.24 ± 0.01 ^{ab}	80.49 ± 4.55	107.07 ± 1.14 ^c

Values are expressed as mean ± SEM. Values are not significantly different at $P < 0.05$ in week 0. NC: normal diet group, PC: positive control, HS, HPO, HKO, HF, and HD: hypercholesterolemic group treated with 10 mg/kg/day simvastatin, 20 g kg⁻¹ of pulp oil, 20 g kg⁻¹ kernel oil, 50 g kg⁻¹ fullfat pulp, or 50 g kg⁻¹ defatted pulp, respectively.

TABLE 5: Plasma lipid profile and the ratio of TC to HDL-C at week 0 (baseline), week 4, and week 8.

	NC	PC	HS	HPO	HKO	HF	HD
TC (mmol/L)							
Week 0	1.79 ± 0.06 ^{a,1}	1.54 ± 0.06 ^{a,1}	1.58 ± 0.09 ^{a,1}	1.16 ± 0.03 ^{a,1}	0.84 ± 0.03 ^{a,1}	1.23 ± 0.01 ^{a,1}	0.89 ± 0.02 ^{a,1}
Week 4	2.21 ± 0.04 ^{a,2}	19.58 ± 0.81 ^{d,2}	9.54 ± 0.38 ^{b,2}	20.4 ± 0.37 ^{d,2}	21.36 ± 0.59 ^{d,2}	12.33 ± 0.47 ^{c,2}	4.21 ± 0.19 ^{a,2}
Week 8	1.94 ± 0.02 ^{a,1}	34.42 ± 0.84 ^{c,3}	3.74 ± 0.11 ^{a,3}	24.83 ± 0.88 ^{b,3}	24.26 ± 0.61 ^{b,3}	33.61 ± 0.99 ^{c,3}	1.29 ± 0.02 ^{a,1}
LDL-C (mmol/L)							
Week 0	0.66 ± 0.03 ^{a,1}	0.62 ± 0.03 ^{a,1}	0.65 ± 0.02 ^{a,1}	0.53 ± 0.21 ^{a,1}	0.28 ± 0.18 ^{a,1}	0.58 ± 0.04 ^{a,1}	0.29 ± 0.02 ^{a,1}
Week 4	1.02 ± 0.05 ^{a,2}	11.94 ± 0.06 ^{c,2}	5.97 ± 0.12 ^{b,2}	13.17 ± 0.89 ^{c,2}	6.36 ± 0.42 ^{c,2}	14.91 ± 0.61 ^{b,2}	3.00 ± 0.22 ^{ab,2}
Week 8	0.66 ± 0.05 ^{a,1}	14.84 ± 1.26 ^{c,2}	3.99 ± 0.31 ^{a,3}	14.83 ± 1.42 ^{b,2}	17.37 ± 1.14 ^{c,3}	17.97 ± 1.18 ^{c,2}	10.90 ± 0.59 ^{b,3}
HDL-C (mmol/L)							
Week 0	0.59 ± 0.04 ^{c,1}	0.36 ± 0.02 ^{ab,1}	0.49 ± 0.03 ^{bc,1}	0.37 ± 0.03 ^{ab,1}	0.35 ± 0.02 ^{ab,1}	0.55 ± 0.04 ^{c,1}	0.30 ± 0.03 ^{a,1}
Week 4	0.6 ± 0.04 ^{a,1}	2.81 ± 0.11 ^{c,2}	2.46 ± 0.03 ^{c,2}	4.08 ± 0.38 ^{d,2}	1.59 ± 0.07 ^{c,2}	2.62 ± 0.22 ^{b,2}	0.68 ± 0.16 ^{a,1}
Week 8	0.57 ± 0.04 ^{a,1}	3.59 ± 0.19 ^{d,3}	1.29 ± 0.13 ^{a,3}	2.79 ± 0.21 ^{c,3}	3.31 ± 0.11 ^{d,3}	4.12 ± 0.24 ^{e,3}	1.91 ± 0.11 ^{b,2}
TG (mmol/L)							
Week 0	0.64 ± 0.01 ^{a,1}	0.65 ± 0.06 ^{a,1}	0.56 ± 0.02 ^{a,1}	0.69 ± 0.05 ^{a,1}	0.65 ± 0.03 ^{a,1}	0.69 ± 0.05 ^{a,1}	0.75 ± 0.11 ^{a,1}
Week 4	0.54 ± 0.01 ^{c,2}	0.48 ± 0.03 ^{ab,1}	0.59 ± 0.12 ^{a,1}	0.7 ± 0.05 ^{a,1}	0.77 ± 0.07 ^{a,1}	0.43 ± 0.03 ^{b,1}	1.07 ± 0.08 ^{d,1}
Week 8	0.51 ± 0.04 ^{a,1}	1.28 ± 0.09 ^{c,2}	0.56 ± 0.04 ^{a,1}	1.28 ± 0.05 ^{c,2}	1.58 ± 0.07 ^{c,1}	1.18 ± 0.12 ^{b,2}	1.03 ± 0.02 ^{c,1}
TC:HDL ratio							
Week 0	2.99 ± 0.01 ^{b,1}	4.29 ± 0.11 ^{d,1}	3.22 ± 0.08 ^{b,2}	3.13 ± 0.05 ^{b,1}	3.50 ± 0.09 ^{c,2}	1.53 ± 0.06 ^{a,1}	2.91 ± 0.14 ^{b,2}
Week 4	3.68 ± 0.01 ^{a,2}	6.98 ± 0.19 ^{a,2}	3.88 ± 0.07 ^{a,3}	5.01 ± 0.11 ^{b,2}	7.74 ± 0.50 ^{d,3}	8.14 ± 0.70 ^{e,3}	6.22 ± 0.15 ^{c,3}
Week 8	3.39 ± 0.08 ^{b,3}	9.57 ± 0.11 ^{b,3}	1.36 ± 0.14 ^{a,1}	8.88 ± 0.10 ^{d,3}	10.15 ± 0.42 ^{e,1}	5.89 ± 0.09 ^{c,2}	0.67 ± 0.02 ^{a,1}

Value represents the mean ± SEM ($n = 4$). Values for a given parameter in a row that do not share the same superscript letter are significantly different at $P < 0.05$. Values for a given parameter in each column that do not share the same superscript number are significantly different at $P < 0.05$. NC: normal control, PC: positive control, HS, HPO, HKO, HF, and HD: hypercholesterolemic diet treated with simvastatin, 20 g kg⁻¹ of pulp oil, 20 g kg⁻¹ kernel oil, 50 g kg⁻¹ fullfat pulp, or 50 g kg⁻¹ defatted pulp, respectively.

lowering effect of defatted pulp in the HD group in the present study might have been due to the binding of dietary fibre in the defatted pulp with bile acids which in turn increases the faecal excretion [46, 47].

HDL-C plays an important role in protection against cardiovascular diseases and is responsible for transporting cholesterol from cells and arteries to the liver for catabolism. In the CO supplemented groups (HPO, HKO, HF, and HD), the increment of HDL-C was higher (6.4–9.5 times) than the statin receiving group (HS) (2.6 times). Thus, it can be suggested that the effect of CO fruit parts on lowering plasma lipid cholesterol is superior to that of simvastatin.

Triglycerides (TGs) circulate in the blood are stored in the body fat and are used when the body needs extra energy. Excessive TG is related to the occurrence of coronary artery disease [49]. In this study, feeding rabbits a high cholesterol diet (PC) increased the plasma TG by two-fold from week 0 to week 8. Meanwhile, supplementation of fullfat pulp in rabbits resulted in 8% a significant decrease ($P < 0.05$) in TG after 8 weeks of treatment. No significant changes ($P > 0.05$) were observed in groups supplemented with pulp oil (HPO), kernel oil (HKO), and defatted pulp (HD), compared to PC.

Generally, it is difficult to detect the CVD risk factor based on individual lipoproteins (TC, LDL-C, HDL-C) and

TG levels. Consequently, the atherogenic index (TC to HDL-C ratio) was used for this purpose. This ratio is a good marker for identifying and minimizing the risk of CVD [50]: an increase in this ratio increases the risk of cardiovascular diseases. The value for the TC to HDL-C ratio in the PC group was three times higher compared to animals in the normal group, which clearly showed that PC is associated with a very high risk of CVD. After treatment with simvastatin, this value decreased by two-fold. In the blood, statins lower TC, LDL-C, and TG. Interestingly, supplementation of both fullfat pulp and defatted pulp of CO decreased the ratio of TC to HDL by 36% and 93%, respectively, with no significant differences from the statin group.

Besides dietary content and other nutrients, the fatty acid content can influence plasma lipid and lipoprotein types and concentrations. Saturated fatty acids (SFAs) are well known to increase CVD by elevating plasma TC and LDL, while a diet rich in monounsaturated fatty acids (MUFAs) and polyunsaturated fatty acids (PUFAs) is able to reduce plasma TC and LDL in normolipidemic subjects [51]. The plasma TC was reduced by 28% and 30% in the HPO and HKO groups, respectively. The preventive roles of pulp and kernel oils of CO were attributed to their MUFA contents. A diet high in MUFA is able to suppress LDL oxidation and oxidative stress [52]. However, the plasma LDL-C levels were slightly higher in HKO. This could be explained by higher levels of SFAs in kernel oil. A study by Mensink et al. [51] showed that vegetable oils rich in SFAs can increase plasma LDL-C.

4.5. Lipid Peroxidation by Thiobarbituric Acid Reactive Substances (TBARS). Lipid peroxidation can be evaluated by the thiobarbituric acid reactive substances method (TBARS) which evaluates oxidative stress by assaying for MDA (malondialdehyde), a product of lipid breakdown [9]. Table 6 shows the effect of CO fruit parts on the TBARS level at different time points where initial values of plasma TBARS were not significantly different to each other. In rabbits, a fed high cholesterol diet, the plasma TBARS was significantly higher ($P < 0.05$) than in rabbits on a normal diet, which clearly indicates elevated production of free radicals which enhance the process of lipid peroxidation [8].

The TBARS level was diminished significantly ($P < 0.05$) in groups supplemented with the fruit parts of CO. The reductions in the HPO, HKO, HF, and HD groups were 14%, 13%, 15%, and 36%, respectively; the highest reduction in TBARS was observed in the defatted pulp supplemented group. The reduction in the lipid peroxidation level could be related to strong antioxidant properties of the defatted pulp against OFRs in biological systems. CO fruit pulp has been demonstrated to have a high polyphenols contents with potent antioxidant capacity *in vitro* [16, 17]. The antifree radical activities of phenolics are well established, act as free radical scavengers and slow down oxidative stress-related lipid peroxidation.

4.6. Atheroma Plaques. Atherosclerosis is characterized by the accumulation of cholesterol deposits in the macrophages

TABLE 6: Plasma malondialdehyde (MDA) level in experimental rabbits.

Groups	Plasma MDA (mol/L)		
	Week 0	Week 4	Week 8
NC	2.60 ± 0.04 ^{a,1}	2.67 ± 0.08 ^{b,2}	3.74 ± 0.15 ^{b,2}
PC	2.92 ± 0.32 ^{a,1}	3.10 ± 0.17 ^{ab,1}	4.37 ± 0.18 ^{c,2}
HS (simvastatin)	2.80 ± 0.10 ^{a,1}	2.87 ± 0.07 ^{c,1}	4.17 ± 0.17 ^{bc,2}
HPO (pulp oil)	2.96 ± 0.08 ^{a,1}	3.42 ± 0.03 ^{b,2}	3.78 ± 0.08 ^{b,3}
HKO (kernel oil)	3.03 ± 0.18 ^{a,1}	3.44 ± 0.15 ^{b,1}	3.79 ± 0.05 ^{b,2}
HF (fullfat)	3.06 ± 0.12 ^{a,1}	3.06 ± 0.11 ^{b,1}	3.70 ± 0.09 ^{b,2}
HD (defatted)	2.92 ± 0.18 ^{a,1}	3.77 ± 0.09 ^{a,2}	2.81 ± 0.04 ^{a,1}

NC: normal diet group, PC: positive control, HS, HPO, HKO, HF, and HD: hypercholesterolemic group treated with 10 mg/kg/day simvastatin, 20 g kg⁻¹ of pulp oil, 20 g kg⁻¹ kernel oil, 50 g kg⁻¹ fullfat pulp, or 50 g kg⁻¹ defatted pulp, respectively. Values are expressed as mean ± SEM. Values within column followed by the same superscript letter are not significantly different at $P > 0.05$. Values within groups followed by the same superscript number are not significantly different at $P > 0.05$.

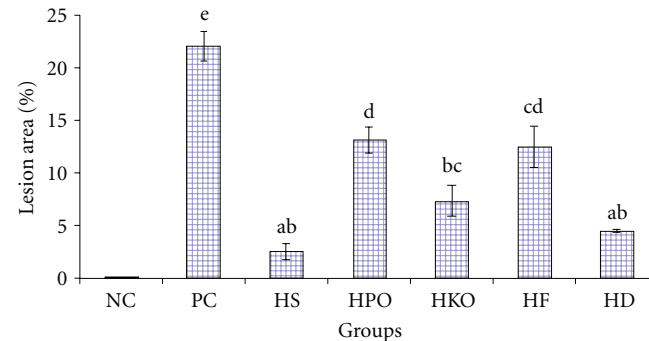


FIGURE 1: Percentage of lesion area in the experimental groups. Each value represents the mean ± SEM for $n = 7$. Values with different letters are significantly different ($P < 0.05$) between groups.

of arteries [53] which become disrupted through the physical forces in arterial walls. The severity of atheromatous lesions is associated with hypercholesterolemia [54, 55]. The percentages of lesions on the intimal surface of aortas from the PC, HS, HPO, HKO, HF, and HD groups are shown in Figure 1. The plaques were severe in animals fed a high cholesterol diet (PC) (22.08% ± 2.76) (Figure 2). A hypercholesterolemic diet produced intimal thickening that contained foam cells similar to those observed by many researchers [54, 56, 57].

Among the treated groups, HD exhibited the greatest reduction in atherosclerotic plaque formation by nearly 80%. The pronounced effect in HD compared to HF could be due to the higher level of dietary fiber in defatted compared to fullfat pulp (Table 1). Pulp oil had higher MUFA compared to kernel oil. However, lower plaque formation was found in HKO compared to HPO which could be due to higher level of cholesterol-lowering agents such as phytosterols [58], antioxidant vitamins [59], and flavonoids [2] which were not measured in this study.

The protective effect of the defatted pulp could be attributed to the high antioxidant capacity of the fraction that reduced the plasma MDA level (Table 6). It has been well

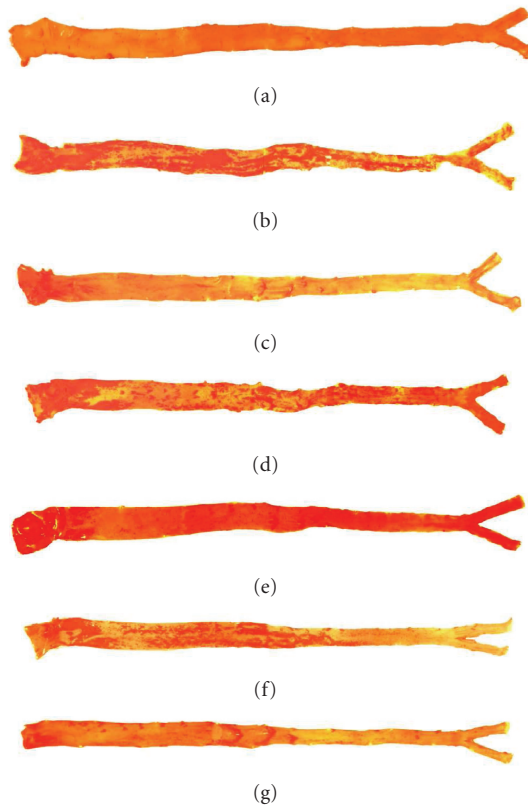


FIGURE 2: Photograph of intimal surface of aorta of each group. Representative photograph of intimal surface of aortas stained with Sudan IV. Atherosclerotic lesions were indicated by concentrated brick red colours. Atherosclerotic lesion is absent in the NC group. (a) NC, (b) PC, (c) HS, (d) HPO, (e) HKO, (f) HF, (g) HD followed the respective diet for 8 weeks.

established that an increased MDA level is positively correlated with the progression of atherosclerosis [60]. The high polyphenolic contents of the defatted pulp [16, 40] used in the present study might have prevented the development of atherosclerosis by its free radical-scavenging antioxidant activity. Instead of having high antioxidant activity, the protective effect of the defatted pulp could also be attributed to its lipid lowering ability. Animals fed defatted pulp had reduced (significant, $P < 0.05$) plasma TC and a lower atherogenic index (TC to HDL-C ratio). Several epidemiological studies have demonstrated that increased dietary intake of natural phenolic antioxidants plays an essential role in the prevention of cardiovascular diseases, cancer, and neurodegenerative diseases. Similarly, the pulp of CO fruits has been shown to possess tremendous *in vitro* antioxidant capacity estimated from extracts of the fruit [16, 17, 40]. In addition, a high correlation was reported between the phenolic content and antioxidant capacities in these studies. Thus, this suggests that the protective effect of CO defatted pulp against the formation of atherosclerotic lesions may be mainly attributed to the high antioxidant content of this fruit part.

5. Conclusions

Among the CO fruit parts, defatted pulp was associated with the greatest reduction in atherosclerotic plaque formation, induced by a significant reduction in LDL-C, TC, and lipid peroxidation levels. The presence of high dietary fiber and high levels of antioxidants with potent activity was essential factor contributing to the retardation of atherosclerosis and a reduction in coronary artery disease risk. Consequently, these results indicate the potential use of CO defatted pulp as a hypocholesterolemic and antioxidative agent apart from its ability to slow the progression of atherosclerosis.

Acknowledgments

The financial support of ScienceFund from Ministry of Agriculture, Malaysia (Vote no. 5450555, is gratefully acknowledged. The authors like to thank the assistance of laboratory staffs from the Department of Nutrition and Dietetic and the use of laboratories facilities of Universiti Putra Malaysia throughout the research project.

References

- [1] D. D. Heistad, Y. Wakisaka, J. Miller, Y. Chu, and R. Pena-Silva, "Novel aspects of oxidative stress in cardiovascular diseases," *Circulation Journal*, vol. 73, no. 2, pp. 201–207, 2009.
- [2] K. Prasad, "Hypocholesterolemic and antiatherosclerotic effect of flax lignan complex isolated from flaxseed," *Atherosclerosis*, vol. 179, no. 2, pp. 269–275, 2005.
- [3] S. I. Toshima, A. Hasegawa, M. Kurabayashi et al., "Circulating oxidized low density lipoprotein levels: a biochemical risk marker for coronary heart disease," *Arteriosclerosis, Thrombosis, and Vascular Biology*, vol. 20, no. 10, pp. 2243–2247, 2000.
- [4] P. J. Barter, S. Nicholls, K. A. Rye, G. M. Anantharamaiah, M. Navab, and A. M. Fogelman, "Antiinflammatory properties of HDL," *Circulation Research*, vol. 95, no. 8, pp. 764–772, 2004.
- [5] G. Assmann and A. M. Gotto, "HDL cholesterol and protective factors in atherosclerosis," *Circulation*, vol. 109, no. 23, pp. III8–III14, 2004.
- [6] P. Barter, J. Kastelein, A. Nunn et al., "High density lipoproteins (HDLs) and atherosclerosis; the unanswered questions," *Atherosclerosis*, vol. 168, no. 2, pp. 195–211, 2003.
- [7] R. Albertini, R. Moratti, and G. De Luca, "Oxidation of low-density lipoprotein in atherosclerosis from basic biochemistry to clinical studies," *Current Molecular Medicine*, vol. 2, no. 6, pp. 579–592, 2002.
- [8] P. O. Bonetti, L. O. Lerman, and A. Lerman, "Endothelial dysfunction: a marker of atherosclerotic risk," *Arteriosclerosis, Thrombosis, and Vascular Biology*, vol. 23, no. 2, pp. 168–175, 2003.
- [9] J. M. Mates, C. Rerez-Gomez, and I. N. Castro, "Antioxidant enzymes and human disease," *Clinical Biochemistry*, vol. 32, pp. 595–603, 1999.
- [10] C. C. Chai, G. K. Teo, C. Y. Lau, and A. M. A. Powoven, "Conservation and sustainable utilization of indigenous vegetables of Sarawak," in *Agrobiodiversity in Malaysia*, pp. 42–55, Kuala Lumpur, Malaysia, 1st edition, 2008.
- [11] W. W. W. Wong, T. C. Chong, and J. Tananak, "Conservation and sustainable utilization of fruit species of Sabah," in *Agrobiodiversity in Malaysia*, pp. 30–42, Kuala Lumpur, Malaysia, 2008.

- [12] P. Ding and Y. K. Tee, "Physicochemical characteristics of dabai (*Canarium odontophyllum* Miq.) fruit," *Fruits*, vol. 66, no. 1, pp. 47–52, 2011.
- [13] V. B. Hoe, "The nutritional value of indigenous fruits and vegetables in Sarawak," *Asia Pacific Journal of Clinical Nutrition*, vol. 8, no. 1, pp. 24–31, 1999.
- [14] M. T. G. Hierro, M. C. Tomas, F. Fernandez-Martin, and G. Santa-Maria, "Determination of the triglyceride composition of avocado oil by high-performance liquid chromatography using a light-scattering detector," *Journal of Chromatography*, vol. 607, no. 2, pp. 329–338, 1992.
- [15] M. D. Salvador, F. Aranda, and G. Fregapane, "Influence of fruit ripening on 'Cornicabra' virgin olive oil quality: a study of four successive crop seasons," *Food Chemistry*, vol. 73, no. 1, pp. 45–53, 2001.
- [16] F. H. Shakirin, K. N. Prasad, A. Ismail, L. C. Yuon, and A. Azlan, "Antioxidant capacity of underutilized Malaysian *Canarium odontophyllum* (dabai) Miq. fruit," *Journal of Food Composition and Analysis*, vol. 23, no. 8, pp. 777–781, 2010.
- [17] A. Azrina, M. N. Nurul Nadiah, and I. Amin, "Antioxidant properties of methanolic extract of *Canarium odontophyllum* fruit," *International Food Research Journal*, vol. 17, no. 2, pp. 319–326, 2010.
- [18] L. Y. Chew, H. E. Khoo, I. Amin, A. Azrina, and C. Y. Lau, "Analysis of phenolic compounds of dabai (*Canarium odontophyllum* Miq.) fruits by high-performance liquid chromatography," *Food Analytical Methods*, vol. 5, pp. 1–12, 2011.
- [19] E. Hainida, A. Ismail, N. Hashim, N. Mohd, and A. Zakiah, "Effects of defatted dried roselle (*Hibiscus sabdariffa* L.) seed powder on lipid profiles of hypercholesterolemia rats," *Journal of the Science of Food and Agriculture*, vol. 88, no. 6, pp. 1043–1050, 2008.
- [20] E. Lecumberri, L. Goya, R. Mateos et al., "A diet rich in dietary fiber from cocoa improves lipid profile and reduces malondialdehyde in hypercholesterolemic rats," *Nutrition*, vol. 23, no. 4, pp. 332–341, 2007.
- [21] J. A. Buege and S. D. Aust, "Microsomal lipid peroxidation," *Methods in Enzymology*, vol. 52, pp. 302–310, 1978.
- [22] R. L. Holman, H. C. McGill, J. P. Strong, and J. C. Geer, "The natural history of atherosclerosis: the early aortic lesions as seen in New Orleans in the middle of the of the 20th century," *The American Journal of Pathology*, vol. 34, no. 2, pp. 209–235, 1958.
- [23] T. M. A. Bocan, S. B. Mueller, M. J. Mazur, P. D. Uhlendorf, E. Q. Brown, and K. A. Kieft, "The relationship between the degree of dietary-induced hypercholesterolemia in the rabbit and atherosclerotic lesion formation," *Atherosclerosis*, vol. 102, no. 1, pp. 9–22, 1993.
- [24] A. N. Georges, C. K. Olivier, and R. E. Simard, "*Canarium schweinfurthii* Engl.: chemical composition of the fruit pulp," *Journal of the American Oil Chemists' Society*, vol. 69, no. 4, pp. 317–320, 1992.
- [25] L. Y. Chew, K. N. Prasad, I. Amin, A. Azrina, and C. Y. Lau, "Nutritional composition and antioxidant properties of *Canarium odontophyllum* Miq. (dabai) fruits," *Journal of Food Composition and Analysis*, vol. 24, no. 4-5, pp. 670–677, 2011.
- [26] A. Jimenez, R. Rodriguez, I. Fernandez-Caro, R. Guilen, J. Fernandez-Bolanos, and A. Heredia, "Dietary fibre content of tables olives processed under different European styles: study of physico-chemical characteristics," *Journal of the Science of Food and Agriculture*, vol. 80, pp. 1903–1908, 2000.
- [27] S. Gorinstein, A. Caspi, I. Libman, E. Katrich, H. T. Lerner, and S. Trakhtenberg, "Preventive effects of diets supplemented with sweetie fruits in hypercholesterolemic patients suffering from coronary artery disease," *Preventive Medicine*, vol. 38, no. 6, pp. 841–847, 2004.
- [28] H. J. F. Zunft, W. Lüder, A. Harde et al., "Carob pulp preparation rich in insoluble fibre lowers total and LDL cholesterol in hypercholesterolemic patients," *European Journal of Nutrition*, vol. 42, no. 5, pp. 235–242, 2003.
- [29] M. L. Sudha, V. Baskaran, and K. Leelavathi, "Apple pomace as a source of dietary fiber and polyphenols and its effect on the rheological characteristics and cake making," *Food Chemistry*, vol. 104, no. 2, pp. 686–692, 2007.
- [30] A. Nurnadia, *The Determination of Fatty Acid Composition and Vitamin E Content in Oils Extracted from Flesh and Kernel of *Canarium odontophyllum**, Department of Nutrition and Dietetics, Universiti Putra Malaysia, Kuala Lumpur, Malaysia, 2007.
- [31] C. C. Chen, L. K. Liu, J. D. Hsu, H. P. Huang, M. Y. Yang, and C. J. Wang, "Mulberry extract inhibits the development of atherosclerosis in cholesterol-fed rabbits," *Food Chemistry*, vol. 91, no. 4, pp. 601–607, 2005.
- [32] H. S. Lee, H. C. Ahn, and S. K. Ku, "Hypolipemic effect of water extracts of picrorrhiza rhizoma in PX-407 induced hyperlipemic ICR mouse model with hepatoprotective effects: a prevention study," *Journal of Ethnopharmacology*, vol. 105, no. 3, pp. 380–386, 2006.
- [33] H. Weintraub, "Simvastatin 80mg: if you can't go lower, go elsewhere," *Medscape News*, 2011.
- [34] F. B. Hu and W. C. Willett, "Optimal diets for prevention of coronary heart disease," *Journal of the American Medical Association*, vol. 288, no. 20, pp. 2569–2578, 2002.
- [35] W. W. Xing, J. Z. Wu, M. Jia, J. Du, H. Zhang, and L. P. Qin, "Effects of polydatin from *Polygonum cuspidatum* on lipid profile in hyperlipidemic rabbits," *Biomedicine and Pharmacotherapy*, vol. 63, no. 7, pp. 457–462, 2009.
- [36] M. L. Garg, R. J. Blake, and R. B. H. Wills, "Macadamia nut consumption lowers plasma total and LDL cholesterol levels in hypercholesterolemic men," *Journal of Nutrition*, vol. 133, no. 4, pp. 1060–1063, 2003.
- [37] U. Rauch, J. I. Osende, J. H. Chesebro et al., "Statins and cardiovascular diseases: the multiple effects of lipid-lowering therapy by statins," *Atherosclerosis*, vol. 153, no. 1, pp. 181–189, 2000.
- [38] T. P. Johnston, L. B. Nguyen, W. A. Chu, and S. Shefer, "Potency of select statin drugs in a new mouse model of hyperlipidemia and atherosclerosis," *International Journal of Pharmaceutics*, vol. 229, no. 1-2, pp. 75–86, 2001.
- [39] R. S. Rosenson, "Statins in atherosclerosis: lipid-lowering agents with antioxidant capabilities," *Atherosclerosis*, vol. 173, no. 1, pp. 1–12, 2004.
- [40] H. E. Khoo, A. Azlan, A. Ismail, and F. Abas, "Influence of different extraction media on phenolic contents and antioxidant capacity of defatted dabai (*Canarium odontophyllum*) fruit," *Food Analytical Methods*, vol. 5, no. 3, pp. 339–350, 2012.
- [41] K. N. Prasad, L. Y. Chew, H. E. Khoo, B. Yang, A. Azlan, and A. Ismail, "Carotenoids and antioxidant capacities from *Canarium odontophyllum* Miq. fruit," *Food Chemistry*, vol. 124, no. 4, pp. 1549–1555, 2011.
- [42] D. A. J. M. Kerckhoffs, G. Hornstra, and R. P. Mensink, "Cholesterol-lowering effect of β -glucan from oat bran in mildly hypercholesterolemic subjects may decrease when β -glucan is incorporated into bread and cookies," *American Journal of Clinical Nutrition*, vol. 78, no. 2, pp. 221–227, 2003.

- [43] P. M. Kris-Etherton, K. D. Hecker, A. Bonanome et al., "Bioactive compounds in foods: their role in the prevention of cardiovascular disease and cancer," *American Journal of Medicine*, vol. 113, pp. 71S–88S, 2002.
- [44] M. H. Kang, Y. Kawai, M. Naito, and T. Osawa, "Dietary defatted sesame flour decreases susceptibility to oxidative stress in hypercholesterolemic rabbits," *Journal of Nutrition*, vol. 129, no. 10, pp. 1885–1890, 1999.
- [45] K. M. Queenan, M. L. Stewart, K. N. Smith, W. Thomas, R. G. Fulcher, and J. L. Slavin, "Concentrated oat β -glucan, a fermentable fiber, lowers serum cholesterol in hypercholesterolemic adults in a randomized controlled trial," *Nutrition Journal*, vol. 6, article 6, 2007.
- [46] W. W. Chu and P. G. Hanson, "Dietary fiber and coronary artery disease," *Wisconsin Medical Journal*, vol. 99, no. 7, pp. 32–36, 2000.
- [47] S. Ramos, L. Moulay, A. B. Granado-Serrano et al., "Hypolipidemic effect in cholesterol-fed rats of a soluble fiber-rich product obtained from cocoa husks," *Journal of Agricultural and Food Chemistry*, vol. 56, no. 16, pp. 6985–6993, 2008.
- [48] J. W. Anderson, P. Baird, R. H. Davis et al., "Health benefits of dietary fiber," *Nutrition Reviews*, vol. 67, no. 4, pp. 188–205, 2009.
- [49] G. Yuan, K. Z. Al-Shali, and R. A. Hegele, "Hypertriglyceridemia: its etiology, effects and treatment," *Canadian Medical Association Journal*, vol. 176, no. 8, pp. 1113–1120, 2007.
- [50] B. C. T. Leudeu, C. Tchiegang, M. D. Gadet et al., "Effect of *Canarium Schweinfurthii* and *Dacrydodes edulis* oils on blood lipids, lipid peroxidation and oxidative stress in rats," *Journal of Food Technology*, vol. 41, pp. 385–390, 2006.
- [51] R. P. Mensink, P. L. Zock, A. D. M. Kester, and M. B. Katan, "Effects of dietary fatty acids and carbohydrates on the ratio of serum total to HDL cholesterol and on serum lipids and apolipoproteins: a meta-analysis of 60 controlled trials," *American Journal of Clinical Nutrition*, vol. 77, no. 5, pp. 1146–1155, 2003.
- [52] J. J. Moreno and M. T. Mitjavila, "The degree of unsaturation of dietary fatty acids and the development of atherosclerosis," *Journal of Nutritional Biochemistry*, vol. 14, no. 4, pp. 182–195, 2003.
- [53] R. Stocker and J. F. Keaney, "Role of oxidative modifications in atherosclerosis," *Physiological Reviews*, vol. 84, no. 4, pp. 1381–1478, 2004.
- [54] Z. Amom, Z. Zakaria, J. Mohamed et al., "Lipid lowering effect of antioxidant alpha-lipoic acid in experimental atherosclerosis," *Journal of Clinical Biochemistry and Nutrition*, vol. 43, no. 2, pp. 88–94, 2008.
- [55] K. Prasad, S. V. Mantha, A. D. Muir, and N. D. Westcott, "Reduction of hypercholesterolemic atherosclerosis by CDC-flaxseed with very low alpha-linolenic acid," *Atherosclerosis*, vol. 136, no. 2, pp. 367–375, 1998.
- [56] A. Triviño, A. I. Ramírez, J. J. Salazar et al., "A cholesterol-enriched diet induces ultrastructural changes in retinal and macroglial rabbit cells," *Experimental Eye Research*, vol. 83, no. 2, pp. 357–366, 2006.
- [57] F. Hakimoğlu, G. Kizil, Z. Kanay, M. Kizil, and H. Isi, "The effect of ethanol extract of *Hypericum lysimachoides* on lipid profile in hypercholesterolemic rabbits and its *in vitro* antioxidant activity," *Atherosclerosis*, vol. 192, no. 1, pp. 113–122, 2007.
- [58] S. Gonçalves, A. V. Maria, A. S. Silva-Herdade, J. Martins e Silva, and C. Saldanha, "Milk enriched with phytosterols reduces plasma cholesterol levels in healthy and hypercholesterolemic subjects," *Nutrition Research*, vol. 27, no. 4, pp. 200–205, 2007.
- [59] K. Prasad, "Effects of vitamin e on serum enzymes and electrolytes in hypercholesterolemia," *Molecular and Cellular Biochemistry*, vol. 335, no. 1-2, pp. 67–74, 2010.
- [60] D. C. Schwenke and S. R. Behr, "Vitamin E combined with selenium inhibits atherosclerosis in hypercholesterolemic rabbits independently of effects on plasma cholesterol concentrations," *Circulation Research*, vol. 83, no. 4, pp. 366–377, 1998.

Research Article

Ganoderma tsugae Induces S Phase Arrest and Apoptosis in Doxorubicin-Resistant Lung Adenocarcinoma H23/0.3 Cells via Modulation of the PI3K/Akt Signaling Pathway

Yang-Hao Yu,^{1,2} Han-Peng Kuo,³ Hui-Hsia Hsieh,⁴ Jhy-Wei Li,⁵ Wu-Huei Hsu,² Shih-Jung Chen,⁶ Muh-Hwan Su,⁷ Shwu-Huey Liu,⁸ Yung-Chi Cheng,⁹ Chih-Yi Chen,¹⁰ and Ming-Ching Kao^{3,11}

¹ Graduate Institute of Clinical and Medical Science, School of Medicine, China Medical University, Taichung 40402, Taiwan

² Division of Pulmonary and Critical Care, China Medical University Hospital, Taichung 40447, Taiwan

³ Department of Biological Science and Technology, College of Life Sciences, China Medical University, Taichung 40402, Taiwan

⁴ Pharmacy Department, China Medical University Hospital, Taichung 40447, Taiwan

⁵ Department of Pathology, Da-Chien General Hospital, Miaoli 36052, Taiwan

⁶ Luo-Gui-Ying Fungi Agriculture Farm, Taoyuan 33043, Taiwan

⁷ Sinphar Group R&D Center, Yilan 26944, Taiwan

⁸ Division of Drug Development, PhytoCeutica, Inc., New Haven, CT 06511-1989, USA

⁹ Department of Pharmacology, Yale University School of Medicine, New Haven, CT 06520-8066, USA

¹⁰ Division of Chest Surgery, China Medical University Hospital, Taichung 40447, Taiwan

¹¹ Department of Biochemistry, National Defense Medical Center, Taipei 11490, Taiwan

Correspondence should be addressed to

Chih-Yi Chen, micc@www.cmuh.org.tw and Ming-Ching Kao, mckao@mail.cmu.edu.tw

Received 14 March 2012; Accepted 26 April 2012

Academic Editor: William C. S. Cho

Copyright © 2012 Yang-Hao Yu et al. This is an open access article distributed under the Creative Commons Attribution License, which permits unrestricted use, distribution, and reproduction in any medium, provided the original work is properly cited.

Ganoderma tsugae (GT) is a traditional Chinese medicine that exhibits significant antitumor activities against many types of cancer. This study investigated the molecular mechanism by which GT suppresses the growth of doxorubicin-resistant lung adenocarcinoma H23/0.3 cells. Our results reveal that GT inhibits the viability of H23/0.3 cells *in vitro* and *in vivo* and sensitizes the growth suppression effect of doxorubicin on H23/0.3 cells. The data also show that GT induces S phase arrest by interfering with the protein expression of cyclin A, cyclin E, CDK2, and CDC25A. Furthermore, GT induces cellular apoptosis via induction of a mitochondria/caspase pathway. In addition, we also demonstrate that the suppression of cell proliferation by GT is through down-regulation of the PI3K/Akt signaling pathway. In conclusion, this study suggests that GT may be a useful adjuvant therapeutic agent in the treatment of lung cancer.

1. Introduction

Lung carcinoma is the most predominant form of cancer and has surpassed breast carcinoma as the leading cause of cancer mortality in the United States; it accounts for approximately 26% and 28% of all female and male cancer deaths, respectively [1]. Lung carcinoma was also the leading cause of cancer death in Taiwan for women and men in 2010 [2]. Moreover, an apparent increasing death rate of lung carcinoma from 1986 to 2010 has also been observed in Taiwan [2].

The two most aggressive forms of lung cancer are non-small-cell lung cancer (NSCLC) and small-cell lung cancer (SCLC), which account for approximately 85% and 15%, respectively, of all lung cancers [3]. Both forms of lung cancer frequently cause drug resistance leading to poor survival [4]. Therefore, alternative medicines and more treatment modalities to overcome drug resistance and to improve the patients' outcomes of this serious disease are urgently desired.

Ganoderma, a traditional Chinese medicine (TCM), has been widely used for medicinal purposes in oriental

countries for centuries. *Ganoderma lucidum* (GL) and *Ganoderma sinense* (GS), listed as Lingzhi in China pharmacopeia, are two of the most representative species of *Ganoderma* and have a long history of use in folk medicine in China. The biological activities of GL and GS, especially their immunomodulatory and antitumor properties, have been well documented [5]. In addition, *Ganoderma tsugae* (GT), another well-cultivated species of *Ganoderma*, has been investigated and found to possess many biological and pharmacological properties, such as antiinflammation [6], antifibrosis [7], antiautoantibody formation [8], and antioxidation [9]. A number of reports show that GT possess growth inhibition effects on a variety of tumor cells, such as sarcoma 180 cells [10], breast cancer MDA-MB-231 and MCF-7 cells [11], hepatoma Hep3B cells [12], and colorectal cancer COLO 205 cells [13]. Moreover, GT also exerts antiangiogenesis effects on epidermoid carcinoma A431 cells by modulating the EGFR/PI3K/Akt/mTOR signaling pathway [14]. Although GT exhibits anticancer activities in many human cancer cells, the molecular mechanisms that govern its inhibitory effect on the growth of lung cancer cells are still not clear and need to be explored.

The quality and quantity of TCMs, including *Ganoderma*, are potentially influenced by many factors, including the cultivation methods, the cultivated regions, the growth conditions, the processing procedures, and the formulated preparations [15]. Therefore, the quality control of TCMs must be established scientifically in terms of both the chemical and biological aspects; but to date, this has not been achieved. A newly established and actively progressed Chinese medicine-based academic organization, called the Consortium for Globalization of Chinese Medicine (CGCM; <http://www.tcmedicine.org>), is promoting and requesting the quality control of TCMs and also striving to explore the functional use of herbonomics.

In this study, we provide a quality assured ethanol extract of GT (GTE) and demonstrate its anticancer effects and related molecular mechanisms in doxorubicin-resistant NSCLC H23/0.3 cells *in vitro* and *in vivo*. Our results indicate that the GTE inhibits cellular growth and induces S phase arrest and apoptosis by modulating the PI3K/Akt signaling pathway. Furthermore, we also show that GTE sensitizes H23/0.3 cells to doxorubicin, indicating a potential use of GTE in the treatment of lung cancer with drug resistance.

2. Materials and Methods

2.1. Cell Culture. Two non-small-cell lung cancer (NSCLC) cell lines were used in this study. H23 (CRL-5800, ATCC), a lung adenocarcinoma cell line, was purchased from ATCC (American Type Culture Collection). H23/0.3, a doxorubicin-resistant H23 cell line, was a gift from Dr. Chun-Ming Tsai (Department of Chest, Veterans General Hospital, Taipei, Taiwan); the cell line was generated by the stepwise exposure of H23 to increasing concentrations of doxorubicin up to 0.3 $\mu\text{g}/\text{mL}$. All cells were cultured in RPMI-1640 medium (Gibco BRL) supplemented with 10%

fetal bovine serum in a humidified atmosphere with 5% CO_2 at 37°C.

2.2. Chemicals and Antibodies. The anticytochrome c antibody and propidium iodide (PI) were obtained from Sigma-Aldrich Co. (St. Louis, MO, USA). The antibodies against cyclin A, cyclin E, Akt1, Bax, and caspase-3 were purchased from Santa Cruz Biotechnology (Santa Cruz, CA, USA). The anti-PARP antibody was obtained from Biovision Inc. (Mountain View, CA, USA). The antibodies against Bcl-2, CDK2, CDC25A, CDC25B, and CDC25C were purchased from Abcam, Inc. (Cambridge, MA, USA). The anti-phospho-Akt (Thr473) antibody, the horseradish peroxidase-conjugated anti-rabbit and anti-mouse IgG antibodies, and the PI3K inhibitor (LY294002) were purchased from Cell Signaling Technology, Inc. (Beverly, MA, USA). The anti- β -actin antibody was purchased from Chemicon International, Inc. (Temecula, CA, USA). The IRDye 800-conjugated affinity purified anti-rabbit and anti-mouse IgGs were purchased from Rockland Immunochemicals, Inc. (Gilbertsville, PA, USA). Doxorubicin was purchased from Pharmacia (Pharmacia & Upjohn S.P.A. Milan, Italy).

2.3. Preparation of *Ganoderma tsugae* Extracts. *Ganoderma tsugae* (GT) was kindly provided by the Luo-Gui-Ying Fungi Agriculture Farm (with a registered name of Tien-Shen Lingzhi), Taoyuan, Taiwan. Briefly, the powder of the GT fruiting body (20 g) was soaked in 99.9% ethanol (400 mL), mixed, and shaken for 24 h with a rotating shaker. After centrifugation, the supernatant was filtered through filter paper (Whatman, Cat. No. 1001-110), and the residues were extracted with alcohol two additional times as mentioned above. The filtrates were collected and subjected to concentration under reduced pressure (i.e., evaporated to dryness under reduced pressure) to produce a brown gel-like GT extract (GTE). The yield was approximately 10%. The GTE was then prepared as a stock solution with ethanol solvent (200 mg/mL) and stored at -20°C until use.

2.4. High-Performance Liquid Chromatography (HPLC). Sample preparation: the sample was diluted, by the addition of ethanol to 1.0 mg/mL, and filtered through a 0.2 μm Millipore filter; then, 10 μL of the sample was subjected to HPLC analysis. Sample separation: the sample (10 μL) was automatically delivered into a C-18 column (LiChroCART, 250 \times 4.6 mm, 5 μm , Merck, Germany) for separation via an HPLC system (L-7100 pump and L-7400 UV-vis detector, Hitachi, Tokyo, Japan). The initial mobile phase comprised acetonitrile (30%) and phosphoric acid (0.11%, pH 2.2) with a flow rate of 1 mL/min; the percentage of acetonitrile in the mobile phase was increased from 30% to 100% in a linear gradient for the first 20 minutes and then maintained at 100% until the end of the experiment. The detection of signals was set at wavelength of 288 nm.

2.5. Electrospray Ionization Mass Spectrometry (ESI-MS). GTE was dissolved in ethanol (10 ng/ μL), and the resulting solution was directly injected into the ion source (Esquire

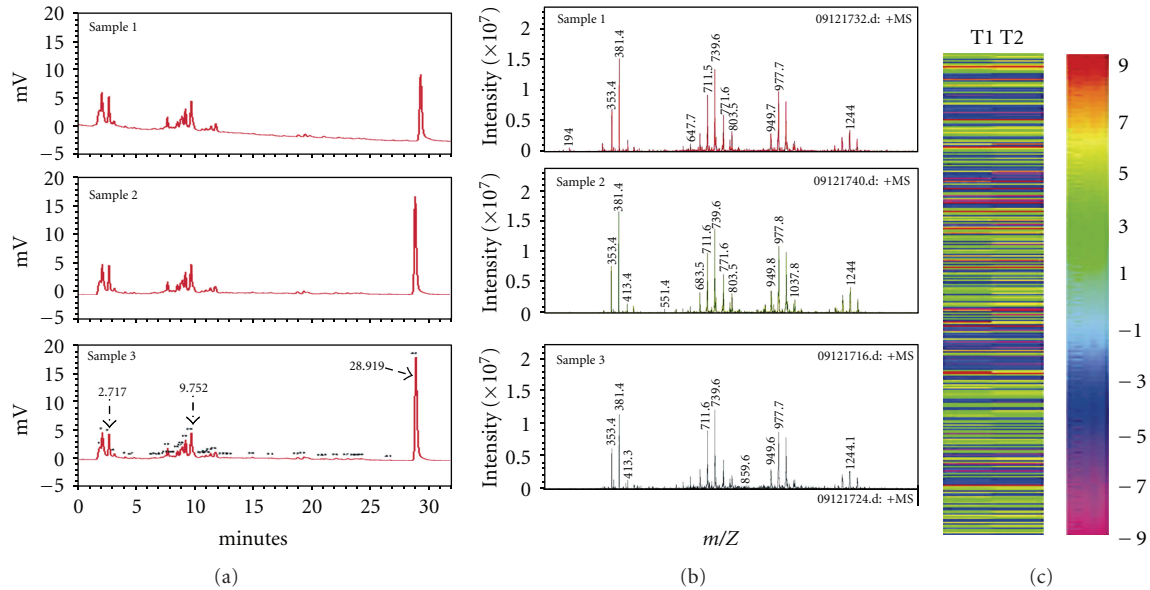


FIGURE 1: Quality control of GTE. (a) The 3 GTE samples were derived from the fruiting bodies of an improved strain of *Ganoderma tsugae* that were collected at three different times. The HPLC chromatogram shows all of the peaks of the components that eluted before 32 minutes. The chemical fingerprints were found to be identical for the 3 batches, and the specific retention time was given in one example. (b) The identical mass fingerprints were also confirmed using ESI-MS. (c) The biological responses for GTE acting on H23/0.3 analyzed by Phytoviewer QC using the whole genomic approach in duplicate experiments (T1, T2) show highly concordant bioresponse fingerprints with a PSI value of 0.98.

HCT ultra PTM, Bruker) using ESI (positive mode) at a flow rate of 240 $\mu\text{L}/\text{min}$. The mass range was acquired from 100 to 1,000 m/z .

2.6. Quality Control of GTEs via Bioresponse Fingerprinting. To maintain and assess the quality of the GT extracts (GTEs), a comprehensive platform for quality control of botanical drugs, named PhytomicsQC [16], was used in this study. In addition to the chemical fingerprinting method (e.g., HPLC & ESI-MS) as mentioned above, a biological response fingerprinting method from the PhytomicsQC technology [16] was also performed in this study. Briefly, the bioresponse is measured by defining the set of genes that are significantly regulated in cell cultures treated with the GTE. We used optimized standard operating procedures at every step, including cell banking, tissue culture, botanical extractions, cell culture treatments, and RNA extractions. The RNA is used to obtain transcription profiles in GeneChip hybridization studies using Affymetrix technology. The changes in the individual gene expression levels obtained by the GeneChip experiments were measured by Affymetrix MAS 5.0 software. A statistical pattern comparison method from the PhytomicsQC platform, phytomics similarity index (PSI), was applied to determine the batch-to-batch similarity of the botanical products. In general, clinically similar batches have a PSI of 0.95 or more. The genomic bioresponse to the GTEs was determined in H23/0.3 cells treated with a single IC_{50} dose of GTE for 24 h. The total RNA was extracted from the GTE-treated cells and cleaned with a commercial kit (Qiagen RNA extraction kit, cat# 75144). The quality of the GTEs was then assessed, and the samples were submitted to the

National Yang-Ming University Genome Core Laboratory (Taipei, Taiwan) for GeneChip Hybridization experiments. These experiments were repeated independently in duplicate.

2.7. Cell Proliferation Assay. Cell proliferation was determined using the MTT metabolic assay as described previously [17]. Briefly, cells were plated onto 96-well microtiter plates (1×10^3 – 1×10^4 cells/well, depending on the cancer cells used). After the cells adhered to the plates, various doses of GTE were applied to the cells, and the cells were incubated at 37°C for 72 h. At the end of the GTE treatment, the media were aspirated, and the cells were incubated for 4 h in fresh media containing MTT reagent (0.5 mg/mL). Finally, the solution was measured spectrophotometrically at 545 nm against a reference wavelength of 690 nm.

2.8. Flow Cytometric Analysis. For the analysis of the cell cycle, the phase distribution was detected by flow cytometry as described previously [17]. After the GTE treatment, the cells were trypsinized, washed with PBS, and fixed with 75% ethanol overnight at -20°C . The fixed cells were washed with PBS and treated with a working solution of propidium iodide (PI) (50 $\mu\text{g}/\text{mL}$ PI in PBS plus 1% Tween-20 and 10 μg RNase) for 30 min in the dark at room temperature to stain the cells for subsequent analysis. The DNA contents were measured using flow cytometry (BD FACS Canto). The cell cycle distribution was analyzed with the FCS Express v2.0 software. For the analysis of apoptosis, the cells were stained using the Annexin V-FITC Apoptosis Detection Kit I (BD Biosciences, San Diego, CA) according

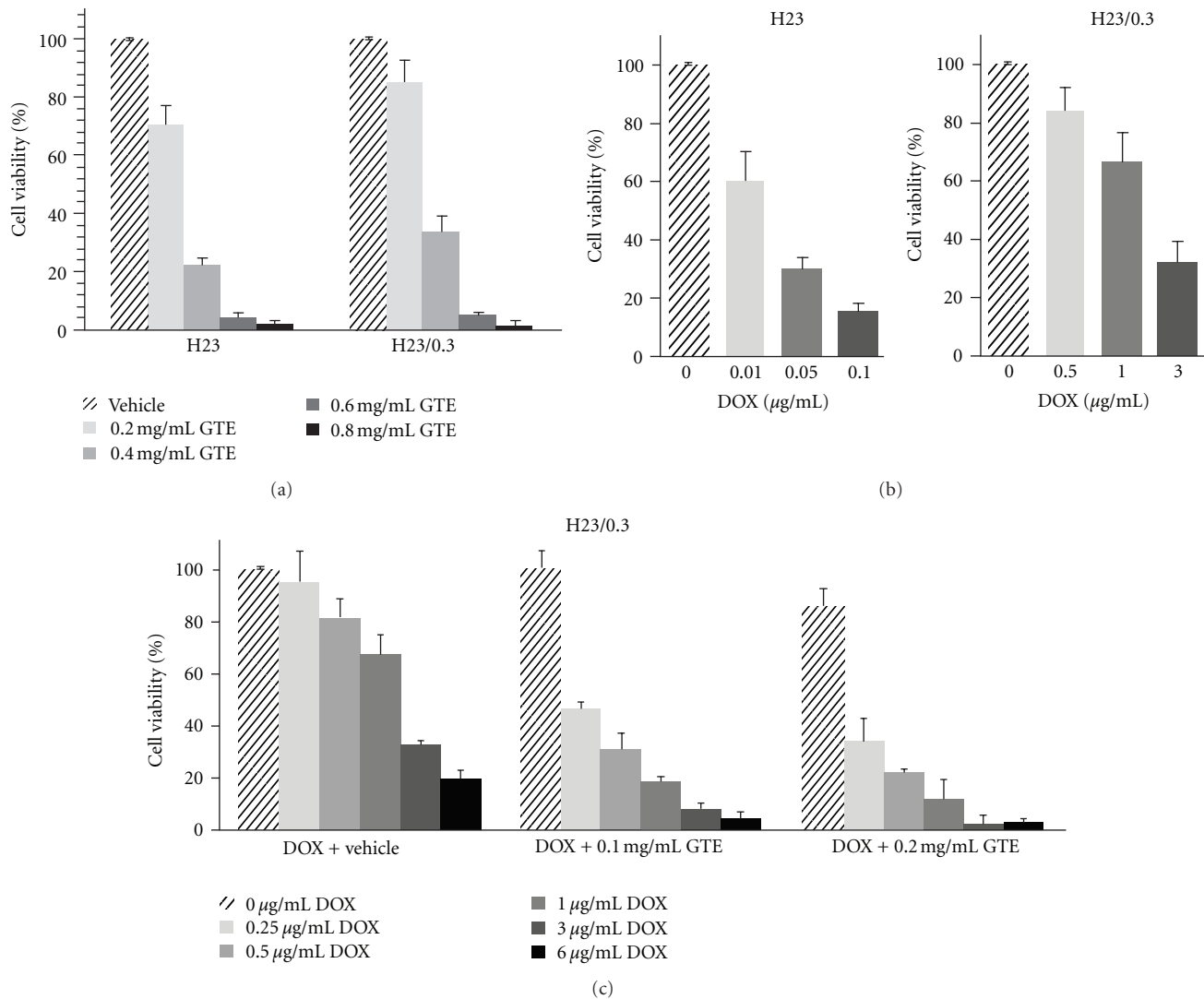


FIGURE 2: Effect of GTE on cell viability in doxorubicin-resistant lung adenocarcinoma H23/0.3 cells. (a) H23 and H23/0.3 cells were treated with either vehicle control or GTE (0.2 mg/mL, 0.4 mg/mL, 0.6 mg/mL, or 0.8 mg/mL) for 72 h. Cell viability was determined using the MTT assay as described in the Section 2. (b) H23 and H23/0.3 cells were treated with various concentrations of doxorubicin (0.01–0.1 µg/mL in H23 cells; 0.5–3 µg/mL in H23/0.3 cells) for 72 h. Cell viability was determined using the MTT assay. (c) H23/0.3 cells were treated with various concentrations of doxorubicin (0 µg/mL, 0.25 µg/mL, 0.5 µg/mL, 1 µg/mL, 3 µg/mL, and 6 µg/mL) with or without GTE (0.1 mg/mL or 0.2 mg/mL) for 72 h. Cell viability was determined by the MTT assay. Results are expressed as the mean \pm SD of three independent experiments.

to the manufacturer's recommendation. The amount of apoptotic cells was determined by flow cytometry (BD FACS Canto) and analyzed by the FCS Express v2.0 software.

2.9. Immunofluorescence Microscopy. H23/0.3 cells (2×10^5 cells) were treated with GTE for 24 h and washed with cold DPBS. Then, the Annexin V-FITC Apoptosis Detection Kit I reagent was added to the cells according to the manufacturer's protocol and incubated for 15 min at room temperature in the dark. Photomicrographs were obtained with a Leica TCS SP2 Confocal Spectral Microscope [18]. We also used a fluorescence microscope (Leica DMR) to identify

the fragmented and condensed nuclei that were stained with DAPI (4',6'-diamidino-2-phenylindole).

2.10. Western Blot Analysis. To determine the changes at the protein level after the GTE treatment, the cells were lysed in RIPA buffer (50 mM Tris-HCl, pH 7.2, 150 mM EDTA, 1% Nonidet P-40, 0.05% SDS, 1 mM PMSF and 1 mM leupeptin). The cell lysates were centrifuged at $14,000 \times g$ for 10 min at 4°C. The supernatant was analyzed by SDS-PAGE and blotted onto a polyvinylidene difluoride (PVDF) membrane. The membrane was subsequently incubated with the specified primary antibody and then incubated with the HRP-conjugated or the IRDye 800-conjugated secondary

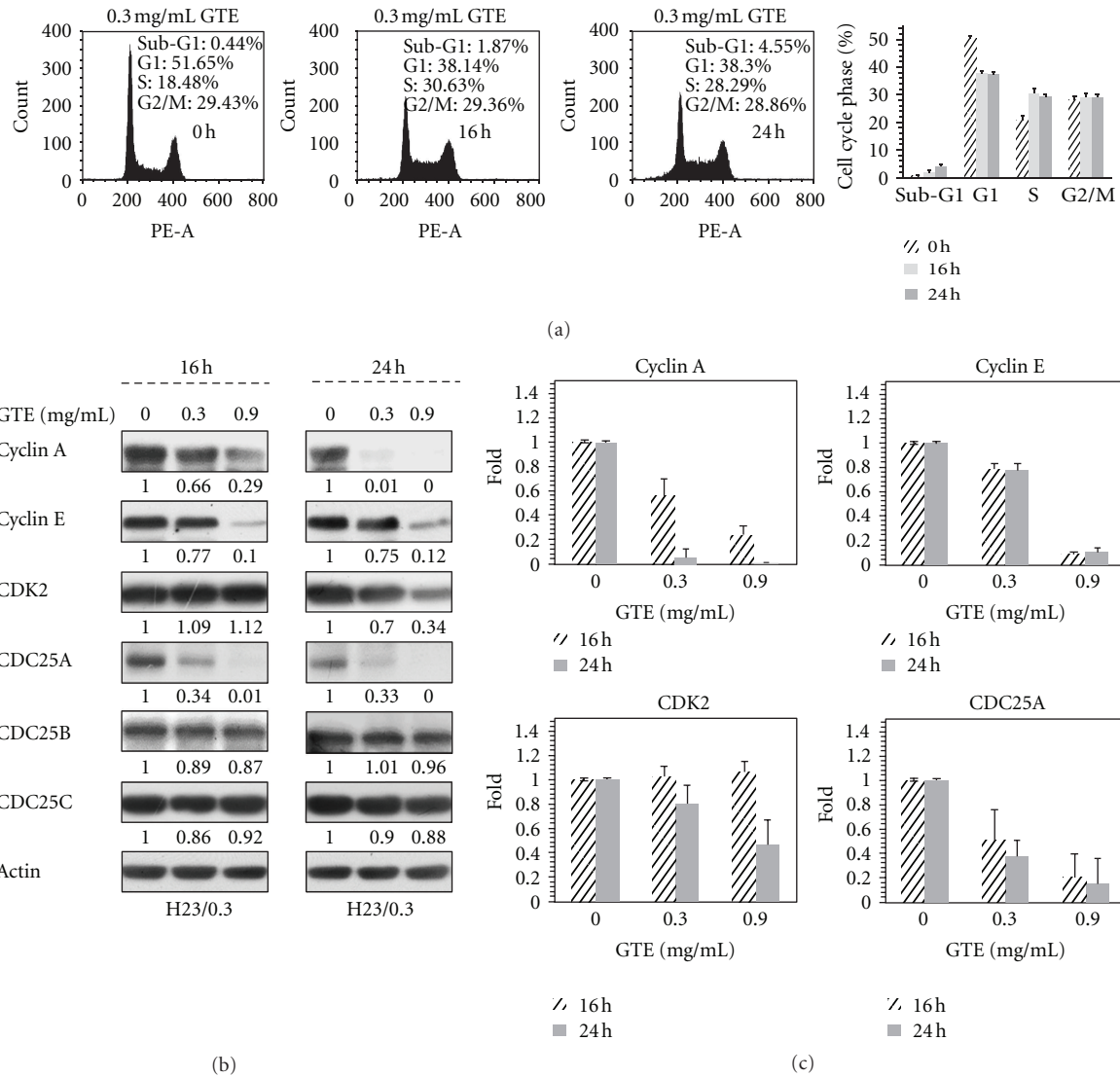


FIGURE 3: Effect of GTE on cell cycle distribution in H23/0.3 cells. (a) H23/0.3 cells were treated with GTE (0.3 mg/mL) for 16 and 24 h. The cell cycle distribution was measured by flow cytometry as described in Section 2. The error bars indicate the standard deviations of each phase (%), which were the means of three independent experiments. (b) H23/0.3 cells were treated with various concentrations of GTE (0 mg/mL, 0.3 mg/mL, and 0.9 mg/mL) for 16 h and 24 h. The expression of S phase regulators was determined by Western blotting as described in Section 2. (c) A histogram showing the relative protein levels from (b). Results are expressed as the mean \pm SD of three independent experiments.

antibody. Reactive signals were visualized with an Enhanced Chemiluminescence Kit (Amersham Biosciences, Arlington Heights, IL) or the Odyssey Infrared Imaging System (LI-COR Biosciences, Cambridge, UK).

2.11. Release of Cytochrome c. The release of cytochrome c (Cyt-c) from the mitochondria to the cytosol was detected as described previously [17]. Briefly, the cells were gently lysed in lysis buffer (1 mM EDTA, 20 mM Tris-HCl, pH 7.2, 250 mM sucrose, 1 mM dithiothreitol, 1.5 mM MgCl₂, 10 mM KCl, 10 μ g/mL leupeptin, 5 μ g/mL pepstatin A, and 2 μ g/mL aprotinin). The cell lysates were centrifuged at 12,000 \times g at 4°C for 10 min to obtain the pellets (the

fractions that contained mitochondria) and the supernatants (cytosolic extracts free of mitochondria). The protein content of the supernatant was determined by the Bio-Rad protein assay kit. The protein (20 μ g) was resolved by SDS-PAGE (14%) and then transferred onto PVDF membranes for the detection of Cyt-c.

2.12. Animal Experiments. The animal experiments were performed as described previously [13] with slight modifications. Briefly, 1 \times 10⁶ H23/0.3 cells were subcutaneously implanted into the flank region of nude mice. In total, 26 mice were enrolled in this experiment, 20 tumor-implanted mice were treated with ($n = 10$) and without ($n = 10$) GTE,

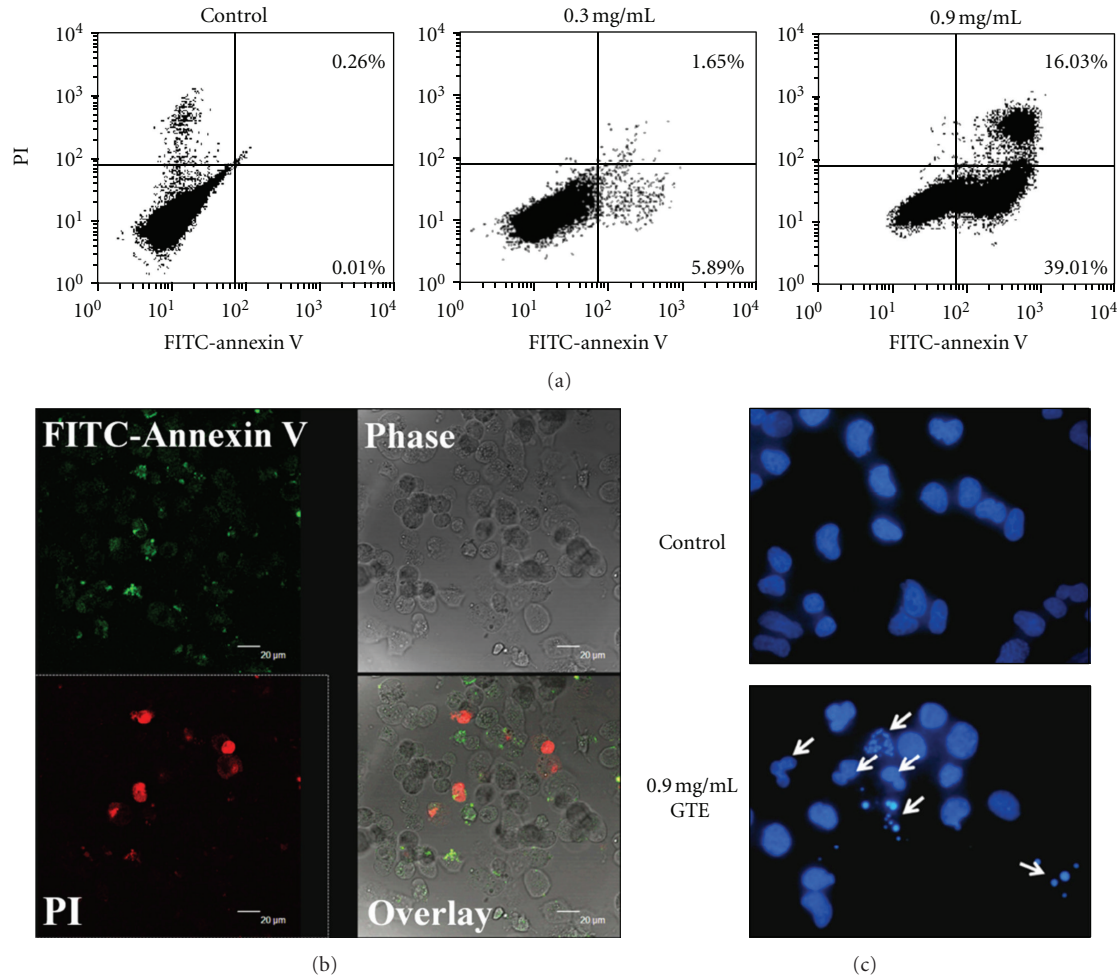


FIGURE 4: Effect of GTE on cellular apoptosis in H23/0.3 cells. (a) H23/0.3 cells were treated with various concentrations of GTE (0 mg/mL, 0.3 mg/mL, and 0.9 mg/mL) for 24 h. Cellular apoptosis was measured by flow cytometry using the FITC-conjugated annexin V and PI double stains as described in Section 2. (b) H23/0.3 cells were treated with 0.9 mg/mL of GTE for 24 h. The exposure of phosphatidylserine (PS) was measured by confocal microscopy with annexin V-FITC (green color, stained for early asymmetry membrane) and PI (red color, stained for nuclear chromosome after cell membrane disruption) double stains. (c) H23/0.3 cells were treated with 0.9 mg/mL of GTE for 24 h. Fragmented condensed nuclei were measured using a DAPI staining assay.

respectively, and the remaining 6 mice were neither tumor-implanted nor GTE-treated and were used as a reference control. The GTE-treated mice were fed with GTE daily at a dose of 100 mg/kg body weight; this feeding schedule was initiated when the developed tumor was approximately 50 mm³ in volume (usually 2-3 weeks after the cancer cells were implanted). The tumor volume and body weight were measured every 3 days. The mice were sacrificed for pathological examination when the tumor volume exceeded 2,000 mm³. The tumors were then completely excised from the subcutaneous tissue and weighed. Biochemical and hematological measurements were evaluated for the toxicity test of the drug.

2.13. Immunohistochemical Staining. Fourteen H23/0.3-xenografted tumors (seven for each of the GTE-free and GTE-treated groups) and the surrounding mouse tissues were completely excised, fixed in 10% neutral buffered

formalin, embedded in paraffin, and sliced for hematoxylin and eosin (H&E) staining to measure the extent of mitotic and necrotic figures. The preparation of samples for H&E staining was performed as described previously [13]. Five high-power fields (5 HPFs, 400X) of H&E-stained slides were counted using the image selection function of Adobe Photoshop, Version 7.0 (Adobe Systems, CA). The number of mitotic figures was counted in 5 HPFs of H&E-stained, necrosis-free areas.

2.14. Statistical Analysis. For statistical analysis, the items of cell death percentage and mitoses were calculated with the Mann-Whitney *U* test. The differences in tumor growth were determined by multiple response models, and the tumor weights were compared by the two sample *t*-test. Statistical Products and Services Solution software (SPSS, version 10.0, SPSS UK Ltd., Woking, Surrey, UK) was used for the analysis. Significant levels were set as $P < 0.05$.

3. Results

3.1. Quality Control of GTE Using Chemical and Bioresponse Fingerprint Analyses. Three batches of GT fruiting bodies that were collected from the same fungi farm at different times were extracted with ethanol. The chemical profiles of the GTEs were analyzed using high-performance liquid chromatography (HPLC). The fingerprints of the 3 batches of GTE were almost identical in triplet experiments. Three representative fingerprints located at 2.717 minutes, 9.752 minutes, and 28.919 minutes were indicated based on their retention times (Figure 1(a)). The last part of the chromatogram corresponded with the major compounds of GTE and had a peak area of 47% (the specific elution time and peak area are based on one representative sample, sample 2). We further verified the chemical profiles of the GTEs with electrospray ionization mass spectrometry (ESI-MS). Similarly, the MS fingerprints for the 3 batches of samples were also indistinguishable (Figure 1(b)). In addition, the bioresponse fingerprints were analyzed by the pattern comparison method of the PhytomicsQC platform, which showed highly concordant biological responses for GTE acting on H23/0.3 cells with a PSI value of 0.98. Under this PSI value, the bioresponse fingerprints contain 338 specifically altered expressed genes with 178 upregulations and 160 downregulations (Figure 1(c)). These results suggest that the GT powder products used in this study have stable, consistent, and high quality.

3.2. GTE Suppresses the Growth of Doxorubicin-Resistant H23/0.3 Cells. To ascertain whether GTE inhibits the growth of lung adenocarcinoma H23 and H23/0.3 cells, we first determined the viability of cells exposed to GTE using the MTT assay. As shown in Figure 2(a), the GTE treatment resulted in a dose-dependent inhibition of cell viability, accounting for a 28–97% and 5–98% reduction in the number of viable cells after treatment with various concentrations of GTE (0.2–0.8 mg/mL) for 72 h in H23 and H23/0.3 cells, respectively. The IC_{50} of GTE was approximately 0.29 mg/mL for H23 cells and 0.34 mg/mL for H23/0.3 cells. The results suggest that GTE is capable of suppressing the proliferation of lung adenocarcinoma H23 and H23/0.3 cells with no selectivity on either cell.

Resistance to anticancer drugs (e.g., doxorubicin and cisplatin) is a major problem in the treatment of patients with lung cancer [19]. We, therefore, examined whether GTE could enhance/sensitize the growth inhibition effects of the anticancer drug doxorubicin in the doxorubicin-resistant H23/0.3 cells (Figure 2(b)), by incubating that cell line with both doxorubicin and GTE. As illustrated in Figure 2(c), GTE significantly enhanced/sensitized the growth suppression effect of doxorubicin on H23/0.3 cells. We found that the number of viable cells was reduced by 14% in cells exposed to GTE (0.2 mg/mL) alone, by 18% in cells exposed to doxorubicin (0.5 μ g/mL) alone, and by 78% in cells exposed to both agents combined. Similarly, we also discovered that GTE could enhance the chemotherapeutic efficacy of anticancer drugs against other lung cancer cell lines, for example, H23, A549, and CL1-0 (our unpublished

data). These results clearly demonstrate that GTE is able to chemosensitize lung cancer cells to anticancer drugs such as doxorubicin.

3.3. GTE Induces S Phase Arrest by Modulating the Expression of Cell Cycle Regulatory Proteins. As mentioned above, our results showed a growth suppression effect of GTE on H23/0.3 cells (Figure 2(a)). To verify that the growth inhibition effect of GTE was due to the disruption of the cell cycle, flow cytometry was used to analyze the cell cycle distribution of H23/0.3 cells. As shown in Figure 3(a), the GTE treatment resulted in a marked cell cycle arrest at S phase, which accounted for 12% and 10% increases in the numbers of S phase cells after 16 h and 24 h of treatment with GTE, respectively. This increase in the population of S phase cells was accompanied by an attendant decrease in the G1 phase cell population. These findings suggest that GTE suppresses the growth of H23/0.3 cells by modulating the progression of the cell cycle.

Different regulatory proteins, such as cyclins, cyclin-dependent kinases (CDKs), and cell division cycle 25 (CDC25), work in multiple pathways to tightly modulate the progression of the cell cycle [20]. To identify the molecular mechanisms that govern the GTE-induced S phase arrest, we assessed the effect of GTE on the expression of cell cycle regulators involving in S phase progression. We found that treatment with GTE had a marked dose- and time-dependent inhibitory effect on the protein expression of cyclin A, cyclin E, CDK2, and CDC25A (Figures 3(b) and 3(c)). However, GTE treatment did not cause significant changes in the protein levels of CDC25B and CDC25C (Figures 3(b) and 3(c)). These results suggest that GTE induces S phase cell cycle arrest by modulating the protein expression of cell cycle regulatory proteins in H23/0.3 cells.

3.4. GTE Induces Cellular Apoptosis. The suppression of cell proliferation can be achieved by inhibiting cell cycle progression or by inducing cellular apoptosis [21, 22]. To further determine if GTE also induced cellular apoptosis, we analyzed the percentages of apoptotic cells by flow cytometry in H23/0.3 cells following staining with annexin V-FITC and PI. Apoptotic cells were shown in the upper right (as late apoptotic cells) or lower right (as early apoptotic cells) quadrants of the FACS histogram. We found that the treatment of H23/0.3 cells with 0.9 mg/mL of GTE resulted in a marked induction of apoptosis at both the early (39%) and late (16%) stages of apoptosis (Figure 4(a)). Confocal images clearly demonstrated that the translocation of phosphatidylserine (PS) from the inner leaflet of the plasma membrane to the cell surface, an early feature of cellular apoptosis, was induced by GTE treatment (Figure 4(b)). Additionally, fragmented and condensed nuclei were also identified by fluorescence microscopy with DAPI staining (Figure 4(c)). These observations suggest that GTE induces cell apoptosis in H23/0.3 cells.

3.5. GTE Activates the Mitochondria/Caspase Pathway. To determine the underlying molecular mechanisms that are

TABLE 1: A comparison of the organ toxicity of the control and GTE treatment.

	Heart			Lung			Kidney			Brain			Liver			Spleen			Intestines		
	H	N	I	H	N	I	H	N	I	H	N	I	H	N	I	H	N	I	H	N	I
A1	-	-	-	++	-	-	+	-	-	-	-	-	+	-	-	+	-	-	-	-	-
A2	-	-	-	+	-	-	+	-	-	-	-	-	+	-	-	+	-	-	-	-	-
A3	+	-	-	++	-	-	+	-	-	-	-	-	+	-	-	+	-	-	-	-	+
A4	+	-	-	+++	-	-	+	-	-	-	-	-	+	-	-	+	-	-	-	-	-
A5	+	-	-	++	-	-	-	-	-	-	-	-	+	-	-	+	-	-	-	-	-
A6	++	-	-	++	-	-	+	-	-	-	-	-	+	-	-	+	-	-	-	-	+
B1	+	-	-	++	-	-	+	-	-	-	-	-	++	-	-	+	-	-	-	-	+
B2	++	-	-	+++	-	-	+	-	-	-	-	-	+	-	-	+	-	-	-	-	-
B3	-	-	-	++	-	-	-	-	-	-	-	-	+	-	-	+	-	-	-	-	+
B4	+++	-	-	++	-	-	+	-	-	-	-	-	+	-	-	+	-	-	-	-	-
B5	+	-	-	+++	-	-	-	-	-	-	-	-	+	-	-	+	-	-	-	-	-
B6	++	-	-	+	-	-	+	-	-	-	-	-	+	-	-	+	-	-	-	-	-
B7	+	-	-	++	-	-	+	-	-	-	-	-	+	-	-	+	-	-	-	-	-
C1	+	-	-	++	-	-	+	-	-	-	-	-	+	-	-	+	-	-	-	-	+
C2	+	-	-	+++	-	-	+	-	-	-	-	-	+	-	-	+	-	-	-	-	+
C3	+	-	-	++	-	-	+	-	-	-	-	-	+	-	-	+	-	-	-	-	-
C4	+	-	-	++	-	-	+	-	-	-	-	-	+	-	-	+	-	-	-	-	-
C5	+++	-	-	+++	-	-	+	-	-	-	-	-	+	-	-	+	-	-	-	-	+
C6	+	-	-	+++	-	-	-	-	-	-	-	-	+	-	-	+	-	-	-	-	-
C7	-	-	-	++	-	-	+	-	-	-	-	-	+	-	-	+	-	-	-	-	-

A1–6: mice that received neither a tumor implant nor GTE treatment; B1–7: mice that received a tumor implant but did not receive GTE treatment; C1–7: mice that received both a tumor implant and GTE treatment; H: hemorrhage; N: necrosis; I: Inflammation. The severity of the visual scoring system represented by “-” and “+”; - stands for none, + stands for minimal, ++ stands for visible, and +++ stands for apparent pathological change.

responsible for GTE-induced cell apoptosis, we examined the influence of GTE on the protein levels of members of the Bcl-2 family that mediate the activation of the mitochondria/caspase pathway [23]. As shown in Figure 5(a), GTE treatment resulted in a marked increase in the protein level of the proapoptotic protein Bax; however, treatment did not cause significant changes in the protein expression of the antiapoptotic protein Bcl-2. Moreover, we examined the effect of GTE on the release of Cyt-c and found that GTE caused a significant increase of Cyt-c protein in the cytosolic fractions (Figure 5(b)). In addition, treatment with GTE also caused a significant cleavage of caspase-3 and PARP (Figure 5(c)). These results demonstrate that GTE induces cell apoptosis by activating the mitochondria/caspase pathway in H23/0.3 cells.

3.6. GTE Inhibits Cell Proliferation via the PI3K/Akt Signaling Pathway. The PI3K/Akt signaling pathway is associated with cell proliferation, survival, and drug resistance in lung cancer [24]; therefore, we analyzed the influence of GTE on the PI3K/Akt signaling pathway. As shown in Figure 6(a), GTE exhibited dose- and time-dependent inhibitory effects on the levels of phospho-Akt and Akt. We next tested the validity of our results by incubating H23/0.3 cells with the PI3K inhibitor LY294002. The results revealed that LY294002 downregulated not only the protein levels of cyclin A but also the expression of cyclin E protein in H23/0.3 cells (Figure 6(b)). In other words, LY294002 exhibited an

inhibitory effect that was similar to that of GTE on H23/0.3 cells. These data indicate that GTE inhibits cell proliferation by inhibiting the PI3K/Akt signaling pathway in H23/0.3 cells.

3.7. GTE Inhibits the Growth of H23/0.3 Xenografted Tumors.

To verify the *in vivo* antitumor effect of GTE, we used xenografted tumor-bearing nude mice to examine the differences in tumor growth with and without GTE treatment. After the volume of the H23/0.3 xenografted tumor reached approximately 100–200 mm³, the nude mice were treated with either GTE (100 mg/kg/day) or vehicle orally (p.o.) for 45 days. As shown in Figure 7(a), the nude mice treated with GTE exhibited a significant suppression in H23/0.3 tumor growth relative to that of the control group. There was no significant difference in the body weights of the mice with and without GTE treatment (data not shown). In addition, as illustrated in Figure 7(b), we found that the numbers of mitotic cancer cells were significantly suppressed by the GTE treatment compared to those of the control group (85.43 ± 21.68 versus 58.71 ± 12 in 5 HPFs, $P = 0.048$). These results indicate that GTE suppresses the growth of H23/0.3 xenografted tumors *in vivo*.

We also evaluated the possibility of a toxic effect of GTE by conducting a pathological examination of all of the sacrificed and dissected mouse organs; the brain, heart, lung, liver, spleen, kidney, and intestines from 7 cases with and 7 cases without GTE treatment were examined. Toxicity was

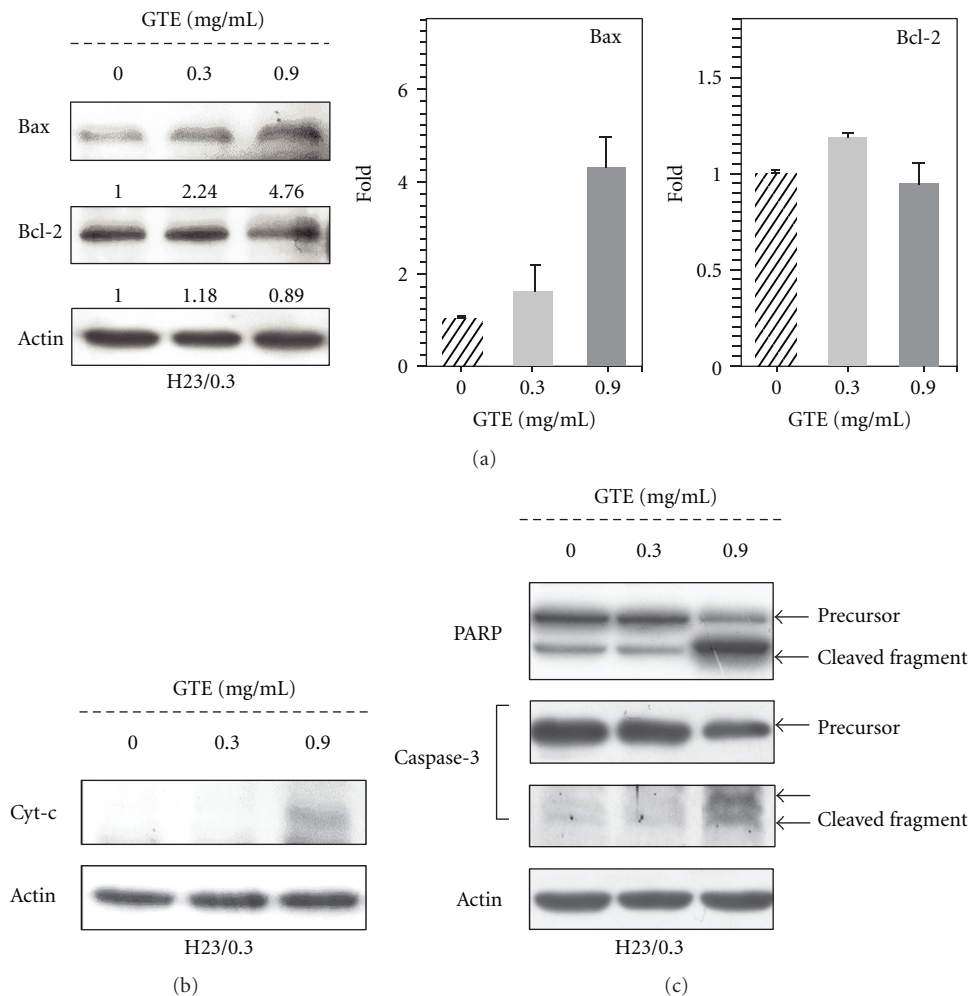


FIGURE 5: Effect of GTE on the mitochondria/caspase pathway in H23/0.3 cells. (a) H23/0.3 cells were treated with various concentrations of GTE (0 mg/mL, 0.3 mg/mL, and 0.9 mg/mL) for 24 h. The protein expression of Bcl-2 and Bax was measured by western blotting. (b) H23/0.3 cells were treated with various concentrations of GTE (0 mg/mL, 0.3 mg/mL, and 0.9 mg/mL) for 24 h. The release of cytochrome c (Cyt-c) into the cytoplasm was detected by western blotting. (c) H23/0.3 cells were treated with various concentrations of GTE (0 mg/mL, 0.3 mg/mL, and 0.9 mg/mL) for 24 h. The cleavage of caspase-3 and PARP was detected by western blotting. Results are expressed as the mean \pm SD of three independent experiments.

evaluated in terms of the severity of hemorrhage, necrosis, and inflammation on microscopic visual scales from “–” to “+++” that stand for none, mild, moderate, and severe, respectively. There were no significant differences in the aforementioned organ toxicities between the controls and the GTE-treated mice (Table 1).

4. Discussion

A number of Chinese herbal medicines have demonstrated significant potential as anticancer therapeutic agents due to their growth suppression effects on tumor cells [25, 26]. Among these medicines, *Ganoderma* is the most widely used herbal medicine in Asia and has been used for centuries. *Ganoderma tsugae* (GT), one of the most major species cultivated in Taiwan, has been shown to exhibit anti-proliferative effects against human tumor cells [12, 13]. In

this study, we investigated the anticancer effects of the GT on the NSCLC H23/0.3 cells *in vitro* (Figure 2(a)) and *in vivo* (Figure 7(a)).

Botanical products, especially TCMs, are mixtures of phytochemicals that are not defined by the standard formula as pure chemical compounds, thus presenting a difficult issue for the scientific requirements of quality control (QC). Chemical fingerprinting is usually viewed as a gold standard to identify TCMs [27]; however, this method may not be the best method to achieve this core purpose. In comparison with the classification of botanical products by chemical fingerprints, the biological response will be more appropriate in characterizing the therapeutic effects, particularly for those products with mixed compounds, such as TCM [16]. In this study, we used a comprehensive PhytomicsQC platform as a scientific approach for the QC of TCMs (e.g., GTE). Both the bioresponse fingerprint and the chemical

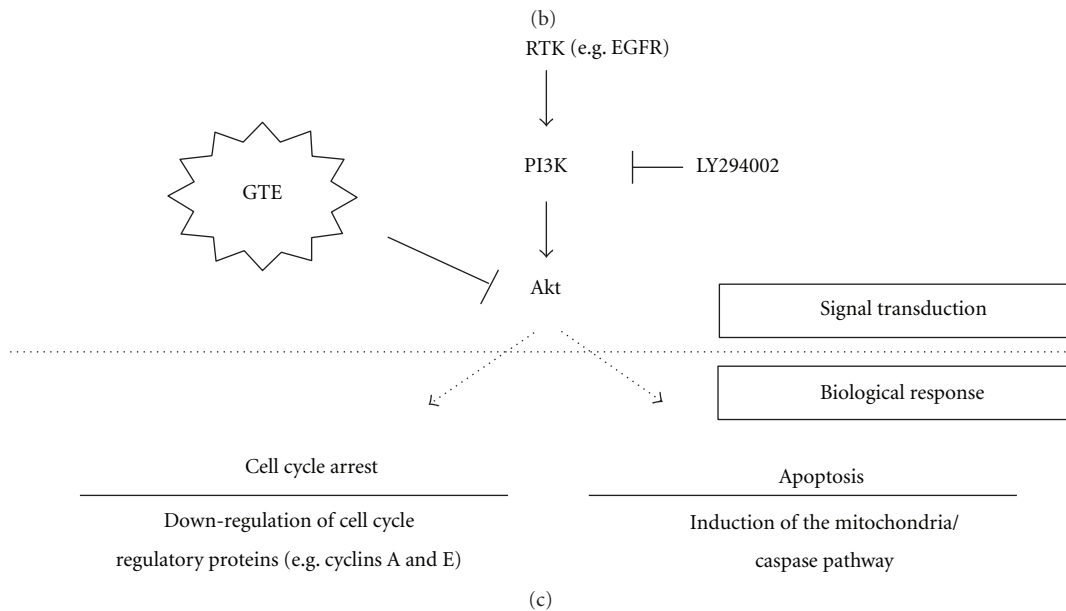
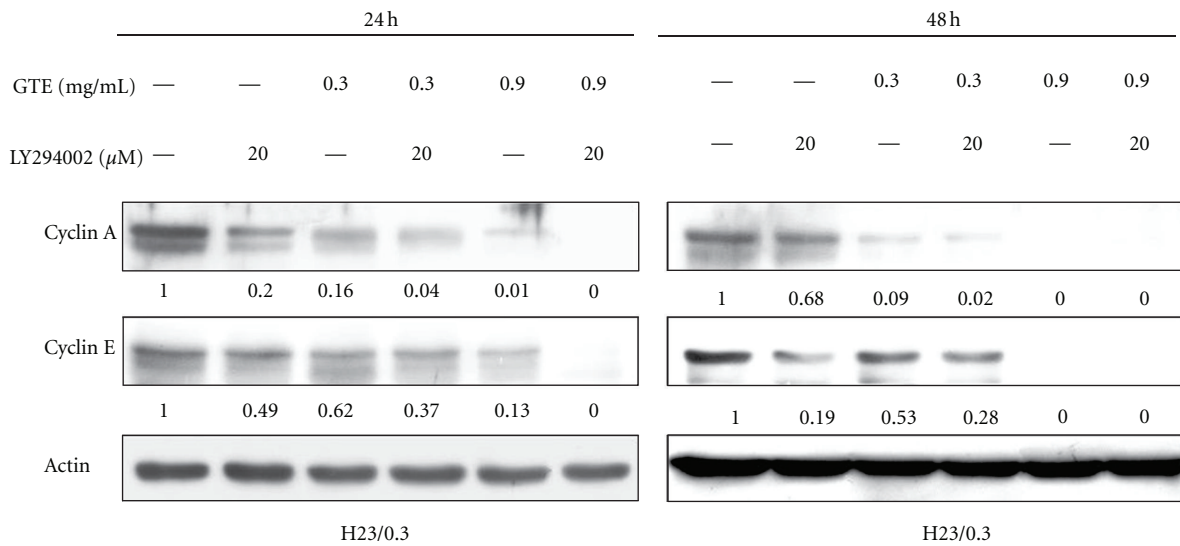
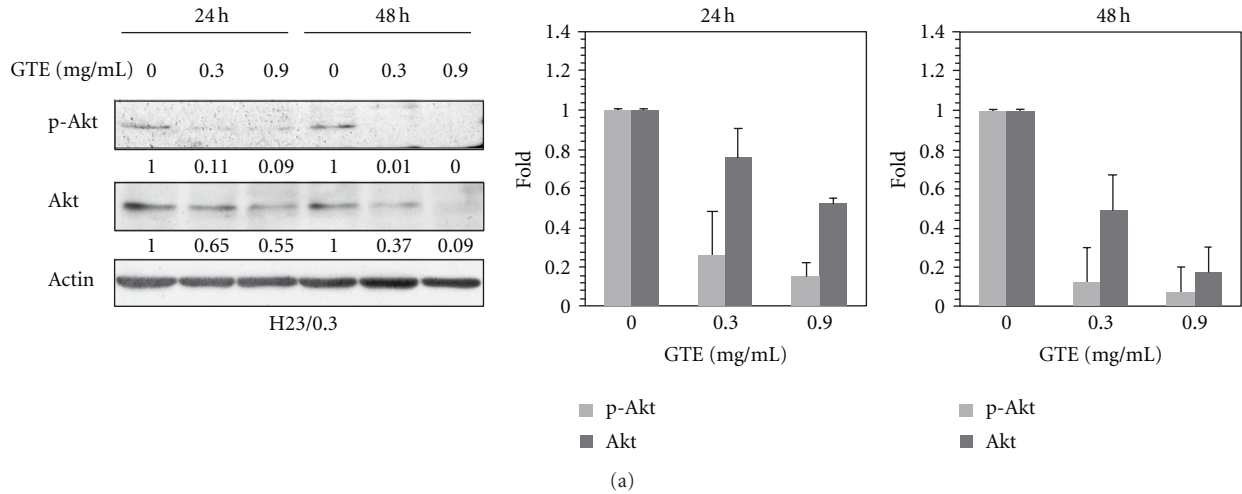


FIGURE 6: Effect of GTE on PI3K/Akt pathways in H23/0.3 cells. (a) H23/0.3 cells were treated with various concentrations of GTE (0 mg/mL, 0.3 mg/mL, and 0.9 mg/mL) for 24 h and 48 h. The protein levels of p-Akt and Akt were measured by western blotting. (b) H23/0.3 cells were treated with 20 μM LY294002 (a PI3K inhibitor) alone or in combination with GTE (0.3 mg/mL or 0.9 mg/mL) for 24 h and 48 h. The expression levels of proteins (cyclins A and E) were measured by western blotting. (c) A proposed model for the GTE-mediated antiproliferation of doxorubicin-resistant lung adenocarcinoma H23/0.3 cells. Results are expressed as the mean ± SD of three independent experiments.

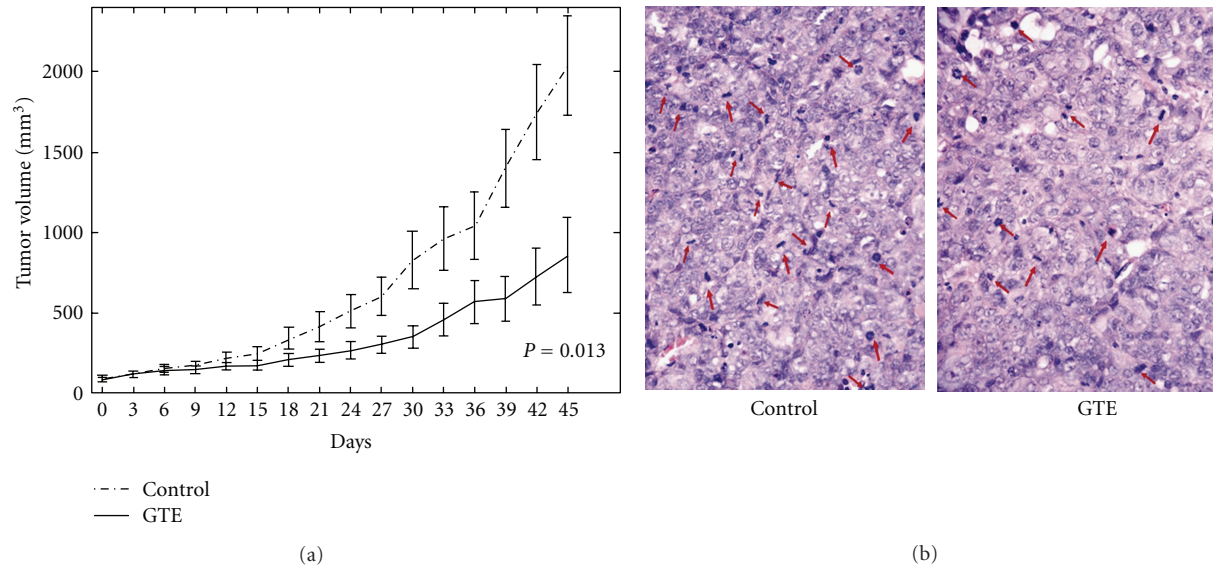


FIGURE 7: Effect of GTE on the growth of H23/0.3 xenografted tumors *in vivo*. (a) The tumor growth rate was significantly retarded in the GTE-treated group (100 mg/kg/day). The tumor volumes were estimated from the caliper measurements of three dimensions of the tumor. The estimated tumor volumes were calculated as $L \times W^2 \times 0.5$, where L is the major axis and W is tumor width. The data are represented as the mean \pm SE ($n = 10$). (b) The tumor sections from the control mice showed more mitotic cells compared to those from the GTE-treated mice. The red arrows indicate mitotic figures in the H&E-stained areas (400X).

fingerprint [16] of GTEs were determined and revealed the high quality and consistency among different batches of GTE (Figures 1(a)–1(c)).

Perturbation of progression of the cell cycle in tumor cells is a helpful strategy to halt tumor growth [21]. Furthermore, the cell cycle arrest of tumor cells also provides an occasion for cells to undergo either repair or cellular apoptosis. A number of TCMs exhibit significant inhibitory effects on lung cancer cells via disruption of cell cycle progression and/or induction of cell apoptosis [25, 26]. Previous reports showed that a G2/M cell cycle arrest was induced in Hep3B cells treated with the chloroform extract of GT [9] and in COLO 205 cells exposed to the methanol extract of GT [10]. In this study, our *in vitro* data indicated that the treatment of H23/0.3 cells with ethanol extract of GT induced S phase arrest (Figure 3(a)) via modulation of the expression of S phase regulatory proteins (Figures 3(b) and 3(c)) in H23/0.3 cells. The various effects of GT on the distribution of cell cycle may be due to cell-type specificity and/or result from variations in preparation process of GT extract.

Many anticancer drugs/agents exert their anticancer activities by inducing the cellular apoptosis of tumor cells [28]. Resistance to cellular apoptosis, therefore, results in a decrease in the sensitivity of cancer cells to drugs and the failure of chemotherapy [22, 29]. Several TCMs have been reported to induce cellular apoptosis in lung cancer [25, 26]. For example, *Typhonium blumei* extract induces cellular apoptosis via the mitochondrial/caspase pathway by upregulating the expression of proapoptotic proteins (e.g., Bax, Bad, and Bak), downregulating the expression of anti-apoptotic proteins (e.g., Bcl-2 and Bcl-xL), and activating caspase-9 and caspase-3 in lung cancer A549 cells [26], whereas *Scutellaria baicalensis* extract induces apoptosis by

upregulating the expression of the proteins p53 and Bax in lung cancer A549 cells [25]. In this study, our results indicated that GTE not only perturbed cell cycle progression but also induced cellular apoptosis in lung cancer H23/0.3 cells (Figures 4(a)–4(c)). Furthermore, we also found that the treatment of H23/0.3 cells with GTE resulted in a marked increase in the expression of Bax (Figure 5(a)). This increase may be responsible for the concomitant execution phase of cellular apoptosis such as an increase in the release of Cyt-c from the mitochondria to the cytosol and the activation/cleavage of caspase-3 and PARP (Figure 5(c)).

The PI3K/Akt signaling pathway plays a critical role in cell proliferation, survival, and drug resistance in lung cancer [24]. Therefore, the suppression of the PI3K/Akt signaling pathway may be an effective approach to the treatment of lung cancer [30, 31]. In this study, we found that GTE inhibits the protein levels of Akt and phospho-Akt in H23/0.3 cells (Figure 6(a)). The inhibitory influence of GTE on phospho-Akt levels may be governed by its ability to suppress the expression of the Akt protein. We incubated H23/0.3 cells with LY294002, a PI3K-specific inhibitor, to confirm that GTE inhibits the proliferation of lung cancer H23/0.3 cells via modulation of the PI3K/Akt signaling pathway (Figure 6(b)). These results suggest that GTE may be a useful Akt-targeting agent for the treatment of lung cancer.

A number of reports show that the combined usage of some extracts from herbs (such as coptis rhizoma and glycyrrhizae radix) with anticancer agents results in a synergistic growth inhibitory effect on cancer cells [32, 33]. It has also been reported that a combination of *Ganoderma* with anticancer agents significantly slows the growth rate of cancer cells [13, 34]. For example, the combined treatment of taxol with *Ganoderma tsugae* (GT) extract results in a

synergistic growth suppression effect on colorectal cancer COLO205 cells [13], and *Ganoderma lucidum* enhances the chemotherapeutic efficacy of doxorubicin against SCLC H69 and VPA cells (a multidrug resistant cell line derived from H69 cells) [34]. Similarly, we demonstrated that a combination of doxorubicin with GTE resulted in a marked reduction in the number of viable NSCLC H23/0.3 cells (Figure 2(c)). These results suggest that GTE may be a promising adjuvant to anticancer agents in the treatment of drug resistant NSCLC cells.

In conclusion, we have demonstrated that GTE induces S phase arrest and the cellular apoptosis of H23/0.3 cells via regulation of the PI3K/Akt signaling pathways (Figure 6(c)). In addition, we have also shown that a combination of GTE and doxorubicin exerts an enhanced growth inhibitory effect on H23/0.3 cells. Our results suggest that GTE may be a safe and effective adjuvant therapeutic agent for the treatment of NSCLC cells with drug resistance.

Acknowledgments

The authors are grateful to Mr. Fon-Chang Liu for his technical assistance in conducting chromatography. This work was supported by grants from the National Science Council (NSC99-2320-B-039-023, and NSC100-2313-B-039-005-MY3) and Department of Health Clinical Trial and Research Center of Excellence (DOH101-TD-C-111-005), and China Medical University (Taichung) (CMU99-NTU-11), Taiwan, Republic of China. We also wish to thank members of the Medical Research Core Facilities Center (Office of Research & Development, China Medical University, Taichung, Taiwan) for their excellent technical support. H.-P. Kuo, H.-H Hsieh are contributed equally to this study.

References

- [1] R. Siegel, E. Ward, O. Brawley, and A. Jemal, "Cancer statistics, 2011: the impact of eliminating socioeconomic and racial disparities on premature cancer deaths," *CA Cancer Journal for Clinicians*, vol. 61, no. 4, pp. 212–236, 2011.
- [2] E. Y. Department of Health, Taiwan, "Health and vital statistics," 2011, <http://www.doh.gov.tw>.
- [3] R. S. Herbst, J. V. Heymach, and S. M. Lippman, "Molecular origins of cancer: lung cancer," *New England Journal of Medicine*, vol. 359, no. 13, pp. 1367–1380, 2008.
- [4] D. J. Stewart, "Tumor and host factors that may limit efficacy of chemotherapy in non-small cell and small cell lung cancer," *Critical Reviews in Oncology/Hematology*, vol. 75, no. 3, pp. 173–234, 2010.
- [5] X. Zhou, J. Lin, Y. Yin, J. Zhao, X. Sun, and K. Tang, "*Ganoderma taceae*: natural products and their related pharmacological functions," *American Journal of Chinese Medicine*, vol. 35, no. 4, pp. 559–574, 2007.
- [6] H. H. Ko, C. F. Hung, J. P. Wang, and C. N. Lin, "Antiinflammatory triterpenoids and steroids from *Ganoderma lucidum* and *G. tsugae*," *Phytochemistry*, vol. 69, no. 1, pp. 234–239, 2008.
- [7] Y. W. Wu, K. D. Chen, and W. C. Lin, "Effect of *Ganoderma tsugae* on chronically carbon tetrachloride-intoxicated rats," *American Journal of Chinese Medicine*, vol. 32, no. 6, pp. 841–850, 2004.
- [8] N. S. Lai, R. H. Lin, R. S. Lai, U. C. Kun, and S. C. Leu, "Prevention of autoantibody formation and prolonged survival in New Zealand Black/New Zealand White F1 mice with an ancient Chinese herb, *Ganoderma tsugae*," *Lupus*, vol. 10, no. 7, pp. 461–465, 2001.
- [9] J. L. Mau, H. C. Lin, and C. C. Chen, "Antioxidant properties of several medicinal mushrooms," *Journal of Agricultural and Food Chemistry*, vol. 50, no. 21, pp. 6072–6077, 2002.
- [10] G. Wang, J. Zhang, T. Mizuno et al., "Antitumor active polysaccharides from the Chinese mushroom Songshan lingzhi, the fruiting body of *Ganoderma tsugae*," *Bioscience, biotechnology, and biochemistry*, vol. 57, no. 6, pp. 894–900, 1993.
- [11] G. G. L. Yue, K. P. Fung, G. M. K. Tse, P. C. Leung, and C. B. S. Lau, "Comparative studies of various *Ganoderma* species and their different parts with regard to their antitumor and immunomodulating activities in vitro," *Journal of Alternative and Complementary Medicine*, vol. 12, no. 8, pp. 777–789, 2006.
- [12] K. H. Gan, Y. F. Fann, S. H. Hsu, K. W. Kuo, and C. N. Lin, "Mediation of the cytotoxicity of lanostanoids and steroids of *Ganoderma tsugae* through apoptosis and cell cycle," *Journal of Natural Products*, vol. 61, no. 4, pp. 485–487, 1998.
- [13] S. C. Hsu, C. C. Ou, J. W. Li et al., "*Ganoderma tsugae* extracts inhibit colorectal cancer cell growth via G2/M cell cycle arrest," *Journal of Ethnopharmacology*, vol. 120, no. 3, pp. 394–401, 2008.
- [14] S. C. Hsu, C. C. Ou, T. C. Chuang et al., "*Ganoderma tsugae* extract inhibits expression of epidermal growth factor receptor and angiogenesis in human epidermoid carcinoma cells: in vitro and in vivo," *Cancer Letters*, vol. 281, no. 1, pp. 108–116, 2009.
- [15] B. Boh, M. Berovic, J. Zhang, and L. Zhi-Bin, "*Ganoderma lucidum* and its pharmaceutically active compounds," *Biotechnology Annual Review*, vol. 13, pp. 265–301, 2007.
- [16] R. Tilton, A. A. Paiva, J. Q. Guan et al., "A comprehensive platform for quality control of botanical drugs (PhytomicsQC): a case study of Huangqin Tang (HQT) and PHY906," *Chinese Medicine*, vol. 5, article no. 30, 2010.
- [17] H. P. Kuo, T. C. Chuang, M. H. Yeh et al., "Growth suppression of HER2-overexpressing breast cancer cells by berberine via modulation of the HER2/PI3K/Akt signaling pathway," *Journal of Agricultural and Food Chemistry*, vol. 59, no. 15, pp. 8216–8224, 2011.
- [18] M. H. Hsu, C. J. Chen, S. C. Kuo et al., "2-(3-Fluorophenyl)-6-methoxyl-4-oxo-1,4-dihydroquinoline-3-carboxylic acid (YJC-1) induces mitotic phase arrest in A549 cells," *European Journal of Pharmacology*, vol. 559, no. 1, pp. 14–20, 2007.
- [19] K. Nishio, T. Nakamura, Y. Koh, T. Suzuki, H. Fukumoto, and N. Saijo, "Drug resistance in lung cancer," *Current Opinion in Oncology*, vol. 11, no. 2, pp. 109–115, 1999.
- [20] R. Boutros, V. Lobjois, and B. Ducommun, "CDC25 phosphatases in cancer cells: key players? Good targets?" *Nature Reviews Cancer*, vol. 7, no. 7, pp. 495–507, 2007.
- [21] K. Collins, T. Jacks, and N. P. Pavletich, "The cell cycle and cancer," *Proceedings of the National Academy of Sciences of the United States of America*, vol. 94, no. 7, pp. 2776–2778, 1997.
- [22] F. H. Igney and P. H. Krammer, "Death and anti-death: tumour resistance to apoptosis," *Nature Reviews Cancer*, vol. 2, no. 4, pp. 277–288, 2002.

- [23] S. Cory and J. M. Adams, "The BCL2 family: regulators of the cellular life-or-death switch," *Nature Reviews Cancer*, vol. 2, no. 9, pp. 647–656, 2002.
- [24] C. X. Xu, H. Jin, J. Y. Shin, J. E. Kim, and M. H. Cho, "Roles of protein kinase B/Akt in lung cancer," *Frontiers in Bioscience*, vol. 2, pp. 1472–1484, 2010.
- [25] J. Gao, W. A. Morgan, A. Sanchez-Medina, and O. Corcoran, "The ethanol extract of *Scutellaria baicalensis* and the active compounds induce cell cycle arrest and apoptosis including upregulation of p53 and Bax in human lung cancer cells," *Toxicology and Applied Pharmacology*, vol. 254, no. 3, pp. 221–228, 2011.
- [26] H. F. Hsu, K. H. Huang, K. J. Lu et al., "Typhonium blumei extract inhibits proliferation of human lung adenocarcinoma A549 cells via induction of cell cycle arrest and apoptosis," *Journal of Ethnopharmacology*, vol. 135, no. 2, pp. 492–500, 2011.
- [27] S. Li, Q. Han, C. Qiao, J. Song, C. L. Cheng, and H. Xu, "Chemical markers for the quality control of herbal medicines: an overview," *Chinese Medicine*, vol. 3, article no. 7, 2008.
- [28] T. Ohmori, E. R. Podack, K. Nishio et al., "Apoptosis of lung cancer cells caused by some anti-cancer agents (MMC, CPT-11, ADM) is inhibited by BCL-2," *Biochemical and Biophysical Research Communications*, vol. 192, no. 1, pp. 30–36, 1993.
- [29] R. J. Arceci, "Mechanisms of resistance to therapy and tumor cell survival," *Current opinion in hematology*, vol. 2, no. 4, pp. 268–274, 1995.
- [30] S. C. Park, H. S. Yoo, C. Park et al., "Induction of apoptosis in human lung carcinoma cells by the water extract of *Panax notoginseng* is associated with the activation of caspase-3 through downregulation of Akt," *International Journal of Oncology*, vol. 35, no. 1, pp. 121–127, 2009.
- [31] E. Nam and C. Park, "Maspin suppresses survival of lung cancer cells through modulation of Akt pathway," *Cancer Research and Treatment*, vol. 42, no. 1, pp. 42–47, 2010.
- [32] J. Liu, C. He, K. Zhou, J. Wang, and J. X. Kang, "Coptis extracts enhance the anticancer effect of estrogen receptor antagonists on human breast cancer cells," *Biochemical and Biophysical Research Communications*, vol. 378, no. 2, pp. 174–178, 2009.
- [33] K. Takara, S. Horibe, Y. Obata, E. Yoshikawa, N. Ohnishi, and T. Yokoyama, "Effects of 19 herbal extracts on the sensitivity to paclitaxel or 5-fluorouracil in HeLa cells," *Biological and Pharmaceutical Bulletin*, vol. 28, no. 1, pp. 138–142, 2005.
- [34] D. Sadava, D. W. Still, R. R. Mudry, and S. E. Kane, "Effect of *Ganoderma* on drug-sensitive and multidrug-resistant small-cell lung carcinoma cells," *Cancer Letters*, vol. 277, no. 2, pp. 182–189, 2009.

Research Article

Norcantharidin Induces HL-60 Cells Apoptosis In Vitro

You-Ming Jiang,¹ Zhen-Zhi Meng,¹ Guang-Xin Yue,² and Jia-Xu Chen^{1,3}

¹ School of Pre-Clinical Medicine, Beijing University of Chinese Medicine, Beijing 100029, China

² Institute of Basic Theory of TCM, China Academy of Chinese Medical Sciences, P.O. Box 83, Beijing 100700, China

³ Department of Basic Theory in Chinese Medicine, Henan University of Traditional Chinese Medicine, Zhengzhou 450008, China

Correspondence should be addressed to Jia-Xu Chen, chenjiaxu@hotmail.com

Received 29 February 2012; Revised 3 May 2012; Accepted 3 May 2012

Academic Editor: Vincenzo De Feo

Copyright © 2012 You-Ming Jiang et al. This is an open access article distributed under the Creative Commons Attribution License, which permits unrestricted use, distribution, and reproduction in any medium, provided the original work is properly cited.

Norcantharidin (NCTD) is the demethylated form of cantharidin, which is the active substance of mylabris, and is known to have anticancer potentials. The aim of this paper was to assess the apoptosis-inducing effect of NCTD on HL-60 cells. *Methods.* The effects of NCTD were detected by flow cytometer on the cell toxicity, cell cycle, and apoptosis of HL-60 cells cultured in vitro. *Results.* After 48-hour treatment with NCTD, the growth of HL-60 cells was inhibited significantly. The summit of apoptosis appeared after 24 hours. The percentage of the cells in G₁ phase decreased and then increased in S and G₂ + M phase, while the S and G₂ + M phases were blocked after treatment with 5, 10, and 50 μmol/L NCTD for 24 hours. *Conclusions.* NCTD can induce the apoptosis of HL-60 cells and inhibit the fission, and the domino effect was obviously correlated with the time and dosage.

1. Introduction

Mylabris, the polypide of *Mylabris phalerata* Pall or *Mylabris cichorii* Linnaeus, characterized by being cold in nature, acrid in flavor, and toxic, has the effect of removing toxic substance for cellulites, breaking blood stasis, and dispersing accumulation. It has been showed that cantharidin is the main ingredient for anticarcinogenic effect of mylabris, chemical structure of which is exo-1,2-syn-dimethyl-3,6-oxidohydrophthalic anhydride. Norcantharidin (NCTD) is the demethylated form of cantharidin, which is the active substance of mylabris, and is known to have anticancer potentials. NCTD is a kind of new-type anticancer drug with the effect of increasing white cells. It was synthesized with furan and maleic anhydride through Diels-Alder reaction [1] and was currently used as an anticancer drug in China. Many experiments including our previous study [2] have demonstrated that NCTD can inhibit the growth of tumor cells in vitro and in vivo [3–9]. However, the exact anticancer mechanism of NCTD on human cancer cells remains poorly understood. In the present study, flow cytometer and cytomorphology staining were used to study the effect of NCTD on apoptosis and cell cycle of HL-60 cells.

2. Materials and Methods

2.1. Cell Strain. HL-60 cells were cultivated in pure RPMI-1640 (purchased from GBICO), placed in a temperature-controlled CO₂ incubator (37°C), transfer of culture one time every 2-3 days. Experiment started when cells entered exponential growth stage, the best state.

2.2. Drugs and Agent. Calf serum was provided by Institute of Hematologic Disease in Tianjin affiliated to Chinese Academy of Medical Sciences; NCTD was purchased from the Forth Pharmaceutical Factory in Beijing and was dissolved by DMSO. RNA enzyme was purchased from Huamei Company, the concentration of which used in this experiment was 0.02 g/L. Propidium iodide (PI) (Sigma Company), the concentration of which used in this experiment was 0.05 g/L.

2.3. Flow Cytometer. Fluorescence-activated cell sorter, being manufactured by USA Becton Dickinson Company, type of 420, was provided by Institute of Basic Theory, China Academy of TCM.

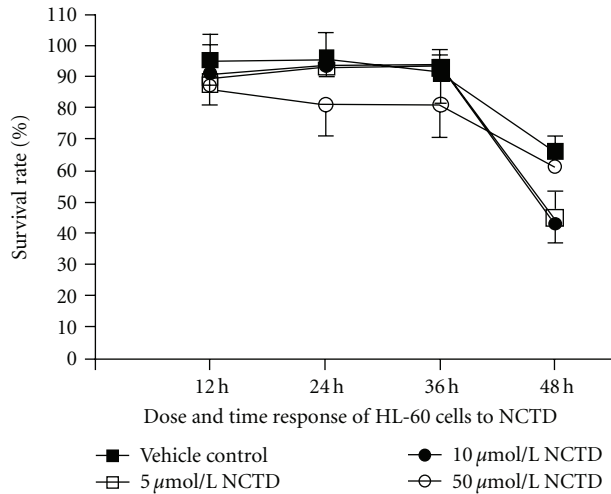


FIGURE 1: Cytotoxic effect of NCTD on HL-60 cells.

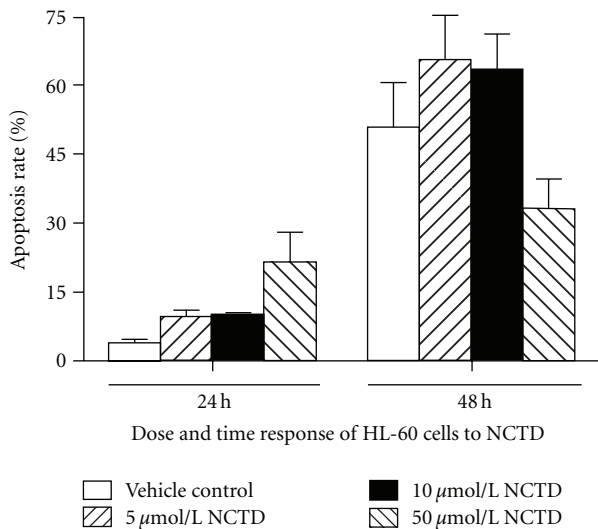


FIGURE 2: Effect of NCTD on HL-60 cells apoptosis.

2.4. Experiment of Dose and Time Response on HL-60 Cells by NCTD. Cell concentration was adjusted into $5 \times 10^8/\text{L}$ when HL-60 cells were at the logarithmic increasing phase; then the cells were inoculated on 12-well plates. Each well added 1 mL cell suspension and 3 mL RPMI-1640 containing 10% calf serum, then added NCTD (the final concentrations were $5 \mu\text{mol/L}$, $10 \mu\text{mol/L}$, $50 \mu\text{mol/L}$, resp.), and DMSO as control group; each group had 3 parallel wells. Specimens were collected at 24 h, 48 h after the cell suspension was cultured in temperature-controlled incubator (37°C , 0.05CO_2). Adding $200 \mu\text{L}$ cell suspension into $100 \mu\text{L}$ 1.8% NaCl and $100 \mu\text{L}$ 4% trypan blue stock solution to stain. Stained specimens were put into centrifugal machine for 1 min at 1000 r/min, sucking the supernatant. The supernatant was washed by PBS (pH 7.4, 0.05mol/L) two times and centrifuged for 1 min at 1000 r/min to count the alive cells and dead cells

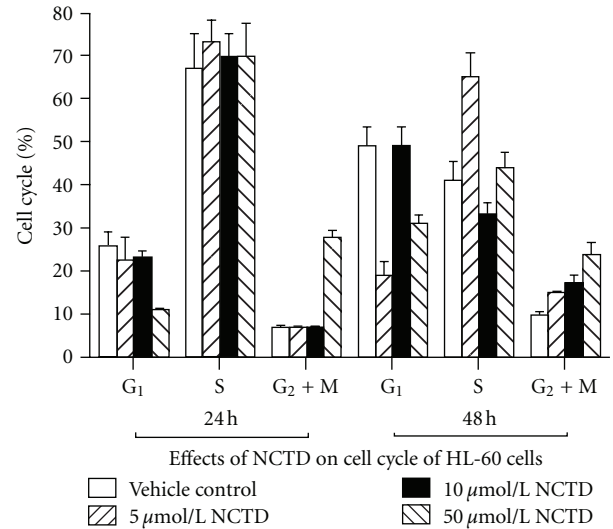


FIGURE 3: Effects of NCTD on HL-60 cell cycle.

under the invert microscope after the colorless supernatant was dropped on slide.

2.5. Experiment of Dose and Time Response on HL-60 Cells Apoptosis and Cell Cycle by NCTD. The concentration and action time of NCTD were the same as mentioned above. To collect cells after medication treatment, wash the cells with PBS not containing Ca^{2+} , Mg^{2+} and centrifuge them for 5 min at 800 r/min twice, respectively. Then use syringe with TB pinhead to infuse cells precipitation into 70% alcohol (4°C), shake until cells homogeneous dispersion, and fix the cells more than 18 h. Concentration of cells was adjusted into $1 \times 10^9/\text{L}$ after being centrifuged and washed. $500 \mu\text{L}$ cell sap were lucifuge strained with $50 \mu\text{L}$ 0.1% PI (50 mg/L Propidium iodide, 0.1% Sodium-cit-rate, 0.1% triton X-100) for 30 min. Specimen was filtered with 400 holes net, exciting wavelength was set at 488 nm, and blocking filter was 585 nm. Photomultiplier tube and multichannel pulse analyzer were used to show apoptosis scatterplot. Flow cytometer analysis showed that near diploid cell mass peak appeared at the left of G1 phase during cell apoptosis. Flow cytometer was used to determine the change of percentage of cell at G1 phase, S phase, and G2 + M phase. Each group had 1×10^6 cells and 3 parallel wells.

2.6. Observation on Cytomorphology of HL-60 Cells after NCTD. The apoptotic morphology was observed by using staining reagent Wright-Giemsa. Collected HL-60 cells treated with NCTD at 1000 r/min for 5 min used PBS to rinse the collected cells one time. Collected cells were then resuspended in PBS and dropped on slide. Collected cells were fixed in Colonial spirit for 2-3 min after air drying, then open-air drying. Collected cells were stained in Giemsa stain. The stained cells were separated according to color in 95% alcohol for 30 s and dehydrated in absolute alcohol for 10-30 s, cleared in dimethyl benzene, and enveloped with neutral gum. Cellular shape was observed and photographed under type 2 Leitz-ORTHOLUX light microscope (German).

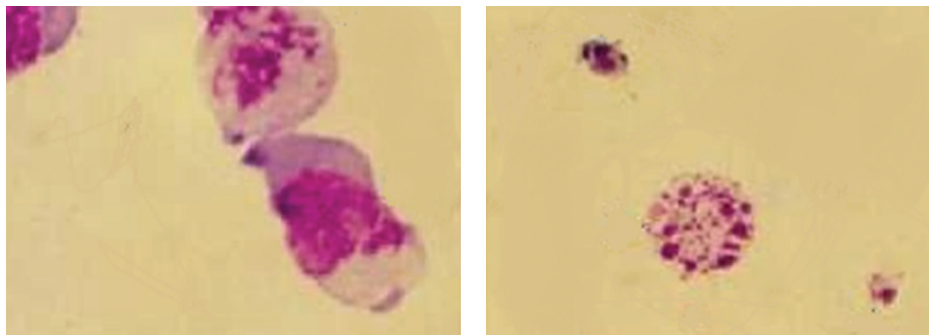


FIGURE 4: Cytomorphology of HL-60 cells after NCTD treatment ($\times 500$).

2.7. Statistical Method. Data were analyzed by analysis of variance (ANOVA) followed by post hoc *t* tests for comparisons between groups. Significance was accepted as $P < 0.05$. Data are expressed as mean \pm standard deviation (SD).

3. Results

3.1. Dose and Time Response on HL-60 Cells by NCTD. Trypan blue staining showed that the cytotoxic effect of NCTD on HL-60 cells increased with increase of time ($P < 0.01$); survival rate of HL-60 cells decreased with increase of the concentration of NCTD ($P < 0.05$). Results showed that cytotoxic effect of NCTD on HL-60 cells was time and dose concentration response (Figure 1).

3.2. Dose and Time Response on HL-60 Cells Apoptosis by NCTD. Apoptosis of HL-60 appeared at 48 h ($P < 0.01$). Apoptosis of HL-60 induced by $5 \mu\text{mol/L}$ NCTD for 48 h was more apparent than those induced by other concentrations and also was time dependent. Apoptosis of HL-60 induced by $50 \mu\text{mol/L}$ NCTD for 24 h was obvious (Figure 2).

3.3. Effects of NCTD on Cell Cycle of HL-60 Cells. Compared with blank control group, the percentages of HL-60 cells of G_1 phase decrease after being treated by NCTD, while the percentages of HL-60 cells of S phase and $G_1 + M$ phase increased, the cell cycle was dramatically arrested at G_2/M phase ($P < 0.01$). Effect of NCTD on HL-60 cells cycle was specially obvious with $50 \mu\text{mol/L}$ for 24 h and 48 h (Figure 3).

3.4. Change of Cytomorphology of HL-60 Cells after NCTD Treatment. Under inverted microscope, the HL-60 cells growth was round. After treatment with NCTD, the cell growth was inhibited, the growth velocity decreased, and the cell changed from round into ellipse, horseshoe shape, gradually. There were several ecthyma on edge of cell membrane, the cell clarity decreased apparently. Above phenomena became more obvious with the increase of the concentration of NCTD. Wright-Giemsa staining showed that apparent change of morphology appeared after treating with different concentrations of NCTD for 24 h. Its expression was that the chromosome movement was abnormal at mitosis anaphase,

nucleoplasm condensed into one or several big boluses, and cell nucleus split into shivers; thus ganoid apoptotic bodies encapsulated by cell membrane appeared to be intracellular (Figure 4 represents apoptosis cell and/or apoptotic body; left: $5 \mu\text{mol/L}$ NCTD treatment group; right: $50 \mu\text{mol/L}$ NCTD treatment group).

4. Discussion

The development of tumor is closely related to apoptosis. An important foundation of tumor development is reinforcement of cell multiplication or apoptosis blocking or multiplication and apoptosis reinforcement, but the reinforcement of multiplication exceeded that of apoptosis significantly. In recent years, it has been paid attention to apoptosis induced by Chinese materia medica at home and abroad [10]. It has been proved that lots of anticancer drug originated from Chinese materia medica such as taxol [11], camptothecin, teniposide, harringtonine [12], and trichosanthin [13] can induce tumor cell apoptosis.

Mylabris, characterized by being acrid in flavor, and cold in nature, is toxiferous; it should be processed before being used as decoction. Much attention has been attached to study on curative feasibility of toxiferous Chinese crude drug by the exploitation of its so-called function of fight fire with fire. Whether the mechanism of toxiferous Chinese crude drug is related to inducing apoptosis has been indefinite yet.

This study showed that the depressant effect of NCTD on HL-60 cells was apparent and had time and dose effect response. Flow cytometer showed that HL-60 cells appeared as apoptosis after treatment with $5 \mu\text{mol/L}$, $10 \mu\text{mol/L}$, $50 \mu\text{mol/L}$ NCTD for 24 h and 48 h, and the effect of NCTD on HL-60 cells was dose dependent. After treating by NCTD, the percentage of HL-60 cells decreased at G_1 phase, the percentage at S phase and G_2/M phase increased, and the cell cycle was dramatically arrested at G_2/M phase and S phase. It indicated that NCTD could inhibit the DNA synthesis of HL-60 cell at S phase obviously, interfere with karyokinesia, and thus, restrain the proliferation of tumor cells. In conclusion, NCTD can inhibit the growth of HL-60 cells by interfering with cell proliferation and inducing apoptosis. This has been proved by morphology staining, and its mechanism needs further investigation.

Acknowledgment

This work was supported by Program for Innovative Research Team in Beijing University of Chinese Medicine (2011CXTD-07).

References

- [1] B. J. Cao and J. Z. Wang, "Improvement on synthesis of norcantharidin," *Tianjin Pharmacy*, vol. 7, no. 2, pp. 35–36, 1995.
- [2] J. X. Chen, X. L. Liu, and Y. Liu, "Influence of norcantharidin on apoptosis of K562," *China Journal of Traditional Chinese Medicine and Pharmacy*, vol. 15, no. 2, pp. 21–23, 2000.
- [3] W. W. An, X. F. Gong, M. W. Wang, S. I. Tashiro, S. Onodera, and T. Ikejima, "Norcantharidin induces apoptosis in HeLa cells through caspase, MAPK, and mitochondrial pathways," *Acta Pharmacologica Sinica*, vol. 25, no. 11, pp. 1502–1508, 2004.
- [4] W. W. An, M. W. Wang, S. I. Tashiro, S. Onodera, and T. Ikejima, "Norcantharidin induces human melanoma A375-S2 cell apoptosis through mitochondrial and caspase pathways," *Journal of Korean Medical Science*, vol. 19, no. 4, pp. 560–566, 2004.
- [5] Y. J. Chen, C. J. Shieh, T. H. Tsai et al., "Inhibitory effect of norcantharidin, a derivative compound from blister beetles, on tumor invasion and metastasis in CT28 colorectal adenocarcinoma cells," *Anti-Cancer Drugs*, vol. 16, no. 3, pp. 293–299, 2005.
- [6] Y. Z. Fan, J. Y. Fu, Z. M. Zhao, and C. Q. Chen, "Effect of norcantharidin on proliferation and invasion of human gallbladder carcinoma GBC-SD cells," *World Journal of Gastroenterology*, vol. 11, no. 16, pp. 2431–2437, 2005.
- [7] S. H. Kok, S. J. Cheng, C. Y. Hong et al., "Norcantharidin-induced apoptosis in oral cancer cells is associated with an increase of proapoptotic to antiapoptotic protein ratio," *Cancer Letters*, vol. 217, no. 1, pp. 43–52, 2005.
- [8] J. L. Li, Y. C. Cai, X. H. Liu, and L. J. Xian, "Norcantharidin inhibits DNA replication and induces apoptosis with the cleavage of initiation protein Cdc6 in HL-60 cells," *Anti-Cancer Drugs*, vol. 17, no. 3, pp. 307–314, 2006.
- [9] H. F. Liao, S. L. Su, Y. J. Chen, C. H. Chou, and C. D. Kuo, "Norcantharidin preferentially induces apoptosis in human leukemic Jurkat cells without affecting viability of normal blood mononuclear cells," *Food and Chemical Toxicology*, vol. 45, no. 9, pp. 1678–1687, 2007.
- [10] Z. H. Zhou, "Research progress on chinese materia medica induces tumor cell apoptosis," *Foreign Medical Science*, vol. 20, no. 3, pp. 3–6, 1988.
- [11] L. Milas, N. R. Hunter, B. Kurdoglu et al., "Kinetics of mitotic arrest and apoptosis in murine mammary and ovarian tumors treated with taxol," *Cancer Chemotherapy and Pharmacology*, vol. 35, no. 4, pp. 297–303, 1995.
- [12] M. Fang, H. Q. Zhang, S. B. Xue et al., "Harringtonine induces HL-60 cells apoptosis," *Chinese Science Bulletin*, vol. 39, no. 12, pp. 1125–1129, 1994.
- [13] L. Bi, H. Li, and Y. Zhang, "Effect of trichosanthin of cell cycle and apoptosis of murine melanoma cells," *Chinese Journal of Integrated Traditional and Western Medicine*, vol. 18, no. 1, pp. 35–37, 1998.

Research Article

Caffeic Acid Phenylethyl Amide Protects against the Metabolic Consequences in Diabetes Mellitus Induced by Diet and Streptozocin

Yi-Chun Weng,¹ Sung-Ting Chuang,¹ Yen-Chu Lin,¹ Cheng-Fung Chuang,¹
Tzong-Cherng Chi,² Hsi-Lin Chiu,³ Yueh-Hsiung Kuo,³ and Ming-Jai Su¹

¹Institute of Pharmacology, College of Medicine, National Taiwan University, Taipei 10051, Taiwan

²Graduate Institute of Medical Sciences, Chang Jung Christian University, Tainan 71101, Taiwan

³Tsuzuki Institute for Traditional Medicine, China Medical University, Taichung 40402, Taiwan

Correspondence should be addressed to Ming-Jai Su, mingja@ntu.edu.tw

Received 7 February 2012; Revised 2 May 2012; Accepted 6 May 2012

Academic Editor: William C. S. Cho

Copyright © 2012 Yi-Chun Weng et al. This is an open access article distributed under the Creative Commons Attribution License, which permits unrestricted use, distribution, and reproduction in any medium, provided the original work is properly cited.

Caffeic acid phenyl ester is distributed widely in nature and has antidiabetic and cardiovascular protective effects. However, rapid decomposition by esterase leads to its low bioavailability in vivo. In this study, chronic metabolic and cardiovascular effects of oral caffeic acid phenylethyl amide, whose structure is similar to caffeic acid phenyl ester and resveratrol, were investigated in ICR mice. We found that caffeic acid phenylethyl amide protected against diet or streptozocin-induced metabolic changes increased coronary flow and decreased infarct size after global ischemia-reperfusion in Langendorff perfused heart. Further study indicated that at least two pathways might be involved in such beneficial effects: the induction of the antioxidant protein MnSOD and the decrease of the proinflammatory cytokine TNF α and NF κ B in the liver. However, the detailed mechanisms of caffeic acid phenylethyl amide need further studies. In summary, this study demonstrated the protective potential of chronic treatment of caffeic acid phenylethyl amide against the metabolic consequences in diabetes mellitus.

1. Introduction

Diabetes mellitus (DM) is a metabolic disease with hyperglycemia and usually accompanied with many complications [1–5]. Lifestyle patterns in industrialized societies comprise an increasing availability and ingestion of high-caloric food in the presence of a sedentary living, and these factors are emerging as the fundamental causes of the fast-spread diabetes. Since the incidence of acute myocardial infarction and coronary heart disease is pretty high in the population of metabolic syndrome, the identification of new pharmacological approaches to effectively prevent and treat metabolic syndrome and its cardiovascular complications is of crucial importance.

Streptozocin (STZ) is a pancreatic β -cell toxin that induces rapid and irreversible necrosis of β cells. It is widely used in making experimental animal models of type 1 DM [6]. Since insulin secretion is deficient in STZ-induced type 1

diabetic mice, it is also a good model for research on insulin-independent antidiabetic mechanisms of the compounds. For type 2 DM, transgenic [7, 8] and chemical-induced [9] animals are widely used in hypoglycemic drug screen for many years, but these animals are not so similar to most clinical patients. Recently, the usage of diet-induced type 2 DM animal models in studies has increased [10–15]. Higher similarity in the cause and the pathology of DM in these diet-induced animal models are observed as compared to those in patients. According to our previous results, two stages were observed in high-fat and high-fructose diet-induced diabetic mice: hyperglycemia and hyperlipidemia without insulin resistance occurred at week 2 and systemic insulin resistance owing to low insulin sensitivity in main metabolic tissues occurred at week 4 [16]. Since systemic insulin resistance and specific reduction of insulin sensitivity in major metabolic tissue could be induced in a short time, diet-induced diabetic BLTW:CD1(ICR) mice could be an

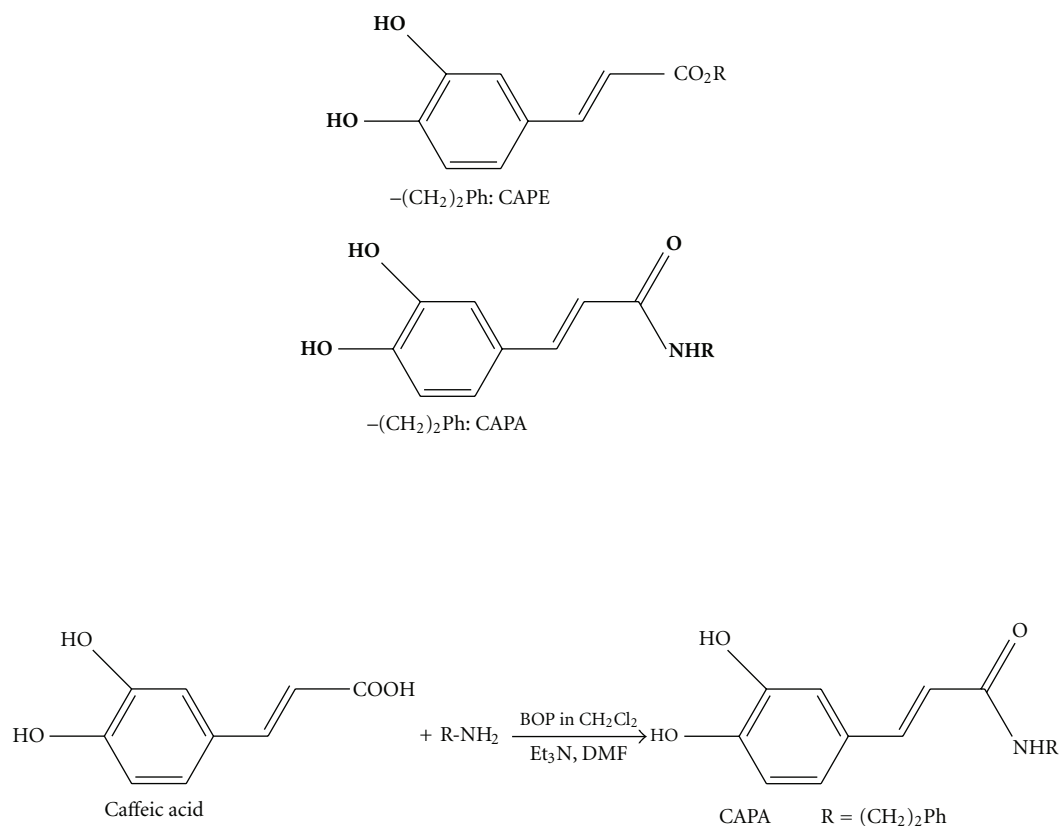


FIGURE 1: The chemical structures of CAPE and CAPA used in the present study. CAPA was obtained from the amide binding coupling method, beginning with caffeic acid.

efficient model for medical research with an advantage of ruling out strain-specific gloss.

Many natural polyphenolic compounds are demonstrated to have anti-inflammatory, antioxidant, anticarcinogenic, antithrombotic, and cardiovascular protective effects [17–19]. Resveratrol and curcumin are successfully employed in the prevention and treatment of a variety of diseases, including metabolic dysfunction, coronary artery disease, pressure-overload hypertrophy, and heart failure [20, 21]. Caffeic acid and caffeic acid phenylethyl ester (CAPE) are also widely distributed in nature, especially the plant kingdom. However, the rapid metabolism of CAPE by esterase leads to its low bioavailability. Caffeic acid phenylethyl amide (CAPA) was a caffeic acid amide derivative and structurally similar to CAPE and resveratrol (Figure 1). Since amide is more resistant to esterase, it is foreseeable that CAPA is more stable than CAPE in vivo. In this study, the protective potential of chronic oral CAPA against the metabolic consequences in type 1 and type 2 diabetic mice model was investigated and the known antidiabetic agent metformin was taken as a positive control.

2. Materials and Methods

2.1. Chemical. Beginning with caffeic acid, CAPA was obtained from the following amide binding coupling

method. The solution of benzotriazol-1-yloxytris (dimethylamino)phosphonium hexafluorophosphate (BOP) (1.2 eq) in dichloromethane (CH₂Cl₂) (5 mL) was added to a mixture of caffeic acid (100 mg), R-NH₂ (1.2 eq), and triethylamine (Et₃N) (0.08 mL) in dimethylformamide (DMF) (1.0 mL). The mixture was stirred at 0°C for 30 min, then allowed to stir at room temperature for 12 h. This reaction mixture was evaporated under in vacuo, and the residue was partitioned between ethyl acetate (AcOEt) and H₂O. Successively, the AcOEt layer was washed with 3 N aqueous HCl and 10% NaHCO₃(aq), dried over MgSO₄ and concentrated in vacuo. The residue was further purified by column chromatography with eluting solution (CH₂Cl₂–AcOEt 1 : 1, v/v) on silica gel (70–230 and 230–400 mesh, Merck 7734). The final products (82–88% yield) were recrystallized from AcOEt to obtain pure crystals. ¹H and ¹³C NMR spectra were recorded on a Bruker Avance 500 spectrometer. Electron impact mass spectrometries (EIMS) were determined on a Finnigan TSQ-46C mass spectrometer. IR spectra were recorded on a Nicolet Magna-IR 550 spectrophotometer.

Caffeic acid phenylethyl amide: solid. mp 148–149°C. IR ν_{\max} (cm⁻¹): 3288, 1642, 1591, 1523, 1361, 1279, 1036, 975, 849. ¹H NMR (CD₃COCD₃, 500 MHz): δ 2.84 (2H, *t*, *J* = 6.8 Hz), 3.53 (2H, *q*, *J* = 6.8 Hz), 6.43 (1H, *d*, *J* = 15.2 Hz), 6.83 (1H, *d*, *J* = 8.1 Hz), 6.92 (1H, *dd*, *J* = 8.1, 1.8 Hz), 7.07 (1H, *d*, *J* = 1.8 Hz), 7.15–7.30 (5H, *m*), 7.35 (1H, *br. s*, –NH),

7.43 (1H, *d*, *J* = 15.2 Hz), 8.20 (1H, *s*, –OH), 8.42 (1H, *s*, –OH). EI-MS *m/z*(%): 283 (M^+ , 17), 178 (22), 163 (100).

2.2. Animals. 4-week-old male BLTW: CD1(ICR) mice were acquired from BioLasco Taiwan Co., Ltd. and maintained at National Taiwan University College of Medicine Experimental Animal Center, in a temperature- and humidity-controlled ($22 \pm 1^\circ\text{C}$ and $60 \pm 5\%$) environment with a strict 12 hour light-dark cycle and given free access to food and water. After the acclimatizing period (at least 3 days), mice with fasting plasma glucose levels higher than 130 mg/dL or lower than 70 mg/dL were excluded.

Type 1 diabetic mice were induced by modifying the previous method [6]. In brief, an intraperitoneal injection of streptozocin (STZ, Sigma Chemical Co.; St. Louis, MO, USA) at 150 mg/kg dissolved in 1% citrate buffer was performed in 4-week-old mice fasted for 48 hours. Mice with plasma glucose level of 350 mg/dL or greater were considered as type 1 diabetic. Type 2 diabetic mice were induced by high-fat and high-fructose diet according to previous method [22] and our previous study [16]. Mice with fasting plasma glucose level of 150 mg/dL or greater were considered as type 2 diabetic.

Caffeic acid phenylethyl amide (10 mg/kg) or metformin (300 mg/kg) was given once a day orally. The investigation followed the University guidelines for the use of animals in experimental studies and conformed to the Guide for the Care and Use of Laboratory Animals published by the US National Institutes of Health (NIH publication no. 85-23, revised 1996). The animal experiments were approved by the IACUC of National Taiwan University (IACUC no. 20100007).

2.3. High-Fat and High-Fructose Diet. Additional 24.18% w/w palm oil and 2.56% w/w soybean oil were added to powder of Purina Laboratory Rodent Diet 5001 standard chow (Purina; PMI Nutrition International, St. Louis, MO, USA) and this high-fat diet mixture was reconstituted in small pellets. High fat diet and fructose-sweetened water (containing 20% fructose) were used to induce type 2 diabetes in ICR mice. Metabolizable energy of standard rodent chow, HF diet, and fructose water was 3.04 kcal/gm, 4.63 kcal/gm, and 0.8 kcal/mL, respectively.

2.4. Blood Sampling. Mice were anesthetized with pentobarbital (80 mg/kg, intraperitoneal, Sigma), and blood was withdrawn from the orbital venous plexus using a heparinized capillary tube. Blood samples were centrifuged at 10000 $\times g$ for 5 min, and plasmas were placed on ice or stored at -20°C until assay [23].

2.5. Determination of Plasma Parameters. An aliquot of plasma was added to glucose kit reagent (Biosystems S.A., Barcelona, Spain) and incubated at 37°C for 5 min. The concentration of plasma glucose was then estimated via a spectrophotometer with samples run in duplicate [24]. Determination of serum insulin concentration adopted ELISA (Mammalian Insulin ELISA; Mercodia AB, Uppsala,

Sweden) [25]. Plasma triglycerides and total cholesterol were measured using commercially available cholesterol kit (Randox, UK) and triglycerides kit (Randox, UK), respectively. Plasma retinol binding protein 4 (RBP4) and adiponectin levels were measured using commercially available ELISA kits (AdipoGen and Linco, resp.). All assays were performed according to the manufacturer's instructions.

2.6. Insulin Tolerance Test (ITT) and Intraperitoneal Glucose Tolerance Test (IPGTT). Intraperitoneal glucose tolerance test (IPGTT) and insulin tolerance test (ITT) were performed according to the method described previously [12, 26]. Briefly, intraperitoneal insulin (0.5 IU/kg) and glucose (2 g/kg) tolerance tests were performed after 3 hr and overnight of fast, respectively, and blood samples were collected at 0, 15, 30, and 60 minute for ITT and at 0, 30, 60, 120, and 150 minute for IPGTT. Areas between glucose curves after glucose or insulin injection and baseline glucose level curve (ΔAUC) were also calculated.

2.7. Glycogen Content Assay. About 50 mg of tissue sample was dissolved in 1 N KOH at 70°C for 30 min. Dissolved homogenate was neutralized by glacial acetic acid and incubated overnight in acetate buffer (0.3 M sodium acetate, pH 4.8) containing amyloglucosidase (Sigma, St. Louis, MO, USA). Samples were then analyzed by measuring glucosyl units using Trinder reaction. The reaction mixture was neutralized with 1 N NaOH [27].

2.8. Histological Analysis. Tissues were immersion-fixed in neutral 10% buffered formalin. Sections were paraffin-embedded, cut at $4\ \mu\text{m}$, and mounted onto slides. HE staining was performed for histological analysis. Tissue sections were examined using a microscope and were photographed with a digital camera.

2.9. Cell Culture. HepG2 cell lines were grown, as a monolayer, in Dulbecco's modified Eagle's medium (DMEM) supplemented with 10% (v/v) fetal bovine serum (FBS), 100 U/mL penicillin G, and 100 $\mu\text{g}/\text{mL}$ streptomycin in a humidified atmosphere with 5% CO_2 at 37°C . The cells were cultured at 90% confluence and then seeded onto 6 cm culture dishes to perform the experiments [28]. Cells were starved for 24 h before the experiments. After starvation, cells were incubated in DMEM medium containing 10% FBS and treated with various concentrations of caffeic acid phenylethyl amide at 1 h prior to and during treatment with human recombinant TNF- α (tumor necrosis factor-alpha, CytoLab Ltd., Rehovot, Israel) or H_2O_2 (100 to 500 μM). Incubation with TNF- α was conducted for 60 min for IKK (I κ B kinase) phosphorylation as described by others [29].

2.10. HepG2 Triglyceride Content Assay. Cells were lysed in lysis buffer (20 mM HEPES (pH 7.6), 150 mM NaCl, 1% Triton X-100, 0.1% SDS) and total fat was extracted by Bligh and Dyer method [28]. Briefly, the cell extract was incubated with methanol and chloroform for 1 h, and then chloroform and sterile water were added, centrifuged briefly to collect

chloroform phase. This extract was dried for overnight, and was dissolved in 10% Triton-isopropanol solution. According to a manual of triglycerides kit, the quantity of triglyceride was measured.

2.11. Western Blotting. Protein contents were measured by Western blotting using commercially available polyclonal antibodies specific for TNF α (Millipore, USA), MnSOD (Millipore, USA), p-p65 (Cell Signaling, USA), p-IKK α/β (Santa Cruz, USA), PEPCK (a kind gift from Professor DK Granner), and GLUT4 (R&D systems). To adjust for loading differences, blots were reprobed with a monoclonal antibody to β -actin (ABS, USA). Densities of the obtained immunoblots were quantified using ImageQuant.

2.12. Langendorff Perfused Heart Model. Isolated perfused mouse heart model was set as previously described with minor modification [30]. In brief, the aorta was cannulated with a 20-gauge cannula. The aorta was perfused in the Langendorff System (ADInstruments) at constant pressure (80 ± 3 mmHg). The hearts were perfused with a buffer consisting of (in mM) 118.5 NaCl, 25 NaHCO $_3$, 4.7 KCl, 1.2 MgSO $_4$, 1.2 KH $_2$ PO $_4$, and 2.5 CaCl $_2$, 11 glucose and gassed with 95% O $_2$ -5% CO $_2$ (pH 7.4). Hearts were allowed to beat spontaneously; basal coronary flow and heart rate were recorded after a 30-minute balance period. Then hearts were subjected to a 30-minute global ischemia (area at risk equaled to whole heart mass) and 2-hour reperfusion. The infarct sizes were analyzed by TTC stain method and expressed as percentage of AAR.

2.13. Statistical Analysis. Data were represented as the means \pm SEM for the number (n) of animals in the group as indicated in figures. Statistical analysis was performed by one-way analysis of variance (ANOVA) with Dunnett's post-hoc test. $P < 0.05$ was regarded as statistically significant.

3. Results

3.1. CAPA Protected Mice from Diet-Induced Metabolic Dysfunction. Continuous exposure to a high-fat and high-fructose diet for 4 weeks led to significant increases in body weight (Figure 2(a)) and fat mass (Figures 2(b) and 2(c)) in ICR mice. Significant lower body weight and fat mass accompanied by decreased calorie intake (Table 1) were observed in mice treated with 10 mg/kg CAPA or 300 mg/kg metformin compared with nontreated ones. Plasma retinol binding protein 4 (RBP4) and adiponectin levels were increased after exposure to the high-fat and high-fructose diet, and both levels were lowered after CAPA treatment (Figures 2(d) and 2(e)).

3.2. CAPA Protected Mice from Glucose Intolerance. Chronic exposure to high-fat and high-fructose diet for 4 weeks increased glucose, insulin, triglyceride, and cholesterol levels (Figure 3(a) to 3(d)). To assess the impact of chronic high-fat and high-fructose diet exposure on glucose homeostasis in more detail, the mice were subjected to a glucose tolerance

test (GTT) (Figure 4(a)). Intraperitoneal administration of glucose led to a more rapid increase of blood glucose levels in mice fed a high-fat and high-fructose diet, indicating the expected diet-induced systemic glucose intolerance. Both CAPA and metformin treated mice had lower blood glucose levels than nontreated mice on the same glucose tolerance test. Δ AUC (area-under-the-curve) values revealed a significantly preserved glucose tolerance of mice treated with CAPA (Figure 4(b)). An insulin tolerance test (ITT) after chronic exposure to high-fat and high-fructose diet for 4 weeks showed lower glucose levels and bigger Δ AUC values in CAPA and metformin treated mice (Figures 4(c) and 4(d)). Glycogen content assay also showed that CAPA and metformin preserved the insulin induced glycogen synthesis in skeletal muscle (Figure 4(e)).

Noteworthy, even when hyperglycemia, hyperinsulinemia, and higher plasma level of adiponectin had been developed after two weeks of exposure to high-fat and high-fructose diet, treatment with CAPA for another 2 weeks significantly ameliorated the metabolic dysfunctions and prevented glucose intolerance (Table 2). Similarly, mice with plasma glucose levels higher than 350 mg/dL measured at two weeks after STZ injection were seen as type 1 diabetic mellitus model. CAPA treatment for another two weeks ameliorated STZ-induced hyperglycemia and body weight (Table 3). According to these results, we concluded that chronic oral administration of CAPA could protect mice from diet and STZ-induced metabolic dysfunctions, even when hyperglycemia had been developed.

3.3. CAPA Preserved Basal Coronary Flow and Decreased Infarct Size in Langendorff Perfused Heart. Since the incidence of acute myocardial infarction and coronary heart disease is pretty high in the population of metabolic syndrome, we investigated the effects of 2-week treatment with CAPA or metformin on basal coronary flow and infarct size after global ischemia-reperfusion in Langendorff perfused heart. Four weeks of continuous exposure to high-fat and high-fructose diet decreased basal coronary flow, but CAPA or metformin treatment (introduced after 2 weeks exposure to the diet) for two weeks preserved the basal flow (Table 2). After a 30-minute global ischemia and 2-hour reperfusion, mice fed on high-fat and high-fructose diet had larger infarct size. Treatment of CAPA or metformin protected mice on high-fat and high-fructose diet from severe ischemic and reperfusion injury (Table 2). Besides, CAPA treatment could also improve basal coronary flow and decreased infarct size in STZ-induced type 1 diabetic mice (Table 3).

3.4. CAPA Protected Liver from Inflammation and Decreased Gluconeogenesis. A high-fat and high-fructose diet-induced obesity can induce and lead to a chronic inflammatory reaction, which is believed to be critical for the development of glucose intolerance and insulin resistance [31]. Correspondingly, the expression of TNF α , a major proinflammatory cytokine, was significantly enhanced in livers of mice on a chronic high-fat and high-fructose diet (Figure 5(a)). However, CAPA or metformin treated mice exhibited lower

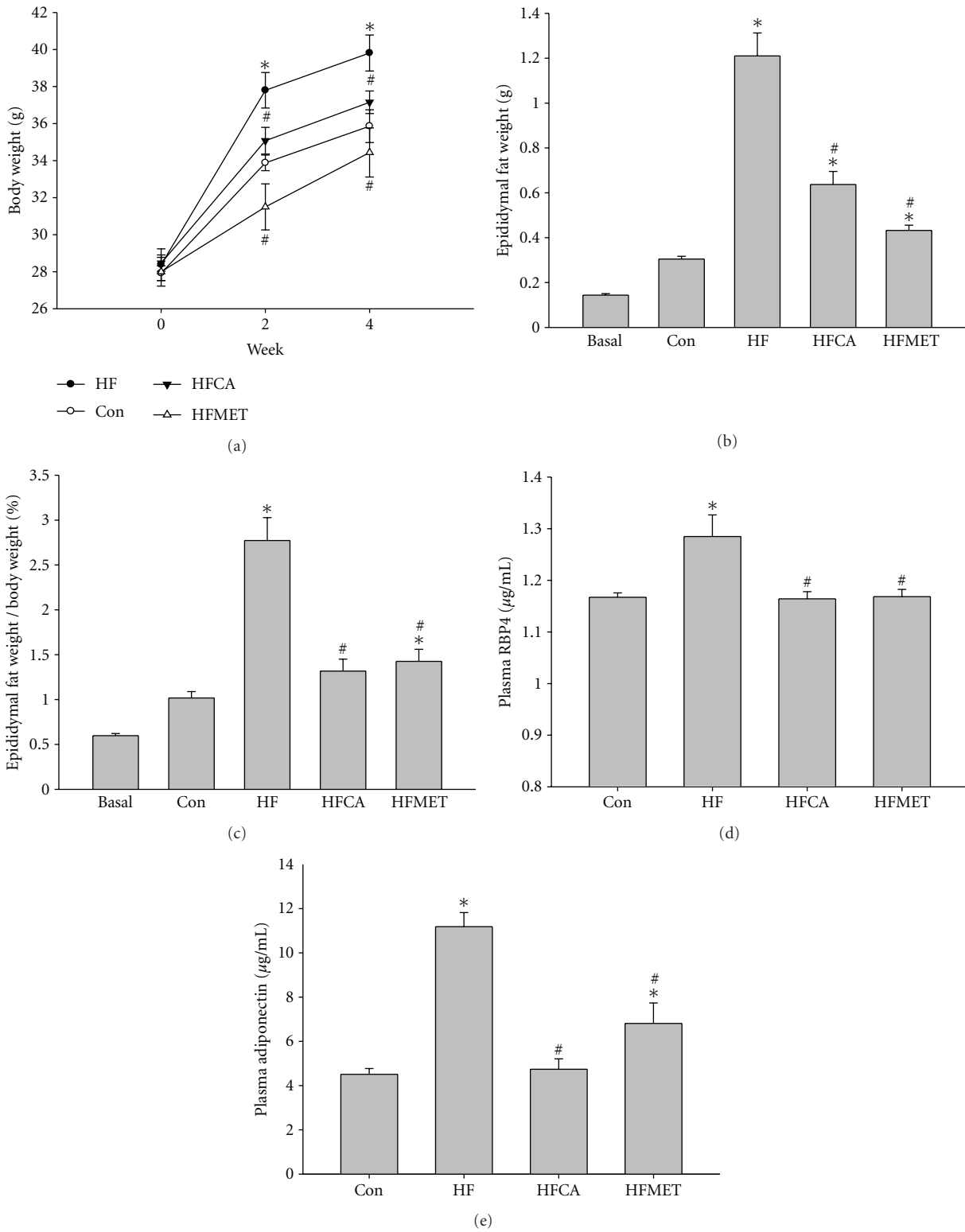


FIGURE 2: Fat metabolism of mice. (a) Body weight before (0W) and after two (2W) and four (4W) weeks of diet exposure. (b and c) Fat mass and fat to body weight ratio after 4 weeks of diet exposure. (d and e) Plasma levels of retinol binding protein 4 (RBP4) and adiponectin after 4 weeks of diet exposure. $n = 6-8$ per group; means \pm SEM; Con: control mice; HF: mice fed with high fat and diet; HFCA: HF mice treated with CAPA; HFMET: HF mice treated with metformin; *, $P < 0.05$ versus Con; #, $P < 0.05$ versus HF.

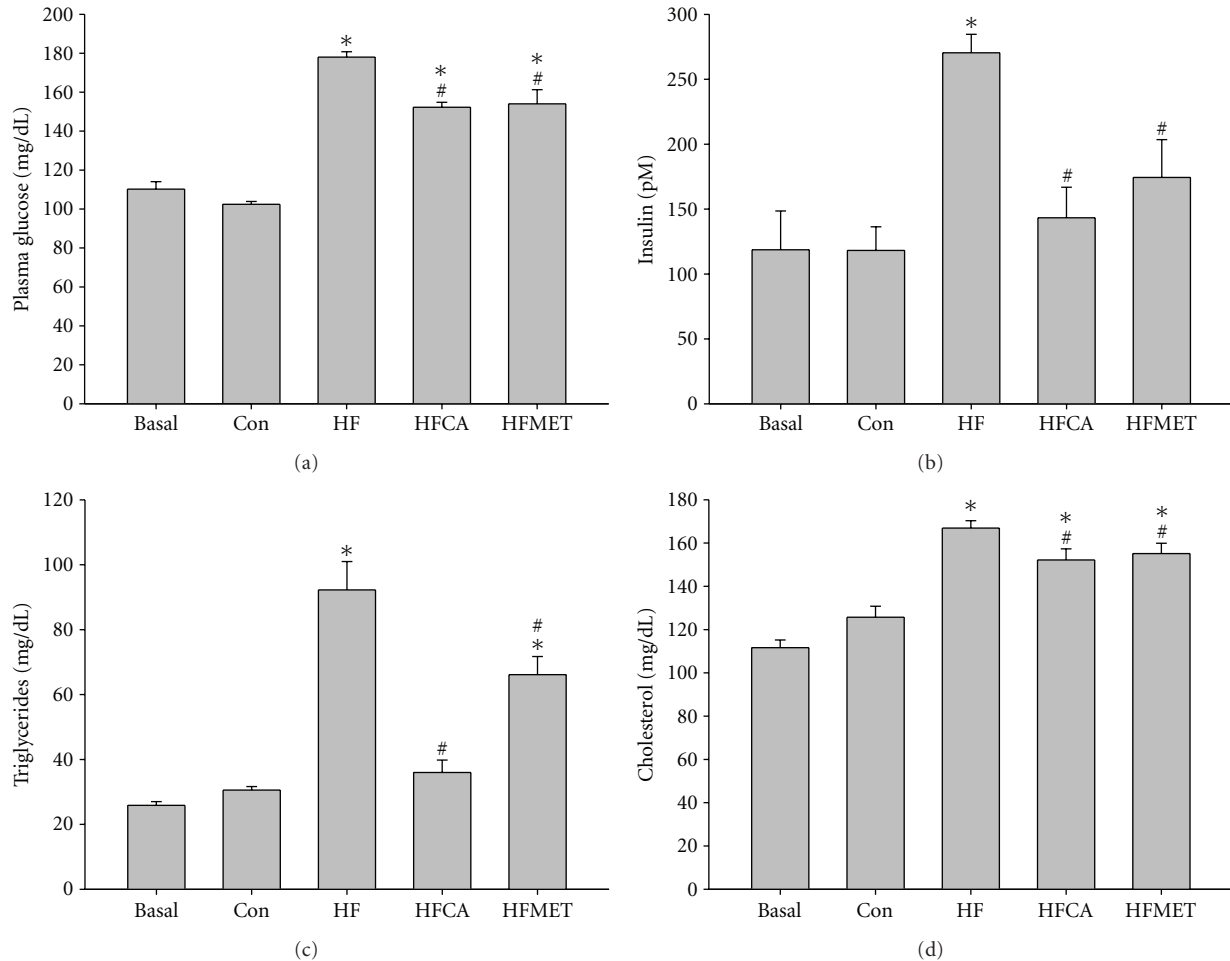


FIGURE 3: Diet-induced hyperglycemia and hyperlipidemia were reduced by CAPA treatment in BLT_W:CD1(ICR) mice. (a) Plasma glucose levels after 4 weeks of diet exposure. (b) Plasma insulin levels after 4 weeks of diet exposure. (c) Plasma triglycerides levels after 4 weeks of diet exposure. (d) Plasma total cholesterol levels after 4 weeks of diet exposure. $n = 6-8$ per group; means \pm SEM; Con: control mice; HF: mice fed with high fat and diet; HFCA: HF mice treated with CAPA; HFMET: HF mice treated with metformin; *: $P < 0.05$ versus Con; #: $P < 0.05$ versus HF.

TABLE 1: Food and water intake of mice after 4 weeks of diet exposure.

	Basal		After 4 weeks of diet exposure		
		Con	HF	HC	HM
Body weight (g)	25.6 \pm 0.4	35.5 \pm 0.8	40.2 \pm 1.0*	37.2 \pm 0.6 [#]	35.0 \pm 1.1 [#]
Night food intake (g)	4.5 \pm 0.5	6.0 \pm 0.5	4.3 \pm 0.8*	2.4 \pm 0.3 [#]	2.4 \pm 0.4 [#]
Night water intake (mL)	10.5 \pm 0.6	12.2 \pm 0.2	6.4 \pm 0.6*	5.9 \pm 0.3	6.4 \pm 0.5
Night calorie intake					
Food (kcal)	14.4 \pm 1.3	18.1 \pm 1.4	19.8 \pm 2.2	12.5 \pm 0.9 [#]	11.1 \pm 1.7 [#]
Water (kcal)	—	—	5.5 \pm 0.3	4.1 \pm 0.5	5.1 \pm 0.4
Total (kcal)	14.4 \pm 1.3	18.1 \pm 1.4	25.3 \pm 2.2*	16.6 \pm 0.8 [#]	15.9 \pm 4.4 [#]

Con: control mice; HF: mice fed with high fat and diet; HC: HF mice treated with CAPA; HM: HF mice treated with metformin; *: $P < 0.05$ versus Con; #: $P < 0.05$ versus HF; $n = 6-8$ per group.

levels of TNF α . Consistent with the inhibition of TNF α expression, both CAPA and metformin treatment resulted in lower p-p65 expression (Figure 5(b)). In contrast to the suppression of TNF α expression, the antioxidant proteins manganese superoxide dismutase (MnSOD) expression was

increased in CAPA or metformin treated mice on high-fat and high-fructose diet (Figure 5(c)).

RBP4 is known as a key regulator in obesity-related insulin resistance and type 2 DM. RBP4 secreted from adipocytes is increased when GLUT4 is downregulated.

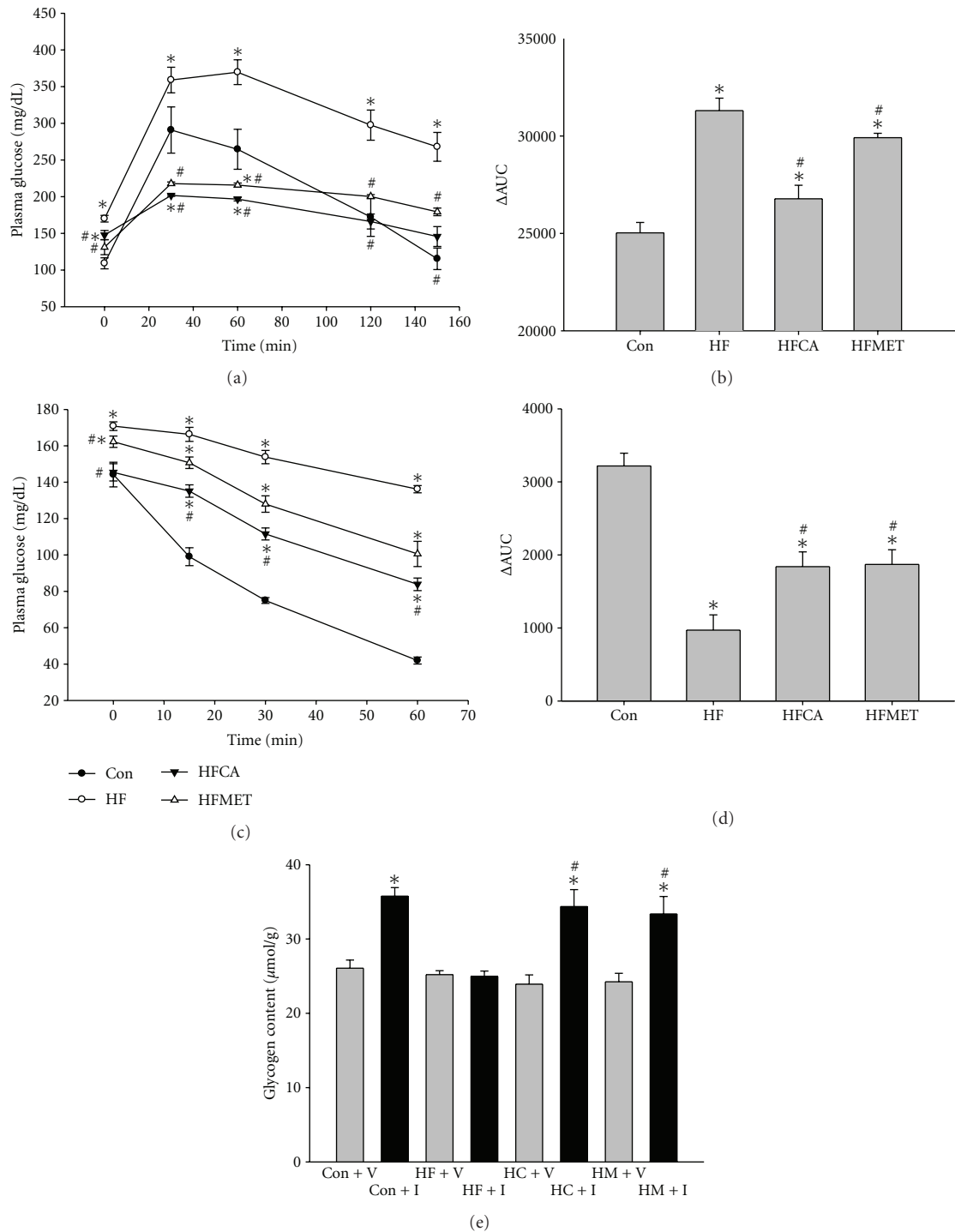


FIGURE 4: BLTW: CD1(ICR) mice are protected from diet-induced glucose intolerance. (a) Glucose tolerance test (GTT) after 4 weeks of diet exposure by using an i.p. dose of 2 g of glucose per kg of body weight. (b) Values of the area under the curve (AUC) during GTT since the different basal plasma glucose levels, areas between glucose curves after glucose or insulin injection, and baseline glucose level curve (Δ AUC) were calculated. (c) Insulin tolerance test (ITT) after 4 weeks of diet exposure by using 0.5 IU/kg insulin. (d) Δ AUC during ITT. $n = 6-8$ per group; means \pm SEM; *: $P < 0.05$ versus Con; #: $P < 0.05$ versus HF. (e) Glycogen content assay after 4 weeks of diet exposure by using 0.5 IU/kg insulin. $n = 6-8$ per group; means \pm SEM; *: $P < 0.05$ versus those treated with vehicle (V, grey bars); #: $P < 0.05$ versus HF treated with insulin (I, black bars); Con: control mice; HF: mice fed with high fat and diet; HFCA or HC: HF mice treated with CAPA; HFMET or HM: HF mice treated with metformin.

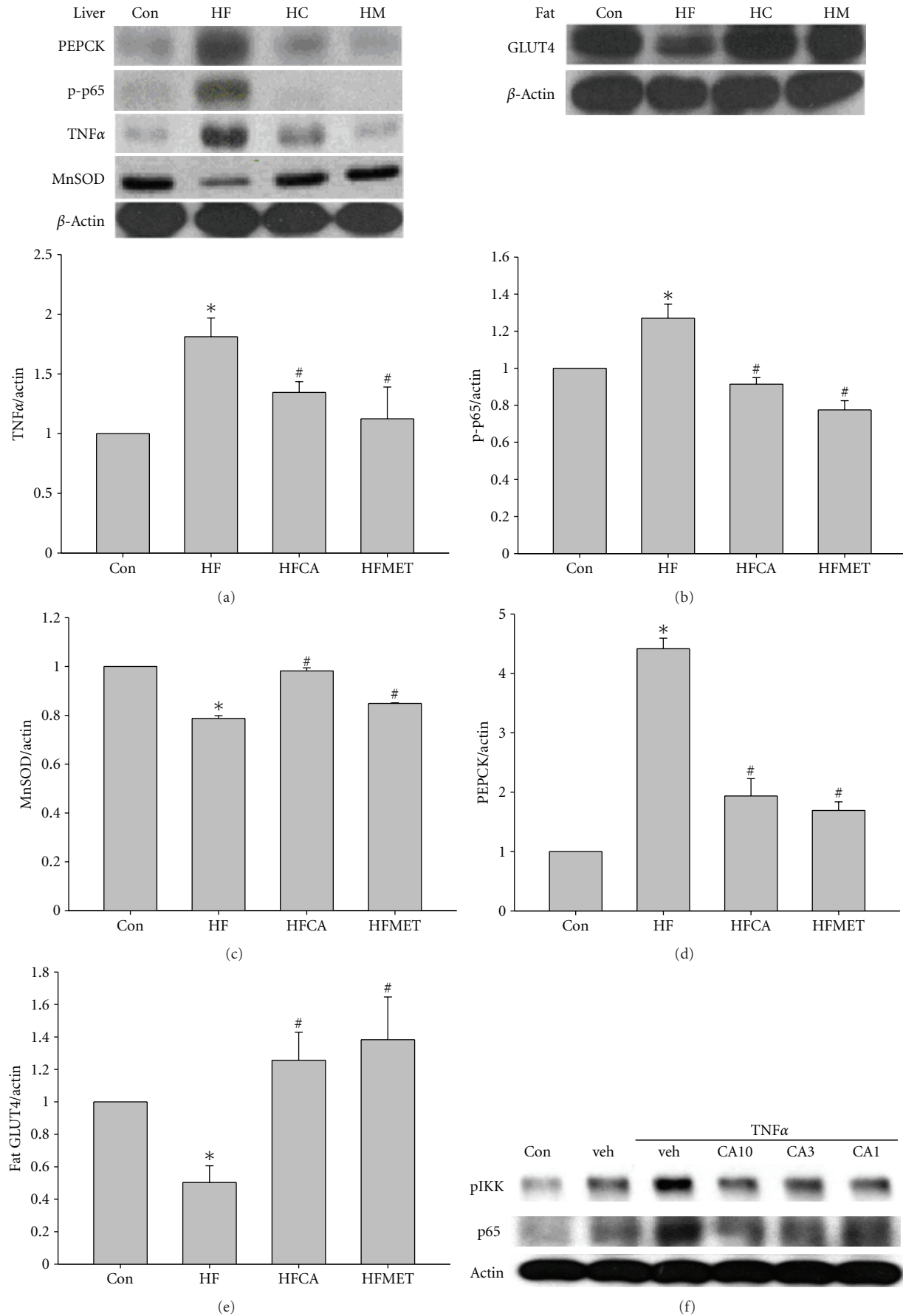


FIGURE 5: Continued.

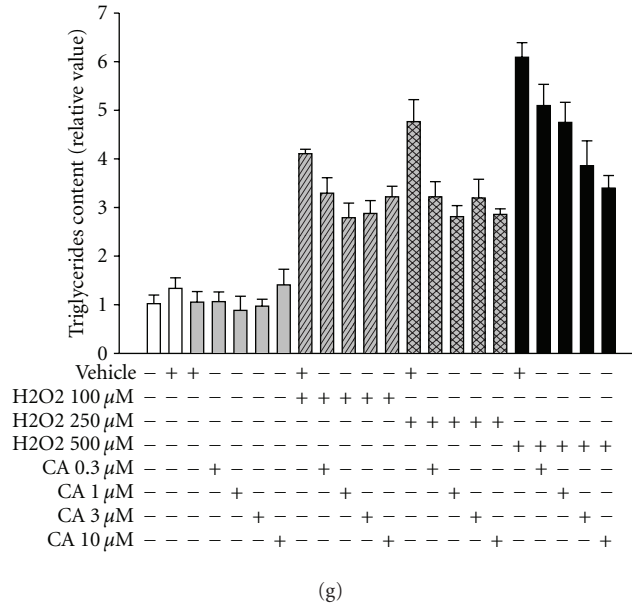


FIGURE 5: Protein expressions in the livers and fats of BLTW : CD1(ICR) mice after 4 weeks of diet exposure and triglycerides accumulation in HepG2 cells. (a) Protein expression of TNF α in livers of mice. (b) Protein expression of p-p65 in livers of mice. (c) Expression of the antioxidant protein MnSOD in livers of mice. (d) Expression of PEPCK in livers of mice. (e) Expression of GLUT4 in fats of mice. (f) Protein expression of pIKK α/β and p-p65 in HepG2 cells. (g) H₂O₂ induced triglycerides accumulation in HepG2 cells. *n* = 3 per group; means \pm SEM; Con: control mice; HF: mice fed with high fat and diet; HFCA or HC: HF mice treated with CAPA (CA); HFMET or HM: HF mice treated with metformin; *: *P* < 0.05 versus Con; #: *P* < 0.05 versus HF.

PEPCK is an important protein for gluconeogenesis and RBP4 increases gluconeogenesis in liver via upregulating PEPCK and inhibit insulin signaling [32]. After treatment of CAPA or metformin for four weeks, expression of PEPCK in the livers decreased and expression of GLUT4 in the fats increased (Figures 5(d) and 5(e)).

In summary, treatment with CAPA appears to protect mice from high-fat and high-fructose diet-induced hepatic inflammation and glucose intolerance associated with decreasing the NF κ B-mediated induction of inflammatory cytokines and increasing the expression of antioxidant protein. We used HepG2 as cell models for further investigation. Incubation with TNF α increased pIKK α/β expression and NF κ B activation in HepG2, and cotreatment with CAPA could ameliorate TNF α induced pIKK α/β expression (Figure 5(f)). In addition, we analyzed triglyceride content in HepG2 cells treated with H₂O₂. Cells were stimulated with H₂O₂ (100, 250, and 500 μ M) for 3 hours and then cultured for another 48 hours in fresh DMEM without H₂O₂ for triglyceride assay. The triglyceride levels rose with increasing H₂O₂ concentrations. Incubation with CAPA (1, 3, and 10 μ M) 1 h before H₂O₂ prevent triglycerides accumulation in HepG2 cells (Figure 5(g)).

4. Discussion and Conclusion

Our study addresses the potential of CAPA in arresting the development of glucose intolerance and cardiac ischemic injury in BLTW : CD1(ICR) mice. Our data show that CAPA improves lipid and glucose metabolism and basal coronary

flow and protects myocardium from damage inflicted by high-fat and high-fructose diet or STZ. The induction of the antioxidant protein MnSOD and the decrease of NF κ B activation in the liver were also observed after CAPA treatment. Since CAPA also decreased plasma glucose levels and protected cardiac ischemic injury in insulin deficient STZ mice, insulin-independent mechanisms might be involved.

White adipose tissue is now recognized as a secretory organ and secretes adipocytokines, such as RBP4 and adiponectin, which are involved in the regulation of glucose and lipids metabolism. Though it is reported that plasma adiponectin level is lower in obese, insulin resistant, or diabetic patients, in this study we found that high fat and fructose diet did not cause lower plasma adiponectin level. Liu et al. [33] observed that plasma adiponectin levels were higher when wild type mice were fed with high-fat diet less than 12 weeks. However, plasma adiponectin levels decreased after wild type mice were fed with high-fat diet longer than 12 weeks. Our finding is consistent with Liu’s report that mice fed with high-fat diet for two and four weeks had higher plasma adiponectin levels than control mice and might lead to the conclusion that a low plasma adiponectin level might be a result instead of a cause in insulin resistance. Liu et al. also showed that compared with wild type, adiponectin receptor 2 deficient mice always had higher plasma adiponectin levels and suffered less from diet-induced insulin resistance, yet deteriorated glucose homeostasis as high-fat feeding continued, which resulted from the failure of pancreatic beta-cells to adequately compensate for the moderate insulin resistance.

TABLE 2: Metabolism and ischemic injury of mice after 4 weeks of diet exposure.

	After 4 weeks of diet exposure			
	Con	HF	HF2WCA2W	HF2WMET2W
Body weight (g)	35.5 ± 0.8	40.2 ± 1.0*	39.7 ± 1.2*	38.3 ± 0.7*
Plasma insulin (pM)	117.5 ± 8.8	203.5 ± 21.1*	148.3 ± 29.2 [#]	131.1 ± 20.5 [#]
Plasma glucose during IPGTT (mg/dL)				
0 min after injection	109.2 ± 7.5	169.9 ± 4.5*	149 ± 6.9* [#]	151.4 ± 8.5* [#]
30 min after injection	290.8 ± 31.5	359.0 ± 17.5*	291.7 ± 2.4* [#]	271.8 ± 2.3* [#]
120 min after injection	172.2 ± 26.3	297.5 ± 20.5*	166.7 ± 10.2* [#]	179.3 ± 5.2* [#]
Basal coronary flow (mL/min)	3.4 ± 0.5	1.6 ± 0.3*	3.6 ± 0.4 [#]	2.5 ± 0.4 [#]
Infarct size of the heart after global ischemia/reperfusion (AAR%)	30.6 ± 5.1	39.4 ± 6.6*	29.9 ± 4.8 [#]	30.0 ± 3.8 [#]

CAPA was introduced after 2 weeks of diet exposure and orally treated once a day for another 2 weeks. Con: control mice; HF: mice fed with high fat and diet; HF2WCA2W: HF mice treated with CAPA for another 2 weeks; HF2WMET2W: HF mice treated with metformin for another 2 weeks; AAR: area at risk; *: $P < 0.05$ versus Con; [#]: $P < 0.05$ versus HF; $n = 6-8$ per group.

TABLE 3: Metabolism and ischemic injury of mice after 4 weeks of STZ injection.

	After 4 weeks of STZ injection		
	Con	STZ	S2WCA2W
Body weight (g)	35.5 ± 0.8	21.2 ± 2.9*	24.0 ± 0.6* [#]
Plasma glucose (mg/dL)	113.5 ± 4.5	588.0 ± 34.5*	483.2 ± 24.0* [#]
Plasma insulin (pM)	117.5 ± 8.8	8.3 ± 1.5*	5.8 ± 1.0*
Basal coronary flow (mL/min)	3.4 ± 0.5	1.5 ± 0.2*	1.83 ± 0.3* [#]
Infarct size of the heart after global ischemia/reperfusion (% AAR)	30.6 ± 5.1	51.3 ± 2.5*	37.1 ± 5.8* [#]

CAPA was introduced after 2 weeks of STZ injection and orally treated once a day for another 2 weeks. Con: control mice; STZ: streptozocin-induced type 1 diabetic mice; S2WCA2W: STZ mice treated with CAPA for another 2 weeks; AAR: area at risk; *: $P < 0.05$ versus Con; [#]: $P < 0.05$ versus STZ; $n = 6-8$ per group.

However, we could not tell whether adiponectin receptors are involved in diet-induced insulin resistance in our study yet. Another limitation is that we did not analyze high molecular weight adiponectin (HMW adiponectin). A decrease level of HMW adiponectin is a predictor of progression to metabolic syndrome. Lifestyle modification for three months or administrating thiazolidinediones induced an increase in serum HMW adiponectin in patients with metabolic syndrome [34]. We did not know how plasma levels of HMW adiponectin changed after high-fat diet exposure or CAPA treatment in this study.

Yang et al. [35] showed that RBP4 secretion from adipocytes is increased when GLUT4 is downregulated. In this study, increased RBP4 secretion and decreased GLUT4 expression in fat were observed after 4 weeks exposure to the high-fat and high-fructose diet, confirming that insulin resistance occurred in adipose tissue of mice fed with high-fat and high-fructose diet. Obvious increased PEPCK expression in liver, an important index of insulin resistance, was observed in HF mice. Chronic treatment of CAPA and metformin significantly decreased body weight gain, fat mass and plasma levels of adipocytokines induced by high-fat and high-fructose. These data indicated that insulin resistance had occurred in liver of mice after four weeks of high fat and high fructose diet feeding and oral CAPA (10 mg/kg) exerted similar protection in mice against these metabolic dysfunctions as metformin (300 mg/kg) did.

However, it is noteworthy that CAPA preserved MnSOD in the liver at a higher level than metformin did ($P < 0.05$). Since oxidative stress is reported to induce triglycerides accumulation in hepatocytes and might play important role in hepatic insulin resistance [28], we stimulated HEPG2 with H_2O_2 and found that CAPA decreased the triglycerides accumulation in HEPG2 after H_2O_2 stimulation. This observation is correlated with the prominent reduction of plasma triglycerides by CAPA in diet-induced diabetic mice. However, whether induction of MnSOD was required in this effect of CAPA needs further studies.

Hepatic inflammation is an established risk factor for the development of insulin resistance and glucose intolerance [36]. Insulin resistance and glucose intolerance, in turn, can stimulate the development and progression of hepatic inflammation and hepatosteatosis [37], thereby fueling and promoting a detrimental cycle that is believed to represent a key role in metabolic syndrome. In this study, daily oral CAPA results in protection of mice from diet-induced glucose intolerance. Hepatic NF κ B signaling is activated by high-fat and high-fructose diet exposure and triggers insulin resistance [38], thereby linking inflammation with obesity-induced insulin resistance [39]. Conjunction with the activation of antioxidant protein MnSOD, inhibition of NF κ B by CAPA may explain the prevention from hepatic inflammation and diet-induced glucose intolerance.

Most importantly, clinical diabetes mellitus is usually diagnosed when hyperglycemia occurs; thus, it is important

to find out antidiabetic compounds that can treat, not prevent, metabolic dysfunctions after hyperglycemia has occurred. CAPA can arrest the development of diabetes mellitus and the metabolic consequences in type 1 and type 2 diabetic mice model even when hyperglycemia has developed. After blood glucose levels were raised, daily oral CAPA for two weeks prevented body weight gain and hyperglycemia and preserved basal coronary flow in Langendorff perfused hearts. When subjected to global ischemia and reperfusion, larger infarct sizes were observed in the hearts from type 1 and type 2 diabetic mice. Chronic oral CAPA prevented severe ischemic injury in diabetic hearts.

In summary, chronic oral CAPA protects against diet-induced metabolic damage, such as obesity, hyperglycemia, insulin resistance and liver inflammation. CAPA also increased coronary flow and decreased infarct size after global ischemia-reperfusion in Langendorff perfused heart. In addition, CAPA protects mice from metabolic consequences by STZ-induced type 1 diabetes, indicating that some effects of CAPA were insulin independent. Prevention of activation of the proinflammatory NF κ B pathway and increase in expression of antioxidant proteins such as MnSOD in the liver were also involved in the action of CAPA. Together, these results highlighted the protective potential of chronic treatment of CAPA against the metabolic consequences in diabetes mellitus.

However, there are still lots of work to do. Whether decreased calorie intake contributed to these beneficial metabolic effects after CAPA treatment and whether CAPA protected cardiovascular system directly were still left unclarified. Changes were still taking place and steady state was not reached after four weeks of feeding. Thus, short study period might be a limitation in our present study. A long study period, such as 12 weeks or longer, should be taken to estimate the long-term effects of CAPA in ICR mice. Moderate Sirt1 (mammalian silent information regulator 2) overexpression under control of its natural promoter in mice prevents high-fat diet-induced glucose intolerance, and this effect may result, in part, from prevention of high-fat diet-induced activation of the proinflammatory NF κ B pathway together with upregulation of PGC1 α and its antioxidant targets such as MnSOD or Nrf1 [40]. Since CAPA is structurally similar to the Sirt1 activator, resveratrol, further study was needed to clarify whether Sirt1 activation was involved in the beneficial effects of CAPA. In addition, CAPA had AMPK (AMP-activated protein kinase) activating activities in C2C12 skeletal muscle cells and in HEP3B hepatocytes (our unpublished data), but further investigations should be done to know whether and how AMPK activation was involved in the protective effects of CAPA. Finally, the anti-inflammatory effects of CAPA open up aspects that could link caffeic acid phenylethyl amide with other diseases such as aging and cancer. Although the detailed mechanisms need to be clarified, the protective potential of chronic treatment of CAPA against diabetes mellitus and other diseases is undeniable.

Conflict of Interests

The authors declare that they have no conflict of interests.

Acknowledgments

The authors thank Professor DK Granner (Department of Molecular Physiology and Biophysics, Vanderbilt University School of Medicine, Nashville, TN, USA) for the supply of antibodies specific to PEPCK. This study was supported by the National Science Council Grants no. NSC 98-2323-B-002-014-CC2, NSC 99-2323-B-002-005, and NSC 100-2325-B-002-066.

References

- [1] D. P. Macfarlane, K. R. Paterson, and M. Fisher, "Oral antidiabetic agents as cardiovascular drugs," *Diabetes, Obesity and Metabolism*, vol. 9, no. 1, pp. 23–30, 2007.
- [2] L. A. Olatunji and A. O. Soladoye, "Increased magnesium intake prevents hyperlipidemia and insulin resistance and reduces lipid peroxidation in fructose-fed rats," *Pathophysiology*, vol. 14, no. 1, pp. 11–15, 2007.
- [3] M. Golubovic-Arsovska, "Correlation of diabetic maculopathy and level of diabetic retinopathy," *Prilozi*, vol. 27, no. 2, pp. 139–150, 2006.
- [4] E. Ritz, "Diabetic nephropathy," *Saudi Journal of Kidney Diseases and Transplantation*, vol. 17, no. 4, pp. 481–490, 2006.
- [5] A. A. F. Sima and H. Kamiya, "Diabetic neuropathy differs in type 1 and type 2 diabetes," *Annals of the New York Academy of Sciences*, vol. 1084, pp. 235–249, 2006.
- [6] K. Hayashi, R. Kojima, and M. Ito, "Strain differences in the diabetogenic activity of streptozotocin in mice," *Biological and Pharmaceutical Bulletin*, vol. 29, no. 6, pp. 1110–1119, 2006.
- [7] T. M. Chan, K. M. Young, and N. J. Hutson, "Hepatic metabolism of genetically diabetic (db/db) mice. I. Carbohydrate metabolism," *American Journal of Physiology*, vol. 229, no. 6, pp. 1702–1712, 1975.
- [8] Y. Ohta, T. Kitazaki, and M. Tsuda, "Thermogenesis in brown adipose tissue of genetically obese, diabetic (KKA(Y)) mice," *Endocrinologia Japonica*, vol. 35, no. 1, pp. 83–92, 1988.
- [9] P. Masiello, C. Broca, R. Gross et al., "Experimental NIDDM: development of a new model in adult rats administered streptozotocin and nicotinamide," *Diabetes*, vol. 47, no. 2, pp. 224–229, 1998.
- [10] C. Messier, K. Whately, J. Liang, L. Du, and D. Puissant, "The effects of a high-fat, high-fructose, and combination diet on learning, weight, and glucose regulation in C57BL/6 mice," *Behavioural Brain Research*, vol. 178, no. 1, pp. 139–145, 2007.
- [11] S. Ikemoto, M. Takahashi, N. Tsunoda, K. Maruyama, H. Itakura, and O. Ezaki, "High-fat diet-induced hyperglycemia and obesity in mice: differential effects of dietary oils," *Metabolism*, vol. 45, no. 12, pp. 1539–1546, 1996.
- [12] S. A. Schreyer, D. L. Wilson, and R. C. Leboeuf, "C57BL/6 mice fed high fat diets as models for diabetes-accelerated atherosclerosis," *Atherosclerosis*, vol. 136, no. 1, pp. 17–24, 1998.
- [13] H. Jürgens, W. Haass, T. R. Castañeda et al., "Consuming fructose-sweetened beverages increases body adiposity in mice," *Obesity Research*, vol. 13, no. 7, pp. 1145–1156, 2005.
- [14] Z. Asghar, D. Yau, F. Chan, D. LeRoith, C. B. Chan, and M. B. Wheeler, "Insulin resistance causes increased beta-cell mass but defective glucose-stimulated insulin secretion in a murine model of type 2 diabetes," *Diabetologia*, vol. 49, no. 1, pp. 90–99, 2006.
- [15] S. Y. Park, Y. R. Cho, H. J. Kim et al., "Unraveling the temporal pattern of diet-induced insulin resistance in individual organs

- and cardiac dysfunction in C57BL/6 mice," *Diabetes*, vol. 54, no. 12, pp. 3530–3540, 2005.
- [16] Y. C. Weng, H. L. Chiu, Y. C. Lin, T. C. Chi, Y. H. Kuo, and M. J. Su, "Antihyperglycemic effect of a caffeamide derivative, KS370G, in normal and diabetic mice," *Journal of Agricultural and Food Chemistry*, vol. 58, no. 18, pp. 10033–10038, 2010.
- [17] W. Guo, E. Kong, and M. Meydani, "Dietary polyphenols, inflammation, and cancer," *Nutrition and cancer*, vol. 61, no. 6, pp. 807–810, 2009.
- [18] W. Wongcharoen and A. Phrommintikul, "The protective role of curcumin in cardiovascular diseases," *International Journal of Cardiology*, vol. 133, no. 2, pp. 145–151, 2009.
- [19] J. T. Hwang, D. Y. Kwon, and S. H. Yoon, "AMP-activated protein kinase: a potential target for the diseases prevention by natural occurring polyphenols," *New Biotechnology*, vol. 26, no. 1-2, pp. 17–22, 2009.
- [20] P. Wojciechowski, D. Juric, X. L. Louis et al., "Resveratrol arrests and regresses the development of pressure overload-but not volume overload-induced cardiac hypertrophy in rats," *Journal of Nutrition*, vol. 140, no. 5, pp. 962–968, 2010.
- [21] T. Morimoto, Y. Sunagawa, T. Kawamura et al., "The dietary compound curcumin inhibits p300 histone acetyltransferase activity and prevents heart failure in rats," *Journal of Clinical Investigation*, vol. 118, no. 3, pp. 868–878, 2008.
- [22] B. W. Huang, M. T. Chiang, H. T. Yao, and W. Chiang, "The effect of high-fat and high-fructose diets on glucose tolerance and plasma lipid and leptin levels in rats," *Diabetes, Obesity and Metabolism*, vol. 6, no. 2, pp. 120–126, 2004.
- [23] S. H. Park, S. K. Ko, and S. H. Chung, "Euonymus alatus prevents the hyperglycemia and hyperlipidemia induced by high-fat diet in ICR mice," *Journal of Ethnopharmacology*, vol. 102, no. 3, pp. 326–335, 2005.
- [24] T. C. Chi, S. S. Lee, and M. J. Su, "Antihyperglycemic effect of aporphines and their derivatives in normal and diabetic rats," *Planta Medica*, vol. 72, no. 13, pp. 1175–1180, 2006.
- [25] L. Jansson, P.-O. Carlsson, B. Bodin, A. Andersson, and O. Källskog, "Neuronal nitric oxide synthase and splanchnic blood flow in anaesthetized rats," *Acta Physiologica Scandinavica*, vol. 183, no. 3, pp. 257–262, 2005.
- [26] E. Bonora, V. Manicardi, I. Zavaroni, C. Coscelli, and U. Butturini, "Relationships between insulin secretion, insulin metabolism and insulin resistance in mild glucose intolerance," *Diabetes & Metabolism*, vol. 13, no. 2, pp. 116–121, 1987.
- [27] C. H. Chou, Y. L. Tsai, C. W. Hou et al., "Glycogen overload by postexercise insulin administration abolished the exercise-induced increase in GLUT4 protein," *Journal of Biomedical Science*, vol. 12, no. 6, pp. 991–998, 2005.
- [28] M. Sekiya, A. Hiraishi, M. Touyama, and K. Sakamoto, "Oxidative stress induced lipid accumulation via SREBP1c activation in HepG2 cells," *Biochemical and Biophysical Research Communications*, vol. 375, no. 4, pp. 602–607, 2008.
- [29] N. L. Huang, S. H. Chiang, C. H. Hsueh, Y. J. Liang, Y. J. Chen, and L. P. Lai, "Metformin inhibits TNF- α -induced I κ B kinase phosphorylation, I κ B- α degradation and IL-6 production in endothelial cells through PI3K-dependent AMPK phosphorylation," *International Journal of Cardiology*, vol. 134, no. 2, pp. 169–175, 2009.
- [30] F. J. Sutherland, M. J. Shattock, K. E. Baker, and D. J. Hearse, "Mouse isolated perfused heart: characteristics and cautions," *Clinical and Experimental Pharmacology and Physiology*, vol. 30, no. 11, pp. 867–878, 2003.
- [31] G. S. Hotamisligil, "Inflammation and metabolic disorders," *Nature*, vol. 444, no. 7121, pp. 860–867, 2006.
- [32] Y. Tamori, H. Sakaue, and M. Kasuga, "RBP4, an unexpected adipokine," *Nature Medicine*, vol. 12, no. 1, pp. 30–31, 2006.
- [33] Y. Liu, M. D. Michael, S. Kash et al., "Deficiency of adiponectin receptor 2 reduces diet-induced insulin resistance but promotes type 2 diabetes," *Endocrinology*, vol. 148, no. 2, pp. 683–692, 2007.
- [34] H. Hirose, Y. Yamamoto, Y. Seino-Yoshihara, H. Kawabe, and I. Saito, "Serum high-molecular-weight adiponectin as a marker for the evaluation and care of subjects with metabolic syndrome and related disorders," *Journal of Atherosclerosis and Thrombosis*, vol. 17, no. 12, pp. 1201–1211, 2010.
- [35] Q. Yang, T. E. Graham, N. Mody et al., "Serum retinol binding protein 4 contributes to insulin resistance in obesity and type 2 diabetes," *Nature*, vol. 436, no. 7049, pp. 356–362, 2005.
- [36] S. E. Shoelson, L. Herrero, and A. Naaz, "Obesity, Inflammation, and Insulin Resistance," *Gastroenterology*, vol. 132, no. 6, pp. 2169–2180, 2007.
- [37] T. Ota, T. Takamura, S. Kurita et al., "Insulin resistance accelerates a dietary rat model of nonalcoholic steatohepatitis," *Gastroenterology*, vol. 132, no. 1, pp. 282–293, 2007.
- [38] D. Cai, M. Yuan, D. F. Frantz et al., "Local and systemic insulin resistance resulting from hepatic activation of IKK- β and NF- κ B," *Nature Medicine*, vol. 11, no. 2, pp. 183–190, 2005.
- [39] M. C. Arkan, A. L. Hevener, F. R. Greten et al., "IKK- β links inflammation to obesity-induced insulin resistance," *Nature Medicine*, vol. 11, no. 2, pp. 191–198, 2005.
- [40] P. T. Pfluger, D. Herranz, S. Velasco-Miguel, M. Serrano, and M. H. Tschöp, "Sirt1 protects against high-fat diet-induced metabolic damage," *Proceedings of the National Academy of Sciences of the United States of America*, vol. 105, no. 28, pp. 9793–9798, 2008.

Research Article

6-Gingerol Inhibits Growth of Colon Cancer Cell LoVo via Induction of G2/M Arrest

Ching-Bin Lin,^{1,2} Chun-Che Lin,^{1,3} and Gregory J. Tsay^{2,4}

¹Division of Hepatology and Gastroenterology, Department of Internal Medicine, Chung Shan Medical University Hospital, Taichung 402, Taiwan

²Institute of Microbiology and Immunology, Chung Shan Medical University, Taichung 402, Taiwan

³Institute of Medicine, Chung Shan Medical University, Taichung 402, Taiwan

⁴Department of Medicine, Chung Shan Medical University (CSMU), Taichung 402, Taiwan

Correspondence should be addressed to Gregory J. Tsay, lin.yuying@gmail.com

Received 22 November 2011; Revised 10 March 2012; Accepted 25 March 2012

Academic Editor: William C. S. Cho

Copyright © 2012 Ching-Bin Lin et al. This is an open access article distributed under the Creative Commons Attribution License, which permits unrestricted use, distribution, and reproduction in any medium, provided the original work is properly cited.

6-Gingerol, a natural component of ginger, has been widely reported to possess antiinflammatory and antitumorogenic activities. Despite its potential efficacy against cancer, the anti-tumor mechanisms of 6-gingerol are complicated and remain sketchy. In the present study, we aimed to investigate the anti-tumor effects of 6-gingerol on colon cancer cells. Our results revealed that 6-gingerol treatment significantly reduced the cell viability of human colon cancer cell, LoVo, in a dose-dependent manner. Further flow cytometric analysis showed that 6-gingerol induced significant G2/M phase arrest and had slight influence on sub-G1 phase in LoVo cells. Therefore, levels of cyclins, cyclin-dependent kinases (CDKs), and their regulatory proteins involved in S-G2/M transition were investigated. Our findings revealed that levels of cyclin A, cyclin B1, and CDK1 were diminished; in contrast, levels of the negative cell cycle regulators p27^{Kip1} and p21^{Cip1} were increased in response to 6-gingerol treatment. In addition, 6-gingerol treatment elevated intracellular reactive oxygen species (ROS) and phosphorylation level of p53. These findings indicate that exposure of 6-gingerol may induce intracellular ROS and upregulate p53, p27^{Kip1}, and p21^{Cip1} levels leading to consequent decrease of CDK1, cyclin A, and cyclin B1 as result of cell cycle arrest in LoVo cells. It would be suggested that 6-gingerol should be beneficial to treatment of colon cancer.

1. Introduction

Colorectal cancer (CRC) is one of the most prevalent cancers with high mortality in the western world and Taiwan [1]. CRC is inclined to evolve into invasive cancer from adenomatous polyps through mutations in various genes [2]. Although early diagnosis improves patients' clinical outcomes, 5-year survival rate of patients diagnosed with CRC is poor. Current therapeutic regimens for CRC constitute predominantly of surgical procedures and chemotherapy [3, 4]. Despite improvements in the prognosis of CRC patients receiving appropriate clinical modularity, resistance to advanced therapy does occur in many patients suffering from incomplete eradication of malignant cells and metastasis.

Of various phytochemicals showing various biochemical and pharmacologic activities, 6-gingerol, a major pharmacologically active component of ginger, has been reported

to exhibit antioxidant and anti-inflammatory properties and exert substantial anticarcinogenic and antimutagenic activities [5]. Mounting evidence suggests that 6-gingerol is effective in suppressing the transformation, hyperproliferation, and inflammatory processes that initiate and promote carcinogenesis, as well as the later steps of carcinogenesis, namely, angiogenesis and metastasis [6–10]. Despite awareness to its activity against several human cancers, the exact molecular mechanism underlying anti-tumoral effects of 6-gingerol remains sketchy.

Accumulating evidence suggests that induction of reactive oxygen species (ROS) by phytochemicals are critically involved in their anti-tumoral activity [11, 12]. Increase of intracellular ROS usually leads to DNA damage, and the subsequent phosphorylation of p53 contributes to cell cycle arrest and further apoptosis of cancer cell. The role of cell

cycle mediators in cancer development is now well documented. Critical genes responsible for cell cycle regulation as checkpoints have been demonstrated to be lost and/or aberrant in a variety of cancers in human [13]. Cell cycle is under sophisticated regulation through the interactions of different cyclins with their specific kinases, cyclin-dependent kinases (CDKs) [14]. Two classes of CDK inhibitors, inhibitors of CDK4 (INK4) and kinase inhibitor proteins (KIPs), have been reported to negatively modulate the activity of CDKs. The latter include p21^{Cip1} [15], p27^{Kip1} [16], and p57^{Kip2} [17, 18]. It has been reported that overexpression of p21^{Cip1} leads to inhibited proliferation of mammalian cells and inactivation of all cyclin-CDK complexes, indicating that it is a universal cyclin-CDK inhibitor [19]. p27^{Kip1}, a negative regulator of protein kinases, interacts with cyclin E-CDK2 and cyclin A-CDK2 which drive cells into the S phase of the cell division cycle [20]. Moreover, p27^{Kip1} has been reported to play important roles in G2/M checkpoint as tumor suppressor [21].

In the present study, we focused on the mechanism underlying anticancer effects of 6-gingerol on colon cancer with emphasis on cell viability alteration and cell cycle disruption. To investigate the alteration of cell viability and cell cycle distribution induced by 6-gingerol, MTT assay and flow cytometric analysis were performed. Expression level of important cell cycle regulators was determined by immunoblotting. Intracellular ROS was determined by using spectrofluorometrical analysis.

2. Materials and Methods

2.1. Materials. 6-gingerol, 2-propanol, 3-(4,5-Dimethylthiazol-2-yl)-2,5-diphenyltetrazolium bromide (MTT), 1-butanol, dimethyl sulfoxide (DMSO), 2',7'-dichlorofluorescein diacetate (DCF-DA), deoxycholic acid, dithiothreitol, EDTA, glycerol, Igepal CA-630, phenylmethylsulfonyl fluoride (PMSF), sodium chloride (NaCl), potassium chloride (KCl), sodium dodecyl sulfate (SDS), sodium phosphate, Tris-HCl, and trypsin/EDTA were purchased from Sigma (St. Louis, MO, USA). Antibodies against cyclin A, cyclin B1, cyclin D1, cyclin E, CDK1, p53, p21^{Cip1}, p27^{Kip1}, and β -actin were purchased from Santa Cruz Biotechnology (Santa Cruz, CA, USA). Peroxidase-conjugated antibodies against mouse IgG or rabbit IgG were purchased from Cell Signaling Technology (Beverly, MA, USA).

2.2. Cell Culture. Colon cancer cell line LoVo was obtained from the American Type Culture Collection (ATCC; Rockville, MD, USA) and maintained in Dulbecco's modified Eagle's medium (DMEM) supplemented with 10% v/v fetal bovine serum, 1% nonessential amino acid, 1% L-glutamine (Gibco BRL, Gaithersburg, MD, USA), and 100 μ g/mL penicillin/streptomycin (Sigma) at 37°C in a humidified atmosphere with 5% CO₂. Cells were seeded in 10 cm Petri dishes at an initial density of 2×10^5 cells/mL and grown to approximately 80% confluence. Then, the cells were collected for the subsequent analyses including cell viability, flow cytometric analysis, and immunoblotting analysis.

For 6-gingerol treatments, cells were starved for 24 hours (h) in serum-free DMEM and then incubated with 6-gingerol at a series of concentrations in serum-free DMEM (1, 5, 10, and 15 μ g/mL) for 24 h or 48 h.

2.3. Cell Viability Assay. Cell viability was determined by MTT assay as previously described [20]. Briefly, cells were seeded at a density of 4×10^4 cells/well in a 24-well plate and cultured with serum-free DMEM for 16 h. Then, the cells were treated with serial concentrations of 6-gingerol (0, 5, 10, and 15 μ g/mL) for 24 h or 48 h. Treatment at each concentration was performed in triplicate. After treatments, the medium was aspirated and cells were washed with PBS. Cells were subsequently incubated with MTT solution (5 mg/mL) for 4 h. The supernatant was removed, and formazan was solubilized in isopropanol and measured spectrophotometrically at 563 nm. The percentage of viable cells was estimated in comparison with untreated cells.

2.4. Determination of Cell Cycle Distribution. Cell cycle distribution was analyzed by flow cytometry. After 6-gingerol treatment, cells were collected, fixed with 1 mL of ice-cold 70% ethanol, incubated at -20°C for at least 24 h, and centrifuged at $380 \times g$ for 5 min at room temperature. Cell pellets were treated with 1 mL of cold staining solution containing 20 μ g/mL propidium iodide (PI), 20 μ g/mL RNase A, and 1% Triton X-100 and incubated for 15 min in dark at room temperature. Subsequently, the samples were analyzed in a FACS Calibur system (version 2.0, BD Biosciences, Franklin Lakes, NJ, USA) using Cell Quest software. Results were representative of at least three independent experiments.

2.5. Protein Extraction. After 6-gingerol treatments, cells were trypsinized and homogenized in ice-cold lysis buffer (50 mM Tris-HCl, pH 7.5, 150 mM NaCl, 0.1% (v/v) Igepal CA-630, 0.5% (w/v) sodium deoxycholate, 0.1% (w/v) SDS, 1 mM dithiothreitol, 0.1 mM EDTA, and 1 mM PMSF). After sonication at 4°C for 30 min, the homogenate was centrifuged at $14,000 \times g$ for 10 min, and then the supernatant was transferred into a new 1.5 mL eppendorf and stored at -70°C for subsequent analysis. Protein concentration was quantitated by the Bradford method (protein assay reagent; Bio-Rad Laboratory, Hercules, CA, USA) according to the manufacturer's instruction.

2.6. Immunoblotting. Crude proteins (30 μ g of protein) were subjected to a 12.5% SDS-polyacrylamide gel and transferred onto a nitrocellulose membrane as previously described [21]. The blot was subsequently incubated with 5% nonfat milk in PBS for 1 h, probed with a primary antibody against cyclin A, cyclin B1, CDK1, p21^{Cip1}, p27^{Kip1}, p53, or β -actin for 2 h and then reacted with an appropriate peroxidase-conjugated secondary antibody for 1 h. All incubations were carried out at 30°C, and intensive PBS washing was performed between incubations. After the final PBS wash, the signal was developed by ECL chemiluminescence, and the relative photographic density was quantitated by image analysis system (Fuji Film, Tokyo, Japan).

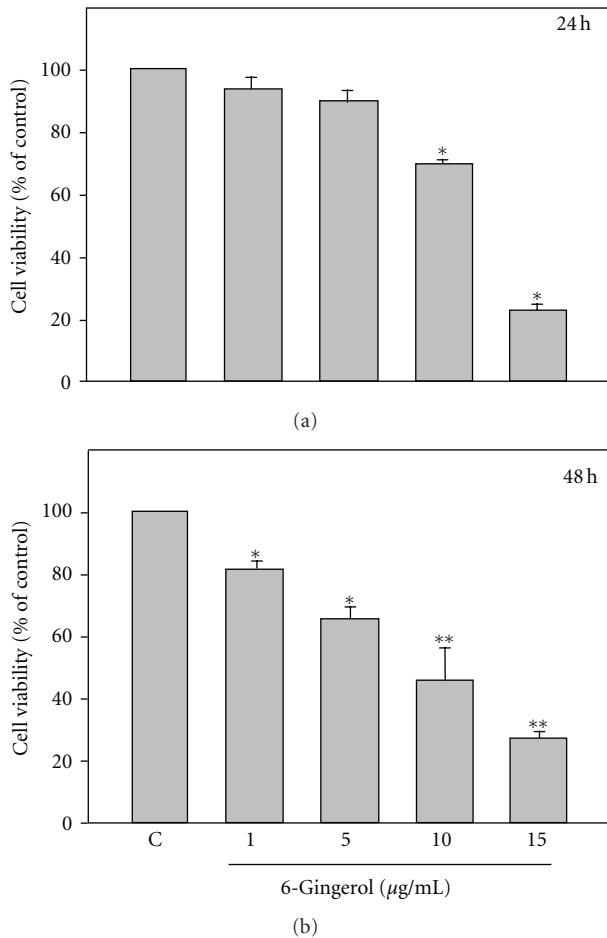


FIGURE 1: 6-Gingerol inhibited the cell viability of LoVo cells. Cells were treated with indicated concentration of 6-gingerol for 24 h or 48 h, and the cell viability was analyzed by MTT assay. Data were shown as the means \pm SD. Three independent experiments were performed for statistical analysis. * $P < 0.05$ and ** $P < 0.005$ as compared to control (C).

2.7. Determination of Intracellular Reactive Oxygen Species (ROS). Production of ROS was determined by spectrofluorometrical method using 2',7'-dihydrodichlorofluorescein diacetate (DCFH-DA) assay with modification [22]. DCFH-DA diffuses through the cell membrane and is enzymatically hydrolyzed by intracellular esterases to the nonfluorescent DCFH, which can be rapidly oxidized to the highly fluorescent DCF, the fluorescent product, in the presence of ROS. After exposure to LPS and PFE, DCFH-DA was added to the culture plates at a final concentration of $5 \mu\text{M}$ and incubated for 40 min at 37°C in darkness. DCF fluorescence intensity was detected with emission wavelength at 530 nm and excitation wavelength at 485 nm using a SpectraMax Plus microplate reader (Molecular Devices Corporation, Sunnyvale, CA, USA). The values were expressed as the mean absorbance normalized to the ratio of control value.

2.8. Statistical Analysis. Data were expressed as mean \pm standard deviation (SD) of the three independent experiments.

Statistical significance analysis was determined by using 1-way ANOVA followed by Dunnett for multiple comparisons with the control. The differences were considered significant for P values less than 0.05.

3. Results

3.1. 6-Gingerol Inhibited the Cell Viability of LoVo Cells. To examine the inhibitory effects of 6-gingerol on colon cancer cells, LoVo cells were treated with a serial concentration of 6-gingerol (1, 5, 10, and $15 \mu\text{g/mL}$) for 24 or 48 h, respectively, and then cell viability of LoVo cells was determined. As shown in Figure 1, the cell viability in presence of 6-gingerol was found decreased in association with the concentration of 6-gingerol in a dose-dependent fashion. 6-Gingerol treatments at concentrations of 10 and $15 \mu\text{g/mL}$ significantly decreased cell viability to $68.7 \pm 4.3\%$ and $24.6 \pm 2.1\%$ of control for 24 h and to $40.4 \pm 1.4\%$ and $24.5 \pm 1.4\%$ of control for 48 h, respectively ($P < 0.05$ as compared to control).

3.2. 6-Gingerol Induced G2/M Phase Arrest but Not Apoptosis in LoVo Cells. As a significant suppression of cell viability of LoVo occurred after 6-gingerol treatments resulted, cell cycle distribution of 6-gingerol-treated LoVo cell was consequently analyzed and quantitated using flow cytometry. As shown in Figure 2, percentages of cells in sub-G1 phase, ranging from $1.36 \pm 0.23\%$ to $2.58 \pm 0.36\%$, were not significantly influenced by the treatments of 6-gingerol for 24 h. However, an increase in population of cells in G2/M phase after the treatment was observed in a dose-dependent manner, ranging from $45.7 \pm 3.6\%$ to $58.8 \pm 5.4\%$, (5, 10 and $15 \mu\text{g/mL}$, $P < 0.05$). Additionally, a number of G0/G1 phase cells, ranging from $43.8 \pm 2.9\%$ to $33.7 \pm 3.2\%$, were significantly decreased with the concentration of 6-gingerol. The similar change in population of G2/M phase and G0/G1 phase was also found in LoVo cells treated with the serial concentrations of 6-gingerol for 48 h. These results revealed that 6-gingerol treatments increased the ratios of G2/M phase but decreased G0/G1 phase of LoVo cells in a dose-dependent manner. Moreover, $15 \mu\text{g/mL}$ 6-gingerol treatment resulted in an 1.29-fold increase in number of cells in G2/M phase compared with that after DMSO treatment. Amongst 4 phases of cell cycle, G2/M phase arrest of LoVo cells was significant in response to 6-gingerol treatment.

As a slight change in percentage of sub-G1 phase of 6-gingerol-treated LoVo cells was observed, a further experiment was performed to investigate the involvement of apoptosis in inhibited viability of LoVo cells upon exposure to 6-gingerol. Caspase 3, and 8 that are situated at pivotal junction in apoptosis pathway were monitored after 6-gingerol treatment. No significant change in the level of precursor form and activated form of caspase 3 was observed in response to 6-gingerol treatments (5, 10, and $15 \mu\text{g/mL}$) as well as caspase 8 (Figure 3).

3.3. 6-Gingerol Diminished Levels of CDK1, Cyclin A, and Cyclin B1 in LoVo Cells. Having observed 6-gingerol-induced G2/M phase arrest, the effects of 6-gingerol treatments on cell cycle progress of LoVo cells were further investigated. Levels

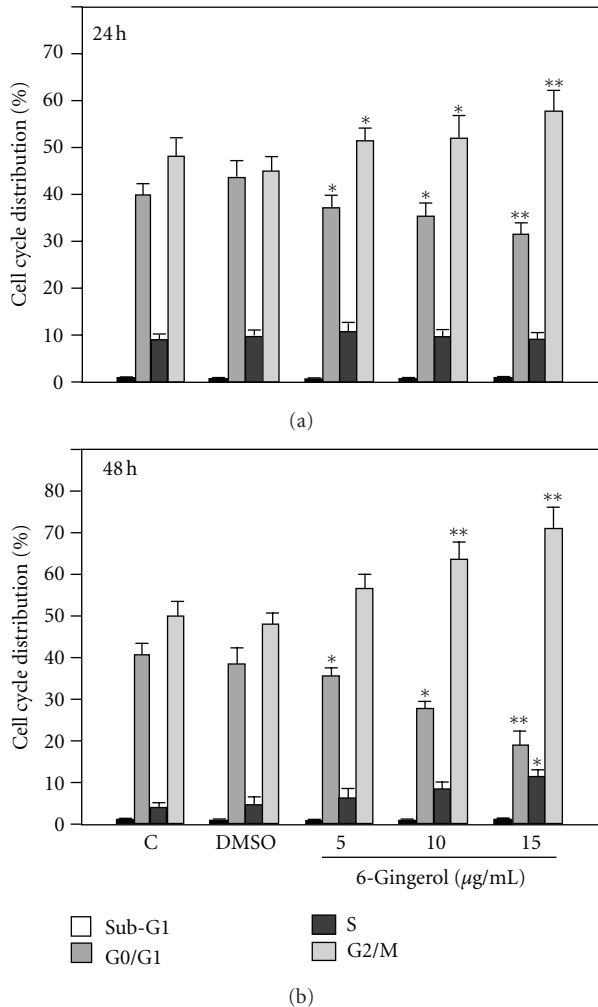


FIGURE 2: 6-Gingerol induced G2/M phase arrest of LoVo cells. Cells were treated with indicated concentration of 6-gingerol for 24 h or 48 h, and the percentages of various cell cycle phases, including sub-G1, G0/G1, S, and G2/M, were analyzed and quantitated by flow cytometry. Data were shown as the means \pm SD. Three independent experiments were performed for statistical analysis. * $P < 0.05$ and ** $P < 0.005$ as compared to corresponding control.

of important cell cycle mediators, including CDK1, cyclin A, cyclin B1, cyclin D1, and cyclin E, were determined by immunoblotting and relatively quantitated by densitometric analysis. Our results showed that 6-gingerol treatments (5, 10, and 15 $\mu\text{g}/\text{mL}$) dose-dependently decreased the levels of CDK1, cyclin A, and cyclin B1 but slightly affected the levels of cyclin D1 and cyclin E (Figure 4). With the 6-gingerol treatment at concentration of 15 $\mu\text{g}/\text{mL}$ for 24 h, the levels of CDK1, cyclin A, and cyclin B1 were reduced to 64%, 71%, and 68% of control, respectively, by densitometric quantitation (Figure 4).

3.4. 6-Gingerol Increased Levels of p21^{Cip1} and p27^{Kip1} in LoVo Cells. Observing diminished levels of CDK1, cyclin A, and cyclin B1 upon 6-gingerol treatments, we further investigated the effects of 6-gingerol treatments on cell cycle

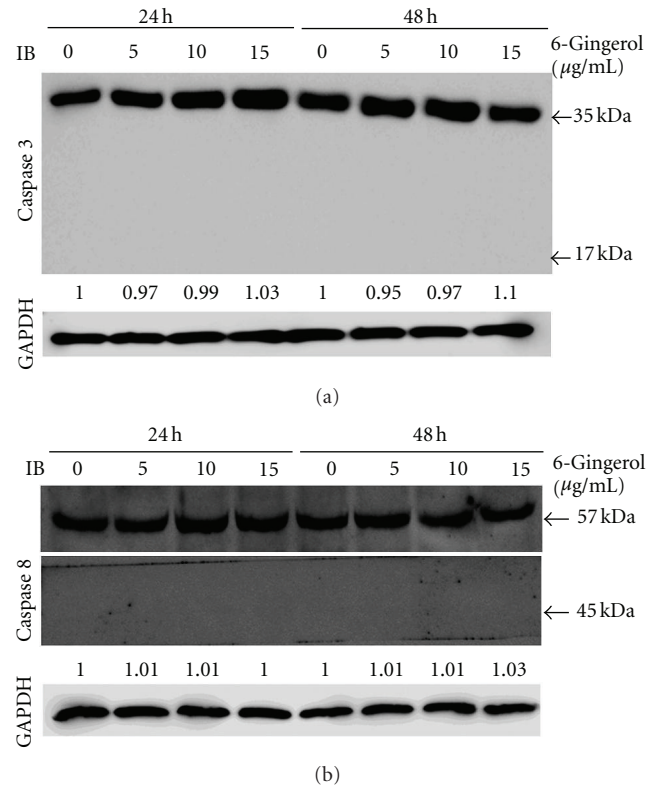


FIGURE 3: Effects of 6-gingerol on activation of caspase 3 and caspase 8 of LoVo cells. Cells were treated with indicated concentration of 6-gingerol for 24 h or 48 h, and then the cell lysates were subjected to immunoblot for detection of caspase 3 and caspase 8. Protein levels were relatively quantitated by densitometric analysis using GAPDH as control.

regulators, p21^{Cip1} and p27^{Kip1}. As shown in Figure 5, 6-gingerol treatments (24 h) dose-dependently increased levels of p21^{Cip1} and p27^{Kip1} up to 1.65- and 1.46-fold, respectively, compared to that of control. The trend of increase in p21^{Cip1} and p27^{Kip1} level was continuous in LoVo cells for further 24 h. These findings revealed that 6-gingerol treatments significantly induced both of negative cell cycle regulators p21^{Cip1} and p27^{Kip1}.

3.5. 6-Gingerol Elevated p53 Level and Intracellular ROS in LoVo Cells. Basing on that 6-gingerol treatment elevated negative cell cycle regulator p21^{Cip1}, the upstream regulator of p21^{Cip1}, p53 was further investigated. As shown in Figure 6(a), 6-gingerol treatments (24 h) elevated level of p53 up to 1.89-fold as compared to that of control. The trend of increase in p53 level was continuous in LoVo cells for further 24 h. These findings revealed that 6-gingerol treatments significantly induced the important cell cycle regulator p53 in LoVo cells.

ROS has been reported to play pivotal roles in phytochemical-induced cell cycle arrest and apoptosis [23, 24]. Therefore, whether 6-gingerol induced ROS production in LoVo cells was also analyzed. As shown in Figure 6(b), 6-gingerol dose-dependently increased intracellular ROS up to

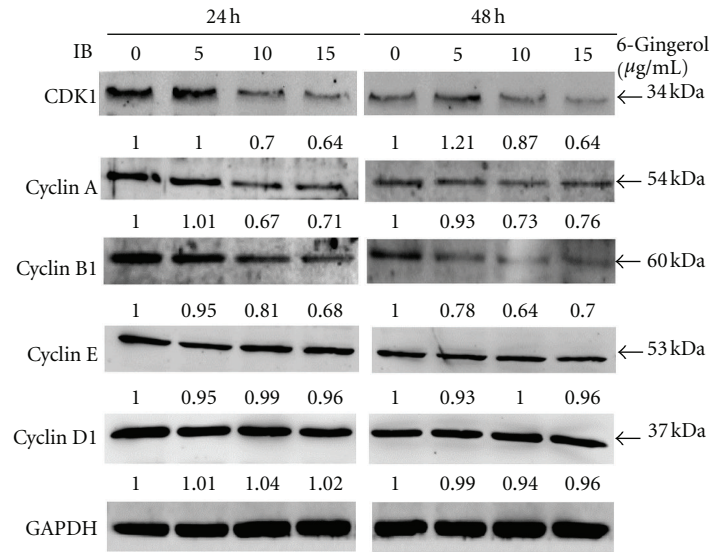


FIGURE 4: Effects of 6-gingerol on CDK1 and cyclins of LoVo cells. Cells were treated with indicated concentration of 6-gingerol for 24 h or 48 h, and then the cell lysates were subjected to immunoblot for detection of indicated proteins. Protein levels were relatively quantitated by densitometric analysis using GAPDH as control.

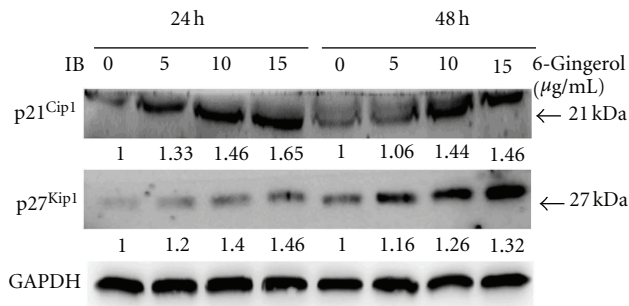


FIGURE 5: Effects of 6-gingerol on p21^{Cip1} and p27^{Kip1} of LoVo cells. Cells were treated with indicated concentration of 6-gingerol for 24 h or 48 h, and then the cell lysates were subjected to immunoblot for detection of p21^{Cip1} and p27^{Kip1}. Protein levels were relatively quantitated by densitometric analysis using GAPDH as control.

1.89-fold as compared to the control, and the increase of ROS was diminished by NAC pretreatment. These results showed that 6-gingerol significantly increased level of p53 as well as elevated intracellular ROS in LoVo cell.

4. Discussion

Previous studies have shown that treatment of 200 μM 6-gingerol induced G1 phase arrest and apoptosis in several human colorectal cancer cells, including HCT-116, SW480, HT-29, LoVo, and Caco-2 [25]. It is also reported that 6-gingerol (60 μM) shows a weaker effect on induction of apoptosis of colorectal carcinoma COLO 205 than its analogue, 6-shogaol [26]. Similarly, our results demonstrate that a relative low concentration of 6-gingerol (up to 50 μM) significantly suppresses the viability, induces G2/M phase arrest, but does not provoke apoptosis of LoVo cells. Therefore, it

is suggested that low concentration of 6-gingerol tends to inhibit growth of LoVo cells through induction of cell cycle arrest instead of apoptosis.

Cyclin A2, an originally identified A-type cyclin, is ubiquitously expressed in mitotically dividing cells and is upregulated in a variety of cancers [27, 28]. In late G1 phase, cyclin A binds to CDK2 to promote transition to S phase and plays important roles in replication of DNA and centromere in S phase [29]. Another type of cyclin is discovered and coined as B-type cyclin of which the biological role is not fully understood; however, the B-type cyclins generally emerge during the G2-M phase transition of the cell cycle. During G2-M phase transition, cyclin B1 binds to CDK1 (*cdc2*) to form mitosis-promoting factor that facilitates the transition from G2 to M phase of the cell cycle [30]. Therefore, reduced levels of cyclin A and cyclin B1 attenuate the activation of both CDK1 and CDK2, consequently leading to the cell cycle arrest at S phase and G2/M phase. In consistency with the phenomenon, our flow cytometric analysis showed a significant increased percentage of G2/M phase in 6-gingerol-treated LoVo cells (Figure 2), suggesting that 6-gingerol may trigger the G2/M cell cycle arrest via downregulation of cyclin A, CDK2, cyclin B1, and CDK1.

Generally, the activity of cyclin-CDK complexes is regulated by two different families of proteins known as INK4 and CDK inhibitors [31]. However, the tight regulation of cell cycle progression is compromised in cancer cells, which consequently results in aberrant proliferation of cells [32]. In this regard, both INK4 and CDK inhibitor family members have been reported to lose their functions in various malignant cancers such as CRC, resulting in an uncontrolled cell cycle progression and cancer growth [33, 34]. Therefore, the molecular players such as cyclins, CDKs, and their inhibitors serve as potential targets to halt the uncontrolled

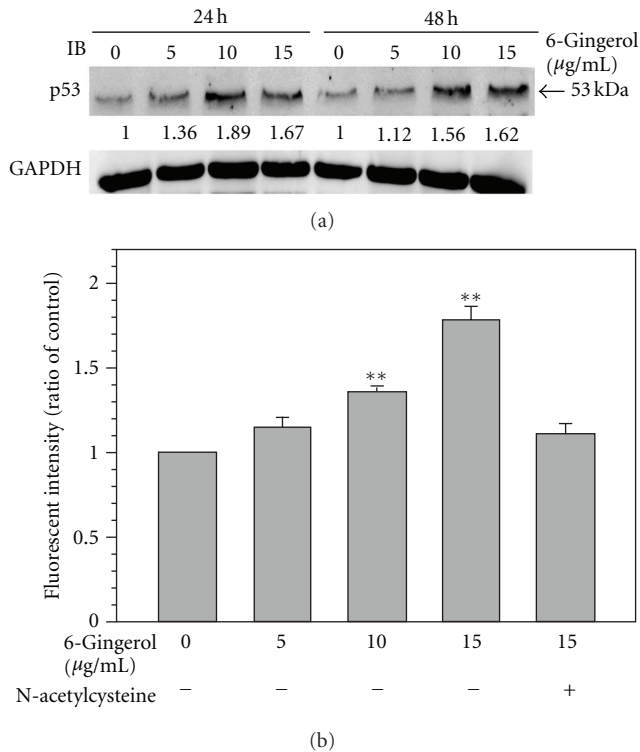


FIGURE 6: Effects of 6-gingerol on p53 and intracellular ROS of LoVo cells. (a) Cells were treated with indicated concentration of 6-gingerol for 24 h or 48 h, and then the cell lysates were subjected to immunoblot for detection of p53. Protein levels were relatively quantitated by densitometric analysis using GAPDH as control. (b) Cells were treated with indicated concentration of 6-gingerol for 24 h, and the intracellular ROS was determined as described in the Section 2.

proliferation [35, 36]. Specifically, it could be argued that the agents inducing the level and/or function of cell cycle inhibitory regulators (INK4 and Cip/Kip family members) might be useful in the control of various malignancies including CRC. In the present study, our results clearly showed an increase in the levels of p21^{Cip1} and p27^{Kip1} in presence of 6-gingerol in LoVo cells, which is in line with the observed G2/M phase arrest. Importantly, 6-gingerol caused a dose- and time-dependent increase in the levels of p27^{Kip1} in LoVo cells, which supports the finding of cell cycle arrest effect in S or G2/M phase in this cell line.

6-gingerol has been reported to exert its anti-tumoral activity via induction of ROS which is also known to trigger activation of p53 and the consequent cell cycle arrest and apoptosis [37]. Our results also showed that 6-gingerol significantly increased intracellular ROS as well as the critical cell cycle regulator p53 in LoVo cells. These findings indicate that 6-gingerol increased p53 level may attribute to induction of ROS. In conclusion, it could be suggested that 6-gingerol induces ROS production and p53 activation as well as inhibits the degradation of p27^{Kip1} and p21^{Cip1} in LoVo cells, by a mechanism yet to be established, which induces the cell cycle arrest at S and G2/M phases.

Conflict of Interests

All the authors confirm that there are no conflicts of interest.

References

- [1] L. T. Chen and J. Whang-Peng, "Current status of clinical studies for colorectal cancer in Taiwan," *Clinical Colorectal Cancer*, vol. 4, no. 3, pp. 196–203, 2004.
- [2] K. W. Kinzler and B. Vogelstein, "Lessons from hereditary colorectal cancer," *Cell*, vol. 87, no. 2, pp. 159–170, 1996.
- [3] R. J. Mayer, "Targeted therapy for advanced colorectal cancer—more is not always better," *New England Journal of Medicine*, vol. 360, no. 6, pp. 623–625, 2009.
- [4] A. P. Zbar, P. J. Kennedy, and V. Singh, "Functional outcome following restorative rectal cancer surgery," *Acta Chirurgica Lugoslavica*, vol. 56, no. 2, pp. 9–16, 2009.
- [5] Y. J. Surh, "Molecular mechanisms of chemopreventive effects of selected dietary and medicinal phenolic substances," *Mutation Research*, vol. 428, no. 1-2, pp. 305–327, 1999.
- [6] A. M. Bode, W. Y. Ma, Y. J. Surh, and Z. Dong, "Inhibition of epidermal growth factor-induced cell transformation and activator protein 1 activation by [6]-gingerol," *Cancer Research*, vol. 61, no. 3, pp. 850–853, 2001.
- [7] S. O. Kim, J. K. Kundu, Y. K. Shin et al., "[6]-Gingerol inhibits COX-2 expression by blocking the activation of p38 MAP kinase and NF-κB in phorbol ester-stimulated mouse skin," *Oncogene*, vol. 24, no. 15, pp. 2558–2567, 2005.
- [8] E. C. Kim, J. K. Min, T. Y. Kim et al., "[6]-Gingerol, a pungent ingredient of ginger, inhibits angiogenesis in vitro and in vivo," *Biochemical and Biophysical Research Communications*, vol. 335, no. 2, pp. 300–308, 2005.
- [9] H. S. Lee, E. Y. Seo, N. E. Kang, and W. K. Kim, "[6]-Gingerol inhibits metastasis of MDA-MB-231 human breast cancer cells," *Journal of Nutritional Biochemistry*, vol. 19, no. 5, pp. 313–319, 2008.
- [10] F. Suzuki, M. Kobayashi, Y. Komatsu, A. Kato, and R. B. Pollard, "Keishi-ka-kei-to, a traditional Chinese herbal medicine, inhibits pulmonary metastasis of B16 melanoma," *Anti-cancer Research*, vol. 17, no. 2, pp. 873–878, 1997.
- [11] W. J. Duan, Q. S. Li, M. Y. Xia, S. I. Tashiro, S. Onodera, and T. Ikejima, "Silibinin activated p53 and induced autophagic death in human fibrosarcoma HT1080 cells via reactive oxygen species-p38 and c-Jun N-terminal kinase pathways," *Biological and Pharmaceutical Bulletin*, vol. 34, no. 1, pp. 47–53, 2011.
- [12] H. M. Chen, F. R. Chang, Y. C. Hsieh et al., "A novel synthetic protoapigenone analogue, WYC02-9, induces DNA damage and apoptosis in DU145 prostate cancer cells through generation of reactive oxygen species," *Free Radical Biology and Medicine*, vol. 50, no. 9, pp. 1151–1162, 2011.
- [13] A. M. Abukhdeir and B. H. Park, "p21 and p27: roles in carcinogenesis and drug resistance," *Expert Reviews in Molecular Medicine*, vol. 10, no. 19, 2008.
- [14] D. O. Morgan, "Principles of CDK regulation," *Nature*, vol. 374, no. 6518, pp. 131–134, 1995.
- [15] J. W. Harper, G. R. Adami, N. Wei, K. Keyomarsi, and S. J. Elledge, "The p21 Cdk-interacting protein Cip1 is a potent inhibitor of G1 cyclin-dependent kinases," *Cell*, vol. 75, no. 4, pp. 805–816, 1993.
- [16] K. Polyak, M. H. Lee, H. Erdjument-Bromage et al., "Cloning of p27^{Kip1}, a cyclin-dependent kinase inhibitor and a potential mediator of extracellular antimitogenic signals," *Cell*, vol. 78, no. 1, pp. 59–66, 1994.

- [17] S. Matsuoka, M. C. Edwards, C. Bai et al., "p57(KIP2), a structurally distinct member of the p21(CIP1) Cdk inhibitor family, is a candidate tumor suppressor gene," *Genes and Development*, vol. 9, no. 6, pp. 650–662, 1995.
- [18] M. H. Lee, I. Reynisdottir, and J. Massague, "Cloning of p57(KIP2), a cyclin-dependent kinase inhibitor with unique domain structure and tissue distribution," *Genes and Development*, vol. 9, no. 6, pp. 639–649, 1995.
- [19] Y. Xiong, G. J. Hannon, H. Zhang, D. Casso, R. Kobayashi, and D. Beach, "p21 is a universal inhibitor of cyclin kinases," *Nature*, vol. 366, no. 6456, pp. 701–704, 1993.
- [20] C. J. Sherr and J. M. Roberts, "Inhibitors of mammalian G1 cyclin-dependent kinases," *Genes and Development*, vol. 9, no. 10, pp. 1149–1163, 1995.
- [21] M. L. Fero, E. Randel, K. E. Gurley, J. M. Roberts, and C. J. Kemp, "The murine gene p27(Kip 1) is haplo-insufficient for tumour suppression," *Nature*, vol. 396, no. 6707, pp. 177–180, 1998.
- [22] R. Liu, M. Gao, Z. H. Yang, and G. H. Du, "Pinocembrin protects rat brain against oxidation and apoptosis induced by ischemia-reperfusion both in vivo and in vitro," *Brain Research*, vol. 1216, no. C, pp. 104–115, 2008.
- [23] S. Fan, M. Qi, Y. Yu et al., "P53 activation plays a crucial role in silibinin induced ROS generation via PUMA and JNK," *Free Radical Research*, vol. 46, no. 3, pp. 310–319, 2012.
- [24] L. Tian, D. Yin, Y. Ren, C. Gong, A. Chen, and F.-J. Guo, "Plumbagin induces apoptosis via the p53 pathway and generation of reactive oxygen species in human osteosarcoma cells," *Molecular Medicine Reports*, vol. 5, no. 1, pp. 126–132, 2012.
- [25] S. H. Lee, M. Cekanova, and J. B. Seung, "Multiple mechanisms are involved in 6-gingerol-induced cell growth arrest and apoptosis in human colorectal cancer cells," *Molecular Carcinogenesis*, vol. 47, no. 3, pp. 197–208, 2008.
- [26] M. H. Pan, M. C. Hsieh, J. M. Kuo et al., "6-Shogaol induces apoptosis in human colorectal carcinoma cells via ROS production, caspase activation, and GADD 153 expression," *Molecular Nutrition and Food Research*, vol. 52, no. 5, pp. 527–537, 2008.
- [27] J. Pines and T. Hunter, "Human cyclin A is adenovirus E1A-associated protein p60 and behaves differently from cyclin B," *Nature*, vol. 346, no. 6286, pp. 760–763, 1990.
- [28] J. Wang, X. Chenivresse, B. Henglein, and C. Brechot, "Hepatitis B virus integration in a cyclin A gene in a hepatocellular carcinoma," *Nature*, vol. 343, no. 6258, pp. 555–557, 1990.
- [29] D. Coverley, H. Laman, and R. A. Laskey, "Distinct roles for cyclins E and A during DNA replication complex assembly and activation," *Nature Cell Biology*, vol. 4, no. 7, pp. 523–528, 2002.
- [30] P. Nurse, "Universal control mechanism regulating onset of M-phase," *Nature*, vol. 344, no. 6266, pp. 503–508, 1990.
- [31] A. Besson, S. F. Dowdy, and J. M. Roberts, "CDK inhibitors: cell cycle regulators and beyond," *Developmental Cell*, vol. 14, no. 2, pp. 159–169, 2008.
- [32] C. H. Goliafs, A. Charalabopoulos, and K. Charalabopoulos, "Cell proliferation and cell cycle control: a mini review," *International Journal of Clinical Practice*, vol. 58, no. 12, pp. 1134–1141, 2004.
- [33] T. Uchida, T. Kinoshita, H. Saito, and T. Hotta, "CDKN2 (MTS1/p16(INK4A)) gene alterations in hematological malignancies," *Leukemia and Lymphoma*, vol. 24, no. 5-6, pp. 449–461, 1997.
- [34] M. Shiohara, K. Koike, A. Komiyama, and H. P. Koeffler, "p21(WAF1) mutations and human malignancies," *Leukemia and Lymphoma*, vol. 26, no. 1-2, pp. 35–41, 1997.
- [35] W. Li, A. Sanki, R. Z. Karim et al., "The role of cell cycle regulatory proteins in the pathogenesis of melanoma," *Pathology*, vol. 38, no. 4, pp. 287–301, 2006.
- [36] K. Vermeulen, D. R. Van Bockstaele, and Z. N. Berneman, "The cell cycle: a review of regulation, deregulation and therapeutic targets in cancer," *Cell Proliferation*, vol. 36, no. 3, pp. 131–149, 2003.
- [37] G. Yang, L. Zhong, L. Jiang et al., "Genotoxic effect of 6-gingerol on human hepatoma G2 cells," *Chemico-Biological Interactions*, vol. 185, no. 1, pp. 12–17, 2010.

Research Article

The Effect of *Labisia pumila* var. *alata* on Postmenopausal Women: A Pilot Study

Azidah Abdul Kadir,¹ Nik Hazlina Nik Hussain,¹ Wan Mohammad Wan Bebakar,¹ Dayang Marshitah Mohd,¹ Wan Mohd Zahiruddin Wan Mohammad,¹ Intan Idiana Hassan,² Norlela Shukor,³ Nor Azmi Kamaruddin,³ and Wan Nazaimoon Wan Mohamud⁴

¹ School of Medical Sciences, Universiti Sains Malaysia, Kubang Kerian, 16150 Kelantan, Malaysia

² School of Health Sciences, Universiti Sains Malaysia, Kubang Kerian, 16150 Kelantan, Malaysia

³ Department of Medicine, Universiti Kebangsaan Malaysia, Kuala Lumpur, 56000 Cheras, Malaysia

⁴ Institute for Medical Research, 50588 Kuala Lumpur, Malaysia

Correspondence should be addressed to Azidah Abdul Kadir, azidah@kb.usm.my

Received 17 January 2012; Revised 2 April 2012; Accepted 4 April 2012

Academic Editor: William C. S. Cho

Copyright © 2012 Azidah Abdul Kadir et al. This is an open access article distributed under the Creative Commons Attribution License, which permits unrestricted use, distribution, and reproduction in any medium, provided the original work is properly cited.

This is a randomized, double-blind, placebo-controlled study comparing the effects of a water extract of *Labisia pumila* var. *alata* at 280 mg/day with placebo, given for 6 months in postmenopausal Malay women. There were 29 patients treated with *Labisia pumila* and 34 patients in the placebo group. Menopausal symptoms were assessed at baseline and at 6 months. The blood pressure, body mass index, waist circumference, fasting blood sugar, lipid profile, and hormonal profile (follicle stimulating hormone/luteinizing hormone/estradiol) were measured during visits every two months. ANCOVA model analysis showed significantly lower triglycerides levels in LP subjects at 6 months after treatment as compared to placebo (1.4 versus 1.9 mmol/L; adj. mean difference 0.5, 95% CI: 0.02, 0.89 after adjusted for the baseline values, age, BMI, and duration of menopause placebo). Other parameters in both groups did not differ significantly. In conclusion, daily intake of *Labisia pumila* at 280 mg/day for six months was found to provide benefit in reducing the triglyceride (TG) values.

1. Introduction

The number of women entering menopause has increased worldwide due to the increment of life expectancy. One of the important issues affecting postmenopausal women is the risk and benefits of estrogens replacement therapy. Many of the women who are prescribed hormone replacement therapy stop taking it or never commence taking it due to fear of associations with malignancy, unacceptable bleeding, or its side effects. Instead, they search for alternative ways of self-managing the postmenopausal symptoms or its long term consequences, such as increased risk of coronary artery disease (CAD) and osteoporosis.

Labisia pumila (LP) or more commonly known as Kacip Fatimah has been used widely in South East Asian communities for a variety of illnesses and in food supplements. This plant has been widely used by Malaysian

women for generations to ease childbirth and also for its postpartum rejuvenating properties [1]. Traditionally, LP extract is prepared by boiling the roots, leaves, or the whole plant in water, and the extract is consumed orally [1]. Its exclusive use by women has led to the belief that it is a phytoestrogen, a compound with similar chemical structures to estrogen [2], and is therefore able to relieve menopausal symptoms [3].

L. pumila is from the genus Myrsinaceae. Three different varieties of *L. pumila* were identified in Malaysia: var. *alata*, var. *pumila*, and var. *lanceolata* [4]. The term Kacip Fatimah is used to describe the plant in general. Preliminary studies have shown that the var. *alata* and var. *pumila* are more commonly used medicinal plants than var. *lanceolata*.

Phytochemical studies of the roots and leaves of *L. pumila* var. *alata* have shown the presence of three C₁₅ monoene

resorcinols that are (Z)-5-(pentadec-4-enyl) benzene-1-3,3-diol, (Z)-5-5-(pentadec-8-enyl) benzene-1-3,3-diol, and (Z)-5-5-(pentadec-10-enyl) benzene-1-3,3-diol [5]. In addition, it also contains two novel benzoquinoid compounds 1, 2 as major components [6].

Research has demonstrated the estrogenic activity of LP. It is possible that it acts as selective estrogen receptor modulators (SERMs) which is active in certain tissues, [7]. A study showed that water extracts of LP were able to displace estradiol binding to antibodies raised against estradiol, making it similar to other estrogens such as estrone and estradiol [7]. The extract has also been found to produce a dose-response effect on the reproductive hormones of female rats, notably on the estradiol and free testosterone levels [7].

Recently, study has showed that *Labisia pumila* (LP) is a potential alternative agent for hormone replacement therapy in postmenopausal women [8]. In that study, a group of researchers [8] had conducted a study comparing the effect of LP aqueous extract to estrogen on reproductive hormones using ovariectomised rat model. *Labisia pumila* supplementation had been shown to resemble the effect of estrogen replacement therapy on reproductive hormones [8]. In the study, it showed that 60-day treatment with LP significantly reduced luteinizing hormone (LH) and follicle stimulating hormone (FSH). It also elevates the estradiol and testosterone levels. These results resembled the effect of estrogen in the ovariectomised rats.

Currently, *L. pumila* is manufactured in the form of tonics or capsules by local companies, and various claims have been made that *L. pumila* can improve the well-being of women. It is imperative that all these declarations regarding the benefits and advantages of *L. pumila* or any herbal formulations containing *L. pumila* are proven scientifically, and that any possible toxicity arising from its consumption is evaluated.

In view of the initial evidence, it is postulated that this plant has a beneficial effect on postmenopausal women in terms of the positive impact on the lipids and hormonal profiles. The present study was designed to investigate the effect of LP on menopausal symptoms, cardiovascular risk factors, and hormonal profiles in Malay postmenopausal women.

2. Materials and Methods

2.1. Study Design and Setting. This randomised, parallel-group, placebo-controlled study to compare the effects of *Labisia pumila* var. *alata* extract at 280 mg/day was carried out amongst postmenopausal Malay women at the Clinical Trial Unit, Hospital Universiti Sains Malaysia (HUSM) from June 2004 until May 2005.

2.2. Study Participants. Malay women aged between 48 to 55 years with the body mass index ranging from 18 to 35 kg/m² were eligible for the study if they had been postmenopausal for at least six months. The women were not assessed on whether they had any menopause symptoms. The exclusion criteria included a history of taking hormone

replacement therapy or any herbal products for at least 6 months, a history of oophorectomy, a history of alcohol or drug abuse, a history of breast or cervical cancer, any active medical illnesses making the implementation of the study protocol or interpretation of the results difficult, or the presence of endometrium thickness of more than 0.5 cm detected with a pelvic ultrasonography.

The study participants were identified from the Obstetrics & Gynaecology Clinic or from the outpatients' clinic of HUSM. They were invited to come to the Clinical Trial Unit for the study explanation and screening procedure. Informed consent was obtained once they agreed to participate in the study. A detailed history including past medical history and gynaecology history was assessed at baseline. The physical examination including blood pressure, weight, height, and waist hip ratio measurement, and cardiovascular, breast, abdomen, and pelvic examinations including Pap smear and pelvic ultrasound were performed at the initial and the last visit.

2.3. Randomization and Interventions. Study participants were randomly allocated to either LP or placebo by means of computer-generated randomization numbers issued by the Institute for Medical Research (IMR). Subject eligibility was established before treatment randomization which was done after the baseline visit and after the patient agreed to participate and signed the informed consent. The research nurse determined the treatment allocation by drawing a sealed nonopaque envelope containing instructions on the treatment allocations.

2.4. Plant Material. The raw material of *Labisia pumila* var. *alata* was identified and authenticated by ethno botanist of the Forest Research Institute of Malaysia (FRIM). The preparation of water extract of *Labisia pumila* var. *alata* is done by subjecting the dried plant material to water to form a water-soluble extract and then desiccating the extract. The process for preparation of *Labisia pumila* extract is by extracting dried *Labisia pumila* plant material with water at a ratio of 1:6 of dried *Labisia pumila* plant material:water to form a water-soluble extract and drying the extract wherein the extracting is carried out at 80°C for 3 hours and with continuous stirring. The starting material is fully dehydrated by drying it at 40°C for three days. The process wherein the extracting is repeated and the ratio of *Labisia pumila* plant material:water is 1:6. Then the *Labisia pumila* extract is dried by spray drying and wherein the spray drying comprises concentrating and drying. The spray drying is performed using a spray tower having a tower inlet and outlet, wherein tower inlet temperature is 185°C, and wherein tower outlet temperature is 107°C, respectively. Then a process for isolating a marker compound by semipreparative reverse-phase high-performance liquid chromatography was done from *Labisia pumila* extract. The marker compound is 3,4,5-trihydroxybenzoic acid.

The extract that was used in this study was similar with most of the animal studies [7–10] conducted since it was a big research project planned by the Malaysia government under the grant provided by the Ministry of Science,

Technology and Innovation (MOSTI). *Labisia pumila* var. *alata* extract was prepared and packed in a sachet form by a Good Manufacturing Practice (GMP) certified herbal company that has been approved by the Drug Control Authority, Ministry of Health, Malaysia.

2.5. Dosage and Study Protocol. The dosage used was based on animal studies carried out by the Institute for Medical Research Malaysia (IMR). Based on the study, a significant response in estradiol and testosterone levels were seen when the rats received 16 mg/kg body weight of *L. pumila* var. *alata* extract. Using the conversion dose as suggested by Freireich et al. [11] where the dose conversion used was 1/7 of rat dose equals to a 60 kg man dose, the minimum dose of *L. pumila* var. *alata* extract to be tested was 140 mg. In this study, we used the double dose of the minimum dose needed because we did not know the dose that will give significant response in human. Due to budget constraint to do study for all three doses that is 140 mg, 280, or 560 mg, we decided to use 280 mg of *L. Pumila* extract per day for this study.

The study subjects were required to take two sachets of the extract of *L. Pumila* daily at night for six months. The compliance was measured using the numbers of sachets taken. The sachets were supplied to the patients every month, and subjects were asked to return all unused medication. The number of sachets issued minus the number of sachets returned was used to calculate the compliance.

2.6. Outcome Measures and Followups. The women were given questionnaires to assess their menopausal symptoms. This questionnaire was validated and based on previous study [12]. It consisted of a list of symptoms which comprised of classical vasomotor symptoms, physical symptoms, and psychological symptoms. Each of the symptoms was assessed using the Likert scale from 0 to 5. They were asked to fill in this questionnaire at baseline and at the end of six months. Blood samples to measure fasting glucose levels, total cholesterol, low density lipoprotein (LDL), high density lipoprotein (HDL), triglycerides, luteinizing hormone (LH), follicle stimulating hormone (FSH), and estradiol levels as study outcomes were taken at baselines and at two-month intervals. The subjects were followed up every two months for the total duration of six months. At each visit, the subjects were examined by medical specialists who were part of the clinical trial team, and they were asked for feedback regarding any side effects.

2.7. Approval by the Research and Ethics Committee. Ethical approval was obtained from the Research and Ethics Committee, Universiti Sains Malaysia prior to the study implementation. The protocol was approved by the Research and Ethical Committee, School of Medical Sciences, University Sains Malaysia (USM/PPSP/Ethics Com./2004 (125.4(6))).

2.8. Statistical Analyses. Analyses were done by using SPSS for windows version 12.0, and all numerical variables were expressed as mean and standard deviation (SD) and categorical data as frequencies and percentages. Randomized groups were compared for any possible differences at baseline using

independent *t*- and chi-square tests. To show the effectiveness of the treatment group, analysis of covariance (ANCOVA) was used to compare the difference of the outcome variables at 6-month postintervention after controlling the age, BMI, duration of menopause, and the baseline values as the covariates. Summary changes were reported as means, standardizing changes for possible covariate imbalances between groups. All reported *P* values are 2-tailed with a value of less than 0.05 which is considered significant.

3. Results

A total of 63 patients completed the 6-month study. The baseline characteristic of the study participants is shown in Table 1. There were no statistical significant differences between the treatment group and placebo at baseline in terms of age, duration of menopause, parity, clinical, biochemical, and hormonal parameters.

3.1. Table 2. It displays the mean of the menopausal symptoms scores of both groups comparing the baseline and the last visit. Both groups showed a reduced trend within the groups. However, there was no significant difference observed between the placebo and the verum (treatment) group.

3.2. Table 3. It shows the cardiovascular risk factors and hormonal changes after the 6-month followup trial with placebo and LP at 280 mg. After adjustments were made regarding age, BMI, duration of menopause, and its baseline values, there was a significant main effect of treatment on the TG levels [$F(1,63) = 4.309, P = 0.042$, ANCOVA] where the adjusted mean of TG in LP subjects was significantly lower than placebo (1.4 versus 1.9 mmol/L) (adj. mean difference 0.5, 95% CI: 0.02, 0.89) (Table 3). There were also comparatively lower means of the fasting plasma glucose and total cholesterol in the LP treatment group; however, the differences were not statistically significant.

4. Discussion

Previously, hormone replacement therapy has subsisted as the mainstay of treatment for problems arising from loss of ovarian functions. However, recent studies have changed this practice due to adverse effects as regards to hormone replacement therapy (HRT) [13]. Now, there are many controversial issues regarding prescribing HRT for postmenopausal women. These is a cause for the tremendous growth in the use of alternative therapies to relieve the postmenopausal symptoms. Many women assume that alternative medicine is safe and natural. However, compared to HRT, there are still not sufficient clinical trials to assess the effect of phytoestrogen on cardiovascular risk factors and osteoporosis evidenced by changes in bone mineral density.

There is still very little information about *Labisia pumila* var. *alata* chemical properties and the mechanism of action despite its wide range of use among females in Malaysia. The plant root and leaves were found to contain two novel benzoquinoid compounds 1, 2 as major components [6].

TABLE 1: Baseline characteristics among participants of randomized controlled trial between *Labisia pumila* and placebo groups.

Characteristics	All* (n = 63)	Trial groups*		P value [‡]
		<i>Labisia</i> (n = 29)	Placebo (n = 34)	
Age (years)	52.7 (1.9)	52.9 (1.8)	52.6 (1.9)	0.445
Age at menarche (years)	13.9 (1.7)	13.9 (1.7)	13.9 (1.7)	0.790
Duration of menopause (years)	3.2 (3.1)	3.0 (2.9)	3.6 (3.2)	0.495
Number of parity (%) [†]				
<5	23 (36.5)	8 (27.6)	15 (44.1)	0.174
≥5	40 (63.5)	21 (72.4)	19 (55.9)	
Household income per month (%) [†]				
≤RM 1,000	39 (61.9)	19 (65.5)	20 (58.8)	0.586
>RM 1,000	24 (38.1)	10 (34.5)	14 (41.2)	
Body mass index (BMI) (kg/m ²)	26.5 (3.7)	26.4 (4.5)	26.5 (3.1)	0.814
Waist hip ratio	0.85 (0.08)	0.85 (0.08)	0.86 (0.09)	0.812
Diastolic BP (mm Hg)	82.9 (10.1)	81.8 (10.5)	83.8 (9.9)	0.439
Systolic BP (mm Hg)	125.3 (18.5)	122.8 (18.5)	127.3 (18.4)	0.339
Total cholesterol (mmol/L)	5.2 (1.1)	5.1 (1.1)	5.3 (1.1)	0.601
Triglycerides (mmol/L)	1.7 (1.4)	1.4 (1.1)	1.9 (1.6)	0.095
Fasting glucose (mmol/L)	6.1 (1.9)	5.8 (0.7)	6.2 (2.6)	0.433
Female hormones (IU)				
FSH	49.0 (22.2)	45.8 (23.7)	51.8 (20.8)	0.297
LH	23.6 (13.6)	23.8 (14.8)	23.3 (12.6)	0.877
Estrogen	38.7 (19.0)	35.7 (12.2)	41.2 (22.9)	0.271

* Values are expressed as mean (standard deviation, SD) unless otherwise specified.

[†]Determined by independent *t*-test; [‡]chi-square tests.

Another group of researcher had conducted a study which looked at the adverse effects of the aqueous extract of this plant on the oestrous cycle, reproductive performance, postnatal growth, and the offsprings of rats [9]. In that study, the water-based extracts did not pose any significant reproductive toxicity or complication during pregnancy and delivery in rats. Currently, to our knowledge, the toxicology studies were done only in rats.

Theoretically, phytoestrogens exert their effects primarily through binding to estrogen receptors (ERs) [14]. Reports have shown that the plant displays a nonsignificant response to *in vitro* estrogen activity [5]. The water extract of LP was shown to be able to displace estradiol binding to antibodies raised against estradiol making it similar to other estrogens such as estrone and estradiol [7]. The extract also produced a dose response effect on the reproductive hormones of female rats, notably on estradiol and free testosterone levels [7]. However, in this study, there was no effect of LP on the menopausal symptoms and hormonal profiles in the post menopausal women. The possible explanations are that the sample size in this study is very small, and also it needed to be given in a longer duration before the effects can be seen. In animal study, it showed that estrogen replacement therapy increased estradiol level as early as 30 days of treatment compared to LP which requires 60 days of treatment [8].

There were few limitations in this study. Although the treatment group showed reduced triglyceride levels compared to the placebo group, however the level in both groups was still within the normal range. Therefore, it is of no clinical relevance at this moment. We suggest that further study is required in order to assess this effect. In an animal study, it was revealed that the ovariectomised rats treated with LP extract had decreased in body weight compared to the control group and have postulated that this mechanism occurred due to the presence of phytoestrogen in it [10]. The study postulates that there is a possible role for *Labisia pumila* var. *alata* in modulating postmenopause adiposity in a manner similar to that reported for estrogen through the initiation of the lipolysis process in adipose tissue and thus may have a possible effect on weight management [10].

In the other study [15], which looked at the effect of water extract from *Labisia pumila* on the aorta of ovariectomized rats, it was found that the elastic lamellae architecture of the ovariectomized rat aortae in the treatment group by the plant was maintained in a manner comparable to the normal rat. This result implied that there is a possible role for LP in modulating postmenopausal cardiovascular risks.

This study involved a small sample size which may have had an impact on why some of the results might not be significant. Conducting a bigger study is highly recommended in

TABLE 2: The menopausal symptoms changes after 6-month followup trial with placebo and *Labisia pumila*.

Menopausal symptoms	*Placebo (n = 34)	* <i>Labisia</i> (n = 29)	P value [‡]
Hot flushes	V1 0.96 (1.34)	V1 1.10 (1.32)	0.75
	V2 0.56 (0.93)	V2 0.90 (1.49)	
Night sweats	V1 1.04 (1.43)	V1 1.24 (1.30)	0.49
	V2 0.59 (1.04)	V2 0.79 (1.17)	
Insomnia	V1 1.56 (1.60)	V1 1.31 (1.58)	0.78
	V2 0.89 (1.15)	V2 0.90 (1.34)	
Dyspareunia	V1 1.89 (1.91)	V1 1.72 (1.62)	0.93
	V2 1.37 (1.49)	V2 1.59 (1.66)	
Painful joints	V1 2.56 (1.72)	V1 2.66 (1.57)	0.63
	V2 1.33 (1.44)	V2 2.03 (1.38)	
Mastalgia	V1 0.56 (1.25)	V1 0.17 (0.38)	0.52
	V2 0.19 (0.48)	V2 0.21 (0.62)	
Palpitation	V1 1.48 (1.55)	V1 0.86 (1.56)	0.19
	V2 0.52 (0.80)	V2 0.55 (0.95)	
Irritability	V1 2.15 (1.59)	V1 2.34 (1.54)	0.34
	V2 1.07 (1.17)	V2 1.54 (1.21)	
Difficulty in concentration	V1 1.26 (1.58)	V1 2.07 (1.41)	0.16
	V2 1.15 (1.17)	V2 1.79 (1.37)	
Memory problem	V1 1.89 (1.50)	V1 2.07 (1.41)	0.52
	V2 1.15 (1.17)	V2 1.79 (1.37)	
Lethargic	V1 2.04 (1.69)	V1 1.59 (1.59)	0.75
	V2 0.96 (1.29)	V2 0.97 (1.05)	

* Values are expressed as mean (standard deviation, SD) unless otherwise specified.

[‡]Determined by independent *t*-test; [†]chi-square tests.

TABLE 3: Cardiovascular risk factors and hormonal changes after 6-month followup trial with placebo and *Labisia pumila* at 280 mg.

Study variables	Trial groups [†]			P value [‡]
	Placebo (n = 34)	<i>Labisia</i> (n = 29)	Adjusted mean difference (95% CI)	
Cardiovascular disease risk factors				
Total cholesterol (mmol/L)	5.5 (5.2, 5.9)	5.0 (4.6, 5.4)	0.5 (−0.06, 1.04)	0.082
Triglycerides (mmol/L)	1.9 (1.6, 2.2)	1.4 (1.1, 1.7)	0.5 (0.02, 0.89)	0.042
Fasting glucose (mmol/L)	6.3 (5.8, 6.8)	5.6 (5.1, 6.2)	0.7 (−0.06, 1.38)	0.073
Diastolic BP (mm Hg)	81.2 (78.3, 84.1)	82.1 (78.9, 85.2)	0.9 (−3.4, 5.2)	0.686
Systolic BP (mm Hg)	125.8 (120.9, 130.7)	127.5 (122.1, 132.8)	1.7 (−5.6, 9.0)	0.643
Female hormones (IU)				
FSH	36.3 (29.7, 42.8)	38.4 (31.3, 45.5)	2.11 (−7.62, 11.84)	0.665
LH	26.2 (21.8, 30.5)	24.4 (19.9, 29.0)	1.75 (−4.59, 8.08)	0.583
Estrogen	37.5 (31.4, 43.5)	33.5 (26.7, 40.3)	3.94 (−5.23, 13.10)	0.393

Abbreviations: LH: luteinizing hormone; FSH: follicle stimulating hormone; BP: blood pressure.

[†]Values at 6-month followup are expressed as adjusted means (95% confidence interval, CI) and are adjusted for baseline values, age, BMI, and duration of menopause.

[‡]Determined by analysis of covariance (ANCOVA); *P* value < 0.05 is considered significant.

order to look at the cardiovascular effect of LP and probably its weight reduction effect.

In conclusion, the result showed that *Labisia pumila* has beneficial effect to reduce the triglyceride (TG) values. Thus, it may be a useful phytosupplement for maintaining cardiovascular health in menopausal women. However, there was no effect on the hormonal profiles.

Acknowledgment

This study was supported by Ministry of Science, Technology and Innovation (MOSTI) Grant (IRPA Top Down 305/PPSP/6112233).

References

- [1] I. H. Burkill, *A Dictionary of the Economic Products of the Malay Peninsula*, Crown Agent, London, UK, 1935.
- [2] A. J. Jamia, J. P. Houghton, R. S. Milligan et al., "The oestrogenic and cytotoxic effects of the extracts of *Labisia pumila* var. *alata* and *Labisia pumila* var. *in vitro*," *Journal Sains Kesihatan*, vol. 1, pp. 53–60, 2003.
- [3] S. J. Bhatena and M. T. Velasquez, "Beneficial role of dietary phytoestrogens in obesity and diabetes," *The American Journal of Clinical Nutrition*, vol. 76, no. 6, pp. 1191–1201, 2002.
- [4] B. C. Stone, "Notes on the genus *labisia* lindl. (Myrsinaceae)," *Malayan Nature Journal*, vol. 42, no. 43, p. 51, 1988.
- [5] J. A. Jamal, P. J. Houghton, and S. R. Milligan, "Testing of *Labisia pumila* for oestrogenic activity using a recombinant yeast screen," *Journal of Pharmacy and Pharmacology*, vol. 50, no. 9, p. 79, 1998.
- [6] P. J. Houghton, J. A. Jamal, and R. S. Milligan, "Studies on *Labisia pumila* herb and its commercial products," *Journal of Pharmacy and Pharmacology*, vol. 51, p. 236, 1999.
- [7] Malaysian Herbal Medicine Research Center, "Estrogenic and androgenic activities of Kacip Fatimah (*Labisia pumila*)," Institute for Medical Research (IMR), December 2011, Kuala Lumpur, http://www.imr.gov.my/org/hmrc_r2.htm.
- [8] N. A. Wahab, W. H. W. Yusoff, A. N. Shuib et al., "*Labisia pumila* has similar effects to estrogen on the reproductive hormones of ovariectomized rats," *Internet Journal of Herbal and Plant Medicine*, vol. 1, no. 1, 2011.
- [9] M. F. Ezumi, S. Siti Amrah, A. W. M. Suhaimi, and S. S. J. Mohsin, "Evaluation of the female reproductive toxicity of aqueous extract of *Labisia pumila* var. *alata* in rats," *Indian Journal of Pharmacology*, vol. 39, no. 1, pp. 30–32, 2007.
- [10] A. W. Ayida, W. M. Wan Nazaimoon, H. S. Farihah et al., "Effect of water extract of *Labisia pumila* var *alata* treatment and estrogen replacement therapy morphology of adipose tissue in ovariectomized Sprague Dawley rats," *Journal of Medicinal and Biological Sciences*, vol. 1, no. 1, 2006.
- [11] E. J. Freireich, E. A. Gehan, D. P. Rall, L. H. Schmidt, and H. E. Skipper, "Quantitative comparison of toxicity of anticancer agents in mouse, rat, hamster, dog, monkey, and man," *Cancer Chemotherapy Reports*, vol. 50, no. 4, pp. 219–244, 1966.
- [12] A. Hamid, T. Nai Peng, and R. Nazilah, "A study on the age at menopause and menopausal symptoms among Malaysian women," *Malaysian Journal Reproductive Health*, vol. 7, no. 1, pp. 1–9, 1989.
- [13] Writing Group for the Women's Health Initiative Investigators, "Risk and benefits of estrogen plus progestin in healthy post-menopausal women: principal results from the Women's Health Initiative randomized controlled trial," *The Journal of the American Medical Association*, vol. 288, no. 3, pp. 321–333, 2002.
- [14] J. V. Turner, S. Agatonovic-Kustrin, and B. D. Glass, "Molecular aspects of phytoestrogen selective binding at estrogen receptors," *Journal of Pharmaceutical Sciences*, vol. 96, no. 8, pp. 1879–1885, 2007.
- [15] A. Al-Wahaibi, W. M. Wan Nazaimoon, W. N. Norsyam, H. S. Farihah, and A. L. Azian, "Effect of water extract of *Labisia pumila* Var *Alata* on aorta of ovariectomized Sprague Dawley rats," *Pakistan Journal of Nutrition*, vol. 7, no. 2, pp. 208–213, 2008.

Research Article

Quercetin Protects against Cadmium-Induced Renal Uric Acid Transport System Alteration and Lipid Metabolism Disorder in Rats

Ju Wang, Ying Pan, Ye Hong, Qing-Yu Zhang, Xiao-Ning Wang, and Ling-Dong Kong

Key Laboratory of Pharmaceutical Biotechnology, School of Life Sciences, Nanjing University, Nanjing 210093, China

Correspondence should be addressed to Ying Pan, pany@nju.edu.cn and Ling-Dong Kong, kongld@nju.edu.cn

Received 19 January 2012; Accepted 26 March 2012

Academic Editor: Debprasad Chattopadhyay

Copyright © 2012 Ju Wang et al. This is an open access article distributed under the Creative Commons Attribution License, which permits unrestricted use, distribution, and reproduction in any medium, provided the original work is properly cited.

Hyperuricemia and dyslipidemia are involved in Cd nephrotoxicity. The aim of this study was to determine the effect of quercetin, a dietary flavonoid with anti-hyperuricemic and anti-dyslipidemic properties, on the alteration of renal UA transport system and disorder of renal lipid accumulation in 3 and 6 mg/kg Cd-exposed rats for 4 weeks. Cd exposure induced hyperuricemia with renal XOR hyperactivity and UA excretion dysfunction in rats. Simultaneously, abnormal expression levels of renal UA transport-related proteins including RST, OAT1, MRP4 and ABCG2 were observed in Cd-exposed rats with inhibitory activity of renal Na⁺-K⁺-ATPase. Furthermore, Cd exposure disturbed lipid metabolism with down-regulation of AMPK and its downstream targets PPAR α , OCTN2 and CPT1 expressions, and up-regulation of PGC-1 β and SREBP-1 expressions in renal cortex of rats. We had proved that Cd-induced disorder of renal UA transport and production system might have cross-talking with renal AMPK-PPAR α /PGC-1 β signal pathway impairment, contributing to Cd nephrotoxicity of rats. Quercetin was found to be effective against Cd-induced dysexpression of RST and OAT1 with XOR hyperactivity and impairment of AMPK-PPAR α /PGC-1 β signal pathway, resulting in renal lipid accumulation reduction of rats.

1. Introduction

Cadmium (Cd) is considered to be toxic, heavy metal that causes nephrotoxicity in humans [1–3]. More evidence demonstrates the role of high-serum uric acid (UA) levels in Cd-induced overproduction of endogenous reactive oxygen species (ROS), which subsequently leads to renal injury [4, 5] and lipid metabolism disorder [6]. Xanthine oxidoreductase (XOR), including its initial form xanthine dehydrogenase (XDH, EC1.1.1.204) and xanthine oxidase (XO, EC1.2.3.2), is the key enzyme to catalyze UA production. Cd exposure induces the conversion of XDH into XO [7] and causes XO activation [8]. Renal organic ion transporters of solute carrier (SLC) 22 family are increasingly recognized as important determinants of urate transport. Urate transporter 1 (URAT1, *SLC22A12*) is the major absorptive urate transport protein in the kidney being responsible for regulation of blood urate homeostasis [9]. In addition to URAT1, OAT1 (*SLC22A6*) is a basolateral urate transporter [9]. The efflux transporters of the ATP binding cassette (ABC) family such

as the multidrug resistance protein 4 (MRP4, *ABCC4*) [10] and breast cancer-resistance protein (BCRP, *ABCG2*) [11] seem to be major candidates for urate secretory transport. Therefore, abnormality of these renal organic ion transporters may contribute to the impaired UA excretion and hyperuricemia [9–12].

As important cross-regulators, UA and XOR are directly or indirectly related to lipid metabolism [13]. Dyslipidemia is suggested to be responsible for the progression of chronic kidney disease [14]. Cd exposure can alter serum lipid level and liver lipid metabolism in male Wistar rats [15] and induce lipid accumulation in the tubular lumen of male cat [16]. Therefore, animal studies evaluating Cd exposure-induced dysfunction of renal UA transport and production system are needed to verify its role in lipid metabolism disorder in Cd nephrotoxicity.

A dietary flavonoid quercetin from herbal foods has a variety of biological activities [17, 18]. Our previous studies have demonstrated that quercetin regulated renal

UA transport-related proteins in fructose-induced hyperuricemic rats [19] and reduced hepatic XOR hyperactivity in potassium oxonate-induced hyperuricemic mice [20], being an effective antihyperuricemic agent. Moreover, quercetin enhances lipid metabolism in triton-fed rats [21] and inhibits proinflammatory factors against Cd-induced nephrotoxicity [22]. However, the efficacy of quercetin for hyperuricemia and lipid accumulation involved in Cd nephrotoxicity has not been investigated so far.

Therefore, the present study aimed to explain the effects of Cd exposure on renal UA transport-related proteins including renal-specific transporter (RST, a homolog of hURAT1, identified in rats), OAT1, MRP4, and ABCG2 as well as XOR activity in rats. We also investigated its effects on the expression levels of lipid metabolism-related genes including renal AMP-activated protein kinase (AMPK), its downstream targets peroxisome proliferator-activated receptor α (PPAR α), organic cation transporter 2 (OCTN2), carnitine palmityl transferase 1 (CPT1), PPAR γ coactivators 1 β (PGC-1 β), and sterol regulatory element-binding protein 1 (SREBP-1) in rats, demonstrating renal lipid metabolism disorder involved in renal UA transport system dysregulation and XOR hyperactivity in Cd nephrotoxicity of rats. Furthermore, we evaluated the efficacy of quercetin treatment in ameliorating hyperuricemia and lipid accumulation in Cd-exposed rats and explored its mechanisms.

2. Materials and Methods

2.1. Materials. Cadmium chloride (CdCl₂, AR) and quercetin were obtained from Sigma-Aldrich (St. Louis, MO, USA). Diagnostic kits for the activity or level of n-acetyl- β -glucosaminidase (NAG), Na⁺-K⁺-ATPase, protein, albumin (ALB), creatinine (Cr), and triglyceride (TG) were obtained from Jiancheng Biotech Institution (Nanjing, China). The enzyme-linked immunosorbent assay (ELISA) kits for L-carnitine (KA0860, Abnova), retinol-binding protein (RBP, E90929Ra, Uscn), β 2-microglobulin (β 2-MG, E0260r, EIAab) and uromodulin (UMOD, E96918Ra, Uscn), and very low-density lipoprotein (VLDL, E1847r, EIAab) were used for the study. TRIzol reagent was obtained from Invitrogen (Carlsbad, CA, USA). M-MLV reverse transcriptase was obtained from Promega (Madison, WI, USA). The primers for all the genes were designed and synthesized by Generay Biotech (Shanghai, China). Polyvinylidene difluoride membrane was obtained from Millipore (Bedford, MA, USA). Primary antibodies including rabbit polyclonal antibodies against RST and OAT1 were provided by SaiChi Biotech (Beijing, P. R. China), MRP4 by Santa Cruz (CA, USA), ABCG2 by Cell Signaling Technology (Boston, MA, USA), OCTN2 by Abcam (Cambridge, MA, USA), CPT1 by Bioss Biotech (Beijing, P. R. China), and GAPDH by Jingmei Biotech (Shanghai, P. R. China).

2.2. Animals. Male Sprague-Dawley rats (7-week old, weighing 220–240 g) were purchased from the Laboratory Animal Center (Hangzhou, Zhejiang Province, P. R. China) and housed in plastic cages with a 12:12 h light-dark cycle at a constant temperature of 22–24°C. They were given standard

chow *libitum* for study duration and allowed 1 week to adapt to laboratory environment before experiments. All procedures were carried out in accordance with Chinese legislation on the use and care of laboratory animals and with the guidelines established by the Institute for Experimental Animals of Nanjing University.

2.3. Experimental Protocol. Rats were randomly divided into 7 groups ($n = 8$ animals/group) as described below:

Group I: normal control. Rats were treated with saline (vehicle) by intragastric gavage (i.g.) at 8:00 AM and received saline (i.g.) at 2:00 PM;

Group II: rats were daily exposed to 3 mg/kg Cd at 8:00 am and received saline at 2:00 pm;

Group III: rats were daily exposed to 6 mg/kg Cd at 8:00 am and received saline at 2:00 pm;

Group IV: rats were daily exposed to 3 mg/kg Cd at 8:00 am and received 50 mg/kg quercetin at 2:00 pm;

Group V: rats were daily exposed to 3 mg/kg Cd at 8:00 am and received 100 mg/kg quercetin at 2:00 pm;

Group VI: rats were daily exposed to 6 mg/kg Cd at 8:00 am and received 50 mg/kg quercetin at 2:00 pm;

Group VII: rats were daily exposed to 6 mg/kg Cd at 8:00 am and received 100 mg/kg quercetin at 2:00 pm.

The doses of Cd were selected because that evidently induced changes in renal structure and function in rats [23, 24]. The doses of quercetin were selected because that showed protective effects on Cd-induced nephrotoxicity [22]. Furthermore, our preliminary experiments demonstrated hyperuricemia with dyslipidemia in 3 and 6 mg/kg Cd-exposed rats after 4 weeks, which were restored by the treatment of quercetin.

2.4. Urine, Blood, and Tissue Collection. At periodic intervals (the end of weeks 0, 1, 2, 3, and 4, resp.), rats were placed in metabolic cages individually for 24 h to collect urine over ice. Each urine sample was centrifuged at 3,000 \times g (5 min, 4°C), and the volume was recorded. The supernatant was used for assays of NAG activity as well as UA, RBP, β 2-MG, UMOD, ALB and protein levels. At the end of week 4, blood samples from rat's retroorbital venous plexus at 9:00-10:00 a.m. were centrifuged at 3,000 \times g (5 min, 4°C) to get serum and then stored at 4°C for analyses of UA, Cd, Cr, L-carnitine, TG and VLDL levels, respectively. Then, rats were killed by decapitation, their kidney tissues were dissected quickly on ice and stored at –80°C for assays, respectively.

2.5. Determination of Biochemistry Parameters in Urine, Serum, and Kidney. Urine NAG activity, protein and ALB levels were measured using standard diagnostic kits, respectively. Serum, urine and renal L-carnitine, RBP, β 2-MG and UMOD levels were measured using ELISA kits, respectively. UA levels in serum (Sur) and urine (Uur) were determined by the phosphotungstic acid method [25]. Cr levels in serum (Scr) and urine (Ucr) were determined spectrophotometrically

TABLE 1: Summary of the sequences of RT-PCR primers, the appropriate annealing temperature used in experiments, and product size.

Genes	Primer	Annealing temperature (°C)	Product size (bp)
GAPDH	S 5'-TCAACGGCACAGTCAAGG-3'	54	299
	A 5'-ACCAGTGGATGCAGGGAT-3'		
RST	S 5'-CACAGTGGGCAGACTGGACCAGAGC-3'	57	412
	A 5'-CCAAGGATGAGCGAAGGA-3'		
OAT1	S 5'-TAATACCGAAGAGCCATACGA-3'	56	358
	A 5'-TCCTGCTGCTGTTGATTCTGC-3'		
MRP4	S 5'-AAATCGGAATCTCCTGTCTG -3'	56	203
	A 5'-TATGAGGTCGGCGAATGA-3'		
ABCG2	S 5'-TAGCAGCAAGGAAAGAC-3'	54	835
	A 5'-TGATGACAGAACGAGGTA-3'		
XDH	S 5'-CTTTGCGAAGGATGAGGTT-3'	58	412
	A 5'-CACTCGGACTACGATTCTGTT-3'		
CPT1	S 5'-CCACGAAGCCCTCAAACAGA-3'	57	315
	A 5'-AGCACCTTCAGCGAGTAGCG-3'		
OCTN2	S 5'-AGGTTTGGTTCGCAAGAATG-3'	56	458
	A 5'-AACTCACTGGGATCGAAGAT-3'		
PPAR α	S 5'-GGCTCGGAGGGCTCTGTCATC-3'	56	655
	A 5'-ACATGCACTGGCAGCAGTGGGA-3'		
SREBP-1	S 5'-GGAGCGAGCATTGAACTGTAT-3'	58	344
	A 5'-GGGCAGCCTTGAAGGAGTA-3'		
PGC-1 β	S 5'-GGTACAGCTCATTCGCTACAT-3'	58	210
	A 5'-TAGGGCTTGCTAACATCACA-3'		

using standard diagnostic kit (picric acid assay). Fractional excretion of UA (FE_{UA}) is suggested to be a reliable indicator for renal UA excretion. This study calculated FE_{UA} using the formula: $FE_{UA} = (U_{ur} \times S_{cr}) / (S_{ur} \times U_{cr}) \times 100$, expressed as percentage. For TG assay, serum and kidney samples were determined using Van Handel-Caslson method. VLDL levels were measured using ELISA kit. Renal $Na^+ - K^+ - ATPase$ activity was measured using standard diagnostic kit. For XO and XDH activity assays, renal cortex tissues were homogenized in 10 w/v 50 mM ice-cold potassium phosphate buffer (pH7.4) containing 5 mM ethylenediamine tetraacetic acid disodium salt and 1 mM phenylmethanesulfonyl fluoride (AMRESCO Inc, OH, USA) and centrifuged at $12,000 \times g$ (15 min, 4°C). The supernatant fraction was centrifuged at $12,000 \times g$ (15 min, 4°C) once again and then used to detect XO and XDH activity by the method described previously [26].

2.6. RNA Isolation and Reverse Transcription-PCR. Total RNA was extracted from rat kidney using TRIzol reagent. The homogenate was mixed with 200 μ L chloroform and then centrifuged at $12,000 \times g$ for 15 min. Aqueous phase (about 0.5 mL upper layer) was precipitated with equal volume of isopropanol and centrifuging at $12,000 \times g$ for 10 min. The final RNA total pellet was resuspended in 20 μ L DEPC water. Reverse transcription was performed with 1 μ g RNA using M-MLV reverse transcriptase for cDNA synthesis. PCR amplification was carried out using gene-specific PCR primers. The sequences of PCR primers were listed

in Table 1. PCR products were electrophoresed on 1.2% agarose gels, visualized with Bio-Rad ChemiDoc XRS Gel Documentation system, and then quantified using Bio-Rad Quantity One 1D analysis software. Relative quantitation for PCR products was calculated by normalization to the amount of GAPDH mRNA levels.

2.7. Protein Preparation and Western Blot Analysis. Rat renal cortex was homogenized in 10 w/v buffer (10 mM Tris-HCl, 1 mM ethylenediaminetetra-acetic acid and 250 mM sucrose, pH 7.4, containing 15 μ g/mL aprotinin, 5 μ g/mL leupeptin, and 0.1 mM phenylmethyl sulfonyl fluoride), using a Polytron at setting 5 for 20 s, and centrifuged at $3,000 \times g$ for 15 min. The supernatant was centrifuged at $12,000 \times g$ for 20 min. The final peptide samples were dissolved in Tris-HCl buffer (pH 7.5) containing 150 mM NaCl, 0.1% SDS, 1% NP-40, and 1% PMSF. After resolution of 75 μ g protein by 12% SDS-PAGE using Power Pac Basic electrophoresis apparatus (Bio-Rad, Hercules, CA, USA), protein samples were electrophoretically transferred onto PVDF membranes (Millipore, Shanghai, China), respectively. The membranes were blocked with 5% skim milk for 1 h and subsequently incubated with primary and secondary antibodies. Primary antibodies included rabbit polyclonal antibodies against RST (1:2000, NP_001030115), OAT1 (1:2000, NP_058920), MRP4 (1:1000, AAS78928.1) ABCG2 (1:1000, NP_852046.1), OCTN2 (1:200, NP_062142.1), CPT1(1:1000, NP_113747.2), and GAPDH (1:5000, NP_058704.1). Reactivity was detected using an anti-rabbit

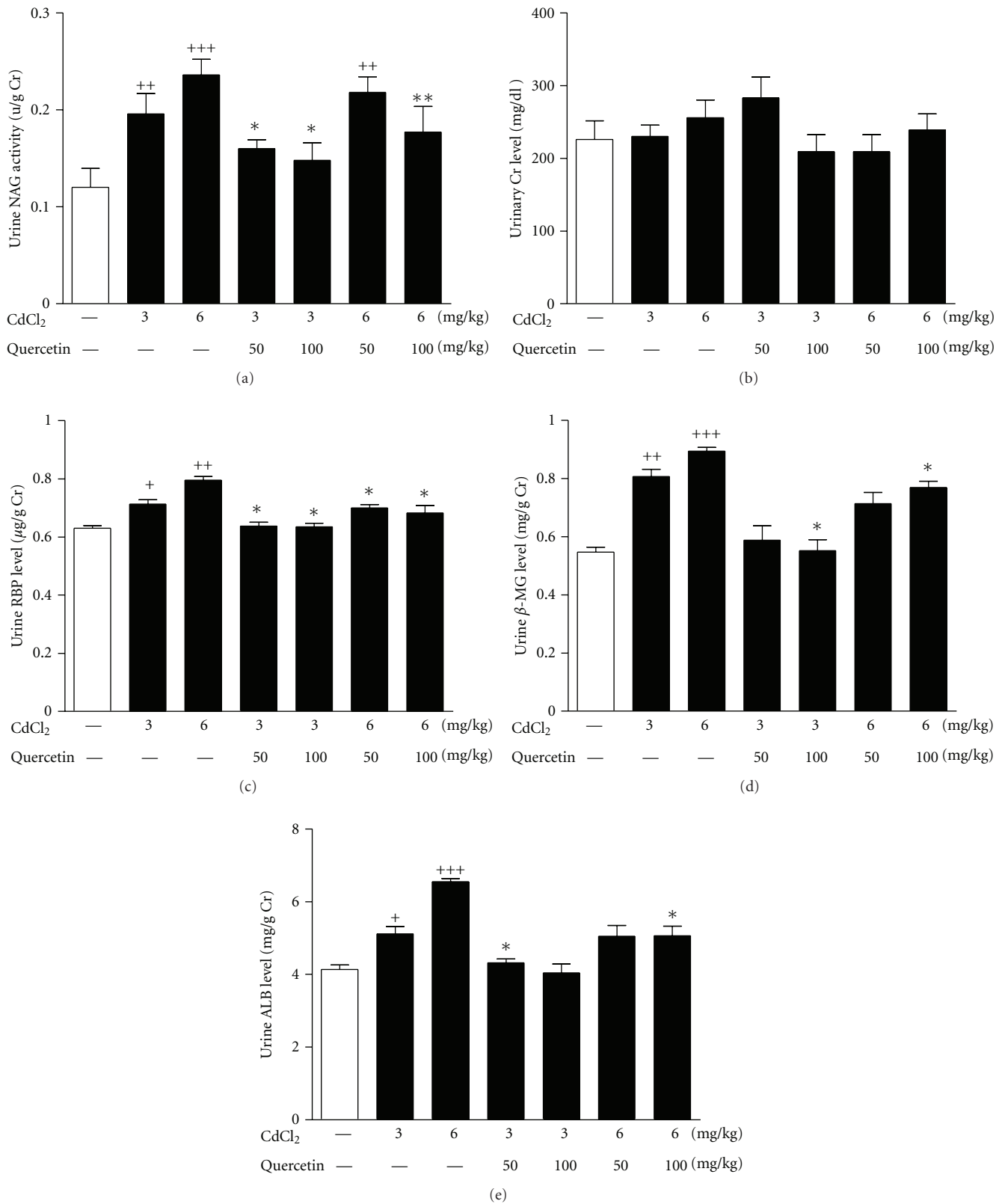


FIGURE 1: Effects of a 4-week treatment of CdCl₂ and coadministration of quercetin on urinary activity of NAG (a), levels of Cr (b), RBP (c), β₂-MG (d), and ALB (e) in rats. Values are mean ± SEM of *n* = 8 in each group. *P* value CdCl₂ versus control at + <0.05, ++ <0.01, and +++ <0.001; treatment versus CdCl₂ at * <0.05 and ** <0.01 for LSD post hoc test.

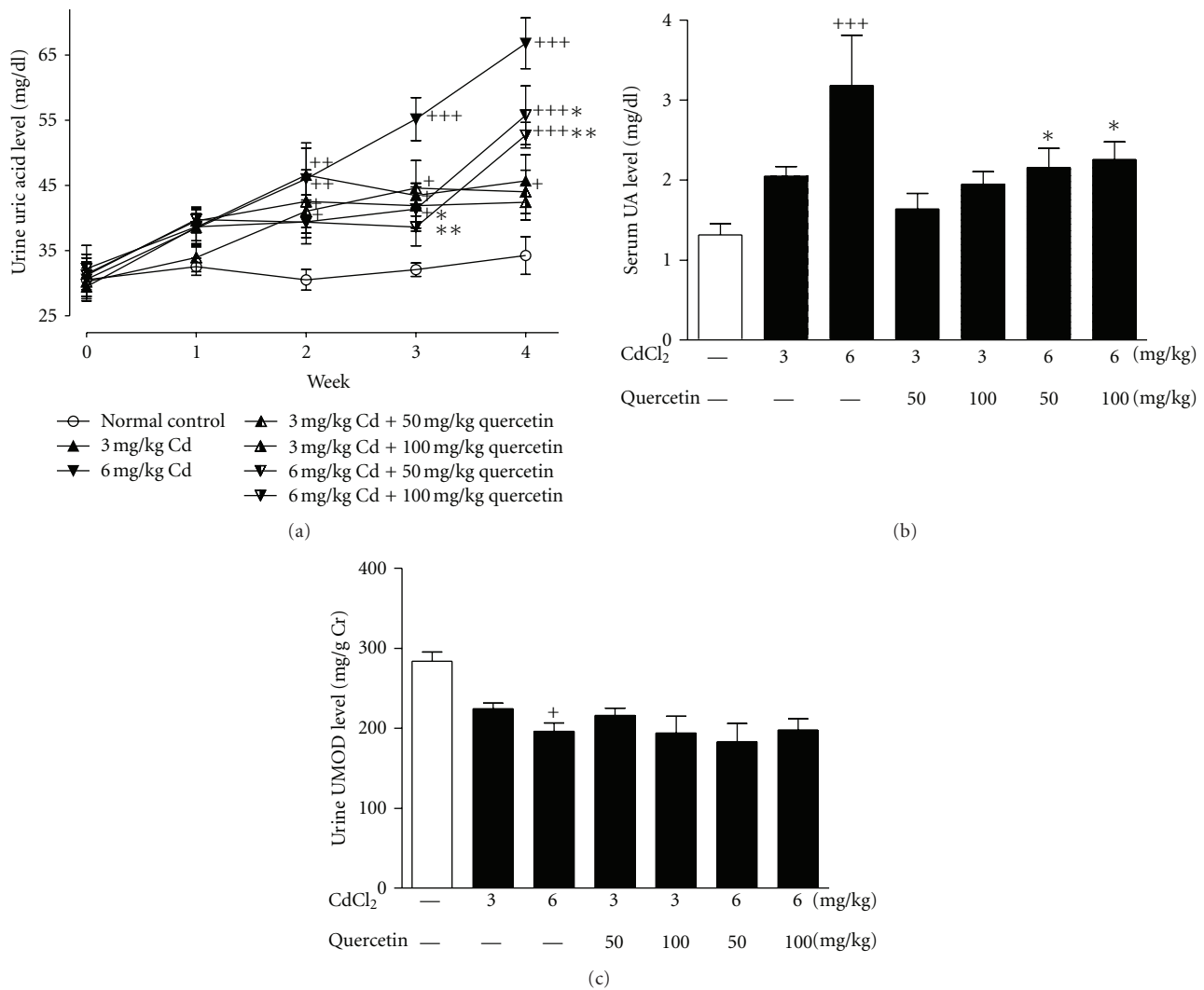


FIGURE 2: Effects of a 4-week treatment of CdCl₂ and coadministration of quercetin on weekly urine UA levels (a), levels of serum UA (b), and urine UMOD (c) at the end of week 4. Values are mean \pm SEM of $n = 8$ in each group. P value CdCl₂ versus control at $^+ < 0.05$, $^{++} < 0.01$, $^{+++} < 0.001$; treatment versus CdCl₂ at $^* < 0.05$ and $^{**} < 0.01$ for LSD post hoc test.

horseradish peroxidase-linked secondary antibody (1 : 1000). Immunoreactive bands were visualized via the Phototope-horseradish peroxidase Western Blot Detection System (Cell Signaling Technologies) and quantified via densitometry using Molecular Analyst software (Bio-Rad Laboratories, Hercules, CA, USA).

2.8. Histological Analyses. Rat kidney cortex was immediately fixed for 1 day at room temperature in 10% neutral buffered formalin for histopathological examination. Renal biopsies were dehydrated with a graded series of alcohol and embedded in paraffin. Specimens were cut in 7 μ m thick sections on a rotary microtome and mounted on APES-coated glass slides. Each section was deparaffinized in xylene, rehydrated in decreasing concentrations of alcohol in water, and stained with hematoxylin-eosin reagent (Sigma). The slide was mounted with neutral balsam. Another kidney cortex was snap-frozen immediately at -70°C . 6 μ m-thick

cryostat sections were prepared on APES-coated glass slides. Each section was washed by distilled water and then stained with oil red O reagent (Sigma) for 5–10 min. After being washed with 60% isopropyl alcohol, the section was restained by hematoxylin.

2.9. Statistical Analysis. All data were expressed as mean \pm SEM. Statistical analysis for experimental groups was performed by using a one-way analysis of variance followed by LSD post hoc test. P value < 0.05 was considered to be statistically significant. Figures were obtained by GraphPad Prism 4 (GraphPad Software, Inc., San Diego, CA, USA).

3. Results

3.1. Body Weight and General Biomarkers of Nephropathy. In order to monitor the efficacy of Cd and subsequent quercetin treatment, body weight as well as urinary macromolecular

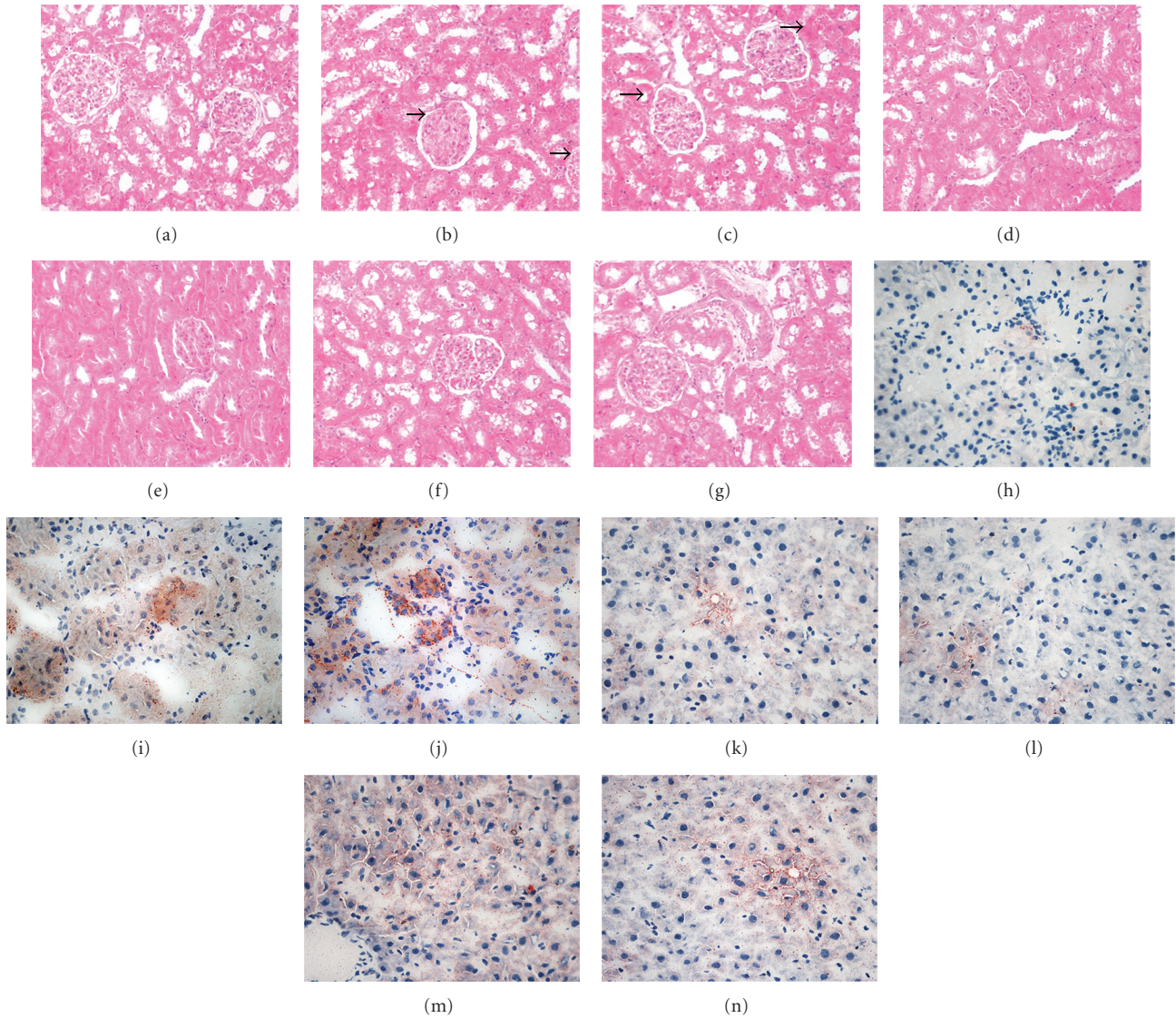


FIGURE 3: Renal cortex morphology in rats of a 4-week treatment of CdCl₂ exposure and coadministration of quercetin. The kidney tissue slices were stained with hematoxylin or oil red O and then observed by microscope (original magnification $\times 200$). Normal rat kidney (a) showed the identical structure of glomerulus and proximal tubules. CdCl₂ exposure at 3 mg/kg (b) and 6 mg/kg (c) induced moderate inflammatory infiltration (black arrows). Quercetin at 50 mg/kg (d; f) and 100 mg/kg (e; g) significantly attenuated CdCl₂-induced inflammatory infiltration around glomerulus and proximal tubules in kidney of rats. Normal rat kidney (h) showed no lipid deposition. CdCl₂ exposure at 3 mg/kg (i) and 6 mg/kg (j) induced moderate lipid deposition (red). Quercetin at 50 mg/kg (k; m) and 100 mg/kg (l; n) significantly attenuated CdCl₂-induced renal lipid deposition in renal tubular epithelial cells by oil red O-stain analysis.

enzyme activity and protein level was measured, respectively. As shown in Table 2, Cd exposure caused body weight reduction in rats ($P < 0.001$) compared with control group during the experimental period; however, quercetin treatment failed to restore this change.

Dysfunction and damage of renal tubules are characterized by the increased activity of urine NAG/Cr [23]. Figure 1(a) showed that Cd at 3 mg/kg ($P < 0.01$) and 6 mg/kg ($P < 0.001$) increased urine NAG activity in rats. Quercetin at 50 and 100 mg/kg significantly inhibited NAG activity ($P < 0.05$) in 3 mg/kg Cd-exposed rats, the latter decreased NAG activity ($P < 0.01$) in 6 mg/kg Cd-exposed

rats. In addition, there were no significant changes of Cr levels in serum (data not shown) and urine (Figure 1(b)) among the tested groups.

As sensitive markers of macromolecular protein for renal tubular injury, urine levels of RBP (3 mg/kg: $P < 0.05$; 6 mg/kg: $P < 0.01$), β_2 -MG (3 mg/kg: $P < 0.01$; 6 mg/kg: $P < 0.001$), and ALB (3 mg/kg: $P < 0.05$; 6 mg/kg: $P < 0.001$) were significantly increased in rats after Cd exposure (Figures 1(c)-1(e)). Urine RBP and β_2 -MG levels in 3 and 6 mg/kg Cd-exposed rats were significantly decreased by the treatment of 100 mg/kg quercetin ($P < 0.05$), so were urine ALB in 6 mg/kg Cd-exposed rats. 50 mg/kg quercetin

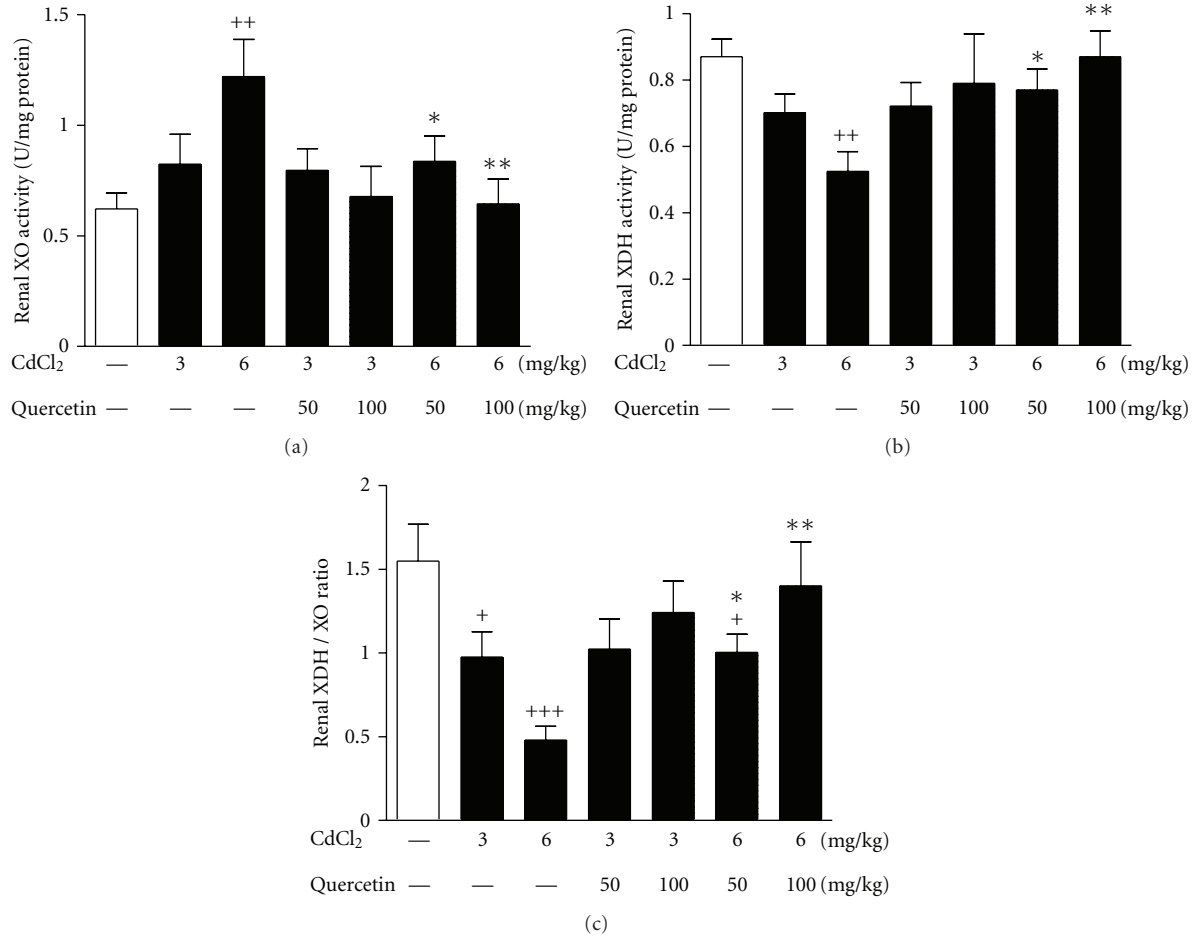


FIGURE 4: Effects of a 4-week treatment of CdCl₂ and coadministration of quercetin on renal XO (a), XDH activity (b) and XDH/XO ratio in rats (c). Values are mean \pm SEM of $n = 6-8$ in each group. P value CdCl₂ versus control at $^+ < 0.05$, $^{++} < 0.01$, and $^{+++} < 0.001$; treatment versus CdCl₂ at $^* < 0.05$ and $^{**} < 0.01$ for LSD post hoc test.

TABLE 2: Effects of a 4-week treatment of cadmium chloride (CdCl₂) and coadministration of quercetin on body weight (g) in rats. (Values are mean \pm SEM from eight rats in each group).

Group	Body weight (g)
Normal control	352.4 \pm 11.9
3 mg/kg CdCl ₂	323.0 \pm 18.5 ⁺
3 mg/kg CdCl ₂ + 50 mg/kg quercetin	309.8 \pm 9.3 ⁺⁺⁺
3 mg/kg CdCl ₂ + 100 mg/kg quercetin	309.7 \pm 9.3 ⁺⁺⁺
6 mg/kg CdCl ₂	305.4 \pm 18.5 ⁺⁺⁺
6 mg/kg CdCl ₂ + 50 mg/kg quercetin	309.3 \pm 14.1 ⁺⁺⁺
6 mg/kg CdCl ₂ + 100 mg/kg quercetin	310.1 \pm 7.6 ⁺⁺⁺

P value CdCl₂ versus control at $^+ < 0.05$ and $^{+++} < 0.001$.

significantly decreased urine RBP levels ($P < 0.05$) in 3 and 6 mg/kg Cd-exposed rats and urine ALB levels ($P < 0.05$) in 3 mg/kg Cd-exposed rats (Figures 1(c)–1(e)).

UA is a biomarker of nephropathy, and its detection is stable and easy. Compared with control group, urine UA levels were increased in rats exposed to Cd from week 2

and maintained until week 4 (3 mg/kg Cd: week 2, $P < 0.01$, week 3, $P < 0.05$, and week 4, $P < 0.05$; 6 mg/kg Cd: week 2, $P < 0.01$, week 3, $P < 0.001$, and week 4, $P < 0.001$) (Figure 2(a)). The decreased urine UA levels were observed in 6 mg/kg Cd-exposed rats receiving quercetin at week 4 (quercetin 50 mg/kg: $P < 0.05$; 100 mg/kg: $P < 0.01$). Furthermore, 6 mg/kg Cd exposure increased serum UA levels in rats compared with normal control ($P < 0.001$), which were significantly restored by the treatment of quercetin ($P < 0.05$) (Figure 2(b)). UMOD is a useful marker of renal dysfunction associated with hyperuricemia. The decreased urine UMOD levels ($P < 0.05$) were observed in 6 mg/kg Cd-exposed rats. Quercetin did not affect urine UMOD levels in Cd-exposed rats (Figure 2(c)).

Microscopically, 3 and 6 mg/kg Cd-induced mild inflammatory infiltration was observed in renal cortex of rats, which was remarkably ameliorated by the treatment of quercetin (Figures 3(a)–3(f)).

3.2. XOR Activity and Expression. We next examined renal activity and expression of XOR, which plays an important role in UA synthesis. 6 mg/kg Cd exposure significantly

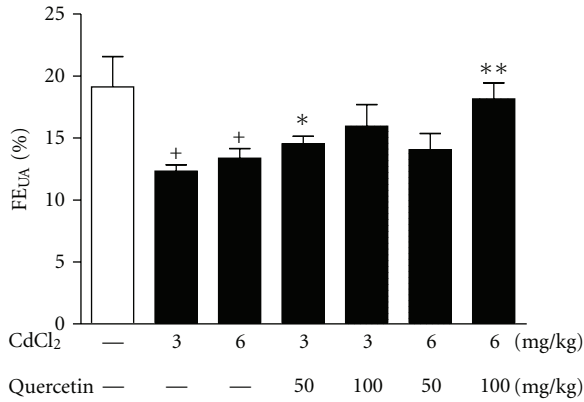


FIGURE 5: Effects of a 4-week treatment of CdCl₂ and coadministration of quercetin on kidney handling fractional excretion of UA (FE_{UA}) in rats. Values are mean ± SEM of $n = 8$ in each group. P value CdCl₂ versus control at + < 0.05 ; treatment versus CdCl₂ at * < 0.05 and ** < 0.01 for LSD post hoc test.

increased renal activity of XO ($P < 0.01$) in rats compared with normal control, which were restored by quercetin at 50 mg/kg ($P < 0.05$) and 100 mg/kg ($P < 0.01$) (Figure 4(a)). However, 6 mg/kg Cd exposure relatively decreased renal activity of XDH ($P < 0.01$) (Figure 4(b)) with significantly decreased XDH/XO ratio ($P < 0.001$) (Figure 4(c)), which were restored by quercetin treatment. Both Cd exposure and quercetin treatment failed to significantly alter renal XDH mRNA levels in rats (data not shown).

3.3. FE_{UA}. FE_{UA} is investigated with the unbalanced bidirectional transport of UA in renal proximal tubules, supporting the predominant mechanism for hyperuricemia and renal UA underexcretion [19, 27]. FE_{UA} in 3 and 6 mg/kg Cd-exposed rats were significant lower than that of normal control ($P < 0.05$) (Figure 5). Quercetin significantly increased FE_{UA} in rats exposed to Cd at 3 mg/kg (50 mg/kg: $P < 0.05$) and 6 mg/kg (50 mg/kg: $P < 0.01$; 100 mg/kg: $P < 0.001$), suggesting that quercetin may enhance renal UA excretion.

3.4. Expression of UA Transport-Related Proteins and Activity of Na⁺-K⁺-ATPase. In order to explore the reasons for renal UA excretion abnormality, we examined the expression levels of renal RST, OAT1, MRP4, and ABCG2 in Cd-exposed rats by RT-PCR and Western blot analyses, respectively. As shown in Figures 6 and 7, Cd exposure significantly increased RST mRNA (3 mg/kg: $P < 0.05$; 6 mg/kg: $P < 0.01$) (Figure 6(a)) and protein (3 mg/kg: $P < 0.05$; 6 mg/kg: $P < 0.001$) (Figure 7(a)) levels and decreased OAT1 mRNA (3 mg/kg: $P < 0.05$; 6 mg/kg: $P < 0.01$) (Figure 6(b)) and protein (6 mg/kg: $P < 0.01$) levels (Figure 7(b)) in the kidney of rats compared with normal control. Cd exposure suppressed renal mRNA levels of MRP4 (6 mg/kg: $P < 0.05$) (Figure 6(c)) and ABCG2 (3 and 6 mg/kg: $P < 0.001$) (Figure 6(d)) and increased renal protein levels of ABCG2 (6 mg/kg: $P < 0.05$) (Figure 7(d)) in rats. Moreover, 100 mg/kg quercetin ameliorated 3 mg/kg Cd-induced changes of RST mRNA levels ($P < 0.05$) in rats

(Figure 6(a)). Meanwhile, quercetin ameliorated 6 mg/kg Cd-induced changes of RST mRNA levels (50 and 100 mg/kg: $P < 0.01$) (Figure 6(a)) and protein levels (100 mg/kg: $P < 0.05$) (Figure 7(a)) in rats. The changed expression levels of renal OAT1 mRNA (100 mg/kg: $P < 0.05$) and protein (50 and 100 mg/kg: $P < 0.05$) in 6 mg/kg Cd-exposed rats were also restored by the treatment of quercetin (Figures 6(b) and 7(b)). However, quercetin performed no effects on renal MRP4 and ABCG2 in Cd-exposed rats.

Na⁺-K⁺-ATPase is an energy supplier for some of UA transport-related proteins such as OAT1 [28]. Cd exposure significantly decreased renal Na⁺-K⁺-ATPase activity in rats compared with normal control (3 mg/kg: $P < 0.05$; 6 mg/kg: $P < 0.001$) (Figure 6(e)). However, quercetin failed to affect the activity in Cd-exposed rats.

3.5. Serum and Renal TG and VLDL Levels. UA and XOR are confirmed to be related to lipid metabolism [13], we addressed the question whether Cd nephrotoxicity was correlated to renal lipid metabolism disorder. Thus, TG and VLDL levels were detected in Cd-exposed rats. Cd exposure increased TG levels in serum (6 mg/kg: $P < 0.001$) and kidney (3 and 6 mg/kg: $P < 0.001$) of rats compared with normal control (Figures 8(a) and 8(b)), exhibiting renal lipid accumulation. 100 mg/kg quercetin significantly reduced serum TG levels ($P < 0.05$) in 6 mg/kg Cd-exposed rats (Figure 8(a)). The increased renal TG levels were ameliorated by the treatment of quercetin at 50 mg/kg ($P < 0.05$) and 100 mg/kg ($P < 0.01$) in 3 and 6 mg/kg Cd-exposed rats (Figure 8(b)). However, Cd exposure did not significantly change serum and renal VLDL levels (Figures 8(c) and 8(d)). 100 mg/kg quercetin reduced renal VLDL levels ($P < 0.01$) in 6 mg/kg Cd-exposed rats (Figure 8(d)).

Moreover, oil red staining analysis revealed moderate lipid deposition observed in tubular epithelial cells in renal tissue sections of Cd-exposed rats, which could be improved by the treatment of quercetin (Figures 3(h)–3(n)).

3.6. L-Carnitine Levels and Expression of Renal Lipid Metabolism-Related Genes. L-carnitine is essential to fatty acid β -oxidation from mitochondrial membrane mediated by CPT1. OCTN2 is an important transporter for L-carnitine reabsorption [29]. However, no significant changes of L-carnitine levels in serum, urine, and kidney cortex were observed in the tested groups (data not shown). Cd exposure reduced renal levels of OCTN2 and CPT1 mRNA (3 mg/kg: $P < 0.05$; 6 mg/kg: $P < 0.001$) (Figures 9(a) and 9(b)) and protein ($P < 0.001$) (Figures 9(g) and 9(h)) in rats compared with normal control. These data indicated that Cd-induced OCTN2 downregulation did not affect L-carnitine levels, which might not be an important factor to cause renal lipid metabolism disorder in Cd nephrotoxicity of rats.

Next, we analyzed whether Cd exposure affected the expression levels of other lipid metabolism-related genes in the kidney of rats. Compared with normal control, Cd exposure significantly suppressed renal mRNA levels of AMPK (Figure 9(c)) and PPAR α (Figure 9(d)) (3 mg/kg: $P < 0.01$; 6 mg/kg: $P < 0.001$). Cd-induced elevation in renal

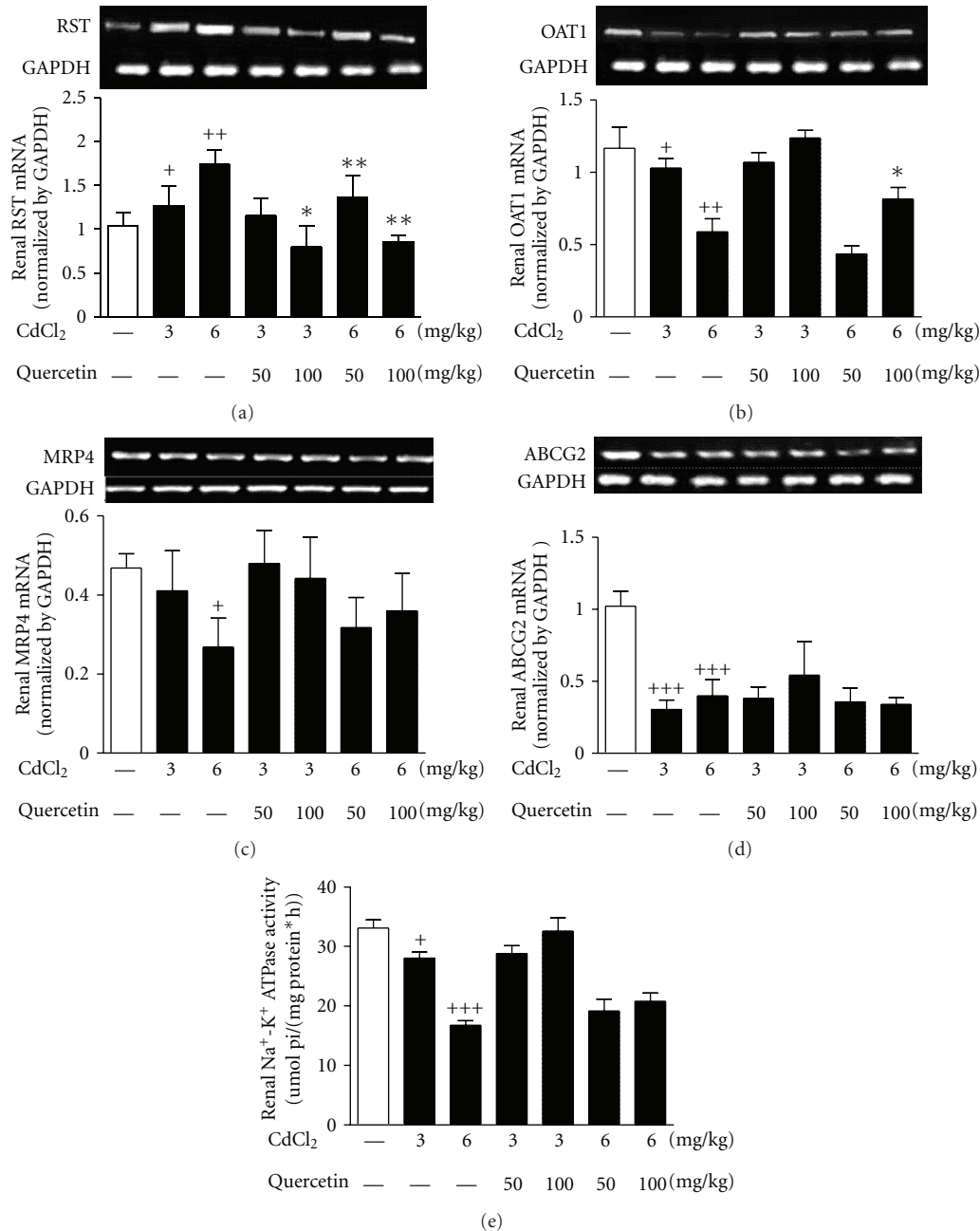


FIGURE 6: Effects of a 4-week treatment of CdCl₂ and coadministration of quercetin on expression of RST (a), OAT1 (b), MRP4 (c), and ABCG2 (d) at mRNA levels and activity of Na⁺-K⁺-ATPase (e) in renal cortex of rats. The mRNA levels were normalized by GAPDH. Values are mean ± SEM of *n* = 4–6 in each group. *P* value CdCl₂ versus control at ⁺ < 0.05, ⁺⁺ < 0.01, and ⁺⁺⁺ < 0.001; treatment versus CdCl₂ at ^{*} < 0.05 and ^{**} < 0.01 for LSD post hoc test.

mRNA levels of and SREBP-1 (Figure 9(e)) and PGC-1β (Figure 9(f)) (3 mg/kg: *P* < 0.05; 6 mg/kg: *P* < 0.001) was observed in rats.

Quercetin treatment increased AMPK in rats exposed to Cd at 3 mg/kg (100 mg/kg: *P* < 0.05) and 6 mg/kg (50 and 100 mg/kg: *P* < 0.05) (Figure 9(c)). Quercetin at 100 mg/kg also ameliorated 3 mg/kg Cd-induced downregulation of renal PPARα mRNA levels (*P* < 0.05) (Figure 9(d)) as well as 6 mg/kg Cd-induced downregulation of renal OCTN2 protein levels (Figure 9(g)), CPT1 mRNA, and protein

levels (*P* < 0.05) in rats (Figures 9(b) and 9(h)). Moreover, quercetin significantly downregulated renal SREBP-1 (50 mg/kg: *P* < 0.05) and PGC-1β (100 mg/kg: *P* < 0.01) (Figures 9(e) and 9(f)) in Cd-exposed rats.

4. Discussion

The main findings of this study were that Cd exposure induced renal UA transport system dysfunction with XOR hyperactivity and impaired renal AMPK-PPARα/PGC-1β

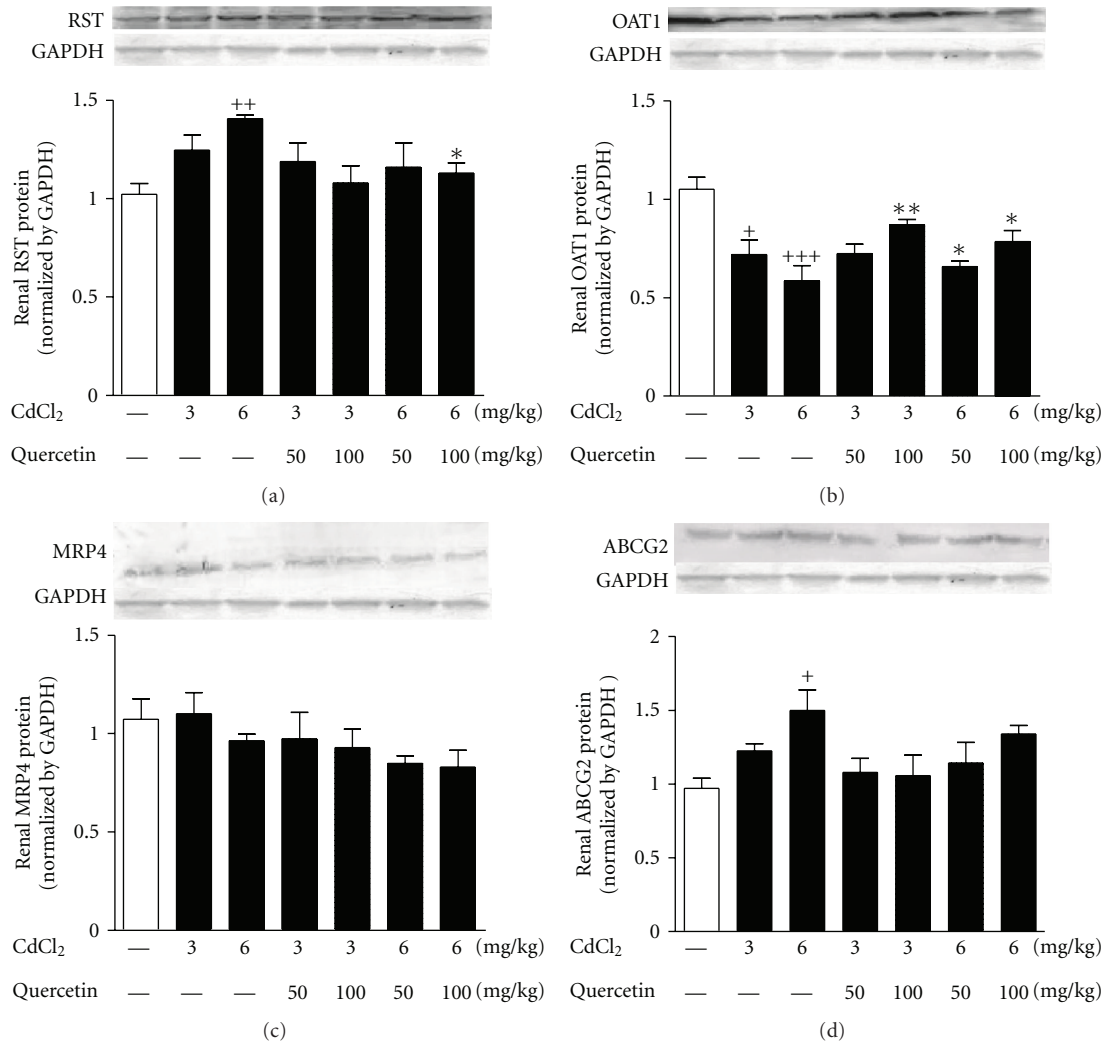


FIGURE 7: Effects of a 4-week treatment of CdCl₂ and coadministration of quercetin on expression of RST (a), OAT1 (b), MRP4 (c), and ABCG2 (d) at protein levels in renal cortex of rats. The protein levels were normalized by GAPDH. Values are mean \pm SEM of $n = 4-6$ in each group. P value CdCl₂ versus control at ⁺ <0.05 , ⁺⁺ <0.01 , ⁺⁺⁺ <0.001 ; treatment versus CdCl₂ at ^{*} <0.05 , and ^{**} <0.01 for LSD post hoc test.

signal pathway, resulting in renal lipid accumulation involved in Cd nephrotoxicity of rats. By administering a dietary flavonoid quercetin to Cd-exposed rats, it ameliorated renal UA transport system dysfunction with XOR hyperactivity and subsequently improved renal AMPK-PPAR α /PGC-1 β signal pathway impairment to restore disorder of renal lipid metabolism, exhibiting its nephroprotection.

The kidney is the primary critical target of toxicity, where Cd accumulation reaches the threshold [23, 30–32], leading to pathological damaged levels of urine enzyme (NAG) and proteins (RBP, β 2-MG, ALB, and UMOD) observed in the present study. Quercetin treatment restored Cd-induced renal dysfunction and toxicity in rats.

In parallel with urine enzyme hyperactivity, a continued rise of serum UA levels was observed in Cd-exposed rats. The UA change could take place in the early stage of Cd exposure, as the urine UA levels increased significantly from week 2. The kidney is a target organ for Cd; therefore,

it was necessary to investigate the effects of Cd on renal XOR activity and UA transport-related proteins in rats. Being consistent with activated renal XO in Cd-exposed Swiss albino mice [33, 34], the present study confirmed activation of renal XO in Cd-exposed Sprague-Dawley rats with a significant reduction of renal XDH/XO ratio, which resulted from the increased XO activity with the relatively decreased XDH activity. These data further demonstrates that Cd enhances the conversion of XDH to XO [7] in the kidney of rats, possibly causing serious renal damage induced by XOR hyperactivity-mediated ROS. Quercetin, as a XOR inhibitor [20, 35, 36], inhibits XOR activation in the kidney of ischemia-reperfusion rat [36]. In the present study, quercetin was confirmed to prevent the conversion of renal XDH to XO, which were consistent with its attenuation of Cd-induced hyperuricemia and renal injury.

More importantly, 6 mg/kg Cd exposure was found to upregulate RST and downregulate OAT1, MRP4, and ABCG2

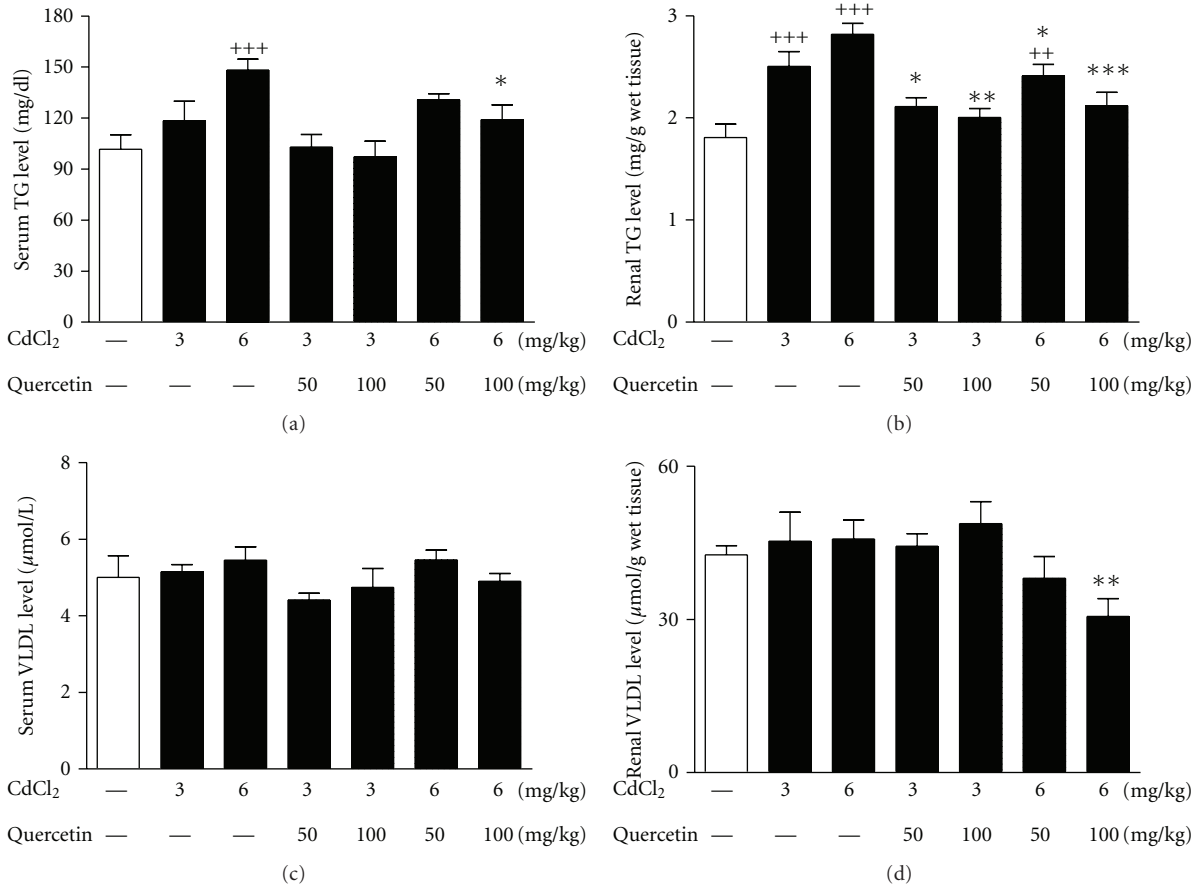


FIGURE 8: Effects of a 4-week treatment of CdCl₂ and coadministration of quercetin on TG levels in serum (a) and kidney (b); VLDL levels in serum (c) and kidney (d) in rats. Values are mean \pm SEM of $n = 8$ in each group. P value CdCl₂ versus control at ++ <0.01 and +++ <0.001; treatment versus CdCl₂ at * <0.05, ** <0.01, and *** <0.001 for LSD post hoc test.

in the kidney of rats, indicating that Cd exposure may alter renal function for UA transport. Na⁺-K⁺-ATPase is the energy supplier for some organic ion transporters such as OAT1 [28]. The altered Na⁺-K⁺-ATPase activity is incriminated to play a role in renal tubular syndrome associated with Cd-induced nephrotoxicity [37, 38]. Hypoactivity of renal rNa⁺-K⁺-ATPase was observed in the present study. Therefore, renal UA transport system dysfunction with XOR hyperactivity may be involved in the mechanisms of Cd-induced hyperuricemia and renal dysfunction in rats. Our previous study showed that quercetin restored fructose-induced dyexpression of renal RST and OAT1 in hyperuricemic rats [19]. In this study, although no effect on renal Na⁺-K⁺-ATPase activity, quercetin reduced serum UA levels, possibly through its amelioration of Cd-induced abnormality of renal RST and OAT1 to enhance renal UA excretion, resulting in relief of hyperuricemia and kidney dysfunction in rats. Thus, renal UA transport system is suggested to be target for quercetin's action in Cd nephrotoxicity.

As important cross-regulators, UA and XOR are associated with lipid metabolism [13]. XOR inhibitors allopurinol and quercetin are confirmed to prevent fructose-induced hypertriglyceridemia in rats [19, 39]. Lipids play

an important role in the progression and development of kidney diseases [14]. The present study demonstrated that Cd induced moderate lipid accumulation and deposition in renal cortex of rats with high TG levels, which were restored by the treatment of quercetin. These results indicate that alteration of renal UA transport system with XOR hyperactivity may be associated with renal lipid metabolism disorder of Cd nephrotoxicity in rats.

Lipid metabolism regulator PPAR α and its target genes OCTN2 and CPT1 are involved in mitochondrion fatty acid β -oxidation, playing an important role in nonadipose tissue [40]. PPAR α can protect renal tubular cells from doxorubicin-induced ROS [41]. Its agonists prevent renal oxidative stress and damage to improve proteinuria in hypertensive patients with renal disease [42]. Furthermore, XOR activation and ROS increase expression of PGC-1 [43], which is suggested to enhance PPAR α -mediated transcriptional activity [44, 45]. Hepatic PGC-1 β overexpression reduces the beneficial effects of PPAR α activation on gene expression, leading to hyperlipidemia [45]. In addition, PGC-1 β activates expression of lipogenic genes via direct coactivation of SREBP-1, a major regulator of fatty acids synthesis [46]. Interestingly, the present study found that

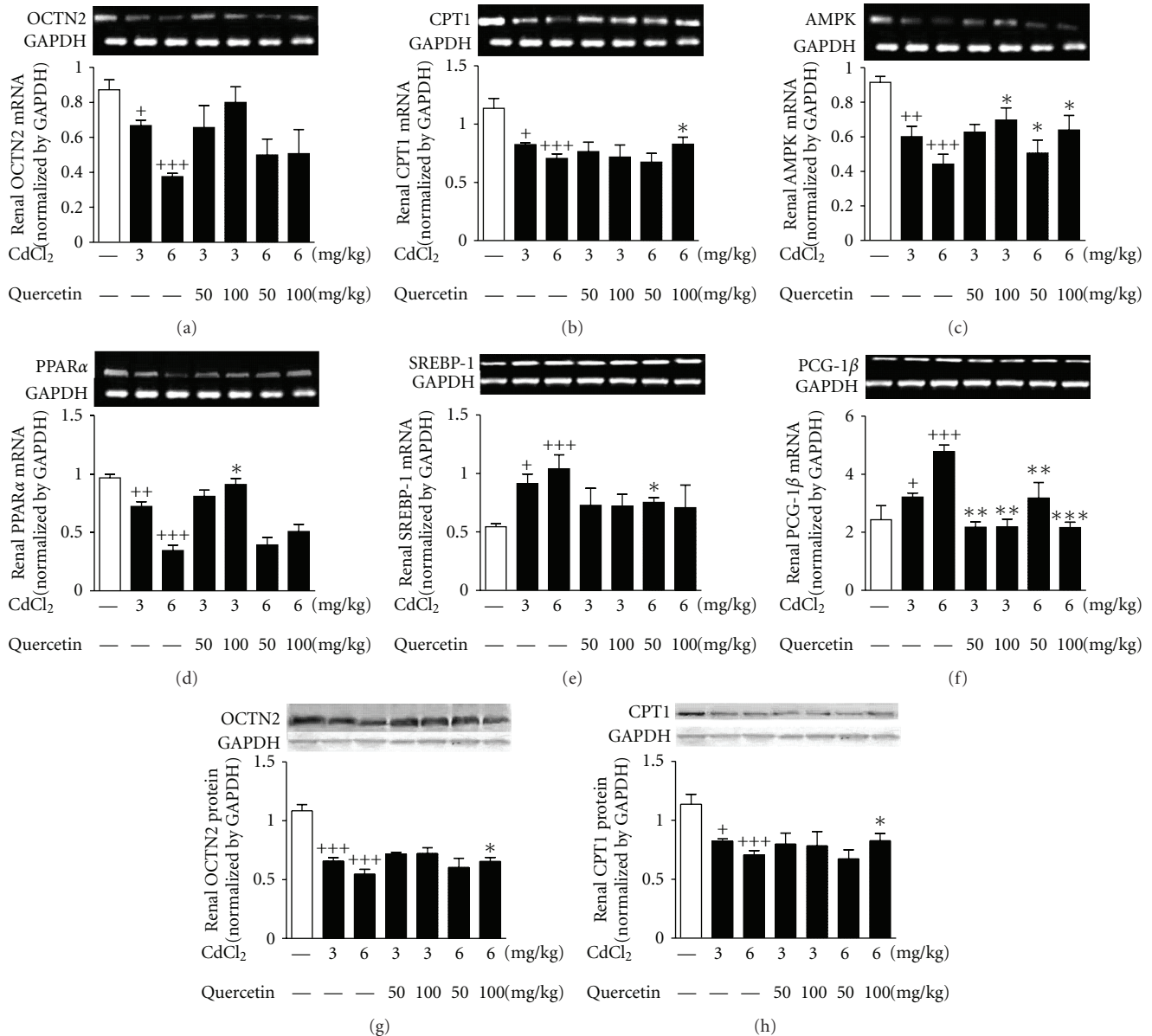


FIGURE 9: Effects of a 4-week treatment of CdCl₂ and coadministration of quercetin on expression of OCTN2 (a), CPT1 (b), AMPK (c), PPARα (d), SREBP-1 (e), PGC-1β (f) at mRNA levels, and OCTN2 (g) and CPT1 (h) at protein levels in renal cortex of rats. The mRNA levels or protein levels were normalized by GAPDH, respectively. Values are mean ± SEM of $n = 4-6$ in each group. P value CdCl₂ versus control at + < 0.05, ++ < 0.01, and +++ < 0.001; treatment versus CdCl₂ at * < 0.05, ** < 0.01, and *** < 0.001 for LSD post hoc test.

Cd exposure decreased PPARα, OCTN2, and CPT1 and increased PGC-1β expression, which possibly activated SREBP-1 in the kidney of rats. These results indicate that renal downregulation of PPARα and its target genes mediated by PGC-1β overexpression may be involved in renal reduction of fatty acid β-oxidation and disorder of lipid metabolism in Cd-exposed rats with renal UA transport function impairment with XOR hyperactivity.

It is well known that AMPK regulates downstream PPARα to affect the transcription of numerous genes including OCTN2 and CPT1 [47]. AMPK activation enhances fatty acid β-oxidation in skeletal muscle by activating PPARα

and PGC-1 [48]. Additionally, SREBP-1 is negatively regulated by AMPK. Interestingly, renal AMPK expression was downregulated in Cd-exposed rats in the present study. PPARα and its target genes are involved in cross-talking of lipid metabolism with oxidative stress by Cd-induced UA overproduction and ROS synthesis. Thus, the ability of Cd to affect renal lipid metabolism-related AMPK-PPARα/PGC-1β signal pathway possibly mediated by renal UA transport function impairment with renal XO hyperactivity may have significant implication for the pathophysiology of Cd-induced renal injury in rats. The precise mechanisms need to be further explored in suitable cell models.

Quercetin, as an activator of AMPK [49], was confirmed to upregulate AMPK, PPAR α , CPT1, and OCTN2, as well as downregulate PGC-1 β and SREBP-1 in the kidney of Cd-exposed rats, which were parallel with its restoration of renal lipid accumulation. Thus, quercetin with regulation of renal UA transport system and XOR activity may reduce renal lipid accumulation partly mediated by improving renal AMPK-PPAR α /PGC-1 β signal pathway impairment in Cd nephrotoxicity of rats.

5. Conclusion

This study demonstrated that Cd-induced UA excretion dysfunction with excess synthesis further aggravated UA congestion and made renal lesion more serious in rats. Abnormality of renal UA transport system with XOR activity may be a key target for disorder of renal lipid metabolism and induction of secondary renal damage process in rats exposed to Cd. This study was the first to focus, and confirm the relative importance of renal UA transport system dysfunction with XOR activation and AMPK-PPAR α /PGC-1 β signal pathway impairment involved in Cd nephrotoxicity of rats. Quercetin was found to ameliorate renal UA transport system dysfunction with XOR hyperactivity and improve renal AMPK-PPAR α /PGC-1 β signal pathway impairment and subsequently reduce renal lipid accumulation in rats. Quercetin may serve as antihyperuricemic and antidyslipidemic agent to prevent Cd-evoked nephrotoxicity.

Acknowledgments

This study is supported by grants from National Basic Research Program of China 973 Program no. 2012CB517600 (no. 2012CB517602), National Natural Science Foundation of China (NSFC 81025025 and J1103512), Jiangsu Natural Science Foundation (BK 2010365), and Program for Changjiang Scholars and Innovative Research Team in University (IRT1020).

References

- [1] K. Nogawa and T. Kido, "Biological monitoring of cadmium exposure in itai-itai disease epidemiology," *International Archives of Occupational and Environmental Health*, vol. 65, no. 1, pp. S43–S46, 1993.
- [2] L. Friberg, "Cadmium and the kidney," *Environmental Health Perspectives*, vol. 54, no. 3, pp. 1–11, 1984.
- [3] J. R. Edwards and W. C. Prozialeck, "Cadmium, diabetes and chronic kidney disease," *Toxicology and Applied Pharmacology*, vol. 238, no. 3, pp. 289–293, 2009.
- [4] J. Renugadevi and S. M. Prabu, "Naringenin protects against cadmium-induced oxidative renal dysfunction in rats," *Toxicology*, vol. 256, no. 1-2, pp. 128–134, 2009.
- [5] J. Renugadevi and S. Milton Prabu, "Quercetin protects against oxidative stress-related renal dysfunction by cadmium in rats," *Experimental and Toxicologic Pathology*, vol. 62, no. 5, pp. 471–481, 2010.
- [6] M. C. Ramirez-Tortosa, C. L. Ramirez-Tortosa, M. D. Mesa, S. Granados, A. Gil, and J. L. Quiles, "Curcumin ameliorates rabbits' steatohepatitis via respiratory chain, oxidative stress, and TNF- α ," *Free Radical Biology and Medicine*, vol. 47, no. 7, pp. 924–931, 2009.
- [7] A. C. Esteves and J. Felcman, "Study of the effect of the administration of Cd(II) cysteine, methionine, and Cd(II) together with cysteine or methionine on the conversion of xanthine dehydrogenase into xanthine oxidase," *Biological Trace Element Research*, vol. 76, no. 1, pp. 19–30, 2000.
- [8] W. Liu, M. Li, F. Huang, J. Zhu, W. Dong, and J. Yang, "Effects of cadmium stress on xanthine oxidase and antioxidant enzyme activities in *Boleophthalmus pectinirostris* liver," *Chinese Journal of Applied Ecology*, vol. 17, no. 7, pp. 1310–1314, 2006.
- [9] A. N. Rizwan and G. Burckhardt, "Organic anion transporters of the SLC22 family: biopharmaceutical, physiological, and pathological roles," *Pharmaceutical Research*, vol. 24, no. 3, pp. 450–470, 2007.
- [10] R. A. M. H. Van Aubel, P. H. E. Smeets, J. J. M. W. Van Den Heuvel, and F. G. M. Russel, "Human organic anion transporter MRP4 (ABCC4) is an efflux pump for the purine end metabolite urate with multiple allosteric substrate binding sites," *American Journal of Physiology*, vol. 288, no. 2, pp. F327–F333, 2005.
- [11] O. M. Woodward, A. Köttgen, J. Coresh, E. Boerwinkle, W. B. Guggino, and M. Köttgen, "Identification of a urate transporter, ABCG2, with a common functional polymorphism causing gout," *Proceedings of the National Academy of Sciences of the United States of America*, vol. 106, no. 25, pp. 10338–10342, 2009.
- [12] A. Dehghan, A. Köttgen, Q. Yang et al., "Association of three genetic loci with uric acid concentration and risk of gout: a genome-wide association study," *The Lancet*, vol. 372, no. 9654, pp. 1953–1961, 2008.
- [13] T. Ohtsubo, K. Matsumura, K. Sakagami et al., "Xanthine oxidoreductase depletion induces renal interstitial fibrosis through aberrant lipid and purine accumulation in renal tubules," *Hypertension*, vol. 54, no. 4, pp. 868–876, 2009.
- [14] C. K. Abrass, "Cellular lipid metabolism and the role of lipids in progressive renal disease," *American Journal of Nephrology*, vol. 24, no. 1, pp. 46–53, 2004.
- [15] E. V. Larregle, S. M. Varas, L. B. Oliveros et al., "Lipid metabolism in liver of rat exposed to cadmium," *Food and Chemical Toxicology*, vol. 46, no. 5, pp. 1786–1792, 2008.
- [16] L. W. Chang and J. A. Sprecher, "Pathological changes in the kidney after methyl cadmium intoxication," *Environmental Research*, vol. 12, no. 1, pp. 92–109, 1976.
- [17] F. Perez-Vizcaino, J. Duarte, R. Jimenez, C. Santos-Buelga, and A. Osuna, "Antihypertensive effects of the flavonoid quercetin," *Pharmacological Reports*, vol. 61, no. 1, pp. 67–75, 2009.
- [18] S. C. Bischoff, "Quercetin: potentials in the prevention and therapy of disease," *Current Opinion in Clinical Nutrition and Metabolic Care*, vol. 11, no. 6, pp. 733–740, 2008.
- [19] Q. H. Hu, C. Wang, J. M. Li, D. M. Zhang, and L. D. Kong, "Allopurinol, rutin, and quercetin attenuate hyperuricemia and renal dysfunction in rats induced by fructose intake: renal organic ion transporter involvement," *American Journal of Physiology*, vol. 297, no. 4, pp. F1080–F1091, 2009.
- [20] J. X. Zhu, Y. Wang, L. D. Kong, C. Yang, and X. Zhang, "Effects of *Biota orientalis* extract and its flavonoid constituents, quercetin and rutin on serum uric acid levels in oxonate-induced mice and xanthine dehydrogenase and xanthine oxidase activities in mouse liver," *Journal of Ethnopharmacology*, vol. 93, no. 1, pp. 133–140, 2004.

- [21] K. F. Santos Ricardo, T. T. De Oliveira, T. J. Nagem, A. Da Silva Pinto, M. G. A. Oliveira, and J. F. Soares, "Effect of flavonoids morin; quercetin and nicotinic acid on lipid metabolism of rats experimentally fed with triton," *Brazilian Archives of Biology and Technology*, vol. 44, no. 3, pp. 263–267, 2001.
- [22] P. Sanchez-Gonzalez, F. Perez-Barriocanal, M. Prieto, J. M. Lopez-Novoa, and A. I. Morales, "Quercetin exerts a protective effect on cadmium-induced nephrotoxicity through its ability to inhibit pro-inflammatory mediators," *Toxicology Letters*, vol. 180, no. 10, pp. S193–S193, 2008.
- [23] M. M. Brzóska, M. Kamiński, D. Supernak-Bobko, K. Zwierz, and J. Moniuszko-Jakoniuk, "Changes in the structure and function of the kidney of rats chronically exposed to cadmium. I. Biochemical and histopathological studies," *Archives of Toxicology*, vol. 77, no. 6, pp. 344–352, 2003.
- [24] M. M. Brzóska, M. Kamiński, M. Dziki, and J. Moniuszko-Jakoniuk, "Changes in the structure and function of the kidney of rats chronically exposed to cadmium. II. Histochemical studies," *Archives of Toxicology*, vol. 78, no. 4, pp. 226–231, 2004.
- [25] J. J. Carroll, H. Coburn, R. Douglass, and A. L. Babson, "A simplified alkaline phosphotungstate assay for uric acid in serum," *Clinical Chemistry*, vol. 17, no. 3, pp. 158–160, 1971.
- [26] M. Mazzali, J. Hughes, Y. G. Kim et al., "Elevated uric acid increases blood pressure in the rat by a novel crystal-independent mechanism," *Hypertension*, vol. 38, no. 5, pp. 1101–1106, 2001.
- [27] F. Perez-Ruiz, M. Calabozo, G. García Erasquin, A. Ruibal, and A. M. Herrero-Beites, "Renal underexcretion of uric acid is present in patients with apparent high urinary uric acid output," *Arthritis Care and Research*, vol. 47, no. 6, pp. 610–613, 2002.
- [28] M. A. Hediger, R. J. Johnson, H. Miyazaki, and H. Endou, "Molecular physiology of urate transport," *Physiology*, vol. 20, no. 2, pp. 125–133, 2005.
- [29] M. Matera, G. Bellinghieri, G. Costantino, D. Santoro, M. Calvani, and V. Savica, "History of L-carnitine: implications for renal disease," *Journal of Renal Nutrition*, vol. 13, no. 1, pp. 2–14, 2003.
- [30] H. Roels, A. M. Bernard, A. Cardenas et al., "Markers of early renal changes induced by industrial pollutants—III. Application to workers exposed to cadmium," *British Journal of Industrial Medicine*, vol. 50, no. 1, pp. 37–48, 1993.
- [31] A. Bernard, R. Lauwerys, and A. O. Amor, "Loss of glomerular polyanion correlated with albuminuria in experimental cadmium nephropathy," *Archives of Toxicology*, vol. 66, no. 4, pp. 272–278, 1992.
- [32] K. Nogawa, R. Honda, T. Kido et al., "A dose-response analysis of cadmium in the general environment with special reference to total cadmium intake limit," *Environmental Research*, vol. 48, no. 1, pp. 7–16, 1989.
- [33] T. Jahangir, T. H. Khan, L. Prasad, and S. Sultana, "Reversal of cadmium chloride-induced oxidative stress and genotoxicity by *Adhatoda vasica* extract in Swiss albino mice," *Biological Trace Element Research*, vol. 111, no. 1–3, pp. 217–228, 2006.
- [34] T. Jahangir, T. H. Khan, L. Prasad, and S. Sultana, "Pluchea lanceolata attenuates cadmium chloride induced oxidative stress and genotoxicity in Swiss albino mice," *Journal of Pharmacy and Pharmacology*, vol. 57, no. 9, pp. 1199–1204, 2005.
- [35] J. M. Pauff and R. Hille, "Inhibition studies of bovine xanthine oxidase by luteolin, silibinin, quercetin, and curcumin," *Journal of Natural Products*, vol. 72, no. 4, pp. 725–731, 2009.
- [36] J. Sanhueza, J. Valdes, R. Campos, A. Garrido, and A. Valenzuela, "Changes in the xanthine dehydrogenase/xanthine oxidase ratio in the rat kidney subjected to ischemia-reperfusion stress: preventive effect of some flavonoids," *Research Communications in Chemical Pathology and Pharmacology*, vol. 78, no. 2, pp. 211–218, 1992.
- [37] H. C. Gonick, "Nephrotoxicity of cadmium & lead," *Indian Journal of Medical Research*, vol. 128, no. 4, pp. 335–352, 2008.
- [38] F. Thévenod and J. M. Friedmann, "Cadmium-mediated oxidative stress in kidney proximal tubule cells induces degradation of Na⁺/K⁺-ATPase through proteasomal and endo-lysosomal proteolytic pathways," *FASEB Journal*, vol. 13, no. 13, pp. 1751–1761, 1999.
- [39] T. Nakagawa, H. Hu, S. Zharikov et al., "A causal role for uric acid in fructose-induced metabolic syndrome," *American Journal of Physiology*, vol. 290, no. 3, pp. F625–F631, 2006.
- [40] S. Eaton, "Control of mitochondrial β -oxidation flux," *Progress in Lipid Research*, vol. 41, no. 3, pp. 197–239, 2002.
- [41] H. Lin, C. C. Hou, C. F. Cheng et al., "Peroxisomal proliferator-activated receptor- α protects renal tubular cells from doxorubicin-induced apoptosis," *Molecular Pharmacology*, vol. 72, no. 5, pp. 1238–1245, 2007.
- [42] P. Gelosa, C. Banfi, A. Gianella et al., "Peroxisome proliferator-activated receptor α agonism prevents renal damage and the oxidative stress and inflammatory processes affecting the brains of stroke-prone rats," *Journal of Pharmacology and Experimental Therapeutics*, vol. 335, no. 2, pp. 324–331, 2010.
- [43] L. R. Silveira, H. Pilegaard, K. Kusuhara, R. Curi, and Y. Hellsten, "The contraction induced increase in gene expression of peroxisome proliferator-activated receptor (PPAR)- γ coactivator 1 α (PGC-1 α), mitochondrial uncoupling protein 3 (UCP3) and hexokinase II (HKII) in primary rat skeletal muscle cells is dependent on reactive oxygen species," *Biochimica et Biophysica Acta*, vol. 1763, no. 9, pp. 969–976, 2006.
- [44] R. B. Vega, J. M. Huss, and D. P. Kelly, "The coactivator PGC-1 cooperates with peroxisome proliferator-activated receptor α in transcriptional control of nuclear genes encoding mitochondrial fatty acid oxidation enzymes," *Molecular and Cellular Biology*, vol. 20, no. 5, pp. 1868–1876, 2000.
- [45] C. J. Lelliott, A. Ljungberg, A. Ahnmark et al., "Hepatic PGC-1 β overexpression induces combined hyperlipidemia and modulates the response to PPAR α activation," *Arteriosclerosis, Thrombosis, and Vascular Biology*, vol. 27, no. 12, pp. 2707–2713, 2007.
- [46] J. Lin, R. Yang, P. T. Tarr et al., "Hyperlipidemic effects of dietary saturated fats mediated through PGC-1 β coactivation of SREBP," *Cell*, vol. 120, no. 2, pp. 261–273, 2005.
- [47] P. Gervois, I. P. Torra, J. C. Fruchart, and B. Staels, "Regulation of lipid and lipoprotein metabolism by PPAR activators," *Clinical Chemistry and Laboratory Medicine*, vol. 38, no. 1, pp. 3–11, 2000.
- [48] W. J. Lee, M. Kim, H. S. Park et al., "AMPK activation increases fatty acid oxidation in skeletal muscle by activating PPAR α and PGC-1," *Biochemical and Biophysical Research Communications*, vol. 340, no. 1, pp. 291–295, 2006.
- [49] J. Ahn, H. Lee, S. Kim, J. Park, and T. Ha, "The anti-obesity effect of quercetin is mediated by the AMPK and MAPK signaling pathways," *Biochemical and Biophysical Research Communications*, vol. 373, no. 4, pp. 545–549, 2008.

Research Article

The Crude Extract from *Puerariae* Flower Exerts Antiobesity and Antifatty Liver Effects in High-Fat Diet-Induced Obese Mice

Tomoyasu Kamiya,¹ Mayu Sameshima-Kamiya,¹ Rika Nagamine,¹ Masahito Tsubata,¹ Motoya Ikeguchi,¹ Kinya Takagaki,¹ Tsutomu Shimada,² and Masaki Aburada²

¹Research and Development Division, Toyo Shinyaku Co. Ltd., 7-28 Yayoigaoka, Tosu-shi, Saga 841-0005, Japan

²Research Institute of Pharmaceutical Sciences, Musashino University, Nishitokyo-shi, Tokyo 202-8585, Japan

Correspondence should be addressed to Tomoyasu Kamiya, kamiyat@toyoshinyaku.co.jp

Received 17 January 2012; Accepted 28 March 2012

Academic Editor: Mohamed Eddouks

Copyright © 2012 Tomoyasu Kamiya et al. This is an open access article distributed under the Creative Commons Attribution License, which permits unrestricted use, distribution, and reproduction in any medium, provided the original work is properly cited.

Kudzu, a leguminous plant, has long been used in folk medicine. In particular, its flowers are used in Japanese and Chinese folk medicine for treating hangovers. We focused on the flower of Kudzu (*Puerariae thomsonii*), and we previously reported the antiobesity effect of *Puerariae thomsonii* flower extract (PFE) in humans. In this study, we conducted an animal study to investigate the effect of PFE on visceral fat and hepatic lipid levels in mice with diet-induced obesity. In addition, we focused on gene expression profiles to investigate the antiobesity mechanism of PFE. Male C57BL/6J mice were fed a high-fat diet (HFD) or an HFD supplemented with 5% PFE for 14 days. PFE supplementation significantly reduced body weight and white adipose tissue (WAT) weight. Moreover, in the histological analysis, PFE supplementation improved fatty liver. Hepatic reverse transcription-polymerase chain reaction revealed that PFE supplementation downregulated acetyl-CoA carboxylase expression. For adipose tissue, the expressions of hormone-sensitive lipase in WAT and uncoupling protein 1 in brown adipose tissue (BAT) were significantly upregulated. These results suggest that PFE exerts antiobesity and antifatty liver effects in high-fat diet-induced obese mice through suppressing lipogenesis in the liver, stimulating lipolysis in WAT, and promoting thermogenesis in BAT.

1. Introduction

Puerariae flower extract (PFE) is a crude extract from the flowers of Kudzu (*Puerariae thomsonii*). It contains approximately 20 percent of isoflavones as the major ingredient. In Japan, PFE is utilized as nutritional supplement for treatment of hangovers and obesity.

Kudzu, a leguminous plant distributed in Japan, China, and other areas, has long been used in folk medicine. In particular, *Puerariae* flowers are used in Japanese and Chinese folk medicine for treating hangovers [1–3]. Niiho et al. confirmed that the *Puerariae lobata* flower exerts hepatoprotective effects in individuals with liver injury induced by carbon tetrachloride or a high-fat diet in animal studies [1, 3]. Recently, research of the effects of Kudzu on lipid metabolism and obesity was reported. Wang et al. confirmed that flavones derived from *Radix Puerariae* exert inhibitory effects on body weight, abdominal fat content, and lipid levels in the liver [4]. In addition, we preliminarily investigated the effect of PFE

on body weight in humans and found that PFE intake might reduce body weight and abdominal fat content in mildly obese subjects [5]. However, the antiobesity mechanism of PFE is not known.

Obesity is a well-established risk factor for the development of hypertension, diabetes, dyslipidemia, and cancers, and it causes premature death [6]. An increase in visceral fat is responsible for many of the metabolic abnormalities, such as impaired glucose tolerance, insulin resistance, and increased very-low-density lipoprotein triglyceride (VLDL-TG) levels, associated with abdominal obesity [7–9]. In addition, it is reported that approximately 50% of cases of obesity involving visceral fat accumulation are complicated by fatty liver [10]. Fatty liver is a reversible condition in which triglycerides accumulate in large vacuoles in hepatocytes. Severe fatty liver is occasionally accompanied by inflammation, a situation that is referred to as steatohepatitis. When inflammation and steatohepatitis occur in people who do not drink alcohol, the condition is called nonalcoholic steatohepatitis

(NASH), and it is known to correlate strongly with obesity [11]. Sources of fatty acids stored in the liver are as follows: 59% of fatty acids are stored in white adipose tissue (WAT); 26% are produced by lipogenesis in hepatocytes; and 15% are obtained from the diet [12]. Accordingly, it is considered that both reducing WAT content and suppressing lipogenesis in the liver are very important for controlling fatty liver.

WAT is a specialized connective tissue that functions as the major storage site for fat in the form of triglycerides. For use as energy, triglycerides are metabolized into fatty acids and transported by the bloodstream to tissues such as the liver and brown adipose tissue (BAT). Therefore, to prevent obesity, it is important to stimulate lipolysis in WAT and increase energy utilization in the liver and BAT.

Thus, in this study, we conducted an animal study to investigate the effect of PFE on visceral fat levels and hepatic lipid accumulation in mice with diet-induced obesity. In addition, we focused on the expression profiles of genes related to beta-oxidation and lipogenesis in the liver, lipolysis in WAT, and thermogenesis in BAT to investigate the anti-obesity mechanism of PFE.

2. Materials and Methods

2.1. Experimental Materials. PFE was purchased from Ohta's Isan Co. Ltd. (Ushiku city, Japan). PFE contains 7 isoflavones (4 isoflavone glucosides: tectoridin (4.70%), tectorigenin 7-O-xylosylglucoside (8.37%), 6-hydroxygenistein-6,7-diglucoside (3.38%), and glycitin (0.17%); 3 aglycones: tectorigenin (0.83%), glycitein (0.10%), and genistein (0.06%)). All isoflavone standard preparations were purchased from Nagara Science Co., Ltd. (Gifu, Japan) and Tokiwa Phytochemical Co., Ltd. (Chiba, Japan).

2.2. Experimental Animals. All procedures using animals were performed in accordance with the Guidelines for the Care and Use of Experimental Animals of the Japanese Association for Laboratory Animal Science and were approved by the Ethical Committee of TOYO SHINYAKU Co., Ltd. Male C57BL/6J mice were purchased from Charles River Laboratories Japan Inc. (Yokohama, Japan) at the age of 6 weeks.

2.3. Test Environment. During the acclimation period, mice were housed in polycarbonate animal cages (260 × 420 × 180 mm; CLEA Japan, Inc., Tokyo, Japan) in groups of 4 and administered the MF diet (Oriental Yeast Co. Ltd., Tokyo, Japan). During the test period, mice were housed in individual stainless steel wire mesh cages (750 × 210 × 150 mm; Tokiwa, Tokyo, Japan) under a 12 h light : dark cycle.

2.4. Experimental Design. After acclimation for 1 week, C57BL/6J mice were weighed and assigned to one of 2 groups so that the mean body weight of each group was uniform. The control group was given a high-fat diet (HFD), and the treatment group was given the HFD containing 5% PFE (HFD + PFE) (Table 1). The animals were restricted-fed and given water *ad libitum* for 14 days.

2.5. Body Weight and Food Intake. During the experiment, the animals were weighed every 4 days. Food intake was

TABLE 1: Composition of the experimental diets.

Ingredient	HFD	HFD + PFE
Casein	20.0	20.0
Alpha-potato starch	28.2	23.2
Sucrose	13.0	13.0
Corn oil	20.0	20.0
Lard	10.0	10.0
Cellulose	4.0	4.0
Mineral mixture	3.5	3.5
Vitamin mixture	1.0	1.0
dl-Methionine	0.3	0.3
PFE	0.0	5.0
Total	100.0	100.0

Mineral mixture, AIN-76; Vitamin mixture, AIN-76 (g/100 g diet).

determined daily by determining the amount of feed remaining from the previous day, and the mean daily food intake for each animal was calculated.

2.6. Measurement of Fecal Lipids. All feces were collected daily on days 11–14 after the start of the experiment. The collected feces were dried for at least 3 days at 100°C and weighed. After dry feces were crushed and homogenized, fecal lipids were extracted using the Folch extraction protocol [13]. The total lipid content was determined by measuring the total dry extract weight.

2.7. Measurement of Tissue Weight. Fourteen days after the start of the experiment, mice were sacrificed, and then the liver and interscapular brown, mesenteric, epididymal, and retroperitoneal adipose tissues were removed. All samples excluding BAT samples were weighed. Each sample was cut into small pieces, dipped in RNAlater (Ambion, Tokyo, Japan), and stored at –80°C until RNA extraction. Another piece of each liver sample was stored at –80°C for subsequent analysis.

2.8. Hepatic Histological Analysis. Oil Red-O staining was performed in frozen liver sections to detect the presence of fat. The degree of fatty liver was assessed by expert pathologists. We entrusted all analyses to Narabyouri Research Co., Ltd. (Nara, Japan).

2.9. Real-Time Quantitative Reverse Transcription-Polymerase Chain Reaction (RT-PCR). The total RNAs from the liver, epididymal adipose tissue, and BAT were isolated using the RNeasy Mini Kit (QIAGEN, Tokyo, Japan) according to the manufacturer's directions. Total RNA (1.0 µg) was reverse-transcribed into cDNA in a reaction mixture using the QuantiTect Reverse Transcription kit (QIAGEN) according to the manufacturer's directions. The gene expression levels in the liver, epididymal adipose tissue, and BAT were determined using a real-time PCR system (MiniOpticon System; Bio-Rad Laboratories, Inc., Tokyo, Japan), the QuantiTect SYBR Green PCR kit (QIAGEN), and specific sets of primers (Table 2). The relative gene expression level was calculated

TABLE 2: Polymerase chain reaction primer sequences.

Gene name	Function	GenBank ID	Direction	Sequences
Fatty acid synthase (FAS)	Lipogenesis	NM_007988.3	Forward	TCCTGGGAGGAATGTAAACAGC
			Reverse	CACAAATTCATTCACTGCAGCC
Acetyl-CoA carboxylase (ACC)	Lipogenesis	NM_133904.2	Forward	TGGATCCGCTTACAGAGACTTT
			Reverse	GCCGGAGCATCTCATTCG
Carnitine palmitoyltransferase I (CPT1)	Beta-oxidation	NM_013495.2	Forward	CTCCAAGGCAGAAGAGTGG
			Reverse	GAACCTTGGCTGCGGTAAGAC
Medium-chain acyl dehydrogenase (MCAD)	Beta-oxidation	NM_007382.4	Forward	TCGAAAGCGGCTCACAAGCAG
			Reverse	CACCGCAGCTTCCGGAATGT
Acyl-CoA oxidase (ACO)	Beta-oxidation	AF006688.1	Forward	TCTTCTTGAGACAGGGCCAG
			Reverse	GTTCCGACTAGCCAGGCATG
Hormone-sensitive lipase (HSL)	Lipolysis	BC021642.1	Forward	CCTACTGCTGGGCTGTCAA
			Reverse	CCATCTGGCACCCCTCACT
Uncoupling protein 1 (UCP1)	Thermogenesis	NM_009463.2	Forward	CTGGGCTTAACGGGTCTCTC
			Reverse	CTGGGCTAGGTAGTGCCAGTG
PPAR γ coactivator alpha (PGC α)	Mitochondriogenesis	BC066868.1	Forward	TCGATGTGTGCGCTTCTTGC
			Reverse	ACGAGAGCGCATCCTTTGG
GAPDH	Housekeeping	XM_001478412.1	Forward	ATGACATCAAGAAGGTGGTG
			Reverse	CATACCAGGAAATGAGCTTG

with real-time PCR data relative to glyceraldehyde-3-phosphate dehydrogenase (GAPDH).

2.10. Statistical Analysis. Data were expressed as the mean \pm SEM. For comparisons between groups, analyses were performed using unpaired *t*-tests on all test items. All statistical analyses were performed using Statview ver. 5.0 (SAS Institute Japan Ltd., Tokyo, Japan), and significance was set at $P < 0.05$.

3. Results

3.1. Body Weight and Food Intake. Table 3 shows the body weight and amount of food intake 14 days after the start of the experiment. There was no significant difference between the 2 groups regarding food intake. Conversely, both the final body weight and body weight gain in the HFD + PFE group were significantly lower than those in the HFD group.

3.2. Liver and Adipose Tissue Weight. Table 3 shows the liver weight and epididymal, mesenteric, and retroperitoneal adipose tissue weights on day 14 after the start of the experiment. There were no significant differences between the 2 groups regarding liver weight and mesenteric adipose tissue

weight. However, epididymal and retroperitoneal adipose tissue weights in the HFD + PFE group were significantly lower than those in the HFD group. These data indicate that PFE reduces body weight by decreasing fat weight in high-fat diet-induced obese mice.

3.3. Fecal Lipid Levels. There was no significant difference between the 2 groups regarding fecal lipid levels (Table 3). In addition, food intake was not significantly different between the 2 groups (Table 3), and thus, it was believed that energy intake did not differ substantially between the 2 groups.

3.4. Hepatic Histological Analysis. Table 4 and Figure 1 show the hepatic histological analysis data on day 14 after the start of the experiment. In the HFD + PFE group, the development of fatty liver was apparently suppressed.

3.5. Real-Time Quantitative RT-PCR. Table 5 shows the effect of PFE on mRNA expression in the liver, WAT, and BAT. The expression of hepatic genes involved in lipogenesis such as acetyl-CoA carboxylase (ACC) in the HFD + PFE group was significantly lower than that in the HFD group. For WAT, hormone-sensitive lipase (HSL) was significantly upregulated in epididymal adipose tissue in the HFD + PFE group. Similarly, uncoupling protein1 (UCP1) in BAT was

TABLE 3: Effects of PFE on food intake, body weight, liver weight, adipose tissue weight, and fecal total lipids.

	HFD	HFD + PFE
Food intake, g/day	2.83 ± 0.04	2.79 ± 0.11
Final body weight, g	26.4 ± 0.5	24.9 ± 0.3*
Body weight gain, g	2.8 ± 0.3	1.4 ± 0.3**
Liver weight, g/100 g body weight	4.54 ± 0.08	4.73 ± 0.12
White adipose tissue weight		
Epididymal, g/100 g body weight	3.22 ± 0.18	2.49 ± 0.14**
Mesenteric, g/100 g body weight	1.31 ± 0.07	1.11 ± 0.10
Retroperitoneal, g/100 g body weight	0.36 ± 0.03	0.26 ± 0.02*
Fecal total Lipids, g/day	0.015 ± 0.001	0.017 ± 0.001

The data represent the mean ± SEM values ($n = 8$).

* and ** indicate significantly different at $P < 0.05$, $P < 0.01$, respectively.

TABLE 4: Results of hepatic histological analysis.

	HFD								HFD + PFE							
	Animal no.								Animal no.							
	1	2	3	4	5	6	7	8	1	2	3	4	5	6	7	8
Fatty liver	+++	+	++	+++	+++	+++	+	+++	-	-	-	-	-	-	-	-

-: no abnormality, ±: minor, +: slight, ++: moderate, +++: severe.

TABLE 5: Effect of PFE on mRNA levels in the liver, WAT, and BAT.

	HFD	HFD + PFE
Liver		
FAS	1.00 ± 0.28	0.58 ± 0.10
ACC	1.00 ± 0.11	0.70 ± 0.06*
CPT1	1.00 ± 0.14	1.21 ± 0.14
MCAD	1.00 ± 0.23	1.51 ± 0.26
ACO	1.00 ± 0.14	1.35 ± 0.20
Epididymal adipose tissue		
HSL	1.00 ± 0.14	1.84 ± 0.15**
Brown adipose tissue		
UCP1	1.00 ± 0.23	2.15 ± 0.38*
PGC1a	1.00 ± 0.15	1.30 ± 0.08

The data represent the mean ± SEM values ($n = 8$).

* and ** indicate significantly different at $P < 0.05$, $P < 0.01$, respectively.

significantly upregulated in the HFD + PFE group. The expression of genes related to beta-oxidation, such as carnitine palmitoyltransferase1 (CPT1), medium-chain acyl-CoA dehydrogenase (MCAD), and acyl-CoA oxidase (ACO), was not significantly different between the 2 groups, although their expressions were higher in the HFD + PFE group. These results suggest that PFE has antiobesity effects in high-fat diet-induced obese mice through suppressing lipogenesis in the liver, stimulating lipolysis in WAT, and promoting thermogenesis in BAT.

4. Discussion

The Kudzu flower is a rich source of isoflavones [14], and soy isoflavones such as genistein and daidzein have been reported to exert antiobesity effects [15–17]. Recently, Kim

et al. reported that daidzein supplementation prevented non-alcoholic fatty liver disease in an animal study [18], and thus, it is believed that isoflavones are promising compounds for preventing obesity and fatty liver disease.

In this study, PFE supplementation significantly reduced body weight, body weight gain, and WAT weight without affecting energy intake (i.e., food intake and fecal lipid content). It is known that obesity develops when energy intake exceeds energy expenditure. Therefore, PFE was believed to exert antiobesity effects by increasing energy expenditure.

In our unpublished data, the isoflavone fraction from *Puerariae thomsonii* stimulated body weight loss in mice. Soy isoflavone is reported to exert antiobesity effects through suppressing lipogenesis in the liver by increasing protein kinase A activity [18] and promoting lipolysis in WAT by increasing cAMP levels [19, 20]. Moreover, tectoridin, an isoflavone characteristic of PFE, has been reported to modulate the expression of beta-oxidation genes such as MCAD and ACO in mice with ethanol-induced liver steatosis [21]. In this study, PFE suppressed the expression of ACC and FAS, which are rate-limiting enzymes in fatty acid biosynthesis, in the liver. In addition, the expression of HSL, the predominant lipase effector of catecholamine-stimulated lipolysis, was also upregulated in WAT. Moreover, insignificant increases in the expression of beta-oxidation genes such as CPT1, MCAD, and ACO were observed (Table 5). These results are similar to the antiobesity effects of isoflavones [18–20]; therefore, the active ingredient of PFE may be an isoflavone.

In addition, PFE supplementation significantly upregulated UCP1 expression in BAT. UCP1 is a key factor that determines the level of thermogenesis in BAT, and peroxisome proliferator-activated receptor gamma coactivator1a (PGC1a) is known to control UCP1 expression and mitochondrial biogenesis. A number of studies using mice revealed

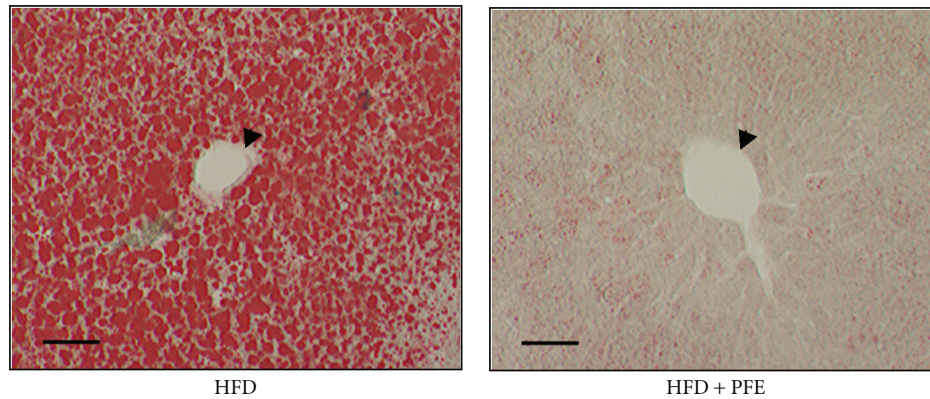


FIGURE 1: Histological analysis of the liver (Oil Red-O staining). The liver was extracted 14 days after commencing the treatment. Oil Red-O staining was performed in frozen liver sections to detect the presence of fat. Lipid droplets are stained red with Oil Red-O. The arrowhead shows the lumen of a blood vessel. These images are representative of observations made on 8 mice per group. (Scale bar: 50 μm).

that UCP1 in BAT controls body fat levels by promoting energy expenditure [22–24]. Research about the effects of isoflavones on UCP1 expression in BAT is sparse; however, it is generally known that cAMP promotes UCP1 expression in BAT [25]. Therefore, PFE may promote UCP1 expression by increasing cAMP levels in BAT as observed in WAT. These results suggest that PFE affects energy expenditure; however, we have to validate this hypothesis by measuring oxygen consumption.

NASH is associated with progressive liver disease, fibrosis, and cirrhosis. Its pathogenesis is considered to include 2 steps. The first step is the development of hepatic steatosis due to the accumulation of free fatty acids in the liver, and the second step involves additional biochemical insults, including oxidative stress, the upregulation of inflammatory mediators, and dysregulated apoptosis [26, 27]. Currently, therapeutic options for NASH are limited to medications that reduce the risk factors. Therefore, suppressing hepatic lipid accumulation, the first step of the pathogenesis of NASH, appears to be very important for preventing this hepatic disorder. In this study, PFE supplementation suppressed the development of fatty liver (Table 4). In addition, genes related to lipogenesis were significantly downregulated in the liver by PFE ingestion (Table 5). Thus, PFE might be expected to prevent NASH by suppressing hepatic lipid accumulation. In fact, GOT, GPT, and gamma-GTP expressions were significantly reduced by PFE ingestion in our preliminary clinical study [5]. This result supports the possibility that PFE supplementation provides the dual effects of preventing both obesity and hepatic disorders.

5. Conclusion

In the present study, the flower extract of *Puerariae thomsonii* has been demonstrated to possess antiobesity and antifatty liver by in vivo assay. In addition, the flower extract of *Puerariae thomsonii* appears to exert these effects through suppressing lipogenesis in the liver and promoting lipolysis in white adipose tissue and thermogenesis in brown adipose

tissue. In future research, we must clarify the detailed mechanism of PFE and its effects on energy expenditure.

Acknowledgment

The authors sincerely thank Professor Teruo Kawada, Laboratory of Molecular Function of Food Division of Food Science and Biotechnology, Graduate School of Agriculture Kyoto University, for the instruction and encouragement throughout the course of this work.

References

- [1] Y. Niho, T. Yamazaki, Y. Nakajima et al., “Pharmacological studies on puerariae flos. II. The effects of puerariae flos on alcohol-induced unusual metabolism and experimental liver injury in mice,” *Yakugaku Zasshi*, vol. 110, no. 8, pp. 604–611, 1990.
- [2] Y. Niho, T. Yamazaki, Y. Nakajima et al., “Pharmacological studies on Puerariae Flos. I. The effects of Puerariae Flos on alcoholic metabolism and spontaneous movement in mice,” *Yakugaku Zasshi*, vol. 109, no. 6, pp. 424–431, 1989.
- [3] T. Yamazaki, Y. Nakajima, Y. Niho et al., “Pharmacological studies on Puerariae flos III: protective effects of kakkalide on ethanol-induced lethality and acute hepatic injury in mice,” *Journal of Pharmacy and Pharmacology*, vol. 49, no. 8, pp. 831–833, 1997.
- [4] J. F. Wang, Y. X. Guo, J. Z. Niu, J. Liu, L. Q. Wang, and P. H. Li, “Effects of Radix Puerariae flavones on liver lipid metabolism in ovariectomized rats,” *World Journal of Gastroenterology*, vol. 10, no. 13, pp. 1967–1970, 2004.
- [5] T. Kamiya, Y. Matsuzuka, N. Kusaba et al., “Preliminary research for the anti-obesity effect of Puerariae flos extract in Humans,” *Journal of Health Science*, vol. 57, no. 6, pp. 521–531, 2011.
- [6] N. S. Joo, S. M. Kim, K. M. Kim, C. W. Kim, B. T. Kim, and D. J. Lee, “Changes of body weight and inflammatory markers after 12-Week intervention trial: results of a double-blind, placebo-control pilot study,” *Yonsei Medical Journal*, vol. 52, no. 2, pp. 242–248, 2011.

- [7] M. Adiels, M. R. Taskinen, C. Packard et al., "Overproduction of large VLDL particles is driven by increased liver fat content in man," *Diabetologia*, vol. 49, no. 4, pp. 755–765, 2006.
- [8] J. P. Després, "The insulin resistance-dyslipidemic syndrome of visceral obesity: effect on patients' risk," *Obesity Research*, vol. 6, supplement 1, pp. 8S–17S, 1998.
- [9] J. P. Després and I. Lemieux, "Abdominal obesity and metabolic syndrome," *Nature*, vol. 444, no. 7121, pp. 881–887, 2006.
- [10] M. Ono, N. Okamoto, and T. Saibara, "Prospect of treatment based on pathogenesis and epidemiology," *Adiposcience*, vol. 7, no. 1, pp. 68–75, 2010.
- [11] S. H. Caldwell, D. H. Oelsner, J. C. Iezzoni, E. E. Hespeneide, E. H. Battle, and C. J. Driscoll, "Cryptogenic cirrhosis: clinical characterization and risk factors for underlying disease," *Hepatology*, vol. 29, no. 3, pp. 664–669, 1999.
- [12] Y. Sumida, M. Yoneda, and H. Hyogo, "Current status and agenda in the diagnosis of nonalcoholic steatohepatitis," *Adiposcience*, vol. 7, no. 1, pp. 54–60, 2011.
- [13] J. Folch, M. Lees, and G. H. Sloane-Stanley, "A simple method for the isolation and purification of total lipides from animal tissues," *The Journal of Biological Chemistry*, vol. 226, no. 1, pp. 497–509, 1957.
- [14] T. Nohara, "Search for functions of natural oligoglycosides—solanaceae and Leguminosae origin glycosides," *Yakugaku Zasshi*, vol. 124, no. 4, pp. 183–205, 2004.
- [15] S. Kim, I. Sohn, Y. S. Lee, and Y. S. Lee, "Hepatic gene expression profiles are altered by genistein supplementation in mice with diet-induced obesity," *Journal of Nutrition*, vol. 135, no. 1, pp. 33–41, 2005.
- [16] E. D. Lephart, J. P. Porter, T. D. Lund et al., "Dietary isoflavones alter regulatory behaviors, metabolic hormones and neuroendocrine function in Long-Evans male rats," *Nutrition and Metabolism*, vol. 1, no. 1, p. 16, 2004.
- [17] S. Kim, H. J. Shin, S. Y. Kim et al., "Genistein enhances expression of genes involved in fatty acid catabolism through activation of PPAR α ," *Molecular and Cellular Endocrinology*, vol. 220, no. 1-2, pp. 51–58, 2004.
- [18] M. H. Kim, J. S. Park, J. W. Jung et al., "Daidzein supplementation prevents non-alcoholic fatty liver disease through alteration of hepatic gene expression profiles and adipocyte metabolism," *International Journal of Obesity*, vol. 35, no. 8, pp. 1019–1030, 2011.
- [19] M. R. Peluso, "Flavonoids attenuate cardiovascular disease, inhibit phosphodiesterase, and modulate lipid homeostasis in adipose tissue and liver," *Experimental Biology and Medicine*, vol. 231, no. 8, pp. 1287–1299, 2006.
- [20] K. Szkudelska, L. Nogowski, and T. Szkudelski, "Genistein, a plant-derived isoflavone, counteracts the antilipolytic action of insulin in isolated rat adipocytes," *Journal of Steroid Biochemistry and Molecular Biology*, vol. 109, no. 1-2, pp. 108–114, 2008.
- [21] Y. Xiong, Y. Yang, J. Yang et al., "Tectoridin, an isoflavone glycoside from the flower of *Pueraria lobata*, prevents acute ethanol-induced liver steatosis in mice," *Toxicology*, vol. 276, no. 1, pp. 64–72, 2010.
- [22] D. Ricquier and F. Bouillaud, "The uncoupling protein homologues: UCP1, UCP2, UCP3, StUCP and AtUCP," *Biochemical Journal*, vol. 345, no. 2, pp. 161–179, 2000.
- [23] M. Saito, Y. Minokoshi, and T. Shimazu, "Brown adipose tissue after ventromedial hypothalamic lesions in rats," *American Journal of Physiology*, vol. 248, no. 1, pp. E20–E25, 1985.
- [24] K. I. Inokuma, Y. Okamatsu-Ogura, A. Omachi et al., "Indispensable role of mitochondrial UCP1 for antiobesity effect of β 3-adrenergic stimulation," *American Journal of Physiology*, vol. 290, no. 5, pp. E1014–E1021, 2006.
- [25] J. S. Rim and L. P. Kozak, "Regulatory motifs for CREB-binding protein and Nfe212 transcription factors in the upstream enhancer of the mitochondrial uncoupling protein 1 gene," *Journal of Biological Chemistry*, vol. 277, no. 37, pp. 34589–34600, 2002.
- [26] P. Portincasa, I. Grattagliano, V. O. Palmieri, and G. Palasciano, "Nonalcoholic steatohepatitis: recent advances from experimental models to clinical management," *Clinical Biochemistry*, vol. 38, no. 3, pp. 203–217, 2005.
- [27] J. R. Lewis and S. R. Mohanty, "Nonalcoholic fatty liver disease: a review and update," *Digestive Diseases and Sciences*, vol. 55, no. 3, pp. 560–578, 2010.

Research Article

Antimicrobial Activity of Essential Oils against *Streptococcus mutans* and their Antiproliferative Effects

Lívia Câmara de Carvalho Galvão,¹ Vivian Fernandes Furletti,²
Salete Meyre Fernandes Bersan,¹ Marcos Guilherme da Cunha,¹ Ana Lúcia Tasca Góis Ruiz,²
João Ernesto de Carvalho,² Adilson Sartoratto,² Vera Lúcia Garcia Rehder,² Glyn Mara
Figueira,² Marta Cristina Teixeira Duarte,² Masarahu Ikegaki,³ Severino Matias de Alencar,⁴
and Pedro Luiz Rosalen¹

¹ Department of Pharmacology, Anesthesiology and Therapeutics, Piracicaba Dental School, University of Campinas (UNICAMP), 13414-903 Piracicaba, SP, Brazil

² Research Center for Chemistry, Biology and Agriculture, University of Campinas (UNICAMP), P.O. Box 6171, 13083-970 Campinas, SP, Brazil

³ School of Pharmacy and Dentistry, Federal University of Alfenas, 37130-000 Alfenas, MG, Brazil

⁴ Department of Agri-food Industry, Food and Nutrition, Escola Superior de Agricultura "Luiz de Queiroz" (ESALQ), University of São Paulo, P.O. Box 9, 13418-900 Piracicaba, SP, Brazil

Correspondence should be addressed to Pedro Luiz Rosalen, rosalen@fop.unicamp.br

Received 26 January 2012; Accepted 26 February 2012

Academic Editor: William C. S. Cho

Copyright © 2012 Lívia Câmara de Carvalho Galvão et al. This is an open access article distributed under the Creative Commons Attribution License, which permits unrestricted use, distribution, and reproduction in any medium, provided the original work is properly cited.

This study aimed to evaluate the activity of essential oils (EOs) against *Streptococcus mutans* biofilm by chemically characterizing their fractions responsible for biological and antiproliferative activity. Twenty EO were obtained by hydrodistillation and submitted to the antimicrobial assay (minimum inhibitory (MIC) and bactericidal (MBC) concentrations) against *S. mutans* UA159. Thin-layer chromatography and gas chromatography/mass spectrometry were used for phytochemical analyses. EOs were selected according to predetermined criteria and fractionated using dry column; the resulting fractions were assessed by MIC and MBC, selected as active fractions, and evaluated against *S. mutans* biofilm. Biofilms formed were examined using scanning electron microscopy. Selected EOs and their selected active fractions were evaluated for their antiproliferative activity against keratinocytes and seven human tumor cell lines. MIC and MBC values obtained for EO and their active fractions showed strong antimicrobial activity. Chemical analyses mainly showed the presence of terpenes. The selected active fractions inhibited *S. mutans* biofilm formation ($P < 0.05$) did not affect glycolytic pH drop and were inactive against keratinocytes, normal cell line. In conclusion, EO showed activity at low concentrations, and their selected active fractions were also effective against biofilm formed by *S. mutans* and human tumor cell lines.

1. Introduction

Despite the implementation of measures to control and treat dental caries with fluoride, they remain the most prevalent dental disease in many countries [1]. Caries are a multifactorial infectious disease caused by accumulation of biofilm on tooth surface [2]. Manifestations of the disease occur when there is an imbalance between the biofilm and

the host due to changes in biofilm matrix pH caused by diet, microorganisms, or salivary flow and their components [3, 4].

Streptococcus mutans is considered the most cariogenic of all oral streptococci [5]. *S. mutans* is able to colonize the tooth surface and to produce large amounts of extra and intra-cellular polysaccharides. This microorganism is also highly acidogenic and aciduric, and it metabolizes several

salivary glycoproteins, thus being responsible for the initial stage of oral biofilm formation and caries lesions [6].

Several products have been used to control dental caries, such as fluoride, chlorhexidine, and their associations [7]. However, natural products have contributed significantly to the discovery of chemical structures to create new medicaments to be used as innovative therapeutic agents against this prevalent disease [8, 9].

Essential oils (EOs) are important for their detected antimicrobial activity [10–12] including that against *S. mutans* [13]. They are complex, volatile, natural compounds formed by aromatic plants as secondary metabolites [14]. They are known for their bactericidal, virucidal, fungicidal, sedative, anti-inflammatory, analgesic, spasmolytic, and locally anesthetic properties [14]. The presence of complex chemical structures constituted of several groups, such as terpenes and terpenoids, aromatic and aliphatic constituents, all characterized by low molecular weight, may explain their successful bacteriostatic and bactericidal action [14].

Additionally, it was attested that the antimicrobial activity of a natural product, such as EO, is important to evaluate its effects on human normal cell lines and also against human tumor cell lines in order to evidence potential toxicity on human healthy and tumor cell lines [15]. For this reason, it is important that extensive studies involving EO as well as other sources of natural medicines are carried out.

The aim of this study was to evaluate the activity of EO and fractions against planktonic cells of *S. mutans* and also the selected active fractions of EO were chemically characterized and evaluated against mutans biofilm and antiproliferative activity on human cells.

2. Materials and Methods

2.1. Medicinal Plants. We studied 20 medicinal and aromatic plants (Table 1), which were obtained from the germoplasm bank of the Collection of Medicinal and Aromatic Plants (CPMA) of the Research Center for Chemistry, Biology and Agriculture (CPQBA), University of Campinas (UNICAMP), São Paulo, Brazil (<http://www.cpqba.unicamp.br/>), and identified by Glyn M. Figueira, curator of CPMA.

The plants were collected from November 2009 to January 2011, during the morning, after the dew point has been reached. The vouchers of each species were deposited in the herbarium of the Institute of Biology, at UNICAMP-UEC, and also registered in the herbarium of CPQBA, receiving identification numbers (CPMA number).

2.2. Essential Oil Extraction. EOs were obtained from 100 g of aerial fresh plant parts by hydrodistillation using a Clevenger-type system, for 3 hours. The aqueous phase was extracted with 50 mL of dichloromethane. Then, the organic layer was separated, dried over anhydrous sodium sulphate (Na_2SO_4), and filtered; the solvent was removed by vacuum evaporation at room temperature, resulting in EO. Oil samples were stored at -25°C in sealed glass vials [11].

2.3. Fractionation of Essential Oils. In order to select the EO that should be fractionated, we predetermined some criteria: best antimicrobial activity ($\text{MIC} < 250 \mu\text{g/mL}$), extract yield ($>0.5\%$, except for *Coriandrum sativum* EO), commercial availability, presence of the EO in aerial parts of plants, and easy cultivation. The resulting fractions were also submitted to the antimicrobial assay.

Fractionation was performed using dry column chromatography (cellulose 2 cm \times 20 cm) with Si gel 60 (Merck, Darmstadt, Germany) as the stationary phase and dichloromethane as the mobile phase, previously chosen by thin-layer chromatography (TLC), visualized under UV 254 nm, followed by anisaldehyde solution application and drying at 105°C for 5 min. After elution, columns were cut into different parts for each EO, according to polarity and extraction, using dichloromethane. The fractions so obtained were analyzed using TLC and gas chromatography coupled to mass spectrometry (GC-MS) and then bioguided using the antimicrobial assays [16]. All chemical wastes generated during this study were treated according to the Environmental Ethics Committee of UNICAMP (324/2009).

2.4. Analyses of the Selected Active Fractions using GC-MS. The chemical composition of each selected active fraction was evaluated using a Hewlett-Packard 6890 gas chromatograph equipped with an HP-5975 mass selective detector and HP-5 capillary column (30 m \times 0.25 mm \times 0.25 μm). GC-MS was performed using split injection with the injector set at 220°C , the column set at 60°C with a heating ramp of $3^\circ\text{C}/\text{min}$ and a final temperature of 240°C , and the MS detector set at 250°C . Helium was used as a carrier gas at 1 mL/min. The GC-MS electron ionization system was set at 70 eV. The quantitative analyses were performed using a Hewlett-Packard 5890 gas chromatograph equipped with a flame ionization detector under the same conditions previously described. A sample of each EO or its selected active fraction was solubilized in ethyl acetate (15 mg/mL) for the analysis. Retention indices (RIs) were determined using injection of hydrocarbon standards and EO samples under the same conditions described above. The oil components were identified by comparison with data described in the literature and the profiles in the NIST 05 mass spectral library [11, 17].

2.5. Microorganisms. For the development of this study, *Streptococcus mutans* UA159 was used.

2.6. Antimicrobial Assay. We tested 20 EOs using the antimicrobial assay and selected them according to pre-determined criteria (item 2.3) before being fractionated and continuing the bioguided study.

MIC test was carried out using tissue culture microplates (96 wells) containing 100 μL /well BHI (Brain Heart Infusion, Difco, Franklin Lakes, NJ, USA) medium [18]. The stock solutions of EO and fractions from selected EO (item 2.3) were diluted with propylene glycol (4 mg/mL), transferred to the first well, and serial dilutions were performed to obtain concentrations ranging from 7.81 to 1000 $\mu\text{g/mL}$. We

TABLE 1: Medicinal and aromatic plants from the germplasm bank of the CPMA/CPQBA/UNICAMP selected for this study with their yield, MIC and MBC values, and MBC : MIC ratio.

Medicinal species	Family	Popular name	Source	CPMA number	Voucher number ¹	Yield (%)	MIC ($\mu\text{g/mL}$)	MBC ($\mu\text{g/mL}$)	MBC : MIC ratio ²	Popular use
<i>Aloysia gratissima</i> (Gillies & Hook)	Verbenaceae	Brazilian lavender	Leaf	714	UEC 121.393	1.1	125–250	250–500	2 : 1	Digestive; antispasmodic
<i>Aloysia triphylla</i> (L'Hér.) Britton	Verbenaceae	Aloisia	Leaf	274/700	UEC 121.412	0.3	125–250	125–250	1 : 1	Sedative; antispasmodic
<i>Alpinia speciosa</i> (Pers.) Burt & Smith	Zingiberaceae	Colony	Root	447	UEC 145.185	0.2	125–250	250–500	2 : 1	Antimicrobial
<i>Baccharis dracunculifolia</i> DC	Asteraceae	Broom weed	Leaf	1841	—	0.8	62.5–125	250–500	4 : 1	Tonic; eupaptic, antipyretic
<i>Cinnamomum zeylanicum</i> Blume	Lauraceae	Cinnamon	Leaf	455	IAC 19624	0.2	250–500	500–1000	2 : 1	Carminative; antispasmodic
<i>Coriandrum sativum</i> L.	Apiaceae	Coriander	Leaf	664	—	0.3	31.2–62.5	62.5–125	2 : 1	Antimicrobial; antifungal
<i>Cymbopogon citratus</i> (DC) Stapf.	Poaceae	Lemon grass	Leaf	503	UEC 85.210	1.1	125–250	250–500	2 : 1	Sedative; analgesic; anticough
<i>Cymbopogon martini</i> (Roxb.) J. F. Watson	Poaceae	Palmarosa	Leaf	354	UEC 127.115	0.6	125–250	250–500	2 : 1	Antiseptic; antifungal
<i>Cymbopogon winterianus</i> Jowitt	Poaceae	Lemon verbena	Leaf	712	UEC 121.414	1.5	125–250	250–500	2 : 1	Repellent, insecticide
<i>Cyperus articulatus</i> Vahl	Cyperaceae	Priprioca	Bulbs	222	UEC 121.396	0.5	125–250	250–500	2 : 1	Anti-inflammatory
<i>Elyonurus muticus</i> Spreng	Poaceae	Agripalma	Leaf	1701	UEC 20.580	0.6	125–250	125–250	1 : 1	Antibacterial
<i>Eugenia florida</i> DC.	Myrtaceae	Guamirim-cereja	Leaf	1685	IAC 49207	0.3	125–250	500–1000	4 : 1	Anti-inflammatory
<i>Eugenia uniflora</i> L.	Myrtaceae	Pitanga	Leaf	1816	—	0.7	125–250	250–500	2 : 1	Antihypertensive; diuretic

TABLE 1: Continued.

Medicinal species	Family	Popular name	Source	CPMA number	Voucher number ¹	Yield (%)	MIC ($\mu\text{g/mL}$)	MBC ($\mu\text{g/mL}$)	MBC:MIC ratio ²	Popular use
<i>Lippia alba</i> (Mill.) N.E. Brown	Verbenaceae	False lemon balm	Leaf	467/509	UEC 121.413	0.3	125–250	250–500	2 : 1	Treatment of migraines
<i>Lippia sidoides</i> Cham.	Verbenaceae	Rosemary	Leaf	398/399	—	4.7	62.5–125	125–250	2 : 1	Bactericide; fungicide
<i>Mentha piperita</i> L.	Lamiaceae	Mint	Leaf	560	UEC 127.110	2.2	250–500	250–500	1 : 1	Antifungal; antibacterial
<i>Mikania glomerata</i> Spreng.	Asteraceae	Guaco	Leaf	766	UEC 102.047	0.4	62.5–125	125–250	2 : 1	Anti-inflammatory; bronchodilator
<i>Siparuna guitanenses</i> Aubl.	Monimiaceae	Wild lemon	Leaf	2025	—	0.3	62.5–125	125–250	2 : 1	Tranquilizer; diuretic
<i>Syzygium aromaticum</i> (L.) Merr. & L. M. Perry	Myrtaceae	Cloves	Leaf	455	IAC 19624	0.5	62.5–125	250–500	4 : 1	Seasoning; antibacterial
<i>Ziziphus joazeiro</i> Mart.	Rhamnaceae	Joazeiro fruit	Leaf	2119	—	0.5	250–500	500–1000	2 : 1	Astringent; anti-inflammatory

¹ A voucher herbarium specimen is a pressed plant sample deposited for future reference. Vouchers deposited at UEC herbarium (<http://www.ib.unicamp.br/herbario/>) at Biology Institute (IB) of UNICAMP, SP, Brazil. (—) Species with no voucher number registered. ²The EOs were considered bactericidal when the MBC:MIC ratio was between 1 : 1 to 2 : 1, and bacteriostatic if this ratio was higher than 2 : 1.

used 0.12% chlorhexidine (Sigma-Aldrich, St. Louis, MO, USA) as positive control and propylene glycol 6.25% as negative control. The bacterial inoculum (1×10^6 UFC/mL) was added to all wells, and the plates were incubated at 37°C and 5% CO₂ for 24 hours. MIC was defined as the lowest concentration of EO or fraction from selected EO that inhibited microorganism visible growth indicated by resazurin 0.01% (Sigma-Aldrich, St. Louis, MO, USA) [19].

To determine MBC, an aliquot of each incubated well with concentrations higher than MIC was subcultured on BHI medium supplemented with 5% defibrinated sheep blood using a Whitley Automatic Spiral Plater (Don Whitley Scientific Limited, Shipley, West Yorkshire, UK). MBC was defined as the lowest concentration of EO or fraction that allowed no visible growth on the test medium.

To determine the nature of antibacterial effect of EO and fractions, the MBC:MIC ratio for bacteria was used [20]. When MBC:MIC ratio for *S. mutans* was between 1:1 and 2:1, the EO or fraction from selected EO was considered bactericidal against this microorganism [20], and when the ratio was higher than 2:1, it was considered bacteriostatic.

2.7. Action of Selected Active Fractions from Selected EO against *S. mutans* Biofilm. We tested 20 EOs, and those that fulfilled the pre-determined criteria (item 2.3) were selected to be chemically fractionated. The resulting fractions were also tested using the antimicrobial assay and selected according to MIC and MBC results and yields. The selected active fractions were then assessed regarding their action against *S. mutans* biofilm.

2.7.1. Inhibition of *S. mutans* Biofilm Growth. In order to evaluate the antimicrobial activity of EO selected active fractions against the formation of *S. mutans* biofilm, the samples were placed, at different concentrations (7.81–1000 µg/mL), in the wells of sterile polystyrene U-bottom microtiter plates, previously treated with saliva (the use of human saliva in this study was approved by the Research Ethics Committee of the Piracicaba Dental School, State University of Campinas (UNICAMP) (Approval 087/2011)) [21]. *S. mutans* cells (1.0×10^7 cells/mL in BHI medium) were added to wells containing BHI medium with 2% sucrose and the samples were incubated at 37°C for 18 hours. Biofilm growth was revealed and quantified using the crystal violet staining method and measuring absorbance at 575 nm [11, 22].

After 18 hours of incubation, the spent medium was aspirated, nonadhered cells were removed, the wells were washed three times with sterile distilled water, and the plates were dried for 45 min before carrying out biofilm quantification [22].

2.7.2. Glycolytic pH-Drop Assay. The effect of EO selected active fractions against *S. mutans* biofilm was measured using the standard glycolytic pH-drop assay [23]. Biofilm growth was carried out as previously described (item 2.7.1), in sterile polystyrene U-bottom microtiter plates without fractions. The biofilms so obtained were washed twice with

0.9% NaCl solution and salt solution (50 mM KCl + 1.0 mM MgCl₂), containing EO selected active fractions at different concentrations (1000, 500, and 250 µg/mL), and vehicle (25% propylene glycol, v/v) was added. The pH was adjusted to 7.2 with 0.1 M KOH solution, and glucose was added to a final concentration of 1%, and pH-drop was assessed using Orion pH glass electrode attached to Orion 290 A⁺ pHmeter (Orion Scientific, Houston, TX, USA) for 90 min.

2.8. Scanning Electron Microscopy (SEM). In order to evaluate *S. mutans* integrity using SEM, biofilms were first developed in Lab-Tek chambered coverglass (Nunc, Naperville, IL, USA), as described previously (item 2.7.1), were treated with vehicle (6.12% propylene glycol) or had their active fractions selected at concentrations able to inhibit more than 90% of *S. mutans* biofilm formation. Samples were fixed in 4% glutaraldehyde (v/v) in phosphate-buffered saline (PBS) at room temperature for 12–24 hours. After this procedure, the biofilms were dehydrated through a graded series of ethanol (50% to 100%), dried to a critical point, coated with gold, and observed using a scanning electron microscope JEOL JSM5600LV (JEOL Ltd., Tokyo, Japan) [11, 24].

2.9. Antiproliferative Assay. The *in vitro* antiproliferative assay [25] was performed in the present study using a human keratinocyte (HaCat) cell line, kindly donated by Dr. Ricardo Della Coletta (FOP, UNICAMP, Brazil), and seven human tumor cell lines (U251 (glioma), MCF-7 (breast), NCI-ADR/RES (ovarian expressing phenotype multiple drugs resistance), 786-0 (renal), NCI-H460 (lung, nonsmall cells), PC-3 (prostate), and OVCAR-03 (ovarian), kindly provided by M. A. Frederick (National Cancer Institute, USA). Stock and experimental cultures were grown in medium containing 5 mL RPMI-1640 (Gibco-BRL, Grand Island, NY, USA) supplemented with 5% fetal bovine serum (Gibco-BRL, Grand Island, NY, USA). A penicilline-streptomycin mixture (1000 U/mL:1000 mg/mL, 1 mL/L RPMI) was added to experimental cultures. Cells in 96-well plates (100 µL cells/well) were exposed to each EO and selected active fractions in dimethyl sulfoxide (DMSO, Sigma-Aldrich, St. Louis, MO, USA) (0.25, 2.5, 25, and 250 µg/mL) at 37°C and 5% CO₂ for 48 hours. Final DMSO concentration did not affect cell viability. Before (T₀ plate) and after sample addition (T₁ plates), cells were fixed with 50% trichloroacetic acid and cell proliferation was determined by spectrophotometric quantification (540 nm) of cellular protein content using sulforhodamine B assay. Using the concentration-response curve for each cell line, the total growth inhibition (TGI) was determined by nonlinear regression analysis using the software Origin 8.0 (OriginLab Corporation, Northampton, MA, USA) [26, 27].

2.10. Statistical Analysis. An exploratory data analysis was performed to determine the most appropriate statistical test. Inhibition of biofilm growth, and glycolytic pH-drop data were compared using the nonparametric Kruskal-Wallis test. *P* value < 0.05 was considered statistically significant.

Triplicates from at least three separated experiments were conducted in each assay.

3. Results

3.1. Essential Oils and Fraction Yields. The EO yields, expressed in relation to dry weight of plant material (% w/w), are shown in Table 1.

According to pre-determined criteria (item 2.3), four EOs were selected to be fractionated using dry column as follows: *A. gratissima*, *B. dracunculifolia*, *C. sativum*, and *L. sidoides*.

The yields of the fractions from selected EO were expressed as a function of the respective EO yield (% w/w) and are shown in Table 2. The yields of *A. gratissima* fractions ranged from 14.4% to 29%, *B. dracunculifolia* from 20.1% to 30.6%, *C. sativum* from 4.9% to 30.9%, and *L. sidoides* from 1.7% to 33.3%.

3.2. Antimicrobial Activity. MIC and MBC values for all tested EO are shown in Table 1. MIC values ranged from 31.2 to 500 $\mu\text{g/mL}$, and MBC values ranged from 62.5 to 1000 $\mu\text{g/mL}$. The highest activities were observed for *A. gratissima* and *A. triphylla* (125–250 $\mu\text{g/mL}$), *B. dracunculifolia*, *L. sidoides*, *M. glomerata*, *S. guianenses*, *S. aromaticum* (62.5–125 $\mu\text{g/mL}$), and *C. sativum* (31.2–62.5 $\mu\text{g/mL}$).

Based on pre-determined criteria (item 2.3), four EOs (*A. gratissima*, *B. dracunculifolia*, *C. sativum*, and *L. sidoides*) were selected to be fractionated. MIC and MBC values of fractions from selected EO are shown in Table 2. MIC values obtained for all fractions ranged from 15.6 to 500 $\mu\text{g/mL}$, and MBC values ranged from 31.2 to 1000 $\mu\text{g/mL}$. The highest activities were observed for the fractions Ag_4 (31.2–62.5 $\mu\text{g/mL}$), Bd_2 (15.6–31.2 $\mu\text{g/mL}$), Cs_4 (15.6–31.2 $\mu\text{g/mL}$), and Ls_3 (62.5–125 $\mu\text{g/mL}$).

The MBC:MIC ratio (Table 1) showed that most EOs are bactericidal, except for *B. dracunculifolia*, *E. florida*, and *S. aromaticum*, which are considered bacteriostatic against *S. mutans*. Among the selected EO chosen to be fractionated, only that obtained from *B. dracunculifolia* was bacteriostatic. Most fractions from selected EO were bactericidal, except for Ag_4 , Cs_1 , Ls_2 , and Bd_2 , considered bacteriostatic against *S. mutans* (Table 2). Based on yield and antimicrobial activity, Ag_4 , Bd_2 , Cs_4 , and Ls_3 fractions were selected for further evaluations.

3.3. Selected Active Fractions Activity against *Smutans* Biofilm. Figure 1 shows the development of *S. mutans* biofilm inhibitor after treatment with selected active fractions. Their growth was measured by optic density at 575 nm. The result showed that the selected active fractions tested at different concentrations were significantly different ($P < 0.05$) from the vehicle. Moreover, Cs_4 and Bd_2 fractions presented a better performance since they inhibited more than 90% of biofilm formation at lower concentrations (31.2 $\mu\text{g/mL}$).

3.4. pH-Drop Assay. The influence of selected active fractions from EO on glycolytic pH-drop of *S. mutans* biofilm

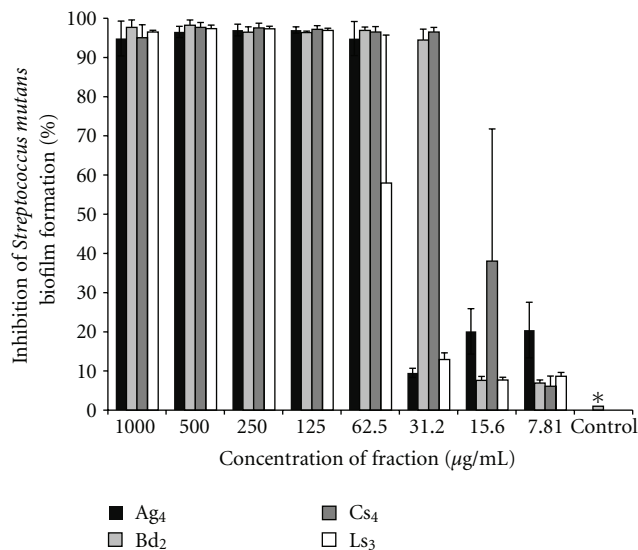


FIGURE 1: Influence of selected active fractions Ag_4 , Bd_2 , Cs_4 , and Ls_3 from selected essential oils at different concentrations against *Streptococcus mutans* biofilm formation. All fractions tested were significantly different from the vehicle at all concentrations tested. Kruskal-Wallis test ($P < 0.05$).

formation in the presence of excess glucose was not significant ($P > 0.05$) for all fractions tested (Ag_4 , Bd_2 , Cs_4 , and Ls_3).

3.5. Chemical Characterization of Fractions Constituents. The chemical composition of the selected EO and the selected active fractions is shown in Table 3.

The analyses of EO and fractions indicated the presence of volatile compounds, mainly mono- and sesquiterpenes.

We identified 28 compounds in the EO of *A. gratissima*, representing 92.73% of the EO, 25 compounds in the EO of *B. dracunculifolia*, representing 93.45% of the EO, 15 compounds in the EO of *C. sativum*, representing 91.93% of the EO, and four compounds in the EO of *L. sidoides*, representing 100% of the EO. We also identified 19 compounds in fraction Ag_4 , representing 94.6% of the fraction, 10 compounds in fraction Bd_2 , representing 83.06% of the fraction, nine compounds in fraction Cs_4 , representing 89.71% of the fraction, and five compounds in fraction Ls_3 , representing 99.7% of the fraction.

The major compounds identified in each selected EO were: trans- and cis-pinocamphone, beta-pinene, and guaial in *A. gratissima*; trans-nerolidol and spathulenol in *B. dracunculifolia*; 2-decen-1-ol and 1-decanol in *C. sativum*; and thymol in *L. sidoides*. The major compounds identified in each selected fraction were trans- and cis-pinocamphone and guaial in Ag_3 ; trans-nerolidol, spathulenol, and ethyl ester benzenepropanoic in Bd_2 ; 2-decen-1-ol and 1-decanol in Cs_4 ; thymol in Ls_3 .

3.6. Scanning Electron Microscopy (SEM). The effect of selected active fractions against *S. mutans* biofilm formation was evaluated by SEM. Figure 2 shows a reduction in

TABLE 2: Selected EO and their fractions with yield results, MIC and MBC values, and MBC : MIC ratio.

Essential oil			Fraction				
Identification	MIC ($\mu\text{g/mL}$)	MBC ($\mu\text{g/mL}$)	Identification	Yield (%)	MIC ($\mu\text{g/mL}$)	MBC ($\mu\text{g/mL}$)	MBC : MIC ratio ¹
<i>Aloysia gratissima</i> (Ag)	125–250	250–500	Ag ₁	28.9	250–500	500–1000	2 : 1
			Ag ₂	17.9	250–500	500–1000	2 : 1
			Ag ₃	20.1	62.5–125	500–1000	8 : 1
<i>Baccharis dracunculifolia</i> (Bd)	62.5–125	250–500	Ag₄²	14.4	31.2–62.5	62.5–125	2 : 1
			Bd ₁	30.5	250–500	500–1000	2 : 1
			Bd₂	22.1	15.6–31.2	125–250	8 : 1
<i>Coriandrum sativum</i> (Cs)	31.2–62.5	62.5–125	Cs ₁	6.6	125–250	500–1000	4 : 1
			Cs ₂	4.9	125–250	250–500	2 : 1
			Cs ₃	12.7	15.6–31.2	31.2–62.5	2 : 1
			Cs₄	30.9	15.6–31.2	31.2–62.5	1 : 1
<i>Lippia sidoides</i> (Ls)	62.5–125	125–250	Ls ₁	13.6	250–500	500–1000	2 : 1
			Ls ₂	33.3	62.5–125	250–500	4 : 1
			Ls₃	26	62.5–125	125–250	2 : 1
			Ls ₄	6.1	62.5–125	125–250	2 : 1
			Ls ₅	1.7	62.5–125	125–250	2 : 1

¹The fractions from selected EO were considered bactericidal when the MBC:MIC ratio was between 1 : 1 to 2 : 1, and bacteriostatic if this ratio was higher than 2 : 1. ²The fractions in bold font were selected as active fractions and evaluated against *S. mutans* biofilm and for their antiproliferative action. The subscript numbers of the fractions represent the numbers of parts obtained using the dry column fractionation.

biofilm formation. Biofilms were first developed as described previously (Section 2.7.1), were treated with vehicle, or had their active fractions selected at concentrations able to inhibit more than 90% of *S. mutans* biofilm formation (Ag₄ at 62.5 $\mu\text{g/mL}$, Bd₂ and Cs₄ at 31.2 $\mu\text{g/mL}$, and Ls₃ at 125 $\mu\text{g/mL}$).

3.7. Antiproliferative Assay. Most EOs and their selected active fractions did not present activity against the human normal cell line evaluated in this study or presented high concentrations to totally inhibit its growth. TGI values are shown in Table 4.

Among the EO evaluated, *B. dracunculifolia* and *C. sativum* were the most active inhibitors of human tumor cell lines growth, presenting selectivity for U251 (TGI = 38.2 $\mu\text{g/mL}$ and TGI = 8.3 $\mu\text{g/mL}$, resp.) and OVCAR-3 (TGI < 0.25 $\mu\text{g/mL}$ for both). On the other hand, *A. gratissima* and *L. sidoides* displayed the lowest activity, both presenting selectivity for OVCAR-3 (TGI < 0.25 $\mu\text{g/mL}$ for both) and *L. sidoides* for PC-3 (TGI = 26.7 $\mu\text{g/mL}$). The reference compound, doxorubicin, presented antiproliferative activity against all cell lines, except for kidney (Table 4).

Table 4 also shows the activity of selected active fractions. Ag₄ and Ls₃ fractions presented better results than *A. gratissima* and *L. sidoides* EO, respectively, since these fractions were not active against human normal cell lines (TGI > 250 $\mu\text{g/mL}$) and showed lower TGI values, being selective for 786-0 (TGI = 5.9 $\mu\text{g/mL}$ and TGI = 26.7 $\mu\text{g/mL}$, resp.). Cs₄ fraction had better results than *C. sativum* EO only against NCI-ADR/RES (TGI = 13.1 $\mu\text{g/mL}$ and TGI

= 90 $\mu\text{g/mL}$, resp.). Bd₂ displayed a better performance than *B. dracunculifolia* EO against NCI-ADR/RES (TGI = 10.5 $\mu\text{g/mL}$ and TGI = 59.2 $\mu\text{g/mL}$, resp.), 786-0 (TGI = 47.1 $\mu\text{g/mL}$ and TGI = 49.5 $\mu\text{g/mL}$, resp.), and NCI-H460 (TGI = 76.8 $\mu\text{g/mL}$ and TGI = 87.6 $\mu\text{g/mL}$, resp.).

4. Discussion

The activity of natural products, especially EO, against microorganisms has been recently confirmed by several studies focusing on antimicrobial activity of EO against planktonic cells. However, bacteria growing in biofilms exhibit a specific phenotype and are often, but not always, more resistant to antimicrobial agents than their planktonic counterparts [10, 11]. Thus, it is important to search for natural products that have antibiofilm properties and antimicrobial activity against oral pathogens [28].

This study aimed to evaluate the activity of EO and their fractions against planktonic cells of *S. mutans*, and the active fractions were evaluated against biofilm formed by *S. mutans*. Also, EO and their active fractions were chemically characterized and their activity against human normal and tumor cell lines proliferation were determined.

The antimicrobial assay revealed low MIC values for almost all 20 EOs and 15 fractions from the selected EO tested. EO and the selected active fractions presented strong activity against *S. mutans*, since natural products are considered strong inhibitors of microbial activity, when MIC values are lower than 500 $\mu\text{g/mL}$ [29].

TABLE 3: Major compounds of the selected active fractions from essential oils with their retention time (Rt), retention index (RI), and relative percentage.

Rt (min)	RI	Compound	Relative percentage ¹							
			Ag EO	Ag ₄	Bd EO	Bd ₂	Cs EO	Cs ₄	Ls EO	Ls ₃
4.02	899	Cyclohexanone	—	—	—	—	—	—	6.5	—
4.22	850	3-hexen-1-ol	—	—	—	0.8	3.6	5.1	—	—
5.87	977	Beta-pinene	12.0	—	—	—	—	—	—	—
7.2	1024	p-cymene	—	—	—	—	—	—	17.3	—
13.08	1140	Trans-pinocarveol	—	4.9	—	—	—	—	—	—
14.09	1165	Trans-pinocamphone	16.0	36.7	—	—	—	—	—	—
14.61	1177	Cis-pinocamphone	6.0	17.0	—	—	—	—	—	—
16.7	1274	2-decen-1-ol <E>	—	—	—	—	23.6	26.9	—	—
16.86	1277	1-decanol	—	—	—	—	33.9	35.4	—	—
17.76	1299	Trans-pinocarvyl acetate	8.2	—	—	—	—	—	—	—
19.74	1300	Thymol	—	—	—	—	—	—	65.8	97.8
19.95	1303	Carvacrol	—	—	—	—	—	—	—	0.6
21.84	1349	Ethyl ester benzenepropanoic	—	—	—	11.7	—	—	—	—
22.57	1416	Trans-caryophyllene	7.2	—	10.7	—	—	—	10.5	—
24.86	1473	2-dodecen-1-ol	—	—	—	—	13.1	14.5	—	—
25.04	14.78	Germacrene D	—	—	4.9	—	—	—	—	—
25.66	1493	Bicyclgermacrene	4.2	—	6.8	—	—	—	—	—
27.97	1553	M ² = 204	6.4	—	—	—	—	—	—	—
30.59	1566	Trans-nerolidol	—	—	31.7	52.2	—	—	—	—
31.05	1578	Spathulenol	—	—	13.6	11.5	—	—	—	—
31.23	1582	Caryophyllene oxide	6.4	7.0	—	6.3	—	—	—	0.7
31.9	1600	Guaiol	8.5	12.7	—	—	—	—	—	—
33.44	1641	Epi alpha cadinol	—	—	—	3.1	—	—	—	—
32.47	1674	2-tetradecen-1-ol <E>	—	—	—	—	5.5	5.2	—	—
34.40	1668	Bulnesol	—	3.5	—	—	—	—	—	—

¹The selected active fractions Ag₄, Bd₂, Cs₄, and Ls₃ had their actions against *S. mutans* biofilm and their antiproliferative activity evaluated. Ag EO, Bd EO, Cs EO, and Ls EO correspond to the following essential oils: *Aloysia gratissima*, *Baccharis dracunculifolia*, *Coriandrum sativum*, and *Lippia sidoides*, respectively. Only the compounds with relative percentage above 3% are listed. ²M: molecular weight of a nonidentified compound.

These results demonstrate that the EO studied and especially those selected (*A. gratissima*, *B. dracunculifolia*, *C. sativum*, and *L. sidoides*) have potential for bioprospection of new active biomolecules. The fractionation process adopted showed good results, since the fractions obtained were more active than the original EO (Table 2). This bioguided study is a model for bioprospecting new drugs [30], and it can be considered successful since we found active fractions presenting higher activity than their respective EO.

Most EO and fractions studied showed MBC: MIC ratio that enables them to be classified as bactericidal compounds. This could be explained by their hydrophobicity, an important characteristic that exists in EO and their fractions [31] and may allow them to partition the lipids of the bacterial cell membrane, turning them more permeable and leading to leakage of ions and other cell constituents [32, 33]. On the other hand, *B. dracunculifolia* EO and its selected active

fraction (Bd₂) present compounds that could be capable of infiltrating the cell and interact with cellular metabolic mechanisms [34], demonstrating their bacteriostatic effect. Nevertheless, despite presenting bactericidal or bacteriostatic effect, the selected EO proved to be active against both *S. mutans* planktonic cells and biofilm, demonstrating the effectiveness of the substances present in these EO, since it is difficult to disrupt *S. mutans* biofilm [35].

The selected active fractions were also tested against *S. mutans* biofilm, and they were able to disrupt its formation at all tested concentrations. This disruption was observed using SEM, which showed the change the selected active fractions caused in the structure of *S. mutans* biofilm.

At the concentrations tested, it was possible to observe huge failures in *S. mutans* biofilm surface treated with the active fractions when compared with the treatment with the vehicle, which presented a more homogeneous

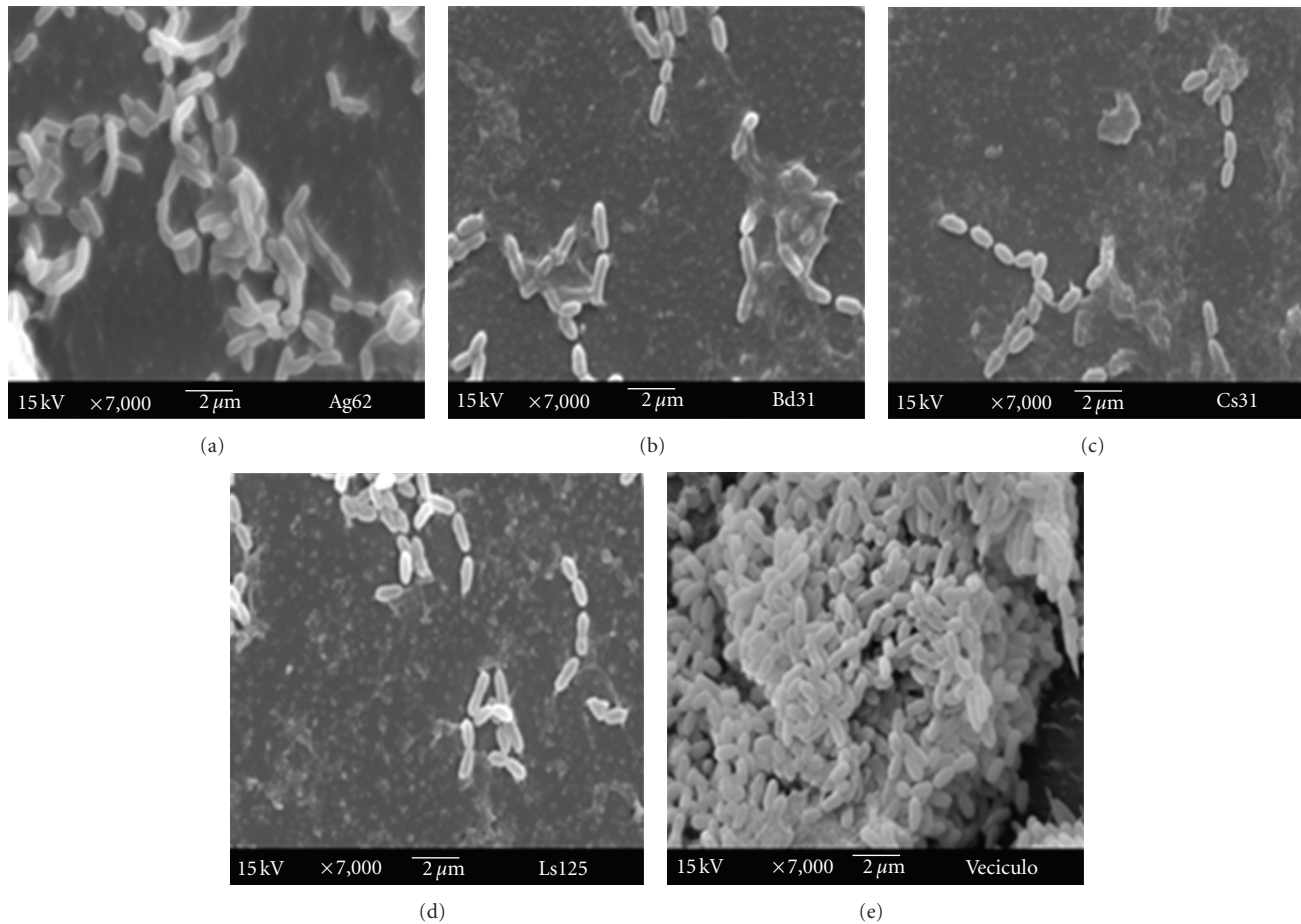


FIGURE 2: Scanning electron microscopy of *Streptococcus mutans* biofilms treated with the selected active fractions from selected essential oils and the vehicle. Images a, b, c, and d show the reduction of biofilm formation after treatment with Ag₄, Bd₂, Cs₄, and Ls₃ fractions, respectively, compared with the treatment with the vehicle (image (e)) (magnification of 7000x).

TABLE 4: Total growth inhibition (TGI) of selected essential oils and their selected active fractions tested against normal human cell and tumor cell lines.

Cell line	TGI ($\mu\text{g/mL}$) ¹								
	Ag EO	Ag ₄	Bd EO	Bd ₂	Cs EO	Cs ₄	Ls EO	Ls ₃	Dox
Glioma (U251)	>250	55.6	38.2	51.4	8.3	61.5	>250	94.9	0.92
Breast (MCF-7)	>250	45.2	46.0	67.7	13.6	111.6	>250	56.6	3.3
Ovarian (NCI-ADR/RES)	>250	50.6	59.2	10.5	90.0	13.1	>250	112.3	1.6
Kidney (786-0)	>250	5.9	49.5	47.1	29.8	72.1	>250	26.7	>250
Lung (NCI-H460)	>250	42.7	87.6	76.8	105.0	110.3	>250	79.8	4.9
Prostate (PC-3)	99.9	>250	>250	>250	118.1	141.9	26.7	>250	11.7
Ovarian (OVCAR-3)	<0.25	47.6	<0.25	58.0	<0.25	73.7	<0.25	60.4	7.6
Keratinocytes (HaCaT)	>250	>250	92.3	95.7	129.4	145.6	>250	>250	2.3

¹ Data result from three replicates per treatment in two independent tests at 25°C for 48 hours. Ag EO, Bd EO, Cs EO, and Ls EO correspond to the following essential oils: *Aloysia gratissima*, *Baccharis dracunculifolia*, *Coriandrum sativum*, and *Lippia sidoides*, respectively. Ag₄, Bd₂, Cs₄, and Ls₃ are the selected active fractions evaluated. Dox: doxorubicin (positive control).

biofilm surface. These changes were also observed in another study that tested the action of *C. sativum* and its bioactive fraction against *Candida albicans* [11]. Moreover, the simple conformational change in biofilm, caused by the action of the selected active fractions, could make it more susceptible and less virulent [4].

However, when the selected active fractions were tested in order to evaluate their ability to reduce *S. mutans* acid production, no significant results were observed ($P > 0.05$). Therefore, the selected active fractions could not act on this important virulence factor of *S. mutans*, different from the findings of another work with *B. dracunculifolia* extracts, which showed significant reduction in production of acid by this microorganism [36]. The difference between *B. dracunculifolia* EO and the active extracts from this plant may be attributed to the extraction method, which results in different compound mixtures with different mechanisms of action [37].

It is known that EOs are composed of numerous different chemical compounds, and their antimicrobial activity might be attributed to several different mechanisms, which could explain the variations in their mode of action [38].

The present data suggest the occurrence of a separation during the fractionation process of the selected EO in such a way that the selected active fractions presented higher amounts of bioactive compounds than their respective EO. The main biologically active compounds found in the selected active fractions were thymol, carvacrol, 2-decen-1-ol, trans-nerolidol, spathulenol, ethyl ester benzene-propanoic, trans-pinocamphone, cis-pinocamphone, and guaïol. These compounds have been extensively described in the literature for their effect on microorganisms [39, 40].

Both forms of trans- and cis-pinocamphone are major constituents of Ag₄ fraction and were also found in *Hyssopus officinalis* L. EO [41]. These compounds are responsible for the antibacterial, antifungal, and antioxidant activities of *H. officinalis* EO, demonstrating that they pass through the cell wall and the plasma membrane, disrupting their structure [41]. The bactericidal activity of Ag₄ fraction observed in the present study may be a consequence of this mode of action.

Trans-nerolidol and spathulenol, two compounds present in Bd₂ fraction, have been considered active against unknown Gram-positive and Gram-negative bacteria [13]. Although spathulenol shows activity against *S. mutans*, its mechanism of action still remains unknown [13].

Other studies showed that certain alcohols, such as 2-decen-1-ol, have higher antimicrobial activity than aldehydes against *Candida* spp. [11, 16]. These alcohols were found in Cs₄ fraction and may be responsible for the action against *S. mutans* biofilm. Furthermore, considering the mode of action of *C. sativum* EO, it seems to result in bacterial cell permeabilization, leading to the impairment of other cell functions, such as membrane potential, respiratory activity, or efflux pump activity [42].

Thymol is an optic isomer of carvacrol, and both substances seem to make bacterial membrane more permeable [43]. In our study, both were found in Ls₃ fraction as its major components. Previous studies have shown that these compounds present antimicrobial activity against fungi and

bacteria [44], including species of the genus *Streptococcus* [12].

After determining the antimicrobial activity of a natural product, it is important to verify if it also exhibits antiproliferative activity, mainly after its fractionation, a procedure that may concentrate toxic compounds in the fractions that present biological activity.

Based on TGI values, the selected EO and selected active fractions could be classified as inactive (TGI > 50 µg/mL), weakly active (15 µg/mL < TGI < 50 µg/mL), moderately active (6.25 µg/mL < TGI < 15 µg/mL), and strongly active (TGI < 6.25 µg/mL) [45]. The absence of activity was clearly observed in this study since all selected EO and selected active fractions were inactive against the human normal cell line tested.

All EOs tested were selective against the ovarian tumor cell line, showing potent activity. Ag₄ showed potent activity against the kidney tumor cell line, and Bd₂ and Cs₄ fractions showed only moderate activity against the ovarian tumor cell line. These results show the specificity of these EO and their fractions against some tumor cell lines, an important and desired characteristic for potential new chemotherapeutic drugs [15].

It is known that EO compounds, such as monoterpenes, have shown effects on mevalonate metabolism, linked to the maintenance of cell membrane, which could contribute to terpene tumor suppressive action [46]. Thereby, the presence of monoterpenes in the selected active fractions of our study may explain their antiproliferative actions against some tumor cell lines [47]; however, more studies are required to find the compounds of EO responsible for their anticancer activity, since little is known about essential oils and their antiproliferative activity.

5. Conclusion

The results of the present study indicate that all EO and fractions tested showed good antimicrobial activity, but only those showing activity at low concentrations were taken into consideration and fractionated for bioprospection of new agents against *S. mutans*. Among these fractions, the selected active fractions were able to disrupt *S. mutans* biofilm formation, did not inhibit normal cell line growth, and were more specific against human tumor cell lines. These features enable them to be tested in further studies and help the discovery of new bioactive molecules.

Acknowledgment

The authors thank São Paulo Research Foundation (FAPESP, no. 2009/12353-0 and no. 2011/14757-0) and the National Council for Scientific and Technological Development (CNPq, no. 308644/2011-5) for the financial support.

References

- [1] Brasil, Ministério da Saúde, Departamento de Atenção Básica, Coordenação Nacional de Saúde Bucal, Projeto SB Brasil

- 2010—Pesquisa Nacional de Saúde Bucal, Primeiros resultados, Brasília, Brazil, 2011.
- [2] P. D. Marsh, "Are dental diseases examples of ecological catastrophes?" *Microbiology*, vol. 149, no. 2, pp. 279–294, 2003.
 - [3] W. H. Bowen, S. M. Amsbaugh, S. Monell-Torrens, J. Brunelle, H. Kuzmiak-Jones, and M. F. Cole, "A method to assess cariogenic potential of foodstuffs," *The Journal of the American Dental Association*, vol. 100, no. 5, pp. 677–681, 1980.
 - [4] J. K. Kajfasz, I. Rivera-Ramos, J. Abranches et al., "Two Spx proteins modulate stress tolerance, survival, and virulence in *Streptococcus mutans*," *Journal of Bacteriology*, vol. 192, no. 10, pp. 2546–2556, 2010.
 - [5] D. Ajdić, W. M. McShan, R. E. McLaughlin et al., "Genome sequence of *Streptococcus mutans* UA159, a cariogenic dental pathogen," *Proceedings of the National Academy of Sciences of the United States of America*, vol. 99, no. 22, pp. 14434–14439, 2002.
 - [6] T. M. S. Alves, C. A. Silva, N. B. Silva, E. B. Medeiros, and A. M. G. Valença, "Atividade antimicrobiana de produtos fluoretados sobre bactérias formadoras do biofilme dentário: estudo *in vitro*," *Pesquisa Brasileira em Odontopediatria e Clínica Integrada*, vol. 10, no. 2, pp. 209–216, 2010.
 - [7] J. D. Bader, D. A. Shugars, and A. J. Bonito, "Systematic reviews of selected dental caries diagnostic and management methods," *Journal of Dental Education*, vol. 65, no. 10, pp. 960–968, 2001.
 - [8] J. Clardy and C. Walsh, "Lessons from natural molecules," *Nature*, vol. 432, no. 7019, pp. 829–837, 2004.
 - [9] J. G. Jeon, P. L. Rosalen, M. L. Falsetta, and H. Koo, "Natural products in caries research: current (limited) knowledge, challenges and future perspective," *Caries Research*, vol. 45, no. 3, pp. 243–263, 2011.
 - [10] M. Simões, "Antimicrobial strategies effective against infectious bacterial biofilms," *Current Medicinal Chemistry*, vol. 18, no. 14, pp. 2129–2145, 2011.
 - [11] V. F. Furlletti, I. P. Teixeira, G. Obando-Pereda et al., "Action of *Coriandrum sativum* L. essential oil upon oral *Candida albicans* biofilm formation," *Evidence-Based Complementary and Alternative Medicine*, vol. 2011, Article ID 985832, 9 pages, 2011.
 - [12] M. A. Botelho, N. A. P. Nogueira, G. M. Bastos et al., "Antimicrobial activity of the essential oil from *Lippia sidoides*, carvacrol and thymol against oral pathogens," *Brazilian Journal of Medical and Biological Research*, vol. 40, no. 3, pp. 349–356, 2007.
 - [13] F. Silva, "Efeito antimicrobiano *in vitro* dos compostos isolados da *Mikania glomerata* sobre os patógenos orais," [Senior Research Project], Faculdade de Odontologia de Piracicaba, UNICAMP, Piracicaba, Brazil, 2005.
 - [14] F. Bakkali, S. Averbeck, D. Averbeck, and M. Idaomar, "Biological effects of essential oils—a review," *Food and Chemical Toxicology*, vol. 46, no. 2, pp. 446–475, 2008.
 - [15] J. E. Carvalho, "Atividade antiulcerogênica e anticâncer de produtos naturais e de síntese," *Construindo a História dos Produtos Naturais*, vol. 7, pp. 1–18, 2006.
 - [16] A. F. Begnami, M. C. T. Duarte, V. Furlletti, and V. L. G. Rehder, "Antimicrobial potential of *Coriandrum sativum* L. against different *Candida* species *in vitro*," *Food Chemistry*, vol. 118, no. 1, pp. 74–77, 2010.
 - [17] R. P. Adams, *Identification of Essential Oils Components by Gas Chromatography/Mass Spectrometry*, Allured, Carol Stream, Ill, USA, 2007.
 - [18] Clinical and Laboratory Standards Institute, *Methods for Dilution Antimicrobial Susceptibility Tests for Bacteria that Grow Aerobically; Approved Standard*, vol. 26, no. 2, CLSI document M07-A7, Fort Wayne, Ind, USA, 7th edition, 2006.
 - [19] S. P. Soares, A. H. C. Vinholis, L. A. Casemiro, M. L. A. Silva, W. R. Cunha, and C. H. G. Martins, "Atividade antibacteriana do extrato hidroalcoólico bruto de *Stryphnodendron adstringens* sobre microorganismos da cárie dental," *Revista Odonto Ciência*, vol. 23, no. 2, pp. 141–144, 2008.
 - [20] Clinical and Laboratory Standards Institute, *Methods for Dilution Antimicrobial Susceptibility Tests for Bacteria that Grow Aerobically*, vol. 29, no. 2, CLSI document M07-A8, Wayne, Pa, USA, 8th edition, 2009.
 - [21] H. Koo, M. F. Hayacibara, B. D. Schobel et al., "Inhibition of *Streptococcus mutans* biofilm accumulation and polysaccharide production by apigenin and *tt*-farnesol," *Journal of Antimicrobial Chemotherapy*, vol. 52, no. 5, pp. 782–789, 2003.
 - [22] R. O. Mattos-Graner, S. Jin, W. F. King, T. Chen, D. J. Smith, and M. J. Duncan, "Cloning of the *Streptococcus mutans* gene encoding glucan binding protein B and analysis of genetic diversity and protein production in clinical isolates," *Infection and Immunity*, vol. 69, no. 11, pp. 6931–6941, 2001.
 - [23] S. Duarte, P. L. Rosalen, M. F. Hayacibara et al., "The influence of a novel propolis on mutans streptococci biofilms and caries development in rats," *Archives of Oral Biology*, vol. 51, no. 1, pp. 15–22, 2006.
 - [24] S. P. Hawser and L. J. Douglas, "Biofilm formation by *Candida* species on the surface of catheter materials *in vitro*," *Infection and Immunity*, vol. 62, no. 3, pp. 915–921, 1994.
 - [25] A. Monks, D. Scudiero, P. Skehan et al., "Feasibility of a high-flux anticancer drug screen using a diverse panel of cultured human tumor cell lines," *Journal of the National Cancer Institute*, vol. 83, no. 11, pp. 757–766, 1991.
 - [26] R. H. Shoemaker, "The NCI60 human tumour cell line anticancer drug screen," *Nature Reviews Cancer*, vol. 6, no. 10, pp. 813–823, 2006.
 - [27] C. Denny, M. E. Zacharias, A. L. T. G. Ruiz et al., "Antiproliferative properties of polyketides isolated from *Virola sebifera* leaves," *Phytotherapy Research*, vol. 22, no. 1, pp. 127–130, 2008.
 - [28] H. Koo, B. P. F. A. Gomes, P. L. Rosalen, G. M. B. Ambrosano, Y. K. Park, and J. A. Cury, "*In vitro* antimicrobial activity of propolis and *Arnica montana* against oral pathogens," *Archives of Oral Biology*, vol. 45, no. 2, pp. 141–148, 2000.
 - [29] M. C. T. Duarte, E. E. Leme, C. Delarmelina, A. A. Soares, G. M. Figueira, and A. Sartoratto, "Activity of essential oils from Brazilian medicinal plants on *Escherichia coli*," *Journal of Ethnopharmacology*, vol. 111, no. 2, pp. 197–201, 2007.
 - [30] L. M. C. Simões, L. E. Gregório, A. A. Silva Filho et al., "Effect of Brazilian green propolis on the production of reactive oxygen species by stimulated neutrophils," *Journal of Ethnopharmacology*, vol. 94, no. 1, pp. 59–65, 2004.
 - [31] S. Burt, "Essential oils: their antibacterial properties and potential applications in foods—a review," *International Journal of Food Microbiology*, vol. 94, no. 3, pp. 223–253, 2004.
 - [32] K. Knobloch, H. Weigand, N. Weis, H. M. Schwarm, and H. Vigerschow, "Action of terpenoids on energy metabolism," in *Proceedings of the Progress in essential oil research: 16th International Symposium on Essential*, E. J. B. Oils, Ed., pp. 429–445, De Gruyter, 1986.
 - [33] A. Ultee, M. H. J. Bennik, and R. Moezelaar, "The phenolic hydroxyl group of carvacrol is essential for action against the

- food-borne pathogen *Bacillus cereus*," *Applied and Environmental Microbiology*, vol. 68, no. 4, pp. 1561–1568, 2002.
- [34] M. Marino, C. Bersani, and G. Comi, "Impedance measurements to study the antimicrobial activity of essential oils from *Lamiaceae* and *Compositae*," *International Journal of Food Microbiology*, vol. 67, no. 3, pp. 187–195, 2001.
- [35] P. D. Marsh, "Dental plaque: biological significance of a biofilm and community life-style," *Journal of Clinical Periodontology*, vol. 32, no. 6, pp. 7–15, 2005.
- [36] D. P. S. Leitão, A. A. Silva Filho, A. C. M. Polizello, J. K. Bastos, and A. C. C. Spadaro, "Comparative evaluation of in-vitro effects of Brazilian green propolis and *Baccharis dracunculifolia* extracts on cariogenic factors of *Streptococcus mutans*," *Biological and Pharmaceutical Bulletin*, vol. 27, no. 11, pp. 1834–1839, 2004.
- [37] J. N. Eloff, "Which extractant should be used for the screening and isolation of antimicrobial components from plants?" *Journal of Ethnopharmacology*, vol. 60, no. 1, pp. 1–8, 1998.
- [38] S. Calsamiglia, M. Busquet, P. W. Cardozo, L. Castillejos, and A. Ferret, "Invited review: essential oils as modifiers of rumen microbial fermentation," *Journal of Dairy Science*, vol. 90, no. 6, pp. 2580–2595, 2007.
- [39] I. H. N. Bassole, R. Nebie, A. Savadogo, C. T. Ouattara, N. Barro, and S. A. Traore, "Composition and antimicrobial activities of the leaf and flower essential oils of *Lippia chevalieri* and *Ocimum canum* from Burkina Faso," *African Journal of Biotechnology*, vol. 4, no. 10, pp. 1156–1160, 2005.
- [40] N. A. Parreira, L. G. Magalhães, D. R. Morais et al., "Antiprotozoal, schistosomicidal, and antimicrobial activities of the essential oil from the leaves of *baccharis dracunculifolia*," *Chemistry and Biodiversity*, vol. 7, no. 4, pp. 993–1001, 2010.
- [41] S. Kizil, N. Haşimi, V. Tolun, E. Kilinç, and H. Karataş, "Chemical composition, antimicrobial and antioxidant activities of hyssop (*Hyssopus officinalis* L.) essential oil," *Notulae Botanicae Horti Agrobotanici Cluj-Napoca*, vol. 38, no. 3, pp. 99–103, 2010.
- [42] F. Silva, S. Ferreira, J. A. Queiroz, and F. C. Domingues, "Coriander (*Coriandrum sativum* L.) essential oil: its antibacterial activity and mode of action evaluated by flow cytometry," *Journal of Medical Microbiology*, vol. 60, no. 10, pp. 1479–1486, 2011.
- [43] R. J. W. Lambert, P. N. Skandamis, P. J. Coote, and G. J. E. Nychas, "A study of the minimum inhibitory concentration and mode of action of oregano essential oil, thymol and carvacrol," *Journal of Applied Microbiology*, vol. 91, no. 3, pp. 453–462, 2001.
- [44] E. Lacoste, J. P. Chaumont, D. Mandin, M. M. Plumel, and F. J. Matos, "Antiseptic properties of the essential oil of *Lippia sidoides* Cham: application to the cutaneous microflora," *Annales Pharmaceutiques Francaises*, vol. 54, no. 5, pp. 228–230, 1996.
- [45] G. Fouche, G. M. Cragg, P. Pillay, N. Kolesnikova, V. J. Maharaj, and J. Senabe, "In vitro anticancer screening of South African plants," *Journal of Ethnopharmacology*, vol. 119, no. 3, pp. 455–461, 2008.
- [46] K. M. Swanson and R. J. Hohl, "Anti-cancer therapy: targeting the mevalonate pathway," *Current Cancer Drug Targets*, vol. 6, no. 1, pp. 15–37, 2006.
- [47] A. E. Edris, "Pharmaceutical and therapeutic potentials of essential oils and their individual volatile constituents: a review," *Phytotherapy Research*, vol. 21, no. 4, pp. 308–323, 2007.

Research Article

Chronic Treatment with Squid Phosphatidylserine Activates Glucose Uptake and Ameliorates TMT-Induced Cognitive Deficit in Rats via Activation of Cholinergic Systems

Hyun-Jung Park,¹ Seung Youn Lee,² Hyun Soo Shim,¹ Jin Su Kim,³
Kyung Soo Kim,² and Insop Shim¹

¹Acupuncture and Meridian Science Research Center, Kyung Hee University, Seoul 130-701, Republic of Korea

²Department of Family Medicine, The Catholic University of Korea, Seoul 137-701, Republic of Korea

³Molecular Imaging Research Center, Korea Institute of Radiological & Medical Sciences,
University of Science & Technology, Republic of Korea

Correspondence should be addressed to Kyung Soo Kim, kskim@catholic.ac.kr and Insop Shim, ishim@catholic.ac.kr

Received 28 November 2011; Revised 6 February 2012; Accepted 6 February 2012

Academic Editor: William C. S. Cho

Copyright © 2012 Hyun-Jung Park et al. This is an open access article distributed under the Creative Commons Attribution License, which permits unrestricted use, distribution, and reproduction in any medium, provided the original work is properly cited.

The present study examined the effects of squid phosphatidylserine (Squid-PS) on the learning and memory function and the neural activity in rats with TMT-induced memory deficits. The rats were administered saline or squid derived Squid-PS (Squid-PS 50 mg kg⁻¹, *p.o.*) daily for 21 days. The cognitive improving efficacy of Squid-PS on the amnesic rats, which was induced by TMT, was investigated by assessing the passive avoidance task and by performing choline acetyltransferase (ChAT) and acetylcholinesterase (AChE) immunohistochemistry. 18F-Fluorodeoxyglucose and performed a positron emission tomography (PET) scan was also performed. In the passive avoidance test, the control group which were injected with TMT showed a markedly lower latency time than the non-treated normal group ($P < 0.05$). However, treatment of Squid-PS significantly recovered the impairment of memory compared to the control group ($P < 0.05$). Consistent with the behavioral data, Squid-PS significantly alleviated the loss of ChAT immunoreactive neurons in the hippocampal CA3 compared to that of the control group ($P < 0.01$). Also, Squid-PS significantly increased the AChE positive neurons in the hippocampal CA1 and CA3. In the PET analysis, Squid-PS treatment increased the glucose uptake more than twofold in the frontal lobe and the hippocampus ($P < 0.05$, resp.). These results suggest that Squid-PS may be useful for improving the cognitive function via regulation of cholinergic enzyme activity and neural activity.

1. Introduction

Trimethyltin (TMT) is an organotin compound with potent neurotoxicant effects. This substance is regarded as being particularly useful for studying the response to injury on account of the distinct pattern of degeneration it causes in rodent brain. In particular, the rat hippocampus constitutes the most suitable model for TMT-induced brain injury [1–4]. The molecular basis for the selective vulnerability of specific neuronal populations to neuronal insults has been a key focus in the fields of neurology and neuropathology [5]. TMT-induced neurodegeneration is characterized by massive neuronal death that is mainly localized in the limbic system and especially in the hippocampus, and this

is accompanied by reactive gliosis, epilepsy, and marked neurobehavioral alterations, and so this is considered a useful model of neurodegeneration and selective neuronal death [5–11]. Also, in rats, TMT induces the degeneration of pyramidal neurons in the hippocampus and the cortical areas (pyriform cortex, entorhinal cortex, and subiculum) connected to the hippocampus, but there is also neuronal loss in the association areas [6, 12, 13]. Furthermore, behavioral studies have shown increased locomotor activity, disruption in self-grooming, and learning deficits in TMT-intoxicated rats [1, 5, 14–21]. TMT intoxication impairs the performance of learning acquisition of water maze and Biel maze (water avoidance) tasks as well as the performance of Hebb-Williams maze and radial arm maze tasks. In addition, TMT

intoxication produces deficits in passive avoidance retention, but not in the acquisition of the passive avoidance response [2–4, 10, 21, 22]. Furthermore, deficits in the acquisition of active avoidance at the beginning of training have been reported [16]. Moreover, TMT has been shown to produce effects on operant behavior since TMT-intoxicated rats had higher rates of lever pressing under a fixed-ratio schedule of food presentation [20], and TMT impaired the performance of differential reinforcement at low response rates in an operant schedule [23]. These anatomical and behavioral findings have made TMT-intoxicated rats an attractive model for degenerative diseases such as AD, which is the most common cause of dementia [16].

Phosphatidylserine (PS), a phospholipid nutrient, is active in cell membranes and is the major acidic phospholipid component in the membranes of the brain. Membranes are the working surfaces of every cell, carrying out the essential functions of cellular communication and hormonal signal transduction [24, 25]. Nerve cells, in particular, depend on healthy membrane function for normal neurotransmitter metabolism and nerve signal transmission [26]. Also, PS assists in maintaining adequate glucose utilization in the brain. Glucose is the preferred energy substrate for nerve cells which, unlike other cells, are unable to use fatty acids or proteins for energy production. Brain glucose utilization, an indicator of brain activity, often declines during aging [27].

The present study was undertaken to evaluate the neuroprotective effect of Squid-PS on the TMT-induced memory deficit in rats and to elucidate the mechanism underlying these protective effects in rats. Rats were tested on a passive avoidance test for learning and memory. The analyzed parameters included the expression of cholinergic neurons and neural activity in the hippocampus.

2. Materials and Methods

2.1. Animals and the Experimental Design. Male Sprague-Dawley rats weighting 250–280 g (8 weeks old) each were purchased from Samtaco Animal Corp. (Kyungki-do, Korea). The animals were housed in individual cages under light-controlled conditions (12/12-hour light/dark cycle) and at 23°C room temperature. Food and water were made available ad libitum. All the experiments were approved by the Kyung Hee University institutional animal care and use committee. Also, this experimental protocol was approved by an Institutional Review Committee for the Use of Human or Animal Subjects or that procedures are in compliance with at least the Declaration of Helsinki for human subjects, the National Institutes of Health Guide for Care and Use of Laboratory Animals (Publication no. 85-23, revised 1985), the UK Animals Scientific Procedures Act 1986, or the European Communities Council Directive of 24 November 1986 (86/609/EEC). The rats were allowed at least 1 week to adapt to their environment before the experiments.

The rats were injected intraperitoneally (i.p.) with TMT (8.0 mg/kg, body weight) dissolved in 0.9% saline, and then they were returned to their home cages.

The rats were randomly assigned to three groups of six individuals each as follows: nontreated, naïve normal group

(normal); saline-treated group (control); 50 mg kg⁻¹ Squid-PS-treated group (Squid-PS 50) used in this study, which were manufactured and kindly provided by Doosan Co. Glonet BU (Youngin, Korea). The rats were orally administered with PS, daily for 21 days.

2.2. Passive Avoidance Task (PAT). A passive avoidance task was performed after 21 days of the administration of Squid-PS. Rats were trained in a step-through inhibitory avoidance task. On the training trial, each rat was placed on a lighted platform outside a hole leading to a dark compartment. When the rat stepped into the dark compartment, a constant current foot shock (5 V, 0.5 mA, 10 seconds) was delivered twice. For the retention test, at 24 hours (day1), and at 2 and 3 days later, each rat was again placed on the platform, and the latency to step through was recorded.

2.3. Immunohistochemistry. Briefly, the rats were anesthetized (sodium pentobarbital, 100 mg/kg, IP) and then perfused transcardially with heparinized phosphate-buffered saline (PBS; pH 7.4) for 30 min followed by 4% paraformaldehyde in 0.1 M phosphate buffer (pH 7.4) for 10–15 min. The brains were postfixed in the same fixative overnight, cryoprotected in 30% sucrose solution in PBS, embedded and serially sectioned on a cryostat (Leica, Germany) at 30 μm thickness in the coronal plane, and were collected in PBS. The primary antibodies against the following specific antigen were used: cholinacetyl transferase (sheep polyclonal ChAT, concentration 1 : 2000; Cambridge Research Biochemicals, Cleveland, UK) and acetylcholinesterase (rabbit polyclonal AchE, concentration 1 : 1000; Cambridge Research Biochemicals, Cleveland, UK). The primary antibody was prepared and diluted in 0.3% PBST, 2% blocking serum, and 0.001% kehole limpet hemocyanin (Sigma, USA). The sections were incubated in the primary antiserum for 72 h at 4°C. Following rinsing in PBST, sections were incubated for 2 hr at room temperature in biotinylated rabbit anti-sheep or antirabbit serum (Vector Laboratories, Burlingame, CA, USA) diluted 200X in PBST containing 2% normal rabbit serum. Following a further rinsing in PBS, the tissue was developed using diaminobenzidine (Sigma, USA) as the chromogen. The images were captured using a DP2-BSW imaging system (Olympus, CA, USA), and they were processed using Adobe Photoshop. For measuring the cells that were positive for ChAT and AchE, the grid was placed on CA1 and CA3 in the hippocampus area according to the method of Paxinos et al. [28]. The number of cells was counted at 100x magnification using a microscope rectangle grid that measured 200 × 200 mm. The cells were counted in three sections per rat within the hippocampal CA1 and CA3 areas. The brain sections were visually inspected at 3 different anteroposterior levels extending from -2.12 to -6.04 mm [28].

2.4. [F-18]FDG Micro-PET Scan. All the rats were deprived of food for 12–15 h before the experiments to enhance the [F-18] FDG uptake in the brain [20]. Each animal was placed on a heating pad in a cage and warmed for at least 30 min before the [F-18] FDG injection. The temperature of the cages was kept at 30°C throughout the uptake period in accordance

with an optimized [F-18] FDG uptake protocol [20]. [F-18] FDG (500 μ Ci/100 g body weight) was injected through a tail vein, and the rats were anesthetized with 2% isoflurane in 100% oxygen (Forane solution; ChoongWae Pharma). For the PET imaging, a Siemens Inveon PET scanner (Siemens Medical Solutions, USA) was used throughout the study. The transverse resolution that was used was <1.8 mm at the center [20, 29].

The transmission PET data was acquired for 15 min using a Co-57 point source with an energy window of 120~125 keV. One mCi of [F-18] FDG was injected. After allowing for 30 min of tracer uptake time, 30 min of emission PET data was acquired within an energy window of 350~650 keV. The emission list-mode PET data was sorted into 3D sinograms and reconstructed using 3 DRP methods. The pixel size of the reconstructed image was $0.15 \times 0.15 \times 0.79 \text{ mm}^3$. Attenuation and scatter corrections were performed for all the datasets. Automated regions of interest (ROI) were used to sample cerebral metabolic rate for glucose from the spatially normalized PET within specific AD-related brain regions (hippocampus, prefrontal cortex).

2.5. Voxel-Based Statistical Analysis. Voxel-based statistical analysis was performed to compare the cerebral glucose metabolism of the Squid-PS and control datasets. The procedure used for SPM analysis of the animal PET data was as previously described in our previous study [29]. Briefly, for efficient spatial normalization, only the brain region was extracted. A study-specific template was then constructed using all the datasets. The PET data was spatially normalized onto a rat brain template and smoothed using a 3 mm Gaussian kernel. Count normalization was performed. A voxel-wise *t*-test between the Squid-PS and normal datasets was performed using the Statistical Parametric Mapping 5 program ($P < 0.05$, $K > 50$).

2.6. Statistical Analysis. Statistical comparisons were done for the behavioral and histochemical studies using one-way or two-way ANOVA and repeated measures of ANOVA, respectively, and Tukey's *post hoc* test was done. All of the results are presented as means \pm SEM, and SPSS 15.0 for Windows was used for analysis of the statistics. The significance level was set at $P < 0.05$.

3. Results

3.1. Effect of Squid-PS on the Performance of the Passive Avoidance Task. As shown in Figure 1, the control group showed a memory deficit in the passive avoidance test compared to the normal group ($F_{2,11} = 2.68$, $P < 0.05$). However, the Squid-PS group showed improved memory compared to the control (Day 3, $P < 0.01$).

3.2. ChAT Immunoreactive Neurons of the Hippocampus. ChAT immunoreactive cells in the different hippocampal subregions are shown in Figure 2. Post-hoc comparisons indicated that the ChAT immunoreactivity in the hippocampal CA1 and CA3 of the control group was significantly reduced compared with that of the normal group ($F_{2,16} = 5.4$,

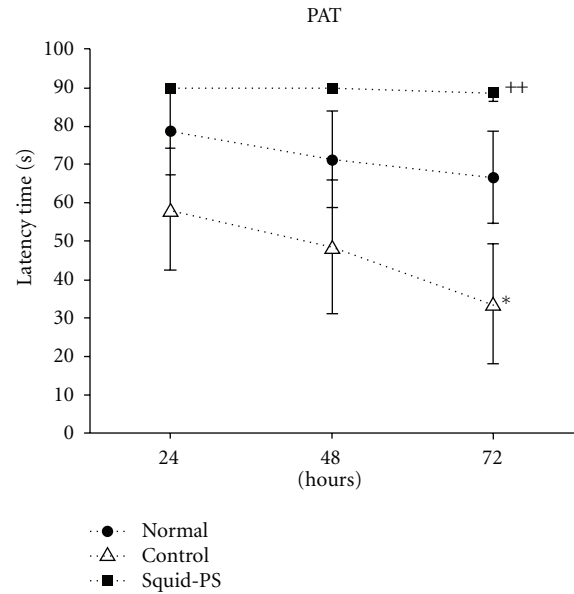


FIGURE 1: The effect of Squid-PS on passive avoidance task. Data represent means \pm SEM of the latency in the passive avoidance task, on learning and memory performance. Rats were exposed to the acquisition trial (DAY1), and retention tests were performed on the following two days (DAY2-3). Statistics: one-way ANOVA test, followed by LSD test. * $P < 0.05$ as compared with the corresponding data of normal group. ** $P < 0.01$ as compared with the corresponding data of control group.

$P < 0.05$; $F_{2,16} = 15.6$, $P < 0.001$). Also, ChAT reactivity in the Squid-PS group was higher than that of the control group, and particularly in CA3 ($P < 0.01$).

3.3. AchE Immunoreactive Neurons of the Hippocampus. AchE immunoreactive cells in the different hippocampal subregions are shown in Figure 3. Post hoc comparisons indicated that the AchE activity in the hippocampus of the control group was significantly lower than that of the normal group ($P < 0.01$). In particular, there were significant differences in both CA1 ($F_{2,13} = 7.3$, $P < 0.01$) and CA3 ($F_{2,13} = 7.6$, $P < 0.01$). However, the AchE reactivity in the Squid-PS group was higher than that of the control group, and particularly in CA1 ($P < 0.01$) and CA3 ($P < 0.05$).

3.4. Change in Brain Glucose Metabolism. The analysis of the brain glucose metabolism analysis was shown in Figure 4, and Table 1. The result of voxel-wise shows comparison between the Squid-PS and control datasets. FDG-PET image scans indicated differences in the cerebral metabolic rate of glucose from the hippocampus to prefrontal cortices between the control and Squid-PS group. On the SPM analysis, the glucose metabolism of the Squid-PS datasets was significantly increased in the hippocampus and frontal lobe compared to that of the control ($P < 0.05$).

4. Discussion

The present study demonstrated that TMT injections produced severe deficits in the rats' performances in a passive

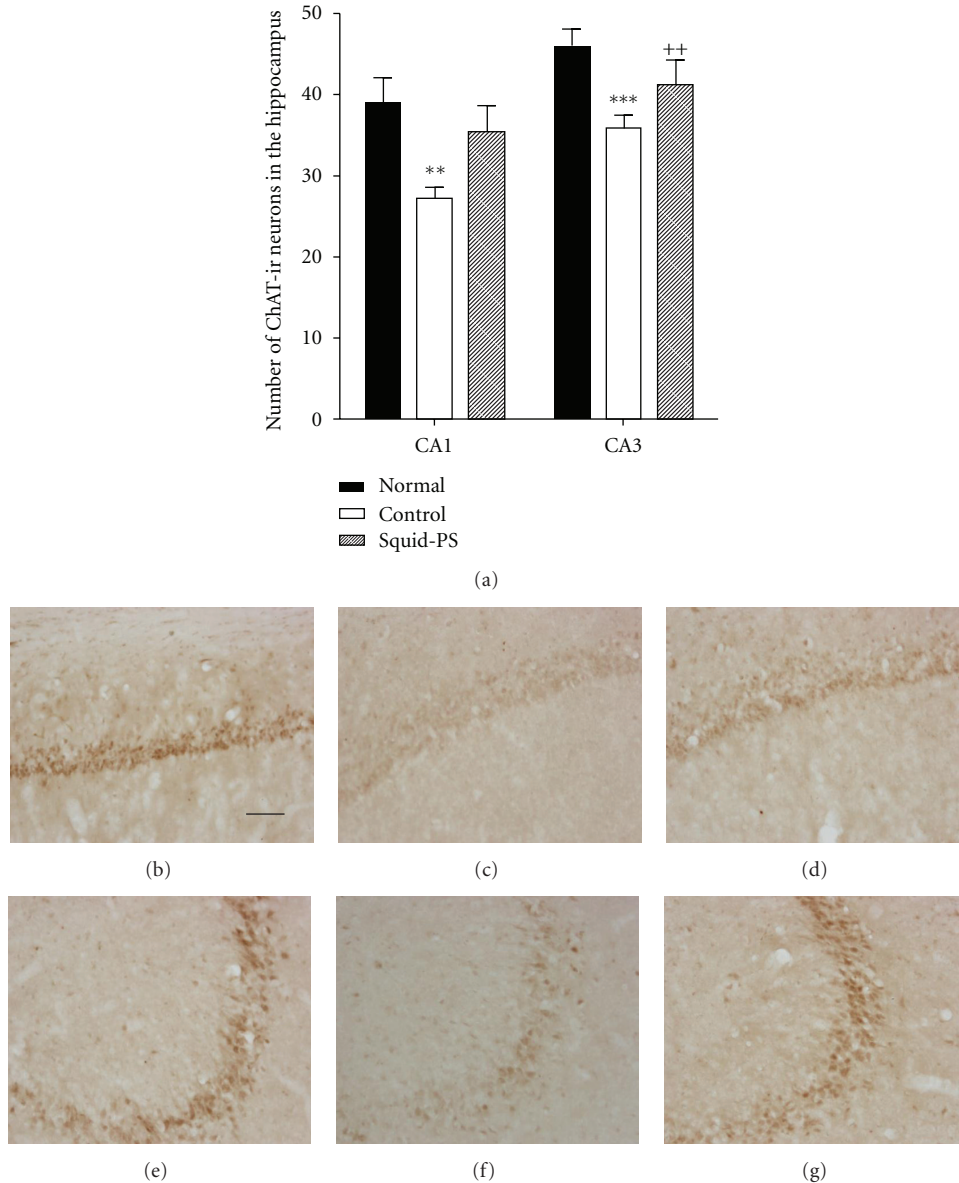


FIGURE 2: (a) The photograph of ChAT immunoreactivity on hippocampus. (b, e) normal group, (c, f) control group, and (d, g) Squid-PS group ChAT expression on the hippocampus. Each column represents the mean value \pm SEM per group. Statistics: one-way ANOVA test, followed by LSD test. ** $P < 0.01$, *** $P < 0.001$ as compared with the corresponding data of normal group. ++ $P < 0.01$ as compared with the corresponding data of control group.

avoidance task along with signs of neurodegeneration, including decreased cholinergic neurons and neural glucose activity in the hippocampus. Repeated treatment with Squid-PS attenuated the TMT-induced learning and memory deficits in the passive avoidance task, and it had a protective effect against the TMT-induced decrease in cholinergic positive neurons. Also, Squid-PS increased the glucose uptake approximately twofold in the frontal lobe and hippocampus.

Intoxication with trimethyltin (TMT) leads to profound behavioral and cognitive deficits in both humans [30] and experimental animals [7, 10]. TMT is known to be widely used as plastic stabilizers, wood preservatives, anti-corrosion

coatings, pesticides, and kill snails, as well as applied by chemical disinfectant and sterilization. So it is clinically meaningful that humans as well as animals can be exposed to it in living environment. In rats, TMT induced the degeneration of the pyramidal neurons in the hippocampus and the cortical areas (pyriform cortex, entorhinal cortex, and subiculum) connected to the hippocampus, but there was also neuronal loss in the association areas [6, 11, 12, 14, 15]. Furthermore, behavioral studies have shown increased disruption of the memory, and learning deficits of TMT-intoxicated rats [20]. TMT intoxication impairs the acquisition of water maze performance [31]. The memory

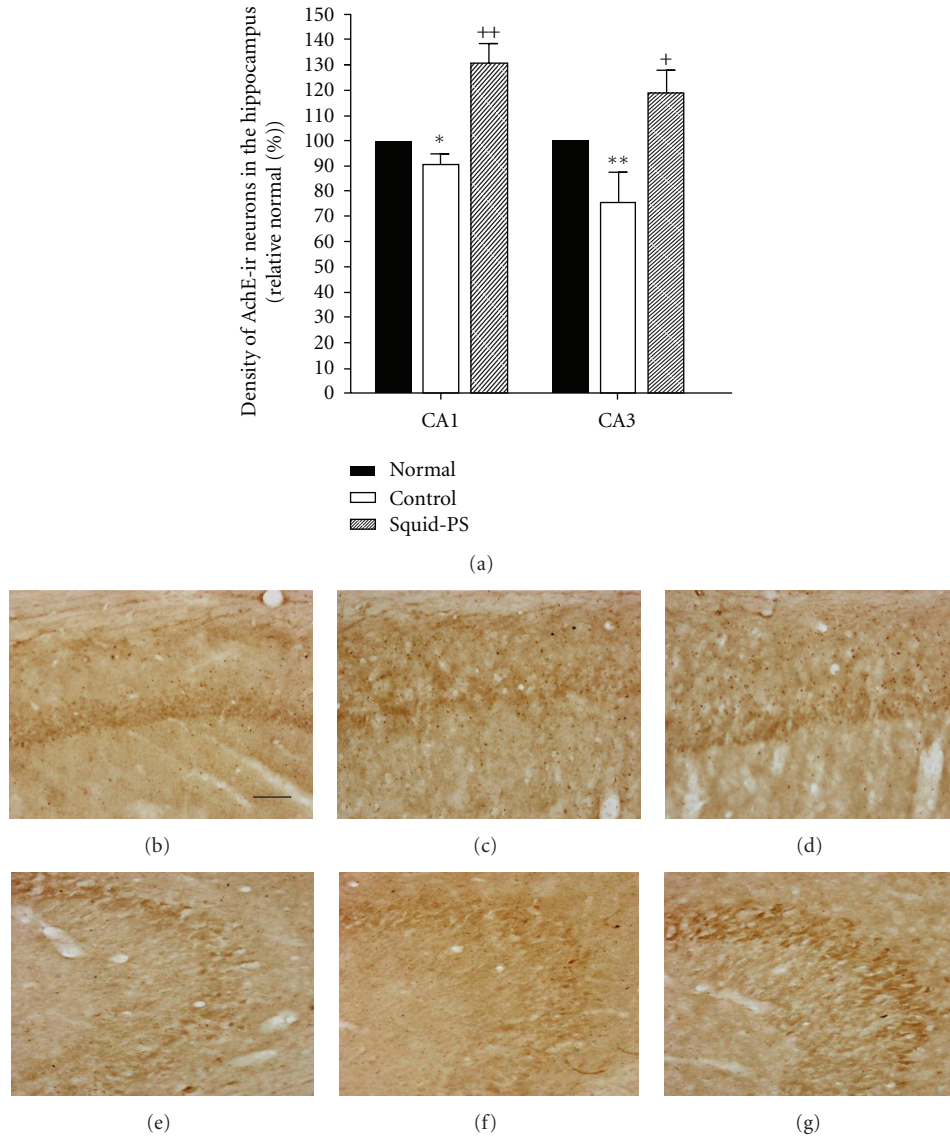


FIGURE 3: (a) The photograph of AchE immunoreactivity on hippocampus. (b, e) normal group, (c, f) control group, and (d, g) Squid-PS group AchE expression on the hippocampus. Each column represents the mean value \pm SEM per group. Statistics: one-way ANOVA test, followed by LSD test. * $P < 0.05$, ** $P < 0.01$ as compared with the corresponding data of normal group. + $P < 0.05$, ++ $P < 0.01$ as compared with the corresponding data of control group.

impairment produced by TMT in the current study is consistent with the previous reports of learning impairments [14, 31–33]. During the training trial in a step-through inhibitory avoidance task after shock, there were no differences among the groups. Treatment of Squid-PS seems to be more effective in reversing the memory impairment of late phase, rather than early phase, suggesting that it may facilitate process of memory consolidation. It has been previously reported that PS has profound curative effects on improving the memory and cognitive function of an Alzheimer's disease-like animal model [22, 34]. Zanotti et al. also showed that the treatment of PS in a scopolamine-induced animal model enhanced the learning and memory abilities of the rats [34]. But there was no study using Squid-PS in TMT intoxication model yet.

TABLE 1: It shows the results of voxelwise comparison between Squid-PS and control datasets. In SPM analysis, the cerebral glucose metabolism of Squid-PS datasets was increased significantly in the hippocampus and frontal lobe compared to control.

Brain area	Coordinates (x, y, z)	Z value
Frontal lobe	(-2.4, 2.7, 8.1)	2.14
Hippocampus (Right)	(7.5, 2.1, 2.4)	2.85
Hippocampus (Left)	(-6.5, 2.1, 2.5)	2.13

The effects of Squid-PS on the central acetylcholine system were also examined by performing immunohistochemistry of the hippocampal neurons. The degeneration of

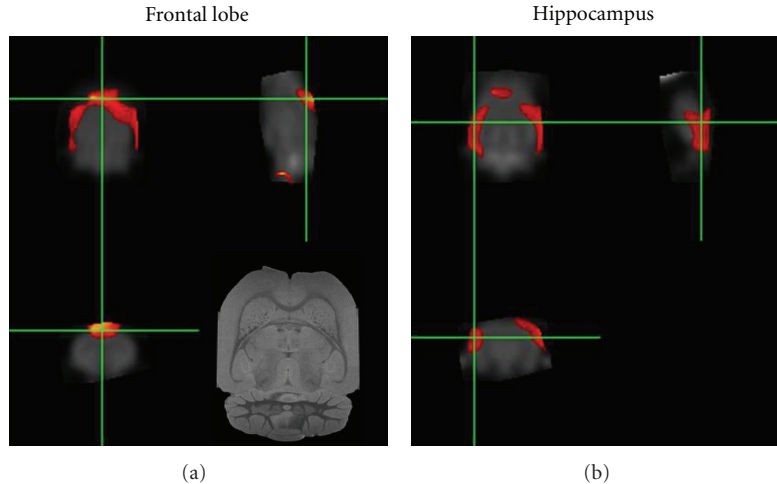


FIGURE 4: Brain regions where regional FDG uptakes in Squid-PS were significantly higher than in control (hippocampus and frontal lobe).

the cholinergic innervation from the basal forebrain to the hippocampal formation in the temporal lobe is thought to be one of the factors determining the progression of memory decay, both during normal aging and AD [35]. The best available marker for cholinergic neurons in the basal forebrain is ChAT activity. ChAT synthesizes the neurotransmitter acetylcholine in the basal forebrain, cortex, hippocampus, and amygdala. A significant reduction in ChAT activity in the postmortem brains of demented patients has been reported. In addition, there was a 20–50% decrease in ChAT activity in the hippocampus of the TMT-induced rats in this current study. However, the present results show that Squid-PS exerts beneficial effects on cholinergic neurotransmission in the brain by increasing the hippocampus ChAT activities. Also, acetylcholine esterase (AChE) is an enzyme which breaks down acetylcholine and is a well-known target and biomarker for memory dysfunction or dementia [20]. In AChE histochemistry, the Squid-PS group showed higher AChE reactivity in both hippocampal CA1 and CA3. These results are consistent with previous reports showing that the cholinergic neurons in the brain are involved in learning and memory in humans and animals [36, 37]. In particular, the hippocampal cholinergic neurons are involved in the formation and maintenance of short-term working memory or retention and retrieval processes in long-term reference memory [16, 18, 38–41]. Based on a previous study, this result suggests that the Squid-PS treatment can promote the memory function.

The name “PET” comes from Positron Emission Tomography. It is a new scanning technique in medical research. Small animal PET experiments can be performed using a variety of dedicated small animal scanners (ATLAS, RatPET, microPET). It is a functional imaging modality at molecular level and provides valuable insights into biochemical, physiological, pathological or pharmacological process in vivo. Recent research efforts find its application in a wide area, ranging from basic insights into the normal physiology and disease processes to drug and radiotracer development and gene therapy. The present study showed that the PET

analysis, the cerebral glucose metabolism of the Squid-PS datasets was significantly increased in the hippocampus and frontal lobe as compared to the control. An obvious limitation of our study is that the spatial resolution of the present micro-PET system is not high enough to permit more specific analysis of the activity changes within certain brain structures. Nevertheless, there have been several studies that have investigated the brain activity changes in small animals using micro-PET technology [2, 20]. Thus, an important point of our study is that in spite of the limited spatial resolution of the micro-PET system, we were able to detect the TMT-induced focal brain changes.

In summary, treatment with Squid-PS attenuated the TMT-induced learning and memory deficits in the passive avoidance test, and Squid-PS treatment had a protective effect against a TMT-induced decrease of the cholinergic neurons and neural activation. Thus, Squid-PS is a good candidate of neuroprotective agent for treatment of Alzheimer’s disease. Further studies that will examine the effects of Squid-PS activation on additional behavioral test will help to elucidate whether increasing the central cholinergic signaling may also improve other types of memory.

Conflict of Interests

The authors declare that there is no conflict of interests.

Authors’ Contribution

Hyun-Jung Park and Seung Youn Lee are equally contributed to this work.

Acknowledgments

This research was supported by the Original Technology Research Program for Brain Science through the National Research Foundation of Korea (NRF) funded by the Ministry of Education, Science and Technology (2011-0030091) and this research was supported by a grant from the Korea

Healthcare Technology R&D Project, Ministry for Health, Welfare & Family Affairs (Grant no. A091037), Republic of Korea.

References

- [1] R. L. Cannon, D. B. Hoover, and M. L. Woodruff, "Trimethyltin increases choline acetyltransferase in rat hippocampus," *Neurotoxicology and Teratology*, vol. 13, no. 2, pp. 241–244, 1991.
- [2] A. O'Connell, B. Earley, and B. E. Leonard, "The neuroprotective effect of tacrine on trimethyltin induced memory and muscarinic receptor dysfunction in the rat," *Neurochemistry International*, vol. 25, no. 6, pp. 555–566, 1994.
- [3] A. O'Connell, B. Earley, and B. E. Leonard, "Changes in muscarinic (M1 and M2 subtypes) and phencyclidine receptor density in the rat brain following trimethyltin intoxication," *Neurochemistry International*, vol. 25, no. 3, pp. 243–252, 1994.
- [4] A. W. O'Connell, B. Earley, and B. E. Leonard, "The σ ligand JO 1784 prevents trimethyltin-induced behavioural and σ -receptor dysfunction in the rat," *Pharmacology and Toxicology*, vol. 78, no. 5, pp. 296–302, 1996.
- [5] C. Brabeck, F. Michetti, M. C. Geloso et al., "Expression of EMAP-II by activated monocytes/microglial cells in different regions of the rat hippocampus after trimethyltin-induced brain damage," *Experimental Neurology*, vol. 177, no. 1, pp. 341–346, 2002.
- [6] C. D. Balaban, J. P. O'Callaghan, and M. L. Billingsley, "Trimethyltin-induced neuronal damage in the rat brain: comparative studies using silver degeneration stains, immunocytochemistry and immunoassay for neuronotypic and gliotypic proteins," *Neuroscience*, vol. 26, no. 1, pp. 337–361, 1988.
- [7] R. S. Dyer, "Physiological methods for assessment of trimethyltin exposure," *Neurobehavioral Toxicology and Teratology*, vol. 4, no. 6, pp. 659–664, 1982.
- [8] M. C. Geloso, V. Corvino, V. Cavallo et al., "Expression of astrocytic nestin in the rat hippocampus during trimethyltin-induced neurodegeneration," *Neuroscience Letters*, vol. 357, no. 2, pp. 103–106, 2004.
- [9] M. C. Geloso, A. Vercelli, V. Corvino et al., "Cyclooxygenase-2 and caspase 3 expression in trimethyltin-induced apoptosis in the mouse hippocampus," *Experimental Neurology*, vol. 175, no. 1, pp. 152–160, 2002.
- [10] N. Ishida, M. Akaike, S. Tsutsumi et al., "Trimethyltin syndrome as a hippocampal degeneration model: temporal changes and neurochemical features of seizure susceptibility and learning impairment," *Neuroscience*, vol. 81, no. 4, pp. 1183–1191, 1997.
- [11] D. Koczyk, M. Skup, M. Zaremba, and B. Oderfeld-Nowak, "Trimethyltin-induced plastic neuronal changes in rat hippocampus are accompanied by astrocytic trophic activity," *Acta Neurobiologiae Experimentalis*, vol. 56, no. 1, pp. 237–241, 1996.
- [12] A. W. Brown, W. N. Aldridge, B. W. Street, and R. D. Verschoyle, "The behavioral and neuropathologic sequelae of intoxication by trimethyltin compounds in the rat," *American Journal of Pathology*, vol. 97, no. 1, pp. 59–81, 1979.
- [13] L. W. Chang and R. S. Dyer, "Septotemporal gradients of trimethyltin-induced hippocampal lesions," *Neurobehavioral Toxicology and Teratology*, vol. 7, no. 1, pp. 43–49, 1985.
- [14] R. L. Cannon, D. B. Hoover, R. H. Baisden, and M. L. Woodruff, "Effects of trimethyltin (TMT) on choline acetyltransferase activity in the rat hippocampus: influence of dose and time following exposure," *Molecular and Chemical Neuropathology*, vol. 23, no. 1, pp. 27–45, 1994.
- [15] R. L. Cannon, D. B. Hoover, R. H. Baisden, and M. L. Woodruff, "The effect of time following exposure to trimethyltin (TMT) on cholinergic muscarinic receptor binding in rat hippocampus," *Molecular and Chemical Neuropathology*, vol. 23, no. 1, pp. 47–62, 1994.
- [16] B. Earley, M. Burke, B. E. Leonard, C. J. Gouret, and J. L. Junien, "A comparison of the psychopharmacological profiles of phencyclidine, ketamine and (+) SKF 10,047 in the trimethyltin rat model," *Neuropharmacology*, vol. 29, no. 8, pp. 695–703, 1990.
- [17] J. J. Hagan, J. H. M. Jansen, and C. L. E. Broekkamp, "Selective behavioural impairment after acute intoxication with trimethyltin (TMT) in rats," *NeuroToxicology*, vol. 9, no. 1, pp. 53–74, 1988.
- [18] R. B. Messing, V. Devauges, and S. J. Sara, "Limbic forebrain toxin trimethyltin reduces behavioral suppression by clonidine," *Pharmacology Biochemistry and Behavior*, vol. 42, no. 2, pp. 313–316, 1992.
- [19] M. Segal, "Behavioral and physiological effects of trimethyltin in the rat hippocampus," *NeuroToxicology*, vol. 9, no. 3, pp. 481–489, 1988.
- [20] H. S. Swartzwelder, R. S. Dyer, W. Holahan, and R. D. Myers, "Activity changes in rats following acute trimethyltin exposure," *NeuroToxicology*, vol. 2, no. 3, pp. 589–593, 1981.
- [21] M. L. Woodruff, R. H. Baisden, and A. J. Nonneman, "Anatomical and behavioral sequelae of fetal brain transplants in rats with trimethyltin-induced neurodegeneration," *NeuroToxicology*, vol. 12, no. 3, pp. 427–444, 1991.
- [22] T. J. Walsh, D. B. Miller, and R. S. Dyer, "Trimethyltin, a selective limbic system neurotoxicant, impairs radial-arm maze performance," *Neurobehavioral Toxicology and Teratology*, vol. 4, no. 2, pp. 177–183, 1982.
- [23] M. L. Woodruff, R. H. Baisden, R. L. Cannon, J. Kalbfleisch, and J. N. Freeman, "Effects of trimethyltin on acquisition and reversal of a light-dark discrimination by rats," *Physiology and Behavior*, vol. 55, no. 6, pp. 1055–1061, 1994.
- [24] S. Chen and K. W. Li, "Comparison of molecular species of various transphosphatidylated phosphatidylserine (PS) with bovine cortex PS by mass spectrometry," *Chemistry and Physics of Lipids*, vol. 152, no. 1, pp. 46–56, 2008.
- [25] Z. Hossain, M. Konishi, M. Hosokawa, and K. Takahashi, "Effect of polyunsaturated fatty acid-enriched phosphatidylcholine and phosphatidylserine on butyrate-induced growth inhibition, differentiation and apoptosis in Caco-2 cells," *Cell Biochemistry and Function*, vol. 24, no. 2, pp. 159–165, 2006.
- [26] J. G. Kay, M. Koivusalo, X. Ma, T. Wohland, and S. Grinstein, "Phosphatidylserine dynamics in cellular membranes," *Molecular Biology of the Cell*. In press.
- [27] X. Bustamante-Marín, C. Quiroga, S. Lavandero, J. G. Reyes, and R. D. Moreno, "Apoptosis, necrosis and autophagy are influenced by metabolic energy sources in cultured rat spermatocytes," *Apoptosis*, vol. 17, no. 6, pp. 539–550, 2012.
- [28] G. Paxinos, C. Watson, M. Pennisi, and A. Topple, "Bregma, lambda and the interaural midpoint in stereotaxic surgery with rats of different sex, strain and weight," *Journal of Neuroscience Methods*, vol. 13, no. 2, pp. 139–143, 1985.
- [29] Q. Bao, D. Newport, M. Chen, D. B. Stout, and A. F. Chatziioannou, "Performance evaluation of the inveon dedicated PET preclinical tomograph based on the NEMA NU-4 standards," *Journal of Nuclear Medicine*, vol. 50, no. 3, pp. 401–408, 2009.
- [30] K. Mizoguchi, M. Yuzurihara, A. Ishige, H. Sasaki, and T. Tabira, "Chronic stress impairs rotarod performance in rats:

- implications for depressive state," *Pharmacology Biochemistry and Behavior*, vol. 71, no. 1-2, pp. 79–84, 2002.
- [31] B. Earley, M. Burke, and B. E. Leonard, "Behavioural, biochemical and histological effects of trimethyltin (TMT) induced brain damage in the rat," *Neurochemistry International*, vol. 21, no. 3, pp. 351–366, 1992.
- [32] B. J. Fueger, J. Czernin, I. Hildebrandt et al., "Impact of animal handling on the results of 18F-FDG PET studies in mice," *Journal of Nuclear Medicine*, vol. 47, no. 6, pp. 999–1006, 2006.
- [33] D. Koczyk, "How does trimethyltin affect the brain: facts and hypotheses," *Acta Neurobiologiae Experimentalis*, vol. 56, no. 2, pp. 587–596, 1996.
- [34] A. Zanotti, L. Valzelli, and G. Toffano, "Chronic phosphatidylserine treatment improves spatial memory and passive avoidance in aged rats," *Psychopharmacology*, vol. 99, no. 3, pp. 316–321, 1989.
- [35] B. Lee, B. J. Sur, J. J. Han et al., "Krill phosphatidylserine improves learning and memory in Morris water maze in aged rats," *Progress in Neuro-Psychopharmacology and Biological Psychiatry*, vol. 34, no. 6, pp. 1085–1093, 2010.
- [36] C. N. Pope, B. T. Ho, and A. A. Wright, "Neurochemical and behavioral effects of N-ethyl-acetylcholine aziridinium chloride in mice," *Pharmacology Biochemistry and Behavior*, vol. 26, no. 2, pp. 365–371, 1987.
- [37] H. Sun, Y. Hu, J.-M. Zhang, S.-Y. Li, and W. He, "Effects of one Chinese herbs on improving cognitive function and memory of Alzheimer's disease mouse models," *China Journal of Chinese Materia Medica*, vol. 28, no. 8, pp. 751–754, 2003.
- [38] C. A. Cohen, R. B. Messing, and S. B. Sparber, "Selective learning impairment of delayed reinforcement autoshaped behavior caused by low doses of trimethyltin," *Psychopharmacology*, vol. 93, no. 3, pp. 301–307, 1987.
- [39] I. Izquierdo, L. A. Izquierdo, D. M. Barros et al., "Differential involvement of cortical receptor mechanisms in working, short-term and long-term memory," *Behavioural Pharmacology*, vol. 9, no. 5-6, pp. 421–427, 1998.
- [40] H. Kim, H. J. Park, H. S. Shim et al., "The effects of acupuncture (PC6) on chronic mild stress-induced memory loss," *Neuroscience Letters*, vol. 488, no. 3, pp. 225–228, 2011.
- [41] K. Mizoguchi, M. Yuzurihara, A. Ishige, H. Sasaki, and T. Tabira, "Effect of chronic stress on cholinergic transmission in rat hippocampus," *Brain Research*, vol. 915, no. 1, pp. 108–111, 2001.

Research Article

The Immunomodulatory Effect of You-Gui-Wan on *Dermatogoides-pteronyssinus*-Induced Asthma

Li-Jen Lin,¹ Chin-Che Lin,² Shulhn-Der Wang,³ Yun-Peng Chao,⁴ and Shung-Te Kao^{1,5}

¹ School of Chinese Medicine, College of Chinese Medicine, China Medical University, Taichung 40402, Taiwan

² Graduate Institute of Chinese Medicine, China Medical University, Taichung 40402, Taiwan

³ School of Post-Baccalaureate Chinese Medicine, College of Chinese Medicine, China Medical University, Taichung 40402, Taiwan

⁴ Department of Chemical Engineering, Feng Chia University, Taichung 40724, Taiwan

⁵ Department of Chinese Medicine, China Medical University Hospital, Taichung 40402, Taiwan

Correspondence should be addressed to Shung-Te Kao, stkao@mail.cmu.edu.tw

Received 22 December 2011; Revised 19 March 2012; Accepted 19 March 2012

Academic Editor: William C. S. Cho

Copyright © 2012 Li-Jen Lin et al. This is an open access article distributed under the Creative Commons Attribution License, which permits unrestricted use, distribution, and reproduction in any medium, provided the original work is properly cited.

The traditional Chinese medicine You-Gui-Wan (YGW) contains ten species of medicinal plants and has been used to improve health in remissive states of asthma for hundreds of years in Asia. However, little is known about the immunomodulatory mechanisms in vivo. Therefore, this study investigated the pathologic and immunologic responses to YGW in mice that had been repeatedly exposed to *Dermatogoides-pteronyssinus* (Der p). YGW reduced Der-p-induced airway hyperresponsiveness and total IgE in serum. It also inhibited eosinophil infiltration by downregulating the protein expression of IL-5 in serum and changed the Th2-bios in BALF by upregulating IL-12. Results of the collagen assay and histopathologic examination showed that YGW reduced airway remodeling in the lung. In addition, after YGW treatment there was a relative decrease in mRNA expression of TGF- β 1, IL-13, eotaxin, RANTES, and MCP-1 in lung in the YGW group. The results of EMSA and immunohistochemistry revealed that YGW inhibited NF- κ B expression in epithelial lung cells. YGW exerts its regulative effects in chronic allergic asthmatic mice via its anti-inflammatory activity and by inhibiting the progression of airway remodeling.

1. Introduction

Asthma is a public health problem worldwide, but particularly in developed countries [1, 2]. Allergic asthma is defined as an acute-on-chronic inflammatory disease of the airway with characteristic eosinophilic recruitment, airway hyperresponsiveness (AHR), hyperplasia of goblet cells, mucus hypersecretion, deposition of collagen, smooth muscle cell hypertrophy, and subepithelial fibrosis [3, 4]. T-cell subsets such as T_H1, T_H2, T_H17, and T_H9 cells as well as regulatory T cells regulate immune responses to allergens in the allergic lung. Moreover, asthma is considered a T helper 2 (T_H2)-cell-driven inflammatory disease [5, 6]. Therefore, drugs that can suppress T_H2 cytokine production would prove useful as allergen immunotherapy agents [7].

Although corticosteroids and β -agonists can improve asthma symptoms, they do not cure the disease [8]. These agents also have side effects, particularly in children. Many

drugs used in Traditional Chinese Medicine (TCM) have been used for centuries to treat asthma and are still widely used in modern medical practice in Asian countries. Recently, many studies have provided evidence of the therapeutic mechanism of numerous herbal formulas that are useful for treating allergic asthma [9].

YGW, a standard yang-tonic decoction, has been used clinically by practitioners of TCM for more than 400 years. Many clinical observations indicate that YGW is capable of enhancing the body's immune system to defend against pathogens [10]. Moreover, some of the herbs in YGW have been demonstrated to promote blood circulation and to have cardioprotective effects [11]. In addition, YGW has been traditionally used to regulate remissive states of asthma. However, the mechanisms governing the modulatory effects of YGW in asthma are not known.

A great deal of information on allergic airway inflammation comes from murine model systems using artificial

TABLE 1: Components of herbal medicines in YGW.

TCM materia medica	Pharmacognostic nomenclature	Amount (g)	Part used
(1) Shou Di Huang	<i>Rehmanniae glutinosa</i>	8.0	root
(2) Shan Yao	<i>Dioscorea opposita</i>	4.0	root
(3) Shan Zhu Yu	<i>Cornus officinalis</i>	4.0	fruit
(4) Gou Qi Zi	<i>Lycium chinensis</i>	4.0	fruit
(5) Yu Si Zi	<i>Cuscuta chinensis</i>	4.0	seed
(6) Lu Jiao Jiao	<i>Cervus elaphus Linnaeus</i>	3.0	horn
(7) Du Zhong	<i>Eucommia ulmoides</i>	4.0	cortex
(8) Dang Gui	<i>Angelica sinensis</i>	3.0	root
(9) Rou Gui	<i>Cinnamomun cassia</i>	2.0	cortex
(10) Fu Zi	<i>Aconitum Carmichaeli</i>	2.0	root
Total amounts		38.0	

ovalbumin (OVA) combined with adjuvants [5]. However, OVA is not a major allergen in human asthma. Up to 85% of patients with allergic asthma are sensitized to house dust mite (HDMs) allergens, such as *Dermatogoides-pteronyssinus* (Der p) [12]. More than ten allergens are found in mites themselves and their fecal pellets [13–18]. These allergens are classified into diverse protein families with various biological functions [19, 20]. For instance, Group 1 allergens are cysteine proteases that cleave intercellular epithelial tight junctions, permitting the transmission of allergens to the submucosal of antigen-presenting cells. Group 2 allergens are interaction with the innate immune system [21]. Repeated dust mite allergen exposure can activate T_H2 and T_H1 , which together orchestrate subsequent allergic responses resulting in pulmonary inflammation characteristic of chronic allergic inflammation [22].

We developed a mouse model of allergic asthma by repeatedly exposing BALB/c mice to Der p via intratracheal exposure to assess the pattern of airway remodeling and the alteration of inflammatory cells and cytokines in BALF after treatment with YGW. Finally, this study was to determine the immunomodulatory effect of YGW and understand the mechanisms by which YGW modulates T_H1 - T_H2 responses at the molecular level. Mice that are chronically exposed to Der p exhibit several symptoms that are similar to those found in patients with allergic asthma, including high levels of immunoglobulin E (IgE) in serum, increased AHR, airway inflammation, and remodeling [22].

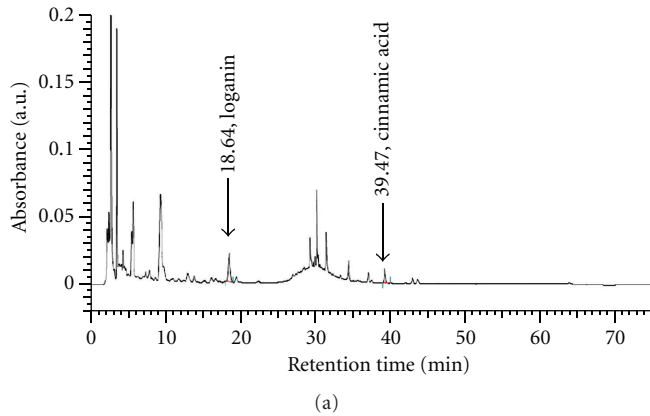
2. Materials and Methods

2.1. Mice and Reagents. Animal experiments were carried out in agreement with the principles outlined by the Institutional Animal Care and Use Committee of the China Medical University (number 97-93-N). Specific pathogen-free, male, 6- to 8-wk-old BALB/c mice were purchased from the National Laboratory Animal Center, Republic of China. The mice were housed in a microisolator cage (Laboratory Products, Inc., Maywood, NJ, USA) and were fed sterile food and water ad libitum. Animal care and all experimental

treatments followed the guidelines set-up by the National Science Council of the Republic of China. Lyophilized Der p was used in this study (Allergon, Sweden). The crude Der p preparation was extracted with ether and dialysis with deionized water. The extracts were lyophilized and stored at -80°C before use. LPS concentration in the Der p preparation was <0.96 EU/mg of Der p (Limulus amoebocyte lysate test; E-Toxate; Sigma-Aldrich).

2.2. YGW Preparation. YGW (batch number 98041022) was supplied by Koda Pharmaceuticals Ltd (Taoyuan, Taiwan). This preparation was a mixture of ten common Chinese herbal medicines as indicated in Table 1. In brief, these were extracted with 17.5 L and 12.5 L of boiled water for 1 hour, respectively. Poaching liquid was mixed two times. After filtering the liquid, the dregs of the decoction were removed. The filtered liquid was lyophilized and crushed into a thin powder. The yield of dried extract from starting crude material was estimated to be 36.31 (w/w). YGW was dissolved in distilled water and stored at -20°C before administration to mice.

2.3. HPLC Analysis of Standard Materials in Test Samples. YGW (1.00 g) was accurately weighed and dissolved in 10 mL of methanol. After sonication for 60 min at room temperature, the solution was filtered through the $0.45\ \mu\text{m}$ membrane filter. YGW was then analyzed by HPLC with Loganin and Cinnamic acid as standards. HPLC analyses were conducted with a system consisting of a Hitachi D-7000 Interface, an L-7100 pump, an L-7420 UV/VIS Detector, an L-7200 Autosampler, and a Mightysil RP-18 (GP) $250 \times 4.6\ \text{mm}$ ($5\ \mu\text{m}$) column. The mobile phase containing Acetonitrile and 0.03% H_3PO_4 (10:90) was pumped at a flow rate of 1.0 mL/min and the product (eluant) was detected at 254 nm. A typical HPLC chromatogram is shown in Figure 1(a). The R^2 values from the calibration curve of two standards were 1.0000 and 0.9999. The quantity of standard materials in YGW was calculated as follows: the amount (mg/g) of standard materials = measured standard materials (mg/ μL) \times the HPLC injection volume



Oriental medicines	Standard materials	Content (mg/g)
Shan Zhu Yu	Loganin	0.3801
Rou Gui	Cinnamic acid	0.0242

(b)

FIGURE 1: (a) The HPLC chromatogram of YGW. (b) Contents of standard materials in YGW (unit: mg/YGW ex. 1 g).

(μL) of YGW \times dilution factor/the amount (g) of YGW. The amounts of standard materials in YGW are given in Figure 1(b).

2.4. Allergen Challenge and Assessment of Airway Inflammation. In the Der p group of BALA/c mice ($n = 6$), allergic airway inflammation and remodeling were provoked by subjecting mice to intratracheally administered Der p (1 mg/mL, 50 μL) in phosphate-buffered saline (PBS) once a week for 4 weeks (total 5 doses). In the YGW group, mice were orally administered YGW (1 g/kg) 30 min before exposure to Der p. In parallel experiments, naïve mice were orally administered water and intratracheally administered PBS.

Mice were sacrificed by i.p. injection of xylazine (200 $\mu\text{g}/\text{mice}$) and ketamine (2 mg/mice) three days after the last challenge as reported previously [23]. Serum and BALF samples were collected and stored at -80°C until assay. Differential counts were performed on cytospin preparations (1×10^5 cells/100 μL of BALF) stained with Liu stain (Biotech, Taiwan) in a blind manner after total leukocyte counting.

2.5. Measurement of Airway Hyperresponsiveness. We used Methacholine-induced pause (Penh) values in live mice as a marker of airway responsiveness to bronchoconstrictors. Airway responsiveness was measured in mice using a single-chamber, whole-body plethysmograph (Buxco Electronics, Inc., Troy, NY) according to the manufacturer's protocol. The enhanced pause (Penh) variable was used to estimate airway resistance. Mice were serially exposed to increasing doses of nebulized methacholine (0, 3.125, 6.25, 12.5, 25, and 50 mg/mL) (Sigma-Aldrich, St. Louis, MO) in PBS for 3 minutes, respectively, and Penh values were measured for 3 minutes following the end nebulization of methacholine.

2.6. Flow Cytometric Analysis. Monoclonal antibodies used for fluorescence-activated cell-scan (FACScan) staining included PE and/or FITC-conjugated anti-mouse CD4 (BD Pharmingen), FITC-conjugated anti-mouse CD8 (BD

Pharmingen), Percp-conjugated anti-mouse CD3 (BD Pharmingen), and FITC-conjugated anti-mouse CD25. BALF cells (1×10^5) were stained with mAb for 30 min on ice. After washing, stained cells were quantified by FACScan (Becton-Dickinson Immunocytometry system, San Jose, CA, USA).

2.7. Measurement of Total IgE. Serum samples of total IgE (1:2 dilution) were measured by ELISA. Briefly, 96-well plates were coated with purified anti-mouse IgE (2 $\mu\text{g}/\text{mL}$, R35-72; BD Pharmingen). After incubation overnight at 4°C , the plates were washed and then exposed to serum samples in duplicate for 2 h. After washing, biotin anti-mouse IgE Ab (2 $\mu\text{g}/\text{mL}$; BD Pharmingen) was added to individual wells and allowed to incubate for 1 h, followed by washings and the addition of streptavidin-HRP conjugate (1:1000 dilution, BD Pharmingen). The plates were washed and developed with a TMB microwell peroxidase substrate system (Kirkegaard & Perry Laboratories, Gaithersburg, MD) and read at OD_{450} . Total IgE concentrations were calculated by comparison with commercial mouse IgE standards.

2.8. ELISA of Cytokine Levels. IL-4, IL-5, IL-6, IL-12, and TNF- α levels were measured with an ELISA Ready-SET-Go! Kit (eBioscience, San Diego, CA), and IL-13, IFN- γ , and TGF- β levels were measured with an ELISA DuoSet! Kit (R&D System, Abingdon, UK) according to the manufacturer's protocols. Standards were run in parallel with recombinant cytokines.

2.9. Histology and Immunohistochemistry of Lung Specimens. Paraffin-embedded tissue was cut into 5 μm sections and stained with H&E and periodic acid-Schiff (PAS) stain. Light microscopy was used for histologic assessment. The degree of inflammatory changes was evaluated with a semiquantitative scale of 0–5 for inflammatory cell infiltration, perivascular spaces, and peribronchial spaces. The scale was graded as follows: 0 (none), 1 (minimal, <1%), 2 (slight, 1–25%), 3 (moderate, 26–50%), 4 (moderate/severe, 51–75%), and 5 (severe/high, 76–100%). Meanwhile, change in goblet-cell

TABLE 2: The total cell number and cellular distributions in BALF of mice 72 h after repetitive Der p challenge.

	Total cells ($\times 10^4/\text{mL}$)	Macrophages (%)	Lymphocytes (%)	Neutrophils (%)	Eosinophils (%)
Naïve	13.6 \pm 2.19	12.60 \pm 1.91 (92.8 \pm 3.27%)	0.52 \pm 0.21 (4.2 \pm 1.79%)	0.48 \pm 0.37 (3.4 \pm 2.51%)	0 (0%)
Der p	69.0 \pm 12.25*	52.99 \pm 9.25* (77.0 \pm 4.69%)	4.49 \pm 1.26* (6.6 \pm 1.81%)	6.81 \pm 5.05* (9.4 \pm 6.43%)	4.68 \pm 1.50* (7.0 \pm 2.55%)
YGW	39.2 \pm 3.11#	33.17 \pm 4.00# (84.6 \pm 7.23%)	2.99 \pm 1.53 (7.6 \pm 3.78%)	2.59 \pm 1.20 (6.6 \pm 3.21%)	0.52 \pm 0.56# (1.4 \pm 1.52%)

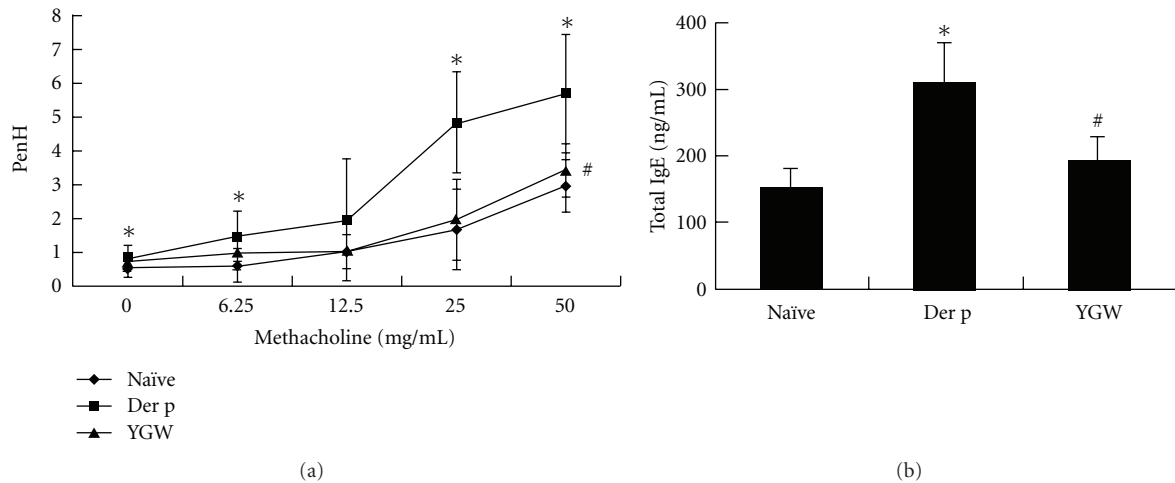


FIGURE 2: The effects of YGW on anti-airway hyperresponsiveness and downregulation of total IgE in a chronic asthmatic mouse model. (a) Airway hyperresponsiveness was determined two days after the last challenge. (b) YGW significantly inhibited the overexpression of IgE in serum. Values represent the mean \pm SD of 6 mice. * P < 0.05 (versus naïve group); # P < 0.05 (between nontreated and YGW-treated groups).

metaplasia was assessed for mucification and the presence of goblet cells in bronchioles as reported previously [24]. The two scores were summed up for individual lesion in each animal. In the immunohistochemical analysis, the Abs against the RelA subunit of NF- κ B (Santa Cruz Biotechnology, Santa Cruz, CA, USA) was used as the primary antibody and HRP-conjugated goat anti-rabbit polyclonal IgG (ZYMED, San Francisco) was used as the secondary antibody. Identification of tissue sites was determined at 100x and 400x magnification.

2.10. Collagen Analysis. Lung tissue (100 mg) from each group was homogenized mechanically in liquid nitrogen and then extracted in 2 mL HBSS. The supernatant collagen was quantified with a Sircol collagen assay kit (Biocolor, Belfast, UK).

2.11. Reverse Transcription and Quantitative PCR. Total RNA was extracted from right lung tissue using Trizol reagent following the manufacturer's protocol (Invitrogen Life Technologies). Total RNA was quantified using a spectrophotometer at 260 nm. Total RNA samples (1 $\mu\text{g}/\text{mL}$) were reverse-transcribed with an ImProm-II Reverse Transcription System kit (Promega). Quantitative PCR was carried out with the FastStart Universal SYBR Green Master

kit (Roche). β -actin was used as a control. The primers (sense and antisense) for each gene were synthesized as follows: β -actin, 5'-GGAAATCGTG CGTGACA-3' and 5'-CACAGGATTCACATACCCAAG-3'; TGF- β , 5'-GAGCAACATGTGGAACCTCTAC-3' and 5'-GCAGTGAGCGCTGAATC-3'; IL-13, 5'-TTATGGTTGTGTGTTATTTAAATGAGTCT-3' and 5'-TGGAGGCTACAGTGAGGT-3'; RANTES, 5'-AGAAGTGGGTTCAAGAATACAT-3' and 5'-GGACCGAGTGGGAGTAG-3'; Eotaxin, 5'-ACATGTTACATTTAAGAAATTGGAGTT-3' and 5'-AGGTCAGCCTGGTCTAC-3'; and MCP-1, 5'-AGAAGGAATGGGTCCAGACATA-3' and 5'-TTAAGGCATCACAGTCCGAG-3'.

2.12. Nuclear Extracts and EMSA. Nuclear extracts were prepared from left lung tissue according to the manufacturer's instructions (Panomics, Redwood). A LightShift Chemiluminescent EMSA Kit (PIERCE, Rockford) was used to detect NF- κ B expression according to the manufacturer's instructions.

2.13. Statistical Analysis. Data are presented as means \pm SD. Differences between mean values were estimated using a Student's t -test. A P value < 0.05 was considered significant. For comparisons of data that were not normally distributed, a Mann-Whitney U -test was performed.

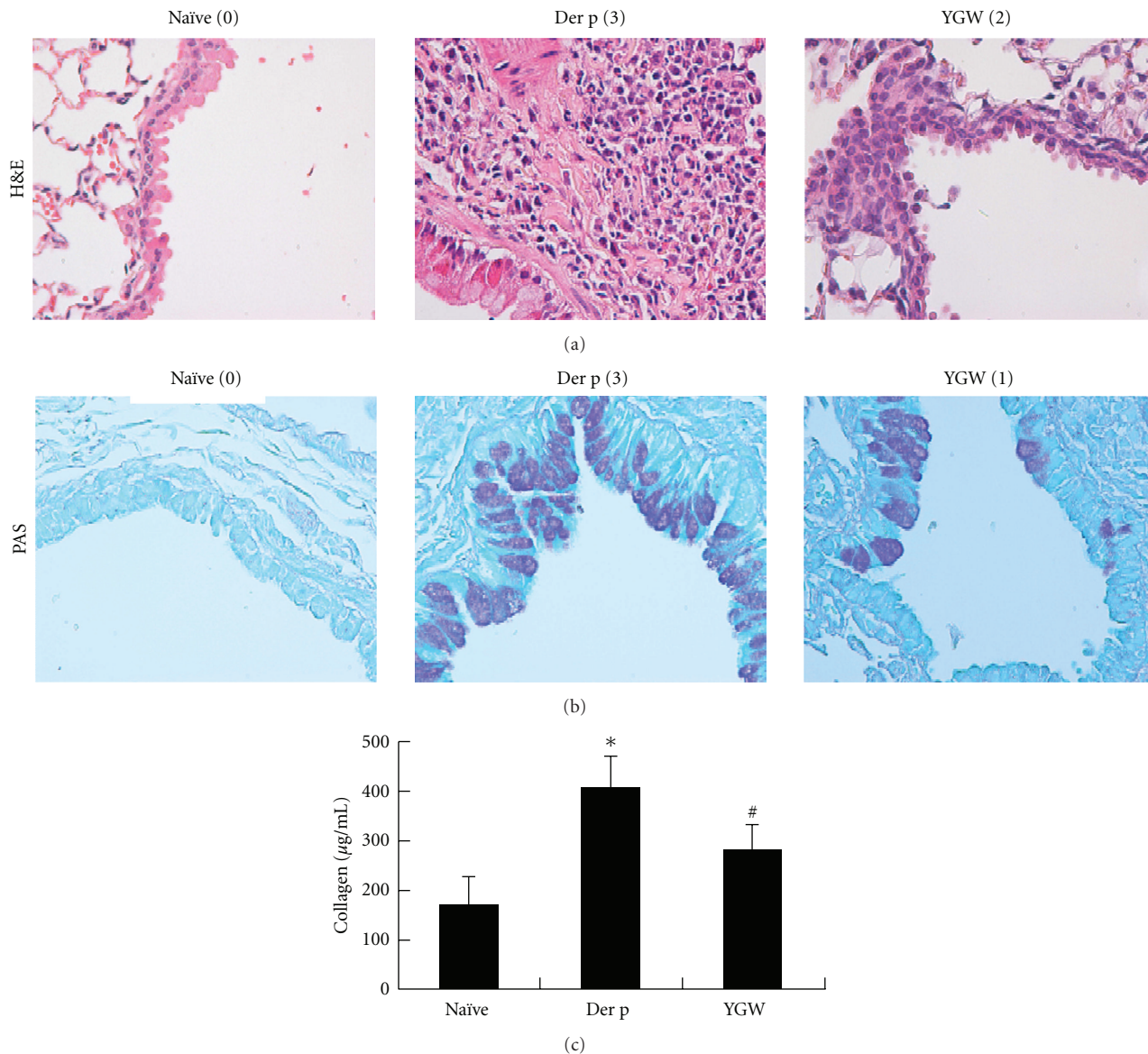


FIGURE 3: The effects of YGW on Der-p-induced airway inflammation, goblet cell hyperplasia, mucus hypersecretion, and collagen deposition in lung tissue of mice. Airway hyperresponsiveness was determined three days after the last challenge. Histopathologic studies of inflammatory cells around the blood vessels (H&E stain; original magnification, $\times 400$) (a) and activity of goblet cells (PAS; original magnification, $\times 400$) in airway epithelial cells (b). Degrees of airway inflammation and goblet cell hyperplasia were estimated as described in Section 2. (c) Collagen levels in lung tissue were significantly higher in the Der p group. Values represent the means \pm SD of 6 mice. * $P < 0.05$ (versus naïve group); # $P < 0.05$ (between nontreated and YGW-treated groups). Values represent the means \pm SD of 6 mice.

3. Results

3.1. Effects of YGW on Antiairway Inflammation, Antiairway Hyperresponsiveness, and Downregulation of Total IgE in a Chronic Asthmatic Mouse Model. We used a repetitive Der p challenge experiment to test the effects of YGW on allergen-induced chronic airway inflammation in a mouse model. Table 2 shows the total and different cell counts in BALF from mice that had been treated with or without YGW during repeated Der p intratracheal inoculation periods (at 1-week intervals). In naïve mice, the cells in BALF were mostly macrophages, and no eosinophils were detected. However, in

the Der p group, the numbers of total cells, macrophages, and eosinophils in BALF were markedly higher than those in naïve mice. Numbers of total cells, macrophages and eosinophils in BALF after allergen challenge were significantly lower in mice in the YGW group than these in untreated challenged mice.

We determined the correlation between airway inflammation and airway AHR. Mice in the Der p group had higher Penh values than those in the naïve group. In the YGW group, there was a marked decrease in Penh values at maximal dose of methacholine (50 mg/mL) relative to the Der p group (Figure 2(a)).

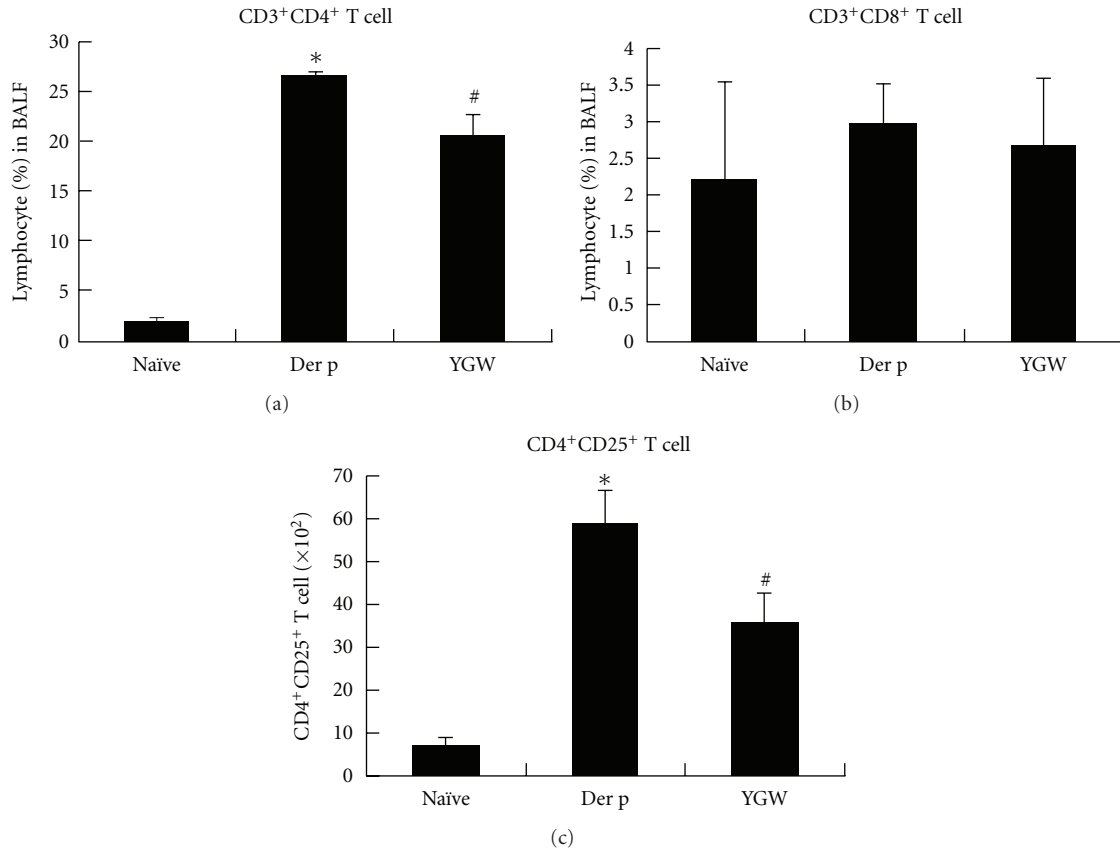


FIGURE 4: The effect of YGW on T-cell subsets in BALF of challenged mice. (a) CD3⁺/CD4⁺, (b) CD3⁺/CD8⁺, and (c) CD4⁺/CD25⁺ lymphocyte levels were determined by flow cytometry with immunofluorescence of monoclonal antibodies. Data are representative of the results from three separate experiments. * $P < 0.05$ (versus naïve group); # $P < 0.05$ (between nontreated and YGW-treated groups).

To determine the effects of YGW treatment on humoral immune responses, we measured serum total IgE. A significant increase in the levels of serum total IgE was observed in the Der p group relative to the naïve group (Figure 2(b)). After treatments with YGW in the sensitization period, the serum concentrations of total IgE decreased significantly.

3.2. YGW Attenuates Der-p-Induced Lung Pathology. The characteristic features of asthmatic airway are cell inflammation, the presence of hyperplastic goblet cells, mucus secretion, and collagen deposition. The left lungs of mice were histologically examined 72 h after the final antigen challenge. Histological sections of lung tissue from Der p-challenged mice exhibited increased airway inflammation, matrix deposition in subepithelial regions, and excessive mucus secretion from hyperplastic goblet cells (Figure 3), relative to mice in the naïve group. In contrast, mice that had been treated with YGW showed significantly less airway inflammation, fewer PAS-positive cells, and less collagen deposition than mice in the Der p group.

3.3. The Effect of YGW on T-Cell Subsets in BALF of Challenged Mice. The effect of YGW on the percentage change of T-cell subsets was determined by flow cytometry with immunofluorescence of monoclonal antibodies to CD3⁺, CD4⁺, CD8⁺,

and CD25⁺, respectively (Figure 4). There was a significant increase in the percentage of CD3⁺/CD4⁺ and numbers of CD4⁺/CD25⁺ lymphocytes in Der p group mice relative to the naïve group. YGW group mice showed a significantly lower percentage of CD3⁺/CD4⁺ and CD4⁺/CD25⁺ lymphocytes than Der p mice. However, there was no significant difference in CD3⁺/CD8⁺ lymphocyte levels in BALF among the three groups of mice.

3.4. YGW Attenuates Cytokine Production in BALF and Serum. To determine the possible effect of YGW on T-cell responses, we evaluated the effects of YGW on T-cell cytokine secretion in BALF and serum. The production of IL-4, IL-5, IL-12, IL-13, TNF- α , TGF- β , and IFN- γ was analyzed by ELISA (Figure 5). YGW significantly attenuated the expression of Der-p-induced IL-13, TNF- α , and TGF- β in BALF but resulted in an increase in IL-12 production relative to mice in the Der p group. YGW group mice also showed significantly lower levels of IL-5 in serum, but not in BALF, than mice in the Der p group. Similarly, there were no changes in IL-4 or INF- γ levels among the YGW groups of mice.

3.5. Immunoregulation of YGW on Der-p-Induced Proinflammatory Cytokine and Chemokine Gene Expression in Lung Tissues. After Der p allergen challenge, the expression levels

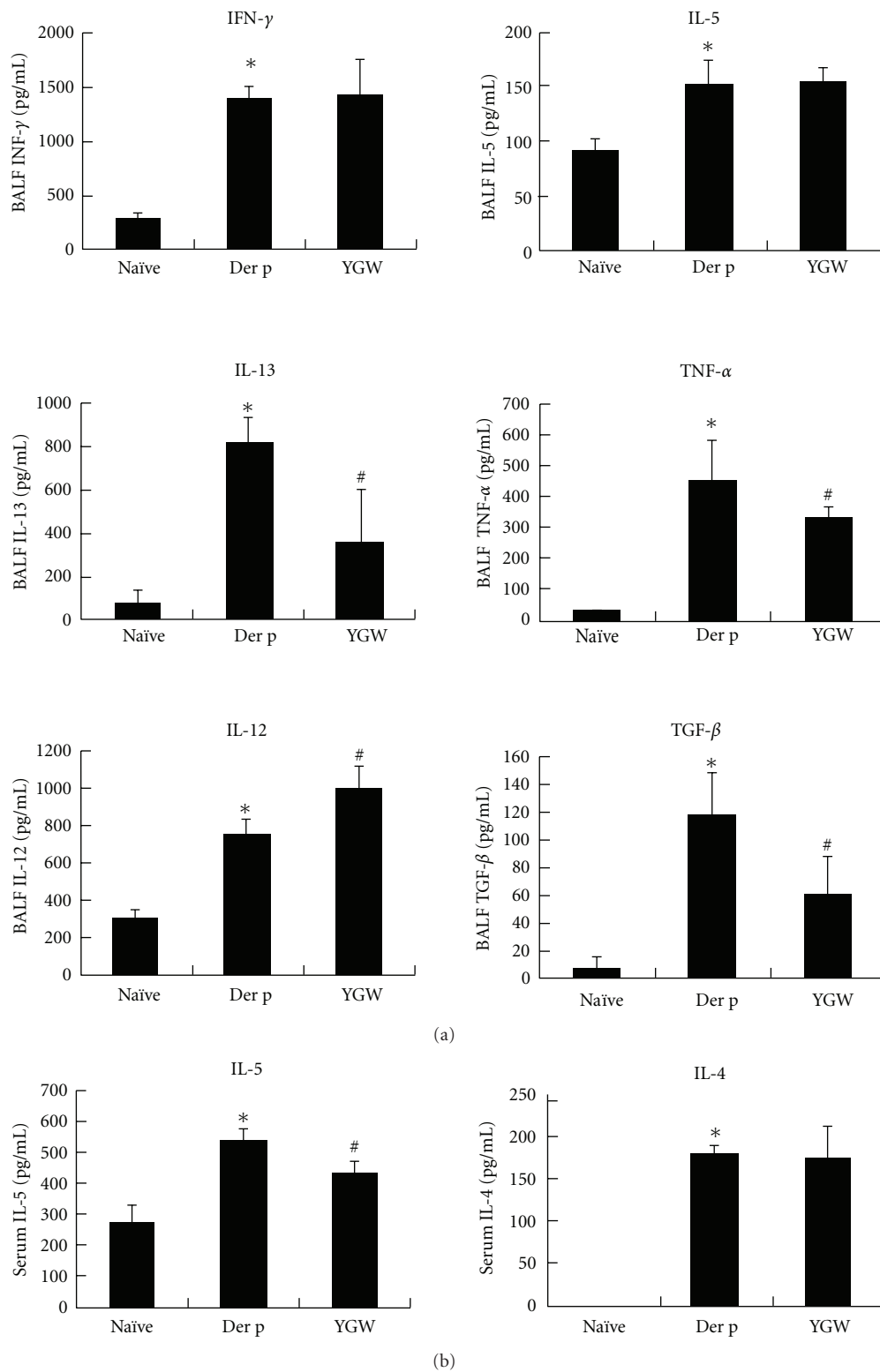


FIGURE 5: The expression levels of IL-13, TGF- β , and TNF- α in BALF were reduced by YGW, but levels of IL-12 increased. YGW resulted in reduced production of IL-5 cytokine in serum. * $P < 0.05$ (versus naïve group); # $P < 0.05$ (between nontreated and YGW-treated groups).

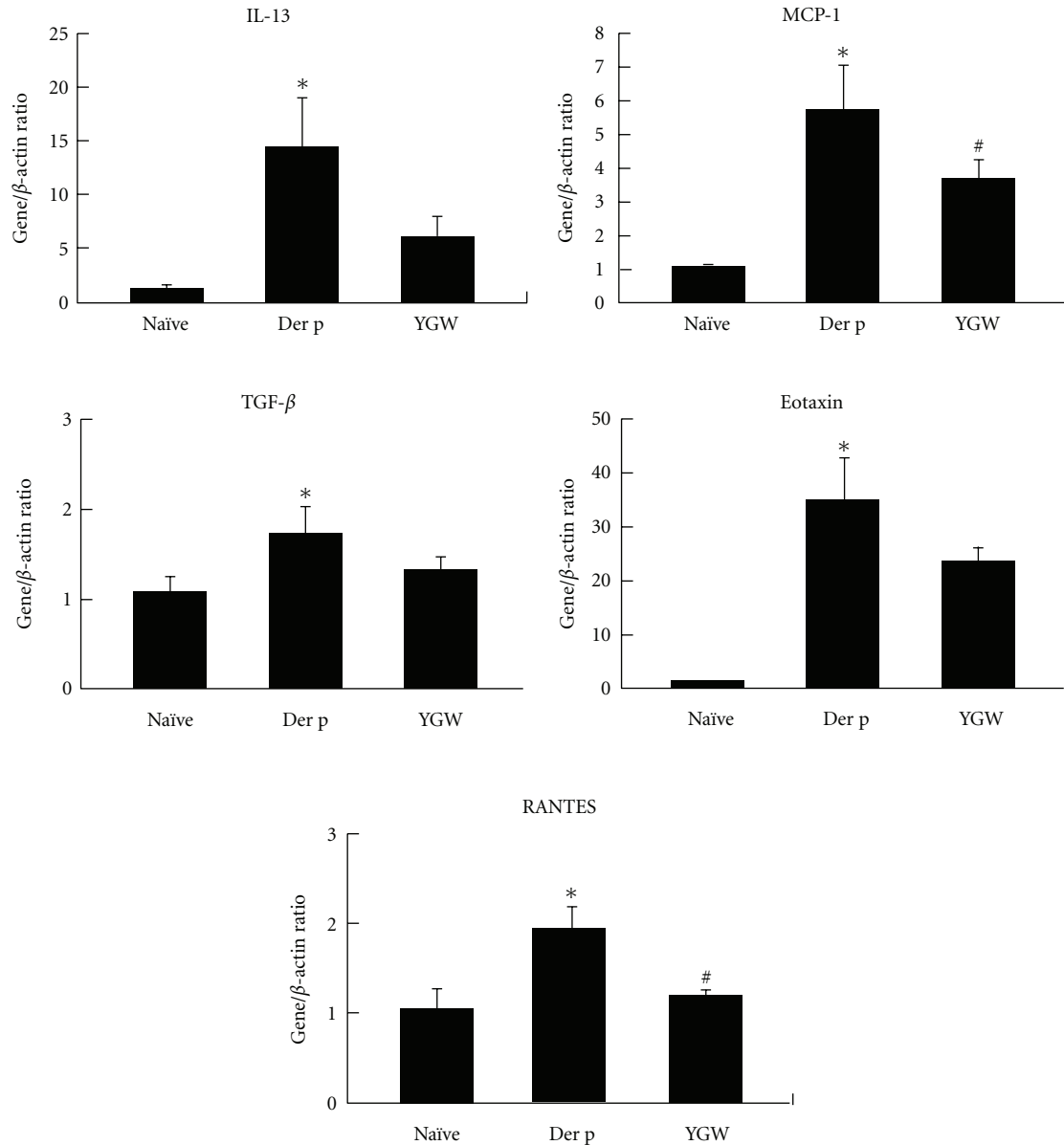


FIGURE 6: Real-time PCR analysis indicated that YGW exerts its suppressive effects by regulating the expression of T_H2 -related genes and chemokines in lung tissue. This real-time PCR profile was representative of three independent experiments.

of IL-13, Eotaxin, RANTES, MCP-1, and TGF- β mRNA in lung tissues from the Der p group were higher than those in the naïve group (Figure 6). Lung tissue from mice pretreated with YGW showed significantly lower levels of IL-13, Eotaxin, RANTES, MCP-1, and TGF- β synthesis than lung tissues from mice in the Der p group.

3.6. NF- κ B Activation Was Suppressed in Der-p-Treated Lung Tissues by YGW. To test whether the inhibitory effect of YGW on Der-p-challenged animals leads to NF- κ B activation, the effects of YGW on expression of NF- κ B were examined by immunohistochemistry and its effects on NF- κ B-specific DNA-protein binding activity were examined using EMSA. Immunohistochemistry staining showed that YGW

inhibited the expression of NF- κ B in bronchiolar epithelial cells of Der-p-challenged mice (Figure 7(a)). EMSA revealed that YGW inhibited NF- κ B-specific DNA-protein binding activity in lung tissues (Figure 7(b)).

4. Discussion

In this study, we provide evidence for the immunoregulatory effects of YGW on allergen-induced airway inflammation and airway hypersensitivity in an established murine model of chronic allergic asthma.

We demonstrated that oral administration of YGW suppressed AHR and reduced the degree of airway inflammation and remodeling. YGW possesses anti-inflammatory effects

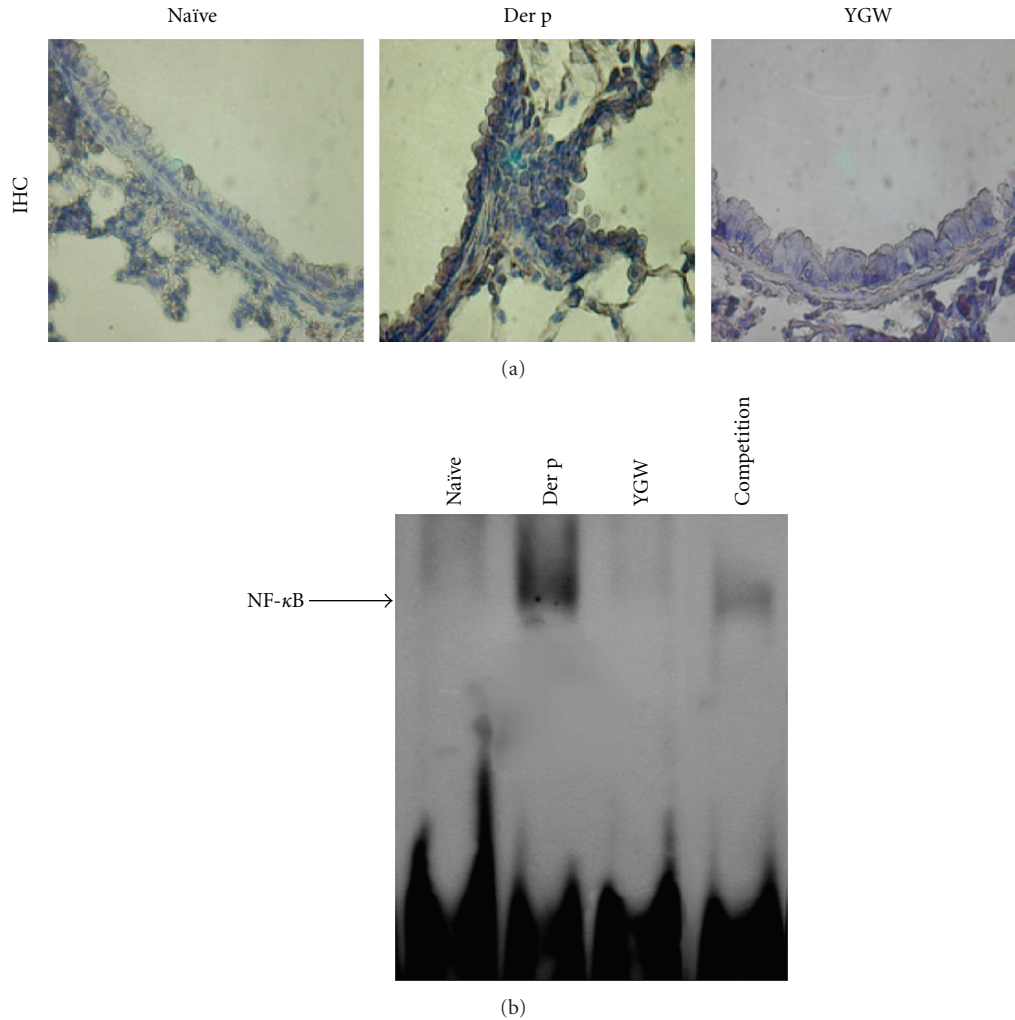


FIGURE 7: (a) In the immunohistochemistry assay, YGW inhibited the expression of NF- κ B (Rel A; $\times 400$) in bronchiolar epithelial cells of mice after repetitive Der p challenge. (b) EMSA showed that YGW decreased NF- κ B activation in whole lung tissue after Der p stimulation. The arrow indicates the specific DNA-probe complex. Data are representative of results from three separate experiments.

as evidenced by the reduction in total numbers of cells and the percent of macrophages and eosinophils in BALF relative to those seen in Der p group mice. Moreover, YGW also reduced inflammation and the number of hyperplastic goblet cells as evidenced by lung histology analysis as well as attenuated deposition of collagen. Therefore, YGW appears to suppress AHR by protecting against airway inflammation, eosinophilia infiltration, and airway remodeling.

It is well established that elevated levels of serum IgE correlate with the incidence or severity of asthma. Therefore, interfering with synthesis of IgE or inhibiting its action has recently become a novel therapeutic approach for development of immunological drugs in asthma, such as omalizumab (Xolair) [3]. In the present study, YGW treatment significantly decreased total IgE in serum. Furthermore, we also found that YGW treatment resulted in a reduction in IgG1 levels and in slight elevation of IgG2a/2b levels (data not show).

T cells with a T_H2 -like phenotype are thought to play an important role in orchestrating the asthmatic inflammatory

response [25]. Therefore, the immunomodulatory role of YGW in allergen-sensitized mice may lie in its ability to regulate T-cell activation. In this study, flow cytometry analysis showed that YGW led to a decrease in the percentage of the $CD3^+CD4^+$ T-cell subset in BALF, but not the $CD3^+CD8^+$ T-cell subset. On the other hand, $CD25^+CD4^+$ regulatory T cells suppress immune responses and are believed to play roles in preventing autoimmune diseases [26]. It has been reported that regulatory T cells downregulate $CD25^-CD4^+$ T-cell-mediated production of IL-12 in antigen-presenting cells [27]. In our study, we found that YGW reduced the number of $CD4^+CD25^+$ T cells in BALF, suggesting that YGW may block this feedback system and shift Th2-bios by increasing IL-12 levels. Further studies are needed to verify the effect of YGW on changing T-cell subsets during allergic inflammation.

Blood and tissue eosinophilia are hallmarks of allergic rhinitis, atopic dermatitis, and atopic asthma. Eosinophils are recruited from the circulation to inflammatory tissues in response to allergic stimuli [28]. Moreover, eosinophils

contribute to the symptomatology of asthma by releasing granule-stored cationic proteins and proinflammatory mediators, including cytokines and chemokines [29]. Therefore, the eosinophil is thought to be a key effector cell in the pathogenesis of allergic disease [29]. Notably, the important regulators of eosinophil trafficking are T_H2 cytokines such as IL-4, IL-5, and IL-13 [29, 30], although chemokines, eotaxis, and RANTES are also involved in recruitment of eosinophils [31]. In addition, only IL-5 is specific for terminal differentiation, growth, and survival of eosinophils [32, 33]. Thus, suppression of these cytokines and chemokines may be effective in reducing eosinophil infiltration into lung, thereby alleviating allergic asthmatic inflammation. In addition, RANTES and MCP-1 are also involved in recruitment of monocytes [34]. In our present study we showed that YGW treatment decreased the secretion of IL-5 in serum and IL-13 in lung tissue but did not affect IL-4 levels in serum. Meanwhile, YGW treatment downregulated mRNA expression of IL-13, eotaxis, RANTES, and MCP-1 in lung tissue. Therefore, we speculate that YGW treatment reduces eosinophil infiltration into lung by modulating T_H2 responses at the molecular level.

In asthmatics, one important feature of airway remodeling is subepithelial fibrosis [35]. TGF- β is a profibrogenic growth factor, which stimulates the differentiation of fibroblast precursors to myofibroblast cells, which in turn induces their proliferation [36]. Moreover, it has been shown to elicit the expression of MMPs and TIMPs [37]. Meanwhile, many studies have shown that TGF- β and eosinophils play important roles in the development of airway remodeling [38–41].

The rate of apoptosis of bronchial epithelial cells is significantly higher in asthma patients than that in healthy people, and TNF- α is suggested to play a crucial role in this process [42, 43]. In addition, TNF- α can regulate overproduction of ECM proteins by inducing epithelial cells, fibroblasts, and ASM cells [44]. Simultaneously, TNF- α and IL-1 β can induce the synthesis of eotaxis [45] and RANTES [46] in human lung epithelial cells.

We found that YGW treatment resulted in decreased secretion of TGF- β and TNF- α in BALF and the downregulation of mRNA expression of TGF- β in lung tissues. Therefore, we propose that YGW treatment reduces airway subepithelial fibrosis by downregulating the expression of TGF- β and TNF- α .

NF- κ B is capable of regulating T_H2 cell differentiation and producing proinflammatory mediators that are required for induction of allergic airway inflammation [47]. Bureau et al. [48] reported that bronchial epithelial and/or airway immune cells displayed augmented NF- κ B activity in OVA/OVA mice [48]. Therefore, targeting of the NF- κ B signaling pathway may be a promising therapy for asthma [48]. However, whether the immunoregulatory activity of YGW against asthma is connected with a diminution of NF- κ B activity in the lung is not clear. To address these issues, we used immunohistochemistry and EMSA to detect NF- κ B expression and activation in lung of repeatedly Der p challenge mice. We found that oral administration of YGW markedly reduced NF- κ B expression, predominantly

in bronchial epithelium. EMSA analysis also revealed a decrease in NF- κ B activation in the whole lung (Figure 7). Taken together, we speculate that inhibition of NF- κ B activation directly or indirectly attenuated IL-5, IL-13, eotaxis, RANTES, TNF- α , and TGF- β gene expression, eosinophilia infiltration, mucus production, collagen deposition, and allergic lung inflammation.

In conclusion, YGW-induced attenuation of AHR, remodeling, and inflammation in this model of chronic asthma is associated with specific downregulation of T_H2 cytokines and inhibition of NF- κ B activation within the bronchial epithelium in lung. To the best of our knowledge, this is the first study to show that YGW has immunoregulatory effects in remissive states of asthma. The pharmacologically active components of YGW, however, have not yet been characterized. Further research will be required to dissect the mechanisms of action of this formula.

Abbreviations

TCM: Traditional Chinese medicine
 YGW: You-Gui-Wan
 HDM: house dust mite
 Der p: Dermatophagoides pteronyssinus
 i.t.: intratracheal
 BALF: Bronchoalveolar lavage fluid (s).

Acknowledgments

This work was supported by grants from the National Science Council, Taiwan (NSC 96-2320-B-039-015 and NSC 97-2320-B-039-014-MY3), and the China Medical University (CMU 96-167).

References

- [1] S. J. Galli, M. Tsai, and A. M. Piliponsky, "The development of allergic inflammation," *Nature*, vol. 454, no. 7203, pp. 445–454, 2008.
- [2] S. Abdureyim, N. Amat, A. Umar, H. Upur, B. Berke, and N. Moore, "Anti-inflammatory, immunomodulatory, and heme oxygenase-1 inhibitory activities of ravan napas, a formulation of uighur traditional medicine, in a rat model of allergic asthma," *Evidence-Based Complementary and Alternative Medicine*, vol. 2011, Article ID 725926, 13 pages, 2011.
- [3] K. F. Rabe, W. J. Calhoun, N. Smith, and P. Jimenez, "Can anti-IgE therapy prevent airway remodeling in allergic asthma?" *Allergy*, vol. 66, no. 9, pp. 1142–1151, 2011.
- [4] S.-K. Jung, J. Ra, J. Seo et al., "An angiotensin I converting enzyme polymorphism is associated with clinical phenotype when using differentiation-syndrome to categorize korean bronchial asthma patients," *Evidence-Based Complementary and Alternative Medicine*, vol. 2011, Article ID 498138, 6 pages, 2011.
- [5] C. M. Lloyd and E. M. Hessel, "Functions of T cells in asthma: more than just T_H2 cells," *Nature Reviews Immunology*, vol. 10, no. 12, pp. 838–848, 2010.
- [6] W. C. Ko, L. H. Lin, H. Y. Shen, C. Y. Lai, C. M. Chen, and C. H. Shih, "Biochanin A, a phytoestrogenic isoflavone with selective inhibition of phosphodiesterase 4, suppresses

- ovalbumin-induced airway hyperresponsiveness," *Evidence-Based Complementary and Alternative Medicine*, vol. 2011, Article ID 635058, 13 pages, 2011.
- [7] S. J. Levine and S. E. Wenzel, "Narrative review: the role of Th2 immune pathway modulation in the treatment of severe asthma and its phenotypes," *Annals of Internal Medicine*, vol. 152, no. 4, pp. 232–237, 2010.
- [8] C. H. Fanta, "Drug therapy: asthma," *New England Journal of Medicine*, vol. 360, no. 10, pp. 1002–1014, 2009.
- [9] X. M. Li and L. Brown, "Efficacy and mechanisms of action of traditional Chinese medicines for treating asthma and allergy," *Journal of Allergy and Clinical Immunology*, vol. 123, no. 2, pp. 297–306, 2009.
- [10] C. Yao, L. Wang, S. Cai et al., "Protective effects of a Traditional Chinese Medicine, You-Gui-Wan, on steroid-induced inhibition of cytokine production in mice," *International Immunopharmacology*, vol. 5, no. 6, pp. 1041–1048, 2005.
- [11] K. M. Ko, D. H. F. Mak, P. Y. Chiu, and M. K. T. Poon, "Pharmacological basis of "Yang-invigoration" in Chinese medicine," *Trends in Pharmacological Sciences*, vol. 25, no. 1, pp. 3–6, 2004.
- [12] W. R. Thomas, B. J. Hales, and W. A. Smith, "House dust mite allergens in asthma and allergy," *Trends in Molecular Medicine*, vol. 16, no. 7, pp. 321–328, 2010.
- [13] L. G. Gregory, B. Causton, J. R. Murdoch et al., "Inhaled house dust mite induces pulmonary T helper 2 cytokine production," *Clinical and Experimental Allergy*, vol. 39, no. 10, pp. 1597–1610, 2009.
- [14] L. G. Gregory, S. A. Mathie, S. A. Walker, S. Pegorier, C. P. Jones, and C. M. Lloyd, "Overexpression of Smad2 drives house dust mite-mediated airway remodeling and airway hyperresponsiveness via activin and IL-25," *American Journal of Respiratory and Critical Care Medicine*, vol. 182, no. 2, pp. 143–154, 2010.
- [15] H. Hammad, M. Chieppa, F. Perros, M. A. Willart, R. N. Germain, and B. N. Lambrecht, "House dust mite allergen induces asthma via Toll-like receptor 4 triggering of airway structural cells," *Nature Medicine*, vol. 15, no. 4, pp. 410–416, 2009.
- [16] J. R. Johnson, R. E. Wiley, R. Fattouh et al., "Continuous exposure to house dust mite elicits chronic airway inflammation and structural remodeling," *American Journal of Respiratory and Critical Care Medicine*, vol. 169, no. 3, pp. 378–385, 2004.
- [17] S. Phipps, E. L. Chuan, G. E. Kaiko et al., "Toll/IL-1 signaling is critical for house dust mite-specific Th1 and Th2 responses," *American Journal of Respiratory and Critical Care Medicine*, vol. 179, no. 10, pp. 883–893, 2009.
- [18] C. Jin, C. P. Shelburne, G. Li et al., "Particulate allergens potentiate allergic asthma in mice through sustained IgE-mediated mast cell activation," *Journal of Clinical Investigation*, vol. 121, no. 3, pp. 941–955, 2011.
- [19] M. D. Chapman, A. Pomés, H. Breiteneder, and F. Ferreira, "Nomenclature and structural biology of allergens," *Journal of Allergy and Clinical Immunology*, vol. 119, no. 2, pp. 414–420, 2007.
- [20] A. Pomés, "Allergen structures and biologic functions: the cutting edge of allergy research," *Current Allergy and Asthma Reports*, vol. 8, no. 5, pp. 425–432, 2008.
- [21] L. G. Gregory and C. M. Lloyd, "Orchestrating house dust mite-associated allergy in the lung," *Trends in Immunology*, vol. 32, no. 9, pp. 402–411, 2011.
- [22] C. K. Yu, C. M. Shieh, and H. Y. Lei, "Repeated intratracheal inoculation of house dust mite (*Dermatophagoides farinae*) induces pulmonary eosinophilic inflammation and IgE antibody production in mice," *Journal of Allergy and Clinical Immunology*, vol. 104, no. 1, pp. 228–236, 1999.
- [23] S. T. Kao, S. T. Wang, C. K. Yu, H. Y. Lei, and J. Y. Wang, "The effect of Chinese herbal medicine, xiao-qing-long tang (XQLT), on allergen-induced bronchial inflammation in mite-sensitized mice," *Allergy*, vol. 55, no. 12, pp. 1127–1133, 2000.
- [24] C. C. Lee, J. W. Liao, and J. J. Kang, "Motorcycle exhaust particles induce airway inflammation and airway hyperresponsiveness in BALB/C mice," *Toxicological Sciences*, vol. 79, no. 2, pp. 326–334, 2004.
- [25] B. D. Medoff, S. Y. Thomas, and A. D. Luster, "T cell trafficking in allergic asthma: the ins and outs," *Annual Review of Immunology*, vol. 26, pp. 205–232, 2008.
- [26] D. S. Robinson, "The role of the T cell in asthma," *Journal of Allergy and Clinical Immunology*, vol. 126, no. 6, pp. 1081–1091, 2010.
- [27] K. Sato, S. Tateishi, K. Kubo, T. Mimura, K. Yamamoto, and H. Kanda, "Downregulation of IL-12 and a novel negative feedback system mediated by CD25⁺CD4⁺ T cells," *Biochemical and Biophysical Research Communications*, vol. 330, no. 1, pp. 226–232, 2005.
- [28] K. D. Stone, C. Prussin, and D. D. Metcalfe, "IgE, mast cells, basophils, and eosinophils," *Journal of Allergy and Clinical Immunology*, vol. 125, no. 2, pp. S73–S80, 2010.
- [29] M. Rådinger and J. Lötvall, "Eosinophil progenitors in allergy and asthma—Do they matter?" *Pharmacology and Therapeutics*, vol. 121, no. 2, pp. 174–184, 2009.
- [30] G. Woltmann, C. A. McNulty, G. Dewson, F. A. Symon, and A. J. Wardlaw, "Interleukin-13 induces PSGL-1/P-selectin-dependent adhesion of eosinophils, but not neutrophils, to human umbilical vein endothelial cells under flow," *Blood*, vol. 95, no. 10, pp. 3146–3152, 2000.
- [31] S. McKay and H. S. Sharma, "Autocrine regulation of asthmatic airway inflammation: role of airway smooth muscle," *Respiratory Research*, vol. 3, no. 1, p. 11, 2001.
- [32] P. S. Foster, A. W. Mould, M. Yang et al., "Elemental signals regulating eosinophil accumulation in the lung," *Immunological Reviews*, vol. 179, pp. 173–181, 2001.
- [33] M. E. Rothenberg and S. P. Hogan, "The eosinophil," *Annual Review of Immunology*, vol. 24, pp. 147–174, 2006.
- [34] R. T. Venkatesha, E. B. Thangam, A. K. Zaidi, and H. Ali, "Distinct regulation of C3a-induced MCP-1/CCL2 and RANTES/CCL5 production in human mast cells by extracellular signal regulated kinase and PI3 kinase," *Molecular Immunology*, vol. 42, no. 5, pp. 581–587, 2005.
- [35] W. R. Roche, J. H. Williams, R. Beasley, and S. T. Holgate, "Subepithelial fibrosis in the bronchi of asthmatics," *The Lancet*, vol. 1, no. 8637, pp. 520–524, 1989.
- [36] M. Michalik, M. Pierzchalska, A. Legutko et al., "Asthmatic bronchial fibroblasts demonstrate enhanced potential to differentiate into myofibroblasts in culture," *Medical Science Monitor*, vol. 15, no. 7, pp. BR194–BR201, 2009.
- [37] W. Mattos, S. Lim, R. Russell, A. Jatakanon, K. F. Chung, and P. J. Barnes, "Matrix metalloproteinase-9 expression in asthma: effect of asthma severity, allergen challenge, and inhaled corticosteroids," *Chest*, vol. 122, no. 5, pp. 1543–1552, 2002.
- [38] J. Y. Cho, M. Miller, K. J. Baek et al., "Inhibition of airway remodeling in IL-5-deficient mice," *Journal of Clinical Investigation*, vol. 113, no. 4, pp. 551–560, 2004.
- [39] E. M. Minshall, D. Y. M. Leung, R. J. Martin et al., "Eosinophil-associated TGF- β 1 mRNA expression and airways fibrosis in

- bronchial asthma," *American Journal of Respiratory Cell and Molecular Biology*, vol. 17, no. 3, pp. 326–333, 1997.
- [40] P. Flood-Page, A. Menzies-Gow, S. Phipps et al., "Anti-IL-5 treatment reduces deposition of ECM proteins in the bronchial subepithelial basement membrane of mild atopic asthmatics," *Journal of Clinical Investigation*, vol. 112, no. 7, pp. 1029–1036, 2003.
- [41] A. M. Vignola, P. Chanez, G. Chiappara et al., "Transforming growth factor- β expression in mucosal biopsies in asthma and chronic bronchitis," *American Journal of Respiratory and Critical Care Medicine*, vol. 156, no. 2 I, pp. 591–599, 1997.
- [42] F. Bucchieri, S. M. Puddicombe, J. L. Lordan et al., "Asthmatic bronchial epithelium is more susceptible to oxidant-induced apoptosis," *American Journal of Respiratory Cell and Molecular Biology*, vol. 27, no. 2, pp. 179–185, 2002.
- [43] A. Trautmann, P. Schmid-Grendelmeier, K. Krüger et al., "T cells and eosinophils cooperate in the induction of bronchial epithelial cell apoptosis in asthma," *Journal of Allergy and Clinical Immunology*, vol. 109, no. 2, pp. 329–337, 2002.
- [44] S. Létuvé, S. Lajoie-Kadoch, S. Audusseau et al., "IL-17E upregulates the expression of proinflammatory cytokines in lung fibroblasts," *Journal of Allergy and Clinical Immunology*, vol. 117, no. 3, pp. 590–596, 2006.
- [45] C. M. Lilly, H. Nakamura, H. Kesselman et al., "Expression of eotaxin by human lung epithelial cells. Induction by cytokines and inhibition by glucocorticoids," *Journal of Clinical Investigation*, vol. 99, no. 7, pp. 1767–1773, 1997.
- [46] C. Stellato, L. A. Beck, G. A. Gorgone et al., "Expression of the chemokine RANTES by a human bronchial epithelial cell line: modulation by cytokines and glucocorticoids," *Journal of Immunology*, vol. 155, no. 1, pp. 410–418, 1995.
- [47] C. Desmet, P. Gosset, B. Pajak et al., "Selective blockade of NF- κ B activity in airway immune cells inhibits the effector phase of experimental asthma," *Journal of Immunology*, vol. 173, no. 9, pp. 5766–5775, 2004.
- [48] F. Bureau, S. Delhalle, G. Bonizzi et al., "Mechanisms of persistent NF- κ B activity in the bronchi of an animal model of asthma," *Journal of Immunology*, vol. 165, no. 10, pp. 5822–5830, 2000.

Research Article

Analgesic and Anti-Inflammatory Activities of Methanol Extract of *Ficus pumila* L. in Mice

Chi-Ren Liao,¹ Chun-Pin Kao,² Wen-Huang Peng,¹ Yuan-Shiun Chang,¹ Shang-Chih Lai,³ and Yu-Ling Ho⁴

¹School of Chinese Pharmaceutical Sciences and Chinese Medicine Resources, College of Pharmacy, China Medical University, Taichung 404, Taiwan

²Department of Nursing, Hsin Sheng College of Medical Care and Management, Taoyuan 325, Taiwan

³Department of Health and Nutrition Biotechnology, Asia University, Taichung 413, Taiwan

⁴Department of Nursing, Hungkuang University, Sha Lu, Taichung 433, Taiwan

Correspondence should be addressed to Yu-Ling Ho, elaine@sunrise.hk.edu.tw

Received 15 November 2011; Revised 29 February 2012; Accepted 29 February 2012

Academic Editor: William C. S. Cho

Copyright © 2012 Chi-Ren Liao et al. This is an open access article distributed under the Creative Commons Attribution License, which permits unrestricted use, distribution, and reproduction in any medium, provided the original work is properly cited.

This study investigated possible analgesic and anti-inflammatory mechanisms of the methanol extract of *Ficus pumila* (FP_{MeOH}). Analgesic effects were evaluated in two models including acetic acid-induced writhing response and formalin-induced paw licking. The results showed FP_{MeOH} decreased writhing response in the acetic acid assay and licking time in the formalin test. The anti-inflammatory effect was evaluated by λ -carrageenan-induced mouse paw edema and histopathological analyses. FP_{MeOH} significantly decreased the volume of paw edema induced by λ -carrageenan. Histopathologically, FP_{MeOH} abated the level of tissue destruction and swelling of the edema paws. This study indicated anti-inflammatory mechanism of FP_{MeOH} may be due to declined levels of NO and MDA in the edema paw through increasing the activities of SOD, GPx, and GRd in the liver. Additionally, FP_{MeOH} also decreased the level of inflammatory mediators such as IL-1 β , TNF- α , and COX-2. HPLC fingerprint was established and the contents of three active ingredients, rutin, luteolin, and apigenin, were quantitatively determined. This study provided evidence for the classical treatment of *Ficus pumila* in inflammatory diseases.

1. Introduction

Inflammatory reaction, typically characterized by redness, swelling, heat, and pain, is one of the most important host defense mechanisms against invading pathogens. However, persistent or overinflammation leads to tissue damage and possibly failure of organs. Proinflammatory cytokines (e.g., TNF- α , IL-1 β , and IL-6) are produced in large quantities by activated macrophages/monocytes that stimulate cellular responses via increasing prostaglandins (PGs) and reactive oxygen species (ROS). Additionally, lipid peroxidation (malondialdehyde, MDA) is produced by free radicals attacking the cell membranes. Thus, inflammatory effect can lead to the accumulation of MDA [1].

Ficus pumila, a creeping vine like fig plant, is native to South China and Malaysia. Several studies have been performed on the composition of *Ficus pumila*, and a number of compounds have been identified such as apigenin, luteolin

[2], rutin, genistein, hesperidin, astragaloside, isoquercitrin, and chrysin [3]. Dried stems and leaves of *Ficus pumila* have been folklorically used in the treatment of rheumatoid arthritis, edema, tonic medicament, throat pain, and postpartum abdominal pain [4]. However, no research has been investigated on the analgesic and anti-inflammatory mechanisms of *Ficus pumila* yet.

In this study, we investigated the analgesic and anti-inflammatory activities of the methanol extract of *Ficus pumila* (FP_{MeOH}). The analgesic activity was evaluated by acetic acid-induced writhing response and formalin test. Anti-inflammatory activity was determined by using λ -carrageenan-induced mouse paw edema model and histopathological analysis. In order to evaluate the mechanism of anti-inflammatory effect, we also analyzed TNF- α , IL-1 β , COX-2, MDA, and NO levels in the edema tissue, as well as antioxidant enzyme activities of SOD (superoxidase dismutase),

GPx (glutathione peroxidase), and GRd (glutathione reductase) in the liver.

Many studies have indicated that flavonoids in herbs possess anti-inflammatory activities via scavenging ROS and reducing proinflammatory cytokines, such as rutin [5], luteolin [6], and apigenin [7]. These three ingredients have also been isolated from *Ficus pumila* in previous studies [2, 3]. In the phytochemical part of this study, not only did we reconfirm the presence of these three compounds in FP_{MeOH} by establishing its fingerprint chromatogram, but also the contents of these active ingredients were quantitatively determined.

2. Materials and Methods

2.1. Chemicals and Drugs. λ -carrageenan, indomethacin, and Griess reagent were purchased from Uni-Onward (distributor of Sigma-Aldrich Chemical Co. in Taipei, Taiwan). Formalin was purchased from Nihon Shiyaku Industry Ltd. (Taipei, Taiwan). SOD, GPx, GRd, and MDA assay kits were purchased from Eugene Chen Co. Ltd. (distributor of Randox Laboratory Ltd. in Taipei, Taiwan). IL-1 β , IL-6, COX-2, and TNF- α were obtained from Blossom Biotechnologies, Inc. (agency of Assay Designs Inc. in Taipei, Taiwan). LC grade acetonitrile was purchased from the branch company of Merck in Taipei, Taiwan. All other reagents used were of analytical grade.

2.2. Plant Material. *Ficus pumila* L. was collected from the herbal garden of China Medical University, Taichung, Taiwan, as described in Flora of Taiwan [8]. A plant specimen has been deposited in the School of Chinese Pharmaceutical Sciences and Chinese Medicine Resources. Dried stems and leaves (1.0 kg) of *Ficus pumila* were sliced into small pieces, soaked with 10 liters of methanol at room temperature for three days. After passing through filter paper, the filtrate was concentrated under reduced pressure to dryness. The above steps were repeated two additional times, and a total of 123.1 g of dry crude extract (yield ratio 12.31%) was produced. The dried crude extract was dissolved in 0.5% CMC (carboxymethyl cellulose) solution into three concentrations (100 mg/mL, 50 mg/mL, and 10 mg/mL) prior to pharmacological testing. Equal volume of 0.1 mL (extract of different concentrations)/10 g B.W. was given to each mouse in all subsequent animal experiments.

2.3. Chromatographic Analysis of FP_{MeOH}. The HPLC system consisted of a Waters 2695 Alliance LC with 996 PDA. Chromatographic separation was performed on X-Bridge RP18 (25 cm \times 4.6 mm I.D., 5 μ m) with an injection volume of 10 μ L. The mobile phase consisted of a mixture of 0.1% formic acid (A) and acetonitrile (B) using a gradient elution. The gradient program was set as follows: 0–15 min, 20% B, 15–30 min, 40% B, 30–45 min, 60% B. The flow rate was set at 0.8 mL/min and the detection wavelength was set to 255 nm. The above conditions were used in both HPLC assay and HPLC fingerprint of FP_{MeOH}.

The contents of rutin, apigenin, and luteolin of FP_{MeOH} were qualified and quantified in the HPLC assay. In qualitative analyses, comparisons were made with the retention time

and maximum absorption of the standards. In quantitative analyses, comparisons were made with peak areas under the standard curves.

2.4. Experimental Animals. Male ICR mice aged between 5–6 weeks and weighing between 20–25 g were obtained from BioLASCO Taiwan Co. Ltd. and were kept in the animal center of China Medical University at a controlled temperature of $22 \pm 1^\circ\text{C}$, relative humidity $55 \pm 5\%$, and with 12 h light/12 h dark cycles for 1 week before the experiment. Animals were provided with rodent diet and clean water *ad libitum*. The experimental protocol was approved by the Committee on Animal Research, China Medical University. Animals were sacrificed by decapitation under ether anesthesia. All studies were conducted in accordance with the National Institutes of Health (NIH) Guide for the Care and Use of Laboratory Animals. All tests were conducted under the guidelines of the International Association for the Study of Pain [9].

2.5. Acute Toxicity Study. The acute toxicology test in mice was carried out according to the method of Liao et al. [10]. Male ICR mice were randomly divided into three groups (10 mice per group). Three groups of mice were administered orally with three concentrations of FP_{MeOH} (2.5 g, 5 g, and 10 g/kg), respectively. The experimental mice were kept under regular observation for 14 days for any mortality or behavioral changes.

2.6. Acetic Acid-Induced Writhing Response. The writhing test in mice was carried out according to the method of Koster et al. [11]. Five randomly-selected groups of mice were orally administered with solvent control (0.5% CMC), positive control (indomethacin at 10 mg/kg) or three different doses of FP_{MeOH} (0.1, 0.5, and 1.0 g/kg) 60 min prior to the chemical stimulus. The number of muscular contractions was counted 5 min after the injection of 1% acetic acid (v/v, 0.1 mL/10 g body weight, i.p.). The data collected represented the total number of writhes observed in a duration of 10 minutes (5–15 min after the injection).

2.7. Formalin Test. The formalin test was conducted based on the method of Tjølsen et al. [12]. Twenty microliters of 5% formalin in saline was injected subcutaneously into the right hind paw of each mouse. The time (in seconds) spent on licking and biting of the injected paw was recorded in both the early phase (0–5 min) and late phase (20–30 min) after the formalin injection. Solvent control (0.5% CMC), positive control (indomethacin at 10 mg/kg), or three different doses of FP_{MeOH} (0.1, 0.5 and 1.0 g/kg) was orally administered to the animals 60 min prior to the formalin injection.

2.8. λ -Carrageenan-Induced Mouse Paw Edema. The test was conducted according to the method of Vinegar et al. [13]. The basal volume of right hind paw was determined before the administration of any drug. Fifty microliters of 1% λ -carrageenan suspended in saline was injected into the plantar side of right hind paw, and the paw volume was measured at the 1st, 2nd, 3rd, 4th, and 5th h after the injection using a

plethysmometer. The degree of swelling was evaluated by the delta volume (a-b), where “a” is the volume of right hind paw after the chemical treatment and “b” is the volume before the treatment. CMC (0.5%), indomethacin (10 mg/kg), and FP_{MeOH} (0.1, 0.5 and 1.0 g/kg) were administered orally 60 min after the λ -carrageenan injection. In the secondary experiment, another set of mice were orally administered with 0.5% CMC, indomethacin, or FP_{MeOH} 1 h after λ -carrageenan had been injected into their right hindpaws. The right hindpaws of the animals were surgically removed under anesthesia 2 h following treatments. The paw tissue was rinsed in ice-cold normal saline and immediately placed in cold normal saline four times its volume before homogenization at 4°C. The homogenate was centrifuged at 12,000 rpm for 5 min. The supernatant was obtained and stored at -20°C for the determinations of MDA, NO, TNF- α , IL-1 β , and COX-2. Similarly, the whole liver tissue was rinsed in ice-cold normal saline and immediately placed in cold normal saline of equal volume before homogenization at 4°C. The homogenate was then centrifuged at 12,000 rpm for 5 min. The supernatant was obtained and stored at -20°C for later analyses of antioxidant enzyme (SOD, GPx, and GRd) activities.

2.9. Histological Analysis. The mice were orally administered with 0.5% CMC, indomethacin, or FP_{MeOH} 1 h after λ -carrageenan had been injected into their right hindpaws. The right hindpaws of the animals were surgically removed under anesthesia 2 h after treatments. Tissue slices were fixed in 10% formalin for 3 days, decalcified overnight and embedded in paraffin and sectioned into 4 μ m tissue sections. Tissue sections were stained with hematoxylin and eosin (H&E stain) before being examined under a BX60 microscope (Olympus, Melville, NY) for pathological changes. Inflammatory reactions induced by λ -carrageenan, including paw swelling and enlarged cavities, were examined. The severity after FP_{MeOH} (0.1, 0.5 and 1.0 g/kg) and indomethacin (10 mg/kg) treatments was also examined. Images were captured with a Macrofire 599831 camera. The results were identified in the Animal Disease Diagnostic Center (ADDC), National Chung Hsing University, Taichung, Taiwan.

2.10. MDA Assay. The production of MDA was induced by λ -carrageenan injection, and evaluated by the thiobarbituric acid reacting substance (TBARS) method [14]. Briefly, MDA reacted with TBARS at high temperature and formed a red-complex TBARS. The absorbance of TBARS was recorded at 532 nm.

2.11. NO Assay. NO was measured according to the method of Moshage et al. [15]. NO₃⁻ was converted into NO₂⁻ by nitrate reductase, NO₂⁻ subsequently reacted with sulfanilic acid to produce diazonium ion and coupled with N-(1-naphthyl) ethylenediamine to form the chromophoric aeroderivative (purplish red) which could be recorded at 540 nm.

2.12. TNF- α and IL-1 β Assay. IL-1 β was measured by an enzyme-linked immunosorbent assay kit (Blossom Biotechnologies Inc.) [16]. The capture antibody of IL-1 β was added

to each well of a 96-well plate overnight. Next day, a second set of biotinylated antibody was incubated with sample tissues or standard antigens in the plate before streptavidin was added. The color of the reaction converted from purple to yellow and was recorded at 450 nm. TNF- α was detected using the same method as IL-1 β . Each sample was presented as pg/mg in TNF- α and IL-1 β concentrations.

2.13. COX-2 Assay. The content of COX-2 was determined by measuring the peroxidase activity of PGHS (prostaglandin endoperoxide H₂ synthase) [17]. Peroxidase activity of PGHS was determined by following the oxidation of N,N,N',N'-tetramethyl-p-phenylenediamine (TMPD) at 37°C using arachidonate as the substrate. The increase in color was recorded at 590 nm.

2.14. Measurement of Antioxidant Enzymes. SOD was measured according to the method of Vani et al. [18]. Xanthine and xanthine oxidase (XOD) generated superoxide radicals reacted with 2-(4-iodophenyl)-3-(4-nitrophenol)-5-phenyl-tetrazolium chloride (I.N.T.) to form a red formazan dye, and the color was recorded at 540 nm. GPx was measured according to the method of Ceballos-Picot et al. by detecting the contents of GR and NADPH [19]. Oxidation of NADPH into NADP⁺ is accompanied by a decrease in absorbance recorded at 340 nm. GRd was measured according to the method of Ahmad and Holdsworth [20] which detects the decrease of glutathione (GSSG) in the presence of NADPH. NADPH oxidized into NADP⁺ would result in a decrease in absorbance recorded at 340 nm.

2.15. Statistical Analysis. All data of each group were expressed as mean \pm SD ($n = 8$). Statistical analyses were performed with SPSS software and were carried out using one-way ANOVA followed by Scheffe's multiple range test.

3. Results

3.1. Chromatographic Analysis of FP_{MeOH}. HPLC fingerprint profile was established for FP_{MeOH} (Figure 1). Three flavonoid components were identified as rutin, luteolin, and apigenin with retention times of 13.8 min, 35.2 min, and 40.4 min, respectively. The maximum absorbance was 255 nm, and the relative amounts for each gram of crude extract were in the order of rutin (24.41 mg), apigenin (14.11 mg), and luteolin (2.72 mg).

3.2. Acute Toxicity Study. Acute toxicity of FP_{MeOH} was evaluated in mice at the doses of 2.5, 5 and 10 g/kg. After 14 days of oral administration, FP_{MeOH} did not cause any behavioral changes, and no mortality was observed. Therefore, the LD₅₀ value of FP_{MeOH} was concluded to be greater than 10 g/kg in mice, indicating it was practically not acutely toxic.

3.3. Acetic Acid-Induced Writhing Response. Figure 2 shows acetic acid-induced writhing responses in mice which serve as an indication of analgesic activities of FP_{MeOH}. Intraperitoneal injection of acetic acid produced 42.2 \pm 5.6 writhes

TABLE 1: Effect of FP_{MeOH} and indomethacin on liver SOD, GPx, and GRd activities in mice injected with λ -carrageenan.

Groups	SOD (U/g protein)	GPx (U/mg protein)	GRd (U/mg protein)
Normal	121.45 \pm 12.53	1.579 \pm 0.136	0.106 \pm 0.012
Car	67.69 \pm 16.43	0.949 \pm 0.144	0.063 \pm 0.014
Car + Indomethacin	99.72 \pm 10.36**	1.222 \pm 0.109	0.085 \pm 0.006**
Car + FP _{MeOH} (0.1 g/kg)	84.94 \pm 13.82*	1.287 \pm 0.133*	0.082 \pm 0.008**
Car + FP _{MeOH} (0.5 g/kg)	93.89 \pm 16.68*	1.332 \pm 0.207**	0.085 \pm 0.007**
Car + FP _{MeOH} (1.0 g/kg)	95.48 \pm 17.87*	1.339 \pm 0.224**	0.078 \pm 0.006*

Each value represents the mean \pm SD ($n = 8$). * $P < 0.05$ and ** $P < 0.01$ as compared with the λ -carrageenan (Car) group (one-way ANOVA followed by Scheffe's multiple range test).

TABLE 2: Effects of FP_{MeOH} and indomethacin on the severity of mouse paw edema.

Groups	Grade (mean \pm SD)
Car	3.6 \pm 0.55
Car + Indomethacin	2.0 \pm 0.71*
Car + FP _{MeOH} (0.1 g/kg)	3.6 \pm 0.55
Car + FP _{MeOH} (0.5 g/kg)	3.0 \pm 0.00
Car + FP _{MeOH} (1.0 g/kg)	2.2 \pm 0.45*

Each value represents the mean \pm SD ($n = 5$). * $P < 0.05$ as compared with the λ -carrageenan (Car) group (one-way ANOVA followed by Scheffe's multiple range test).

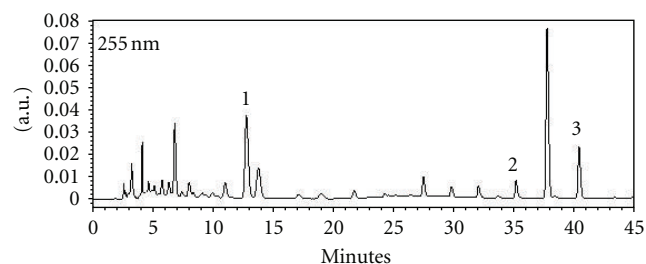


FIGURE 1: HPLC fingerprint of FP_{MeOH}. The peaks represent 1. rutin (13.8 min), 2. luteolin (35.2 min), and 3. apigenin (40.4 min). The contents of rutin, apigenin, and luteolin in FP_{MeOH} were 24.41 mg/g, 14.11 mg/g, and 2.72 mg/g, respectively.

in the solvent control group. The writhing response was significantly reduced by pretreatments with FP_{MeOH} (0.1, 0.5 and 1 g/kg) and indomethacin (10 mg/kg).

3.4. Formalin Test. In the early phase, FP_{MeOH}- and indomethacin-treated groups did not show any significant changes as compared to the solvent control group (Figure 3(a)). In the second phase, subcutaneous injection of formalin induced licking and biting responses in the solvent control group lasted for a period of 155.7 \pm 10.5 seconds. The time was significantly decreased by pretreatment with FP_{MeOH} (0.1, 0.5 and 1 g/kg) and indomethacin (10 mg/kg) (Figure 3(b)).

3.5. Effect of FP_{MeOH} on λ -Carrageenan-Induced Mouse Paw Edema. Following the λ -carrageenan injection, the volume of mouse paw increased as edema developed,

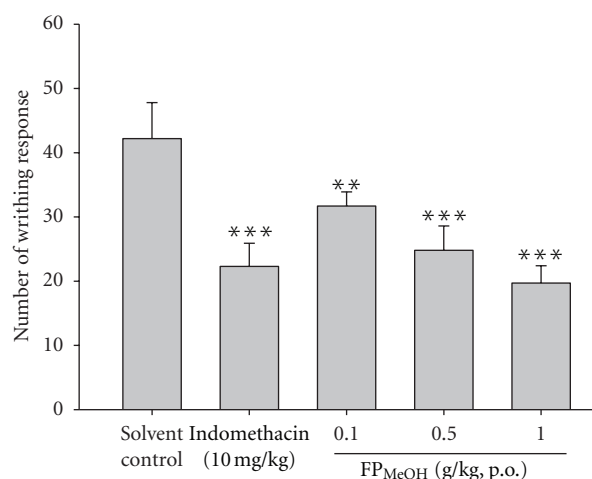


FIGURE 2: Analgesic effects of FP_{MeOH} and indomethacin on acetic acid-induced writhing response in mice. Each value represents mean \pm SD ($n = 8$). The number of abdominal writhes was counted over the time period of 5–15 min after acetic acid injection. ** $P < 0.01$ and *** $P < 0.001$ as compared to the solvent control group (one-way ANOVA followed by Scheffe's multiple range test).

indicating inflammatory activities (Figure 4). However, indomethacin (10 mg/kg) and FP_{MeOH} (0.1–1.0 g/kg) significantly decreased paw edema at the 3rd, 4th, and 5th h after the injection. FP_{MeOH} at the concentrations of 0.5 and 1 g/kg had about equal amount of inhibition as indomethacin.

3.6. Histological Analysis. No inflammation, tissue destruction, and swelling phenomenon were observed in the paws of normal mice (Figure 5(a)). On the other hand, the λ -carrageenan control group displayed enlarged cavities in the paw tissue (Figure 5(b)). Edematous condition was obviously abated by treatment with 10 mg/kg of indomethacin and 1.0 g/kg of FP_{MeOH} (Figures 5(c) and 5(f)). The severity of mouse paw edema was also graded and summarized in Table 2 (mean \pm SD).

3.7. Effect of FP_{MeOH} on MDA Level. MDA level obviously increased in the λ -carrageenan control group (1.120 \pm 0.172 μ M/g); however, pretreatments with FP_{MeOH} (0.1, 0.5 and 1.0 g/kg) and indomethacin (10 mg/kg) significantly inhibited the increase of MDA levels (Figure 6).

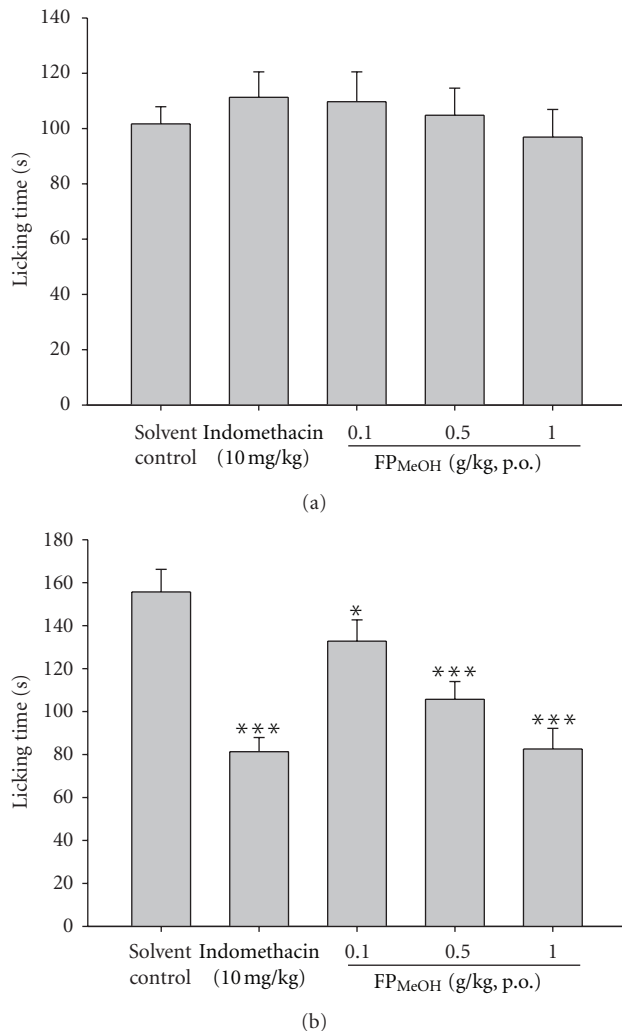


FIGURE 3: Effects of FP_{MeOH} and indomethacin on (a) early and (b) late phases of formalin test in mice. Each value represents mean \pm SD ($n = 8$). The time spent on licking and biting the injected paws was recorded in the time periods of 0–5 min (early phase) and 20–30 min (late phase) as indicators of pain. * $P < 0.05$ and *** $P < 0.001$ as compared to the solvent control group (one-way ANOVA followed by Scheffe's multiple range test).

3.8. Effect of FP_{MeOH} on NO Level. Pretreatments with FP_{MeOH} (0.5 and 1.0 g/kg) and indomethacin (10 mg/kg) significantly inhibited the increase of NO levels in the edema paws of mice, as compared to the λ -carrageenan control group ($10.08 \pm 1.45 \mu\text{M}$), as shown in Figure 7.

3.9. Effect of FP_{MeOH} on TNF- α and IL-1 β . TNF- α and IL-1 β levels in λ -carrageenan-induced edema paws were increased remarkably. FP_{MeOH} (0.5 and 1.0 g/kg) and indomethacin (10 mg/kg) significantly reduced the levels of TNF- α (Figure 8). Similarly, IL-1 β levels were significantly lowered by FP_{MeOH} (0.1, 0.5 and 1.0 g/kg) and indomethacin, as shown in Figure 9.

3.10. Effect of FP_{MeOH} on COX-2 Level. Figure 10 shows that COX-2 level was greatly raised ($37.04 \pm 3.04 \text{ U/mg}$) in λ -carrageenan induced edema paw. However, COX-2 levels

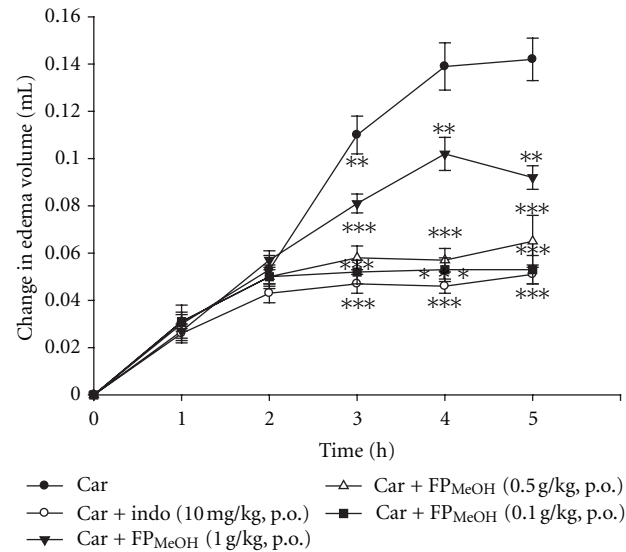


FIGURE 4: Effects of FP_{MeOH} and indomethacin on λ -carrageenan-induced mouse paw edema. The volumes of paw edema were detected at the 1st, 2nd, 3rd, 4th, and 5th h after λ -carrageenan injection. Each value represents mean \pm SD ($n = 8$). ** $P < 0.01$ and *** $P < 0.001$ as compared to the λ -carrageenan control group (one-way ANOVA followed by Scheffe's multiple range test).

were decreased by treating with FP_{MeOH} (0.5 and 1.0 g/kg) as well as indomethacin (10 mg/kg).

3.11. Effect of FP_{MeOH} on the Activities of Antioxidant Enzymes. SOD, GPX, and GRd activities were increased by treating with FP_{MeOH} (0.5 and 1.0 g/kg) and indomethacin (10 mg/kg), as compared to the λ -carrageenan control group (Table 1).

4. Discussion

Ficus is a genus of about 800 species found in tropical and subtropical regions. Several *Ficus* species have been studied for their anti-inflammatory actions, for example, *F. aurantiacea* [20], *F. carica* [21], *F. glomerata* [22], *F. maxima* [23], and *F. obtusifolia* [24].

Traditional medicines have been popularly used in the treatment of various diseases in recent years. Many medicinal plants supply analgesic and anti-inflammatory activities to treat acute, chronic, or recurring illnesses. *Ficus pumila* is a Chinese herbal medicine, its dried stems and leaves have been commonly used in the treatment of rheumatoid arthritis, edema, throat pain, and postpartum abdominal pain [4]. Based on its therapeutic claims in traditional medicine, we investigated possible mechanisms of the analgesic and anti-inflammatory effects of FP_{MeOH}.

Analgesic effect of FP_{MeOH} was evaluated by two animal models, including acetic acid-induced writhing response and formalin test. The results of acetic acid induced writhing test showed that FP_{MeOH} (0.1–1 g/kg) and indomethacin (10 mg/kg) provided antinociceptive effects in mice. Acetic acid indirectly triggers the release of nociceptive endogenous mediators (such as bradykinin, serotonin, and

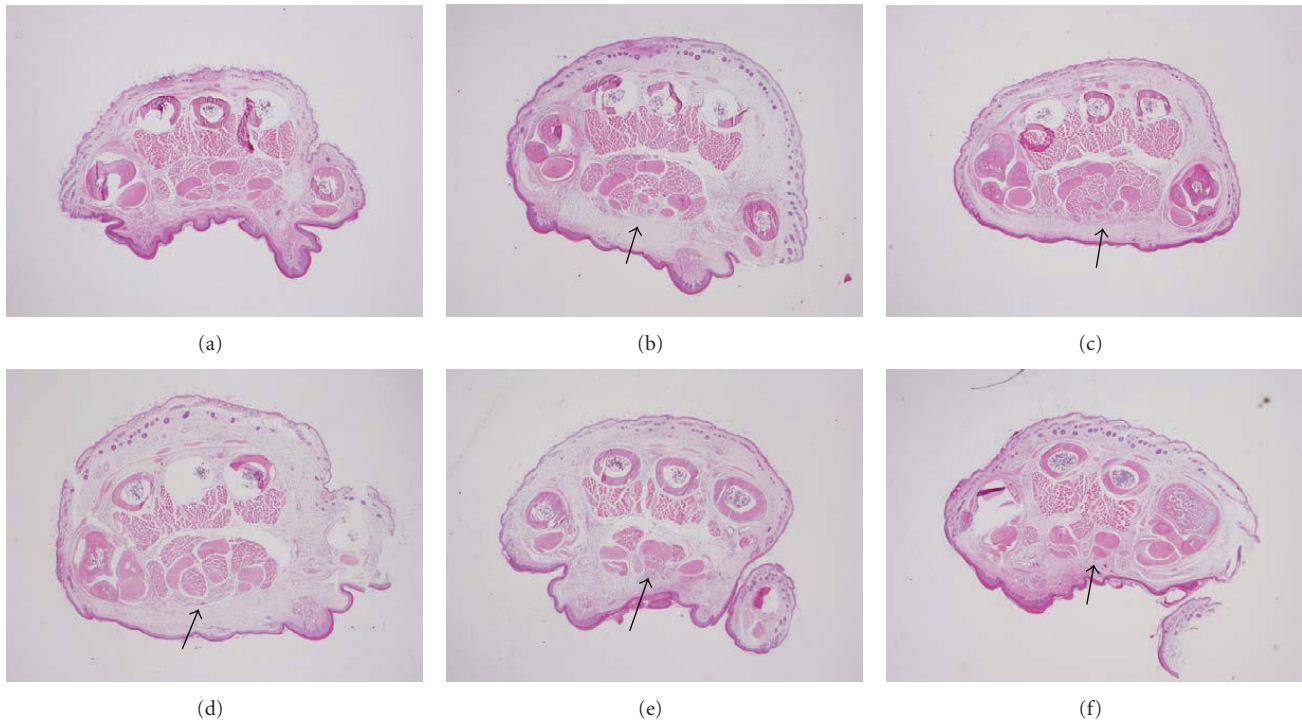


FIGURE 5: Histopathological examinations on λ -carrageenan-induced paw tissue swelling, edema and neutrophil infiltration: (a) normal, (b) λ -carrageenan, (c) indomethacin, (d) FP_{MeOH} (0.1 g/kg), (e) FP_{MeOH} (0.5 g/kg), and (f) FP_{MeOH} (1.0 g/kg).

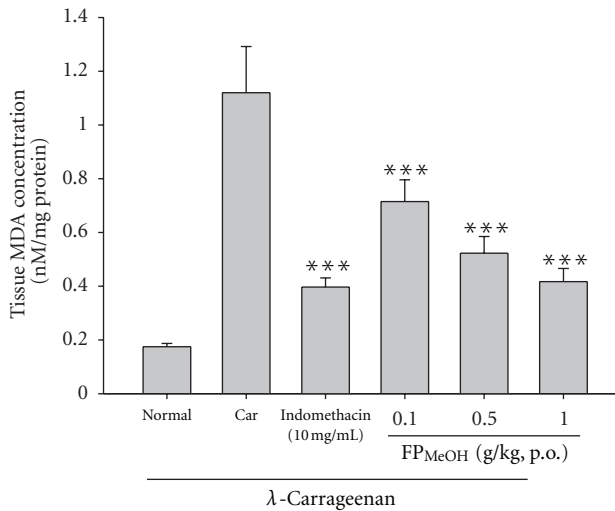


FIGURE 6: Effects of FP_{MeOH} and indomethacin on MDA concentrations in the edema paws. Each value represents mean \pm SD ($n = 8$). *** $P < 0.001$ as compared to the λ -carrageenan control group (one-way ANOVA followed by Scheffe's multiple range test).

prostaglandin) and proinflammatory cytokines (such as $TNF-\alpha$ and $IL-1\beta$) to cause painful sensation [25]. This nociceptive effect can be prevented by analgesic agents with central actions such as morphine as well as peripherally acting drugs like NSAID.

In order to evaluate whether FP_{MeOH} acted centrally or peripherally in the suppression of pain, we also conducted

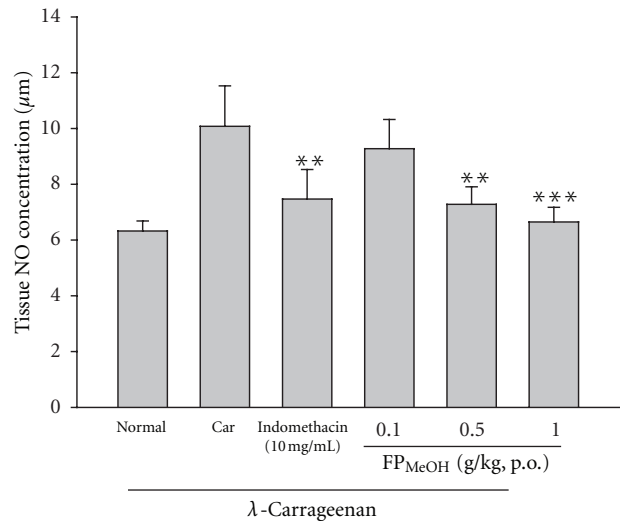


FIGURE 7: Effects of FP_{MeOH} and indomethacin on NO concentrations in the mouse edema paws. Each value represents mean \pm SD ($n = 8$). ** $P < 0.01$ and *** $P < 0.001$ as compared to the λ -carrageenan control group (one-way ANOVA followed by Scheffe's multiple range test).

the formalin test. The formalin test involves a biphasic response: the first phase (neurogenic nociceptive response) occurs in the first 5 min after the formalin injection, while the second phase (inflammatory nociceptive response) occurs between 15 to 30 min after formalin injection. Centrally

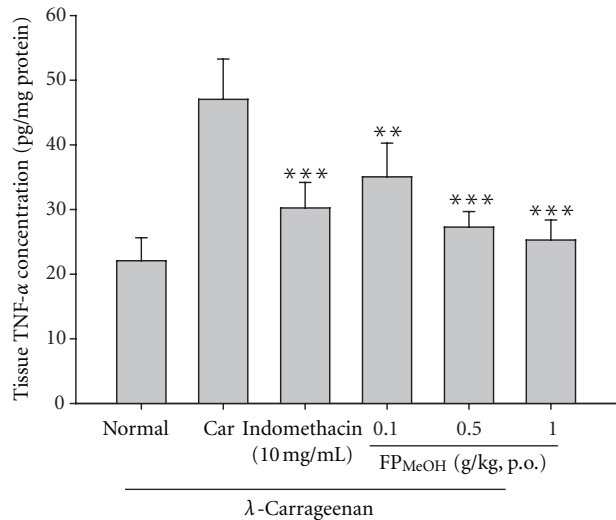


FIGURE 8: Effects of FP_{MeOH} and indomethacin on TNF- α concentrations in mouse paw edema. Each value represents mean \pm SD ($n = 8$). ** $P < 0.01$ and *** $P < 0.001$ as compared to the λ -carrageenan control group (one-way ANOVA followed by Scheffe's multiple range test).

acting drugs can inhibit both phases; however, peripherally acting drugs, such as NSAID, only inhibit the second phase [26]. The treatments of FP_{MeOH} (0.1–1 g/kg) and indomethacin (10 mg/kg) were able to diminish the nociceptive response in the second phase induced by formalin. The results indicated that the antinociceptive effect of FP_{MeOH} was due to its peripheral anti-inflammatory effect.

In the inflammatory model involving λ -carrageenan injection, FP_{MeOH} significantly decreased the volume of paw edema. The anti-inflammatory effect was also evident when we compared histopathological examinations of FP_{MeOH}-treated groups with that of λ -carrageenan control group. Paw biopsy of the λ -carrageenan control group showed obvious edematous condition and enlarged cavities in the connective tissues; on the other hand, the groups that received 10 mg/kg of indomethacin or 1 g/kg of FP_{MeOH} had significant improvement in edematous condition and decreased intercellular spaces in connective tissues as shown in Figure 5 and Table 2.

In our follow-up experiments that explored the mechanisms underlying the anti-inflammatory effect of FP_{MeOH}, we suspected that suppression of inflammatory cytokines may play an important role. λ -Carrageenan-induced paw edema has also been characterized as a biphasic event [13]: histamine, bradykinin, and 5-hydroxytryptamine (5-HT) are released in the first phase of edema (0–1 h), while TNF- α , IL-1 β , COX-2, and PGs are produced more actively in the second phase (1–6 h). TNF- α and IL-1 β have been reported in several studies to be able to recruit leukocytes, such as neutrophils [27, 28]. Additionally, COX-2 is an enzyme responsible for increasing prostaglandin levels in inflammatory reactions, which could in turn worsen the degree of swelling [29]. In this study, FP_{MeOH} (dose dependent)

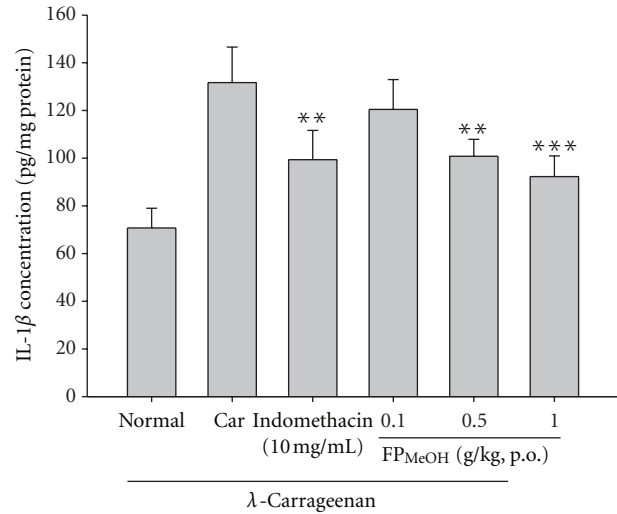


FIGURE 9: Effects of FP_{MeOH} and indomethacin on IL-1 β concentrations in mouse paw edema. Each value represents mean \pm SD ($n = 8$). ** $P < 0.01$ and *** $P < 0.001$ as compared to the λ -carrageenan control group (one-way ANOVA followed by Scheffe's multiple range test).

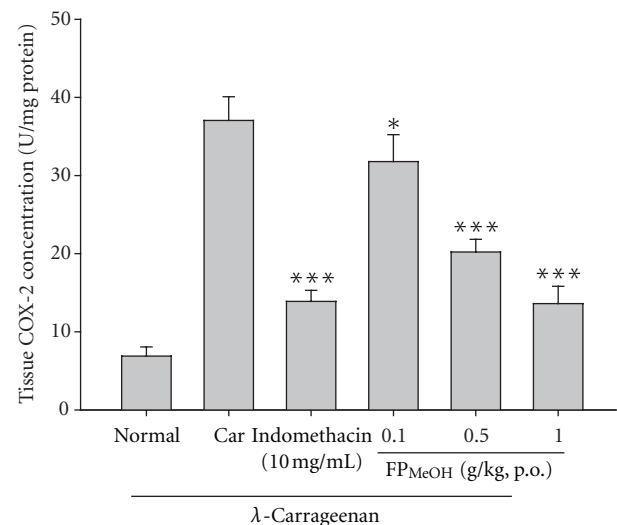


FIGURE 10: Effects of FP_{MeOH} and indomethacin on COX-2 concentrations in mouse paw edema. Each value represented mean \pm SD ($n = 8$). * $P < 0.05$ and *** $P < 0.001$ as compared to the λ -carrageenan control group (one-way ANOVA followed by Scheffe's multiple range test).

and indomethacin (10 mg/kg) showed significant anti-inflammatory effect in λ -carrageenan-induced mouse paw edema from the 3rd to 5th h. Moreover, the levels of TNF- α , IL-1 β , and COX-2 were also decreased by treating with FP_{MeOH} and indomethacin (10 mg/kg). Thus, a putative anti-inflammatory mechanism of FP_{MeOH} could be associated with the inhibition of inflammatory mediators, such as TNF- α , IL-1 β , and COX-2.

Another possible mechanism behind the anti-inflammatory effect of FP_{MeOH} could be due to its antioxidative activity. Increased production of TNF- α , IL-1 β , and other proinflammatory cytokines not only has the capacity to recruit leukocytes, but would also trigger their release of active substances such as ROS [30]. Nitric oxide, hydrogen peroxide, hydroxyl radicals, and superoxide anions play major roles in terms of producing cellular damage [31]. MDA is a reactive aldehyde caused by toxic stress in cells and form covalent protein adducts which are referred to as advanced lipid peroxidation end products (ALE). Inflammation would result in the accumulation of MDA; on the other hand, enhancing the level of GPx, GRd and SOD could reduce MDA production [32]. In this study, SOD, GPx, and GRd activities increased in the liver after treatment with FP_{MeOH}. Conversely, the level of MDA decreased significantly. Therefore, we believe that the suppression of MDA production was likely associated to the increase in SOD, GPx, and GRd activities.

The fingerprint chromatogram of FP_{MeOH} was established, and its three flavonoid contents (rutin, luteolin and apigenin) were quantitatively determined. Three active compounds of FP_{MeOH}, rutin, luteolin, and apigenin, have been previously demonstrated to possess anti-inflammatory and antinociceptive activities which may be responsible, at least in part, to the anti-inflammatory and antinociceptive effects of FP_{MeOH} [5–7].

This study demonstrated that *Ficus pumila* exhibited antinociceptive and anti-inflammatory activities. The anti-inflammatory mechanisms of FP_{MeOH} against λ -carrageenan-induced paw edema involved two possible pathways. The first pathway alleviated the levels of inflammatory factors, such as IL-1 β , TNF- α , and COX-2 in the edema paw induced by λ -carrageenan. The other pathway was likely associated to the decrease in MDA and NO levels in the edema paw via increasing the activities of SOD, GPx, and GRd in the liver. In conclusion, this study supported possible mechanisms of FP_{MeOH} used for mitigating inflammatory pain.

Acknowledgments

The authors would like to thank Dr. Jiunn-Wang Liao from National Chung Hsing University (Taichung, Taiwan) for the histological analysis of tissue biopsy. In addition, we would also like to express our appreciation to Dr. Chao-Lin Chen, former professor in the University of Florida, for his critical reading of the paper and editorial help.

References

- [1] D. R. Janero, "Malondialdehyde and thiobarbituric acid-reactivity as diagnostic indices of lipid peroxidation and peroxidative tissue injury," *Free Radical Biology and Medicine*, vol. 9, no. 6, pp. 515–540, 1990.
- [2] J. B. Harborne, *The Flavonoids: Advances in Research Since 1980*, Chapman and Hall, London, UK, 1986.
- [3] L. Pistelli, E. E. Chiellini, and I. Morelli, "Flavonoids from *Ficus pumila*," *Biochemical Systematics and Ecology*, vol. 28, no. 3, pp. 287–289, 2000.
- [4] Editorial Board of Zhong Hua Ben Cao, *Zhong Hua Ben Cao (China Herbal)*, Shanghai Scientific Technology Press, Shanghai, China, 1999.
- [5] L. Selloum, H. Bouriche, C. Tigrine, and C. Boudoukha, "Anti-inflammatory effect of rutin on rat paw oedema, and on neutrophils chemotaxis and degranulation," *Experimental and Toxicologic Pathology*, vol. 54, no. 4, pp. 313–318, 2003.
- [6] S. Hougee, A. Sanders, J. Faber et al., "Decreased pro-inflammatory cytokine production by LPS-stimulated PBMC upon in vitro incubation with the flavonoids apigenin, luteolin or chrysin, due to selective elimination of monocytes/macrophages," *Biochemical Pharmacology*, vol. 69, no. 2, pp. 241–248, 2005.
- [7] G. S. Jeong, S. H. Lee, S. N. Jeong, Y. C. Kim, and E. C. Kim, "Anti-inflammatory effects of apigenin on nicotine- and lipopolysaccharide-stimulated human periodontal ligament cells via heme oxygenase-1," *International Immunopharmacology*, vol. 9, no. 12, pp. 1374–1380, 2009.
- [8] T. S. Huang, *Flora of Taiwan*, Tah Jinn Printing Company Limited, Taipei, Taiwan, 1998.
- [9] M. Zimmermann, "Ethical guidelines for investigations of experimental pain in conscious animals," *Pain*, vol. 16, no. 2, pp. 109–110, 1983.
- [10] J. W. Liao, Y. C. Chung, J. Y. Yeh et al., "Safety evaluation of water extracts of *Toona sinensis* Roemor leaf," *Food and Chemical Toxicology*, vol. 45, no. 8, pp. 1393–1399, 2007.
- [11] R. Koster, M. Anderson, and E. J. Beer, "Acetic acid for analgesic screening," *Federation Proceeds*, vol. 18, pp. 412–416, 1959.
- [12] A. Tjølsen, O. G. Berge, S. Hunskaar, J. H. Rosland, and K. Hole, "The formalin test: an evaluation of the method," *Pain*, vol. 51, no. 1, pp. 5–17, 1992.
- [13] R. Vinegar, W. Schreiber, and R. Hugo, "Biphasic development of carrageenin edema in rats," *Journal of Pharmacology and Experimental Therapeutics*, vol. 166, no. 1, pp. 96–103, 1969.
- [14] V. L. Tatum, C. Changchit, and C. K. Chow, "Measurement of malondialdehyde by high performance liquid chromatography with fluorescence detection," *Lipids*, vol. 25, no. 4, pp. 226–229, 1990.
- [15] H. Moshage, B. Kok, J. R. Huizenga, and P. L. M. Jansen, "Nitrite and nitrate determinations in plasma: a critical evaluation," *Clinical Chemistry*, vol. 41, no. 6, pp. 892–896, 1995.
- [16] T. Ataoglu, M. Üngör, B. Serpek, S. Halilolu, H. Ataoglu, and H. Ari, "Interleukin-1 β and tumour necrosis factor- α levels in periapical exudates," *International Endodontic Journal*, vol. 35, no. 2, pp. 181–185, 2002.
- [17] N. Petrovic and M. Murray, "Using N,N,N',N'-tetramethyl-p-phenylenediamine (TMPD) to assay cyclooxygenase activity in vitro," *Methods in Molecular Biology*, vol. 594, pp. 129–140, 2010.
- [18] M. Vani, G. P. Reddy, G. R. Reddy, K. Thyagaraju, and P. Reddanna, "Glutathione-S-transferase, superoxide dismutase, xanthine oxidase, catalase, glutathione peroxidase and lipid peroxidation in the liver of exercised rats," *Biochemistry International*, vol. 21, no. 1, pp. 17–26, 1990.
- [19] I. Ceballos-Picot, J. M. Trivier, A. Nicole, P. M. Sinet, and M. Thevenin, "Age-correlated modifications of copper-zinc superoxide dismutase and glutathione-related enzyme activities in human erythrocytes," *Clinical Chemistry*, vol. 38, no. 1, pp. 66–70, 1992.
- [20] F. B. Ahmad and D. K. Holdsworth, "Medicinal plants of Sabah, Malaysia, Part II. The muruts," *International Journal of Pharmacognosy*, vol. 32, no. 4, pp. 378–383, 1994.

- [21] E. Sezik, E. Yesilada, M. Tabata et al., "Traditional medicine in Turkey VIII. Folk medicine in East Anatolia; Erzurum, Erzincan, Agri, Kars, Igridir provinces," *Economic Botany*, vol. 51, no. 3, pp. 195–211, 1997.
- [22] V. K. Singh, Z. A. Ali, S. T. H. Zaidi, and M. K. Siddiqui, "Ethnomedicinal uses of plants from Gonda district forests of Uttar Pradesh, India," *Fitoterapia*, vol. 67, no. 2, pp. 129–139, 1996.
- [23] D. L. Lentz, A. M. Clark, C. D. Hufford et al., "Antimicrobial properties of Honduran medicinal plants," *Journal of Ethnopharmacology*, vol. 63, no. 3, pp. 253–263, 1998.
- [24] X. A. Dominguez and J. B. Alcorn, "Screening of medicinal plants used by Huastec Mayans of North Eastern Mexico," *Journal of Ethnopharmacology*, vol. 13, no. 2, pp. 139–156, 1985.
- [25] M. N. Manjavachi, N. L. M. Quintao, M. M. Campos et al., "The effects of the selective and non-peptide CXCR2 receptor antagonist SB225002 on acute and long-lasting models of nociception in mice," *European Journal of Pain*, vol. 14, no. 1, pp. 23–31, 2010.
- [26] A. J. Reeve and A. H. Dickenson, "The roles of spinal adenosine receptors in the control of acute and more persistent nociceptive responses of dorsal horn neurones in the anaesthetized rat," *British Journal of Pharmacology*, vol. 116, no. 4, pp. 2221–2228, 1995.
- [27] D. Salvemini, Z. Q. Wang, P. S. Wyatt et al., "Nitric oxide: a key mediator in the early and late phase of carrageenan-induced rat paw inflammation," *British Journal of Pharmacology*, vol. 118, no. 4, pp. 829–838, 1996.
- [28] L. C. Loram, A. Fuller, L. G. Fick, T. Cartmell, S. Poole, and D. Mitchell, "Cytokine profiles during carrageenan-induced inflammatory hyperalgesia in rat muscle and hind paw," *Journal of Pain*, vol. 8, no. 2, pp. 127–136, 2007.
- [29] K. Seibert, Y. Zhang, K. Leahy et al., "Pharmacological and biochemical demonstration of the role of cyclooxygenase 2 in inflammation and pain," *Proceedings of the National Academy of Sciences of the United States of America*, vol. 91, no. 25, pp. 12013–12017, 1994.
- [30] A. G. Semb, J. Vaage, and O. D. Mjos, "Oxygen free radical producing leukocytes cause functional depression of isolated rat hearts: role of leukotrienes," *Journal of Molecular and Cellular Cardiology*, vol. 22, no. 5, pp. 555–563, 1990.
- [31] A. Kumaran and R. J. Karunakaran, "Activity-guided isolation and identification of free radical-scavenging components from an aqueous extract of *Coleus aromaticus*," *Food Chemistry*, vol. 100, no. 1, pp. 356–361, 2007.
- [32] S. Cuzzocrea, G. Costantino, B. Zingarelli, E. Mazzon, A. Micali, and A. P. Caputi, "The protective role of endogenous glutathione in carrageenan induced pleurisy in the rat," *European Journal of Pharmacology*, vol. 372, no. 2, pp. 187–197, 1999.

Research Article

Inhibition of NO₂, PGE₂, TNF- α , and iNOS EXpression by *Shorea robusta* L.: An Ethnomedicine Used for Anti-Inflammatory and Analgesic Activity

Chattopadhyay Debprasad,¹ Mukherjee Hemanta,¹ Bag Paromita,¹ Ojha Durbadal,¹
Konreddy Ananda Kumar,² Dutta Shanta,³ Halder Pallab Kumar,⁴ Chatterjee Tapan,⁴
Sharon Ashoke,² and Chakraborti Sekhar^{1,3}

¹ICMR Virus Unit, ID and BG Hospital, GB 4, First Floor, 57 Dr. Suresh C Banerjee Road, Beliaghata, Kolkata 700010, India

²Department of Applied Chemistry, Birla Institute of Technology, Mesra, Ranchi 835215, India

³Division of Microbiology, National Institute of Cholera and Enteric Diseases, Kolkata 700010, India

⁴Division of Pharmacology, Department of Pharmaceutical Technology, Jadavpur University, Kolkata 700032, India

Correspondence should be addressed to Chattopadhyay Debprasad, debprasadc@yahoo.co.in

Received 7 January 2012; Revised 30 January 2012; Accepted 30 January 2012

Academic Editor: Vincenzo De Feo

Copyright © 2012 Chattopadhyay Debprasad et al. This is an open access article distributed under the Creative Commons Attribution License, which permits unrestricted use, distribution, and reproduction in any medium, provided the original work is properly cited.

This paper is an attempt to evaluate the anti-inflammatory and analgesic activities and the possible mechanism of action of tender leaf extracts of *Shorea robusta*, traditionally used in ailments related to inflammation. The acetic-acid-induced writhing and tail flick tests were carried out for analgesic activity, while the anti-inflammatory activity was evaluated in carrageenan- and dextran-induced paw edema and cotton-pellet-induced granuloma model. The acetic-acid-induced vascular permeability, erythrocyte membrane stabilization, release of proinflammatory mediators (nitric oxide and prostaglandin E₂), and cytokines (tumor necrosis factor- α , and interleukins-1 β and -6) from lipopolysaccharide-stimulated human monocytic cell lines were assessed to understand the mechanism of action. The results revealed that both aqueous and methanol extract (400 mg/kg) caused significant reduction of writhing and tail flick, paw edema, granuloma tissue formation ($P < 0.01$), vascular permeability, and membrane stabilization. Interestingly, the aqueous extract at 40 μ g/mL significantly inhibited the production of NO and release of PGE₂, TNF- α , IL-1 β , and IL-6. Chemically the extract contains flavonoids and triterpenes and toxicity study showed that the extract is safe. Thus, our study validated the scientific rationale of ethnomedicinal use of *S. robusta* and unveils its mechanism of action. However, chronic toxicological studies with active constituents are needed before its use.

1. Introduction

Inflammation is a complex biological response of vascular tissues to harmful stimuli as well as a protective attempt to remove the stimuli and initiate the healing process. Inflammation has been classified as *acute* or *chronic*. *Acute inflammation* is the initial response of our body to the harmful stimuli, achieved by the increased movement of plasma and granulocytes from blood to the injured tissues [1]. A cascade of biochemical events involving the vascular system, immune system, and various cells of the injured tissue propagates and matures the response [2]. The affected cells are then activated to release several

mediators (eicosanoids, cytokines, chemokines) at the site, which elicit the inflammatory response from acute to the chronic phase. In prolonged or *chronic inflammation* a progressive shift of injured cells occurs at site and caused simultaneous destruction and healing of the injured tissues [3], during which the release of cyclooxygenase (COX)-mediated prostaglandins leads to pain, oedema, and fever. Thus, COX inhibitors are used as antiinflammatory drugs. However, many COX inhibitors produce serious adverse effects [4] and conventional nonsteroidal antiinflammatory drugs are unsuitable for the management of chronic and silent inflammations. Moreover, most of the modern anti-inflammatory and analgesic drugs are synthetic, costly, and

have several side effects like nephrotoxicity, respiratory problem, constipation, physical dependence, and gastrointestinal irritation in long run. It is therefore essential to search for cost effective antiinflammatory agents with low toxicity and better tolerance from ethnomedicinal source. As the ethnomedicinal plants, in particular, are an important source of drugs and candidate therapeutics [5, 6], their scientific evaluation may provide new drug molecule to combat long-term toxicity and cost.

The Indian ethnomedicine *Shorea robusta* L. (Dipterocarpaceae), popularly known as Sal or Shal, is widely used in Ayurveda and Unani medicine. The resin is used as astringent and detergent, in diarrhoea, dysentery, and gonorrhoea [7]; With Bee wax its act as an ointment base for foot cracks, psoriasis, wounds, ulcers, burns, chronic skin diseases, and ear and eye troubles [8]; while seeds are used for pus forming wounds [9]. A combination of oleoresin with cow ghee is claimed to control burning sensation of haemorrhoids, pain, and swelling [10]. A recent study with methanol extract of mature leaves reported anti-inflammatory and antinociceptive activity [11]. However, till date there is no consistent scientific evidence of those claims with aqueous extract used in ethnomedicinal practice, and its *in vitro* and *in vivo* mechanism of action. Therefore, for the first time, we have evaluated the effect of both aqueous and methanol extracts of *S. robusta* young tender leaves in several *in vivo* and *in vitro* models. The generation of proinflammatory mediators (prostaglandins and nitric oxide) and release of proinflammatory cytokine (TNF- α , IL-1 β , and IL-6) was also studied as markers, to understand the possible mechanism of action of this ethnomedicine used in traditional health care.

2. Materials and Methods

2.1. Plant Material. The young tender leaves of *S. robusta* L. were collected in April, August and December 2008 and 2009, from the nearby forest of tribal area to rule out possible seasonal variation of chemical content of the specimen. The identification and authentication was done by a Taxonomist of the Botanical Survey of India, Shibpur, Howrah, and voucher specimen (Herbarium No. 07/08/17775) has been deposited at the Herbarium and at the host Institute.

2.2. Preparation of Samples and Studies on Their Physicochemical Properties. Following strict standards, the collected part was washed thoroughly, dried in shade, pulverized by a mechanical grinder, and passed through 40-mesh sieve to get the fine powder. The physicochemical characters (total ash, acid insoluble ash, and water content) and the behaviour of powdered sample dissolved in different chemicals and exposed to visible and UV (312 nm) light [12] were studied for constant quality and better yield [13].

2.3. Extraction and Physicochemical Standardization of Extracts. Five hundred grams of powdered young leaves was extracted with distilled water (2.5 L) and 95% methanol (2 L) separately, with maceration upto 48–72 h at room temperature [14]. The extract was repeatedly filtered and

centrifuged (800 \times g for 10 min) to remove the impurities. The collected aqueous extract was lyophilized, while the methanol extract was evaporated to dryness under reduced pressure at 40–45°C to yield crude extract (55.5 g). The % rendement or yield (w/w) of the extracts was determined by standard formula: % yield (w/w) = fixed weights of the extract/Sample weight \times 100.

2.4. Isolation of Fractions from Aqueous Extract. The aforementioned crude extract (50 g) was subjected to phytochemical group tests of tannin (with 10% potassium dichromate/lead acetate/5% ferric chloride), reducing sugar (Benedict's and Fehling's tests), steroids (Liebermann-Burchard test), terpenoids (Salkowski test), flavonoids (extract was hydrolyzed with 10% sulphuric acid, extracted with diethyl ether and divided into three parts to test with sodium carbonate, sodium hydroxide and ammonium solution) and others, following standard methods [15, 16]. The aqueous extract was then extracted with ethyl acetate (7 \times 1 L) and concentrated under reduced pressure to yield a dark brown liquid mass of 1.5 g. The residual material was purified on Silica gel Column using hexane and ethyl acetate as eluent to collect six distinct fractions (F1 to F6), which were monitored by TLC [17]. The yield of fractions 1 to 6 was: 40 mg, 30 mg, 20 mg, 60 mg, 80 mg, and 250 mg, respectively.

For chromatography, the precoated HPTLC silica gel plate (60 F₂₅₄ of 0.2 mm thickness and 20 \times 10 cm size, Merck KGaA, Germany) was used. One mg/mL stock solutions of extracts were prepared in water and methanol separately. Then 100 μ L of each isolated fraction (1–6) was loaded on HPTLC plates at 20 mm distance, using a Linomat IV spotter (Camag, Pvt. Ltd., Switzerland). Plates were dried and developed by ethylacetate:methanol (9:1) solvent system, and further dried to observe under visible and UV (254 nm) light, and scanned by a Camag Scanner III (Switzerland).

The significant biological activity demonstrated by the aqueous extract intended us to further investigate the presence of plausible phytoconstituents, which may be responsible for such potential activities. Therefore, the water extracts were further subjected for purification and chromatographic fractionation.

2.5. Animals. Healthy Swiss albino male mice (18–20 g), and adult male Wistar rats (150–180 g) were housed in the animal house facility of the Department of Pharmaceutical Technology, Jadavpur University, Kolkata, and maintained (23 \pm 4°C, relative humidity 60–70%) on a standard diet with water *ad libitum*. The animals were acclimatized for two weeks before the experiments. All animal experiments were carried out in accordance with the approval (APRO/69/20/08/09; Dated 20-08-2009) and guidelines of the Institutional Animal Ethics Committee.

2.6. Chemicals and Drugs. Dimethylsulfoxide (DMSO), carrageenan, phorbol-12-myristate-13-acetate (PMA), dexamethasone, NS-398 (N-[2-(cyclohexyloxy)-4-nitrophenyl]-methanesulfonamide), and lipopolysaccharide (LPS) of *E. coli* 026:B6 were purchased from Sigma-Aldrich (St. Louis,

Mo, USA). The L-NIL (N6-(-iminoethyl)-L-lysine, dihydrochloride) was obtained from Santa Cruz Biotechnology, Inc., USA; while RPMI 1640, fetal bovine serum (FBS), penicillin and streptomycin, trypsin-EDTA, and Tris-buffer were purchased from Gibco-BRL (Karlsruhe, Germany). The commercial enzyme linked immunosorbent assay (ELISA) kit for TNF- α and PGE2 was purchased from the BD Biosciences, New Jersey, USA, while IL-1 β and IL-6 from the R&D System, Minneapolis, MN, USA, respectively. The Griess reagent, dextran, paracetamol, morphine sulfate, diclofenac disodium, and indomethacin were purchased from the respective manufacturers.

2.7. Acute Toxicity Study. The acute toxicity of *S. robusta* extracts (aqueous and methanol) was evaluated on different groups of mice and male Wistar rats at increasing doses to determine the LD₅₀. The animals were divided into ten groups ($n = 6$) and extracts were administered orally (*p.o.*) at a dose of 0–2500 mg/kg, or by intraperitoneal (*i.p.*) injection at 0–1000 mg/kg. The animals were observed periodically (6, 12, 18 and 24 h) for symptoms of toxicity and death and then daily for next 14 days [18]. No acute toxic effects (agility, muscular tonus, tremors, convulsions, problem in breathing, water or food intake) or mortality was observed following treatment, so the procedure was repeated up to the highest dose of 3.5 gm/kg *p.o.* The dose regimen of the test extracts was selected (200 and 400 mg/kg) on the basis of the acute toxicity data.

2.8. Analgesic Activity

2.8.1. Acetic Acid-Induced Writhing Tests. This was performed following a modified method of Koster and Anderson [19]. Briefly, Swiss albino mice of either sex (18–20 g) were separately divided into six groups of six animals each. The first group served as control; the second group was administered with paracetamol (50 mg/kg), while the third to sixth groups received aqueous and alcoholic extract of *S. robusta*, at doses of 200 and 400 mg/kg as *i.p.* injection. After 30 min of drug treatment, the animals were given 1% v/v acetic acid solution at 10 mL/kg *i.p.* immediately after 5 minutes of acetic acid administration and the numbers of writhing or stretches (a syndrome, characterized by a wave of contraction of the abdominal musculature followed by extension of hind limbs) were counted for 15 minutes. A reduction in the writhing number compared to the control group was considered as the analgesia [15]. The percentage inhibition of writhing was calculated according to the following formula: % Inhibition = $C - T/C \times 100$, Where C is the mean number of writhes produced by the control group and T is the mean number of writhes produced by the test groups.

2.8.2. Tail Flick Test. Swiss albino mice of either sex (18–20 g) were divided into six groups ($n = 6$). The tail of each mouse was placed on the nichrome wire of an analgesiometer (Techno Lab, Lucknow, India) and the time taken by the animal to withdraw (flick) its tail from the

hot wire was taken as a reaction time. The aqueous and alcoholic extract of *S. robusta* at doses of 200 and 400 mg/kg were injected *i.p.*, using Morphine sulphate (5 mg/kg) as standard drug. Analgesic activity was measured after 30 min of administration of extract and drug [15, 20] and the percentage inhibition was calculated by the aforementioned formula.

2.9. Antiinflammatory Activity

2.9.1. Carrageenan-Induced Rat Paw Oedema (Acute Model). Inflammation in the hind paw of Wistar albino rats was induced by the method of Winter et al. [21]. Animals were divided into six groups ($n = 6$). First four groups of animals were pretreated with the aqueous and alcoholic extract at doses of 200 and 400 mg/kg *i.p.*, 1 h prior to subplantar (right hind paw) injection of 0.1 mL of 1% (w/v) fresh carrageenan in normal saline. The 5th group serves as vehicle control, while the 6th group received diclofenac disodium (10 mg/kg) as positive control. The edema volume (linear circumference of the injected paw) was measured by a plethysmometer at 0 h and 1 h interval upto 5 h after carrageenan injection [22]. The antiinflammatory activity was evaluated based on the ratio of the changes in paw diameter in treated and untreated group as per the formula: anti-inflammatory activity (%) = $(1 - D/C) \times 100$, where D is the change in paw diameter in treated group and C is the change in paw diameter in untreated group.

2.9.2. Dextran-Induced Rat Paw Oedema (Subacute Model). The hind paw edema on the right foot of a rat was induced by subplantar injection of 0.1 mL of freshly prepared 1% dextran solution [23]. Paw volumes were measured 30 min before and after dextran injection. The treatment of extracts (test), vehicle (vehicle control), and standard drug (drug control) was the same as described for carrageenan model. The percentage inhibition of edema was calculated by the method of Kavimani et al. [24].

2.9.3. Cotton-Pellet-Induced Granuloma (Chronic Model). The rats were divided into six groups ($n = 6$) and were anaesthetized after shaving of the fur. Sterile preweighed cotton pellets (10 mg) were implanted in the axilla region of each rat through a single needle incision [25]. Aqueous and methanol extracts at 200 and 400 mg/kg were administered *i.p.* 60 min before the cotton pellet implementation to the first four groups. The fifth group served as vehicle control, and the sixth group received diclofenac disodium (10 mg/kg), for consecutive seven days from the day of beginning of implantation. On eighth day, the animals were anaesthetized; the cotton pellets were removed surgically and made free from extraneous tissues. To obtain constant weight, the pellets were incubated at 37°C for 24 h and dried at 60°C. The granuloma weight was calculated by measuring the increase in dry weight of the pellets of the treated and control groups.

2.10. Acetic-Acid-Induced Vascular Permeability in Mice. The vascular permeability in mice was tested by the method of Whittle [26] with modifications. Briefly, randomly selected mice, each with six animals, were divided into six groups. Group I served as vehicle control, groups II to V were treated with 200 and 400 mg/kg of aqueous and alcoholic extract, while group VI received indomethacin (10 mg/kg) orally. One hour after the treatment, 200 μ L of 0.2% Evan's blue in normal saline was injected through tail vein of each mouse (at 0.2 mL/20 gm body weight). Thirty minutes later, the acetic acid (0.6%) in normal saline (0.2 mL) was injected *i.p.* to each mouse. After 1 h, the mice were sacrificed and the abdomen was open to expose the entrails and washed with normal saline (5 mL) to collect the content in a test tube. The content was centrifuged and the absorbance of the supernatant was measured in a spectrophotometer at 500 nm. The vascular permeability effects were expressed as the absorbance (A) of the amount of dye leaked into the intraperitoneal cavity.

2.11. Membrane Stabilizing Activity. Membrane stabilizing activity of the extract was assessed by hypotonic solution-induced human erythrocyte haemolysis [27]. Whole blood was collected from a healthy volunteer (DC) in a heparinized tube and washed thrice with isotonic buffer (154 mM NaCl in 10 mM sodium phosphate buffer, pH 7.4) for 10 minutes at 3000 g. The RBC suspension (0.5 mL) mixed with 5 mL of hypotonic solution (50 mM NaCl in 10 mM PBS, pH 7.4) with or without the extract (0.15–3.0 mg/mL) or indomethacin (0.1 mg/mL) in triplicate was incubated (10 min at room temperature) and centrifuged (3000 g for 10 min), and the absorbance of the supernatant was measured at A_{590} nm. The percentage inhibition of haemolysis was calculated according to the formula: % Inhibition of haemolysis = $100 \times \{OD_1 - OD_2/OD_1\}$, where OD_1 is the Optical density of hypotonic buffered saline solution alone, and OD_2 is the optical density of test sample in hypotonic solution.

2.12. In Vitro Assay of PGE₂, TNF- α , and Nitric Oxide in LPS-Induced THP-1 Cell. Human monocytic THP-1 cells obtained from the National Centre for Cell Science, Pune, India, were grown at 37°C in RPMI 1640 containing heat inactivated FBS (10%), penicillin (100 IU/mL) and streptomycin (100 μ g/mL) at 37°C in 5% CO₂ atmosphere. Cells at the exponential growth phase were trypsinized and suspended in complete medium at 5×10^5 cells/mL [28]. Cell suspension (500 nm) was then activated with PMA (100 ng/mL) for 48 h to obtain transformed macrophages. Cell viability was checked by MTT assay and cytotoxicity of the extract was evaluated in presence or absence of LPS. The transformed cells were incubated with 100 μ L of extracts (0–100 μ g/mL), or dexamethasone (1 μ M) for TNF- α , COX-2 inhibitor N-[2-(cyclohexyloxy)-4-nitrophenyl]-methanesulfonamide, or NS-398 (10 μ M) for PGE₂ as drug control and 0.5% DMSO as vehicle control, respectively. After 30 min of pretreatment cells were further incubated with 1 μ g/mL LPS for 24 h, and cell-free supernatants were collected to

determine PGE₂ and TNF- α level by EIA kits (BD Bioscience, USA) as per manufacturer's instructions.

For measuring nitrite accumulation, an indicator of NO synthesis, 100 μ L of the previous culture was mixed with 100 μ L of Griess reagent (equal volumes of 1% (w/v) sulfanilamide in 5% (v/v) phosphoric acid and 0.1% (w/v) naphthylethylenediamine-HCl) and incubated at room temperature for 10 min. The selective inhibitor of inducible nitric oxide synthetase N6-(1-iminoethyl)-L-lysine, dihydrochloride or L-NIL (10 μ M) was used as positive control. The absorbance was measured at 550 nm in microplate reader using fresh culture media as blank. The amount of nitrite in the sample was calculated from a standard curve prepared with fresh sodium nitrite [29].

2.13. Determination of IL-1 β and IL-6 Production. IL-1 β and IL-6 levels in macrophage culture media were quantified by enzyme immunoassay kits (R&D System, Minneapolis, MN, USA) according to the manufacturer's instructions.

3. Statistical Analysis

The results were expressed as mean, mean \pm SEM (Standard Error Mean), and SD (Standard Deviation). The statistical significance was analyzed by Student's *t*-test for unpaired observations compared with the control, and the significance of difference among the various test and control group was analyzed by one-way ANNOVA followed by Dunnett's *t*-test.

4. Results

In this study anti-inflammatory and analgesic potential of aqueous and alcohol extracts of *S. robusta* young leaves was evaluated by different *in vivo* screening methods, along with the mechanism of action of the most active extract. To find out the mechanism of action, the generation of proinflammatory mediators like NO and PGE₂ and release of cytokines like TNF- α , IL-1 β , and IL-6 from PMA-activated and LPS-stimulated THP-1 cells were measured.

4.1. Physicochemical and Phytochemical Group Tests and Chromatographic Analysis. The physicochemical study, presented in Table 1 indicated that *S. robusta* young leaves collected in August had maximum yield but minimum water (23.69%), total ash (3.55 \pm 0.45) and acid insoluble ash (0.20 \pm 0.3) content, compared to other samples. The fluorescence studies of the powdered samples made from the leaf collected in August showed pale yellow to yellow colour under visible and UV (312 nm) light, while with HCl, H₂SO₄, and HNO₃, the colour was light to deep brown, reddish brown, and orange, respectively. However with acetic acid, chloroform, and n-hexane, the colour varied from yellow green, yellow to pale yellow, and greenish yellow and brown, respectively. The chemical group tests and preliminary HPTLC analysis (*R_f* value, percentage area, and λ max) of the extracts, presented in Table 2, showed that both extracts had two bands with best resolution, when

TABLE 1: The physicochemical properties of *S. robusta* young leave.

Sample	Sample (in gm)	Extract (in gm)	% rendement (yield)	Ash content (% w/w)	Acid insoluble ash (% w/w)	Water content (%)
<i>S. robusta</i> (Aug)	500.00	50.5	10.1 ± 0.51	3.55 ± 0.45	0.20 ± 0.30	23.69 ± 12.51
<i>S. robusta</i> (Dec)	552.80	48.9	8.84 ± 0.47	5.36 ± 0.39	0.35 ± 0.60	26.18 ± 14.47
<i>S. robusta</i> (April)	508.50	42.3	8.31 ± 0.41	6.23 ± 0.27	0.42 ± 0.17	26.56 ± 0.56

TABLE 2: HPTLC and phytochemical analysis of extracts.

Sample	Solvent system	Chromatophore (s)	R_f	Area %	λ max	Phytochemical group
<i>S. robusta</i> extract	Ethyl acetate : Methanol (9 : 1)	Aqueous 1	0.78	19.33	104.3	Tannin, reducing sugar, flavonoids, Steroids
		Aqueous 2	0.87	41.93	155.4	
		Methanol 1	0.78	19.33	104.3	Tannin, flavonoids, steroids, terpenoids
		Methanol 2	0.87	41.33	155.4	
Quercetin	Ethylacetate : Methanol (9 : 1)	Aqueous Q ₁	0.79	19.34	104.5	Flavonoid
		Methanol Q ₁	0.81	19.55	105.1	

TABLE 3: Analgesic activity by acetic-acid-induced writhing and tail flick methods.

Treatment	Dose (mg/kg)	Writhing reflex (Reaction time in sec)	% Inhibition	Tail flick (Reaction time in sec)	% Inhibition
Control		15.00 ± 0.40	0	22.22 ± 0.56	0
Paracetamol	50	3 ± 0.365*	80	—	—
Morphine	5	—	—	5.20 ± 0.10*	76.59
<i>S. robusta</i> aqueous extract	200	5.5 ± 0.763*	63.33	7.68 ± 0.27*	65.43
	400	4.33 ± 0.421*	71.13	6.6 ± 0.15*	70.29
<i>S. robusta</i> methanol extract	200	6 ± 0.516*	60.00	8.14 ± 0.51*	63.36
	400	5 ± 0.365*	66.66	7.46 ± 1.00*	66.42

Results are expressed as mean ± SEM ($n = 6$), * $P < 0.001$ compared to control (2% aqueous Tween 80 v/v).

ethyl acetate:methanol = 9:1 was used as solvent. The detail HPTLC analyses of fractions 1–6 were presented in Figures 1, 2, and 3 using friedelin as reference compound. The HPTLC analysis clearly reveals the significant purity of isolated fraction but absence of friedelin as one of the major compound in the extract.

4.2. Acute Toxicity Study. Oral and *i.p.* treatment of aqueous and methanol extracts upto 14 days showed no manifestation of toxic effects (convulsion, ataxy, diarrhoea, or increased diuresis) or death in treated animals, indicating that both the extracts possess good safety profile. However, the reduced motor activity, ataxia, and hyperventilation were observed in mice, but not in rats, at oral doses of 3500 mg/kg. The LD₅₀ of the orally fed methanolic and aqueous extracts of *S. robusta* was determined as 2.4 gm/kg and 2.7 gm/kg; while it was 1.2 gm/kg and 1.4 gm/kg in *i.p.*, respectively. By comparing with the toxicity-rating chart [30], the extract was classified as nontoxic. Hence, the dose for further study was selected as 200 and 400 mg/kg. Further *in vivo* toxicological study for 21 days with aqueous extract upto 1200 mg/kg (*p.o.*) did not induce mortality or clinical toxicity or reveal

any histopathological changes in kidney, liver and spleen (Figure 4).

4.3. Analgesic Activity

4.3.1. Effect of Extracts on Acetic-Acid-Induced Writhing Test. The results of acetic-acid-induced writhing test with aqueous and methanol extract in mice, presented in Table 3, showed that the maximum inhibition of writhing reflexes was 60% and 63.33% at 200 mg/kg while 66.66% and 71.13% at 400 mg/kg *i.p.* of methanol and aqueous extracts, respectively. Thus, compared to the paracetamol-treated group (80% inhibition), the aqueous extracts at 400 mg/kg have equally significant ($P < 0.001$) inhibition.

4.3.2. Effect of Extracts on Tail Flick Test. The results of tail flick test revealed that the aqueous extract at 400 mg/kg *i.p.* doses had reaction time of 6.6 sec (70.29% inhibition); but with methanol extract it was 7.46 sec (66.42% inhibition). However, with 200 mg/kg dose the reaction time was 7.68 sec and 8.14 sec (65.43% and 63.36% inhibition) respectively. Thus, a dose-dependent significantly ($P < 0.001$) higher effect was recorded with the aqueous extract (400 mg/kg)

TABLE 4: Effect of extracts on carrageenan- and dextran-induced paw edema.

Treatment	Dose (mg/kg)	Carrageenan induced paw edema	% Inhibition	Dextran induced paw edema	% Inhibition
Control	0.1 mL	2.1 ± 0.05	—	2.86 ± 0.01	—
Diclofenac disodium	10	0.51 ± 0.005	75.71	0.68 ± 0.014	76.22
Aqueous extract	200	0.97 ± 0.006	53.80	1.18 ± 0.010	58.74
	400	0.73 ± 0.008	65.23	0.88 ± 0.010	69.23
Methanol extract	200	1.08 ± 0.007	48.57	1.36 ± 0.011	52.44
	400	0.80 ± 0.009	61.90	1.07 ± 0.013	62.58

Results are expressed as mean ± SEM ($n = 6$). The significance level in comparison to control values, $P < 0.001$. Control aqueous Tween-80 solution (2% v/v).

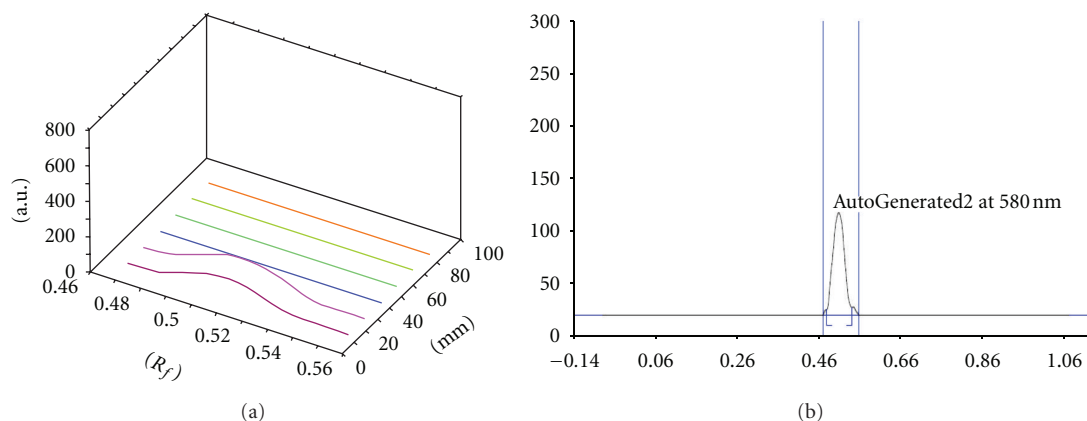


FIGURE 1: The HPTLC spectrogram ($R_f = 0.49$) of the reference compound “friedelin”, used as marker compound to evaluate the isolated fraction for comparative analysis.

compared to the Morphine sulfate (5.20 sec, 76.59% inhibition) after 30 min (Table 3).

4.4. Antiinflammatory Activity

4.4.1. Effect of Extracts on Carrageenan-Induced Rat Paw Oedema. The results of the antiinflammatory activity of the aqueous and methanol extract of *S. robusta* against carrageenan-induced paw oedema in rats showed that there was a gradual increase in the edema volume in the control group during the study period. However, both aqueous and methanol extract at 400 mg/kg *p.o.* produced a significant dose-dependent inhibition (61.90 and 65.23%, $P > 0.001$) of paw oedema, compared to Diclofenac disodium (75.71% inhibition) after 3 h of treatment (Table 4).

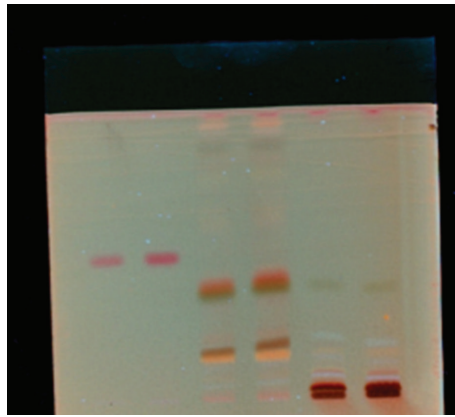
4.4.2. Effect of Extracts on Dextran-Induced Paw Oedema. In dextran-induced paw oedema model, the maximum (69.23%) inhibition of edema swelling was noted with 400 mg/kg *p.o.* aqueous extracts, which are nearly similar to diclofenac disodium (76.22% inhibition at 10 mg/kg after 3 h), while the minimum (52.44%) inhibition was recorded with 200 mg/kg *p.o.* of methanol extract. All these data are significant ($P < 0.0001$) with respect to the control group (Table 4).

4.4.3. Effect of Extracts on Cotton-Pellet-Induced Granuloma. The results presented in Figure 5 showed that both the

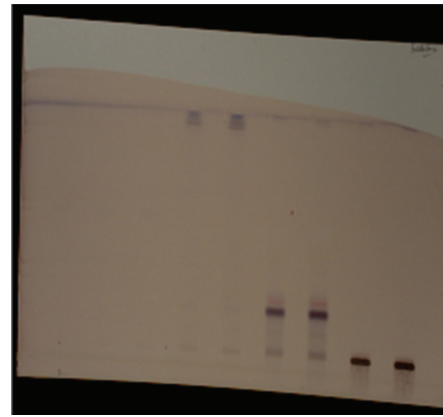
extracts significantly inhibited the granuloma weight in a dose dependent manner. However, the aqueous extract (400 mg/kg *p.o.*) had significantly ($P < 0.001$) higher inhibition (54.12%) of the dry weight of granuloma compared to diclofenac disodium (57.48% at 10 mg/kg; $P < 0.05$). On the otherhand, moderate-to-high inhibitions were recorded with other doses of aqueous and methanol extract.

4.5. Inhibition of Acetic-Acid-Induced Vascular Permeability in Mice. Effects of aqueous and methanolic extract (200 and 400 mg/kg, *p.o.*) and indomethacin (10 mg/kg, *p.o.*) on acetic-acid-induced vascular permeability in mice, presented in Figure 6, revealed that the extract inhibited the vascular permeability by 30% to 54.16%. However, aqueous extract (400 mg/kg) significantly ($P < 0.001$) inhibited vascular permeability (54.16%) compared with vehicle control and indomethacin (60.83%) group.

4.6. Effects of Extracts on Membrane Stabilizing Activity. The aqueous and methanolic extracts at 0.15 mg/mL doses moderately ($P < 0.05$) protect the erythrocyte membrane against lysis induced by hypotonic saline, as it inhibits haemolysis by 39.72–42.46%. However, the aqueous extract at 0.3 mg/mL and indomethacin at 0.1 mg/mL doses offered better ($P < 0.01$) protection (54.79% and 63.69%) compared to the blank (Figure 7).



Spot 1, 2: Friedelin (pink)
Spot 3, 4: Fraction 2
Spot 5, 6: Fraction 4



Spots 1–3: Friedelin (not visible)
Spot 4, 5: Fraction 1
Spot 6, 7: Fraction 3
Spot 8, 9: Fraction 5

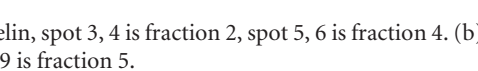
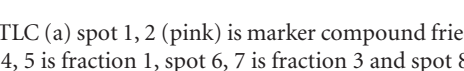
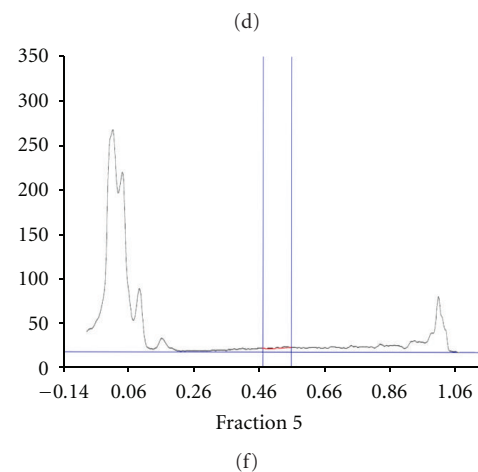
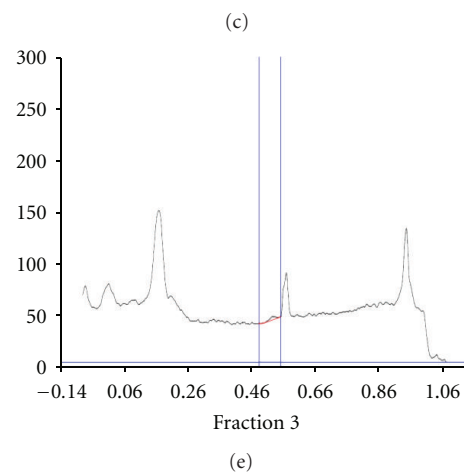
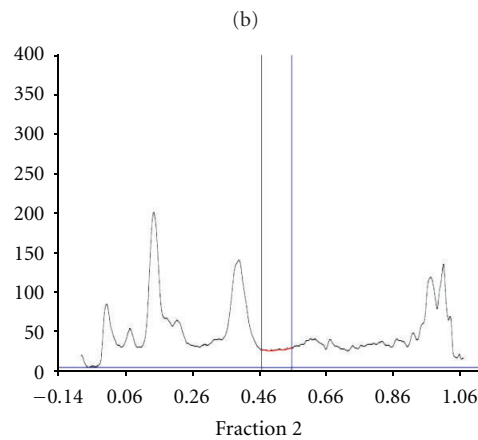
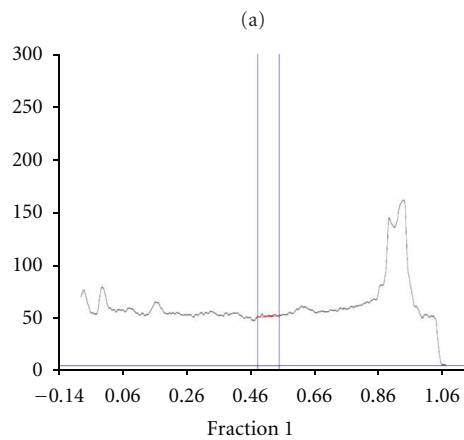
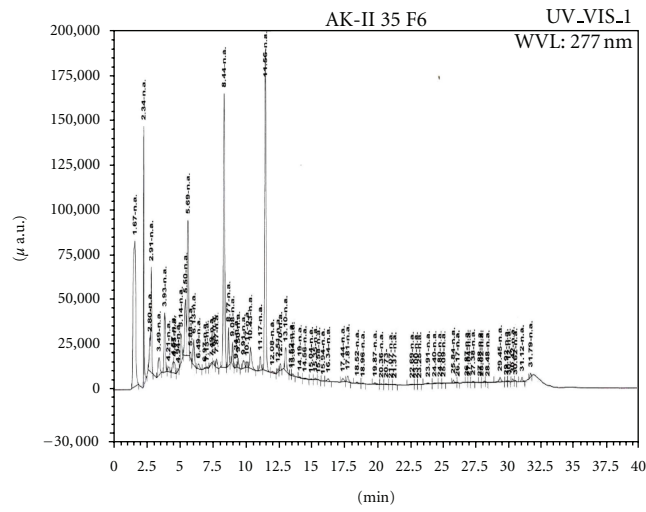


FIGURE 2: The HPTLC (a) spot 1, 2 (pink) is marker compound friedelin, spot 3, 4 is fraction 2, spot 5, 6 is fraction 4. (b) spot 1–3 is friedelin (not visible), spot 4, 5 is fraction 1, spot 6, 7 is fraction 3 and spot 8, 9 is fraction 5.

4.7. Effects of Extracts on Cell Viability, LPS-Induced NO_2 , PGE_2 and $\text{TNF-}\alpha$ Production. Cytotoxic effect of both aqueous and methanol extracts was evaluated in presence or absence of LPS and found that the cell viability was not affected by any of the extract upto $100 \mu\text{g/mL}$ concentration. The effect of the extract on the production of NO , PGE_2 , and $\text{TNF-}\alpha$ in the supernatant of PMA-activated and then

extract-treated and LPS-stimulated THP-1 cells was shown in Figures 8(a), 8(b), and 8(c). The LPS ($1 \mu\text{g/mL}$) induced increased NO_2 -production was significantly suppressed by positive inhibitor L-NIL ($10 \mu\text{M}$); while both the extract showed concentration-dependent inhibitory effect on LPS-induced NO production at noncytotoxic concentrations. However, the aqueous extract was most active. Additionally,

Sample name: AK-II 35 F6
Acquired time: 16/12/2011 22:21:56



Number	Retention time (min)	Area	Area %
1	1.67	1105120	16.02
2	2.34	381889	5.53
3	2.8	100291	1.45
4	2.91	346801	5.03
5	3.49	100638	1.46
6	3.93	241816	3.5
7	4.21	26824	0.39
8	4.57	46084	0.67
9	4.65	41370	0.6
10	4.94	7099	0.1

FIGURE 3: The HPLC chromatogram of fraction 6 with their retention time and area showing 4 major components.

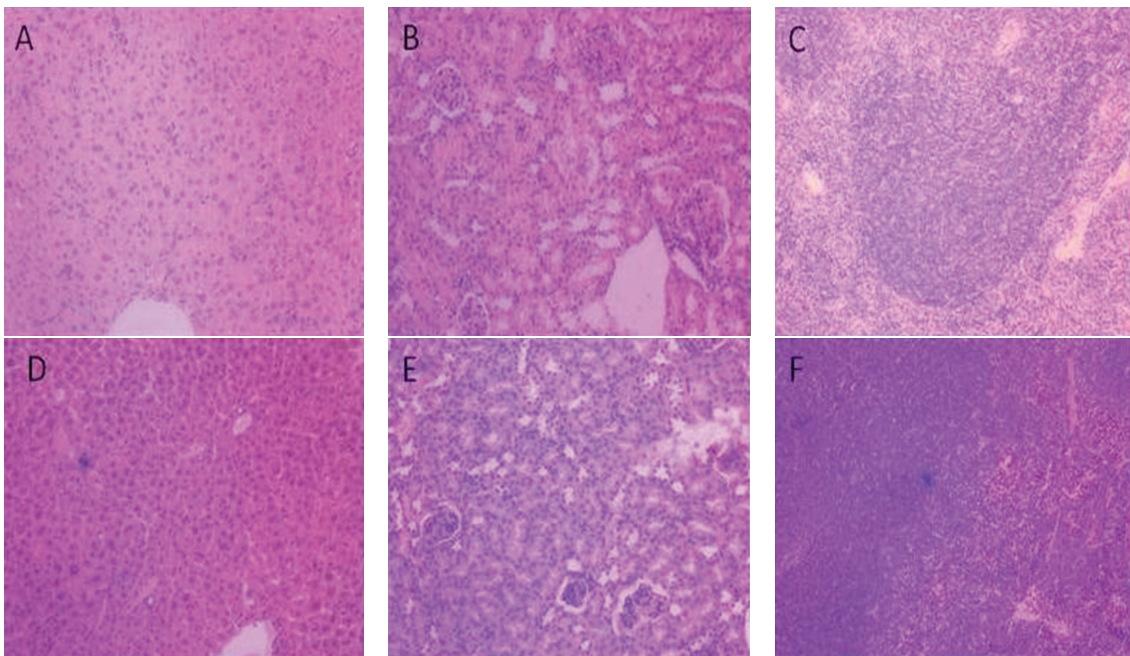


FIGURE 4: Histopathology of liver, kidney, and spleen of Swiss mice treated with aqueous extract (1200 mg/kg body weight orally). Liver (A), kidney (B), and spleen (C): control; liver (D), kidney (E), and spleen (F): treated.

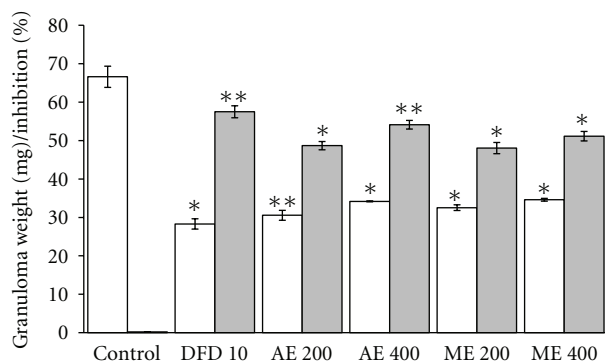


FIGURE 5: Effects of aqueous (AE) and methanol (ME) extracts on the cotton-pellet-induced tissue granulation. DFD: diclofenac disodium. White bars represent the granuloma weight while grey bars showed percentage inhibition of granuloma weight. Values are the mean \pm S.E.M. of six rats. Statistical significance is represented by $*P \leq 0.05$, $**P \leq 0.01$, and $***P \leq 0.001$, respectively (unpaired Student's *t*-test).

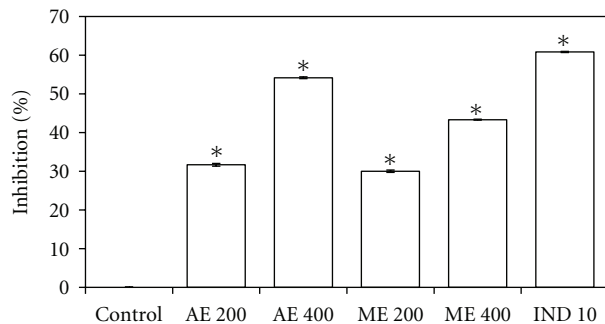


FIGURE 6: Effects of aqueous (AE) and methanol (ME) extracts on the acetic-acid-induced vascular permeability in mice. The animals were pretreated with various concentrations of the extract and indomethacin (IND). Values are the mean \pm S.E.M. of six mice. Statistical significance is represented by $*P \leq 0.05$ (Student's *t*-test).

the extract had no quenching effect on the Griess reagent at the concentrations used (Figure 8(a)). Furthermore, the aqueous extract significantly inhibited PGE2 (Figure 8(b)) and TNF- α production (Figure 8(c)) in a dose-dependent manner and is more active than its alcoholic counterpart.

4.8. Effect of Extract on IL-1 β and IL-6 Production. To investigate the effect of extract on LPS-induced IL-1 β and IL-6 release, we estimated the level of these cytokines in extract-treated THP-1 macrophages by enzyme immunoassay kits. The results showed that the pretreating cells with extract reduced both IL-1 β and IL-6 production (Figures 9(a) and 9(b)) in concentration-dependent manner.

5. Discussion

In the Present study, we have evaluated, for the first time, the anti-inflammatory and analgesic activity of both aqueous and methanol extracts of *S. robusta* young tender leaves, used by two distinct tribes of India for ailments related to inflammation and pain, in different *in vivo* and *in vitro*

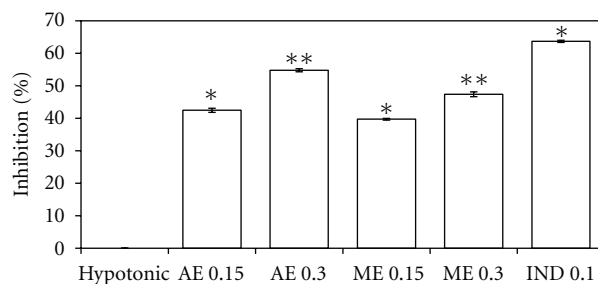


FIGURE 7: Effects of aqueous (AE) and methanol (ME) extracts on membrane stabilization of hypotonic saline-induced human RBC, in compare with indomethacin (IND). Values are the mean \pm S.E.M. of six sets. Statistical significance is represented by $*P \leq 0.05$, and $**P \leq 0.01$ (Student's *t*-test).

model. Moreover, for the first time, the proinflammatory mediators NO and PGE2 and cytokines like TNF- α , IL-1 β , IL-6 have been estimated in presence or absence of the extract to know the possible mechanism of action.

The physicochemical standardization of collected sample and extract(s) was made to achieve better yields and constant quality of the tested extracts [31]. The best quality sample was selected on the basis of physicochemical and behavioral properties, which showed that the post-rainy session sample had the maximum yield (10.1 ± 0.51) with minimum water, total ash, and acid insoluble ash content. The extraction was done by standard protocol and followed by phytochemical group tests and HPTLC analysis. The HPTLC profile of isolated fractions clearly reveals the significant purity of isolated fractions (Figures 2(a), 2(b), 2(c), 2(d), 2(e), and 2(f)). Friedelin was used as marker compound as the preliminary phytochemical tests showed the presence of triterpene and flavonoids in the crude extract. Though the isolated fraction (1–4) did not show friedelin (Figure 1), the fractions 2 and 3 (Figures 2(d) and 2(e)) show that one of the major components is very close to friedelin (parallel blue lines). This result further indicates the possibility of the presence of similar pharmacophores in Fractions 2–3, while fractions 1 and 4 have different profile and contain different nature of compounds. Thus, the HPTLC studies reveal preliminary information and warrant a detail study to establish complete structure activity relationship to demonstrated the biological significance of isolated extract. However, the HPLC profile of Fraction 6 revealed four major compounds. Earlier reports revealed that gum resin of *S. robusta* contain ursolic acid and α -amyrenone [32, 33], bark contains ursonic acid and oleanane [34], seed contains hopeaphenol, leucoanthocyanidin, and 3,7-dihydroxy-8-methoxyflavone-7-*O*- α -1-rhamnopyranosyl-(1 \rightarrow 4)- α -1-rhamnonopyranosyl-(1 \rightarrow 6)- β -d-glucopyranoside [35], while heartwood contains germacrene-D [10]. The isolation of β -amyrin, friedelin, β -sitosterol, pheophytin- α , and dihydroxyisoflavone from mature leaves was also reported [36]. However, our preliminary study indicated that the young tender leaf does not contain friedelin.

Acute toxicity study over 14 days showed that the extract possessed good safety profile and the LD₅₀ of the orally fed methanol and aqueous extracts was 2.4–2.7 gm/kg.

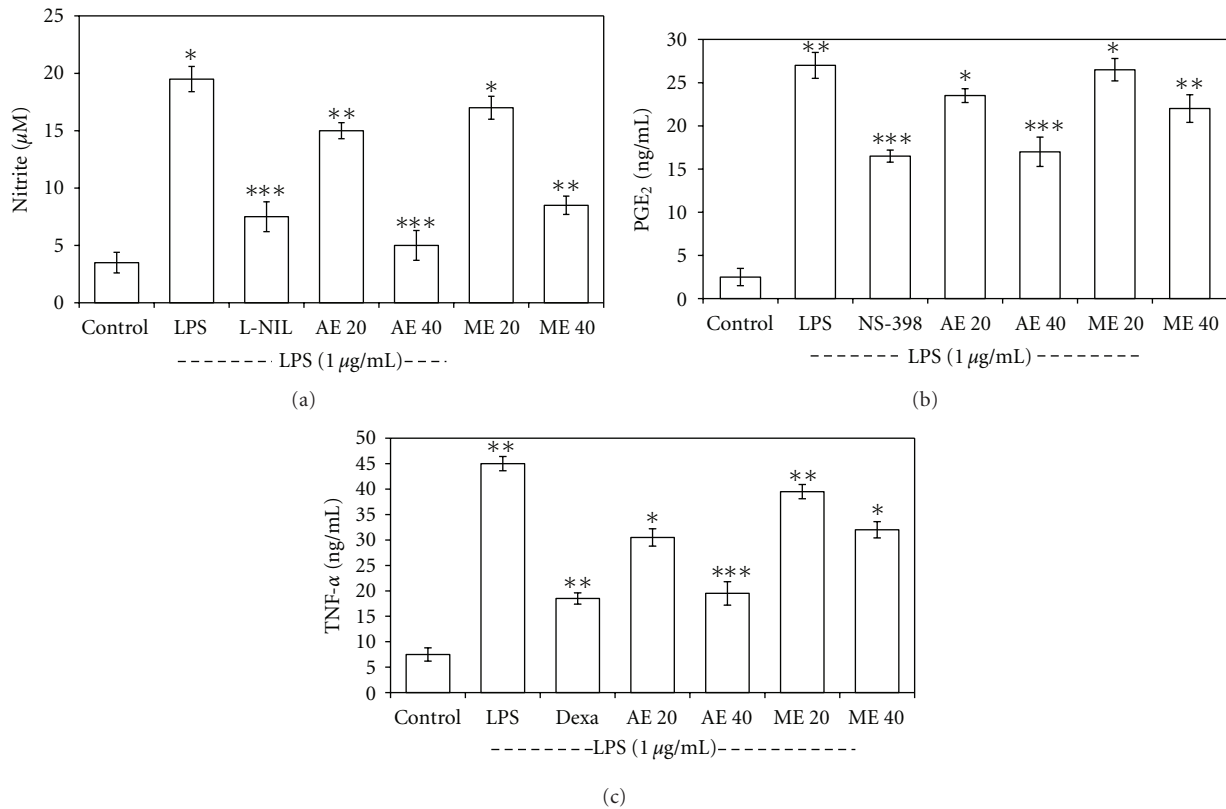


FIGURE 8: Effect of aqueous (AE) and methanol (ME) extract on nitrite (a), PGE₂ (b), and TNF- α (c) production by LPS-induced THP-1 macrophage. (a) The PMA (100 nM) activated cells were pretreated with or without various concentrations of extracts (0–100 $\mu\text{g}/\text{mL}$) for 1 h and then LPS (1 $\mu\text{g}/\text{mL}$) was added and incubated for 24 h. Control values are in the absence of LPS or extract while 10 μM of L-NIL was used as positive control. The values are the means \pm SD from three independent experiments. * P < 0.05; ** P < 0.01; *** P < 0.001 versus LPS-treated group; the significance of the difference between the treated groups was evaluated by Student's t -test. (b) The conditions of sample treatment were identical with Figure 8(a), using 10 μM of COX-2 inhibitor NS-398 as positive control. The values represent the means \pm SD from three independent experiments. * P < 0.05; ** P < 0.01; *** P < 0.001 versus LPS-treated group; the significance of difference between the treated group was evaluated by Student's t -test. (c) The conditions of sample treatment were identical with Figure 8(a), using dexamethasone (Dexa, 1 μM) as positive inhibitor. The values represent the means \pm SD from three independent experiments. ** P < 0.01; *** P < 0.001 versus LPS-treated group; the significance of difference between the treated groups was evaluated by Student's t -test.

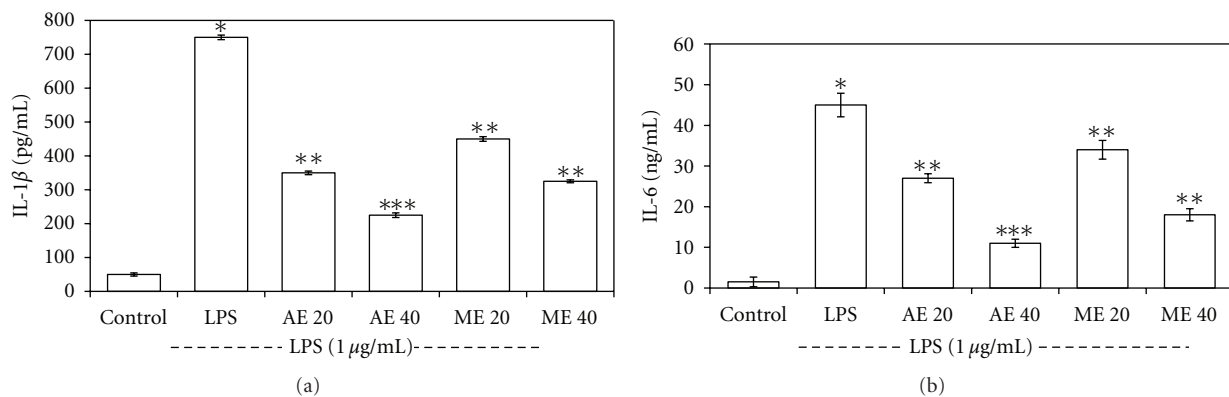


FIGURE 9: The effect of *S. robusta* extracts on LPS-induced IL-1 β (a) and IL-6 (b) in THP-1 macrophage cells. (a) The cells were pretreated for 1 h with two selected concentrations of the extracts (20 and 40 μg), and then LPS (1 $\mu\text{g}/\text{mL}$) was added and incubated for 24 h. Control values were obtained in the absence of LPS or extract. The values represent the means \pm SD of three independent experiments. * P < 0.05 compared with the LPS-treated group; the significance of the difference between the treated groups was evaluated using the Student's t -test.

Hence, for further study the dose was selected as 200 and 400 mg/kg. *In vivo* toxicological study with aqueous extract showed contrasting results, as the oral treatment did not induce mortality or clinical toxicity, or any histopathological changes in organs.

The acetic acid-induced writhing test indicated that the numbers of writhing movements were significantly less in the treated mice, comparable to untreated group. The effect of the extract when compared to paracetamol, suggests that the extract might have peripheral analgesic effect. Furthermore, the analgesic effect produced by the tail flick test was comparable to that of morphine-treated control, suggesting central analgesic effect.

Acute inflammatory agent's carrageenan and dextran induce inflammation through different mechanisms. Carrageenan, a standard phlogistic agent, is used to induce paw edema in animals, as it is known to release histamine, bradykinin, and serotonin (5-hydroxytryptamine) in the early phase, and prostaglandins and kinin in the late phase [37, 38], which induces protein rich exudates with neutrophil at the site of inflammation resulting in increased vascular permeability, and accumulation of fluid in tissues to form edema [39, 40]. The results of the carrageenan-induced edema test revealed that extracts at 400 mg/kg, in 3 h *p.o.* have dose-dependent inhibitory effect on edema formation in both early and late phases, comparable to diclofenac disodium. This suggests that the extract may inhibit the synthesis and/or release of those mediators, particularly the cyclooxygenase. Dextran is a high molecular weight polysaccharide that induces anaphylactic reaction characterized by extravasation and edema formation, as a consequence of liberation of histamine and serotonin [23] to the site of inflammation and the fluid accumulation through mast cell degradation [41]. Moreover, dextran can cause inflammation by activating NF- κ B and inducing the expression of TLR-4, and proinflammatory cytokines IL-1 β , TNF- α and IL-6 in mice [42]. Thus, the inhibition of dextran mediated edema by the extract was probably due to the antihistaminic (inhibition of histamine and serotonin) effects of our extract. Furthermore, the decrease in the cotton-pellet-induced granuloma weight by the extract is due to the inhibition of proliferative phase of inflammation [22], as the inflammatory response induced by the cotton pellet can modulate the release of mediators leading to the tissue proliferation and granuloma formation [43, 44]. The acetic-acid-induced vascular permeability test is a typical capillary permeability assay, used to further confirm the antiinflammatory potential of the extract. The acetic acid is known to cause dilation of arterioles and venules and increase vascular permeability by releasing inflammatory mediators such as histamine, prostaglandins, and leukotrienes by stimulating mast cells [45]. During inflammation histamine, serotonin, and other mediators increase vascular permeability, while acetic acid causes an immediate sustained reaction [46]. Thus, the inhibition of acetic-acid-induced inflammation suggests that the extracts may effectively suppress the exudative phase of acute inflammation.

Further, the protective effect on hypotonic saline-induced RBC lysis is an index of antiinflammatory activity

[47], which leads to the formation of free radical [48] that cause secondary damage through lipid peroxidation [49, 50]. Thus, the compounds with membrane-stabilizing property can protect the cell membrane against injurious substances [27, 51] by interfering the release of phospholipases that trigger the formation of inflammatory mediators [52]. Here, the observed membrane stabilizing activity suggests that the extract may inhibit the release of phospholipases and thereby the formation of inflammatory mediators.

To elucidate the *in vitro* mechanism of action, the estimation of proinflammatory mediators and cytokines, in presence or absence of the extract, was made in LPS-stimulated THP-1 macrophage cells. Macrophages play a crucial role in both nonspecific and acquired immune responses, and its activation by LPS leads to a series of responses like the production of proinflammatory cytokines (TNF- α , IL-1, IL-6) and activation of phospholipase A2 that produce prostaglandin and NO [53] and, thus, can be used as a model to test the potential antiinflammatory compounds [28]. Our results demonstrated that the accumulation of nitrite in the medium (due to enhanced NO production) takes place when THP-1 macrophage was exposed to LPS for hour's, and this LPS-induced NO production was significantly inhibited by the aqueous extract in a time- and concentration-dependent manner without notable cytotoxicity. This inhibition is either through the regulation of inducible nitric oxide (*i*NOS) gene expression, or its direct interference with *i*NOS activity. It is known that various anti-inflammatory drugs inhibit prostaglandins (PGs) synthesis by cyclooxygenase (COX) 1 and 2. COX-1 provides a physiologic level of PGs, while COX-2 is highly induced at inflammatory sites [54, 55]. Here, the significant inhibition of PGE2 production by the extract is probably through COX-2 gene expression in LPS-treated macrophages. However, further investigation is needed to confirm the extract action on NF κ B activities.

Proinflammatory cytokines (TNF- α , IL-1 β , and IL-6) are known to control inflammation *in vitro* and *in vivo* [56, 57] and are probably interlinked in a cascade, produced by macrophages during inflammatory response. Moreover, the development of hyperalgesia during inflammation is probably mediated by proinflammatory cytokines [58]. Therefore, we have investigated the role of our extract in cytokine production and found that the aqueous extract significantly reduced the production of TNF- α , IL-1 β , and IL-6 in dose-dependent manner. TNF- α plays a critical role in both acute and chronic inflammation [59] by infiltration of inflammatory cells through the adhesion of neutrophils and lymphocytes [60], and stimulates neutrophils to release cytokines (IL-1 β and IL-6) and chemokines [61, 62]. Interaction between these mediators enhances further inflammatory reactions [63]. Thus, inhibition of TNF- α , IL-1 β , and IL-6 release can reduce the severity of inflammation. The antichronic inflammatory activity of the extract observed in cotton-pellet-induced granuloma model is further supported by this study, as cellular accumulations of fluids and proinflammatory cytokines were demonstrated within the first 14 days [64–66]. Therefore, the inhibition of tissue granuloma by the extract, at least in part, is through the interference with TNF- α , IL-1 β , and IL-6 release. Thus,

the present study suggests that *S. robusta* young tender leaf extract, particularly the aqueous extract, inhibits LPS-induced iNOS and COX-2 protein expression, along with NO₂, PGE₂, and TNF- α production probably due to its terpenoids, flavonoids, or related compounds alone or in combination, as reported with other plants [67–69], and thereby it is useful in the prevention and treatment of inflammatory conditions.

6. Conclusion

In conclusion, the observed analgesic and anti-inflammatory activity of the aqueous extracts of *S. robusta* young leaves might be through the inhibition of leukocyte activations and reduced release of inflammatory mediators (PGE₂, NO) and proinflammatory cytokines (TNF- α , IL-1, and IL-6). Therefore, our findings support the ethnomedicinal use of *S. robusta* young leaves in the management of inflammatory ailments via multilevel regulation of inflammatory reactions. Additionally its low toxicity encourages clinical trials in primary health care after subchronic and chronic toxicological studies with the active component(s).

Acknowledgments

The authors are thankful to the Head, Department of Pharmaceutical Technology, Jadavpur University, Kolkata, and the Officer in-Charge, ICMR Virus Unit, Kolkata, for their help and support. They are thankful to Arbro Analytical Division, Delhi, for providing analytical service. The financial assistance of the Department of Biotechnology and Indian Council of Medical Research (fellowship to PB), New Delhi is deeply acknowledged.

References

- [1] I. G. Colditz, "Margination and emigration of leucocytes," *Survey and synthesis of pathology research*, vol. 4, no. 1, pp. 44–68, 1985.
- [2] T. Kasama, R. M. Strieter, T. J. Standiford, M. D. Burdick, and S. L. Kunkel, "Expression and regulation of human neutrophil-derived macrophage inflammatory protein 1 α ," *Journal of Experimental Medicine*, vol. 178, no. 1, pp. 63–72, 1993.
- [3] L. Ferrero-Miliani, O. H. Nielsen, P. S. Andersen, and S. E. Girardin, "Chronic inflammation: importance of NOD2 and NALP3 in interleukin-1 β generation," *Clinical and Experimental Immunology*, vol. 147, no. 2, pp. 227–235, 2007.
- [4] A. Gaddi, A. F. G. Cicero, and E. J. Pedro, "Clinical perspectives of anti-inflammatory therapy in the elderly: the lipoxigenase (LOX)/cyclooxygenase (COX) inhibition concept," *Archives of Gerontology and Geriatrics*, vol. 38, no. 3, pp. 201–212, 2004.
- [5] D. Chattopadhyay, G. Arunachalam, A. B. Mandal, R. Bhadra, and S. C. Mandal, "CNS activity of the methanol extract of *Mallotus peltatus* (Geist) Muell Arg. leaf: an ethnomedicine of Onge," *Journal of Ethnopharmacology*, vol. 85, no. 1, pp. 99–105, 2003.
- [6] D. Chattopadhyay and M. T. H. Khan, "Ethnomedicines and ethnomedicinal phytophores against herpesviruses," *Biotechnology Annual Review*, vol. 14, pp. 297–348, 2008.
- [7] D. M. Verma, N. P. Balakrishnan, and R. D. Dixit, *Flora of Madhya Pradesh*, vol. 1, Botanical Survey of India, 1993.
- [8] <http://www.himalayahealthcare.Com/aboutayurveda/cahs.htm#shorea>.
- [9] Y. N. Singh, "Traditional medicine in Fiji: some herbal folk cures used by Fiji Indians," *Journal of Ethnopharmacology*, vol. 15, no. 1, pp. 57–88, 1986.
- [10] S. Kaur, R. Dayal, V. K. Varshney, and J. P. Bartley, "GC-MS analysis of essential oils of heartwood and resin of *Shorea robusta*," *Planta Medica*, vol. 67, no. 9, pp. 883–886, 2001.
- [11] G. Jyothi, W. M. Carey, R. B. Kumar, and K. G. Mohan, "Antinoceptive and antiinflammatory activity of methanolic extract of leaves of *Shorea robusta*," *Pharmacologyonline*, vol. 1, pp. 9–19, 2008.
- [12] World Health Organization Guidelines, *Macroscopic and Microscopic Examination: Quality Control Methods for Medicinal Plant Materials*, World Health Organization, Geneva, Switzerland, 1998.
- [13] P. H. List and P. C. Schmidt, *Phytopharmaceutical Technology*, Heyden, London, UK, 2nd edition, 1989.
- [14] D. Chattopadhyay, K. Maiti, A. P. Kundu et al., "Antimicrobial activity of *Alstonia macrophylla*: a folklore of bay islands," *Journal of Ethnopharmacology*, vol. 77, no. 1, pp. 49–55, 2001.
- [15] D. Chattopadhyay, G. Arunachalam, T. K. Sur, S. K. Bhattacharya, and A. B. Mandal, "Analgesic and antiinflammatory activity of *Alstonia macrophylla* and *Mallotus peltatus* leaf extracts: two popular Ethnomedicines of Onge, A Nigrito Tribes of Little Andaman," *Oriental Pharmacy and Experimental Medicine*, vol. 5, no. 2, pp. 124–136, 2005.
- [16] G. Arunachalam, P. Bag, and D. Chattopadhyay, "Phytochemical and phytotherapeutic evaluation of *Mallotus peltatus* (Geist.) Muell. Arg. var *acuminatus* and *Alstonia macrophylla* wall ex A. DC: Two Ethnomedicine of Andaman Islands, India," *Journal of Pharmacognosy and Phytotherapy*, vol. 1, no. 1, pp. 1–20, 2009.
- [17] H. Wagner and S. Bladt, *Plant Drug Analysis, A Thin Layer Chromatography Atlas*, Springer, Heidelberg, Germany, 2nd edition, 1996.
- [18] D. J. Ecobichon, *The Basis of Toxicology Testing*, CRC Press, New York, NY, USA, 1997.
- [19] R. Koster, M. Anderson, and E. J. de Beer, "Acetic acid for analgesics screening," *Federation Proceedings*, vol. 18, pp. 412–417, 1959.
- [20] D. Chattopadhyay, "Advances in phytomedicine: ethnomedicine and drug discovery (book review)," *Drug Discovery Today*, vol. 8, no. 10, article 535, 2003.
- [21] C. A. Winter, E. A. Risley, and G. W. Nuss, "Carrageenan induced oedema in hind paw of rat as assay for antiinflammatory drugs," *Experimental Biology and Medicine*, vol. 111, pp. 544–547, 1962.
- [22] D. Chattopadhyay, G. Arunachalam, A. B. Mandal, T. K. Sur, S. C. Mandal, and S. K. Bhattacharya, "Antimicrobial and anti-inflammatory activity of folklore: *Mallotus peltatus* leaf extract," *Journal of Ethnopharmacology*, vol. 82, no. 2-3, pp. 229–237, 2002.
- [23] G. Arunachalam, D. Chattopadhyay, S. Chatterjee, A. B. Mandal, T. K. Sur, and S. C. Mandal, "Evaluation of anti-inflammatory activity of *Alstonia macrophylla* Wall ex A. DC. leaf extract," *Phytomedicine*, vol. 9, no. 7, pp. 632–635, 2002.
- [24] S. Kavimani, T. Vetrivelvan, R. Ilango, and B. Jaykar, "Anti-inflammatory activity of the volatile oil of *Toddalia asiatica*," *Indian Journal of Pharmaceutical Sciences*, vol. 58, no. 2, pp. 67–70, 1996.

- [25] P. D. D'Arcy, E. M. Howard, P. W. Muggleton, and S. B. Townsend, "The antiinflammatory action of griseofulvin in experimental animals," *Journal of Pharmacy and Pharmacology*, vol. 12, pp. 659–665, 1960.
- [26] B. A. Whittle, "The use of changes in capillary permeability in mice to distinguish between narcotic and nonnarcotic analgesics," *British Journal of Pharmacology*, vol. 22, no. 2, pp. 246–253, 1964.
- [27] U. A. Shinde, S. A. Phadke, A. M. Nair, A. A. Mungantiwar, V. J. Dikshit, and M. N. Saraf, "Membrane stabilizing activity—a possible mechanism of action for the anti-inflammatory activity of *Cedrus deodara* wood oil," *Fitoterapia*, vol. 70, no. 3, pp. 251–257, 1999.
- [28] U. Singh, J. Tabibian, S. K. Venugopal, S. Devaraj, and I. Jialal, "Development of an *in vitro* screening assay to test the antiinflammatory properties of dietary supplements and pharmacologic agents," *Clinical Chemistry*, vol. 51, no. 12, pp. 2252–2256, 2005.
- [29] H.-J. Jung, S.-G. Kim, J.-H. Nam et al., "Isolation of saponins with the inhibitory effect on nitric oxide, prostaglandin E₂ and tumor necrosis factor- α production from *Pleurosperrum kamtschaticum*," *Biological and Pharmaceutical Bulletin*, vol. 28, no. 9, pp. 1668–1671, 2005.
- [30] R. E. Gosselin, R. P. Smith, and H. C. Hodge, *Clinical Toxicity of Commercial Products*, Williams & Wilkins, Baltimore, Md, USA, 1984.
- [31] R. D. Petry, G. G. Ortega, and W. B. Silva, "Flavonoid content assay: influence of the reagent concentration and reaction time on the spectrophotometric behavior of the aluminium chloride—flavonoid complex," *Pharmazie*, vol. 56, no. 6, pp. 465–470, 2001.
- [32] R. K. Hota and M. Bapuji, "Triterpenoids from the resin of *Shorea robusta*," *Phytochemistry*, vol. 32, no. 2, pp. 466–468, 1993.
- [33] L. N. Misra and A. Ahmad, "Triterpenoids from *Shorea robusta* resin," *Phytochemistry*, vol. 45, no. 3, pp. 575–578, 1997.
- [34] J. B. Harborne, "Recent advances in chemical ecology," *Natural Product Reports*, vol. 16, no. 4, pp. 509–523, 1999.
- [35] E. O. Prakash and J. T. Rao, "A new flavone glycoside from the seeds of *Shorea robusta*," *Fitoterapia*, vol. 70, no. 6, pp. 539–541, 1999.
- [36] S. M. S. Chauhan, M. Singh, and L. Narayan, "Isolation of 3 β -hydroxyolean-12-ene, friedelin and 7-methoxy-4'-5-dihydroxyisoflavone from dry and fresh leaves of *Shorea robusta*," *Indian Journal of Chemistry Section B*, vol. 41, no. 5, pp. 1097–1099, 2002.
- [37] A. Heller, T. Koch, J. Schmeck, and K. van Ackern, "Lipid mediators in inflammatory disorders," *Drugs*, vol. 55, no. 4, pp. 487–496, 1998.
- [38] T. K. Sur, S. Pandit, D. K. Bhattacharya et al., "Studies on anti-inflammatory activity of *Betula alnoides* bark," *Phytotherapy Research*, vol. 16, no. 7, pp. 669–671, 2002.
- [39] T. J. Williams and J. Morley, "Prostaglandins as potentiators of increased vascular permeability in inflammation," *Nature*, vol. 246, no. 5430, pp. 215–217, 1973.
- [40] M. White, "Mediators of inflammation and the inflammatory process," *Journal of Allergy and Clinical Immunology*, vol. 103, supplement 2, no. 3, pp. S378–S381, 1999.
- [41] J. P. van Wauwe and J. G. Goosens, "Arabinogalactan and dextran-induced ear inflammation in mice: differential inhibition by H1-antihistamines, 5-HT-serotonin antagonists and lipoxygenase blockers," *Agents and Actions*, vol. 28, no. 1-2, pp. 78–82, 1989.
- [42] F. X. Zhang, C. J. Kirschning, R. Mancinelli et al., "Bacterial lipopolysaccharide activates nuclear factor- κ B through interleukin-1 signalling mediators in cultured human dermal endothelial cells and mononuclear phagocytes," *The Journal of Biological Chemistry*, vol. 274, no. 12, pp. 7611–7614, 1999.
- [43] L. Tang and J. W. Eaton, "Inflammatory responses to biomaterials," *American Journal of Clinical Pathology*, vol. 103, no. 4, pp. 466–471, 1995.
- [44] W. J. Hu, J. W. Eaton, T. P. Ugarova, and L. Tang, "Molecular basis of biomaterial-mediated foreign body reactions," *Blood*, vol. 98, no. 4, pp. 1231–1238, 2001.
- [45] J. N. Brown and L. J. Roberts, "Histamine, bradykinin, and their antagonists," in *Goodman and Gilman's The Pharmacological Basis of Therapeutics*, L. L. Brunton, J. S. Lazo, and K. L. Parker, Eds., pp. 645–667, McGraw Hill, New York, NY, USA, 11th edition, 2006.
- [46] K. Whaley and A. D. Burt, "Inflammation, healing and repair," in *Muir's Textbook of Pathology*, R. M. N. MacSween and K. Whaley, Eds., pp. 112–165, Arnold, London, UK, 13th edition, 1996.
- [47] O. O. Oyedapo and A. J. Famurewa, "Anti-protease and membrane stabilizing activities of extracts of *Fagra zanthoxiloides*, *Olex subscropioides* and *Tetrapleura tetraptera*," *International Journal of Pharmacognosy*, vol. 33, pp. 65–69, 1995.
- [48] B. Halliwell, J. R. F. Hoult, and D. R. Blake, "Oxidants, inflammation, and anti-inflammatory drugs," *The FASEB Journal*, vol. 2, no. 13, pp. 2867–2873, 1988.
- [49] M. Ferrali, C. Signorini, L. Ciccoli, and M. Comporti, "Iron release and membrane damage in erythrocytes exposed to oxidizing agents, phenylhydrazine, divicine and isouramil," *Biochemical Journal*, vol. 285, no. 1, pp. 295–301, 1992.
- [50] S. R. J. Maxwell, "Prospects for the use of antioxidant therapies," *Drugs*, vol. 49, no. 3, pp. 345–361, 1995.
- [51] R. M. Perez, S. Perez, M. A. Zavala, and M. Salazar, "Anti-inflammatory activity of the bark of *Hippocratea excelsa*," *Journal of Ethnopharmacology*, vol. 47, no. 2, pp. 85–90, 1995.
- [52] M. Aitadafoun, C. Mounier, S. F. Heyman, C. Binistic, C. Bon, and J. Godhold, "4-Alkoxybenzamides as new potent phospholipase A2 inhibitors," *Biochemical Pharmacology*, vol. 51, pp. 737–742, 1996.
- [53] H. J. Park, K. T. Lee, W. T. Jung, J. W. Choi, and S. Kadota, "Protective effects of syringin isolated from *Kalopanax pictum* on galactosamine induced hepatotoxicity," *Natural Medicines*, vol. 53, no. 3, pp. 113–117, 1999.
- [54] K. Seibert, Y. Zhang, K. Leahy et al., "Pharmacological and biochemical demonstration of the role of cyclooxygenase 2 in inflammation and pain," *Proceedings of the National Academy of Sciences of the United States of America*, vol. 91, no. 25, pp. 12013–12017, 1994.
- [55] J. L. Masferrer, B. S. Zweifel, P. T. Manning et al., "Selective inhibition of inducible cyclooxygenase 2 *in vivo* is anti-inflammatory and nonulcerogenic," *Proceedings of the National Academy of Sciences of the United States of America*, vol. 91, no. 8, pp. 3228–3232, 1994.
- [56] A. Harada, N. Sekido, T. A. K. Akahoshi, T. Wada, N. Mukaida, and K. Matsushima, "Essential involvement of interleukin-8 (IL-8) in acute inflammation," *Journal of Leukocyte Biology*, vol. 56, no. 5, pp. 559–564, 1994.
- [57] M. Feldmann, F. M. Brennan, and R. N. Maini, "Role of cytokines in rheumatoid arthritis," *Annual Review of Immunology*, vol. 14, pp. 397–440, 1996.
- [58] L. R. Watkins, S. F. Maier, and L. E. Goehler, "Immune activation: the role of pro-inflammatory cytokines in inflammation,

- illness responses and pathological pain states," *Pain*, vol. 63, no. 3, pp. 289–302, 1995.
- [59] M. H. Holtmann and M. F. Neurath, "Differential TNF-signaling in chronic inflammatory disorders," *Current Molecular Medicine*, vol. 4, no. 4, pp. 439–444, 2004.
- [60] M. Dore and J. Sirois, "Regulation of P-selectin expression by inflammatory mediators in canine jugular endothelial cells," *Veterinary Pathology*, vol. 33, no. 6, pp. 662–671, 1996.
- [61] P. T. Marucha, R. A. Zeff, and D. L. Kreutzer, "Cytokine regulation of IL-1 β gene expression in the human polymorphonuclear leukocyte," *Journal of Immunology*, vol. 145, no. 9, pp. 2932–2937, 1990.
- [62] M. C. Fernandez, J. Walters, and P. Marucha, "Transcriptional and post-transcriptional regulation of GM-CSF-induced IL-1 β gene expression in PMN," *Journal of Leukocyte Biology*, vol. 59, no. 4, pp. 598–603, 1996.
- [63] M. Gouwy, S. Struyf, P. Proost, and J. van Damme, "Synergy in cytokine and chemokine networks amplifies the inflammatory response," *Cytokine and Growth Factor Reviews*, vol. 16, no. 6, pp. 561–580, 2005.
- [64] L. Tang, T. A. Jennings, and J. W. Eaton, "Mast cells mediate acute inflammatory responses to implanted biomaterials," *Proceedings of the National Academy of Sciences of the United States of America*, vol. 95, no. 15, pp. 8841–8846, 1998.
- [65] A. Dalu, B. S. Blaydes, L. G. Lomax, and K. B. Delclos, "A comparison of the inflammatory response to a polydimethylsiloxane implant in male and female Balb/c mice," *Biomaterials*, vol. 21, no. 19, pp. 1947–1957, 2000.
- [66] T. Kato, H. Haro, H. Komori, and K. Shinomiya, "Sequential dynamics of matrix metalloproteinases, tumor necrosis factor- α , vascular endothelial growth factor and plasmin expressions in the resorption process of herniated disc," *The Spine Journal*, vol. 2, no. 5, article 106, 2002.
- [67] E. Middleton, C. Kandaswami, and T. C. Theoharides, "The effects of plant flavonoids on mammalian cells: implications for inflammation, heart disease, and cancer," *Pharmacological Reviews*, vol. 52, no. 4, pp. 673–751, 2000.
- [68] B. H. Havsteen, "The biochemistry and medical significance of the flavonoids," *Pharmacology and Therapeutics*, vol. 96, no. 2-3, pp. 67–202, 2002.
- [69] D. Chattopadhyay, G. Arunachalam, A. B. Mandal, and S. K. Bhattacharya, "Dose-dependent therapeutic anti-infectives from ethnomedicines of bay islands," *Chemotherapy*, vol. 52, no. 3, pp. 151–157, 2006.

Research Article

Ethanol Extract of *Dianthus chinensis* L. Induces Apoptosis in Human Hepatocellular Carcinoma HepG2 Cells *In Vitro*

Kyoung Jin Nho, Jin Mi Chun, and Ho Kyoung Kim

Center of Herbal Resources Research, Korea Institute of Oriental Medicine, Daejeon 305-811, Republic of Korea

Correspondence should be addressed to Ho Kyoung Kim, hkkim@kiom.re.kr

Received 16 November 2011; Accepted 20 February 2012

Academic Editor: William C. S. Cho

Copyright © 2012 Kyoung Jin Nho et al. This is an open access article distributed under the Creative Commons Attribution License, which permits unrestricted use, distribution, and reproduction in any medium, provided the original work is properly cited.

Dianthus chinensis L. is used to treat various diseases including cancer; however, the molecular mechanism by which the ethanol extract of *Dianthus chinensis* L. (EDCL) induces apoptosis is unknown. In this study, the apoptotic effects of EDCL were investigated in human HepG2 hepatocellular carcinoma cells. Treatment with EDCL significantly inhibited cell growth in a concentration- and time-dependent manner by inducing apoptosis. This induction was associated with chromatin condensation, activation of caspases, and cleavage of poly (ADP-ribose) polymerase protein. However, apoptosis induced by EDCL was attenuated by caspase inhibitor, indicating an important role for caspases in EDCL responses. Furthermore, EDCL did not alter the expression of bax in HepG2 cells but did selectively downregulate the expression of bcl-2 and bcl-xl, resulting in an increase in the ratio of bax:bcl-2 and bax:bcl-xl. These results support a mechanism whereby EDCL induces apoptosis through the mitochondrial pathway and caspase activation in HepG2 cells.

1. Introduction

Hepatocellular carcinoma (HCC) is the fifth most commonly diagnosed cancer, with more than 1 million deaths reported annually worldwide [1]. Exposure to aflatoxin B1 and infection with hepatitis B virus and hepatitis C virus are high-risk factors for HCC [2–4]. The high prevalence and high death rate require novel strategies for the prevention and treatment of hepatic cancer. Natural products with antitumor activity are a promising approach to cancer prevention.

Plants are valuable sources of bioactive compounds and are used for medicinal purposes in Asia including Korea. Recently, oriental medicine has been the focus of scientific discovery efforts into novel drugs including anticancer agents [5–9]. Several herb-based components and extracts have been reported to reduce tumor growth and inhibit metastasis in the human HCC HepG2 model *in vitro* and *in vivo* [10, 11].

Dianthus chinensis L. (Caryophyllaceae, Rainbow pink) is commonly known as “Pae-raeng-ee-kot” in Korea. In Korea, this herb is used as a folk remedy for the treatment of menostasis, gonorrhoea, cough, diuretic, and emmenagogue [12].

The chemical components of *Dianthus chinensis* L. are eugenol, phenylethylalcohol [13], melosides A and L [14] and dianthinosides A, B [15], C, and D [16]. Hypotensive, anthelmintic, intestinal peristaltic, antitumor, and antioxidant activity was documented [12, 13, 17, 18]. However, apoptosis induction by this herb was never reported. The ethnomedical information described above formed the basis for the present study, which was conducted to evaluate the cytotoxic activity and mechanism of action of the ethanol extract of *Dianthus chinensis* L. in HepG2 HCC cells.

2. Materials and Methods

2.1. Plant and Preparation of Extracts. *Dianthus chinensis* L. was purchased as a dried herb from OmniHerb Co. (Yeongcheon, Korea) and authenticated based on microscopic and macroscopic characteristics by the Classification and Identification Committee of the Korea Institute of Oriental Medicine (KIOM). The dried herb (30.26 g) was extracted twice with 70% ethanol (with 2 h reflux) and the extract was then concentrated under reduced pressure. The decoction was

filtered, lyophilized, and stored at 4°C. The yield of dried extract from starting crude material was approximately 18.57% (w/w). The lyophilized powder was dissolved in 10% dimethyl sulfoxide and then filtered through a 0.22 µm syringe filter to create a stock solution. EDCL denotes *Dianthus chinensis* L. ethanol extract. EDCL was diluted in culture medium to the final concentration indicated for each experiment.

2.2. Cell Culture. HepG2 human hepatocarcinoma cells were obtained from the American Type Culture Collection (Manassas, VA, USA). Cells were routinely maintained in Minimum Essential Medium with Earle's Balanced Salts and L-glutamine (MEM/EBSS, HyClone, Logan, UT, USA) supplemented with 10% fetal bovine serum (Gibco BRL, Gaithersburg, MD, USA), 100 U/mL penicillin (Gibco BRL), and 100 µg/mL streptomycin (Gibco BRL) at 37°C in a humidified atmosphere of 5% CO₂. The culture medium was replaced every 2 days.

2.3. Cell Viability Assay. Cells were seeded in 96-well culture plates at a density of 2×10^4 cells/well and allowed to adhere at 37°C for 12 h. The following day, several concentrations of EDCL were added and the cells were further incubated for 48 h. Then, cell viability was measured using the CCK-8 assay. 10 µL CCK-8 reagent was added to each well and incubated for 1 h at 37°C. Cell viability determination was based on the bioconversion of tetrazolium into formazan by intracellular dehydrogenase. Absorbance was measured at 450 nm using a Benchmark Plus Microplate Spectrophotometer (Bio-Rad, Hercules, CA, USA). Cytotoxicity was expressed as a percentage of the absorbance measured in control untreated cells.

2.4. Nuclear Staining with Hoechst 33342. Hoechst 33342 (Invitrogen, Eugene, Oregon, USA) staining was used to observe the apoptotic morphology of cells. Briefly, 5×10^5 cells/mL were seeded in six-well plates and incubated for 24 h. Then, the cells were exposed to different concentrations of EDCL (50–400 µg/mL) for 48 h. Next, the cells were collected and fixed with 3.7% formaldehyde in phosphate buffered saline (PBS) for 15 min and stained with Hoechst 33342 (10 µg/mL) at room temperature for 10 min. Finally, after the cells were washed with PBS, morphological changes, including a reduction in volume and nuclear chromatin condensation, were observed by fluorescence microscopy (Olympus Optical, Tokyo, Japan) and photographed at a 400x magnification.

2.5. Flow Cytometric Analysis for Measurement of Sub-G1 Phase. Cells were seeded in six-well plates at 1×10^6 cells/well and allowed to attach overnight. After exposure to EDCL, cells were collected, washed twice with ice-cold PBS buffer (pH 7.4), fixed with 80% ethanol at 4°C for 2 h, and then stained with PI/RNase Staining Buffer (BD Pharmingen, San Diego, CA, USA) for 20 min in the dark at room temperature. Apoptotic cell analysis was conducted on a FACS Calibur flow cytometer (BD Biosciences, San Jose, CA,

USA) and the data were analyzed using the CellQuest software.

2.6. Assay of Caspase-3/7, -8, and -9 Activity. Caspase activity was assayed using Caspase-Glo assay kits (Promega, Madison, WI, USA) according to manufacturer protocols. Briefly, cells were seeded at a density of 2×10^4 per well in triplicate wells onto 96-well plates and incubated for 24 h. Afterwards, the cells were exposed to several concentrations of EDCL (50–400 µg/mL) for 48 h or incubated with 180 µg/mL of EDCL for 6–48 h. After exposure to EDCL, culture supernatant (100 µL) was transferred into a white-walled 96-well plate. An equal volume of caspase substrate was added and samples were incubated at room temperature for 1 h. Culture medium was used as a blank control sample and luminescence was measured using an EnVision 2103 Multilabel Reader (PerkinElmer, Wellesley, MA, USA).

2.7. Protein Preparation and Western Blot Analysis. Cells were seeded in six-well plates at 1×10^6 cells/well and allowed to attach overnight. Afterwards, cells were exposed to different concentrations of EDCL for 48 h. Then, the cells were washed with ice-cold PBS twice and lysed with 1X RIPA lysis buffer (50 mM Tris-HCl, pH 8.0, 150 mM NaCl, 1% NP-40, 0.5% sodium deoxycholate, 0.1% SDS and 1 mM Protease Inhibitor Cocktail) for 30 min on ice. Lysates were cleared by centrifugation and supernatants were collected. The total protein content was quantified using the Bradford method. Proteins (30 µg) were mixed with 2X sample buffer, incubated at 95°C for 5 min, and loaded onto 12% polyacrylamide gels. Electrophoresis was performed using the Mini Protean 3 Cell (Bio-Rad). Proteins separated on the gels were transferred onto nitrocellulose membranes (Schueicher & Schell BioScience, Dassel, Germany). Membranes were blocked for 2 h using blocking buffer (10 mM Tris-HCl, pH 7.5, 150 mM NaCl, 0.1% Tween 20, 3% nonfat dry milk) and incubated at 4°C overnight with primary antibody (all antibodies were purchased from Cell Signaling Technology, Beverly, MA, USA). After washing with blocking buffer three times for 30 min, membranes were probed with horseradish peroxidase-conjugated goat anti-mouse immunoglobulin G (IgG) and anti-rabbit IgG (Cell Signaling Technology) for 2 h. The membranes were washed for 1 h (during which the wash buffer was changed three times) with Tris-buffered saline Tween 20 solution and developed with ECL Advance Western Blotting Detection Kit (GE Healthcare, Little Chalfont, Buckinghamshire, UK) using a LAS-3000 luminescent image analyzer (Fuji Photo Film Co. Ltd., Kanagawa, Japan). Western blot signals were quantified and normalized to β-actin by densitometry analysis using the Multi-Gauge program of the LAS-3000 imaging system.

2.8. Statistical Analysis. Mean data values are presented with their deviation (mean ± SD) from three independent measurements. Statistical analyses were performed according to Prism 5 program (GraphPad, San Diego, USA). Analysis of variance (ANOVA) was followed by Dunnett's test. A value of $P < 0.05$ was considered to be statistically significant.

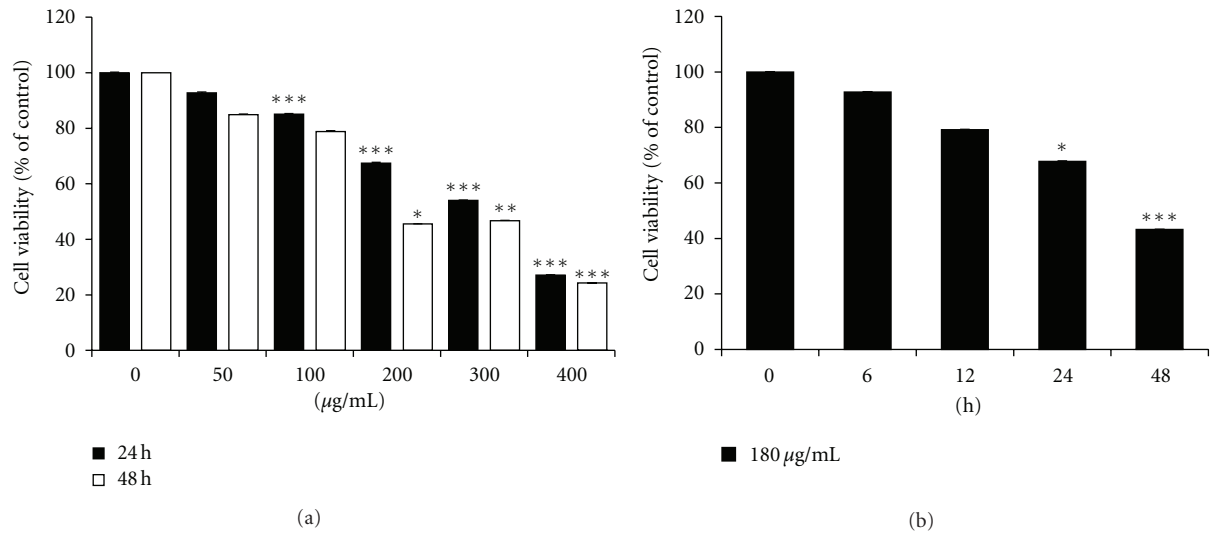


FIGURE 1: Exposure to EDCL induces growth inhibition in HepG2 cells. (a) Concentration response. Cells were incubated in the presence or absence of several concentrations of EDCL for 24 and 48 h. (b) Time course. Cells were exposed to 180 $\mu\text{g/mL}$ EDCL over time (6–48 h). Cell viability was assessed by CCK-8 assay. The data are expressed as the means \pm SD of triplicate samples. * $P < 0.05$, ** $P < 0.01$, and *** $P < 0.001$ versus untreated EDCL.

3. Results

3.1. Effect of EDCL on HepG2 Cell Growth. The effect of EDCL on HepG2 cell growth was assessed using the CCK-8 assay. Figure 1 shows inhibition of HepG2 cell viability by several concentrations (50–400 $\mu\text{g/mL}$) of EDCL and over time (6–48 h). The results show concentration- and time-dependent inhibition, with IC_{50} values ranging from 314.98 $\mu\text{g/mL}$ (24 h) to 186.64 $\mu\text{g/mL}$ (48 h) (Figure 1).

3.2. Effect of EDCL on HepG2 Cell Apoptosis. To investigate the effect of EDCL on the morphology of apoptotic cells, Hoechst 33342 staining was conducted. Very few apoptotic cells were observed in the control culture, while the percentage of apoptotic cells in the presence of EDCL increased in an EDCL concentration-dependent manner (Figure 2(a)). The amount of sub-G1 DNA was analyzed to quantify the number of dead cells, since dead cells have a lower DNA content than cells in the G1 phase. Flow cytometric analysis indicated that exposure to EDCL markedly increased the number of sub-G1 phase cells in a concentration- and time-dependent manner (Figures 2(b) and 2(c)).

3.3. Effect of EDCL on the Apoptotic Mitochondrial Pathway. The expression level of Bcl-2 family members interacting directly with mitochondria was studied. Western blotting (Figure 3(a)) revealed that the translational levels of bax expression, a proapoptotic protein, remained virtually unchanged in response to EDCL, whereas bcl-2, bcl-xl, and mcl-1, which are antiapoptotic proteins, were inhibited by exposure to EDCL. These data show that EDCL alters the bax:bcl-2 and bax:bcl-xl ratios in HepG2 cells in a concentration-dependent manner. Since proteins from the IAP family bind to caspases, leading to caspase inactivation in eukaryotic

cells, the involvement of the IAP family in EDCL-induced apoptosis was further examined. The results indicated that the levels of IAP family members, such as cellular inhibitor-of-apoptosis protein (cIAP)-1, cIAP-2, and X-linked inhibitor of apoptosis protein (XIAP), were downregulated in HepG2 cells exposed to EDCL in a concentration-dependent manner (Figure 3(b)).

3.4. Effect of EDCL on Caspase Activity. To investigate the apoptotic cascade induced by EDCL, HepG2 cells were exposed to several concentrations of EDCL (50–400 $\mu\text{g/mL}$) for 48 h or incubated with 180 $\mu\text{g/mL}$ of EDCL for 6–48 h, after which caspase-3/7, -8, and -9 activity was measured. The level of caspase activation in HepG2 cells exposed to EDCL was compared to that of control untreated cells arbitrarily set to 1.0. Results showed that EDCL markedly increased caspase-3/7, -8, and -9 activity, with maximum increase activity at 200 $\mu\text{g/mL}$. Results also showed that caspase activity increased over time in response to 180 $\mu\text{g/mL}$ EDCL (Figures 4(a) and 4(b)). At the concentration of 200 $\mu\text{g/mL}$, the activity of caspase-3/7, caspase-8, and caspase-9 increased by 16.16-, 7.80-, and 14.17-fold, respectively. Furthermore, EDCL induced the degradation of poly (ADP-ribose) polymerase (PARP, 116 kDa), which is a protein substrate of caspase-3, and PARP cleavage fragments (89 kDa) increased over time (Figure 4(c)).

3.5. Effect of Caspase Inhibitor on EDCL-Induced Apoptosis in HepG2 Cells. To confirm that caspase activation is a key step in EDCL-induced apoptosis, HepG2 cells were pretreated with z-vad-fmk (80 μM), a broad-spectrum caspase inhibitor, for 1 h, and then subsequently exposed to 180 $\mu\text{g/mL}$ EDCL for 48 h. As shown in Figure 5(a), z-vad-fmk did not affect cell viability but inhibited the antiproliferative activity

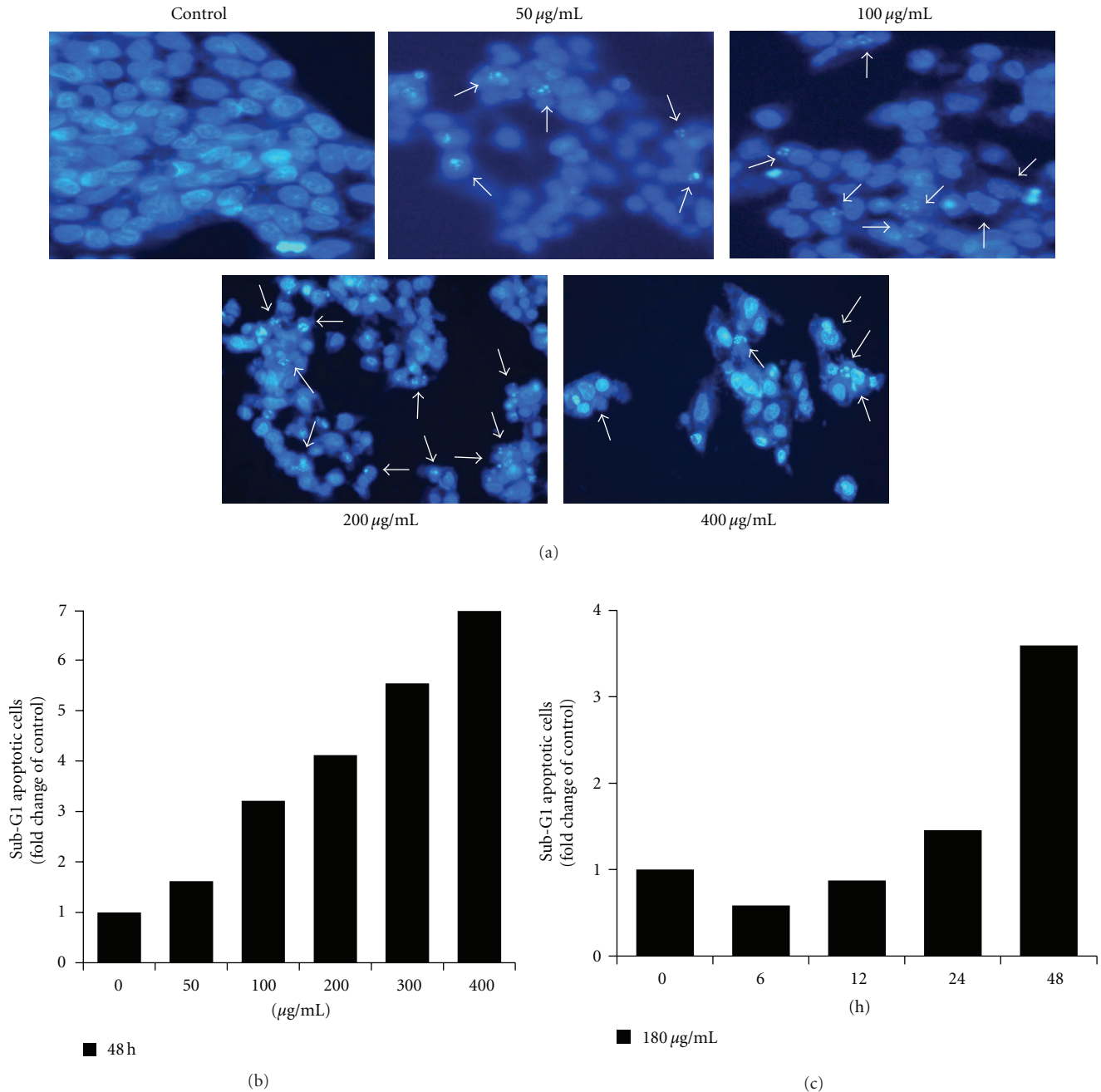


FIGURE 2: Exposure to EDCL induces apoptosis in HepG2 cells. (a) Cells were incubated in the presence or absence of several concentrations of EDCL for 48 h. Hoechst stain showed EDCL-induced chromatin condensation (arrow). Magnification, $\times 400$. (b) Cells were exposed to several concentrations of EDCL for 48 h or (c) exposed to EDCL (180 $\mu\text{g}/\text{mL}$) over time. Apoptosis was measured using PI staining and flow cytometry.

of EDCL. EDCL strongly stimulated caspase protease activity and pretreating cells with z-vad-vmk nearly abolished EDCL-induced caspase activity (Figure 5(b)). Furthermore, blockade of caspase activity by z-vad-vmk prevented EDCL-induced chromatin condensation (Figure 5(c)), PARP degradation (Figure 5(d)), and increase in sub-G1 population (Figure 5(e)). These results clearly show that EDCL-induced apoptosis is associated with caspase activation.

4. Discussion

During the last decade, a considerable amount of research has focused on cancer cell apoptosis. Apoptosis, or programmed cell death, is the major control mechanism by which cells die if DNA damage is not repaired [19]. Apoptosis is also a critical protective mechanism against carcinogenesis, eliminating damaged cells or cells proliferating abnormally in response to carcinogens [20]. Therefore, induction of

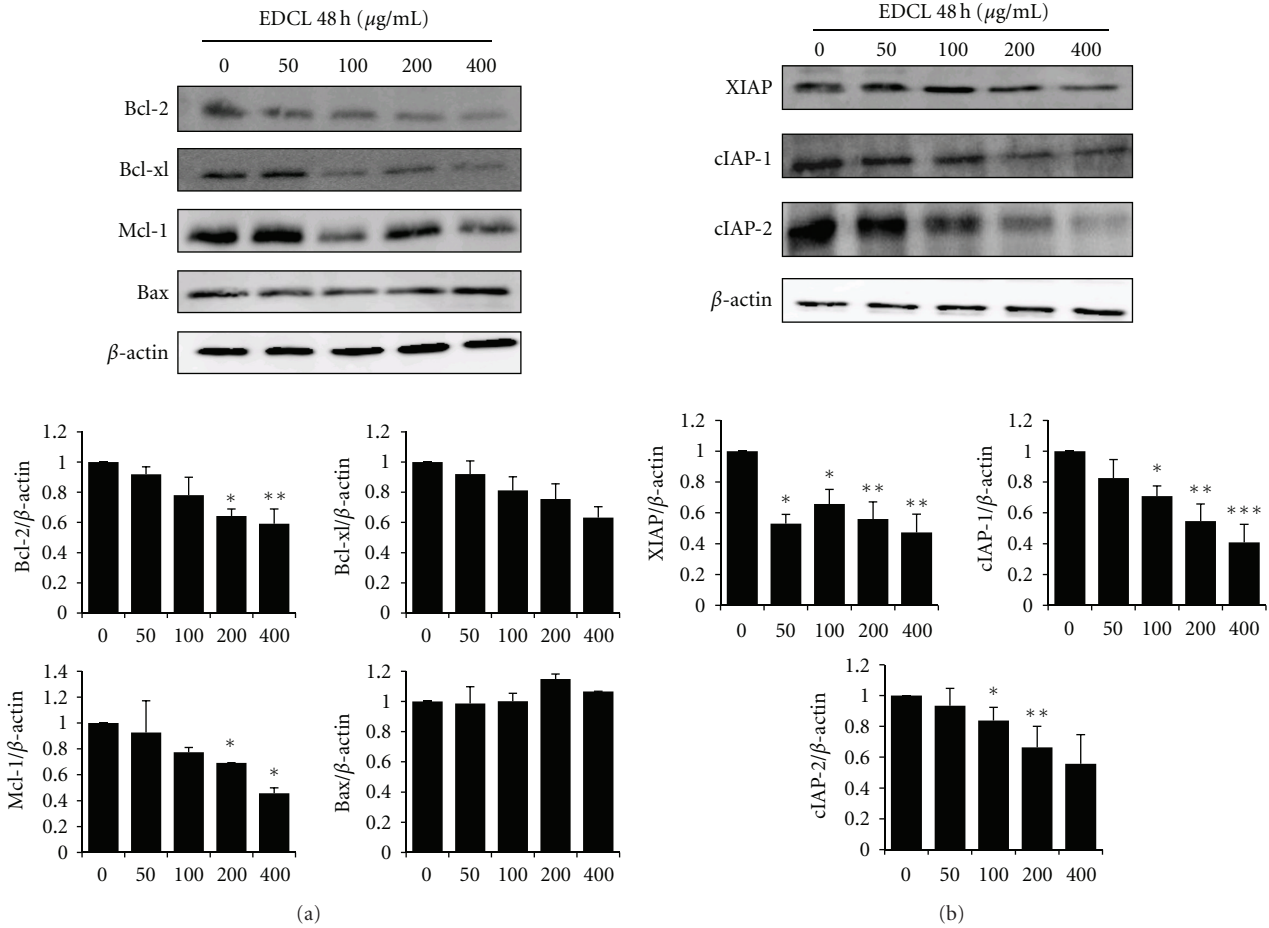


FIGURE 3: Exposure to EDCL downregulates the expression of Bcl-2 and IAP family members in HepG2 cells. Cells were exposed to several concentrations of EDCL for 48 h. Protein levels were monitored by Western blot analysis. Western blot signals were quantified and normalized to β -actin. Values are expressed as means \pm SD. * $P < 0.05$, ** $P < 0.01$, and *** $P < 0.001$ versus untreated EDCL.

apoptotic cell death is a promising emerging strategy for the prevention and treatment of cancer [21]. The results of the present study clearly demonstrate that EDCL suppressed HepG2 cell viability by inducing apoptosis. After exposure to EDCL, chromatin condensation and apoptotic bodies were clearly observed. These results suggest that HepG2 cells exposed to EDCL undergo typical apoptosis. Furthermore, flow cytometric analysis after propidium iodide staining confirmed EDCL-induced apoptosis in HepG2 cells.

Members of the Bcl-2 family of proteins, such as bcl-2, bcl-xl, mcl-1, and bax, are the most prominent actors in controlling the release of cytochrome c and in mitochondria-mediated apoptosis [22]. Thus, it has been suggested that the ratio between the level of proapoptotic bax protein and the level of antiapoptotic bcl-2 protein determines whether a cell responds to an apoptotic signal [23]. In this study, EDCL did not alter the expression of bax in HepG2 cells but did selectively downregulate the expression of bcl-2 and bcl-xl, resulting in an increase in the ratio of bax:bcl-2 and bax:bcl-xl.

The execution of cellular demolition in apoptosis is also carried out by caspases [24]. The caspase family of proteins is one of the main executors of the apoptotic process. Caspases belong to a group of enzymes known as cysteine proteases and exist within the cell as inactive proforms or zymogens. These zymogens can be cleaved to form active enzymes following the induction of apoptosis. The IAP family of proteins blocks apoptosis by directly inhibiting at least two members of the caspase family of cell death proteases, caspase-3, and caspase-7. XIAP, cIAP-1, and cIAP-2 can prevent the proteolytic processing of procaspase-3, -6, and -7 by blocking the cytochrome c-induced activation of procaspase-9 [24, 25]. Studies have shown that exposure of HepG2 cells to EDCL caused proteolytic activation of caspases and down-regulation of XIAP, cIAP-1 and cIAP-2. The enzyme poly(ADP-ribose) polymerase, or PARP, was one of the first proteins identified as a substrate for caspases. PARP is involved in repair of DNA damage and functions by catalyzing the synthesis of poly (ADP-ribose) and by binding to DNA strand breaks and modifying nuclear proteins. PARP helps cells

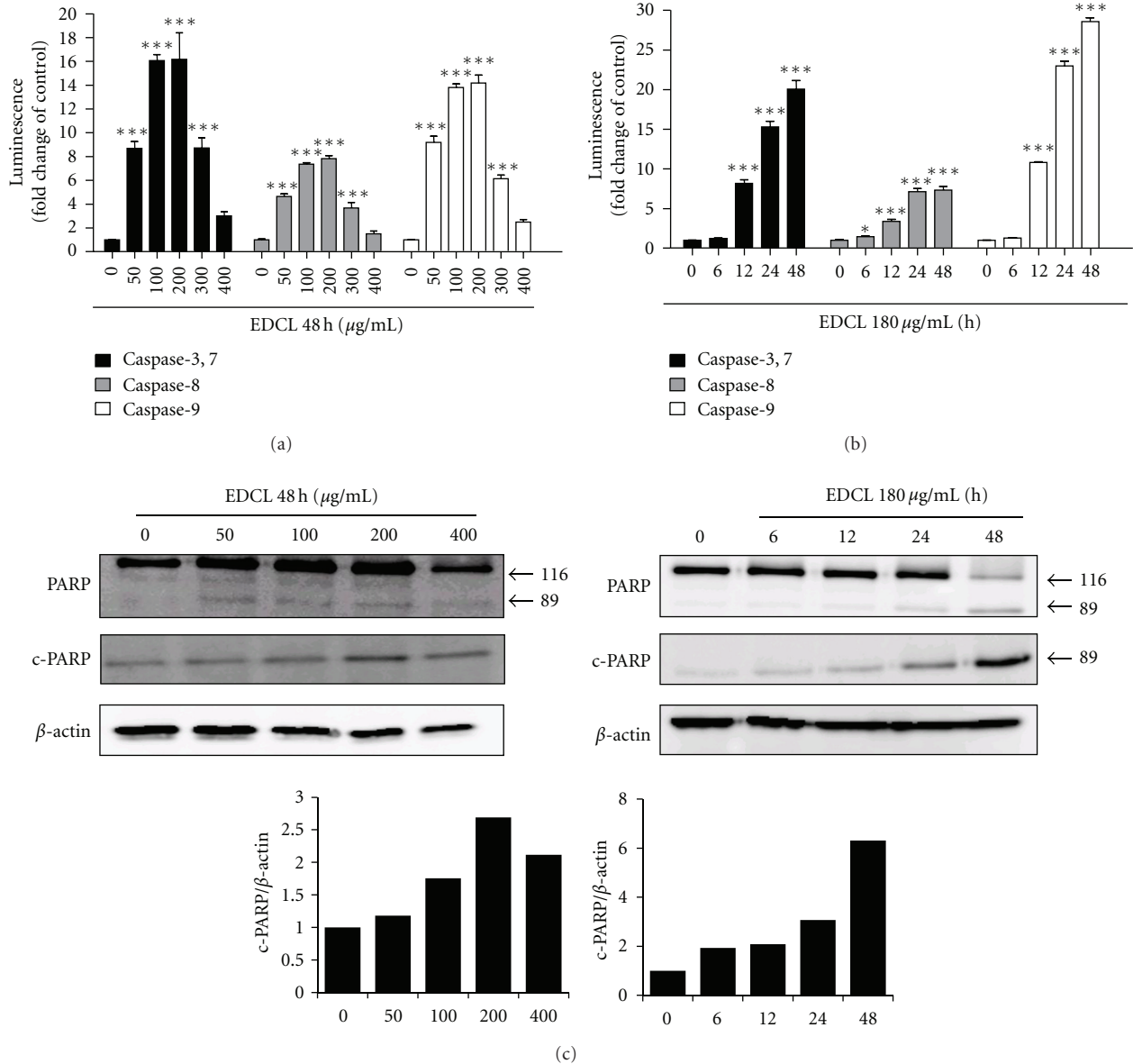


FIGURE 4: Exposure to EDCL shows activation of caspases and degradation of PARP protein in HepG2 cells. (a) Concentration response. Cells were incubated in the presence or absence of several concentrations of EDCL for 48 h. (b) Time course. Cells were incubated in the presence or absence of 180 $\mu\text{g/mL}$ EDCL for different lengths of time. Upon completion of each exposure time, caspase activity was assessed using a Caspase-Glo assay kits assay, as described in Section 2. The data are expressed as the means \pm SD of triplicate samples. $*P < 0.05$ and $***P < 0.001$ versus untreated EDCL. (c) Cells were subjected to Western blot analysis using anti-PARP and anti-c-PARP antibodies. Western blot signals were quantified and normalized to β -actin.

maintain viability, and the cleavage of PARP facilitates cellular disassembly and serves as a marker for cells undergoing apoptosis [26, 27]. In the present study, we examined whether the PARP protein, a substrate of caspase-3 [28], was cleaved in cells exposed to EDCL. As expected, PARP was clearly degraded in a concentration- and time-dependent manner that correlated with caspase activation. Under the same experimental conditions, z-vad-fmk prevented EDCL-induced apoptosis by blocking caspase activation. These data

indicate that caspases are the key molecules mediating EDCL-induced apoptosis in HepG2 cells.

In conclusion, this study clearly demonstrates that EDCL strongly inhibits cell proliferation and induces apoptosis in HepG2 cells. EDCL induced apoptosis through the mitochondrial pathway, involving the activation of caspase-3/7, -8, and -9, the down-regulation of antiapoptotic proteins, and the degradation of PARP protein. Because induction of apoptosis is thought to be a suitable anticancer

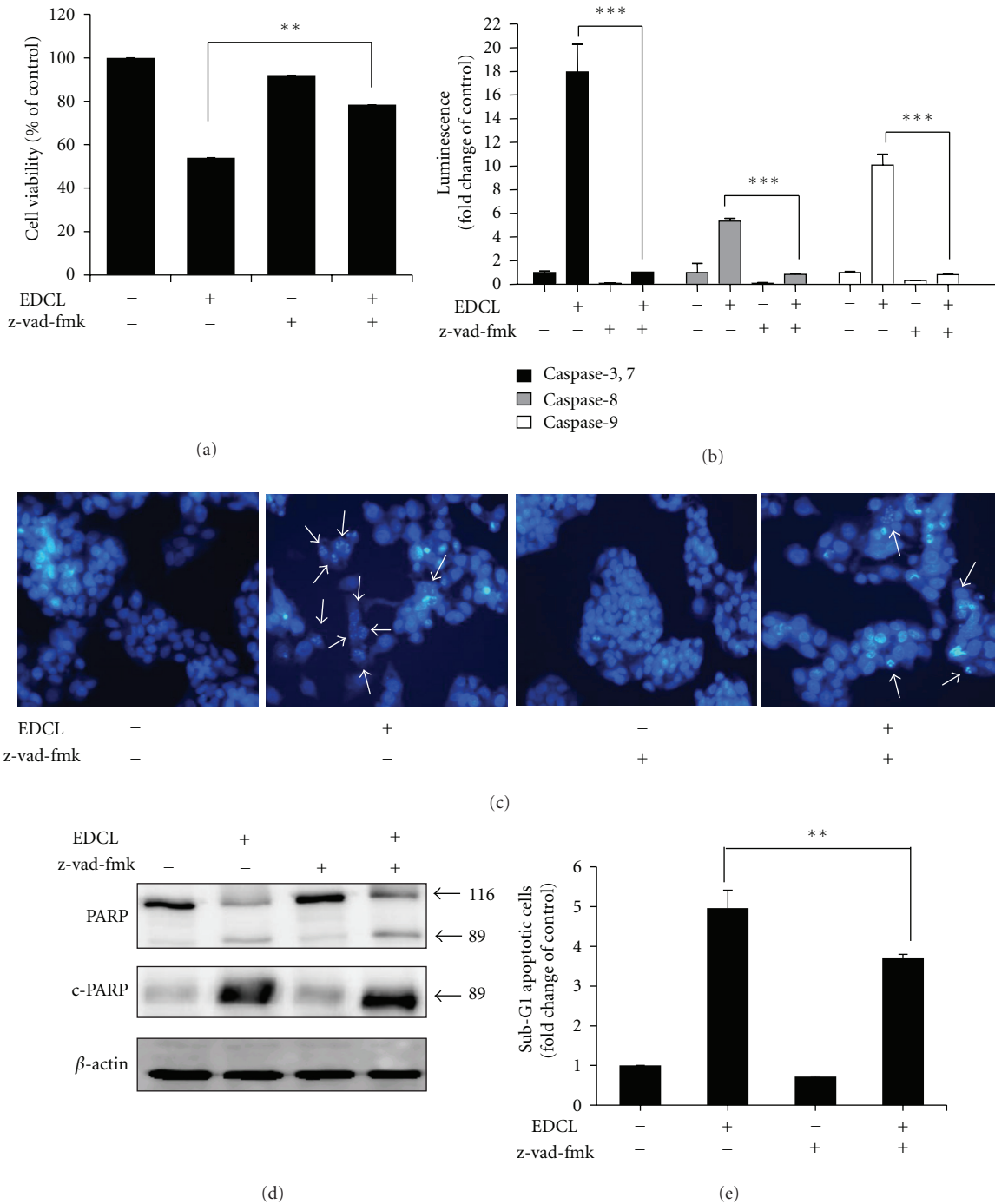


FIGURE 5: Caspase inhibition prevents EDCL-induced apoptosis in HepG2 cells. Cells were incubated in the presence or absence of z-vad-fmk for 1 h before being exposed to EDCL (180 μ g/mL). (a) After 48 h of incubation with EDCL, cell viability was assessed using the CCK-8 assay and (b) caspase activity was measured. (c) Hoechst staining shows EDCL-induced chromatin condensation (arrow). Magnification, \times 400. (d) Cells were subjected to Western blot analysis using anti-PARP and anti-c-PARP antibodies. (e) Cells were evaluated for sub-G1 DNA content by flow cytometry. The data are expressed as the means \pm SD of triplicate samples. * P < 0.05, ** P < 0.01, and *** P < 0.001 versus EDCL+z-vad-fmk.

therapeutic mechanism, these results confirm the potential of EDCL as a chemotherapeutic agent in human hepatocellular carcinoma cells. *In vivo* studies are needed to fully establish the potential of EDCL as a chemopreventive and therapeutic agent in cancer.

Conflict of Interests

The authors have no conflict of interests to declare.

Acknowledgments

This work was supported by the project "Construction of the Basis for Practical Application of Herbal Resources" funded by the Ministry of Education, Science and Technology (MEST) of Korea to the Korea Institute of Oriental Medicine (KIOM). We thank the KIOM Classification and Identification Committee for critical authentication of plants and helpful discussions.

References

- [1] A. Jemal, T. Murray, E. Ward et al., "Cancer statistics, 2005," *Ca-A Cancer Journal for Clinicians*, vol. 55, no. 1, pp. 10–30, 2005.
- [2] K. Okuda, "Hepatocellular carcinoma: recent progress," *Hepatology*, vol. 15, no. 5, pp. 948–963, 1992.
- [3] T. K. Seow, R. C. M. Y. Liang, C. K. Leow, and M. C. M. Chung, "Hepatocellular carcinoma: from bedside to proteomics," *Proteomics*, vol. 1, no. 10, pp. 1249–1263, 2001.
- [4] M. A. Kern, K. Breuhahn, and P. Schirmacher, "Molecular pathogenesis of human hepatocellular carcinoma," *Advances in Cancer Research*, vol. 86, pp. 67–112, 2002.
- [5] H. Hu, N. S. Ahn, X. Yang, Y. S. Lee, and K. S. Kang, "Ganoderma lucidum extract induces cell cycle arrest and apoptosis in MCF-7 human breast cancer cell," *International Journal of Cancer*, vol. 102, no. 3, pp. 250–253, 2002.
- [6] S. M. Y. Lee, M. L. Y. Li, Y. C. Tse et al., "Paeoniae Radix, a Chinese herbal extract, inhibit hepatoma cells growth by inducing apoptosis in a p53 independent pathway," *Life Sciences*, vol. 71, no. 19, pp. 2267–2277, 2002.
- [7] Y. L. Cheng, S. C. Lee, S. Z. Lin et al., "Anti-proliferative activity of *Bupleurum scrozonifolium* in A549 human lung cancer cells in vitro and in vivo," *Cancer Letters*, vol. 222, no. 2, pp. 183–193, 2005.
- [8] D. I. Park, J. H. Lee, S. K. Moon et al., "Induction of apoptosis and inhibition of telomerase activity by aqueous extract from *Platycodon grandiflorum* in human lung carcinoma cells," *Pharmacological Research*, vol. 51, no. 5, pp. 437–443, 2005.
- [9] M. L. Tan, S. F. Sulaiman, N. Najimuddin, M. R. Samian, and T. S. T. Muhammad, "Methanolic extract of *Pereskia bleo* (Kunth) DC. (Cactaceae) induces apoptosis in breast carcinoma, T47-D cell line," *Journal of Ethnopharmacology*, vol. 96, no. 1–2, pp. 287–294, 2005.
- [10] T. W. Chung, S. K. Moon, Y. C. Chang et al., "Novel and therapeutic effect of caffeic acid and caffeic acid phenyl ester on hepatocarcinoma cells: complete regression of hepatoma growth and metastasis by dual mechanism," *The FASEB Journal*, vol. 18, no. 14, pp. 1670–1681, 2004.
- [11] C. S. F. Cheung, K. K. W. Chung, J. C. K. Lui et al., "Leachianone A as a potential anti-cancer drug by induction of apoptosis in human hepatoma HepG2 cells," *Cancer Letters*, vol. 253, no. 2, pp. 224–235, 2007.
- [12] WHO, *Medicinal plants in the Republic of Korea*, World Health Organization, Regional Office for Western Pacific, Manila, Philippines, 1998.
- [13] H. Y. Hsu, Y. P. Chen, C. S. Shen, C. C. Hsu, and H. C. Chang, *Oriental Materia Medica*, Oriental Healing Arts Institute, Long Beach, Calif, USA, 1986.
- [14] B. Monties, M. L. Bouillant, and J. Chopin, "C-diholoylflavones dans les feuilles du melon (*Cucumis melo*)," *Phytochemistry*, vol. 15, no. 6, pp. 1053–1056, 1976.
- [15] H. Y. Li, K. Koike, T. Ohmoto, and K. Ikeda, "Dianchinonides A and B, two new saponins from *Dianthus chinensis*," *Journal of Natural Products*, vol. 56, no. 7, pp. 1065–1070, 1993.
- [16] Li Hong Yu, K. Koike, and T. Ohmoto, "Triterpenoid saponins from *Dianthus chinensis*," *Phytochemistry*, vol. 35, no. 3, pp. 751–756, 1994.
- [17] T. Kosuge, M. Yokota, and K. Sugiyama, "Studies on antitumor activities and antitumor principles of Chinese herbs. I. Antitumor activities of Chinese herbs," *Yakugaku Zasshi*, vol. 105, no. 8, pp. 791–795, 1985.
- [18] S. Y. Kim, J. H. Kim, S. K. Kim, M. J. Oh, and M. Y. Jung, "Antioxidant activities of selected oriental herb extracts," *Journal of the American Oil Chemists' Society*, vol. 71, no. 6, pp. 633–640, 1994.
- [19] S. W. Lowe and A. W. Lin, "Apoptosis in cancer," *Carcinogenesis*, vol. 21, no. 3, pp. 485–495, 2000.
- [20] M. Schuchmann and P. R. Galle, "Sensitizing to apoptosis—sharpening the medical sword," *Journal of Hepatology*, vol. 40, no. 2, pp. 335–336, 2004.
- [21] W. Hu and J. J. Kavanagh, "Anticancer therapy targeting the apoptotic pathway," *Lancet Oncology*, vol. 4, no. 12, pp. 721–729, 2003.
- [22] C. Borner, "The Bcl-2 protein family: sensors and checkpoints for life-or-death decisions," *Molecular Immunology*, vol. 39, no. 11, pp. 615–647, 2003.
- [23] G. S. Salomons, H. J. M. Brady, M. Verwijs-Janssen et al., "The bax:Bcl-2 ratio modulates the response to dexamethasone in leukaemic cells and is highly variable in childhood acute leukemia," *International Journal of Cancer*, vol. 71, no. 6, pp. 959–965, 1997.
- [24] Q. L. Deveraux, E. Leo, H. R. Stennicke, K. Welsh, G. S. Salvesen, and J. C. Reed, "Cleavage of human inhibitor of apoptosis protein XIAP results in fragments with distinct specificities for caspases," *EMBO Journal*, vol. 18, no. 19, pp. 5242–5251, 1999.
- [25] N. Roy, Q. L. Deveraux, R. Takahashi, G. S. Salvesen, and J. C. Reed, "The c-IAP-1 and c-IAP-2 proteins are direct inhibitors of specific caspases," *EMBO Journal*, vol. 16, no. 23, pp. 6914–6925, 1997.
- [26] P. R. Walker and M. Sikorska, "New aspects of the mechanism of DNA fragmentation in apoptosis," *Biochemistry and Cell Biology*, vol. 75, no. 4, pp. 287–299, 1997.
- [27] F. J. Oliver, G. De La Rubia, V. Rolli, M. C. Ruiz-Ruiz, G. De Murcia, and J. Ménissier-De Murcia, "Importance of poly (ADP-ribose) polymerase and its cleavage in apoptosis: lesson from an uncleavable mutant," *Journal of Biological Chemistry*, vol. 273, no. 50, pp. 33533–33539, 1998.
- [28] M. Tewari, L. T. Quan, K. O'Rourke et al., "Yama/ CPP32 β , a mammalian homolog of CED-3, is a CrmA-inhibitable protease that cleaves the death substrate poly(ADP-ribose) polymerase," *Cell*, vol. 81, no. 5, pp. 801–809, 1995.

Research Article

***Ecklonia cava* Inhibits Glucose Absorption and Stimulates Insulin Secretion in Streptozotocin-Induced Diabetic Mice**

Hye Kyung Kim

Department of Food and Biotechnology, Hanseo University, Seosan 356-706, Republic of Korea

Correspondence should be addressed to Hye Kyung Kim, hkkim111@dreamwiz.com

Received 29 December 2011; Accepted 20 February 2012

Academic Editor: Mohamed Eddouks

Copyright © 2012 Hye Kyung Kim. This is an open access article distributed under the Creative Commons Attribution License, which permits unrestricted use, distribution, and reproduction in any medium, provided the original work is properly cited.

Aims of study. Present study investigated the effect of *Ecklonia cava* (EC) on intestinal glucose uptake and insulin secretion. *Materials and methods.* Intestinal Na⁺-dependent glucose uptake (SGU) and Na⁺-dependent glucose transporter 1 (SGLT1) protein expression was determined using brush border membrane vesicles (BBMVs). Glucose-induced insulin secretion was examined in pancreatic β -islet cells. The antihyperglycemic effects of EC, SGU, and SGLT1 expression were determined in streptozotocin (STZ)-induced diabetic mice. *Results.* Methanol extract of EC markedly inhibited intestinal SGU of BBMV with the IC₅₀ value of 345 μ g/mL. SGLT1 protein expression was dose dependently down regulated with EC treatment. Furthermore, insulintrophic effect of EC extract was observed at high glucose media in isolated pancreatic β -islet cells *in vitro*. We next conducted the antihyperglycemic effect of EC in STZ-diabetic mice. EC supplementation markedly suppressed SGU and SGLT1 abundance in BBMV from STZ mice. Furthermore, plasma insulin level was increased by EC treatment in diabetic mice. As a result, EC supplementation improved postprandial glucose regulation, assessed by oral glucose tolerance test, in diabetic mice. *Conclusion.* These results suggest that EC play a role in controlling dietary glucose absorption at the intestine and insulintrophic action at the pancreas contributing blood glucose homeostasis in diabetic condition.

1. Introduction

Diabetes is one of the most prevalent and serious metabolic diseases worldwide. It is characterized by chronic hyperglycemia, impairment of insulin secretion from pancreatic β -cells, and insulin resistance in peripheral tissues. One of the therapeutic approaches for decreasing postprandial hyperglycemia is to retard the absorption of glucose by inhibition of carbohydrate-hydrolyzing enzymes such as α -amylase and α -glucosidase. However, they are not able to prevent glucose absorption when glucose itself has been ingested. Hence, the direct inhibition of intestinal glucose absorption could represent a novel mechanism for an antidiabetic drug.

Intestinal glucose absorption is thought to be regulated by the Na⁺-dependent glucose transporter 1 (SGLT1) at the apical membrane of the intestinal epithelia [1]. It has been shown in diabetic animals and humans that the capacity of the small intestine to absorb glucose increases at the brush border membrane vesicles (BBMVs) due to the enhanced activity and abundance of SGLT1 [2, 3].

In order to prevent or delay the progression of diabetes, insulin should be sufficiently secreted to compensate for insulin resistance in peripheral tissues. Thus, one of the mechanisms for the antidiabetic agents requires the characteristics of insulintrophic action from pancreatic cells [4].

Marine algae have been identified as rich sources of structurally diverse bioactive compounds with great pharmaceutical and biomedical potential. The brown algae, *Ecklonia cava* (EC), are abundant in the south-west coastal region of Japan and Korea. It has been reported that EC extract has numerous biological activities including antioxidative, radical scavenging, immunomodulatory, and antimutagenic activities [5–8]. Recently, Lee et al. demonstrated that polyphenol isolated from EC inhibit α -amylase and α -glucosidase activities and alleviate postprandial hyperglycemia in streptozotocin (STZ-) induced diabetic mice [9]. However, the effect of EC on intestinal glucose uptake or insulintrophic action has not been examined. In this study, we investigated the effects of EC on intestinal Na⁺-dependent glucose uptake, SGLT1 protein expression, and insulin secretion in pancreatic islets.

Furthermore, the antihyperglycemic effects of EC in STZ-induced diabetic mice were also evaluated.

2. Materials and Methods

2.1. Preparation of EC Powder and Extract. EC was obtained from a local market in Seosan, Republic of Korea. Fresh EC was washed, dried, and ground into powder. The EC powder was used for the *in vivo* experiment, and EC extract was used for the *in vitro* experiment. The dried powder was extracted three times with ten volumes of methanol at room temperature for 24 hour. The combined extracts were centrifuged, filtered, concentrated under vacuum, lyophilized, concentrated to 1 mg/mL with deionized water, and subsequently used for the experiment.

2.2. BBMV Isolation. BBMVs were prepared using a previously described method with some modification [10]. All subsequent isolation steps were performed at 4°C. Male ICR mice (8-week old, Joongang Lab Animal Co., Korea) jejunal mucosal scrapings were suspended in 10 mM HEPES/Tris buffer (pH 7.5), containing 300 mM mannitol and 300 mM MgCl₂, and homogenized in a glass-Teflon homogenizer (Glass-Col, Terre Haute, IN, USA) for 2 min at 3,000 rpm. The mixture was stirred for 2 min and centrifuged at 15,000 rpm for 15 min at 4°C. The supernatant was centrifuged at 30,000 rpm for 45 min. The resulting pellets were resuspended in 10 mM HEPES/Tris buffer containing 300 mM mannitol (pH 7.5) to a final protein concentration of 10 mg/mL and stored in liquid nitrogen until use. The degree of purity in BBMV was routinely assessed by the enrichment of alkaline phosphatase (ALP) in the finally prepared BBMV compared to the homogenate of intestinal scrapings. ALP activity was determined with ALP assay kit (Yeongdong Pharmaceutical Co., Seoul, Korea). The specific ALP activities of mucosal homogenate and BBMV suspension were 1.21 ± 0.09 and 6.21 ± 0.48 units/mg protein, respectively, exhibiting 5-fold enrichment in final BBMV fraction. The amount of protein in the BBMV was measured by the Bradford method [11].

2.3. Na⁺-Dependent Glucose Uptake. Measurement of Na⁺-dependent glucose uptake by BBMV was determined by incubating 150 μ L BBMV suspension with 850 μ L uptake buffer containing 100 μ M 2-NBDG (Molecular Probes, Grand Island, NY, USA) and EC extract (0.1 mg/mL) at 37°C for 15 min in a shaking water bath. The uptake reaction was stopped by centrifuging for 20 min at 15,000 rpm, and the BBMV pellet was washed with stop buffer. The uptake and stop buffers were 10 mM HEPES/Tris (pH 7.5) containing 150 mM NaCl and 300 μ M phlorizin (Sigma Co., St. Louis, USA), respectively. Glucose uptake was measured by detecting fluorescence intensity of 2-NBDG with a spectrofluorometer (excitation: 485 nm, emission: 535 nm). The difference between the glucose uptakes in the presence of Na⁺ and phlorizin represents the Na⁺-dependent glucose uptake by SGLT1.

2.4. SGLT1 Expression. Glutaraldehyde was added to Immune well plate and incubated at 37°C for 1 hour. After washing the plate, an antigen of diluted BBMV membrane protein (100 μ L/well) and EC were added and incubated at 37°C for 2 hours. After washing the plate, the coated plates were blocked with blocking solution (0.5% casein) at 37°C for 1 hour. Primary antibody incubation was conducted with 100 μ L of the SGLT1 polyclonal antibody (Chemicon International Inc., Temecula, CA, USA; diluted 1 : 1000 in 0.5% casein) at 37°C for 2 hour. Secondary antibody incubation was conducted with 100 μ L of the anti-rabbit IgG conjugated to horseradish peroxidase (diluted 1 : 2000 in 0.5% casein) at 37°C for 1 hour. For substrate incubation, 200 μ L of substrate solution (TMB 10 mg/L DMSO, 3% H₂O₂, 50 mM sodium acetate buffer, pH 5.1) was added to each well and reacted for 15 min. The enzymatic reaction was stopped by adding 50 μ L of 1 M H₂SO₄ to each well. The absorbance was determined at 450 nm using automated microplate reader (Model 550, BIO-RAD Laboratories, Philadelphia, PA, USA).

2.5. Insulin Secretion. Pancreatic islet cells were isolated from male mice by collagenase digestion [12]. Twenty islets were preincubated in Krebs-Ringer the bicarbonate (KRB) buffer, pH 7.4, supplemented with serum albumin (3 mg/mL) and glucose (3 mM) for 30 min at 37°C under humidified atmosphere of 5% CO₂. The islets were treated with EC extract (50 μ g/mL) in 3, 8, and 16 mM glucose KRB buffer for 60 min at 37°C. Insulin concentration in each medium was determined using an ELISA procedure (Boehringer Mannheim Diagnostics, Germany).

2.6. Animal Study. Male ICR mice (8-week old) were housed in plastic cages under temperature- (24 \pm 2°C) and light- (12-hour light/dark cycle) controlled conditions with constant humidity (55 \pm 5%). The study has been carried out along the Korea National Institutes of Health Guidelines on the care and use of laboratory animals and approved by Hanseo University. The mice were randomly divided into four groups ($n = 10$); normal control (NC), normal mice fed EC powder (NE), diabetic control (DC), and diabetic mice fed EC powder (DE). Normal and diabetic control mice were fed AIN-93-based semipurified standard diet, and experimental groups were supplemented with EC powder (3%, w/w). Diabetes was induced by a single intraperitoneal injection of STZ (Sigma, St. Louis, USA; 95 mg/kg in citrate buffer, pH 4.5). NC group received the buffer only. Tail bleeds were performed 24 hour after injection, and animals with blood glucose concentrations above 300 mg/dL were considered to be diabetic and used in this study.

2.7. Oral Glucose Tolerance Test and Intestinal BBMV Glucose Uptake. At the end of 4 weeks of experimental period, mice were fasted overnight and administered with glucose (1.5 g/kg). Blood samples were collected from the tail at various time points (0~90 min) after glucose loading, and blood glucose levels were measured by one-touch basic glucose measurement system (Lifescan Inc., Milpitas, CA, USA). Mice were killed by decapitation immediately after 90-min

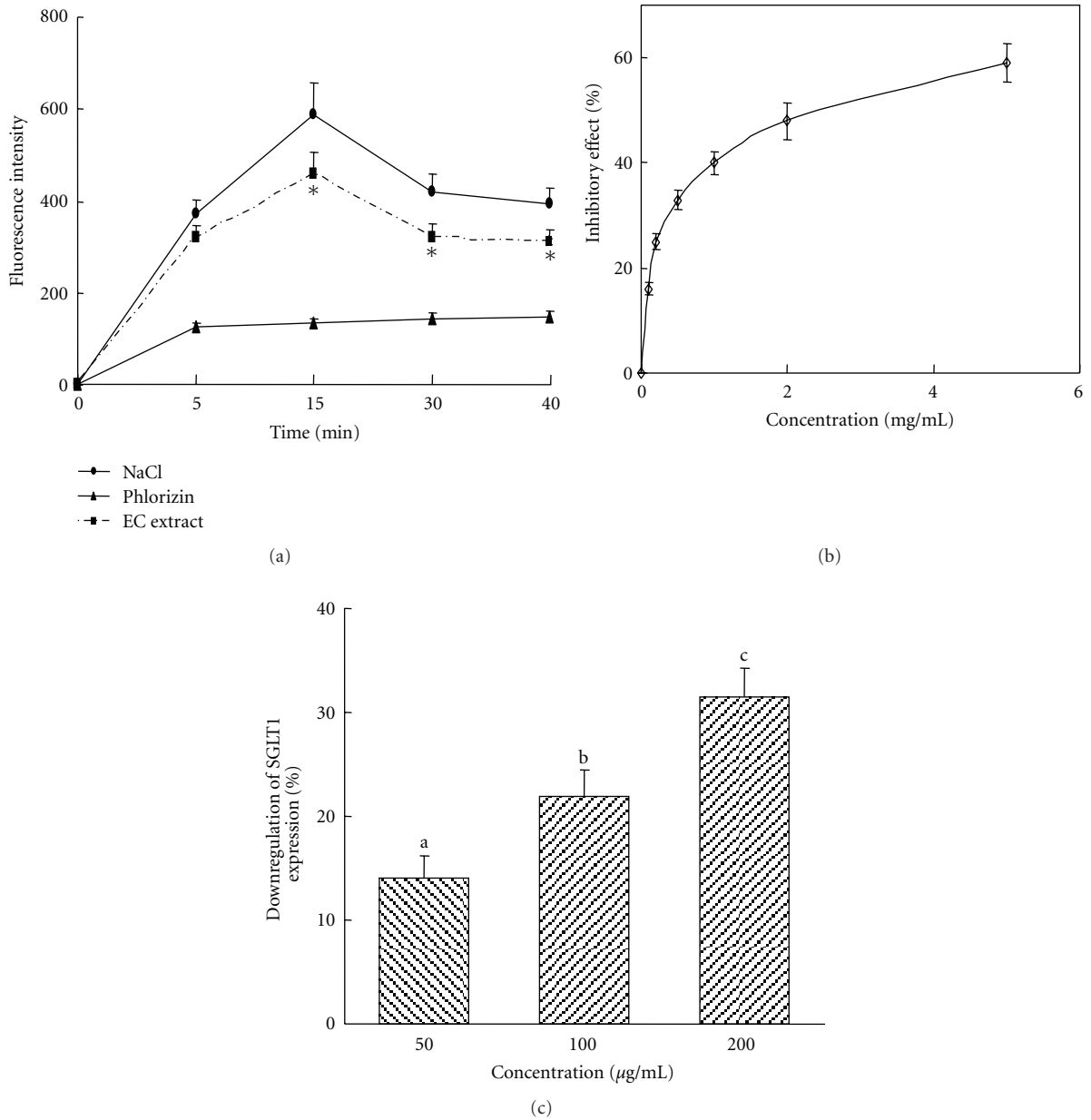


FIGURE 1: Effects of *Ecklonia cava* (EC) on Na^+ -dependent glucose uptake and SGLT1 expression. (a) Time course effects. *Effect of EC (100 $\mu\text{g}/\text{mL}$) at $P < 0.05$. (b) Concentration-dependent inhibitory effects. Data are expressed as the % of inhibitory activity compared to control group. Glucose uptake was measured with 150 mM NaCl or 300 μM phlorizin to evaluate the sodium dependency of the glucose uptake. (c) Downregulation of SGLT1 expression by EC treatment. SGLT1 abundance was determined by ELISA analysis. ^{a-c}Different letters are significantly different at $P < 0.05$. Each value is the mean \pm SE of three different experiments.

blood samples were taken. Preparation of intestinal BBMVs, Na^+ -dependent glucose uptake, and plasma insulin concentrations were determined as described above.

2.8. Statistical Analysis. Results were presented as mean \pm SE, and significant differences ($P < 0.05$) between groups were analyzed by ANOVA followed by Tukey's post hoc test. The 50% inhibitory concentration (IC_{50}) value was calculated using Prism program (GraphPad Software Inc., La Jolla, CA, USA).

3. Results

3.1. Na^+ -Dependent Glucose Uptake and SGLT1 Expression in BBMVs. The intestinal glucose uptake inhibitory activity of EC extract was determined by *in vitro* model of BBMVs using 2-NBDG. Na^+ -dependent 2-NBDG uptake by normal mice intestinal BBMVs was time- and concentration-dependent and almost linear up to 15 min and 200 $\mu\text{g}/\text{mL}$ (Figures 1(a) and 1(b)). The uptake of 2-NBDG into the intestinal BBMVs showed a typical overshoot reaching its peak at 15 min (Figure 1(a)). The overshoot was not observed in

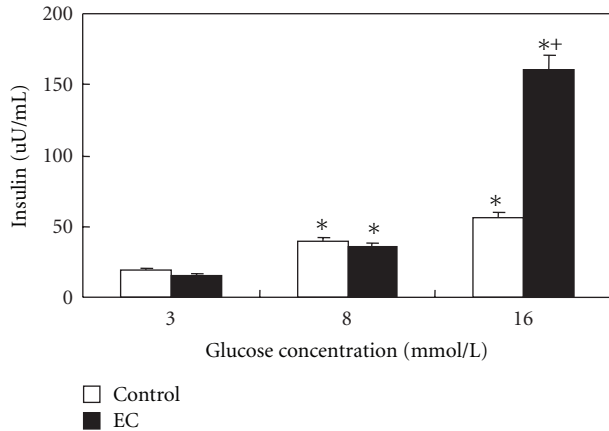


FIGURE 2: Glucose-stimulated insulin secretion in pancreatic islet cells. The incubations were performed with or without EC extract (50 $\mu\text{g}/\text{mL}$) in 3, 8, or 16 mM glucose media. *Significant effect of media glucose concentration and +significant effect of EC treatment at $P < 0.05$.

the presence of phlorizin, a SGLT1 inhibitor. These results suggest that intestinal glucose uptake mediated by SGLT1 actively occurs after glucose ingestion reaching its peak shortly, and SGLT1 inhibitor abolished the active uptake after glucose ingestion. Furthermore, in the presence of phlorizin, glucose uptake was very low showing about 22% of the total glucose uptake at 15 min indicating that BBMVs used SGLT1 as a major mechanism for glucose uptake. EC extract at 100 $\mu\text{g}/\text{mL}$ significantly suppressed the Na^+ -dependent glucose uptake into the BBMVs in the entire uptake profile (Figure 1(a)). The inhibitory effects were 14, 22, 24, and 22% at 5, 15, 30, and 40 min incubation, respectively. The Na^+ -dependent glucose uptake inhibitory activity of BBMVs with various concentrations of EC extract exhibited a dose dependency with IC_{50} at $345 \pm 54 \mu\text{g}/\text{mL}$ (Figure 1(b)).

The abundance of SGLT1, measured by ELISA analysis, was downregulated in a dose-dependent manner and showed 31.4% reduction with 200 $\mu\text{g}/\text{mL}$ EC treatment (Figure 1(c)).

3.2. Glucose-Induced Insulin Secretion in β -Islet Cells. Figure 2 shows the stimulatory effect of the EC extract on insulin secretion in the presence of glucose (3~16 mM). Glucose induced a dose-dependent increase of insulin secretion from pancreatic β -islet cells in both control and EC-treated group. In the presence of 16 mM glucose, insulin secretion increased by 2.9- and 10.4-fold compared to the 3 mM glucose media in control and EC-treated group, respectively. EC extract fails to stimulate insulin output in 3~8 mM glucose media. However, EC extract significantly boosted insulin secretion in 16 mM glucose media exhibiting 2.8-fold increase as compared with control group.

3.3. Intestinal Glucose Uptake in Diabetic Mice. To validate the *in vitro* results, the antihyperglycemic effects of EC supplementation were investigated in STZ-induced diabetic mice. Induction of diabetes caused significant weight loss

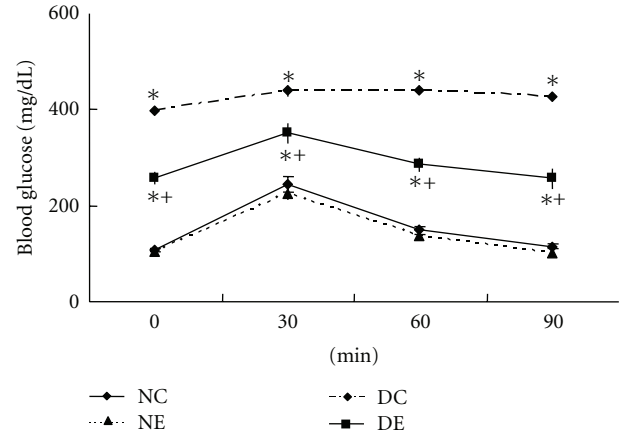


FIGURE 3: Effect of *Ecklonia cava* (EC) on oral glucose tolerance. Glucose (1.5 g/kg) was administered at time zero after 12 hour fasting. Normal control mice (NC); normal mice supplemented with EC powder for 4 weeks (NE); STZ-diabetic control mice (DC); diabetic mice supplemented with EC powder (DE). Values are mean \pm SE of 10 mice in each group. *Significantly different from normal mice and +significant effect of EC treatment at $P < 0.05$.

resulting in negative body weight gain, whereas EC consumption for 4 weeks ameliorated weight loss (Table 1). The Na^+ -dependent glucose uptake by BBMVs prepared from diabetic mice was increased by 39.7% compared with normal mice, and EC supplementation reduced the Na^+ -dependent glucose uptake to near normal value. In normal mice, EC supplementation slightly (14.8%) reduced the Na^+ -dependent glucose uptake without statistical significance. SGLT1 expression in BBMVs was 2.6-fold increased in diabetic mice compared to normal mice. Consumption of EC reduced the SGLT1 protein expressions by 17% and 34% in normal and diabetic mice, respectively, confirming the *in vitro* results. The fasting blood glucose concentrations were markedly decreased by EC supplementation in diabetic mice without any significant differences in normal mice. Plasma insulin concentrations were markedly reduced in diabetic mice, and EC supplementation significantly increased the plasma insulin level reaching 75% of the normal insulin level. However, EC supplementation did not affect the plasma insulin concentrations in normal mice.

The oral glucose tolerance test (OGTT) can be used to evaluate blood glucose homeostasis and also indirectly evaluate glucose absorption. As shown in Figure 3, glucose load in normal mice produced rapid increase in blood glucose levels from 108 ± 4 to $245 \pm 15 \text{ mg}/\text{dL}$ at 30 min and returned to baseline values within 90 min. In contrast, STZ-induced diabetic mice demonstrated basal hyperglycemia ($399 \pm 14 \text{ mg}/\text{dL}$) which remained above 400 mg/dL during all time points determined. The peak increase in serum glucose concentrations in diabetic mice was observed after 60 min of glucose treatment, while that of normal mice observed after 30 min, indicating delayed glucose homeostasis in diabetic mice. Consumption of EC powder slightly reduced fasting blood glucose level in normal mice without any statistical significance. However, EC supplementation in diabetic mice

TABLE 1: Effect of *Ecklonia cava* (EC) on blood glucose regulation.

	NC	NE	DC	DE
Body weight gain (g)	7.8 ± 0.9 ^a	8.4 ± 0.6 ^a	-5.9 ± 0.7 ^b	-2.1 ± 0.4 ^c
Glucose uptake ¹	357 ± 28 ^a	304 ± 17 ^a	499 ± 33 ^b	392 ± 22 ^{a,c}
SGLT1 expression ²	1.00 ± 0.21 ^a	0.83 ± 0.22 ^a	2.61 ± 0.34 ^b	1.72 ± 0.20 ^c
Blood glucose (mg/dL)	112 ± 10 ^a	109 ± 1 ^a	395 ± 13 ^b	240 ± 19 ^c
Plasma insulin (ng/mL)	1.28 ± 0.03 ^a	1.25 ± 0.03 ^a	0.50 ± 0.01 ^b	0.96 ± 0.03 ^c

Values are means ± SE of 10 mice in each group. NC: normal control mice; NE: normal mice supplied with EC powder (3%). DC: STZ-mice; DE: STZ-mice supplied with EC. ¹Na⁺-dependent glucose uptake by BBMV was expressed as fluorescence intensity. ²Relative SGLT1 protein expression.

^{a-c}Different superscript letter means significantly different at $P < 0.05$.

dramatically decreased fasting blood glucose level, and postprandial glucose tolerance showed definite improvement exhibiting similar pattern as normal mice with peak increase at 30 min.

4. Discussion

The importance of postprandial glucose control in the development of diabetic complications is widely recognized based on many epidemiological studies. Several inhibitors of α -amylase or β -glucosidase were proposed to control postprandial hyperglycemia, but the inhibitors of these enzymes are not able to prevent glucose absorption when glucose itself has been ingested. Hence, it might be important to inhibit intestinal glucose absorption as well as glucosidase or amylase activity for the regulation of postprandial blood glucose level.

The capacity of the small intestine to absorb glucose increases in patients with type 2 diabetes and in experimentally induced diabetic animals as a consequence of the enhanced activity and abundance of SGLT1 [2, 3] suggesting SGLT1 as a potential target of drug development for glycemic control in diabetic patients.

In the present study, we conducted an *in vitro* study to examine the effects of EC on intestinal glucose uptake using BBMV. The results revealed that EC reduced SGLT1 activity, assessed by Na⁺-dependent glucose uptake and SGLT1 protein expression in BBMV. Furthermore, the insulinotropic effect of EC extract was observed at high glucose (16 mM) environment. Compared to the results at 3 mM media glucose, insulin secretion at 16 mM glucose with EC extract increased by 10.4-fold. This is consistent with the observation that glucose acts synergistically with antidiabetic plant to promote insulin secretion [13]. The elevated insulin secretion with EC treatment at high glucose environment agrees with *in vivo* results in Table 1, thus strengthening the evidence that the EC acts as a stimulator of insulin secretion. Diabetic mice (blood glucose > 20 mM) markedly increased plasma insulin concentration by 192% while Na⁺-dependent glucose uptake was reduced by 22% in response to EC supplementation. These results suggest that the relative contribution of increased islet cell insulin secretion is more potent than reduced intestinal Na⁺-dependent glucose uptake for the regulation of blood glucose level in EC-supplemented diabetic mice. Therefore, it is significant that the EC extract

could potentiate insulin secretion at higher glucose concentration, which could be useful in situations where chronic hyperglycemia decreases the sensitivity of β -islet cells to glucose-induced insulin secretion [14].

We subsequently examined the *in vivo* effect of EC on glucose uptake by BBMV prepared from STZ-diabetic mice fed EC diet. Recent studies have shown that modifications of systemic glycemia in OGTT reflect the activity of the intestinal glucose transporter SGLT1 [15]. STZ-induced diabetic mice exhibited severe hyperglycemia with increased Na⁺-dependent glucose uptake activity and SGLT1 expression in intestinal BBMV compared with normal mice. EC consumption reduced intestinal Na⁺-dependent glucose uptake and SGLT1 expression in diabetic mice resulting in improvement of OGTT and blood glucose level. The blood glucose and insulin levels in EC supplemented mice were not completely normalized whereas the intestinal Na⁺-dependent glucose uptake was normalized, again suggesting the importance of pancreatic insulin secretion for the regulation of blood glucose homeostasis. The enhancement of intestinal glucose uptake in diabetic mice might be attributed to several factors, such as an increase in mucosal mass, an increase in the turnover of the transporter, and/or an increase in the number of SGLT1. It has been reported that glucose transporter levels including SGLT1 are elevated in diabetic animals and humans [2, 3].

Administration of EC suppressed the body weight loss in diabetic mice suggesting that EC treatment may beneficially affect the metabolic state in diabetes. Indeed, it has been reported that administration of phlorizin or T-1095, Na⁺-dependent glucose transporter inhibitor, leads to a body weight gain in STZ diabetic rats [16, 17].

Seaweeds contain appreciable amounts of polyphenols, and Ahn et al. [18] reported that the content of polyphenols in EC is about 18.3%. It has been suggested that polyphenols modulate hyperglycemia through various mechanisms. First, glucose absorption from intestine was reduced by inhibiting α -glucosidase and/or SGLT1 activity. Catechin [19], flavonoid [20], and quercetin [21] have been reported to inhibit α -glucosidase activity via steric hindrance. The influence of polyphenols on glucose transporters has been studied *in vitro* by using intestinal BBMV or everted sacs and Caco-2 cells. The Na⁺-dependent SGLT1-mediated glucose transport was inhibited by tea catechins [22, 23], tannic acids [24], and quercetin monoglucosides [25]. Kobayashi et al. [22] and Shimizu et al. [23] reported that green tea polyphenols,

especially epicatechin gallate (ECg), inhibit SGLT1 in a competitive manner interacting as antagonist-like molecules, although ECg itself was not transported via the glucose transporters. Oliveira et al. reported that polyphenol-rich Yerba maté decreased intestinal SGLT1 expression in alloxan-induced diabetic rats [26]. Second, polyphenols increase pancreatic insulin secretion. Soy isoflavonoids (genistein and daidzein) preserved insulin production by the β -cells in STZ-induced diabetic mice [27]. EGCG activates IRS2 and AMPK signalling in rat pancreatic β -cells [28]. Genistein augments cAMP accumulation and insulin release in MIN6 cells [29]. Therefore, it is obvious that the pancreas is one of the targets of dietary polyphenol bioactivity although no single mechanism has been identified to be responsible for the response. Although the identity of chemical component responsible for the antidiabetic action of EC in present study is unknown, it would be of considerable interest to further elucidate the mechanism and component(s) underlying the action of EC.

In conclusion, this study demonstrates that EC manifests two important antidiabetic properties: the inhibition of intestinal Na^+ -dependent glucose absorption mediated by reduced expression of SGLT1 and the stimulation of insulin secretion in hyperglycemic environment, resulting in improvement of the glucose regulation in diabetic condition. The present findings identify, for the first time to our knowledge, the inhibitory effect on intestinal glucose uptake and insulinotropic effect of EC.

Abbreviations

EC: *Ecklonia cava*
 SGU: Na^+ -dependent glucose uptake
 SGLT1: Na^+ -dependent glucose transporter 1
 BBMV: Brush border membrane vesicles
 STZ: Streptozotocin
 ALP: Alkaline phosphatase.

Conflict of Interests

The authors declare no conflict of interests.

Acknowledgment

This work was supported by a grant from the 2010 Fundamental R&D Program of Hanseo University.

References

- [1] M. A. Hediger and D. B. Rhoads, "Molecular physiology of sodium-glucose cotransporters," *Physiological Reviews*, vol. 74, no. 4, pp. 993–1026, 1994.
- [2] R. N. Fedorak, C. I. Cheeseman, A. B. R. Thomson, and V. M. Porter, "Altered glucose carrier expression: mechanism of intestinal adaptation during streptozotocin-induced diabetes in rats," *American Journal of Physiology*, vol. 261, no. 4, pp. G585–G591, 1991.
- [3] J. Dyer, I. S. Wood, A. Palejwala, A. Ellis, and S. P. Shirazi-Beechey, "Expression of monosaccharide transporters in intestine of diabetic humans," *American Journal of Physiology*, vol. 282, no. 2, pp. G241–G248, 2002.
- [4] G. Perseghin, A. Caumo, C. Arcelloni et al., "Contribution of abnormal insulin secretion and insulin resistance to the pathogenesis of type 2 diabetes in myotonic dystrophy," *Diabetes Care*, vol. 26, no. 7, pp. 2112–2118, 2003.
- [5] H. C. Shin, H. J. Hwang, K. J. Kang, and B. H. Lee, "An anti-oxidative and anti-inflammatory agent for potential treatment of osteoarthritis from *Ecklonia cava*," *Archives of Pharmacological Research*, vol. 29, no. 2, pp. 165–171, 2006.
- [6] Y. Athukorala, K. N. Kim, and Y. J. Jeon, "Antiproliferative and antioxidant properties of an enzymatic hydrolysate from brown alga, *Ecklonia cava*," *Food and Chemical Toxicology*, vol. 44, no. 7, pp. 1065–1074, 2006.
- [7] G. Ahn, I. Hwang, E. Park et al., "Immunomodulatory effects of an enzymatic extract from *Ecklonia cava* on murine splenocytes," *Marine Biotechnology*, vol. 10, no. 3, pp. 278–289, 2008.
- [8] S. H. Lee, J. S. Han, S. J. Heo, J. Y. Hwang, and Y. J. Jeon, "Protective effects of dieckol isolated from *Ecklonia cava* against high glucose-induced oxidative stress in human umbilical vein endothelial cells," *Toxicology in Vitro*, vol. 24, no. 2, pp. 375–381, 2010.
- [9] S. H. Lee, M. H. Park, S. J. Heo et al., "Dieckol isolated from *Ecklonia cava* inhibits α -glucosidase and α -amylase in vitro and alleviates postprandial hyperglycemia in streptozotocin-induced diabetic mice," *Food and Chemical Toxicology*, vol. 48, no. 10, pp. 2633–2637, 2010.
- [10] E. S. Debnam and P. A. Sharp, "Acute and chronic effects of pancreatic glucagon on sugar transport across the brush-border and basolateral membranes of rat jejunal enterocytes," *Experimental Physiology*, vol. 78, no. 2, pp. 197–207, 1993.
- [11] M. M. Bradford, "A rapid and sensitive method for the quantitation of microgram quantities of protein utilizing the principle of protein dye binding," *Analytical Biochemistry*, vol. 72, no. 1-2, pp. 248–254, 1976.
- [12] P. E. Lacy and M. Kostianovsky, "Method for the isolation of intact islets of Langerhans from the rat pancreas," *Diabetes*, vol. 16, no. 1, pp. 35–39, 1967.
- [13] K. A. Asamoah, D. A. Robb, and B. L. Furman, "Chronic chloroquine treatment enhances insulin release in rats," *Diabetes Research and Clinical Practice*, vol. 9, no. 3, pp. 273–278, 1990.
- [14] J. L. Leahy, S. Bonner-Weir, and G. C. Weir, " β -cell dysfunction induced by chronic hyperglycemia: current ideas on mechanism of impaired glucose-induced insulin secretion," *Diabetes Care*, vol. 15, no. 3, pp. 442–455, 1992.
- [15] R. Ducroc, T. Voisin, A. El Firar, and M. Laburthe, "Orexins control intestinal glucose transport by distinct neuronal, endocrine, and direct epithelial pathways," *Diabetes*, vol. 56, no. 10, pp. 2494–2500, 2007.
- [16] S. M. Brichard, J. C. Henquin, and J. Girard, "Phlorizin treatment of diabetic rats partially reverses the abnormal expression of genes involved in hepatic glucose metabolism," *Diabetologia*, vol. 36, no. 4, pp. 292–298, 1993.
- [17] T. Adachi, K. Yasuda, Y. Okamoto et al., "T-1095, A renal Na^+ -glucose transporter inhibitor, improves hyperglycemia in streptozotocin-induced diabetic rats," *Metabolism*, vol. 49, no. 8, pp. 990–995, 2000.
- [18] G. Ahn, E. Park, W. W. Lee et al., "Enzymatic extract from *Ecklonia cava* induces the activation of lymphocytes by IL-2 production through the classical NF- κ B pathway," *Marine Biotechnology*, vol. 13, no. 1, pp. 66–73, 2011.

- [19] T. Matsui, T. Tanaka, S. Tamura et al., “ α -glucosidase inhibitory profile of catechins and theaflavins,” *Journal of Agricultural and Food Chemistry*, vol. 55, no. 1, pp. 99–105, 2007.
- [20] K. Johnston, P. Sharp, M. Clifford, and L. Morgan, “Dietary polyphenols decrease glucose uptake by human intestinal Caco-2 cells,” *FEBS Letters*, vol. 579, no. 7, pp. 1653–1657, 2005.
- [21] K. Tadera, Y. Minami, K. Takamatsu, and T. Matsuoka, “Inhibition of α -glucosidase and α -amylase by flavonoids,” *Journal of Nutritional Science and Vitaminology*, vol. 52, no. 2, pp. 149–153, 2006.
- [22] Y. Kobayashi, M. Suzuki, H. Satsu et al., “Green tea polyphenols inhibit the sodium-dependent glucose transporter of intestinal epithelial cells by a competitive mechanism,” *Journal of Agricultural and Food Chemistry*, vol. 48, no. 11, pp. 5618–5623, 2000.
- [23] M. Shimizu, Y. Kobayashi, M. Suzuki, H. Satsu, and Y. Miyamoto, “Regulation of intestinal glucose transport by tea catechins,” *BioFactors*, vol. 13, no. 1–4, pp. 61–65, 2000.
- [24] C. A. Welsch, P. A. Lachance, and B. P. Wasserman, “Dietary phenolic compounds: inhibition of Na^+ -dependent D-glucose uptake in rat intestinal brush border membrane vesicles,” *Journal of Nutrition*, vol. 119, no. 11, pp. 1698–1704, 1989.
- [25] R. Cermak, S. Landgraf, and S. Wolfram, “Quercetin glucosides inhibit glucose uptake into brush-border-membrane vesicles of porcine jejunum,” *British Journal of Nutrition*, vol. 91, no. 6, pp. 849–855, 2004.
- [26] D. M. Oliveira, H. S. Freitas, M. F. F. Souza et al., “Yerba Maté (*Ilex paraguariensis*) aqueous extract decreases intestinal SGLT1 gene expression but does not affect other biochemical parameters in alloxan-diabetic wistar rats,” *Journal of Agricultural and Food Chemistry*, vol. 56, no. 22, pp. 10527–10532, 2008.
- [27] M. P. Lu, R. Wang, X. Song et al., “Dietary soy isoflavones increase insulin secretion and prevent the development of diabetic cataracts in streptozotocin-induced diabetic rats,” *Nutrition Research*, vol. 28, no. 7, pp. 464–471, 2008.
- [28] E. P. Cai and J. K. Lin, “Epigallocatechin gallate (EGCG) and rutin suppress the glucotoxicity through activating IRS2 and AMPK signaling in rat pancreatic beta cells,” *Journal of Agricultural and Food Chemistry*, vol. 57, no. 20, pp. 9817–9827, 2009.
- [29] T. Ohno, N. Kato, C. Ishii et al., “Genistein augments cyclic adenosine 3′5′-monophosphate (cAMP) accumulation and insulin release in MIN6 cells,” *Endocrine Research*, vol. 19, no. 4, pp. 273–285, 1993.

Research Article

Xanthohumol, a Prenylated Flavonoid from Hops (*Humulus lupulus*), Prevents Platelet Activation in Human Platelets

Ye-Ming Lee,^{1,2} Kuo-Hsien Hsieh,³ Wan-Jung Lu,² Hsiu-Chu Chou,² Duen-Suey Chou,² Li-Ming Lien,⁴ Joen-Rong Sheu,² and Kuan-Hung Lin^{2,4}

¹ Department of Surgery, Hsinchu Mackay Memorial Hospital, Hsinchu and Mackay Medicine, Nursing and Management College, 92 Zhong-Shan N. Road, Taipei 104, Taiwan

² Department of Pharmacology and Graduate Institute of Medical Sciences, Taipei Medical University, 250 Wu-Hsing Street, Taipei 110, Taiwan

³ Department of Orthopedics, Tungs' Taichung MetroHarbor Hospital, 699 Chung-Chi Road, Taichung 435, Taiwan

⁴ Central Laboratory, Shin-Kong Wu Ho-Su Memorial Hospital, 95 Wen-Chang Road, Taipei 111, Taiwan

Correspondence should be addressed to Joen-Rong Sheu, sheujr@tmu.edu.tw and Kuan-Hung Lin, t010619@ms.skh.org.tw

Received 15 December 2011; Accepted 15 February 2012

Academic Editor: Vincenzo De Feo

Copyright © 2012 Ye-Ming Lee et al. This is an open access article distributed under the Creative Commons Attribution License, which permits unrestricted use, distribution, and reproduction in any medium, provided the original work is properly cited.

Xanthohumol is the principal prenylated flavonoid in the hop plant (*Humulus lupulus* L.). Xanthohumol was found to be a very potent cancer chemopreventive agent through regulation of diverse mechanisms. However, no data are available concerning the effects of xanthohumol on platelet activation. The aim of this paper was to examine the antiplatelet effect of xanthohumol in washed human platelets. In the present paper, xanthohumol exhibited more-potent activity in inhibiting platelet aggregation stimulated by collagen. Xanthohumol inhibited platelet activation accompanied by relative $[Ca^{2+}]_i$ mobilization, thromboxane A_2 formation, hydroxyl radical (OH^*) formation, and phospholipase C (PLC) γ 2, protein kinase C (PKC), mitogen-activated protein kinase (MAPK), and Akt phosphorylation. Neither SQ22536, an inhibitor of adenylate cyclase, nor ODQ, an inhibitor of guanylate cyclase, reversed the xanthohumol-mediated inhibitory effect on platelet aggregation. Furthermore, xanthohumol did not significantly increase nitrate formation in platelets. This study demonstrates for the first time that xanthohumol possesses potent antiplatelet activity which may initially inhibit the PI3-kinase/Akt, p38 MAPK, and PLC γ 2-PKC cascades, followed by inhibition of the thromboxane A_2 formation, thereby leading to inhibition of $[Ca^{2+}]_i$ and finally inhibition of platelet aggregation. Therefore, this novel role of xanthohumol may represent a high therapeutic potential for treatment or prevention of cardiovascular diseases.

1. Introduction

Dietary factors play key roles in developing and preventing various human diseases, including cardiovascular diseases (CVDs). Epidemiological studies showed an inverse relationship between diets rich in fruits, vegetables, and spices, and the risk of all causes of death from cancer and CVD [1]. Hops (*Humulus lupulus* L.) have long been used in the brewing industry as a preservative and flavoring agent to add bitterness and aroma to beer [2]. In traditional Chinese medicine, hops are used to treat insomnia, restlessness, dyspepsia, and lack of an appetite. Alcoholic extracts of hops are clinically used in China to treat leprosy, pulmonary tuberculosis, acute bacterial dysentery, silicosis, and asbestosis with

positive outcomes [2]. Xanthohumol is the principal prenylated flavonoid in the hop plant. Recently, xanthohumol has attracted considerable interest because of its biological activities, including anticancer, antiangiogenesis, anti-inflammation, and antioxidation [3]. Xanthohumol (1~50 μ M) was shown to suppress tumor growth by inhibiting cell proliferation and inducing apoptosis in various carcinoma cells [4–6]. It also exhibited antiangiogenic activity through inhibiting nuclear factor (NF)- κ B and Akt activation in vascular endothelial cells [7]. Furthermore, xanthohumol was reported to regulate the function and survival of immune cells by inhibiting the production of two important cytokines, monocyte chemoattractant protein (MCP)-1, and tumor necrosis factor (TNF)- α , in lipopolysaccharide-stim-

ulated macrophages [8]. Xanthohumol also prevented hepatic inflammation and fibrosis *in vivo* and promoted dendritic cell apoptosis [3, 9]. Furthermore, xanthohumol was able to scavenge reactive oxygen species (ROS) in tissue-plasminogen activator-(TPA-) stimulated differentiated HL-60 cells [4].

Intravascular thrombosis is one of the generators of a wide variety of CVDs. Initiation of an intraluminal thrombosis is believed to involve platelet adherence and aggregation. Thus, platelet aggregation may play a crucial role in the atherothrombotic process [10]. Blood platelet activation and aggregation are common denominators in atherothrombotic events. Platelets are exclusively viewed as mediators of thrombosis and hemostasis. Therefore, investigation of the use of antiplatelet agents that inhibit atherothrombotic events (myocardial infarction, ischemic stroke, and vascular death) is warranted.

Olas et al. [11] reported that the extract of hops significantly reduced oxidative stress in peroxynitrite-stimulated platelets. However, the detailed mechanisms underlying xanthohumol's signaling pathways in regulating platelet functions remain obscure. In the present study, we therefore for the first time examined in detail cellular signaling events associated with xanthohumol-mediated platelet function.

2. Materials and Methods

2.1. Materials. Xanthohumol, collagen (type I), luciferin-luciferase, arachidonic acid (AA), phorbol-12,13-dibutyrate (PDBu), 5,5-dimethyl-1 pyrroline N-oxide (DMPO), SQ22536, ODQ, and thrombin were purchased from Sigma (St. Louis, MO, USA). Fura 2-AM and fluorescein isothiocyanate (FITC) were from Molecular Probe (Eugene, OR, USA). The thromboxane B₂ enzyme immunoassay (EIA) kit was from Cayman (Ann Arbor, MI, USA). The anti-phospho-p38 mitogen-activated protein kinase (MAPK) Ser¹⁸² monoclonal antibody (mAb) was from Santa Cruz (Santa Cruz, CA). The anti-p38 MAPK and anti-phospho-c-Jun N-terminal kinase (JNK) (Thr¹⁸³/Tyr¹⁸⁵) mAbs, and antiphospholipase Cy2 (PLCγ2), anti-phospho (Tyr⁷⁵⁹) PLCγ2, and anti-phospho-p44/p42 extracellular signal-regulated kinase (ERK) (Thr²⁰²/Tyr²⁰⁴) polyclonal antibodies (pAbs) were from Cell Signaling (Beverly, MA, USA). Anti-phospho-Akt (Ser⁴⁷³) and anti-Akt mAbs were from Biovision (Mountain View, CA, USA). The anti-α-tubulin mAb was from NeoMarkers (Fremont, CA, USA). The Hybond-P polyvinylidene difluoride (PVDF) membrane, enhanced chemiluminescence (ECL) western blotting detection reagent, and analysis system, horseradish peroxidase-(HRP-) conjugated donkey anti-rabbit immunoglobulin G (IgG), and sheep anti-mouse IgG were from Amersham (Buckinghamshire, UK). Xanthohumol was dissolved in 0.5% dimethyl sulfoxide (DMSO) and stored at 4°C until used.

2.2. Platelet Aggregation. Human platelet suspensions were prepared as previously described [10]. This study was approved by the Institutional Review Board of Taipei Medical

University and conformed to the principles outlined in the *Helsinki Declaration*, and all human volunteers provided informed consent. In brief, blood was collected from healthy human volunteers who had taken no medication during the preceding 2 weeks, and was mixed with acid-citrate-dextrose solution. After centrifugation, the supernatant (platelet-rich plasma; PRP) was supplemented with 0.5 μM prostaglandin E₁ (PGE₁) and 6.4 IU/mL heparin. Washed platelets were finally suspended in Tyrode's solution containing 3.5 mg/mL bovine serum albumin (BSA). The final concentration of Ca²⁺ in Tyrode's solution was 1 mM.

A turbidimetric method was used to measure platelet aggregation [10], with a Lumi-Aggregometer (Payton, Scarborough, ON, Canada). Platelet suspensions (3.6 × 10⁸ cells/mL) were preincubated with various concentrations of xanthohumol or an isovolumetric solvent control (final concentration, 0.5% DMSO) for 3 min before the addition of agonists. The reaction was allowed to proceed for 6 min, and the extent of aggregation was expressed in light-transmission units. When measuring ATP release, 20 μL of a luciferin/luciferase mixture was added 1 min before the addition of agonists, and ATP release was compared to that of the control.

2.3. Flow Cytometric Analysis. Fluorescence-conjugated tri-flavin, an α_{IIb}β₃ disintegrin, was prepared as previously described [12]. Platelet suspensions (3.6 × 10⁸ cells/mL) were preincubated with 1.5 and 3 μM xanthohumol or a solvent control for 3 min, followed by the addition of 2 μL of 2 μg/mL FITC-triflavin. Suspensions were then assayed for fluorescein-labeled platelets using a flow cytometer (Beckman Coulter, Miami, FL, USA). Data were collected from 50,000 platelets per experimental group, and platelets were identified on the basis of their characteristic forward and orthogonal light-scattering profiles. All experiments were repeated at least four times to ensure reproducibility.

2.4. Measurement of Relative [Ca²⁺]_i Mobilization by Fura 2-AM Fluorescence. Citrated whole blood was centrifuged at 120 × g for 10 min. The supernatant was incubated with 5 μM Fura 2-AM for 1 h. Human platelets were then prepared as described above. Finally, the external Ca²⁺ concentration of the platelet suspensions was adjusted to 1 mM. Relative [Ca²⁺]_i mobilization was measured using a fluorescence spectrophotometer (CAF 110, Jasco, Tokyo, Japan) with excitation wavelengths of 340 and 380 nm, and an emission wavelength of 500 nm [10].

2.5. Measurement of Thromboxane B₂ Formation. Platelet suspensions (3.6 × 10⁸ cells/mL) were preincubated with xanthohumol (1.5–10 μM) or a solvent control for 3 min before the addition of agonists. Six minutes after the addition of agonists, 2 mM EDTA and 50 μM indomethacin were added to the suspensions. Thromboxane B₂ levels of the supernatants were measured using an EIA kit.

2.6. Immunoblotting. Washed platelets (1.2 × 10⁹ cells/mL) were preincubated with 1.5 and 3 μM xanthohumol or a

solvent control for 3 min, followed by the addition of agonists to trigger platelet activation. The reaction was stopped, and platelets were immediately resuspended in 200 μL of lysis buffer. Samples containing 80 μg of protein were separated by a 12% sodium dodecylsulfate polyacrylamide gel electrophoresis (SDS-PAGE); proteins were electrotransferred by semidry transfer (Bio-Rad, Hercules, CA, USA). Blots were blocked with TBST (10 mM Tris-base, 100 mM NaCl, and 0.01% Tween 20) containing 5% BSA for 1 h and then probed with various primary antibodies. Membranes were incubated with HRP-linked anti-mouse IgG or anti-rabbit IgG (diluted 1:3000 in TBST) for 1 h. Immunoreactive bands were detected by an ECL system. The bar graph depicts the ratios of semiquantitative results obtained by scanning reactive bands and quantifying the optical density using vidiodensitometry (Bio-profil; Biolight Windows Application V2000.01; Vilber Lourmat, France).

2.7. Estimation of Nitrate Formation. In brief, platelet suspensions (10^9 cells/mL) were preincubated with 1.5 and 3 μM xanthohumol or a solvent control for 3 min, followed by centrifugation. The amount of nitrate in the platelet suspensions (10 μL) was measured by adding a reducing agent to the purge vessel to convert nitrate to NO which was stripped from the suspensions by purging with helium gas [12]. The NO was then drawn into a Sievers Nitric Oxide Analyzer (Sievers 280 NOA, Boulder, CO, USA). Nitrate concentrations were calculated by comparison to standard solutions of sodium nitrate.

2.8. Measurement of Hydroxyl Radicals by Electron Spin Resonance (ESR) Spectrometry. The ESR method used a Bruker EMX ESR spectrometer as described previously [13]. In brief, platelet suspensions (3.6×10^8 cells/mL) were preincubated with 1.5 and 3 μM xanthohumol or a solvent control for 3 min before the addition of 1 $\mu\text{g}/\text{mL}$ collagen. The reaction was allowed to proceed for 5 min, followed by the addition of 100 μM DMPO for the ESR study. The rate of free radical-scavenging activity was defined by the following equation:

$$\text{inhibition rate} = 1 - \left[\frac{\text{signal height (xanthohumol)}}{\text{signal height (control)}} \right], \quad (1)$$

(see [13]).

2.9. Data Analysis. Experimental results are expressed as the means \pm S.E.M. and are accompanied by the number of observations. Experiments were assessed by an analysis of variance (ANOVA). If this analysis indicated significant differences among group means, then each group was compared using the Newman-Keuls method. $P < 0.05$ was considered statistically significant.

3. Results

3.1. Effects of Xanthohumol on Platelet Aggregation and Relative $[\text{Ca}^{2+}]$; Mobilization in Washed Human Platelets. Xanthohumol (1.5 and 3 μM) exhibited very potent activity in

inhibiting platelet aggregation and the ATP-release reaction stimulated by 1 $\mu\text{g}/\text{mL}$ collagen (Figure 1(a)); it also significantly inhibited platelet aggregation stimulated by 60 μM AA at higher concentrations (3 and 10 μM) (Figure 1(a)). However, it did not significantly inhibit platelet aggregation stimulated by 0.05 U/mL thrombin or 1 μM U46619, a prostaglandin endoperoxide, at the same concentrations (3 and 10 μM) (Figure 1(a)). The 50% inhibitory concentration (IC_{50}) value of xanthohumol for platelet aggregation induced by collagen was approximately 1.5 μM (Figure 1(b)). The solvent control (0.5% DMSO) did not significantly affect platelet aggregation stimulated by agonists (Figure 1(a)). In subsequent experiments, we used collagen as an agonist to explore the inhibitory mechanisms of xanthohumol in platelet activation.

As shown in Figure 1(c), 1 $\mu\text{g}/\text{mL}$ collagen evoked a marked increase in relative Ca^{2+} mobilization, and this increase was markedly inhibited in the presence of xanthohumol (1.5 μM , $50.8 \pm 9.5\%$ and 3 μM , $66.5 \pm 9.6\%$; $n = 3$).

3.2. Influence of Xanthohumol on $\alpha_{\text{IIb}}\beta_3$ Integrin Conformational Changes, Thromboxane B_2 Formation, and PLC γ_2 Phosphorylation. Triflavin is an $\alpha_{\text{IIb}}\beta_3$ disintegrin which inhibits platelet aggregation by directly interfering with fibrinogen binding to the $\alpha_{\text{IIb}}\beta_3$ integrin [12]. Therefore, we further evaluated whether or not xanthohumol directly binds to the platelet $\alpha_{\text{IIb}}\beta_3$ integrin, leading to interruption of platelet aggregation. In this study, the relative intensity of the fluorescence of 2 $\mu\text{g}/\text{mL}$ FITC-triflavin bound directly to 1 $\mu\text{g}/\text{mL}$ collagen-activated platelets was 26.8 ± 0.5 ($n = 5$) (Figure 2(a) (A)), and it was markedly reduced in the presence of 5 mM EDTA (negative control, 9.7 ± 0.5 , $P < 0.001$; $n = 5$) (Figure 2(a) (B)). Xanthohumol (1.5 and 3 μM) did not significantly affect FITC-triflavin binding to the $\alpha_{\text{IIb}}\beta_3$ integrin in platelet suspensions (1.5 μM , 26.9 ± 0.6 ; 3 μM , 28.0 ± 0.7 ; $n = 5$) (Figure 2(a) (C, D)), indicating that the inhibitory effect of xanthohumol on platelet aggregation does not involve binding to the platelet $\alpha_{\text{IIb}}\beta_3$ integrin. Furthermore, resting platelets produced relatively low amounts of thromboxane B_2 compared to agonist-activated platelets (i.e., collagen). At 3 μM , xanthohumol inhibited both 1 $\mu\text{g}/\text{mL}$ collagen- and 60 μM AA-stimulated thromboxane B_2 formation by approximately 56% and 10%, respectively, but it was not significantly affected by 0.05 U/mL thrombin stimulation (Figure 2(b)). PLC hydrolyzes phosphatidylinositol 4,5-bisphosphate (PIP_2) to generate two secondary messengers: inositol 1,4,5-trisphosphate (IP_3) and diacylglycerol (DAG) [14]. DAG activates PKC, which then phosphorylates p47 proteins (p47). Treatment with 1.5 and 3 μM xanthohumol concentration dependently abolished the phosphorylation of PLC γ_2 stimulated by collagen (Figure 2(c)).

3.3. Xanthohumol on PKC Activation. Stimulation of platelets with a number of different agonists (such as collagen) or PDBu, an activator of PKC [15], markedly induces PKC activation (p47 phosphorylation). In the present study, when 1 $\mu\text{g}/\text{mL}$ collagen (Figure 3(a)) or 150 nM PDBu

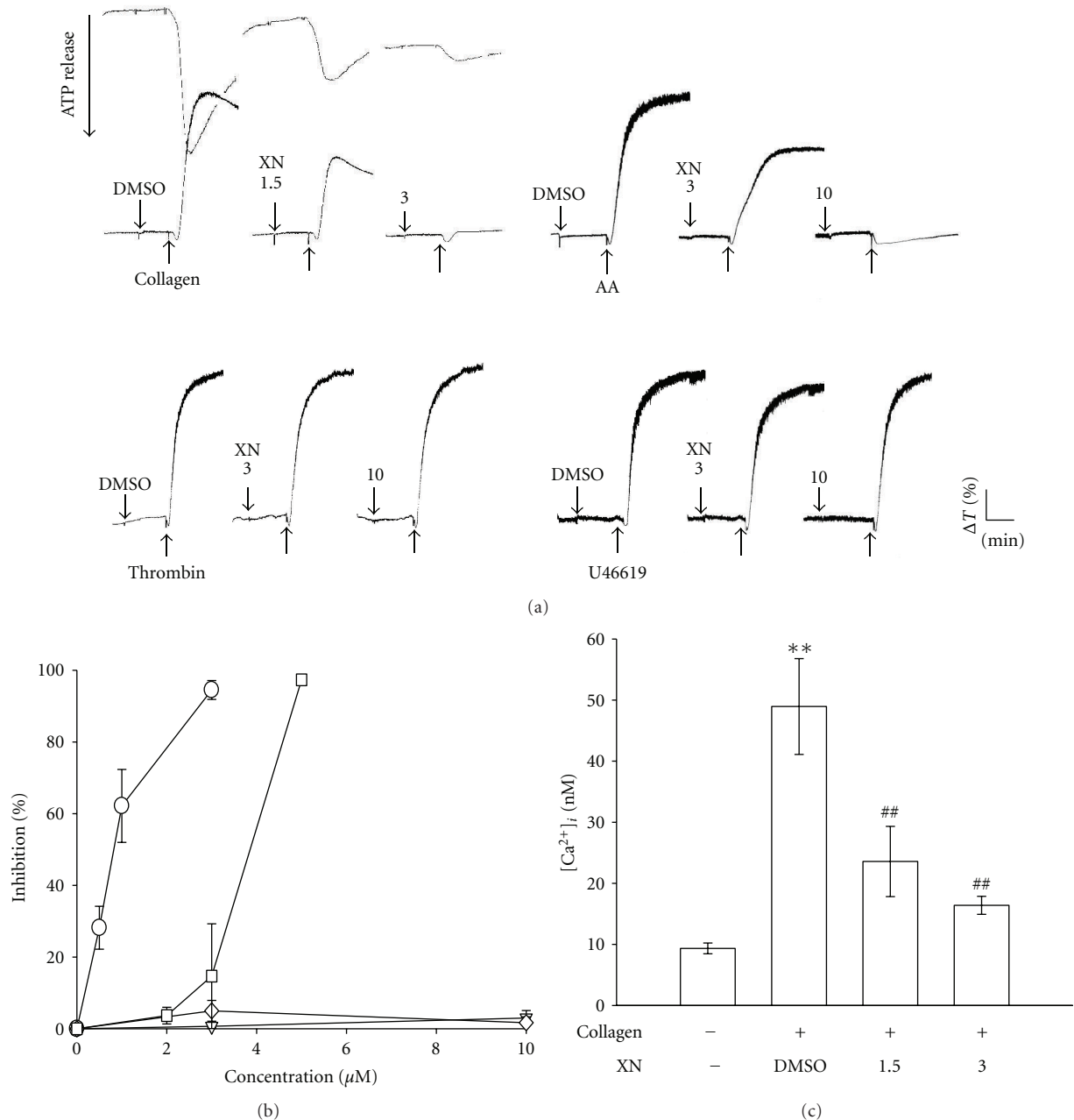


FIGURE 1: Effects of xanthohumol (XN) on the inhibition of platelet aggregation and relative $[\text{Ca}^{2+}]_i$ mobilization in activated platelets. Washed platelets (3.6×10^8 cells/mL) were preincubated with 1.5–10 μM XN or a solvent control (0.5% DMSO), followed by the addition of 1 $\mu\text{g}/\text{mL}$ collagen (\circ), 1 μM U46619 (∇), 60 μM arachidonic acid (AA; \square), or 0.05 IU/mL thrombin (\diamond) to trigger ((a)-(b)) platelet aggregation and an ATP-release reaction ((a), top-left corner) or (c) relative $[\text{Ca}^{2+}]_i$ mobilization. Profiles (a) are representative examples of six similar experiments. Data ((b) and (c)) are presented as the means \pm S.E.M. ((b), $n = 6$; (c), $n = 3$); ** $P < 0.01$, compared to the resting group; ## $P < 0.01$, compared to the control (DMSO) group.

(Figure 3(b)) was added to human platelets, a protein with an apparent molecular weight of 47 kDa (p47) was predominantly phosphorylated compared to resting platelets. Xanthohumol (1.5 and 3 μM) concentration dependently inhibited p47 phosphorylation stimulated by collagen but not by PDBu (Figures 3(a) and 3(b)). As shown in the Figure 3(c), xanthohumol did not significantly affect PDBu-(150 nM) induced platelet aggregation. These results indicate that

xanthohumol abolished PKC activation through inhibiting PLC γ 2 phosphorylation.

3.4. Xanthohumol Attenuates MAPKs and Akt Activation. To further investigate the inhibitory mechanisms of xanthohumol in platelet activation, we detected several signaling molecules such as MAPKs (i.e., p38 MAPK, ERK1/2, and

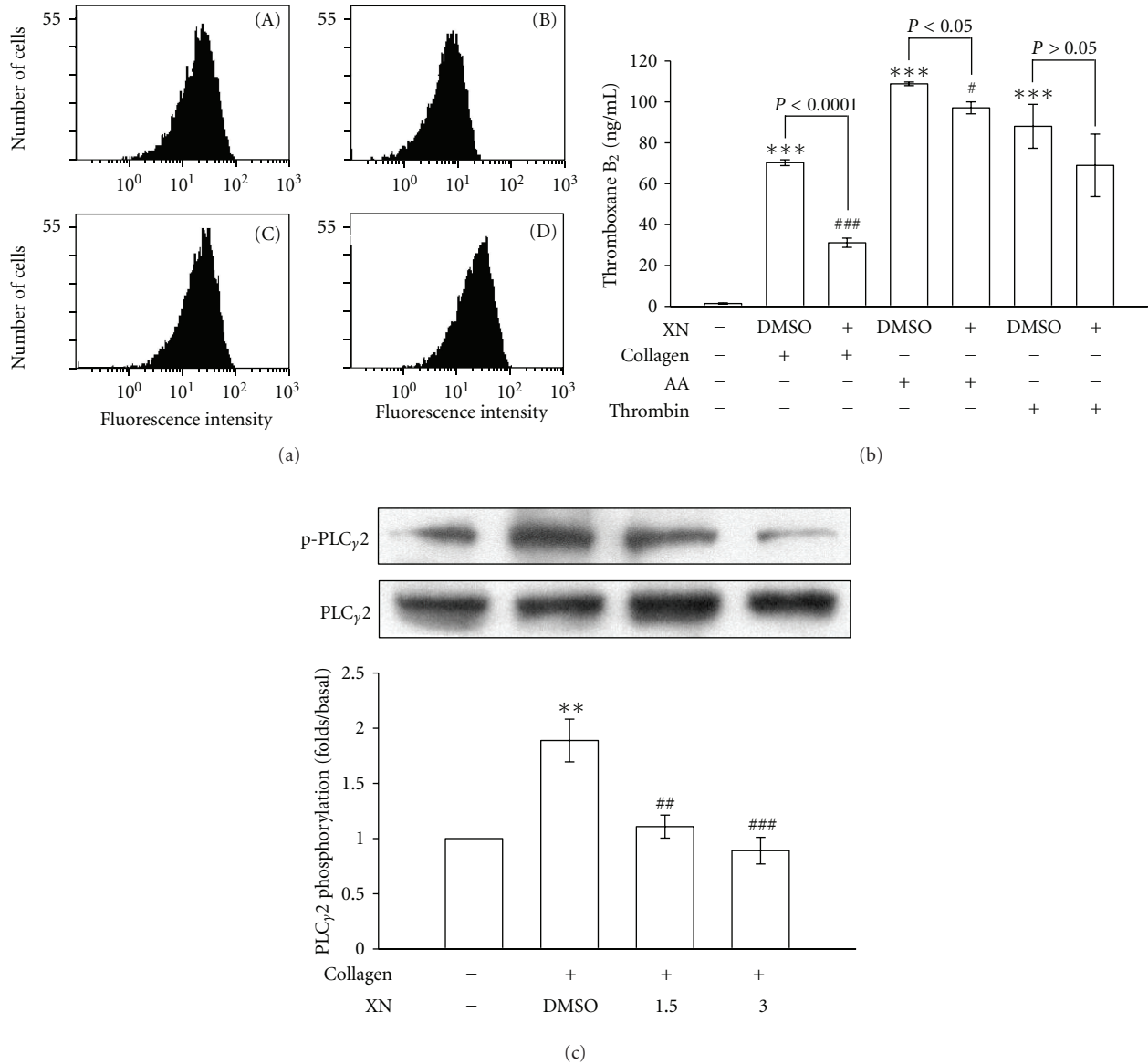


FIGURE 2: Effects of xanthohumol (XN) on FITC-triflavin binding to the $\alpha_{IIb}\beta_3$ integrin, thromboxane B₂ formation, and phospholipase C γ 2 (PLC γ 2) phosphorylation in activated platelets. (a) The solid line represents the fluorescence profiles of (A) 2 μ g/mL FITC-triflavin in the absence of XN as a positive control, (B) in the presence of 5 mM EDTA as a negative control, or in the presence of (C) 1.5 and (D) 3 μ M XN, followed by the addition of 2 μ g/mL FITC-triflavin. For other experiments, washed platelets were preincubated with 3 μ M XN or 0.5% DMSO, followed by the addition of 1 μ g/mL collagen, 60 μ M arachidonic acid (AA), or 0.05 U/mL thrombin to trigger platelet activation. Cells were collected, and subcellular extracts were analyzed for (b) thromboxane B₂ formation, and (c) PLC γ 2 phosphorylation as described in Section 2. Profiles (a) are representative examples of five similar experiments. Data ((b) and (c)) are presented as the means \pm S.E.M. ((b), $n = 4$; (c), $n = 6$). ** $P < 0.01$ and *** $P < 0.001$, compared to the resting group; # $P < 0.05$, ## $P < 0.01$ and ### $P < 0.001$, compared to the control (DMSO) group.

JNK1/2) and Akt. Xanthohumol (3 μ M) attenuated the phosphorylation of p38 MAPK (Figure 4(a)), ERK1/2 (Figure 4(b)), JNK1 (Figure 4(c)), and Akt (Figure 4(d)) stimulated by 1 μ g/mL collagen.

3.5. Effects of Xanthohumol on Cyclic Nucleotides, and Nitrate and Hydroxyl Radical (OH \cdot) Formation in Collagen-Activated Platelets. As shown in Figures 5(a) and 5(b), ODQ (20 μ M)

and SQ22536 (100 μ M), inhibitors of guanylate cyclase and adenylate cyclase, obviously reversed nitroglycerin (NTG; 10 μ M) and PGE₁-(10 μ M) mediated inhibition of platelet aggregation stimulated by collagen, respectively; however, neither inhibitor responded to xanthohumol (3 μ M)-mediated inhibition of platelet aggregation. Xanthohumol (3 μ M) did not significantly increase cyclic AMP or cyclic GMP levels in human platelets (data not shown). Furthermore, NO was quantified using a sensitive

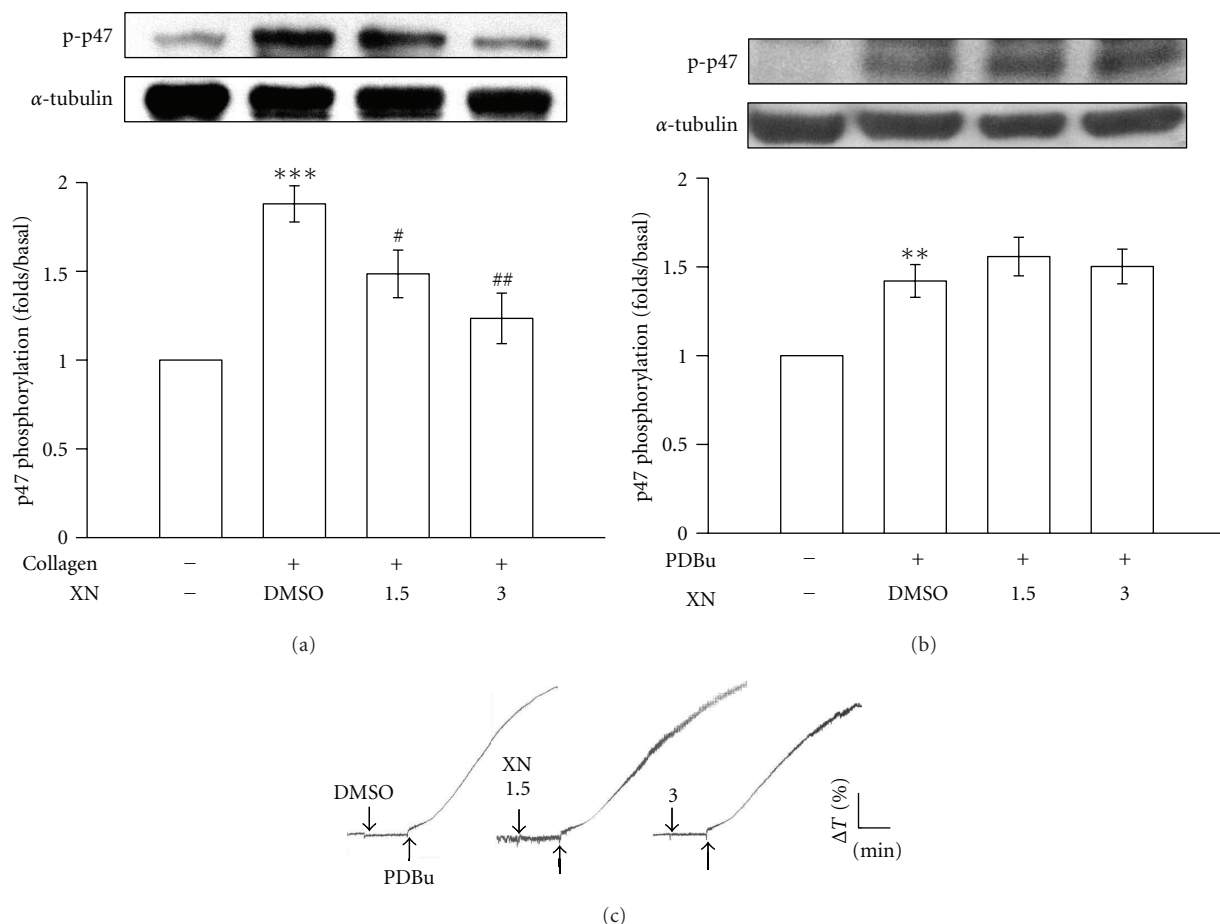


FIGURE 3: Inhibitory activity of xanthohumol (XN) on protein kinase C (PKC) activation in activated platelets. Washed platelets were preincubated with 1.5 and 3 μ M XN or 0.5% DMSO, followed by the addition of 1 μ g/mL collagen or 150 nM PDBu to trigger ((a) and (b)) PKC activation or (c) platelet aggregation. Cells were collected, and subcellular extracts were analyzed for ((a) and (b)) phosphorylation of the PKC substrate (p-p47) as described in Section 2. Data ((a) and (b)) are presented as the means \pm S.E.M. ($n = 5$). ** $P < 0.01$ and *** $P < 0.001$ compared to the resting group; # $P < 0.05$ and ## $P < 0.01$ compared to the control (DMSO) group. Profiles (c) are representative examples of three similar experiments.

and specific ozone redox-chemiluminescence detector as shown in Figure 5(c). The production of nitrate markedly increased with 10 μ M NTG activation compared to the resting group, whereas xanthohumol (1.5 and 3 μ M) did not reach statistical significance. On the other hand, a typical ESR signal of hydroxyl radical (OH^\bullet) formation was triggered in collagen-activated platelets compared to resting platelets (Figure 5(d) (A, B)), and treatment with xanthohumol (1.5 and 3 μ M) obviously reduced hydroxyl radical formation stimulated by collagen (Figure 5(d) (C, D)).

4. Discussion

This study reveals for the first time that xanthohumol, besides its well-known anticancer properties, also possesses potent antiplatelet activity. Xanthohumol is the major prenylflavonoid of hops (0.1% ~ 1% on a dry weight basis) [16], and xanthohumol and its related prenylflavonoids are known to be contained in beer as a dietary source. The average person in the USA consumed 225 mL/day of beer in 2001 [16].

Therefore, the daily intake of total prenylflavonoids would be approximately 0.14 mg. Studies of the pharmacokinetics revealed that the maximal plasma concentration was approximately 180 nM after 4 h of oral administration of 50 mg/kg xanthohumol in rats [16]. Indeed, dietary intake of prenylflavonoids (xanthohumol) through normal beer consumption would not be sufficient to achieve plasma concentrations that could inhibit platelet activation. Ideally, atherothrombotic prevention is achieved by long-term exposure to nontoxic agents, preferably as part of certain food products or nutritional supplements. Xanthohumol showed no toxicity to liver cells nor did it inhibit mitochondrial respiration or uncouple oxidative phosphorylation in isolated rat liver mitochondria at 10 μ M [17]. Therefore, xanthohumol is considered to be the best phytochemical isolated from hops to investigate antiplatelet functions.

Gerhauser et al. [4] reported that xanthohumol can be an effective anti-inflammatory agent by inhibiting endogenous prostaglandin synthesis through inhibition of cyclooxygenases (constitutive COX-1 and inducible COX-2). In the

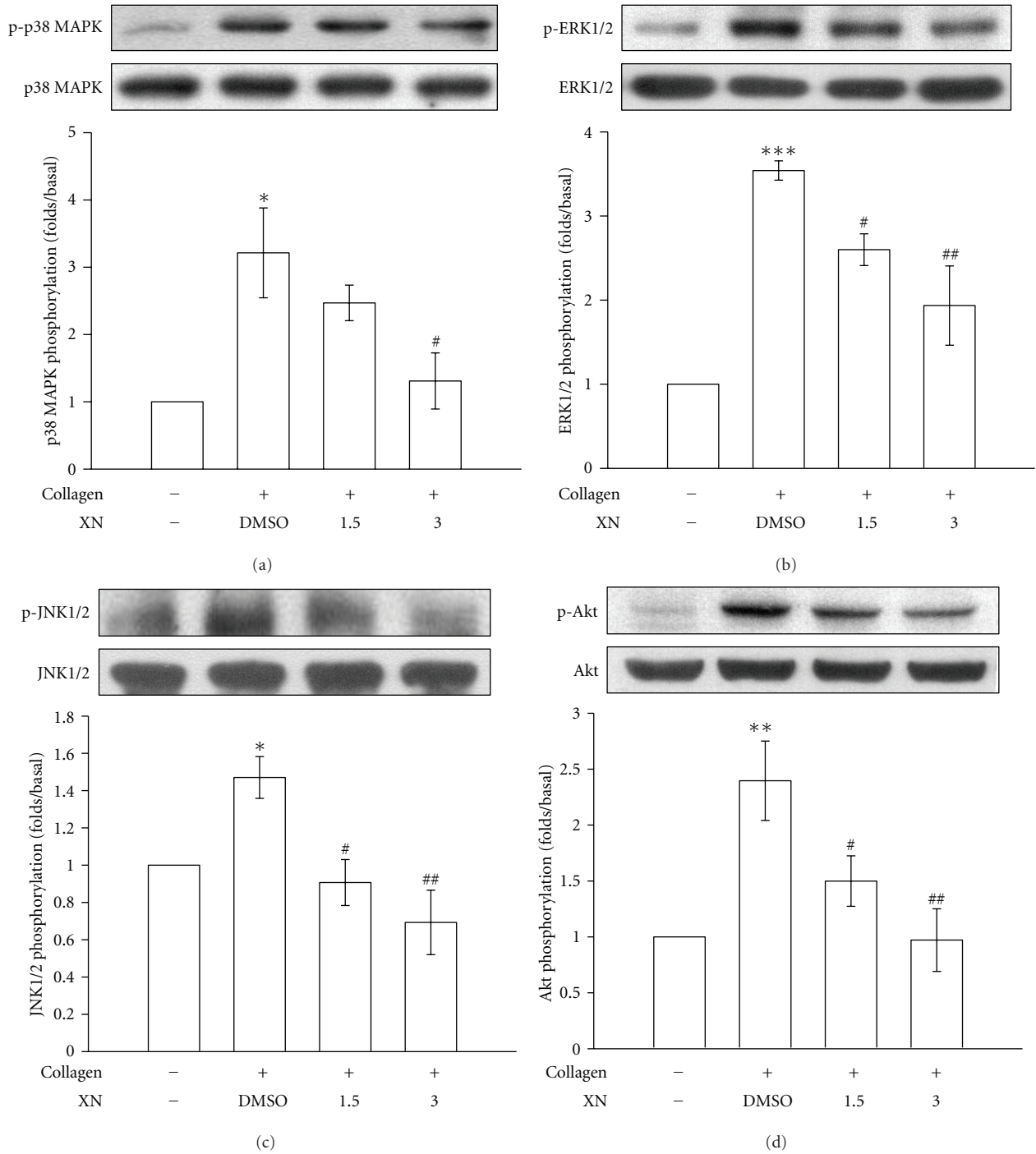


FIGURE 4: Xanthohumol (XN) on p38 MAPK, ERK1/2, JNK1/2, and Akt phosphorylation in collagen-activated platelets. Washed platelets (1.2×10^9 cells/mL) were preincubated with 1.5 and $3 \mu\text{M}$ XN or 0.5% DMSO, followed by the addition of $1 \mu\text{g/mL}$ collagen to trigger platelet activation. Cells were collected, and subcellular extracts were analyzed for (a) p38 MAPK, (b) ERK1/2, (c) JNK1/2, and (d) Akt phosphorylation. Data are presented as the means \pm S.E.M. ($n = 4$). * $P < 0.05$, ** $P < 0.01$, and *** $P < 0.001$, compared to the resting group; # $P < 0.05$ and ## $P < 0.01$, compared to the control (DMSO) group.

present study, collagen-induced thromboxane B₂ formation, a stable metabolite of thromboxane A₂, was also markedly inhibited by xanthohumol. In platelets, AA is released from cell membranes and converted to thromboxane A₂. Thromboxane A₂ is important for collagen- and AA-induced platelet aggregation, which may explain the more-potent activity

of xanthohumol in inhibiting collagen- and AA-induced platelet aggregation than other agonists (i.e., thrombin). Stimulation of platelets by agonists (i.e., collagen) causes marked alterations in phospholipid metabolism. Activation of PLC results in the production of IP₃ and DAG, which activates PKC, inducing protein phosphorylation (p47) [18].

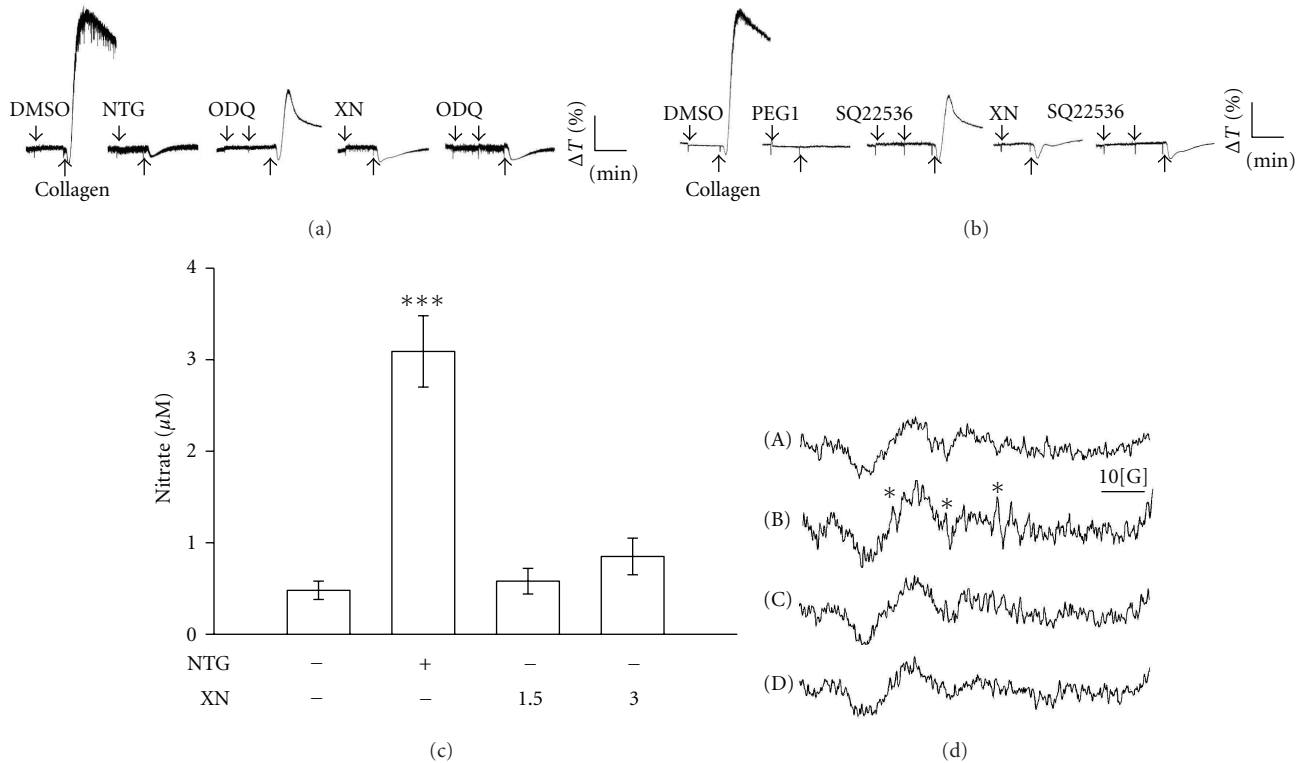


FIGURE 5: Regulation of platelet aggregation, nitrate formation, and hydroxyl radical (OH^\bullet) formation by xanthohumol (XN). ((a) and (b)) Washed platelets (3.6×10^8 cells/mL) were preincubated with $10 \mu\text{M}$ prostaglandin E_1 (PGE_1), $10 \mu\text{M}$ nitroglycerin (NTG), or $3 \mu\text{M}$ XN in the absence or presence of $20 \mu\text{M}$ ODQ or $100 \mu\text{M}$ SQ22536, followed by the addition of $1 \mu\text{g}/\text{mL}$ collagen to trigger platelet aggregation. Profiles are representative examples of three similar experiments. On the other hand, (c) washed platelets (10^9 cells/mL) were incubated with $10 \mu\text{M}$ nitroglycerin (NTG), and 1.5 and $3 \mu\text{M}$ XN. Cells were then collected, and subcellular extracts were analyzed for nitrate formation as described in Section 2. Data are presented as the means \pm S.E.M. ($n = 4$). *** $P < 0.001$, compared to the resting group. (d) For the electron spin resonance (ESR) study, washed platelets (3.6×10^8 cells/mL) were incubated with (A) Tyrode's solution only (resting group), or platelets were preincubated with (B) the control (0.5% DMSO), (C) $1.5 \mu\text{M}$, or (D) $3 \mu\text{M}$ XN followed by the addition of $1 \mu\text{g}/\text{mL}$ collagen to trigger hydroxyl radical formation. Spectra are representative examples of three similar experiments. An asterisk (*) indicates the formation of hydroxyl radicals.

PKC activation represents a strategy adopted by cells to allow selected responses to specific activating signals in distinct cellular compartments [19]. $\text{PLC}\gamma 2$ is involved in collagen-dependent signaling in platelets [20]. In this study, both $\text{PLC}\gamma 2$ phosphorylation and PKC activation were inhibited by xanthohumol, suggesting that xanthohumol-mediated antiplatelet activity is involved in inhibiting the $\text{PLC}\gamma 2$ -PKC signal pathway.

MAPKs consist of three major subgroups. ERKs (p44 ERK1 and p42 ERK2) are involved in proliferation, adhesion, and cell progression [21]. p38 MAPK and JNKs, which include the 46-kDa JNK1 and 55-kDa JNK2 isoforms, are involved in apoptosis [21]. ERK2, JNK1, and p38 MAPK were all identified in platelets [21]. The physiopathological roles of JNK1/2 and ERK1/2 are unclear in platelets, but they were suggested to be suppressors of $\alpha_{\text{IIb}}\beta_3$ integrin activation or negative regulators of platelet activation [22]. On the other hand, p38 MAPK provides a crucial signal for aggregation caused by collagen. We found that SB203580, an inhibitor of p38MAPK, markedly inhibited $1 \mu\text{g}/\text{mL}$ collagen-induced platelet aggregation (data not shown). Among the numerous downstream targets of p38 MAPK,

the most physiologically relevant one in platelets is cytosolic phospholipase A_2 (cPLA_2) which catalyzes AA release to produce thromboxane A_2 [23]; thus, MAPKs (especially p38 MAPK) appear to have a pivotal role in platelet activation. On the other hand, knockout of Akt in mice resulted in defects of platelet activation stimulated by agonists [24, 25]. Akt functions as one of several downstream effectors of PI3-kinase [26]. Recently, we found that both p38 MAPK and PI3-kinase/Akt act in mutual activation as upstream regulators of PKC in activated platelets [27]. Therefore, Akt phosphorylation seems to play a crucial role in platelet activation. On the other hand, activation of human platelets is inhibited by two intracellular pathways regulated by either cyclic AMP or cyclic GMP. The importance of cyclic nucleotides in modulating platelet reactivity is well established [28]. In addition to inhibiting most platelet responses, elevated levels of cyclic nucleotides decrease intracellular Ca^{2+} concentrations by the uptake of Ca^{2+} into the dense tubular system (DTS) which negatively affects the actions of PLC and PKC [28]. Therefore, cyclic AMP and cyclic GMP act synergistically to inhibit platelet aggregation. In addition, platelets produce NO in smaller amounts than do

endothelial cells [29]. Most cellular actions of NO occur via stimulation of intracellular guanylate cyclase, leading to increases in cyclic GMP. In this study, we found that xanthohumol-mediated antiplatelet activity, at least in part, was not regulated by NO or cyclic nucleotides.

Reactive oxygen species (ROS; hydrogen peroxide, hydroxyl radicals, etc.) derived from platelet activation might amplify platelet reactivity during *in vivo* thrombus formation. Free radical species act as secondary messengers that increase cytosolic Ca^{2+} during the initial phase of platelet activation processes, and PKC is involved in receptor-mediated free radical production in platelets [12]. It is also evident that some of the hydrogen peroxide produced by platelets is converted into hydroxyl radicals, as platelet aggregation can be inhibited by hydroxyl radical scavengers [12]. ROS-scavenging activity of xanthohumol was studied by Gerhauser et al. [4] who found that xanthohumol was about 9-fold more potent than trolox at a concentration of $1\ \mu\text{M}$ at scavenging hydroxyl and peroxy radicals as analyzed by an indirect method of an oxygen radical antioxidant capacity (ORAC) assay. In the present study, a similar result, obtained from the ESR study in which xanthohumol scavenges OH^{\bullet} formation, provided direct evidence of its free radical-scavenging activity.

Data generated in this investigation suggest that xanthohumol has a novel role in antiplatelet activation and can likely be used as a nutritional or dietary supplement as a prophylactic. Generally, a nutritional or dietary supplement is required to demonstrate a prophylactic effect in humans which may depend on individual characteristics; hence it may be impossible to delineate a selection of doses for time-course treatment, since it may vary from one individual to another. Nevertheless, this study provides new insights describing the mechanisms of xanthohumol at the studied doses in blocking specific signaling events during agonist-induced platelet activation.

In conclusion, the most important findings of this study demonstrate for the first time that the very potent antiplatelet activity of xanthohumol may initially inhibit the PI3-kinase/Akt, p38 MAPK and PLC γ 2-PKC cascades, followed by inhibition of thromboxane A_2 formation, thereby leading to inhibition of $[\text{Ca}^{2+}]_i$ and finally inhibition of platelet aggregation. Platelet aggregation plays important pathophysiological roles in a variety of thromboembolic disorders. Therefore, the novel role of xanthohumol in antiplatelet activation may represent high therapeutic potential for treating or preventing such diseases, in addition to it originally being considered as a chemopreventive agent.

Acknowledgments

This work was supported by Grants from the National Science Council of Taiwan (NSC97-2320-B-038-016-MY3), Hsinchu Mackay Memorial Hospital (MMH-HB-99-0501 and MMH-HB-100-0301), the Tungs' Taichung MetroHarbor Hospital (TTM-TMU-98-03), and Shin Kong Wu Ho-Su Memorial Hospital (SKH-8302-101-NDR-09). Dr. Y.M. Lee, Dr. K.H. Hsieh, and Dr. W.J. Lu contributed equally to this work.

References

- [1] J. M. Genkinger, E. A. Platz, S. C. Hoffman, G. W. Comstock, and K. J. Helzlsouer, "Fruit, vegetable, and antioxidant intake and all-cause, cancer, and cardiovascular disease mortality in a community-dwelling population in Washington County, Maryland," *American Journal of Epidemiology*, vol. 160, no. 12, pp. 1223–1233, 2004.
- [2] P. Zanoli and M. Zavatti, "Pharmacognostic and pharmacological profile of *Humulus lupulus* L.," *Journal of Ethnopharmacology*, vol. 116, no. 3, pp. 383–396, 2008.
- [3] N. T. Xuan, E. Shumilina, E. Gulbins, S. Gu, F. Götz, and F. Lang, "Triggering of dendritic cell apoptosis by xanthohumol," *Molecular Nutrition and Food Research*, vol. 54, supplement 2, pp. S214–S224, 2010.
- [4] C. Gerhauser, A. Alt, E. Heiss et al., "Cancer chemopreventive activity of Xanthohumol, a natural product derived from hop," *Molecular Cancer Therapeutics*, vol. 1, no. 11, pp. 959–969, 2002.
- [5] K. B. Harikumar, A. B. Kunnumakkara, K. S. Ahn et al., "Modification of the cysteine residues in I κ B α kinase and NF- κ B (p65) by xanthohumol leads to suppression of NF- κ B-regulated gene products and potentiation of apoptosis in leukemia cells," *Blood*, vol. 113, no. 9, pp. 2003–2013, 2009.
- [6] E. C. Colgate, C. L. Miranda, J. F. Stevens, T. M. Bray, and E. Ho, "Xanthohumol, a prenylflavonoid derived from hops induces apoptosis and inhibits NF-kappaB activation in prostate epithelial cells," *Cancer Letters*, vol. 246, no. 1-2, pp. 201–209, 2007.
- [7] A. Albini, R. Dell'Eva, R. Vené et al., "Mechanisms of the antiangiogenic activity by the hop flavonoid xanthohumol: NF- κ B and Akt as targets," *The FASEB Journal*, vol. 20, no. 3, pp. 527–529, 2006.
- [8] E. Lupinacci, J. Meijerink, J. P. Vincken, B. Gabriele, H. Gruppen, and R. F. Witkamp, "Xanthohumol from hop (*Humulus lupulus* L.) Is an efficient inhibitor of monocyte chemoattractant protein-1 and tumor necrosis factor- α release in LPS-stimulated RAW 264.7 mouse macrophages and U937 human monocytes," *Journal of Agricultural and Food Chemistry*, vol. 57, no. 16, pp. 7274–7281, 2009.
- [9] C. Dorn, B. Kraus, M. Motyl et al., "Xanthohumol, a chalcon derived from hops, inhibits hepatic inflammation and fibrosis," *Molecular Nutrition and Food Research*, vol. 54, supplement 2, pp. S205–S213, 2010.
- [10] J. R. Sheu, C. R. Lee, C. H. Lin et al., "Mechanisms involved in the antiplatelet activity of Staphylococcus aureus lipoteichoic acid in human platelets," *Thrombosis and Haemostasis*, vol. 83, no. 5, pp. 777–784, 2000.
- [11] B. Olas, J. Kolodziejczyk, B. Wachowicz, D. Jędrejek, A. Stochmal, and W. Oleszek, "The extract from hop cones (*Humulus lupulus*) as a modulator of oxidative stress in blood platelets," *Platelets*, vol. 22, no. 5, pp. 345–352, 2011.
- [12] J. R. Sheu, W. C. Hung, C. H. Wu et al., "Reduction in lipopolysaccharide-induced thrombocytopenia by triflavin in a rat model of septicemia," *Circulation*, vol. 99, no. 23, pp. 3056–3062, 1999.
- [13] D. S. Chou, G. Hsiao, M. Y. Shen, Y. J. Tsai, T. F. Chen, and J. R. Sheu, "ESR spin trapping of a carbon-centered free radical from agonist-stimulated human platelets," *Free Radical Biology and Medicine*, vol. 39, no. 2, pp. 237–248, 2005.
- [14] W. D. Singer, H. A. Brown, and P. C. Sternweis, "Regulation of eukaryotic phosphatidylinositol-specific phospholipase C and phospholipase D," *Annual Review of Biochemistry*, vol. 66, pp. 475–509, 1997.

- [15] A. S. Kraft and W. B. Anderson, "Phorbol esters increase the amount of Ca^{2+} , phospholipid-dependent protein kinase associated with plasma membrane," *Nature*, vol. 301, no. 5901, pp. 621–623, 1983.
- [16] J. F. Stevens and J. E. Page, "Xanthohumol and related prenylflavonoids from hops and beer: to your good health!," *Phytochemistry*, vol. 65, no. 10, pp. 1317–1330, 2004.
- [17] C. L. Miranda, J. F. Stevens, A. Helmrich et al., "Antiproliferative and cytotoxic effects of prenylated flavonoids from hops (*Humulus lupulus*) in human cancer cell lines," *Food and Chemical Toxicology*, vol. 37, no. 4, pp. 271–285, 1999.
- [18] P. Mangin, Y. Yuan, I. Goncalves et al., "Signaling role for phospholipase $\text{C}\gamma 2$ in platelet glycoprotein $\text{Ib}\alpha$ calcium flux and cytoskeletal reorganization: involvement of a pathway distinct from $\text{Fc}\gamma\text{R}$ chain and $\text{Fc}\gamma\text{RIIA}$," *Journal of Biological Chemistry*, vol. 278, no. 35, pp. 32880–32891, 2003.
- [19] A. Pascale, M. Amadio, S. Govoni, and F. Battaini, "The aging brain, a key target for the future: the protein kinase C involvement," *Pharmacological Research*, vol. 55, no. 6, pp. 560–569, 2007.
- [20] A. Ragab, S. Séverin, M. P. Gratacap et al., "Roles of the C-terminal tyrosine residues of LAT in GPVI-induced platelet activation: insights into the mechanism of $\text{PLC}\gamma 2$ activation," *Blood*, vol. 110, no. 7, pp. 2466–2474, 2007.
- [21] F. Bugaud, F. Nadal-Wollbold, S. Lévy-Toledano, J. P. Rosa, and M. Bryckaert, "Regulation of c-Jun-NH2 terminal kinase and extracellular-signal regulated kinase in human platelets," *Blood*, vol. 94, no. 11, pp. 3800–3805, 1999.
- [22] P. E. Hughes, M. W. Renshaw, M. Pfaff et al., "Suppression of integrin activation: a novel function of a Ras/Raf-initiated MAP kinase pathway," *Cell*, vol. 88, no. 4, pp. 521–530, 1997.
- [23] L. Coulon, C. Calzada, P. Moulin, E. Véricel, and M. Lagarde, "Activation of p38 mitogen-activated protein kinase/cytosolic phospholipase A2 cascade in hydroperoxide-stressed platelets," *Free Radical Biology and Medicine*, vol. 35, no. 6, pp. 616–625, 2003.
- [24] J. Chen, S. De, D. S. Damron, W. S. Chen, N. Hay, and T. V. Byzova, "Impaired platelet responses to thrombin and collagen in AKT-1-deficient mice," *Blood*, vol. 104, no. 6, pp. 1703–1710, 2004.
- [25] D. Woulfe, H. Jiang, A. Morgans, R. Monks, M. Birnbaum, and L. F. Brass, "Defects in secretion, aggregation, and thrombus formation in platelets from mice lacking Akt2," *Journal of Clinical Investigation*, vol. 113, no. 3, pp. 441–450, 2004.
- [26] T. F. Franke, S. I. Yang, T. O. Chan et al., "The protein kinase encoded by the Akt proto-oncogene is a target of the PDGF-activated phosphatidylinositol 3-kinase," *Cell*, vol. 81, no. 5, pp. 727–736, 1995.
- [27] W.-J. Lu, J.-J. Lee, D.-S. Chou et al., "A novel role of andrographolide, an NF-kappa B inhibitor, on inhibition of platelet activation: the pivotal mechanisms of endothelial nitric oxide synthase/cyclic GMP," *Journal of Molecular Medicine*, vol. 89, no. 12, pp. 1261–1273, 2011.
- [28] U. Walter, M. Eigenthaler, J. Geiger, and M. Reinhard, "Role of cyclic nucleotide-dependent protein kinases and their common substrate VASP in the regulation of human platelets," *Advances in Experimental Medicine and Biology*, vol. 344, pp. 237–249, 1993.
- [29] E. Gkaliagkousi, J. Ritter, and A. Ferro, "Platelet-derived nitric oxide signaling and regulation," *Circulation Research*, vol. 101, no. 7, pp. 654–662, 2007.

Research Article

The Observation of Humoral Responses after Influenza Vaccination in Patients with Rheumatoid Arthritis Treated with Japanese Oriental (Kampo) Medicine: An Observational Study

Toshiaki Kogure,¹ Naoyuki Harada,¹ Yuko Oku,² Takeshi Tatsumi,¹ and Atsushi Niizawa³

¹ Department of Japanese Oriental Medicine, Gunma Central and General Hospital, Maebashi Gunma 371-0025, Japan

² Department of Internal Medicine, Gunma Central and General Hospital, Maebashi Gunma 371-0025, Japan

³ Department of Japanese Oriental Medicine, Kobe Century Memorial Hospital, Japan

Correspondence should be addressed to Toshiaki Kogure, gch-kogure@kl.wind.ne.jp

Received 2 December 2011; Accepted 1 February 2012

Academic Editor: Vincenzo De Feo

Copyright © 2012 Toshiaki Kogure et al. This is an open access article distributed under the Creative Commons Attribution License, which permits unrestricted use, distribution, and reproduction in any medium, provided the original work is properly cited.

Objective. The efficacy of influenza vaccination in patients treated with Japanese Oriental (Kampo) Medicine is unknown. The objectives of this study were to observe the efficacy of influenza vaccination in RA patients treated with Kampo. **Methods.** Trivalent influenza subunit vaccine was administered to 45 RA patients who had received Kampo. They were divided into 2 groups: RA patients treated without MTX (“without MTX group”) and treated with MTX (“with MTX group”). Antibody titers were measured before and 4 weeks after vaccination using hemagglutination inhibition assay. **Results.** Geometric mean titers (GMTs) of anti-influenza antibodies significantly increased for all influenza strains. Response to the influenza vaccination in RA patients treated with Kampo was not lower than that of healthy subjects and the response in the “with MTX group” had a tendency to be higher than that in RA patients treated with MTX in the previous study. There was no significant difference in the GMT after 4 weeks between the “with MTX group” and the “without MTX group.” A decreased efficacy in both seroprotection and seroconversion was not found in the “with MTX group.” **Conclusion.** These observations may open the way for further clinical trials to establish the efficacy for the influenza vaccination in RA patients treated with Kampo.

1. Introduction

Rheumatoid arthritis (RA) is a systemic autoimmune disease that is associated with immunologic changes in T cells and B cells. In patients with RA, an impaired ability to react to antigens and an increased peripheral blood CD4/CD8 ratio has been observed in T cells [1, 2]. The presence of soluble interleukin-2 (IL-2) receptors in serum has showed T cell activation [2, 3]. Furthermore, T cell receptor rearrangement excision circles measured from T cells from RA patients were substantially lower than those in healthy controls, because the T cell receptor repertoire has been oligoclonal, which suggests on antigen selection and restriction of the repertoire [4]. There is also a decline in the thymic output of T cells. This premature aging of T cells in RA may have very severe effects on vaccine responses, which are well known to decrease with aging [5]. Additionally, the function of regula-

tory T cells (CD4+, CD25+) may be abnormal in active RA patients, with a lack of suppression of CD4+ or CD8+ T cells [6].

The multiple immunologic effects of the disease process may in part explain why patients with RA are considered immunocompromised and at increased risk of infection [7]. Therefore, although the exact prevalence, morbidity, and mortality of influenza in patients with RA are unknown, a yearly influenza vaccination is recommended [8]. The influenza vaccination is safe and results in protective levels of anti-influenza antibodies in most RA patients, even when they are treated with prednisone, disease-modifying antirheumatic drugs (DMARDs), or tumor necrosis factor-blocking agents [9, 10].

In Japan, Japanese traditional herbal (Kampo) Medicine, which is covered by national health insurance, is often

prescribed in the primary care field and is also applied as an alternative treatment for serious diseases such as RA. Since ancient times, many kinds of Kampo formulae have been used traditionally and are found to be clinically effective for RA treatment. These formulae usually contain components from several medicinal plants that are thought to exert anti-inflammation and immune-regulator effects and are effective for treating RA [11–13]. We have demonstrated that kampo formula possessed antirheumatic effects in vitro and in vivo [14, 15]. Furthermore, we have observed that the administration of kampo formula partially suppressed T cell activation in collagen induced arthritis (CIA) mice [16]. However, the effectiveness of the influenza vaccination in RA patients treated with Kampo remedy is still not known. The purpose of this study is to investigate the response to the influenza vaccination in RA patients treated with Kampo remedy.

2. Patients and Methods

2.1. Patient's Profile. Patients who visited our department in 2010–2011 had to fulfill the American College of Rheumatology 1987 revised criteria for the classification of RA and were selected in a random sampling method. All patients had been treated with Kampo formulae, which were often administered to the patients with RA.

2.2. Study Design. An observational study design was utilized in this study. Forty-five patients were entered into this design. Patients received the influenza vaccine intramuscularly from October 2010 until January 2011. Immediately before and 4 weeks after vaccination, blood was drawn for the measurement of C-reactive protein levels (CRP), erythrocyte sedimentation rate (ESR), and anti-influenza antibodies. The Disease Activity Score in 28 joints (DAS28) [17] was recorded before and 4 weeks after vaccination. Information on previous influenza vaccinations was obtained from all participants, and adverse effects occurring in the first 7 days post-vaccination were recorded. This study was approved by the Ethics Committee of Gunma Central & General Hospital in Aug 2010.

2.3. Vaccine. We used a trivalent influenza subunit vaccine (2010–2011; Daiichi-Sankyo co.ltd Tokyo Japan) containing purified hemagglutinin and neuramidase of the following strains: A/California/7/2009 (H1N1)-like strain (A/H1N1 strain), A/Victoria/210/2009 (H3N2)-like strain (A/H3N2 strain), and B/Brisbane/60/2008-like strain (B strain).

2.4. Hemagglutination Inhibition Assay (HIA). The HIA was used for the detection of anti-influenza antibodies. HIAs were performed with guinea pig erythrocytes in accordance with standard procedures [18]. The following parameters for efficacy of the vaccination based on the anti-influenza antibody response were evaluated: geometric mean titer (GMT), fold increase in titer, 4-fold titer rise resulting in a postvaccination level of 40 (seroconversion), and titer rise to $40 \geq$ (seroprotection). HIA titers 40 are generally considered to be protective in healthy adults [19].

3. Results

3.1. Patient Characteristics. Forty-five RA patients were administered Kampo treatment. They were divided into 2 groups as follows: 16 RA patients treated without MTX (without MTX group) and 23 RA patients treated with MTX (with MTX group). Patients treated with tacrolimus (TAC) or biologics were excluded from the patients in the without MTX group, and patients treated with biologics were excluded from the patients in both the with MTX and without MTX group. Their characteristics were shown in Table 1.

3.2. The Response to the Influenza Vaccination. Each GMT after 4 weeks vaccination was 78.8 ± 119.7 , 35.7 ± 33.6 , and 27.3 ± 27.3 in A/H1N1, A/H3N2, and B strain, respectively (Table 2). Response to the influenza vaccination in RA patients treated with Kampo formulae was not lower than that of healthy subjects in previous studies [20, 21]. There was no significant difference in the GMT after 4 weeks between the “with MTX group” and the “without MTX group.” The GMT in the with MTX group was higher than in the without MTX group (Table 2). The response in the with MTX group had a tendency to be higher than that in RA patients treated with MTX in the previous study [21]. Furthermore, we calculated the fold increase as well as the GMT. The mean fold increase in each group was as follows: 6.5, 2.6, and 2.1, respectively (Table 2). The fold increase in the with MTX group also had a tendency to be higher than in the without MTX group, although this was not significant.

3.3. Seroprotection and Seroconversion. After 4 weeks vaccination, the percentage of patients who possessed the $40 \geq$ titer in A/H1N1 was 53.3, 50.0, and 65.2% in total RA patients, without MTX group and with MTX group, respectively (Figure 1). There was no significant difference between the with MTX and the without MTX groups and a decreased efficacy in seroprotection was not found in the with MTX group. In A/H3N2, the percentage of patients who possessed the $40 \geq$ titer was 46.7, 50.0, and 52.2%, and in the B strain, 28.9, 25.0, and 39.1% in total RA patients, without MTX group, and with MTX group, respectively. The seroprotection effect observed in the with MTX group had a tendency to be higher than results in the previous study [21]. In seroconversion, the percentage of patients who possessed $40 \geq$ titer induced by 4-fold increase was 40.0, 35.6, and 15.6%, respectively (A/H1N1, A/H3N2, and B Strain). There was no significant difference between the with MTX and the without MTX groups also in seroconversion (data not shown).

3.4. The Influence of Influenza Vaccination upon RA Disease Activity. The DAS28 did not change after vaccination. There was no adverse reaction by influenza vaccination.

4. Discussion

Kampo medicine, which is covered by national health insurance in Japan, is often prescribed in the primary care field,

TABLE 1: Characteristics at baseline of RA patients in this study.

	Total	Without MTX group*	With MTX group**
Age, mean \pm SD years	56.2 \pm 13.5	58.6 \pm 10.5	54.1 \pm 12.6
No. (%) female/No. (%) male	42 (93)/3 (7)	15 (94)/1 (6)	22 (92)/2 (8)
Duration of RA mean \pm SD years	12.2 \pm 14.1	13.5 \pm 15.6	10.9 \pm 11.6
MTX dosage, mean \pm mg/week	5.1 \pm 3.8	0	7.6 \pm 2.5
PSL dosage, mean \pm SD mg/day	2.1 \pm 2.0	1.6 \pm 1.5	2.4 \pm 1.9
Taking DMARDs, No.			
Bucillamine	1	1	0
Sulfasalazine	11	8	2
Tacrolimus	4	0	4
DAS28 CRP	3.2 \pm 1.1	2.9 \pm 1.0	3.3 \pm 1.4

*Without MTX group: patients treated with classical DMARDs alone. Patients treated with tacrolimus were excluded. **with MTX group: patients treated with MTX, but not biologics.

TABLE 2: GMTs and fold increase in GMT for influenza A/H3N2, A/H1N1, and B strains in RA patients treated with Kampo formulae before and after administration of influenza vaccines.

	Total	Without MTX group*	With MTX group**
GMT, mean \pm SD			
A/H1N1 strain			
Baseline	12.1 \pm 14.0	11.0 \pm 12.1	14.1 \pm 15.0
4 weeks later	78.8 \pm 119.7	39.6 \pm 39.3	115.9 \pm 148.8
A/H3N2 strain			
Baseline	13.5 \pm 13.9	16.0 \pm 19.7	11.7 \pm 10.2
4 weeks later	35.7 \pm 33.6	33.1 \pm 21.8	39.1 \pm 40.2
B strain			
Baseline	12.8 \pm 10.3	13.9 \pm 9.2	11.4 \pm 11.5
4 weeks later	27.3 \pm 27.8	22.8 \pm 19.2	31.4 \pm 34.0
Fold increase, mean (range)			
A/H1N1 strain	6.5 (1 to 64)	3.6 (1 to 16)	8.2 (1 to 64)
A/H3N2 strain	2.6 (1 to 16)	2.1 (1 to 8)	3.3 (1 to 16)
B strain	2.1 (1 to 16)	1.6 (1 to 4)	2.7 (1 to 16)

*Without MTX group: patients treated with classical DMARDs alone. Patients treated with tacrolimus were excluded. **with MTX group: patients treated with MTX, but not biologics.

and is also applied as an alternative remedy for RA. The efficacy for RA of Kampo medicines has been demonstrated by case or case series reports and several clinical trials. From these reports, the clinical effectiveness of Kampo therapy is almost similar to that of classical DMARDs, such as bucillamine (Bc) and salazosulfapyridine (SASP). Additionally, several investigators have demonstrated the immunomodulatory effects of Kampo medicine in RA patients as well as an arthritis mouse model, such as CIA [11, 12, 14]. We have also reported that Kampo therapy resulted in a decrease in serum IL-6 levels, but not TNF- α levels, as well as the suppression of arthritis development, based on the observations of the CIA mouse model [15]. Furthermore, it has been reported that Kampo medicine is probably effective against infection. The efficacy of Kampo therapy on atypical mycobacterium pneumonia and aspiration bacterial pneumonia has been demonstrated [22, 23], and these effects may be caused by immune-regulator effects, but not direct antibacterial effects. On

the other hand, RA patients are susceptible to both viral and bacterial infections. In Japanese RA patients, major causes of death included malignancies (24.2%), respiratory involvement (24.2%) including pneumonia (12.1%) and interstitial lung disease (ILD) (11.1%), cerebrovascular disease (8.0%), and myocardial infarction (7.6%) [24]. Infectious disease is one of the critical factors in the mortality of RA patients. Therefore, a yearly influenza vaccination is recommended by the Center for Disease Control and Prevention (CDC) [25, 26]. However, the immune response to the influenza vaccination has not been reported in RA patients treated with Kampo medicine. This is the first report demonstrating the titer of anti-influenza antibodies before and after influenza vaccination in RA patients administered Kampo formulae.

The response to the influenza vaccination in our population was almost similar to previous results in healthy subjects. Kampo therapy may be beneficial for RA patients from the clinical viewpoint of protection against influenza

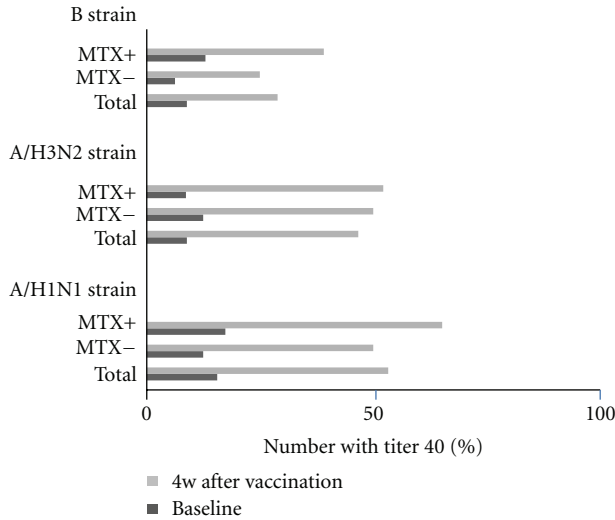


FIGURE 1: Percentage of patients with anti-influenza titers ≥ 40 , as determined by a hemagglutination inhibition assay for each strain after vaccination with a trivalent influenza subunit vaccine, in total RA patients, RA patients treated with MTX, and RA patients treated without MTX. Solid bars represent prevaccination titer ≥ 40 ; open bars represent post vaccination titer ≥ 40 .

virus infection as well as suppression of RA disease activity. However, there are various opinions about the efficacy of the influenza vaccination in RA patients. Some reports demonstrate both no differences and significant differences in the response rate between treatment with and without MTX in RA patients [20, 27–29]. This discrepancy may be caused by the different endpoints when measuring the response to the influenza vaccination and different influenza virus roots. Therefore, our data should be limited in reference to the adjuvant effects of Kampo therapy. However, as the baseline titers in this study were less than previous studies, we consider Kampo therapy to be partially beneficial for RA patients in seroprotection and seroconversion. In addition, it has been reported that the response to vaccination was significantly less in patients treated with anti-TNF- α and anti-CD20 antibody (rituximab) drugs than RA patients without biologics [21, 29]. We have checked the titers of the 5 patients treated with biologics, and they were less than those of other RA patient groups (data not shown). Kampo therapy may not influence the response to the influenza vaccination in RA patients treated with biologics. To analyze this problem, further clinical observational studies will be required using a large number of patients.

The RA disease activity by DAS28 did not change after vaccination in our patients. It is generally thought that the vaccination does not influence the disease activity and the titer of the serological markers. A recent report demonstrates that influenza vaccination did not alter the percentage of healthy adults with positive autoantibodies [30].

We have reported several patients with MTX-resistant RA as being successfully treated with Kampo medicine; however, it is still not clear as to how Kampo medicine acts on arthritis in humans [31]. We previously demonstrated that Kam-

po medicine suppressed polyclonal B cell activation, but not T cell activation, significantly in the CIA mouse model [14, 15]. Recently, it has been clarified that the development of arthritis in the CIA mouse contributed to the differentiation of IL-17 producing cells (Th17), dependent on IL-6 and TGF- β [32, 33]. In our previous study using CIA, Kampo medicine decreased the serum IL-6 levels, but not TNF- α , suggesting that the suppression of Th17 cell activation by Kampo therapy probably improved the development of arthritis. Thus, we suggest that Kampo medicines do not influence the function of antigen presentation in dendrite cells or macrophages. Based on these findings, we suggest that Kampo therapies do not suppress the response to the influenza vaccination in RA patients. Besides, in innate immunity, we have demonstrated that Juzentaihoto enhanced the production of iNOS in macrophages [34] and the upregulation of NK receptor's expression (Killer-cell immunoglobulin-like receptors) in NK cells [35]. Additionally, the direct anti-influenza virus actions of cinnamon cortex and ephedrae herba (the main herbs composing kampo formulae) have been demonstrated, while these actions are not associated with the response to vaccination in RA patients treated with Kampo [36, 37].

In conclusion, we have demonstrated the changes in the titer of each anti-influenza antibody before and after vaccination in RA patients treated with Kampo formula. A low response to the vaccination was not observed compared with previous studies, and in the MTX-treated patients group, the response to vaccination was higher in our study than in previous reports. The present observations may open the way for further clinical trials to establish the efficacy for the influenza vaccination in RA patients treated with Kampo medicines.

Acknowledgment

This paper was supported by a Grant-in-Aid for Scientific Research from the Ministry of Health, Labor, and Welfare in Japan.

References

- [1] J. Verwilghen, S. Vertessen, E. A. Stevens, J. Dequeker, and J. L. Ceuppens, "Depressed T-cell reactivity to recall antigens in rheumatoid arthritis," *Journal of Clinical Immunology*, vol. 10, no. 2, pp. 90–98, 1990.
- [2] J. C. Beckham, D. S. Caldwell, B. L. Peterson et al., "Disease severity in rheumatoid arthritis: relationships of plasma tumor necrosis factor- α , soluble interleukin 2-receptor, soluble CD4/CD8 ratio, neopterin, and fibrin D-dimer to traditional severity and functional measures," *Journal of Clinical Immunology*, vol. 12, no. 5, pp. 353–361, 1992.
- [3] T. Kogure, T. Itoh, Y. Shimada, T. Shintani, H. Ochiai, and K. Terasawa, "Detection of serum soluble markers of immune activation in rheumatoid arthritis," *Mediators of Inflammation*, vol. 5, no. 4, pp. 262–265, 1996.
- [4] K. Koetz, E. Bryl, K. Spickschen, W. M. O'Fallon, J. J. Goronzy, and C. M. Weyand, "T cell homeostasis in patients with rheumatoid arthritis," *Proceedings of the National Academy of Sciences of the United States of America*, vol. 97, no. 16, pp. 9203–9208, 2000.

- [5] T. M. Govaert, C. T. Thijs, N. Masurel, M. J. Sprenger, G. J. Dinant, and J. A. Knottnerus, "The efficacy of influenza vaccination in elderly individuals: a randomized double-blind placebo-controlled trial," *Journal of the American Medical Association*, vol. 272, no. 21, pp. 1661–1665, 1994.
- [6] M. R. Ehrenstein, J. G. Evans, A. Singh et al., "Compromised function of regulatory T cells in rheumatoid arthritis and reversal by anti-TNF α therapy," *Journal of Experimental Medicine*, vol. 200, no. 3, pp. 277–285, 2004.
- [7] F. Wolfe, D. M. Mitchell, J. T. Sibley et al., "The mortality of rheumatoid arthritis," *Arthritis and Rheumatism*, vol. 37, no. 4, pp. 481–494, 1994.
- [8] Centers for Disease Control and Prevention, "Prevention of pneumococcal disease: recommendations of the advisory committee on immunization practices (ACIP)," *Morbidity and Mortality Weekly Report*, vol. 55, pp. 1–42, 2006.
- [9] I. Fomin, D. Caspi, V. Levy et al., "Vaccination against influenza in rheumatoid arthritis: the effect of disease modifying drugs, including TNF α blockers," *Annals of the Rheumatic Diseases*, vol. 65, no. 2, pp. 191–194, 2006.
- [10] A. Chalmers, D. Scheifele, C. Patterson et al., "Immunization of patients with rheumatoid arthritis against influenza: a study of vaccine safety and immunogenicity," *Journal of Rheumatology*, vol. 21, no. 7, pp. 1203–1206, 1994.
- [11] D. M. Chang, W. Y. Chang, S. Y. Kuo, and M. L. Chang, "The effects of traditional antirheumatic herbal medicines on immune response cells," *Journal of Rheumatology*, vol. 24, no. 3, pp. 436–441, 1997.
- [12] K. Asano, J. Matsuishi, Y. Yu, T. Kasahara, and T. Hisamitsu, "Suppressive effects of *Tripterygium wilfordii* Hook f., a traditional Chinese medicine, on collagen arthritis in mice," *Immunopharmacology*, vol. 39, no. 2, pp. 117–126, 1998.
- [13] S. Kobayashi, H. Kobayashi, H. Matsuno, I. Kimura, and M. Kimura, "Inhibitory effects of anti-rheumatic drugs containing magnosalin, a compound from "Shin-I" (*Flos magnoliae*), on the proliferation of synovial cells in rheumatoid arthritis models," *Immunopharmacology*, vol. 39, no. 2, pp. 139–147, 1998.
- [14] A. Niizawa, T. Kogure, L. X. Hai et al., "Clinical and immunomodulatory effects of Fun-boi, an herbal medicine, on collagen-induced arthritis in vivo," *Clinical and Experimental Rheumatology*, vol. 21, no. 1, pp. 57–62, 2003.
- [15] L. X. Hai, T. Kogure, A. Niizawa et al., "Suppressive effect of hochu-ekki-to on collagen induced arthritis in DBA1J mice," *Journal of Rheumatology*, vol. 29, no. 8, pp. 1601–1608, 2002.
- [16] T. Kogure, T. Tatsumi, A. Niizawa, H. Fujinaga, Y. Shimada, and K. Terasawa, "The population of CD40L-expressing cells was slightly but not significant decreased in lymphoid tissues of collagen induced arthritic mice treated with Hochu-Ekki-To," *Yakugaku Zasshi*, vol. 127, no. 3, pp. 547–550, 2007.
- [17] M. L. Prevoo, M. A. van't Hof, H. H. Kuper, M. A. van Leeuwen, L. B. van de Putte, and P. L. van Riel, "Modified disease activity scores that include twenty-eight-joint counts: development and validation in a prospective longitudinal study of patients with rheumatoid arthritis," *Arthritis and Rheumatism*, vol. 38, no. 1, pp. 44–48, 1995.
- [18] A. Holvast, A. Huckriede, J. Wilschut et al., "Safety and efficacy of influenza vaccination in systemic lupus erythematosus patients with quiescent disease," *Annals of the Rheumatic Diseases*, vol. 65, no. 7, pp. 913–918, 2006.
- [19] J. C. de Jong, A. M. Palache, W. E. Beyer, G. F. Rimmelzwaan, A. C. Boon, and A. D. Osterhaus, "Haemagglutination-inhibiting antibody to influenza virus," *Developments in Biologicals*, vol. 115, pp. 63–73, 2003.
- [20] I. Fomin, D. Caspi, V. Levy et al., "Vaccination against influenza in rheumatoid arthritis: the effect of disease modifying drugs, including TNF α blockers," *Annals of the Rheumatic Diseases*, vol. 65, no. 2, pp. 191–194, 2006.
- [21] S. van Assen, A. Holvast, C. A. Benne et al., "Humoral responses after influenza vaccination are severely reduced in patients with rheumatoid arthritis treated with rituximab," *Arthritis and Rheumatism*, vol. 62, no. 1, pp. 75–81, 2010.
- [22] T. Nogami, N. Sekiya, T. Mitsuma, and T. Yamaguchi, "A case of pulmonary Mycobacterium fortuitum infection successfully treated with Kampo treatments," *Kekkaku*, vol. 81, no. 8, pp. 525–529, 2006.
- [23] N. Mantani, Y. Kasahara, T. Kamata et al., "Effect of Seihaito, a Kampo medicine, in relapsing aspiration pneumonia—an open-label pilot study," *Phytomedicine*, vol. 9, no. 3, pp. 195–201, 2002.
- [24] A. Nakajima, E. Inoue, E. Tanaka et al., "Mortality and cause of death in Japanese patients with rheumatoid arthritis based on a large observational cohort, IORRA," *Scandinavian Journal of Rheumatology*, vol. 39, no. 5, pp. 360–367, 2010.
- [25] M. Bijl, N. Agmon-Levin, J. M. Dayer, E. Israeli, M. Gatto, and Y. Shoenfeld, "Vaccination of patients with auto-immune inflammatory rheumatic diseases requires careful benefit-risk assessment," *Autoimmunity Reviews*, *In press*.
- [26] F. Conti, S. Rezai, and G. Valesini, "Vaccination and autoimmune rheumatic diseases," *Autoimmunity Reviews*, vol. 8, no. 2, pp. 124–128, 2008.
- [27] L. Stojanovich, "Influenza vaccination of patients with systemic lupus erythematosus (SLE) and rheumatoid arthritis (RA)," *Clinical and Developmental Immunology*, vol. 13, no. 2–4, pp. 373–375, 2006.
- [28] J. Sibilja and J. F. Maillefert, "Vaccination and rheumatoid arthritis," *Annals of the Rheumatic Diseases*, vol. 61, no. 7, pp. 575–576, 2002.
- [29] S. Oren, M. Mandelboim, Y. Braun-Moscovici et al., "Vaccination against influenza in patients with rheumatoid arthritis: the effect of rituximab on the humoral response," *Annals of the Rheumatic Diseases*, vol. 67, no. 7, pp. 937–941, 2008.
- [30] N. Toplak, T. Kveder, A. Trampus-Bakija, V. Subelj, S. Cucnik, and T. Avcin, "Autoimmune response following annual influenza vaccination in 92 apparently healthy adults," *Autoimmunity Reviews*, vol. 8, no. 2, pp. 134–138, 2008.
- [31] T. Kogure, H. Sato, D. Kishi, T. Ito, and T. Tatsumi, "Serum levels of anti-cyclic citrullinated peptide antibodies are associated with a beneficial response to traditional herbal medicine (Kampo) in rheumatoid arthritis," *Rheumatology International*, vol. 29, no. 12, pp. 1441–1447, 2009.
- [32] C. A. Murphy, C. L. Langrish, Y. Chen et al., "Divergent pro- and antiinflammatory roles for IL-23 and IL-12 in joint autoimmune inflammation," *Journal of Experimental Medicine*, vol. 198, no. 12, pp. 1951–1957, 2003.
- [33] S. Nakae, A. Nambu, K. Sudo, and Y. Iwakura, "Suppression of immune induction of collagen-induced arthritis in IL-17-deficient mice," *Journal of Immunology*, vol. 171, no. 11, pp. 6173–6177, 2003.
- [34] H. Kawamata, H. Ochiai, N. Manlani, and K. Terasawa, "Enhanced expression of inducible nitric oxide synthase by Juzen-Taiho-To in LPS-activated RAW264.7 Cells, a murine macrophage cell line," *American Journal of Chinese Medicine*, vol. 28, no. 2, pp. 217–226, 2000.
- [35] T. Kogure, A. Niizawa, L. X. Hai et al., "Effect of interleukin 2 on killer cell inhibitory receptors in patients with rheumatoid arthritis," *Annals of the Rheumatic Diseases*, vol. 60, no. 2, pp. 166–169, 2001.

- [36] K. Hayashi, N. Imanishi, Y. Kashiwayama et al., "Inhibitory effect of cinnamaldehyde, derived from Cinnamomi cortex, on the growth of influenza A/PR/8 virus in vitro and in vivo," *Antiviral Research*, vol. 74, no. 1, pp. 1–8, 2007.
- [37] N. Mantani, N. Imanishi, H. Kawamata, K. Terasawa, and H. Ochiai, "Inhibitory effect of (+)-catechin on the growth of influenza A/PR/8 virus in MDCK cells," *Planta Medica*, vol. 67, no. 3, pp. 240–243, 2001.

Research Article

Antidepressant-Like Activity of the Ethanolic Extract from *Uncaria lanosa* Wallich var. *appendiculata* Ridsd in the Forced Swimming Test and in the Tail Suspension Test in Mice

Lieh-Ching Hsu,¹ Yu-Jen Ko,¹ Hao-Yuan Cheng,² Ching-Wen Chang,¹ Yu-Chin Lin,³ Ying-Hui Cheng,¹ Ming-Tsuen Hsieh,¹ and Wen Huang Peng¹

¹ School of Chinese Pharmaceutical Sciences and Chinese Medicine Resources, College of Pharmacy, China Medical University, No. 91 Hsueh-Shih Road, Taichung 404, Taiwan

² Department of Nursing, Chung Jen College of Nursing, Health Sciences and Management, No. 1-10 Da-Hu, Hu-Bei Village, Da-Lin Township, Chia-Yi 62241, Taiwan

³ Department of Biotechnology, TransWorld University, No. 1221, Jen-Nang Road, Chia-Tong Li, Douliou, Yunlin 64063, Taiwan

Correspondence should be addressed to Hao-Yuan Cheng, chenghy1974@yahoo.com.tw and Wen Huang Peng, whpeng@mail.cmu.edu.tw

Received 23 November 2011; Revised 30 January 2012; Accepted 30 January 2012

Academic Editor: Vincenzo De Feo

Copyright © 2012 Lieh-Ching Hsu et al. This is an open access article distributed under the Creative Commons Attribution License, which permits unrestricted use, distribution, and reproduction in any medium, provided the original work is properly cited.

This study investigated the antidepressant activity of ethanolic extract of *U. lanosa* Wallich var. *appendiculata* Ridsd (UL_{E_tO_H}) for two-weeks administrations by using FST and TST on mice. In order to understand the probable mechanism of antidepressant-like activity of UL_{E_tO_H} in FST and TST, the researchers measured the levels of monoamines and monoamine oxidase activities in mice brain, and combined the antidepressant drugs (fluoxetine, imipramine, maprotiline, clorgyline, bupropion and ketanserin). Lastly, the researchers analyzed the content of RHY in the UL_{E_tO_H}. The results showed that UL_{E_tO_H} exhibited antidepressant-like activity in FST and TST in mice. UL_{E_tO_H} increased the levels of 5-HT and 5-HIAA in cortex, striatum, hippocampus, and hypothalamus, the levels of NE and MHPG in cortex and hippocampus, the level of NE in striatum, and the level of DOPAC in striatum. Two-week injection of IMI, CLO, FLU and KET enhanced the antidepressant-like activity of UL_{E_tO_H}. UL_{E_tO_H} inhibited the activity of MAO-A. The amount of RHY in UL_{E_tO_H} was 17.12 mg/g extract. Our findings support the view that UL_{E_tO_H} exerts antidepressant-like activity. The antidepressant-like mechanism of UL_{E_tO_H} may be related to the increase in monoamines levels in the hippocampus, cortex, striatum, and hypothalamus of mice.

1. Introduction

Depression, a widespread incapacitating psychiatric ailment, imposes a substantial health burden on society [1]. Affective disorder are characterized by a disturbance of mood associated with alteration in behavior, energy, appetite, sleep, and weight [2]. According to the most accepted hypothesis of depression, the monoamine theory, patients with major depression have symptoms that are reflected changes in brain monoamine neurotransmitters, specifically norepinephrine (NE) and serotonin (5-HT) [3]. Clinical data suggests that dopamine (DA) is also involved in the pathophysiology and treatment of depression [4]. Medications such as tricyclic antidepressants (TCAs), selective

serotonin reuptake inhibitors (SSRIs), monoamine oxidase inhibitors (MAOIs), specific serotonin-norepinephrine reuptake inhibitors (SNRIs), 5-HT₂ receptor antagonists, and other heterocyclics are clinically employed for drug therapy [5]. However, these drugs can impose a variety of side-effects including sedation, apathy, fatigue, sleep disturbance, cognitive impairment, and sexual dysfunction, and so forth. Hence, there remains a pressing need for new effective and better-tolerated antidepressants.

Herbal therapies may be effective alternatives in the treatment of depression, such as *Hypericum perforatum* L. [6], *Cordyceps sinensis* [7], and *Perilla frutescens* [8]. The *Uncaria* species recorded in Chinese Pharmacopoeia and Taiwan Herbal Pharmacopoeia include *Uncaria rhynchophylla*

(Miquel) Jacks (abbrev. as *UR*), *U. macrophylla* Wallich. *U. hirsuta* Haviland (*UH*), *U. sinensis* (Oliver) Havil, and *U. sessilifructus* Roxburgh [9, 10]. According to Flora of Taiwan, there are three different species of *Gouteng* in Taiwan: *UR*, *UH*, and *U. lanosa* Wallich var. *appendiculata* Ridsd (*UL*) [11]. However, *UL* is not recorded in Pharmacopoeia. In traditional Chinese medicine, *Gouteng* is categorized as a herb to extinguish wind, arrest convulsions, clear heat, and pacify the liver [12]. *Gouteng* is mainly used to treat cardiovascular and central nervous system ailments, including light headedness, convulsions, numbness, and hypertension [12]. Several studies demonstrate that the herb extract mainly acts on neuroprotective effect used to treat antiepileptic [13–15], anti-Parkinsonian [16], anti-Alzheimer's disease [17, 18], anxiolytic [19], protective action against ischemia-induced neuronal damage [20, 21], anti-inflammation [22]. Alkaloids are the active pharmacological component in *Gouteng* and comprise components include RHY, isorhynchophylline, hirsutine, hirsuteine, corynantheine, isocorynoxine. RHY exhibited a similar pharmacological activity when compared with *Gouteng* [12]. RHY is an important active component of alkaloids separated from gambir plant (*Gouteng* in Chinese), RHY exerts the protective action primarily by inhibiting of NMDA and 5-HT₂ receptor-mediated neurotoxicity during ischemia [21]. RHY also affects the levels of serotonin in cortex, striatum, hippocampus, and hypothalamus [23, 24]. From the above perspectives, we inferred that RHY is the key component of antidepressant-like activity of *Gouteng*. *Gouteng* possesses neuroprotective effect, regulation of monoamine transporters, macrophage theory [25], and regulation of glutamatergic system [26]. Our preliminary test indicated that ethanolic extract of *U. lanosa* Wallich var. *appendiculata* Ridsd. (*UL*_{EtOH}) contained the largest amount of RHY among *Uncaria* species in Taiwan. However, the antidepressant-like activity of *UL*_{EtOH} has not been investigated, which encouraged us to investigate the effects of *UL*_{EtOH} on depression problems.

In the present study, we aimed to investigate the effect of *UL*_{EtOH} in FST and TST in mice. The behavioral despair tasks have good predictive value for antidepressant potency in humans [27]. Moreover, we investigated whether the effect of *UL*_{EtOH} in FST and TST is dependent on its interaction with the 5-HT, NE, and DA receptors, and the brain monoamine neurotransmitter concentration. MAO activity was also tested by neurochemical and biochemical assays to confirm the participation of monoamine transmitters in treatment involving *UL*_{EtOH}.

2. Materials and Methods

2.1. Animals. Male ICR albino mice (weighing around 22 g), purchased from BioLASCO Taiwan Co., Ltd., were used in the present study. They were maintained at 22 ± 1°C with free access to water and food, under a 12:12 h light/dark cycle (lights on at 08:00 h). All manipulations were carried out between 9:00 and 15:00 h, with each animal used only once. All procedures in this study were performed in accordance with the NIH Guide for the Care and Use of Laboratory

Animals. The experimental protocol was approved by the Committee on Animal Research, China Medical University. The minimum number of animals and duration of observations required to obtain consistent data were used.

2.2. Plant Materials. *Uncaria rhynchophylla* (Miquel) Jacks (*UR*) was collected from SiaoWulai, *U. hirsuta* Haviland (*UH*) was collected from Wulai, and *U. lanosa* Wallich var. *appendiculata* Ridsd (*UL*) was collected from Xuhai, Mudan Township of Taiwan, and was identified by Dr. Chao-Lin Kuo, Leader of the School of Chinese Pharmaceutical Sciences and Chinese Medicine Resources (CPCR). The voucher specimen (Number: CMU-CPCR-UL-10001) was deposited at CPCR.

2.3. Preparation of Plant Extract. Dried 1 kg of *UR*, *UH*, and *UL*, made from the stems and hooks of plants, were sliced into small pieces and ground into a powder, and extracted four times with 5% ammonia solution and 70% ethanol. The extracts were filtered, combined, and concentrated under reduced pressure at 40°C to obtain the *UR*_{EtOH}, *UH*_{EtOH}, *UL*_{EtOH} extracts. The yield ratios of the *UR*_{EtOH}, *UH*_{EtOH}, *UL*_{EtOH} extracts (120 g, 97 g, 115 g) were 12%, 9.7%, 11.5%.

2.4. Drugs and Drug Administration. Imipramine HCl (*IMI*), clorgyline HCl (*CLO*), maprotiline HCl (*MAP*), fluoxetine HCl (*FLU*), bupropion HCl (*BUP*), ketanserin (*KET*), sodium octyl sulfate, norepinephrine HCl (*NE*), dopamine HCl (*DA*), 5-hydroxytryptamine HCl (*5-HT*), 4-Hydroxy-3-methoxyphenylglycol (*MHPG*), 4-dihydroxyphenylacetic acid (*DOPAC*), and 5-hydroxyindoleacetic acid (*5-HIAA*), as well as horseradish peroxidase (*HRP*), benzylamine, amplex red, and phosphate-buffered saline (*PBS*) solution were purchased from Sigma-Aldrich (St. Louis, MO, USA). RHY was purchased from Matsuura Yakugyo Co., Ltd (Japan). Drugs were dissolved in normal saline, except *HRP*, benzylamine, and amplex red that was diluted in *PBS* solution. Citric acid, tri-natriumcitrate-2-hydrate, and EDTA were purchased from Merck. *UR*_{EtOH}, *UH*_{EtOH}, *UL*_{EtOH}, or saline was administered by oral route, whereas the other drugs were administered by i.p. route. The i.p. or p.o. administrations were given in a volume of 10 mL/kg body weight. Tests were performed 1 hr (*UL*_{EtOH}) and 30 min (imipramine, fluoxetine, clorgyline, maprotiline, bupropion, ketanserin) after administration.

2.5. HPLC Analysis of *UR*_{EtOH}, *UH*_{EtOH}, and *UL*_{EtOH}. The HPLC system consisted of a Shimadzu (Kyoto, Japan) LC-10ATvp liquid chromatograph equipped with a DGU-14A degasser, an FCV-10ALvp low-pressure gradient flow control valve, an SIL-10ADvp autoinjector, an SPD-M10Avp diode array detector, and an SCL-10Avp system controller. Peak areas were calculated using Shimadzu Class-LC10 software (Version 6.12 sp5). The column was a Phenomenex Synergi 4_ Fusion-RP 80A column (250 mm × 4.6 mm). The gradient mobile phase was methanol (solvent A) and 0.01 mol/L triethylamine, and adjusted to adjust pH to 7.5 with glacial acetic acid (solvent B) solvent A : B = 60 : 40. The sample was

injected of 10 μ L. The following gradient profile was run at 1.0 mL/min over 60 min. Peaks were detected at 274 nm with SPD-M10AVP (Shimadzu) detector. The peaks of UR_{EtOH}, UH_{EtOH}, and UL_{EtOH} samples were identified by comparison with the standard solutions (RHY). The UR_{EtOH}, UH_{EtOH}, and UL_{EtOH} solutions were quantified by spiking with a known amount of standard and also by comparing the area under curve. The repeatability of the method was evaluated by injecting the solution of UR_{EtOH}, UH_{EtOH}, and UL_{EtOH} and standard solution three times, and the relative standard deviation (RSD) percentage was calculated.

2.6. Behavior Despair Study. For FST and TST, animals were divided into six groups ($n = 10$ /group): control (0.9% saline), the four doses of UL_{EtOH} (0.0625, 0.125, 0.25, 0.5 g/kg) and 10 mg/kg IMI for 14-day treatment.

2.6.1. Forced Swimming Test (FST). The method was carried out on mice according to the method of Porsolt et al. [28]. Mice were placed in an open cylindrical container (diameter 10 cm, height 25 cm), containing 15 cm of water at $25 \pm 1^\circ\text{C}$. The duration of observed immobility was recorded during the last 4 min of the 6-minute testing period [29, 30]. Mice are forced to swim in a restricted space from which they cannot escape and are induced to a characteristic behavior of immobility. Each mouse was judged to be immobile when it ceased struggling and remained floating motionless in the water, making only those movements necessary to keep its head above water. Decrease in the duration of immobility during the FST was taken as a measure of antidepressant activity.

2.6.2. Tail Suspension Test (TST). The total duration of immobility induced by tail suspension was measured according to the method of Steru et al. [31]. Mice both acoustically and visually isolated were suspended 50 cm above the floor by adhesive tape placed approximately 1 cm from the tip of the tail. The time during which mice remained immobile was quantified during a test period of 6 min. Mice were considered immobile only when they hung passively and completely motionless.

2.7. Open-Field Test. For open-field test. Animals were divided into five groups ($n = 6$ /group): control (0.9% saline), the three doses of UL_{EtOH} (0.125, 0.25, 0.5 g/kg), and 10 mg/kg IMI for 14-day treatment.

To assess the effects of UL_{EtOH} on locomotor activity, mice were evaluated in the open-field paradigm as previously described [32]. Animals were individually placed in a box (40 \times 60 \times 50 cm). The mice were placed in the center and their behavior was noted immediately and continued for 5 min. The parameters such as resting time, total movement distance, total movement time, total movement were recorded by video camera and registered in the computer. During the interval of the test the apparatus was cleaned.

2.8. Pharmacological Treatments. We investigated whether the antidepressant-like activity of UL_{EtOH} in FST and TST

is dependent on its interaction with IMI (a tricyclic antidepressant), MAP (a selective NE reuptake inhibitor), FLU (a selective 5-HT reuptake inhibitors), BUP (a selective DA reuptake inhibitor), CLO (a selective MAO-A inhibitor), and KET (a preferential 5-HT_{2A} receptor antagonist). To this end, mice were pretreated with UL_{EtOH} (0.5 g/kg for two weeks' administration) or saline. They received IMI, FLU, KET, CLO (5 mg/kg for two weeks' administration), MAP (20 mg/kg for two weeks' administration), or BUP (4 mg/kg for two weeks' administration) 30 mins before being tested in FST and TST.

The doses of the drugs which do not affect locomotor activity and immobility time were selected on the basis of literature data [33–35] and our preliminary test.

2.9. Determination of Monoamines and Their Metabolites Levels in the Mice Frontal Cortex, Striatum, Hippocampus, and Hypothalamus. Animals were divided into six groups ($n = 6$ /group): control (0.9% saline), control versus FST, the three experiment groups (0.125, 0.25, 0.5 g/kg, for two weeks' administration), and IMI (10 mg/kg for two weeks' administration).

Monoamines were measured according to the method of Renard et al. [36]. Briefly, mice were killed by cervical dislocation without anesthesia just after the FST. The brain was removed after a rapid dissection of frontal cortex, striatum, hippocampus, and hypothalamus were isolated. The four brain tissues were weighed and placed separately in 5 mL of ice-cold homogenizing solution (8.8 mg of ascorbic acid and 122 mg of EDTA in 1000 mL of perchloric acid 0.1 M). After homogenization, the solution was centrifuged at $10,000 \times g$ for 10 min at 4°C . Twenty microliters of the resultant supernatant was injected in the high-performance liquid chromatography (HPLC) system. The levels of monoamines (NE, DA and 5-HT) and their metabolites (MHPG, DOPAC, 5-HIAA) were measured by HPLC (Waters 610) with electrochemical detection in the three brain tissues. The mobile phase [4.2 g/L] citric acid monohydrate, 6.8 g/L sodium acetate trihydrate, 0.8 g/L octanesulfonic acid sodium salt, 0.05 g/L tetrasodium ethylenediamine tetraacetate, 0.02% (v/v) dibutyl amine, and 7% (v/v) methyl alcohol) was delivered at 1.0 mL/min. The reverse-phase column used was a Merk Lichrospher 100 RP-18 endcapped column with a length of 12.5 cm and an internal diameter of 4.0 mm (E. Merk 50734). The compounds were measured at +0.75 V using a Bioanalytical Systems LC-4C electrochemical detector.

2.10. Measurements of Monoamine Oxidase Activity. Animals were divided into five groups ($n = 6$ /group): control (0.9% saline), the three doses of UL_{EtOH} (0.125, 0.25, 0.5 g/kg, for two weeks' administration), and CLO (10 mg/kg for two weeks' administration).

Mice were sacrificed and the brain tissues was rapidly frozen (-80°C) until analyzed. The brain tissues was each homogenized in 50 mM phosphate buffer (pH 7.4) containing 0.5 mM EDTA and 0.25 M sucrose and stored at -80°C . Protein content of the homogenate was determined using the method of Lowry et al. [37]. Mouse brain monoamine

oxidase activity was measured following the method of Zhou and Panchuk-Voloshina [38]. Briefly, For the measurement of each type of MAO, serotonin was used as a substrate for MAO-A and benzylamine for MAO-B. The experiments were conducted at room temperature for 60 min in a reaction mixture with brain homogenates at a final protein concentration of 8 mg/mL. For the sensitivity assay, the brain homogenates with different protein concentrations were incubated in a reaction mixture of 200 mM Amplex Red, 1 mM benzylamine, and 1 U/mL HRP at room temperature for 60 min.

2.11. Statistical Analysis. All results are expressed as mean \pm SEM. Data were analyzed by one-way ANOVA followed by Bonferroni's multiple range test. The criterion for statistical significance was $P < 0.05$. All statistical analyses were carried out by using SPSS for Windows (SPSS Inc.).

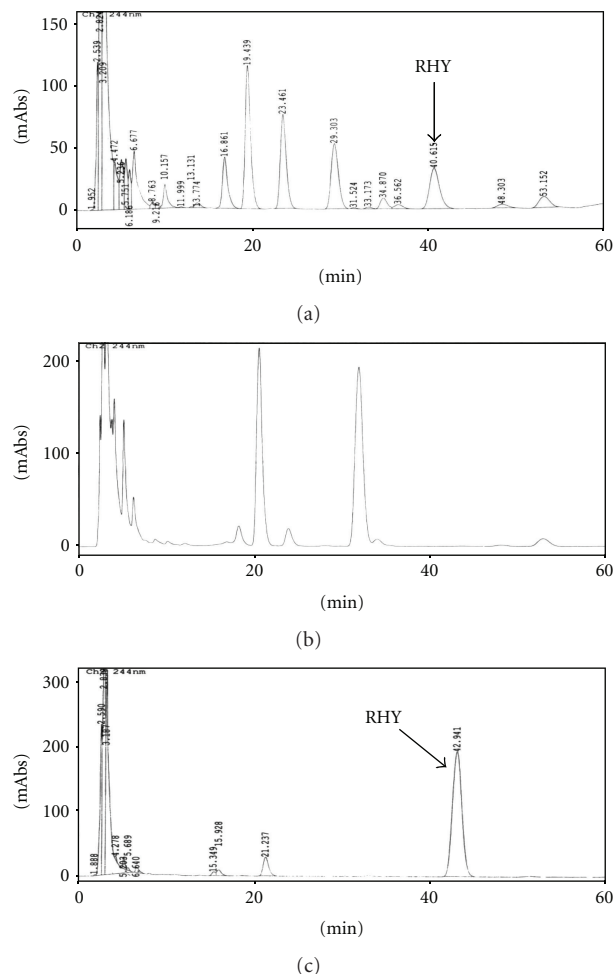
3. Results

3.1. HPLC Analysis of UR_{EtOH} , UH_{EtOH} , and UL_{EtOH} . The HPLC chromatogram shows that RHY is the major components among organic molecules of UR_{EtOH} , UH_{EtOH} , and UL_{EtOH} . As shown in Figure 1, the content of RHY in UR_{EtOH} and UL_{EtOH} were 3.87 mg/g and 17.12 mg/g. UH_{EtOH} did not detect the content of RHY.

3.2. Effect of Repeated Treatment with UL_{EtOH} on the Immobility Time Both in the FST and TST. In order to investigate whether UL_{EtOH} can produce chronic changes in depression-related behavior in FST and TST, we treated mice with different dosages to mice via continuous oral administration for 14 days. UL_{EtOH} decreased significantly the immobility time in FST (dose range: 0.0625–0.5 g/kg, p.o.; Figure 2). UL_{EtOH} also caused a reduction in the immobility time in TST (dose range: 0.0625–0.5 g/kg, p.o.; Figure 3). In both tests, IMI at doses of 10 mg/kg produced a reduction of the immobility time that was stronger than that afforded by UL_{EtOH} (Figure 3).

3.3. Effect of Repeated Treatment with UL_{EtOH} on the Locomotor Activity in Mice. In order to determine whether UL_{EtOH} actually possesses an antidepressant-like activity, we tested the locomotion counts to exclude the excitatory or inhibitory effects after administration of UL_{EtOH} . UL_{EtOH} did not affect locomotor activity at the same doses that significantly reduced immobility response in the FST and TST (Figure 4).

3.4. Effect of Combination of UL_{EtOH} with IMI, FLU, CLO, MAP, BUP, and KET on Immobility Periods in FST and TST. The results depicted in Figure 5 show the effect of treatment of mice with IMI (5 mg/kg for two weeks' administration, a dose that did not affect the immobility time) on the reduction in immobility time elicited by UL_{EtOH} (0.5 g/kg, p.o.). Post-hoc analyses indicated that the treatment of mice with IMI augmented the antidepressant-like activity of UL_{EtOH} in FST and TST.



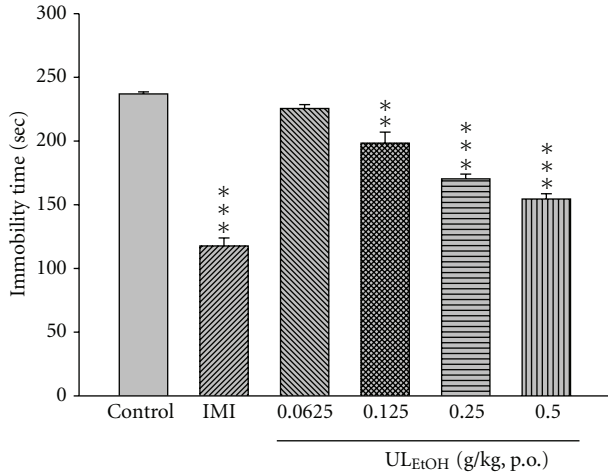


FIGURE 2: The effect of ethanol extracts from *U. lanosa* (UL_{EtOH} , 0.0625–0.5 g/kg, p.o.), or Imipramine (IMI, 10 mg/kg, i.p.) for two weeks' administration on the immobility time in the forced swimming task. The values are mean \pm SEM for each group ($n = 10$). ** $P < 0.01$, *** $P < 0.001$ as compared with control group (one-way ANOVA followed by Bonferroni's multiple range test).

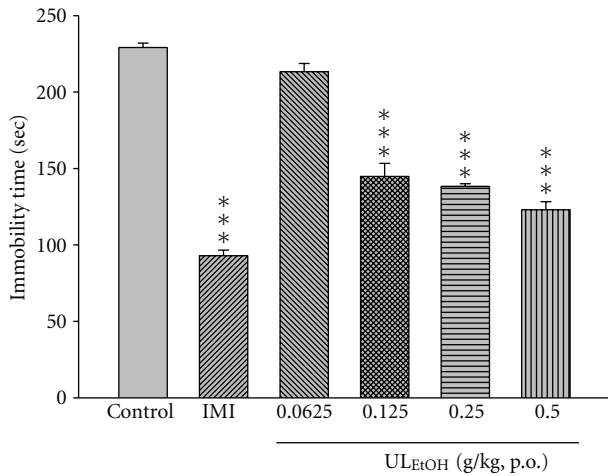
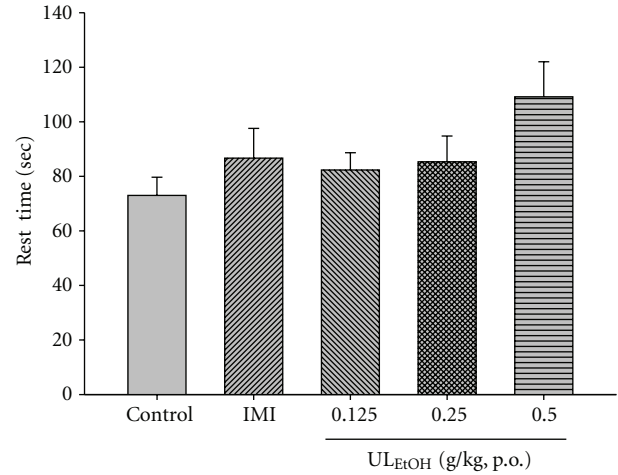


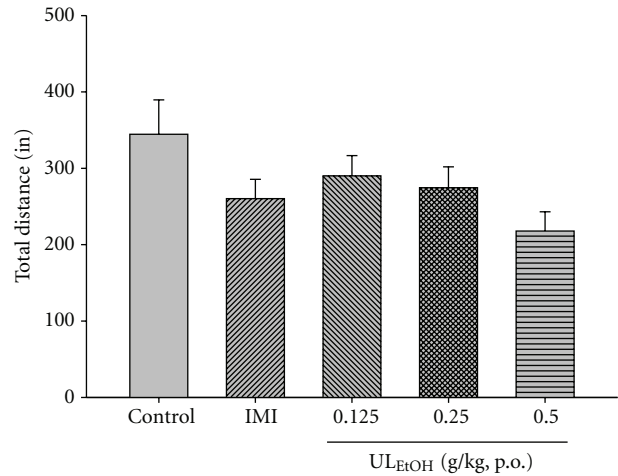
FIGURE 3: The effect of ethanol extracts from (UL_{EtOH} , 0.0625–0.5 g/kg, p.o.), or Imipramine (IMI, 10 mg/kg, i.p.) for two weeks' administration on the immobility time in the tail suspension test. The value are mean \pm SEM for each group ($n = 10$). *** $P < 0.001$ as compared with control group (one-way ANOVA followed by Bonferroni's multiple range test).

The results depicted in Figure 9 show the effect of treatment of mice with BUP (4 mg/kg, for two weeks' administration, a dose that did not affect the immobility time) on the reduction in immobility time elicited by UL_{EtOH} (0.5 g/kg, p.o.). Post-hoc analyses indicated that the treatment of mice with BUP did not augment the antidepressant-like activity of UL_{EtOH} in FST and TST.

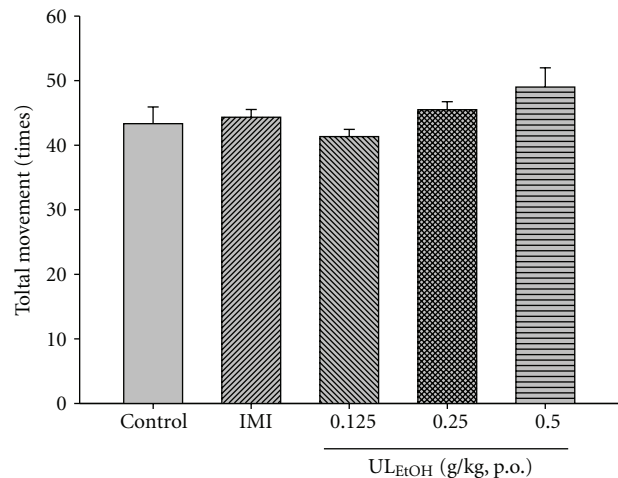
The results depicted in Figure 10 show the effect of treatment of mice with KET (5 mg/kg for two weeks' administration, a dose that did not affect the immobility



(a)



(b)



(c)

FIGURE 4: The effects of UL_{EtOH} for two weeks administration on resting time, total movement distance and total movement time in the locomotor. The value are mean \pm SEM for each group ($n = 6$).

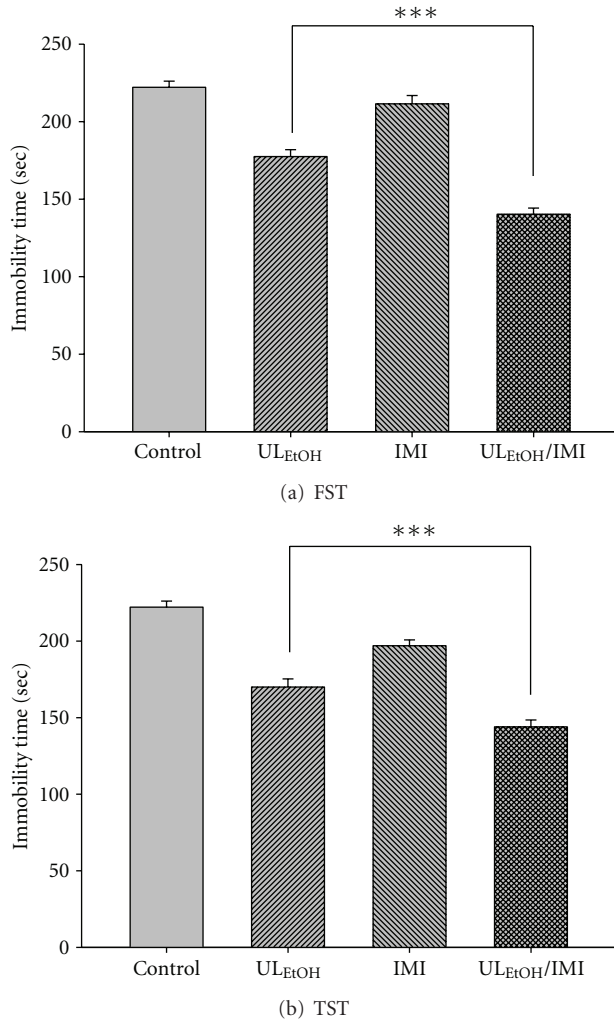


FIGURE 5: Effect of imipramine (IMI) on UL_{EtOH}-induced immobility time in (a) FST and (b) TST. The values are mean \pm SEM for each group ($n = 6$). *** $P < 0.001$ as compared with UL_{EtOH} alone.

time) on the reduction in immobility time elicited by UL_{EtOH} (0.5 g/kg, p.o.). Post-hoc analyses indicated that the treatment of mice with KET augmented the antidepressant-like activity of UL_{EtOH} in FST and TST.

3.5. Determination of Monoamines and Their Metabolites Levels in the Mice Frontal Cortex, Striatum, Hippocampus, and Hypothalamus. The concentrations of NE, DA, 5-HT, and its metabolites in the frontal cortex, striatum, hippocampus, and hypothalamus are presented in Tables 1, 2, 3, and 4. UL_{EtOH} (0.125 g/kg, p.o.) increased the level of NE in hypothalamus, and the level of DOPAC in striatum. UL_{EtOH} (0.25 g/kg, p.o.) increased the level of 5-HT in cortex and striatum, the level of 5-HIAA in striatum, hippocampus, and hypothalamus, and the level of NE in cortex, hippocampus, the level of MHPG in hippocampus, and level of DOPAC in striatum. UL_{EtOH} (0.5 g/kg, p.o.) increased the levels of 5-HT and 5-HIAA in cortex, striatum, hippocampus, and hypothalamus, the levels of NE and MHPG in cortex

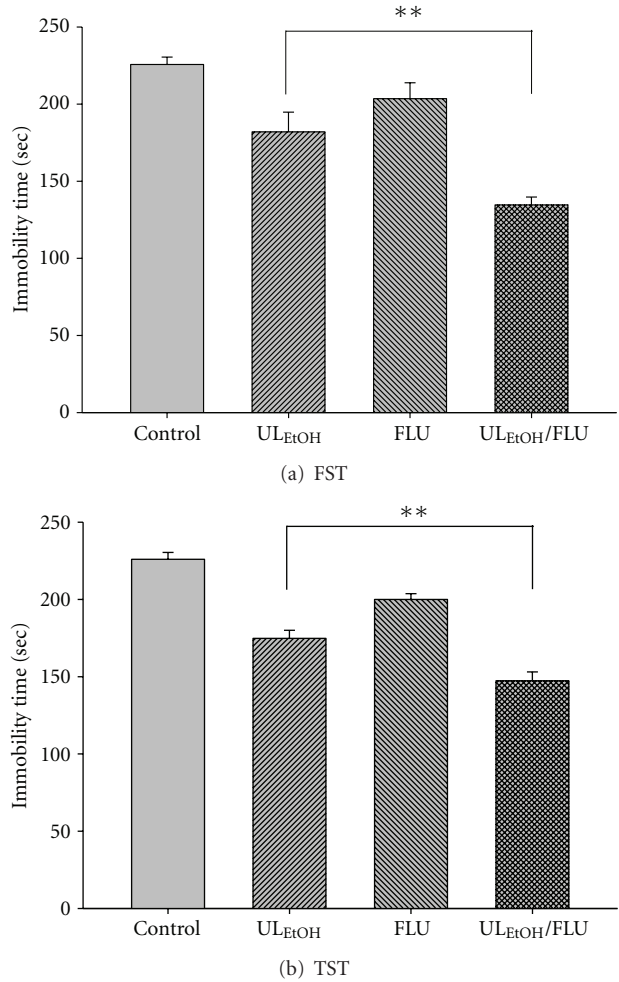


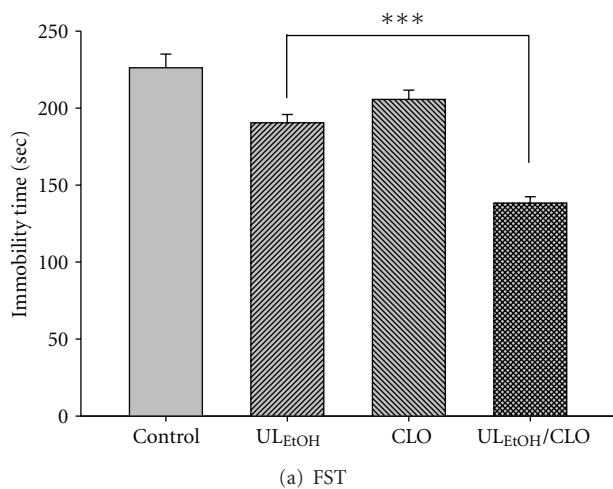
FIGURE 6: Effect of fluoxetine (FLU) on UL_{EtOH}-induced immobility time in (a) FST and (b) TST. The values are mean \pm SEM for each group ($n = 6$). ** $P < 0.01$ as compared with UL_{EtOH} alone.

and hippocampus, the level of NE in striatum, and level of DOPAC in striatum.

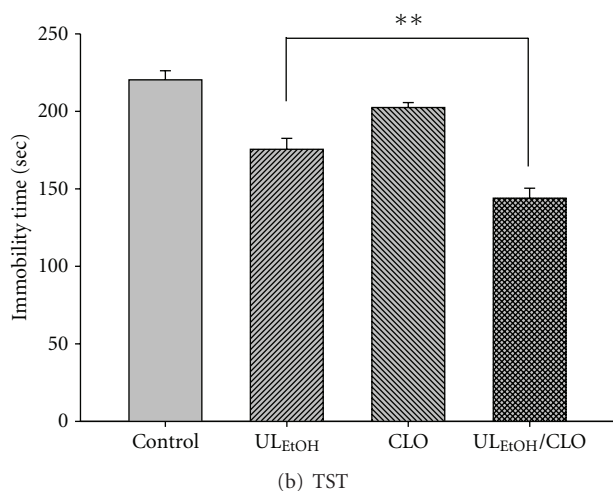
3.6. Measurements of Monoamine Oxidase Activity. Table 5 summarizes the effect of UL_{EtOH} and cloglyline on the activities of type A and type B monoamine oxidase in mouse brain. UL_{EtOH} (0.5 g/kg) and cloglyline (10 mg/kg) inhibited the activity of type A monoamine oxidase in the mouse brain.

4. Discussion

In the present study, we analyzed the RHY content of *Gouteng* grown in Taiwan and chose the UL which has higher amount of RHY as the research sample. To raise the yield ratio of alkaloid, the researcher alkalinized the three species of *Gouteng* by 5% ammonia solution, turning alkaloid salts into free alkaloid, followed by 70% ethanol extracting. After the above procedure, the UR_{EtOH}, UH_{EtOH}, and UL_{EtOH} were produced. Afterwards, the researcher used HPLC method



(a) FST

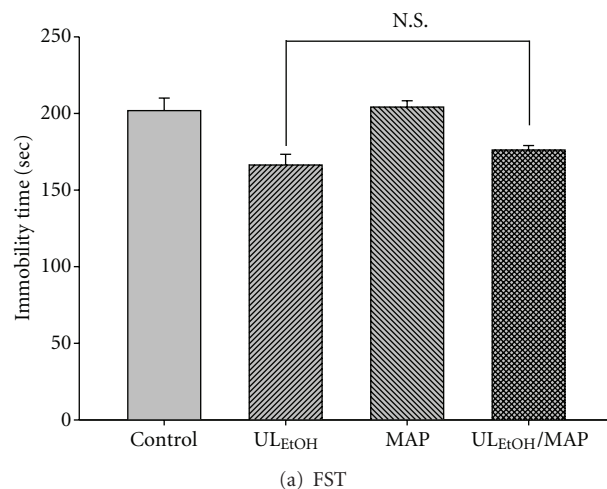


(b) TST

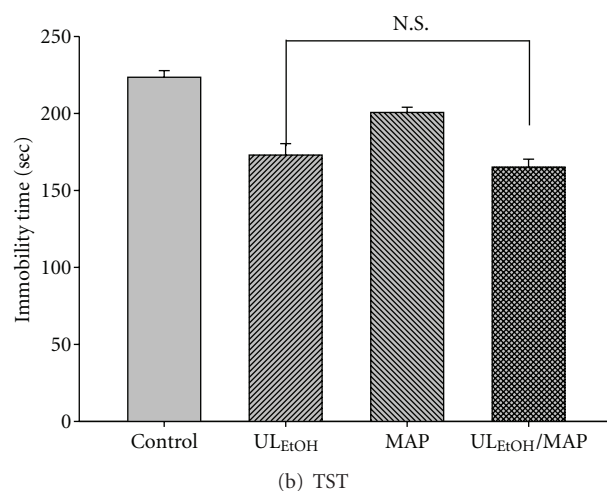
FIGURE 7: Effect of clorgyline (CLO) on UL_{EtOH}-induced immobility time in (a) FST and (b) TST. The value are mean \pm SEM for each group ($n = 6$). ** $P < 0.01$ *** $P < 0.001$ as compared with UL_{EtOH} alone.

to analyse the RHY content of the samples. The analytical result of UL_{EtOH} contained most RHY among all. However, from the study of Jung et al. [19], the aqueous extract of UR (UR_{DDW}) possesses anxiolytic activity by inhibiting WAY1005635 (the compounds that could selective block 5-HT_{1A} presynaptic receptors and prevent the negative feedback might be effective) [34]. In this study, the researcher analysed the RHY content of UR_{DDW}. Result showed that UR_{DDW} did not detect RHY (unpublished data) and suggested that the antianxiety activity of UR_{DDW} was not related to RHY.

The forced swimming and tail suspension tests are behavioral despair tests useful for probing the pathological mechanism of depression and for the evaluation of antidepressant drugs [39]. These tests are sensitive to all major classes of antidepressant drugs including tricyclics, serotonin reuptake inhibitors, monoamine oxidase inhibitors, and atypical [28]. Characteristic behavior scored in both tests is termed immobility, reflecting behavioral despair as seen in human depression [31]. The results presented here show, to



(a) FST



(b) TST

FIGURE 8: Effect of maprotiline (MAP) on UL_{EtOH}-induced immobility time in (a) FST and (b) TST. The value are mean \pm SEM for each group ($n = 6$). N.S.: nonsignificant.

our knowledge for the first time, that UL_{EtOH} given orally is effective in producing significant antidepressant-like activity, when assessed in FST and in TST. The antidepressant-like activity of UL_{EtOH} in FST and TST was not comparable but weaker than that of IMI, used as a standard antidepressant in a dose of 10 mg/kg.

In FST and TST, psychostimulants are also shown to reduce immobility but in contrast to antidepressants they cause a marked motor stimulation. Locomotor activity test was also observed after UL_{EtOH} treatment. We employed an additional locomotor activity test to check the motor stimulating activity of UL_{EtOH} after tests. These results suggested that UL_{EtOH}, at the same doses that produce an antidepressant-like activity, did not show significant locomotor stimulation. The antidepressant-like activity of UL_{EtOH} is specific.

The precise mechanisms by which UL_{EtOH} produced antidepressant-like activity are not completely understood. However, according to our results, the antidepressant-like activity of UL_{EtOH} was additive to the treatment of animals

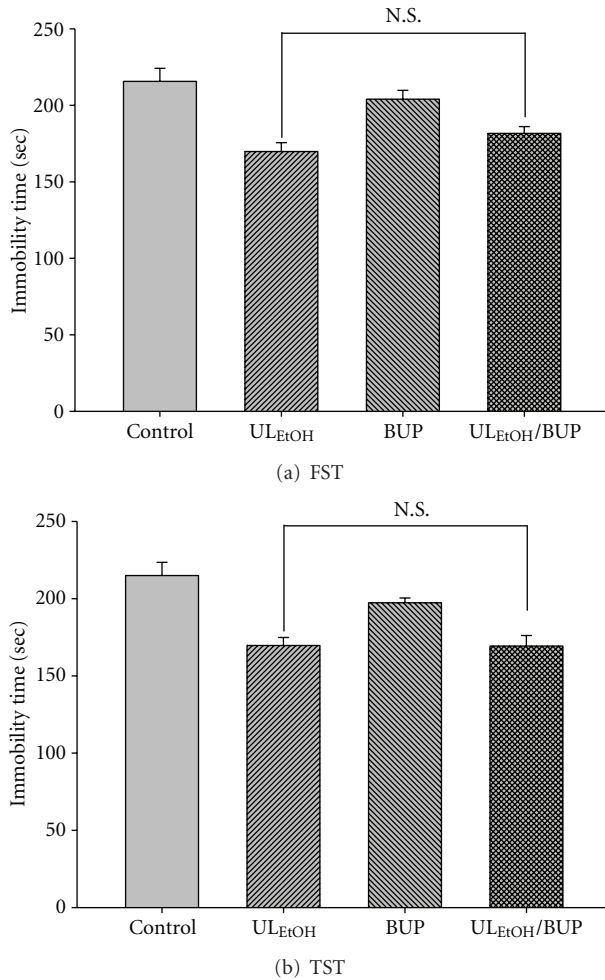


FIGURE 9: Effect of bupropion (BUP) on UL_{EtOH}-induced immobility time in (a) FST and (b) TST. The value are mean \pm SEM for each group ($n = 6$). N.S.: nonsignificant.

with IMI (a-NE/5-HT reuptake inhibitor), FLU (a selective 5-HT reuptake inhibitor), CLO (a selective MAO-A inhibitor), and KET (a preferential 5-HT_{2A} receptor antagonist) when tested in FST and TST. This effect was not accompanied by hyperlocomotion (data not shown) that could produce a false-positive antidepressant-like activity. These suggest that UL_{EtOH} might produce antidepressant-like activity by interaction with monoamines receptors, and monoamine oxidase, thereby increasing the levels NE, 5-HT, and DA in the brains of mice and was related to downregulation of 5-HT_{2A} receptor (inhibition of 5-HT_{2A} receptor expression exerts antidepressant-like activity) [40]. Moreover, this study suggests that the combination of UL_{EtOH} with these antidepressants might be helpful in the treatment of depression.

Intensive research into the neurobiology of depression suggests that an increase in the monoamine levels at the synapse is believed to be the first step in a complex cascade of events that results in antidepressant activity [41]. Four brain regions were studied: the frontal cortex, the striatum, the hippocampus, and the hypothalamus, which

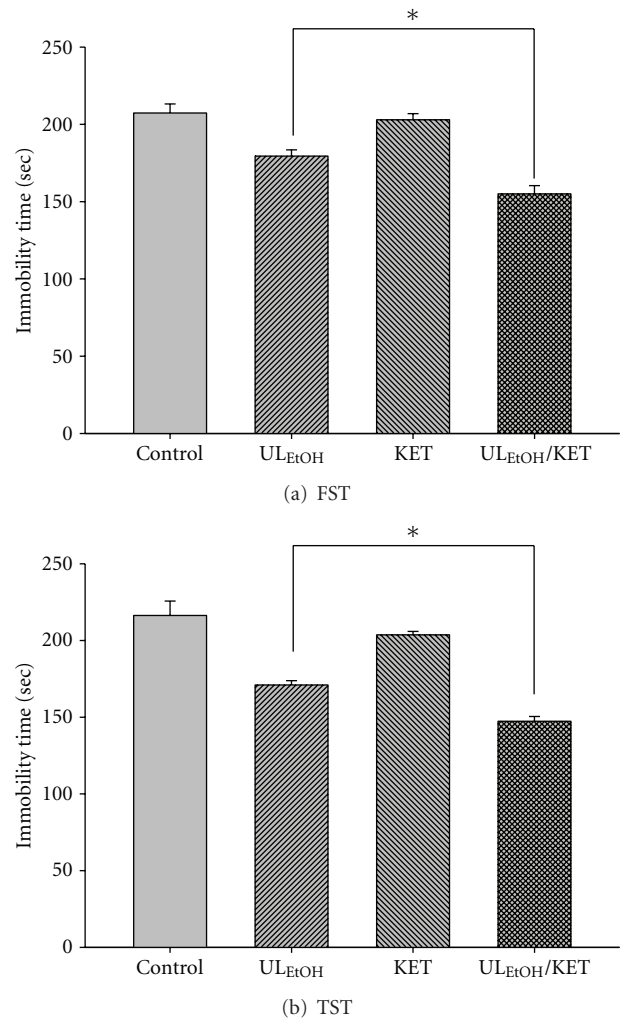


FIGURE 10: Effect of ketanserin (KET) on UL_{EtOH}-induced immobility time in (a) FST and (b) TST. The value are mean \pm SEM for each group ($n = 6$). * $P < 0.05$ as compared with UL_{EtOH} alone.

are involved Integrating in important behavioral functions, such as emotion, motivation, and learning and memory [41, 42]. Abnormal monoamine levels in four brain regions may be relevant to the depressed state. Our results show that UL_{EtOH} increased the levels of 5-HT and 5-HIAA in cortex, striatum, hippocampus, and hypothalamus, the levels of NE and MHPG in cortex and hippocampus, the level of NE in striatum, and the level of DOPAC in striatum. The HPLC assay showed that a significant increase in DOPAC in the striatum was observed after UL_{EtOH} treatment. The results from behavior and HPLC assay were inconsistent possibly because behavioral changes are not significantly sensitive to small changes in dopamine level in the brain. Integrating the HPLC, and pharmacological treatments results, we inferred that the anti-depression mechanism of UL_{EtOH} might be partly due to its influence on the function of 5-HT/NE systems through the regulation of serotonergic and adrenergic receptors and/or the metabolism of 5-HT and NE.

TABLE 1: Effect of UL_{EtOH} on the concentration (ng/g tissue) of monoamines and their metabolites in the cortex of mice brain.

Groups	Cortex (ng/g tissue)					
	NE	MHPG	DA	DOPAC	5-HT	5-HIAA
Normal	525.96 ± 43.71	280.41 ± 12.76	735.26 ± 53.40	625.26 ± 63.78	438.75 ± 36.89	372.32 ± 18.22
Control versus FST	168.49 ± 17.15 ^{###}	119.06 ± 13.32 [#]	596.01 ± 27.13	530.69 ± 49.32	216.67 ± 25.11 ^{##}	143.76 ± 31.54 ^{###}
Imipramine 10 mg/kg	583.92 ± 28.9 ^{***}	233.37 ± 59.00	701.97 ± 56.63	411.47 ± 49.71	711.42 ± 63.27 ^{***}	342.13 ± 18.26 ^{**}
UL _{EtOH} 0.125 g/kg	146.39 ± 10.11	176.81 ± 29.29	834.17 ± 55.66	395.71 ± 26.67	346.30 ± 8.91	167.40 ± 31.30
UL _{EtOH} 0.25 g/kg	292.78 ± 26.93 [*]	145.86 ± 18.35	695.69 ± 29.25	433.10 ± 16.43	499.49 ± 19.78 ^{***}	165.02 ± 46.22
UL _{EtOH} 0.5 g/kg	320.69 ± 20.16 ^{**}	273.19 ± 58.11 [*]	622.98 ± 67.15	577.92 ± 88.01	639.27 ± 49.86 ^{***}	311.63 ± 23.23 ^{**}

Values were the mean ± SEM ($n = 6$). [#] $P < 0.05$, ^{##} $P < 0.01$, ^{###} $P < 0.001$ as compared with the normal group. ^{*} $P < 0.05$, ^{**} $P < 0.01$, ^{***} $P < 0.001$ as compared with the control versus FST group (one-way ANOVA following by Bonferroni's test).

TABLE 2: Effect of UL_{EtOH} on the concentration (ng/g tissue) of monoamines and their metabolites in the striatum of mice brain.

Groups	Striatum (ng/g tissue)					
	NE	MHPG	DA	DOPAC	5-HT	5-HIAA
Normal	408.22 ± 74.25	80.23 ± 84.83	1021.35 ± 74.58	1256.23 ± 160.42	334.60 ± 65.88	242.45 ± 21.90
Control versus FST	331.74 ± 33.07	75.23 ± 45.83	681.62 ± 69.78	927.96 ± 198.73	103.09 ± 44.16 [#]	140.02 ± 50.36
Imipramine 10 mg/kg	696.74 ± 83.8 ^{**}	78.71 ± 17.44	950.93 ± 58.4	1032.17 ± 160.68	426.01 ± 60.75 [*]	352.37 ± 87.32
UL _{EtOH} 0.125 g/kg	466.40 ± 33.77	61.58 ± 7.65	835.30 ± 92.92	1864.85 ± 272.97 [*]	241.71 ± 29.87	254.62 ± 36.12
UL _{EtOH} 0.25 g/kg	467.62 ± 24.12	110.10 ± 38.63	735.40 ± 61.14	1873.61 ± 189.68 [*]	356.64 ± 73.28 [*]	508.37 ± 43.27 ^{***}
UL _{EtOH} 0.5 g/kg	860.02 ± 67.30 ^{***}	129.91 ± 16.13	743.81 ± 86.79	1847.19 ± 182.61 [*]	420.20 ± 94.71 [*]	751.38 ± 34.33 ^{***}

Value were the mean ± SEM ($n = 6$). [#] $P < 0.05$ as compared with the normal group. ^{*} $P < 0.05$, ^{**} $P < 0.01$, ^{***} $P < 0.001$ as compared with the control group (one-way ANOVA following by Bonferroni's test).

TABLE 3: Effect of UL_{EtOH} on the concentration (ng/g tissue) of monoamines and their metabolites in the hippocampus of mice brain.

Groups	Hippocampus (ng/g tissue)					
	NE	MHPG	DA	DOPAC	5-HT	5-HIAA
Normal	581.57 ± 25.89	640.84 ± 44.27	713.98 ± 27.06	639.43 ± 49.15	638.07 ± 31.74	613.67 ± 78.51
Control versus FST	183.67 ± 24.01 [#]	210.34 ± 22.72 ^{##}	275.21 ± 34.86 ^{##}	268.46 ± 26.14	113.72 ± 25.71 ^{###}	192.77 ± 15.70 ^{##}
Imipramine 10 mg/kg	851.76 ± 96.22 ^{***}	682.1 ± 31.39 ^{***}	633.56 ± 63.63	445.35 ± 94.67	898.71 ± 35.47 ^{***}	1028.46 ± 75.43 ^{***}
UL _{EtOH} 0.125 g/kg	431.38 ± 52.01	386.16 ± 27.86	435.43 ± 63.16	360.87 ± 107.15	201.48 ± 73.29	354.73 ± 91.78
UL _{EtOH} 0.25 g/kg	510.95 ± 52.67 ^{**}	515.38 ± 97.48 ^{**}	539.59 ± 72.49	432.42 ± 67.79	229.74 ± 55.82	509.97 ± 44.55 [*]
UL _{EtOH} 0.5 g/kg	824.21 ± 71.69 ^{***}	735.31 ± .84 ^{***}	612.29 ± 84.59	532.09 ± 42.28	381.89 ± 10.25 ^{**}	665.73 ± 42.55 ^{**}

Value were the mean ± SEM ($n = 6$). [#] $P < 0.05$, ^{##} $P < 0.01$, ^{###} $P < 0.001$ as compared with the normal group.

^{*} $P < 0.05$, ^{**} $P < 0.01$, ^{***} $P < 0.001$ as compared with the control group (one-way ANOVA following by Bonferroni's test).

TABLE 4: Effect of UL_{EtOH} on the concentration (ng/g tissue) of monoamines and their metabolites in the hypothalamus of mice brain.

Groups	Hypothalamus (ng/g tissue)					
	NE	MHPG	DA	DOPAC	5-HT	5-HIAA
Normal	162.87 ± 18.84	359.47 ± 42.85	673.24 ± 39.45	632.91 ± 31.21	82.70 ± 1.59	610.04 ± 52.00
Control versus FST	82.12 ± 10.34 [#]	301.73 ± 33.83	368.95 ± 24.42 ^{##}	359.99 ± 20.43	27.61 ± 4.24 ^{###}	250.69 ± 51.46 ^{##}
Imipramine 10 mg/kg	491.34 ± 17.78 ^{**}	750.59 ± 67.95 ^{**}	466.00 ± 49.59	498.45 ± 12.95	72.86 ± 5.06 ^{***}	780.53 ± 78.00 ^{***}
UL _{EtOH} 0.125 g/kg	86.59 ± 20.24	256.23 ± 28.26	311.62 ± 49.34	344.75 ± 46.98	37.00 ± 6.16	612.67 ± 65.72 ^{**}
UL _{EtOH} 0.25 g/kg	161.51 ± 11.41	357.50 ± 22.94	407.61 ± 23.02	564.04 ± 42.35	40.99 ± 3.46	633.35 ± 65.61 ^{**}
UL _{EtOH} 0.5 g/kg	148.62 ± 13.21	501.39 ± 57.27	439.88 ± 51.01	585.68 ± 26.87	86.84 ± 11.23 ^{***}	877.39 ± 75.70 ^{***}

Value were the means ± SEM ($n = 6$). [#] $P < 0.05$, ^{##} $P < 0.01$, ^{###} $P < 0.001$ as compared with the Normal group.

^{**} $P < 0.01$, ^{***} $P < 0.001$ as compared with the control group (one-way ANOVA following by Bonferroni's test).

TABLE 5: Effects of UL_{EtOH} (0.125, 0.25, 0.5 g/kg, p.o.) and clorgyline (10 mg/kg, i.p.) for two weeks' administration on MAO-A, MAO-B activity in mouse brain.

Group	MAO-A activity (% of mouse brain)	MAO-B activity (% of mouse brain)
Control	98.56 ± 4.44	96.89 ± 4.10
Clorgyline 10 mg/kg	45.05 ± 8.02**	102.41 ± 5.50
UL _{EtOH} 0.125 g/kg	107.31 ± 14.21	103.86 ± 7.46
UL _{EtOH} 0.25 g/kg	80.97 ± 7.20	107.70 ± 5.50
UL _{EtOH} 0.5 g/kg	49.84 ± 7.02**	105.94 ± 3.99

Value were the mean ± SEM ($n = 6$). ** $P < 0.01$ as compared with the control group (one-way ANOVA following by Bonferroni's test).

MAO exists in two subtypes, A and B. The original MAOIs are nonselective, inhibiting both forms. The A form of MAO preferentially metabolizes 5-HT and NE, the monoamines most closely linked to depression. The B form preferentially metabolizes trace amines, including phenethylamine. MAO-A and MAO-B metabolize DA and tyramine [43]. Hou et al. [44] concluded that the (+) catechin and (-) epicatechin of methanol extract of *UR* had inhibitory effect on MAO-B activity. However, due to the different extracting methods in this research, we did not detect the contents of (+) catechin and (-) epicatechin in UL_{EtOH}. (unpublished data). Furthermore, based on the same studies have reported a positive correlation between oxidative stress and depression [45], and *Gouteng* has antioxidant activity [46]. We applied two-weeks oral administration of UL_{EtOH} to conduct monoamine oxidase activity test. The results of our study reveal that UL_{EtOH} inhibited MAO-A activity.

Several studies demonstrated that the herb extract and its active component RHY protect neurons against the ischemia, glutamate-, or dopamine-induced damage or death [20, 21, 47], and regulation of monoamine transporters [23, 24]. From the above studies, we inferred that RHY might be the main active component in *Gouteng*'s antidepressant activity. Further studies are needed to verify the antidepressant activity of RHY and underlying mechanisms.

In conclusion, UL_{EtOH} contained most RHY among *Uncaria* species of *Gouteng* in Taiwan. UL_{EtOH} showed antidepressant-like activity in FST and TST. The mechanism of anti-depressive-like activity of UL_{EtOH} was mediated by increasing the monoamines level, particularly 5-HT and NE in different brain regions of mice. Furthermore, UL_{EtOH} was proofed to inhibit the activity of MAO_A. From the present study, we conclude that UL_{EtOH} is a worth developing Taiwanese specific medicinal plant, and thus we suggest that it should be included in Pharmacopoeia.

Abbreviations

5-HIAA: 5-hydroxyindoleacetic acid
 5-HT: Serotonin
 BUP: Bupropion
 CLO: Clorgyline
 DA: Dopamine
 DOPAC: 4-dihydroxyphenylacetic acid

FLU: Fluoxetine
 FST: Forced swimming test
 HPLC: High-performance liquid chromatograph
 HRP: Horseradish peroxidase
 IMI: Imipramine
 KET: Ketanserin
 MAOIs: Monoamine oxidase inhibitors
 MAP: Maprotiline
 MHPG: 4-Hydroxy-3-methoxyphenylglycol
 NE: Norepinephrine
 PBS: Phosphate-buffered saline
 RHY: Rhynchophylline
 SNRIs: Specific serotonin-norepinephrine reuptake inhibitors
 SSRIs: Selective serotonin reuptake inhibitors
 TCAs: Tricyclic antidepressants
 TST: Tail suspension test
 UH: *Uncaria hirsuta* Haviland
 UL: *Uncaria lanosa* Wallich. var. *appendiculata* Ridsd
 UR: *Uncaria rhynchophylla* (Miquel) Jacks.

Acknowledgment

This study is supported in part by the National Science Council, Taiwan (NSC 100-2320-B-039-013) and Taiwan Department of Health Clinical Trial and Research Center of Excellence (DOH100-TD-B-111-004).

References

- [1] C. B. Nemeroff, "The burden of severe depression: a review of diagnostic challenges and treatment alternatives," *Journal of Psychiatric Research*, vol. 41, no. 3-4, pp. 189-206, 2007.
- [2] M. J. Neal, *Medical Pharmacology at a Glance*, Wiley-Blackwell, Singapore, 2009.
- [3] I. Hindmarch, "Beyond the monoamine hypothesis: mechanisms, molecules and methods," *European Psychiatry*, vol. 17, no. 3, pp. 294-299, 2002.
- [4] S. K. Kulkarni, M. K. Bhutani, and M. Bishnoi, "Antidepressant activity of curcumin: involvement of serotonin and dopamine system," *Psychopharmacology*, vol. 201, no. 3, pp. 435-442, 2008.
- [5] J. T. Anthony, G. K. Bertram, and B. M. Susan, *Pharmacology Examination and Board Review Ninth Edition*, McGraw-Hill Medical, Singapore, 2010.
- [6] G. Calapai and A. P. Caputi, "Herbal medicines: can we do without pharmacologist?" *Evidence-based Complementary and Alternative Medicine*, vol. 4, no. 1, pp. 41-43, 2007.
- [7] J. Y. Guo, C. C. Han, and Y. M. Liu, "A contemporary treatment approach to both diabetes and depression by cordyceps sinensis, Rich in Vanadium," *Evidence-Based Complementary and Alternative Medicine*, vol. 7, no. 3, pp. 387-389, 2010.
- [8] N. Ito, T. Nagai, T. Oikawa, H. Yamada, and T. Hanawa, "Antidepressant-like effect of l-perillaldehyde in stress-induced depression-like model mice through regulation of the olfactory nervous system," *Evidence-based Complementary and Alternative Medicine*, vol. 2011, Article ID 512697, 5 pages, 2011.

- [9] Chinese Pharmacopoeia Commission, *Pharmacopoeia of the People's Republic of China*, vol. 1, Chemical Industry Press, Beijing, China, 2010.
- [10] Committee on Chinese Medicine and Pharmacy, *Taiwan Herbal Pharmacopoeia*, Department of Health, Executive Yuan, Taipei City, Taiwan, 2004.
- [11] T. C. Huang and Editorial Committee of the Flora of Taiwan, *Flora of Taiwan*, vol. 4, Editorial Committee of the Flora of Taiwan, Department of Botany, National Taiwan University, Taipei, Taiwan, 2nd edition, 1998.
- [12] J. Zhou and S. Zhou, "Antihypertensive and neuroprotective activities of rhynchophylline: the role of rhynchophylline in neurotransmission and ion channel activity," *Journal of Ethnopharmacology*, vol. 132, no. 1, pp. 15–27, 2010.
- [13] C. L. Hsieh, T. Y. Ho, S. Y. Su, W. Y. Lo, C. H. Liu, and N. Y. Tang, "Uncaria rhynchophylla and rhynchophylline inhibit c-Jun N-terminal kinase phosphorylation and nuclear factor- κ B activity in kainic acid-treated rats," *American Journal of Chinese Medicine*, vol. 37, no. 2, pp. 351–360, 2009.
- [14] N. Y. Tang, C. H. Liu, S. Y. Su et al., "Uncaria rhynchophylla (Miq) Jack plays a role in neuronal protection in kainic acid-treated rats," *American Journal of Chinese Medicine*, vol. 38, no. 2, pp. 251–263, 2010.
- [15] W. Y. Lo, F. J. Tsai, C. H. Liu et al., "Uncaria rhynchophylla upregulates the expression of MIF and cyclophilin A in kainic acid-induced epilepsy rats: a proteomic analysis," *American Journal of Chinese Medicine*, vol. 38, no. 4, pp. 745–759, 2010.
- [16] J. S. Shim, H. G. Kim, M. S. Ju, J. G. Choi, S. Y. Jeong, and M. S. Oh, "Effects of the hook of *Uncaria rhynchophylla* on neurotoxicity in the 6-hydroxydopamine model of Parkinson's disease," *Journal of Ethnopharmacology*, vol. 126, no. 2, pp. 361–365, 2009.
- [17] H. Fujiwara, K. Iwasaki, K. Furukawa et al., "Uncaria rhynchophylla, a Chinese medicinal herb, has potent antiaggregation effects on Alzheimer's β -amyloid proteins," *Journal of Neuroscience Research*, vol. 84, no. 2, pp. 427–433, 2006.
- [18] M. T. Hsieh, W. H. Peng, C. R. Wu, K. Y. Ng, C. L. Cheng, and H. X. Xu, "Review on experimental research of herbal medicines with anti-amnesic activity," *Planta Medica*, vol. 76, no. 3, pp. 203–217, 2010.
- [19] J. W. Jung, N. Y. Ahn, H. R. Oh et al., "Anxiolytic effects of the aqueous extract of *Uncaria rhynchophylla*," *Journal of Ethnopharmacology*, vol. 108, no. 2, pp. 193–197, 2006.
- [20] T. H. Kang, Y. Murakami, K. Matsumoto et al., "Rhynchophylline and isorhynchophylline inhibit NMDA receptors expressed in *Xenopus* oocytes," *European Journal of Pharmacology*, vol. 455, no. 1, pp. 27–34, 2002.
- [21] T. H. Kang, Y. Murakami, H. Takayama et al., "Protective effect of rhynchophylline and isorhynchophylline on in vitro ischemia-induced neuronal damage in the hippocampus: Putative neurotransmitter receptors involved in their action," *Life Sciences*, vol. 76, no. 3, pp. 331–343, 2004.
- [22] D. Yuan, B. Ma, J. Y. Yang et al., "Anti-inflammatory effects of rhynchophylline and isorhynchophylline in mouse N9 microglial cells and the molecular mechanism," *International Immunopharmacology*, vol. 9, no. 13–14, pp. 1549–1554, 2009.
- [23] Y. F. Lu, X. L. Xie, Q. Wu, G. R. Wen, S. F. Yang, and J. S. Shi, "Effects of rhynchophylline on monoamine transmitter contents of striatum and hippocampus in cerebral ischemic rats," *Chinese Journal of Pharmacology and Toxicology*, vol. 18, no. 4, pp. 253–258, 2004.
- [24] J. S. Shi, B. Huang, Q. Wu, R. X. Ren, and X. L. Xie, "Effects of rhynchophylline on motor activity of mice and serotonin and dopamine in rat brain," *Acta Pharmacologica Sinica*, vol. 14, no. 2, pp. 114–117, 1993.
- [25] R. S. Smith, "The macrophage theory of depression," *Medical Hypotheses*, vol. 35, no. 4, pp. 298–306, 1991.
- [26] G. Sanacora, C. A. Zarate, J. H. Krystal, and H. K. Manji, "Targeting the glutamatergic system to develop novel, improved therapeutics for mood disorders," *Nature Reviews Drug Discovery*, vol. 7, no. 5, pp. 426–437, 2008.
- [27] J. F. Cryan, A. Markou, and I. Lucki, "Assessing antidepressant activity in rodents: recent developments and future needs," *Trends in Pharmacological Sciences*, vol. 23, no. 5, pp. 238–245, 2002.
- [28] R. D. Porsolt, A. Bertin, and M. Jalfre, "Behavioral despair in mice: a primary screening test for antidepressants," *Archives Internationales de Pharmacodynamie et de Therapie*, vol. 229, no. 2, pp. 327–336, 1977.
- [29] A. Dias Elpo Zomkowski, A. Oscar Rosa, J. Lin, A. R. S. Santos, J. Batista Calixto, and A. Lúcia Severo Rodrigues, "Evidence for serotonin receptor subtypes involvement in agmatine antidepressant-like effect in the mouse forced swimming test," *Brain Research*, vol. 1023, no. 2, pp. 253–263, 2004.
- [30] A. D. E. Zomkowski, A. R. S. Santos, and A. L. S. Rodrigues, "Evidence for the involvement of the opioid system in the agmatine antidepressant-like effect in the forced swimming test," *Neuroscience Letters*, vol. 381, no. 3, pp. 279–283, 2005.
- [31] L. Steru, R. Chermat, B. Thierry, and P. Simon, "The tail suspension test: a new method for screening antidepressants in mice," *Psychopharmacology*, vol. 85, no. 3, pp. 367–370, 1985.
- [32] A. L. S. Rodrigues, J. B. T. Rocha, C. F. Mello, and D. O. Souza, "Effect of perinatal lead exposure on rat behaviour in open-field and two-way avoidance tasks," *Pharmacology and Toxicology*, vol. 79, no. 3, pp. 150–156, 1996.
- [33] W. H. Peng, K. L. Lo, Y. H. Lee, T. H. Hung, and Y. C. Lin, "Berberine produces antidepressant-like effects in the forced swim test and in the tail suspension test in mice," *Life Sciences*, vol. 81, no. 11, pp. 933–938, 2007.
- [34] A. E. Freitas, J. Budni, K. R. Lobato et al., "Antidepressant-like action of the ethanolic extract from *Tabebuia avellanedae* in mice: evidence for the involvement of the monoaminergic system," *Progress in Neuro-Psychopharmacology and Biological Psychiatry*, vol. 34, no. 2, pp. 335–343, 2010.
- [35] M. Bourin, F. Chenu, C. Prica, and M. Hascoët, "Augmentation effect of combination therapy of aripiprazole and antidepressants on forced swimming test in mice," *Psychopharmacology*, vol. 206, no. 1, pp. 97–107, 2009.
- [36] C. E. Renard, E. Dailly, D. J. P. David, M. Hascoët, and M. Bourin, "Monoamine metabolism changes following the mouse forced swimming test but not the tail suspension test," *Fundamental and Clinical Pharmacology*, vol. 17, no. 4, pp. 449–455, 2003.
- [37] O. H. Lowry, N. J. Rosebrough, A. L. Farr, and R. J. Randall, "Protein measurement with the Folin phenol reagent," *The Journal of Biological Chemistry*, vol. 193, no. 1, pp. 265–275, 1951.
- [38] M. Zhou and N. Panchuk-Voloshina, "A one-step fluorometric method for the continuous measurement of monoamine oxidase activity," *Analytical Biochemistry*, vol. 253, no. 2, pp. 169–174, 1997.
- [39] R. D. Porsolt, A. Bertin, and M. Jalfre, "Behavioral despair in rats and mice: strain differences and the effects of imipramine," *European Journal of Pharmacology*, vol. 51, no. 3, pp. 291–294, 1978.
- [40] E. Sibille, Z. Sarnyai, D. Benjamin, J. Gal, H. Baker, and M. Toth, "Antisense inhibition of 5-hydroxytryptamine(2A)

- receptor induces an antidepressant-like effect in mice,” *Molecular Pharmacology*, vol. 52, no. 6, pp. 1056–1063, 1997.
- [41] Y. Xu, Z. Wang, W. You et al., “Antidepressant-like effect of trans-resveratrol: involvement of serotonin and noradrenaline system,” *European Neuropsychopharmacology*, vol. 20, no. 6, pp. 405–413, 2010.
- [42] M. W. Shiflett and B. W. Balleine, “Contributions of ERK signaling in the striatum to instrumental learning and performance,” *Behavioural Brain Research*, vol. 218, no. 1, pp. 240–247, 2011.
- [43] S. M. Stahl and A. Felker, “Monoamine oxidase inhibitors: a modern guide to an unrequited class of antidepressants,” *CNS Spectrums*, vol. 13, no. 10, pp. 855–870, 2008.
- [44] W. C. Hou, R. D. Lin, C. T. Chen, and M. H. Lee, “Monoamine oxidase B (MAO-B) inhibition by active principles from *Uncaria rhynchophylla*,” *Journal of Ethnopharmacology*, vol. 100, no. 1-2, pp. 216–220, 2005.
- [45] H. Herken, A. Gurel, S. Selek et al., “Adenosine deaminase, nitric oxide, superoxide dismutase, and xanthine oxidase in patients with major depression: impact of antidepressant treatment,” *Archives of Medical Research*, vol. 38, no. 2, pp. 247–252, 2007.
- [46] M. Na, Y. H. Kim, B. S. Min et al., “Cytoprotective effect on oxidative stress and inhibitory effect on cellular aging of *Uncaria sinensis* Haval,” *Journal of Ethnopharmacology*, vol. 95, no. 2-3, pp. 127–132, 2004.
- [47] J. S. Shi and H. G. Kenneth, “Effect of rhynchophylline on apoptosis induced by dopamine in NT2 cells,” *Acta Pharmacologica Sinica*, vol. 23, no. 5, pp. 445–449, 2002.

Research Article

Mechanisms of Gastroprotective Effects of Ethanolic Leaf Extract of *Jasminum sambac* against HCl/Ethanol-Induced Gastric Mucosal Injury in Rats

Ahmed S. AlRashdi,¹ Suzy M. Salama,¹ Salim S. Alkiyumi,¹ Mahmood A. Abdulla,¹
A. Hamid A. Hadi,² Siddig I. Abdelwahab,³ Manal M. Taha,² Jamal Hussiani,⁴ and Nur Asykin⁴

¹ Department of Molecular Medicine, Faculty of Medicine, University of Malaya, 50603 Kuala Lumpur, Malaysia

² Department of Chemistry, Faculty of Science, University of Malaya, 50603 Kuala Lumpur, Malaysia

³ Department of Pharmacy, Faculty of Medicine, University of Malaya, 50603 Kuala Lumpur, Malaysia

⁴ Department of Medical Microbiology, Faculty of Medicine, University Technology, MARA, 40450 Shah Alam, Malaysia

Correspondence should be addressed to Mahmood A. Abdulla, mahmood955@yahoo.com

Received 26 October 2011; Revised 30 January 2012; Accepted 30 January 2012

Academic Editor: Vincenzo De Feo

Copyright © 2012 Ahmed S. AlRashdi et al. This is an open access article distributed under the Creative Commons Attribution License, which permits unrestricted use, distribution, and reproduction in any medium, provided the original work is properly cited.

Jasminum sambac is used in folk medicine as the treatment of many diseases. The aim of the present investigation is to evaluate the gastroprotective effects of ethanolic extracts of *J. sambac* leaves against acidified ethanol-induced gastric ulcers in rats. Seven groups of rats were orally pre-treated with carboxymethylcellulose (CMC) as normal group, CMC as ulcer group, 20 mg/kg of omeprazole as positive group, 62.5, 125, 250, and 500 mg/kg of extract as the experimental groups, respectively. An hour later, CMC was given orally to normal group and acidified ethanol solution was given orally to the ulcer control, positive control, and the experimental groups. The rats were sacrificed after an hour later. Acidity of gastric content, the gastric wall mucus, ulcer areas, and histology and immunohistochemistry of the gastric wall were assessed. Gastric homogenates were determined for prostaglandin E₂ (PGE₂), superoxide dismutase (SOD), and malondialdehyde (MDA) content. Ulcer group exhibited significantly severe mucosal injury as compared with omeprazole or extract which shows significant protection towards gastric mucosal injury the plant promotes ulcer protection as it shows significant reduction of ulcer area grossly, and histology showed marked reduction of edema and leucocytes infiltration of submucosal layer compared with ulcer group. Immunohistochemistry showed overexpression of Hsp70 protein and downexpression of Bax protein in rats pretreated with extract. Significant increased in the pH, mucus of gastric content and high levels of PGE₂, SOD and reduced amount of MDA was observed.

1. Introduction

Peptic ulcer is a common disorder of the stomach and duodenum [1]. The basic physiopathological of gastric ulcer results from an imbalance between some endogenous aggressive factor(s) [hydrochloric acid, pepsin, refluxed bile, leukotrienes, reactive oxygen species (ROS)] and cytoprotective factors, which include the function of the mucus-bicarbonate barrier, surface active phospholipids, prostaglandins (PGs), mucosal blood flow, cell renewal and migration, nonenzymatic and enzymatic antioxidants, and some growth factors [2, 3]. The multifactorial pathogenesis of peptic ulcers is secretion of gastric acid. Therefore, the main therapeutic target is

the control of this secretion using antacids, H₂ receptor blockers (ranitidine, famotidine) or proton pump blockers (omeprazole and lansoprazole) [4]. However, nowadays, gastric ulcer therapy faces a major drawback because most of the drugs currently available in the market show limited efficacy against gastric diseases and are often associated with severe side effects [5]. Thus, there is an urgent need to identify more effective and safe antiulcer agents. In this context, the use of medicinal plants for the prevention and treatment of different pathologies is in continuous expansion worldwide [6]. Natural products are gaining space and importance in the pharmaceutical industry as well as inspiring the search for new potential sources of bioactive

molecules [7]. Herbs, medicinal plants, spices, vegetables, and crude drug substances are considered to be a potential source to combat various diseases including gastric ulcer. In the scientific literature, a large number of medicinal plants with gastric antiulcer potential have been reported [8–10].

Jasminum sambac. Linn (Oleaceae) is commonly known as Jasmine. Traditionally, *J. sambac* is used as the treatment of various illnesses such as rheumatism, paralysis, gallstones, and diabetes mellitus. Flowers of *J. sambac* are used to reduce fever, swollen eyes, and bee stings. Leaf part is usually used to reduce the shortness of breath and as treatment of acne. The root part is used to treat headache and insomnia and is believed can accelerate fracture healing. Essential oil of *J. sambac* is used as fragrance for skin care products as it tones the skin as well as reduces skin inflammation [11]. The *J. sambac* flowers and leaves are largely used in folk medicine to prevent and treat breast cancer. Flowers of *J. sambac* are useful to women when brewed as a tonic as it aids in preventing breast cancer and stopping uterine bleeding [12]. Previous studies done on *J. sambac* reveal that the plant antifungal [13] and anti-cancer [14] works. Essential oil and methanol extract from *Jasminum sambac* have *in vitro* antimicrobial and antioxidant activities which could support the use of the plant by traditional healers to treat various infective diseases [11]. Phytochemical studies showed that the roots contain dotriacontanoic acid, dotriacontanol, oleanolic acid, daucosterol, and hesperidin [15]. Ethyl acetate and water extract of leaves of *Jasminum sambac* showed reduction in plasma glucose level, lipid profile, and serum urea in diabetic rats [16]. However, there is no data reported on antiulcer activities within the plant. Hence, the current study was undertaken to evaluate the gastroprotective effects of ethanolic extracts of this plant against HCl/ethanol-induced gastric ulcers in rats and the effect of acidified ethanol and *J. sambac* extract treatment on Hsp70 and Bax proteins in immunohistochemical staining, and on antioxidant status of gastric tissue homogenate they were assessed by determining MDA levels and antioxidants, PGE₂ and SOD.

2. Materials and Methods

2.1. Omeprazole. In this study, omeprazole was used as the reference antiulcer drug and was obtained from the University Malaya Medical Centre (UMMC) Pharmacy. The drug was dissolved in 0.5% w/v carboxymethylcellulose (CMC) and administered orally to the rats in concentrations of 20 mg/kg body weight (5 mL/kg) according to the recommendation of Mahmood et al. [9].

2.2. Plant Specimen and Preparation of Extraction. Fresh *J. sambac* leaf were obtained from Ethno Resources Sdn Bhd, Selangor, Malaysia, and identified by comparison with the Voucher specimen deposited at the Herbarium of Rimba Ilmu, Institute of Science Biology, University of Malaya, Kuala Lumpur. The dried leaves were powdered using electrical blender. Hundred grams of the fine powder were soaked in 500 mL of 95% ethanol in conical flask for 3 days.

After 3 days, the mixture was filtered using a fine muslin cloth followed by filter paper (Whatman no. 1) and distilled under reduced pressure in an Eyela rotary evaporator (Sigma-Aldrich, USA) and yielded approximately 11.3%. The dry extract was then dissolved in CMC and administered orally to rats at doses of 62.5, 125, 250, and 500 mg/kg body weight (5 mL/kg body weight) [17].

2.3. Acute Toxicity Test and Experimental Animals. Adult healthy male and female Sprague Dawley rats (6–8 weeks old) were obtained from the Animal house, Faculty of Medicine, University of Malaya, Kuala Lumpur (Ethic no. PM/27/07/2010/MAA (R)). The rats weighted between 150–180 g. The animals were given standard rat pellets and tap water. The acute toxicity study was used to determine a safe dose for the extract. Thirty six Sprague Dawley rats (18 males and 18 females) were randomly assigned equally each into 3 groups labeled as vehicle (CMC, 0.5% w/v, 5 mL/kg), 2 g/kg, and 5 g/kg of *J. sambac* extract preparation, respectively [18]. The animals were fasted overnight (food but not water) prior to dosing. Food was withheld for a further 3 to 4 hours after dosing. The animals were observed for 30 min and 2, 4, 8, 24 and 48 h after the administration for the onset of clinical or toxicological symptoms. Mortality, if any, was observed over a period of 2 weeks. The animals were sacrificed on the 15th day. Histology, hematological, and serum biochemical parameters were determined according to the OECD [18]. The study was approved by the ethics Committee for animal experimentation, Faculty of Medicine, University of Malaya, Malaysia. Throughout the experiments, all animals received human care according to the criteria outlined in the Guid for the Care and Use of laboratory Animals prepared by the National Academy of Sciences and published by the national Institute of health.

2.4. Experimental Animals for Gastric Ulcer. Sprague Dawley healthy adult male rats were obtained from the Experimental Animal House, Faculty of Medicine, University of Malaya, and Ethic Number PM/12/05/2010/MAA (R). The rats were divided randomly into 7 groups of 6 rats each. Each rat that weighed between 225–250 g was placed individually in a separate cage (one rat per cage) with wide-mesh wire bottoms to prevent coprophagia during the experiment. The animals were maintained on standard pellet diet and tap water. The study was approved by the Ethics Committee for Animal Experimentation, Faculty of Medicine, University of Malaya, Malaysia.

2.5. Gastric Ulcer Induction by HCl/Ethanol. The rats fasted for 24 hours but were allowed free access to drinking water up till 2 hours before the experiment. A gastric injury model based upon a modification of the method described by Mizui and Doteuchi [19] was induced by acidified ethanol solution (150 mM HCl/absolute ethanol) 40:60 v/v, (HCl/ethanol solution). Normal control groups were orally administered vehicle CMC (5 mL/kg). Ulcer control groups were orally administered vehicle CMC (5 mL/kg). Reference group received oral doses of 20 mg/kg omeprazole.

Experimental groups were orally administered with ethanolic extract of *J. sambac* leaves at doses of 62.5, 125, 250, and 500 mg/kg. One hour after this pretreatment, normal control group was orally administered with CMC, and HCl/ethanol solution (5 mL/kg) was orally administered to ulcer control group, reference group, and experimental group in order to induce gastric ulcers. The rats were euthanized 60 minutes later [10] under an overdose of xylazine and ketamine anesthesia and their stomachs were immediately excised.

2.6. Measurement of Acid Content of Gastric Juice (pH). Samples of gastric contents were analyzed for hydrogen ion concentration by pH metric titration with 0.1 N NaOH solutions using digital pH meter [20].

2.7. Gastric Wall Mucus Determination. The glandular segments of the stomach were removed, weighed, and assessed to determine gastric wall mucus in rats [21]. Each segment was transferred immediately to a 1% Alcian blue solution (in sucrose solution, buffered with sodium acetate at pH 5), and the excess dye was removed by rinsing with sucrose solution. The dye complexes with the gastric wall mucus were extracted with magnesium chloride solution. A 4 mL aliquot of blue extract was then shaken with an equal volume of diethyl ether. The resulting emulsion was centrifuged and the absorbance of the aqueous layer was recorded at 580 nm. The quantity of Alcian blue extracted per gram of glandular tissue (net) was then calculated.

2.8. Gross Gastric Lesions Evaluation. Ulcers of the gastric mucosa appear as elongated bands of black hemorrhagic lesions parallel to the long axis of the stomach. Gastric mucosa of each rat was thus examined for damage. The length and width of the ulcer (mm) were measured by a planimeter ($10 \times 10 \text{ mm}^2 = \text{ulcer area}$) under dissecting microscope (1.8x). The ulcerated area was measured by counting the number of small squares, $2 \text{ mm} \times 2 \text{ mm}$, covering the length and width of each ulcer band. The sum of the areas of all lesions for each stomach was applied in the calculation of the ulcer area (UA) where in the sum of small squares $\times 4 \times 1.8 = \text{UA (mm}^2\text{)}$ according to the recommendation of Mahmood et al., 2011 [17]. The inhibition percentage (I.0%) was calculated by the following formula according to the recommendation of Mahmood et al. [9]:

$$(I\%) = \frac{[(\text{UA}_{\text{control}} - \text{UA}_{\text{treated}}) \div \text{UA}_{\text{control}}]}{\times 100\%} \quad (1)$$

2.9. Histological Evaluation of Gastric Lesions. Specimens of the gastric walls of each rat were fixed in 10% buffered formalin and processed in a paraffin tissue processing machine. Sections of the stomach were made at a thickness of 5μ and stained with Hematoxylin and eosin for histological evaluation [8, 20].

2.10. Immunohistochemistry. Tissue section slides were heated at 60°C for approximately 25 min in hot air oven (Venticell, MMM, Einrichtungen, Germany). The tissue

sections were deparaffinized in xylene and rehydrated using graded alcohol. Antigen retrieval process was performed in 10 mM sodium citrate buffer boiled in microwave. Immunohistochemical staining was conducted according to manufacturer's protocol (Dakocytomation, USA). Briefly, endogenous peroxidase was blocked by peroxidase block (0.03% hydrogen peroxide containing sodium azide) for 5 min. Tissue sections were washed gently with wash buffer, and then incubated with HSP70 (1:500) and Bax (1:200) biotinylated primary antibodies for 15 min. The sections were rinsed gently with wash buffer and placed in buffer bath. The slides were then placed in a humidified chamber and sufficient amount of streptavidin-HRP (streptavidin conjugated to horseradish peroxidase in PBS containing an antimicrobial agent) was added and incubated for 15 min. Then, tissue sections were rinsed gently in wash buffer and place in buffer bath. Diaminobenzidined (DAB-) substrate-chromagen was added to the tissue sections and incubated further for 5 min following washing and counterstaining with hematoxylin for 5 second. The sections were then dipped in weak ammonia (0.037 mol/L) 10 times and then rinsed with distilled water and cover slipped. Positive findings of the immunohistochemical staining should be seen as brown stains under light microscope.

2.11. Antioxidant Activity of Gastric Homogenate

2.11.1. Sample Preparations. For assays of PGE₂, SOD and MDA in gastric tissue of analyzed groups, the tissue homogenates were produced. All the processes were handled at 4°C throughout. Gastric tissue was cut into three small pieces and then weighed (about 200 mg for each) [22]. The tissues were homogenized in teflon homogenizer (Polytron, Heidolph RZR 1, Germany) using the appropriate buffer, depending upon the variable to be measured. After centrifugation at $18,000 \times g$ for 15 min at 4°C , the supernatant was extracted.

2.11.2. Measurement of Superoxide Dismutase (SOD) Activity. SOD activity was measured according to Sun et al. [23]. The activity of the enzyme was evaluated by measuring its capacity to inhibit the photochemical reduction of nitro-blue tetrazolium (NBT). In this assay, the photochemical reduction of riboflavin generates O_2^- that reduces the NBT to produce formazan salt, which absorbs at a wavelength of 560 nm. In the presence of SOD, the reduction of the NBT is inhibited because the enzyme converts the superoxide radical to peroxide. The results are expressed as the quantity of SOD necessary to inhibit the rate of reduction of the NBT by 50% in units of the enzyme per gram of protein. Homogenates (10% of tissue in phosphate buffer) were centrifuged (10 minutes, 3,600 rpm, 4°C), and the supernatant was removed and centrifuged a second time (20 minutes, 12,000 rpm, 4°C). The resulting supernatant was assayed. In a dark chamber, 1 mL of the reactant (50 mM phosphate buffer, 100 nM EDTA, and 13 mM l-methionine, pH 7.8) was mixed with $30 \mu\text{L}$ of the sample, $150 \mu\text{L}$ of $75 \mu\text{M}$ NBT, and $300 \mu\text{L}$ of $2 \mu\text{M}$ riboflavin. The tubes containing the resulting solution

were exposed to fluorescent light bulbs (15 W) for 15 minutes and then read using a spectrophotometer at 560 nm.

2.11.3. Measurement of Membrane Lipids Peroxidation (MDA). The rate of lipoperoxidation in the gastric mucous membrane was estimated by determination of malondialdehyde (MDA) using the thiobarbituric acid reactive substances (TBARSs) test. The stomachs were washed with phosphate buffered saline to minimize the interference of hemoglobin with free radicals and to remove blood adhered to the mucous membrane. The stomachs were homogenized with 10% of the tissue with potassium phosphate buffer. Then, 250 μ L was removed and stored at 37°C for 1 hour, after which 400 μ L of 35% perchloric acid was added, and the mixture was centrifuged at 14,000 rpm for 20 minutes at 4°C. The supernatant was removed, mixed with 400 μ L of 0.6% thiobarbituric acid, and incubated at 95–100°C for 1 hour. After cooling, the absorbance at 532 nm was measured. A standard curve was generated using 1,1,3,3-tetramethoxypropane. The results were expressed as nmol of MDA/mg of protein. The concentration of the proteins was measured using the method described by Bradford method [24]. Measurement of total protein in the stomach sample after ethanol-induced lesions was done, the method is based on the interaction of the Coomassie Blue G250 dye with proteins. At the pH of the reaction, the interaction between proteins of high molecular weight and the dye causes a shift in the dye to the anionic form, which absorbs strongly at 595 nm. Solutions of albumin standard, distilled water, buffer, and each sample were added to the wells. For sample preparation, 2 μ L of a sample and 38 μ L of buffer were added to each well. Then, 200 μ L Bradford's solutions (diluted 5 \times) were added to each well. After 5 minutes, a reading was taken at a wavelength of 595 nm [24].

2.11.4. Measurement of PGE2 Formation Using Enzyme Immunoassays. The gastric mucosa was weighed, minced with scissors, and homogenized at 48°C in PBS buffer. Homogenates were centrifuged at 13 400 g for 10 min, and the supernatants were subjected to a PGE2 assay using a PGE2 Monoclonal Enzyme Immunoassay Kit (Sigma-Aldrich, Malaysia).

2.12. Statistical Analysis. All values were reported as mean \pm S.E.M. The statistical significance of differences between groups was assessed using one-way ANOVA. A value of $P < 0.05$ was considered significant.

3. Results

3.1. Acute Toxicity Study. Acute toxicity is a study in which the animals were treated with the *J. sambac* extract at a dose of 2 g/kg and 5 g/kg and were kept under observation for 14 days. All the animals remained alive and did not manifest any significant visible toxicity at these doses. Thus, clinical observations, serum biochemistry, and histopathology data did not show any significant differences between control and treated groups (Figure 1 and Table 1).

3.2. Gross Evaluation of Gastric Lesions. The antiulcer activity of *J. sambac* leaf extract in HCl/ethanol-induced gastric lesion model is shown in Figures 2 and 3. Results showed that rats pretreated with omeprazole or *J. sambac* extracts before being given HCl/ethanol solution had significantly reduced areas of gastric ulcer formation compared with ulcer control group (Figures 2 and 3). Acidified ethanol solution produced extensive visible black hemorrhagic lesions of gastric mucosa. Moreover, this plant extract significantly suppressed the formation of the ulcers and it was interesting to note the flattening of gastric mucosal folds in rats pretreated with the extract of this plant (500 mg/kg). It was also observed that protection of gastric mucosa was the most prominent in rats pretreated with 500 mg/kg leaf extract (Figures 2 and 3). The significant inhibition of gastric ulcer in rats pretreated with *J. sambac* extract (250 mg/kg) was comparable with omeprazole which is a standard drug used for curing gastric ulcer (Figures 2 and 3).

3.3. Gastric Wall Mucosal Evaluation. Treatment with HCl/ethanol caused a significant decrease in the mucus content of the gastric wall in the untreated animals (ulcer control group, Figure 3). The depleted gastric mucus was significantly replenished after pretreatment with the *J. sambac* extract. It was also found that the pretreatment with *J. sambac* at doses of 62.5, 125, 250, and 500 mg/kg significantly increased the amount of gastric mucus in the acidified ethanol-ulcerated rats (Figure 3).

3.4. pH of Gastric Content. The acidity of gastric content in experimental animals pretreated with omeprazole or *J. sambac* leaf was decreased significantly compared with that of the ulcer control group ($P < 0.05$, Figure 3).

3.5. Histological Evaluation of Gastric Lesions. Histological observation of HCl/ethanol-induced gastric lesions in ulcer control group showed comparatively extensive damage to the gastric mucosa and necrotic lesions penetrate deeply into mucosa and extensive oedema and leucocytes infiltration of the submucosal layer are present (Figure 4). Rats that received pretreatment with *J. Sambac* extract had comparatively better protection of the gastric mucosa as seen by reduction of ulcer area, reduced submucosal oedema, and leucocytes infiltration (Figure 4). This plant has been shown to exert the cytoprotective effects in a dose-dependent manner.

3.6. Immunohistochemistry. Immunohistochemical results demonstrated that treatment of HCl/ethanol induced injury rats with *J. Sambac* extract cause over-expression of Hsp70 protein (Figure 5). In addition to this, the expression of HSP70 protein in normal control and HCl/ethanol-induced gastric tissues (ulcer control group) was found to be downregulated compared to Hsp70 expression in *J. Sambac* extract-treated group (Figure 5). Immunohistochemical staining of Bax protein demonstrated that pretreatment of HCl/ethanol-induced injury rats with *J. Sambac* extract cause downexpression of Bax protein (Figure 5). In addition to

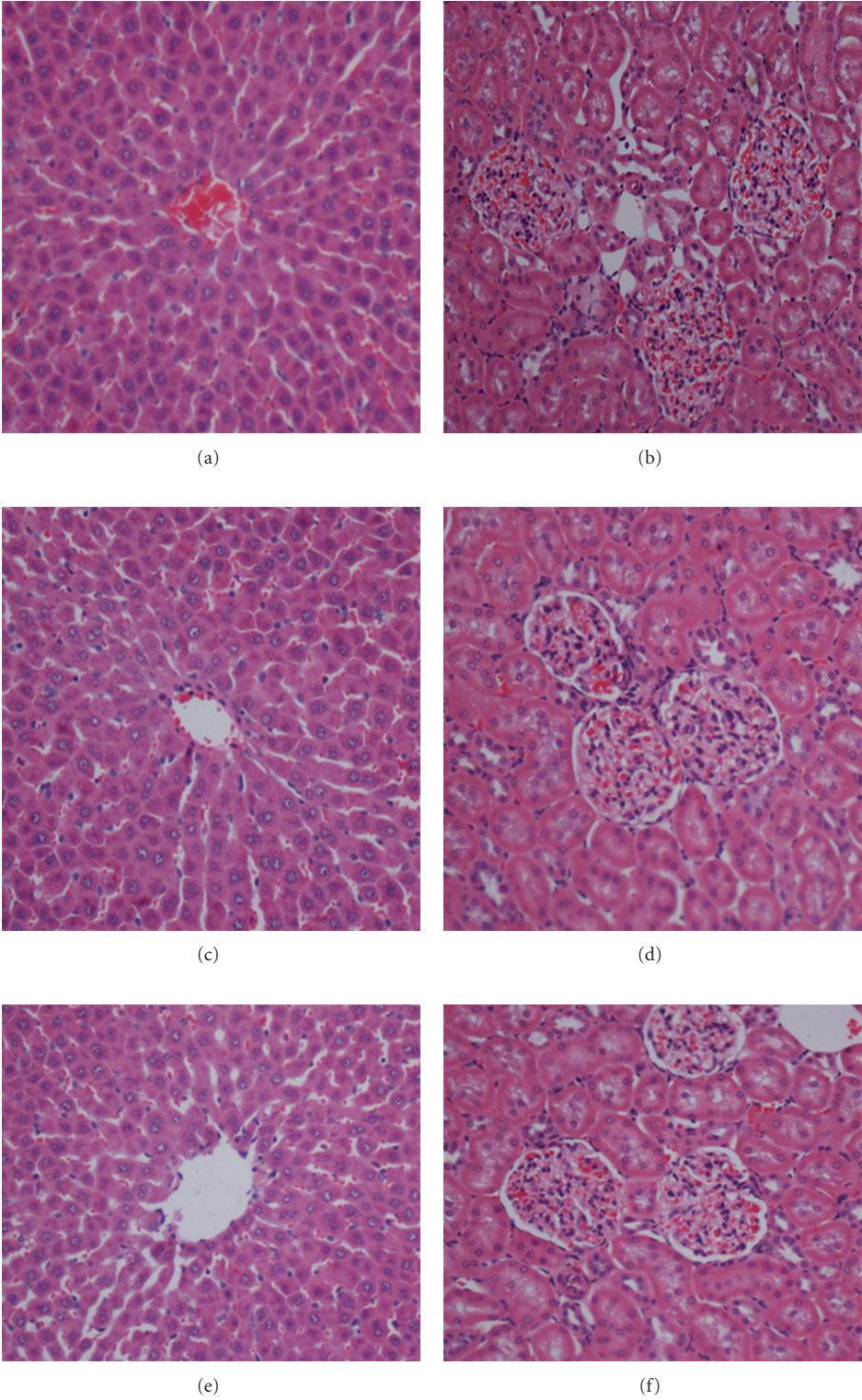


FIGURE 1: Histological sections of the liver and kidney from the acute toxicity test. (a and b) Rats treated with 5 mL/kg of the vehicle (CMC). (c and d) Rats treated with 2000 mg/kg (5 mL/kg) of the *J. sambac* extract. (e and f) Rats treated with 5000 mg/kg (5 mL/kg) of the *J. sambac* extract. There is no significant difference in the structures of the livers and kidneys between the treated and control groups (Hematoxylin and Eosin stain, 20× magnifications).

TABLE 1: (a) Effects of *J. sambac* extract on kidney biochemical parameters in male rats. (b) Effects of *J. sambac* extract on kidney biochemical parameters in female rats. (c) Effects of *J. sambac* extract on liver biochemical parameters in male rats. (d) Effects of *J. sambac* extract on liver biochemical parameters in female rats.

(a)							
Dose	Sodium (mmol/L)	Pottasium (mmol/L)	Chloride (mmol/L)	CO ₂ (mmol/L)	Anion gap (mmol/L)	Urea (mmol/L)	Creatinine (μmol/L)
Vehicle (CMC)	141.33 ± 0.58	4.98 ± 0.04	103.88 ± 0.82	24.12 ± 0.54	18.75 ± 0.46	5.45 ± 0.45	34.83 ± 2.17
LD (2 g/kg)	142.05 ± 0.55	5.02 ± 0.09	105.29 ± 1.02	22.67 ± 0.81	18.55 ± 0.62	6.06 ± 0.83	33.87 ± 2.29
HD (5 g/kg)	143.14 ± 0.68	4.91 ± 0.06	104.35 ± 0.54	23.90 ± 0.64	19.15 ± 0.45	5.63 ± 0.37	35.05 ± 2.26

(b)							
Dose	Sodium (mmol/L)	Pottasium (mmol/L)	Chloride (mmol/L)	CO ₂ (mmol/L)	Anion gap (mmol/L)	Urea (mmol/L)	Creatinine (μmol/L)
Vehicle (CMC)	141.87 ± 0.42	4.83 ± 0.14	105.78 ± 0.67	23.33 ± 0.41	18.00 ± 0.25	7.95 ± 0.33	41.76 ± 2.75
LD (2 g/kg)	142.07 ± 0.56	4.55 ± 0.16	105.85 ± 0.65	22.65 ± 0.42	17.49 ± 0.46	7.97 ± 0.49	42.00 ± 2.36
HD (5 g/kg)	142.15 ± 0.47	4.63 ± 0.18	107.03 ± 0.53	21.96 ± 0.75	17.67 ± 0.48	8.31 ± 0.68	43.13 ± 2.24

Values expressed as mean ± S.E.M. There are no significant differences between groups. Significant value at $P < 0.05$.

(c)									
Dose	Total protein (g/L)	Albumin (g/L)	Globulin (g/L)	TB (μmol/L)	CB (μmol/L)	AP (IU/L)	ALT (IU/L)	AST (IU/L)	GGT (IU/L)
Vehicle (CMC)	60.45 ± 1.25	9.62 ± 0.49	52.02 ± 1.40	2.17 ± 0.17	1.00 ± 0.00	153.00 ± 6.35	50.08 ± 1.62	172.95 ± 6.13	3.26 ± 0.25
LD (2 g/kg)	58.86 ± 0.86	8.81 ± 0.38	50.71 ± 1.21	2.13 ± 0.16	1.00 ± 0.00	154.17 ± 8.10	48.33 ± 0.58	174.23 ± 5.14	3.65 ± 0.42
HD (5 g/kg)	60.15 ± 1.05	9.17 ± 0.46	50.33 ± 1.24	2.02 ± 0.13	1.00 ± 0.00	155.00 ± 7.04	47.87 ± 1.55	175.15 ± 7.02	3.37 ± 0.18

(d)									
Dose	Total protein (g/L)	Albumin (g/L)	Globulin (g/L)	TB (μmol/L)	CB (μmol/L)	AP (IU/L)	ALT (IU/L)	AST (IU/L)	GGT (IU/L)
Vehicle (CMC)	64.33 ± 1.26	11.19 ± 0.17	53.17 ± 1.28	2.00 ± 0.00	1.00 ± 0.00	108.83 ± 4.13	43.17 ± 2.91	171.83 ± 6.38	3.67 ± 0.33
LD (2 g/kg)	63.75 ± 1.19	11.05 ± 0.45	52.33 ± 1.26	2.00 ± 0.00	1.00 ± 0.00	98.83 ± 5.25	42.96 ± 2.70	172.17 ± 6.35	3.50 ± 0.51
HD (5 g/kg)	65.02 ± 2.65	11.30 ± 0.43	53.02 ± 1.25	2.00 ± 0.00	1.00 ± 0.00	102.67 ± 5.17	44.02 ± 1.85	174.28 ± 5.26	3.22 ± 0.44

Values expressed as mean ± S.E.M. There are no significant differences between groups. Significant value at $P < 0.05$.

TB: total bilirubin; CB: conjugated bilirubin; AP: alkaline phosphatase; ALT: alanine aminotransferase; AST: aspartate aminotransferase; GGT: G-glutamyl transferase.

this, the expression of Bax in HCl/ethanol-induced gastric tissues (ulcer control group) was found to be up-regulated compared to *J. Sambac*-treated group (Figure 5).

3.7. Enzymatic Activities in the Gastric Tissue Homogenate.

In gastric tissue homogenate, both PGE₂ and SOD activities in ulcer control group were significantly lower compared with normal control group (Figure 6). Administration of omeprazole or *J. sambac* before HCl/ethanol significantly rise the PGE₂ and SOD compared with ulcer control group (Figure 6). Administration of HCl/ethanol significantly increase the MDA level of gastric homogenate in ulcer control group compared with normal control. Administration of omeprazole or *J. sambac* extract decreased the MDA

level in gastric tissue compared with ulcer control group (Figure 6).

4. Discussion

Peptic ulcers are caused by an imbalance between the protective and the aggressive mechanisms of the mucosa, and are the result of the association of several endogenous factors and aggressive exogenous factors that are related to living conditions [25]. In the HCl/ethanol-induced gastric ulceration model, HCl causes severe damage to gastric mucosa [26], whereas ethanol produces necrotic lesions by direct necrotizing action which in turn reduces defensive factors like the secretion of bicarbonate and production of

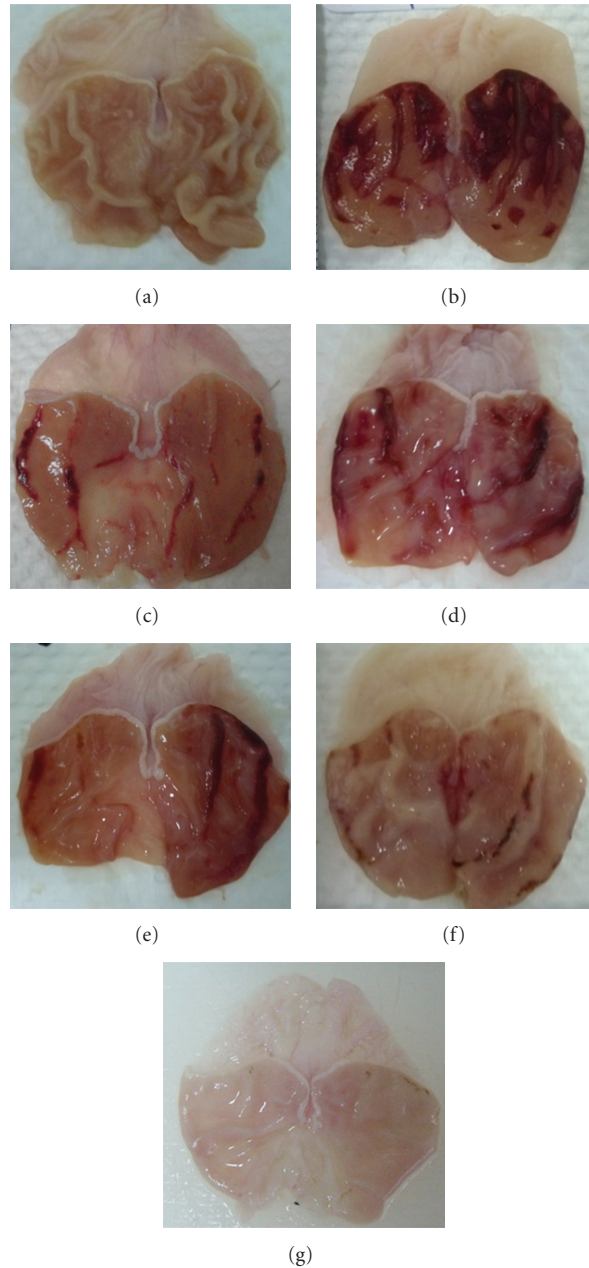


FIGURE 2: Gross appearance of the gastric mucosa in rats. (a) Rats pretreated with 5 mL/kg CMC (normal control). No injuries to the gastric mucosa are seen. (b) Rats pretreated with 5 mL/kg CMC (ulcer control). Severe injuries are seen in the gastric mucosa. HCl/ethanol produced extensive visible hemorrhagic necrosis of gastric mucosa. (c) Rats pretreated with omeprazole (20 mg/kg). Injuries to the gastric mucosa are milder compared to the injuries seen in the ulcer control rats. (d) Rat pretreated with *J. sambac* extract (62.50 mg/kg). Moderate injuries are seen in the gastric mucosa. The extract reduces the formation of gastric lesions induced by acidified ethanol. (e) Rat pretreated with *J. sambac* extract (125 mg/kg). Moderate injuries are seen in the gastric mucosa. The extract reduces the formation of gastric lesions induced by acidified ethanol. (f) Rat pretreated with *J. sambac* extract (250 mg/kg). Mild injuries are seen in the gastric mucosa. The extract reduces the formation of gastric lesions induced by acidified ethanol. (g) rats pretreated with 500 mg/kg of *J. sambac* extract. No injuries to the gastric mucosa are seen instead flattening of gastric mucosa is seen.

mucus [27]. Ethanol-induced gastric lesions impaired gastric defensive factors such as mucus and mucosa circulation [28]. Ethanol causes necrotic lesions of the gastric mucosa in a multifactorial way. It can reach the mucosa by disruption of the mucus-bicarbonate barrier and cause cell rupture in

the wall of blood vessels. These effects are probably due to biological actions, such as of lipid peroxidation, formation of free radicals, intracellular oxidative stress, changes in permeability and depolarization of the mitochondrial membrane prior to cell death [29]. Oral administration

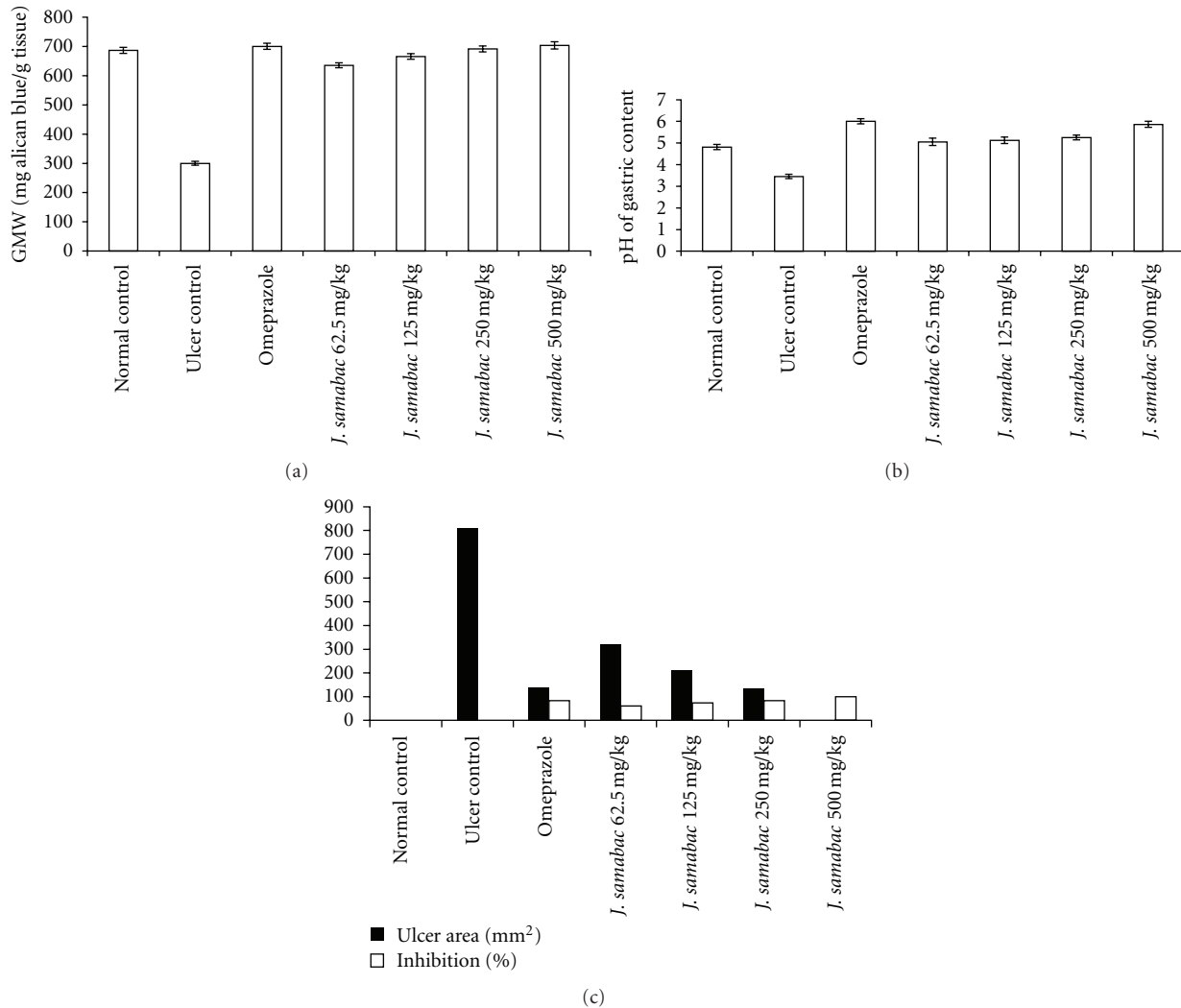


FIGURE 3: (a) Effect of *J. sambac* on GMW. (b) Effect of *J. sambac* on pH of gastric content. (c) Effect of *J. sambac* on Ulcer area and inhibition %.

of absolute ethanol is noxious to the stomach since it affects the gastric mucosa topically by disrupting its barrier and provoking pronounced microvascular changes within a few minutes after its application [30]. In addition, it produces linear hemorrhagic lesions, extensive submucosal edema, mucosal friability, inflammatory cells infiltration, and epithelial cell loss in the stomach, which are typical characteristics of alcohol injury [31]. The pathogenesis of ethanol-induced gastric mucosal damage occurs directly and indirectly through various mediators such as lipoxygenase, cytokines, and oxygen-derived free radicals [32]. Mucus secretion is regarded as a crucial defensive factor in the protection of the gastric mucosa from gastric lesions [33].

In the present study, acute toxicity test did not show any signs of toxicity and mortality. Behavioural changes like irritation, restlessness, respiratory distress, abnormal locomotion, and catalepsy over a period of 14 days were not observed. This revealed that the plant is safe and has no toxicity when administered orally up to 5 g/kg.

Although ulcer etiology is unknown in most cases, it is generally accepted that an imbalance between acid and pepsin production and mucosal integrity would be causative factor acting via endogenous defense mechanisms. The experimental results of the study showed that *J. sambac* extract has an effective antisecretory and antiulcer activity against ethanol-induced gastric mucosal injury. The plant extract decreased the acidity and increased the gastric wall mucus is consistent with results reported by Al-Attar [34]. Similarly, Mahmood et al. [35] discovered a reduction in gastric acidity in treated animals. Pretreatment with *J. sambac* extract could partly reduce the ulcer area and prevent gastric ulceration. Omeprazole exhibits an antisecretory and protective effect [36]. In ulcer control group, it increased the acid secretion resulting into an increase in ulcer area [37]. Omeprazole, as a proton pump inhibitor (PPI), offered a fairly protected gastric mucosa and has been widely used as an acid inhibitor agent for the treatment of disorders related to gastric acid secretion [38]. PPIs are capable of

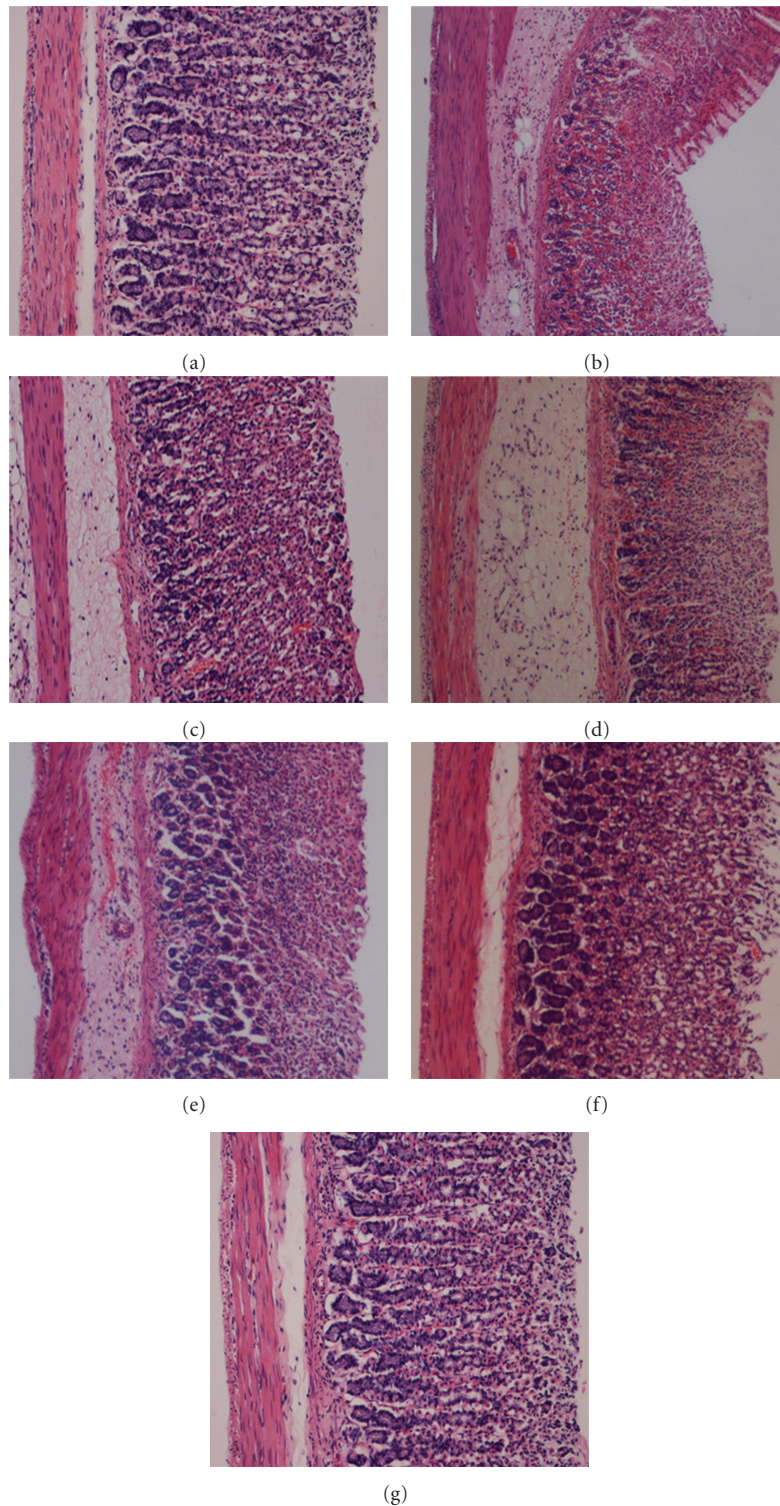


FIGURE 4: Histological study of HCl/ethanol-induced gastric mucosal damage in rats. (a) Rats pretreated with 5 mL/kg of CMC (Normal control group). No injuries to the gastric mucosa are seen. (b) Rats pretreated with 5 mL/kg of CMC (ulcer control group). There is severe disruption to the surface epithelium and necrotic lesions penetrating deeply into mucosa and extensive edema of submucosa layer and leucocytes infiltration is present. (c) Rats pretreated with omeprazole (20 mg/kg). Mild disruption of the surface epithelium mucosa is seen. There is edema and leucocytes infiltration of the submucosal layer. (d) Rat pretreated with *J. sambac* extract (62.50 mg/kg). Moderate disruption of surface epithelium is present. There is submucosal edema and leucocytes infiltration. (e) Rats pretreated with *J. sambac* extract (125 mg/kg). There is mild disruption to the surface epithelium. There is edema with leucocytes infiltration of the submucosal layer. (f) Rats pretreated with *J. sambac* extract (250 mg/kg). There is mild disruption to the surface epithelium. There is no edema or leucocytes infiltration of the submucosal layer. (g) Rats pretreated with *J. sambac* extract (500 mg/kg). There is no disruption to the surface epithelium and no edema or leucocytes infiltration of the submucosal layer (H&E stain 10 \times).

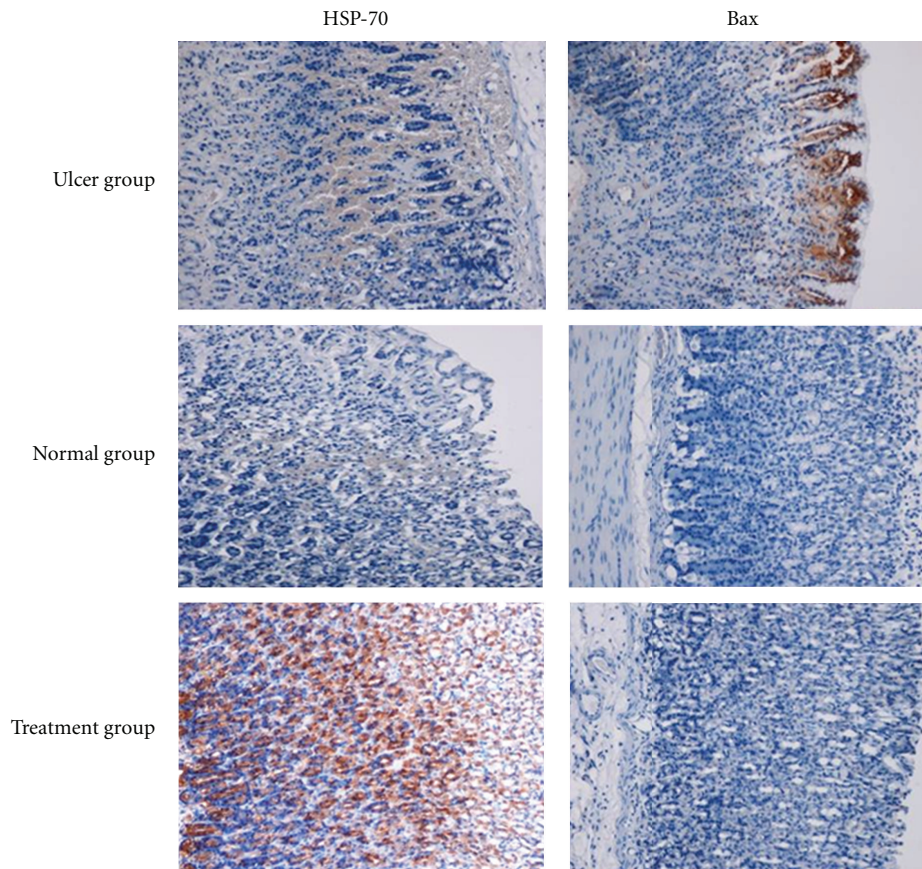


FIGURE 5: Immunohistochemical analysis of expression of Hsp and Bax proteins in the stomach of rats in HCl/ethanol-induced gastric ulcer. Immunohistochemistry staining of Hsp70 and Bax proteins showed overexpression of Hsp70 protein and downexpression of Bax protein in rats pretreated with plant extract (magnification 10 \times).

producing almost complete suppression of acid secretion. The mechanism of action of omeprazole is such that it binds very specifically to a single subunit of the H^+ , K^+ -ATPase at the secretory surface of parietal cell and inactivates it, and it reduces acid secretion regardless of the source of secretory stimulation. Omeprazole are effective in treating peptic ulcer disease and gastroesophageal reflux with both short- and long-term use [39]. The pathogenesis of mucosal damage in the stomach includes the generation of reactive oxygen species (ROS) that seem to play a vital role in the formation of lipid peroxides, accompanied by impairment of antioxidative enzyme activity of cells [2].

Oxidative stress plays important role in the pathogenesis of various diseases including gastric ulcer, with antioxidants being reported to play a significant role in protection of gastric mucosa against various necrotic agents [40]. Antioxidants could help to protect cells from damage caused by oxidative stress and enhanced the body's defense systems against degenerative diseases. Administration of antioxidants inhibits ethanol-induced gastric injury in rat [41]. *J. sambac* extracts have been shown to contain antioxidants [11] and it is likely that gastroprotective activity exerted by this plant extract could be attributed to its antioxidant property.

In addition, *J. sambac* extract are reported to contain flavonoids [42]. Histopathology results of the present study also revealed protection of gastric mucosa and inhibition of leucocytes infiltration of gastric wall in rats pretreated with *J. sambac* extract. Activation and infiltration of neutrophils appear to be involved in the initial processes of formation of the lesion. Similarly, Abdulla et al. [8] demonstrated that the reduction of neutrophil infiltration into ulcerated gastric tissue promotes the prevention of gastric ulcers in rats. Wasman et al. [10] showed that oral administration of plant extract before ethanol administration significantly decreased neutrophil infiltration of gastric mucosa. Absolute alcohol would extensively damage the gastric mucosa leading to increased neutrophil infiltration into the gastric mucosa. Oxygen free radicals derived from infiltrated neutrophils in ulcerated gastric tissues have inhibitory effect on gastric ulcers healing in rats. Neutrophils are a major source of inflammatory mediators and can release potent reactive oxygen species such as superoxide, hydrogen peroxide, and myeloperoxidase derived oxidants as a result they mediate lipid peroxidation [43]. These reactive oxygen species are highly cytotoxic and can induce tissue damage [44]. It is speculated that the gastroprotective effect exerted by this

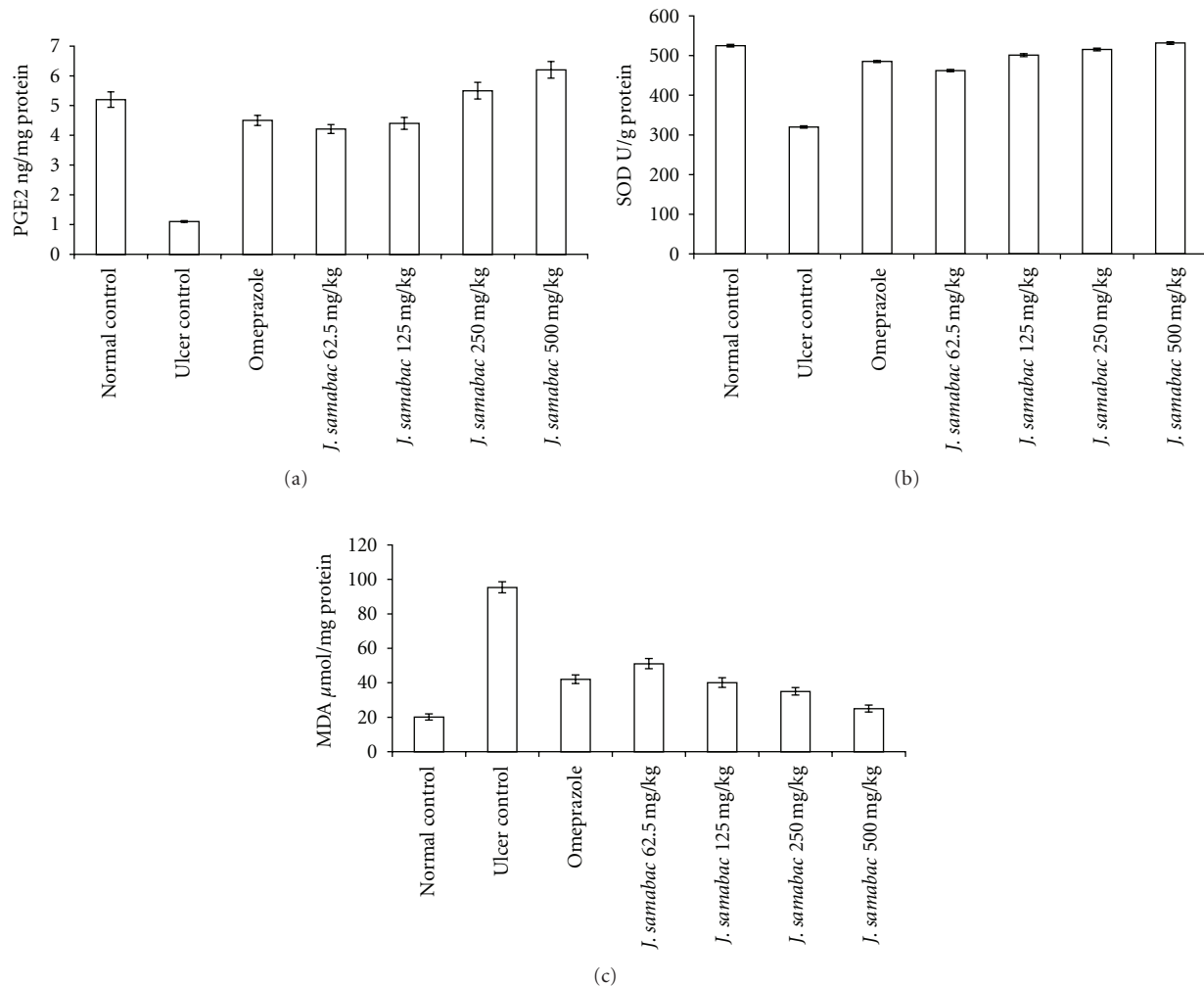


FIGURE 6: (a) Effect of *J. sambac* leaf extract on PGE₂ in gastric tissue homogenate. (b) Effect of *J. sambac* leaf extract on SOD in gastric tissue homogenate. (c) Effect of *J. sambac* leaf extract on MDA in gastric tissue homogenate.

plant extract could be attributed to its anti-inflammatory activity as proved previously [11]. This anti-inflammatory activity could also be a key factor in the prevention of gastric ulcer as reported by Swarnakar et al. [45].

Excessive production of myeloperoxidase (MPO) that exists in neutrophil leukocyte cells and catalyses the formation of toxic hypochlorous acid (HOCl) from hydrogen peroxide causes cell membrane damage by lipid peroxidation. MDA is the final product of lipid peroxidation and is used to determine lipid peroxidation levels in tissues [46]. Gastric MDAs were increased by ulcer control group and decreased by *J. sambac* extract administration, another indicator of a possible antioxidant activity of this plant.

Studies have shown that the excessive recruitment and metabolic activation of neutrophils generate free radicals in several models of gastric damage resulting in inflammation-dependent tissue damage [47]. In the present study, we observed flattening of the mucosal folds which suggests that gastroprotective effect of *J. sambac* leaf extract might be due to a decrease in gastric motility. It is reported that the changes

in the gastric motility may play a role in the development and prevention of experimental gastric lesions [8]. Relaxation of circular muscles may protect the gastric mucosa through flattening of the folds. This will increase the mucosal area exposed to necrotizing agents and reduce the volume of the gastric irritants on rugal crest [8, 10]. Ethanol produces a marked contraction of the circular muscles of rat fundic strip. Such a contraction can lead to mucosal compression at the site of the greatest mechanical stress, at the crests of mucosal folds leading to necrosis and ulceration [17]. Gastric tissue homogenate from animals pretreated with omeprazole or plant extract showed significant antioxidant activity by decreasing the levels of MDA and by elevating the levels of PGE₂ and SOD in response to oxidative stress due to absolute ethanol administration. Free radicals and reactive oxygen species (ROS) that are continuously produced in human body are the cause of cell damage. Therefore, tissues must be protected from oxidative injury through intracellular as well as extracellular antioxidants [48]. SOD converts superoxide to hydrogen peroxide (H₂O₂) which is then transformed into

water by catalase in lysosomes or by glutathione peroxidase (GPx) in mitochondria [49]. SOD-mediated catalysis of superoxide radical anion ($O_2^{\bullet-}$) into less noxious hydrogen peroxide (H_2O_2) represents the first line of antioxidant defense. In our study, SOD activities were significantly reduced after ethanol administration in ulcer control group, and this reduction was prevented by pretreatment with *J. sambac* leaf extract. Reduced activities of SOD in gastric tissue homogenate in ulcer control group that have been observed in our study may be due to increased production of reactive oxygen radicals that can themselves reduce the activity of these enzymes [50]. The reduction of these enzymes in gastric tissue homogenate may lead to a number of deleterious effects. Any compound, natural or synthetic with antioxidant activities might contribute towards the total/partial alleviation of such damage. Lipid peroxidation was found to be an important pathophysiological event in a variety of diseases including gastric ulcer [51]. It is well known that MDA from lipid peroxidation reacts with DNA bases and induces mutagenic lesions [52]. Pratibha et al. [53] showed that the activated oxygen species can in turn induce cellular events such as enzyme inactivation, DNA strands cleavage and also membrane lipid peroxidation. Conclusion, *J. sambac* play a protective role against gastric ulcer. Its antiulcer effect is related to increasing secretion of adherent mucus and pH of gastric content, which may inhibit generation of oxygen-derived free radicals, and decrease the consumption of SOD and maintain content of MDA at normal level.

Prostaglandin E_2 (PGE_2) plays an important role in the regulation of gastric mucus secretion. PGE_2 has protective effects against various gastric injury models [54, 55]. Ethanol has been shown to reduce the mucosal PGE_2 content [56]. PGE_2 is the most abundant gastrointestinal prostaglandin and it regulates functions of the gut, including motility and secretion [57]. PGE_2 has also been shown to exert a protective action on the stomach through the activation of EP receptors [58]. The role of PGE_2 in mediating the gastroprotective effect of *J. sambac* was investigated. The results of the present study suggest that the gastroprotective effect of *J. sambac* is mediated partially by PGE_2 as direct measurement of its mucosal level confirmed that its biosynthesis was significantly enhanced by compound. It has been shown that prostaglandins influence virtually every component of the mucosal defense: stimulating mucus and bicarbonate secretion, maintaining mucosal blood flow, enhancing the resistance of epithelial cells to injury induced by cytotoxins, and inhibiting leukocyte recruitment [59]. Additionally, earlier studies show that prostaglandins exert a gastroprotective action against gastric mucosal lesions through maintenance of gastric mucus synthesis and secretion [60].

Hsp70 proteins defend cells from oxidative stress or heat shock. Ethanol-generated ROS normally act to inhibit the expression of HSP and increase the expression of Bx. Hsp70 prevents these partially denatured proteins from aggregating and allows them to refold. The overexpression of HSP70 noticed in this study could suggest that the plant extract

protected the gastric tissues through the upregulation of Hsp70.

HSP70 is a 70 kDa protein from the HSP family present on mammalian cells. It is the most conserved and abundantly produced protein in response to different forms of stress [61], such as heat, toxic agents, infection, and proliferation [62]. These proteins are responsible to protect cellular homeostatic processes from environmental and physiologic injuries by preserving the structure of normal proteins and repairing or removing damaged proteins [63], which makes the study of this protein an interesting element for possible mechanisms of action elucidation. Our results show significant expression of HSP70 in pretreated plant extract. The HSP70 family functions as a molecular chaperone and reduces stress-induced denaturation and aggregation of intracellular proteins. In addition to its chaperoning activities, Hsp70 has been suggested to exert its cytoprotective action by protecting mitochondria and by interfering with the stress-induced apoptotic program [64].

Tomisato et al. [65] showed the evidence of adaptive cytoprotection through HSP70 induction in animal model experiment that pretreatment of ethanol, which induced Hsp70, made cell to indomethacin injury, and Jin et al. [66] showed that HSP70 could play important role in gastric mucosal adaptation when the PGE_2 level is suppressed by NSAID. Oyake et al. [67] added the data overexpression of Hsp70 confers protection against monochloramine-induced gastric mucosal injury.

Several publications that Hsp70 inductions improved both short-term survival 2-fold and long-term survival 5-fold in mice challenged with ethanol and endotoxin in mice [68]. Hsp70 inductions protected rats against ethanol-induced gastric mucosal damages [69], and Hsp70 inductions led to inactivation of MAPK in alcohol-induced gastric injuries [70] all raised the possibility of the intervention of phytochemicals as novel therapeutics for preventing alcohol-associated gastric damages.

5. Conclusions

In conclusion, an acute toxicity study demonstrated that rats treated with the *J. sambac* (2000 mg or 5000 mg/kg) manifested no abnormal signs. This plant could significantly protect the gastric mucosa against ethanol-induced injury. Such protection was ascertained grossly by significant increase in the gastric wall mucus in comparison with the ulcer control group. Also reduction of ulcer areas in the gastric wall as well as by the reduction or inhibition of edema and leukocytes infiltration of the submucosal layers were shown histologically. Immunohistochemistry staining of Hsp70 and Bax proteins showed overexpression of Hsp70 protein and downexpression of Bax protein in rats pretreated with plant extract. Assays of PGE_2 , SOD and MDA levels of gastric tissue homogenates reveal that this plant significantly increases the PGE_2 and SOD and decreased the level of lipid peroxidation (MDA) in the treated group compared with the ulcer control group. This study provides evidence that the *J. sambac* possesses an antigastric ulcer effect,

which is related partly to a preservation of gastric mucus secretion, to increased production of HSP70 protein, and to the antioxidant enzymes.

Acknowledgment

The authors thank the University of Malaya HIR-MOHE for funding this research study HIR-MOHE (F000009-21001) and (E000045-20001).

References

- [1] D. A. O. V. Araujo, C. Takayama, F. M. De-Faria et al., "Gastro-protective effects of essential oil from *Protium heptaphyllum* on experimental gastric ulcer models in rats," *Brazilian Journal of Pharmacognosy*, vol. 21, no. 4, pp. 721–729, 2011.
- [2] S. J. Konturek, P. C. Konturek, and T. Brzozowski, "Prostaglandins and ulcer healing," *Journal of Physiology and Pharmacology*, vol. 56, no. 5, pp. 5–31, 2005.
- [3] K. S. D. L. Mota, J. C. L. R. Pita, E. C. Estevam et al., "Evaluation of the toxicity and antiulcerogenic activity of the ethanol extract of *Maytenus obtusifolia* Mart. leaves," *Brazilian Journal of Pharmacognosy*, vol. 18, no. 3, pp. 441–446, 2008.
- [4] C. V. Rao, S. K. Ojha, K. Radhakrishnan et al., "Antiulcer activity of *Uleria salicifolia* rhizome extract," *Journal of Ethnopharmacology*, vol. 91, no. 2-3, pp. 243–249, 2004.
- [5] A. Luiz-Ferreira, A. C. A. De Almeida, M. Cola et al., "Mechanisms of the gastric antiulcerogenic activity of *Anacardium humile* St. Hil on ethanol-induced acute gastric mucosal injury in rats," *Molecules*, vol. 15, no. 10, pp. 7153–7166, 2010.
- [6] K. S. De Lira Mota, G. E. N. Dias, M. E. F. Pinto et al., "Flavonoids with gastroprotective activity," *Molecules*, vol. 14, no. 3, pp. 979–1012, 2009.
- [7] G. Schmeda-Hirschmann and E. Yesilada, "Traditional medicine and gastroprotective crude drugs," *Journal of Ethnopharmacology*, vol. 100, no. 1-2, pp. 61–66, 2005.
- [8] M. A. Abdulla, K. A. A. Ahmed, F. H. Al-Bayat, and Y. Masood, "Gastroprotective effect of *Phyllanthus niruri* leaf extract against ethanol-induced gastric mucosal injury in rats," *African Journal of Pharmacy and Pharmacology*, vol. 4, no. 5, pp. 226–230, 2010.
- [9] A. A. Mahmood, A. A. Mariod, F. Al-Bayat, and S. I. Abdel-Wahab, "Anti-ulcerogenic activity of *Gynura procumbens* leaf extract against experimentally-induced gastric lesions in rats," *Journal of Medicinal Plant Research*, vol. 4, no. 8, pp. 685–691, 2010.
- [10] S. Q. Wasman, A. A. Mahmood, H. Salehuddin, A. A. Zahra, and I. Salmah, "Cytoprotective activities of *Polygonum minus* aqueous leaf extract on ethanol-induced gastric ulcer in rats," *Journal of Medicinal Plant Research*, vol. 4, no. 24, pp. 2658–2665, 2010.
- [11] F. Abdoul-Latif, P. Edou, F. Eba et al., "Antimicrobial and antioxidant activities of essential oil and methanol extract of *Jasminum sambac* from Djibouti," *African Journal of Plant Science*, vol. 4, no. 3, pp. 38–43, 2010.
- [12] B. S. Nayak and K. Mohan, "Short communication influence of ethanolic extract of *Jasminum Grandiflorum* linn flower on wound healing activity in rats," *Indian Journal of Physiology and Pharmacology*, vol. 51, no. 2, pp. 189–194, 2007.
- [13] P. Singh, R. Bundiwale, and L. K. Dwivedi, "In-vitro study of antifungal activity of various commercially available itra (Volatile plant oil) against the keratinophilic fungi isolated from soil," *International Journal of Pharma and Bio Sciences*, vol. 2, no. 3, pp. 178–184, 2011.
- [14] W. H. Talib and A. M. Mahasneh, "Antiproliferative activity of plant extracts used against cancer in traditional medicine," *Scientia Pharmaceutica*, vol. 78, no. 1, pp. 33–45, 2010.
- [15] M. A. Rahman, M. S. Hasan, M. A. Hossain, and N. N. Biswas, "Analgesic and cytotoxic activities of *Jasminum sambac* (L.) Aiton," *Pharmacologyonline*, vol. 1, pp. 124–131, 2011.
- [16] Y.-J. Zhang, Y.-Q. Liu, X.-Y. Pu, and C.-R. Yang, "Iridoid glycosides from *Jasminum sambac*," *Phytochemistry*, vol. 38, no. 4, pp. 899–903, 1995.
- [17] A. A. Mahmood, F. H. Al-Bayat, I. Salmah, A. B. Nor Syuhada, H. Harita, and F. F. Mughrabi, "Enhancement of gastric ulcer by *Areca catechu* nut in ethanol-induced gastric mucosal injuries in rats," *Journal of Medicinal Plant Research*, vol. 5, no. 12, pp. 2562–2569, 2011.
- [18] RD Guideline, *OECD guideline for the testing of chemicals*, The Hershberger assay, 2001.
- [19] T. Mizui and M. Doteuchi, "Effect of polyamines on acidified ethanol-induced gastric lesions in rats," *Japanese Journal of Pharmacology*, vol. 33, no. 5, pp. 939–945, 1983.
- [20] K. A. Ketuly, M. A. Abdulla, H. A. Hadi, A. A. Mariod, and S. I. Abdel-Wahab, "Anti-ulcer activity of the 9alpha-bromo analogue of Beclomethasone dipropionate against ethanol-induced gastric mucosal injury in rats," *Journal of Medicinal Plant Research*, vol. 5, no. 4, pp. 514–520, 2011.
- [21] S. J. Corne, S. M. Morrissey, and R. J. Woods, "A method for the quantitative estimation of gastric barrier mucus," *Journal of Physiology*, vol. 242, no. 2, pp. 116P–117P, 1974.
- [22] A. Yildirim, Y. N. Sahin, H. Suleyman, A. Yilmaz, and S. Yildirim, "The role of prednisolone and epinephrine on gastric tissue and erythrocyte antioxidant status in adrenalectomized rats," *Journal of Physiology and Pharmacology*, vol. 58, no. 1, pp. 105–116, 2007.
- [23] Y. Sun, L. W. Oberley, and Y. Li, "A simple method for clinical assay of superoxide dismutase," *Clinical Chemistry*, vol. 34, no. 3, pp. 497–500, 1988.
- [24] M. M. Bradford, "A rapid and sensitive method for the quantitation of microgram quantities of protein utilizing the principle of protein dye binding," *Analytical Biochemistry*, vol. 72, no. 1-2, pp. 248–254, 1976.
- [25] S. Demir, M. Yilmaz, M. Köseoğlu, N. Akalin, D. Aslan, and A. Aydin, "Role of free radicals in peptic ulcer and gastritis," *Turkish Journal of Gastroenterology*, vol. 14, no. 1, pp. 39–43, 2003.
- [26] J. Yamahara, M. Mochizuki, H. Q. Rong, H. Matsuda, and H. Fujimura, "The anti-ulcer effect in rats of ginger constituents," *Journal of Ethnopharmacology*, vol. 23, no. 2-3, pp. 299–304, 1988.
- [27] E. Marhuenda, M. J. Martin, and C. Alarcon De La Lastra, "Antiulcerogenic activity of aescine in different experimental models," *Phytotherapy Research*, vol. 7, no. 1, pp. 13–16, 1993.
- [28] M. D. P. Ferreira, C. M. Nishijima, L. N. Seito et al., "Gastroprotective effect of *Cissus sicyoides* (Vitaceae): involvement of microcirculation, endogenous sulfhydryls and nitric oxide," *Journal of Ethnopharmacology*, vol. 117, no. 1, pp. 170–174, 2008.
- [29] M. Sannomiya, V. B. Fonseca, M. A. Da Silva et al., "Flavonoids and antiulcerogenic activity from *Byrsonima crassa* leaves extracts," *Journal of Ethnopharmacology*, vol. 97, no. 1, pp. 1–6, 2005.

- [30] F. C. Moleiro, M. A. Andreo, R. D. C. D. Santos et al., "Mouriri elliptica: validation of gastroprotective, healing and anti-Helicobacter pylori effects," *Journal of Ethnopharmacology*, vol. 123, no. 3, pp. 359–368, 2009.
- [31] W. Jelski, M. Kozłowski, J. Laudanski, J. Niklinski, and M. Szmitkowski, "The activity of class I, II, III, and IV Alcohol Dehydrogenase (ADH) Isoenzymes and Aldehyde Dehydrogenase (ALDH) in esophageal cancer," *Digestive Diseases and Sciences*, vol. 54, no. 4, pp. 725–730, 2009.
- [32] O. M. E. Abdel-Salam, J. Czimmer, A. Debreceni, J. Szolcsányi, and G. Mózsik, "Gastric mucosal integrity: gastric mucosal blood flow and microcirculation. An overview," *Journal of Physiology Paris*, vol. 95, no. 1–6, pp. 105–127, 2001.
- [33] F. S. Oluwole, J. A. Ayo, B. O. Omolaso, B. O. Emikpe, and J. K. Adesanwo, "Methanolic extract of Tetracera potatoria, an antiulcer agent increases gastric mucus secretion and endogenous antioxidants," *Nigerian Journal of Physiological Sciences*, vol. 23, no. 1–2, pp. 79–83, 2008.
- [34] A. M. Al-Attar, "Protective effect of Avicennia alba leaves extract on gastric mucosal damage induced by ethanol," *Research Journal of Medicinal Plant*, vol. 5, no. 4, pp. 477–490, 2011.
- [35] A. A. Mahmood, K. Sidik, and H. M. Fouad, "Prevention of ethanol-induced gastric mucosal injury by Ocimum basilicum seed extract in rats," *ASM Science Journal*, vol. 1, pp. 1–6, 2007.
- [36] M. L. Schubert, "Gastric secretion," *Current Opinion in Gastroenterology*, vol. 21, no. 6, pp. 636–643, 2005.
- [37] V. C. Devaraj, B. Gopala Krishna, G. L. Viswanatha, V. Satya Prasad, and S. N. Vinay Babu, "Protective effect of leaves of Raphanus sativus Linn on experimentally induced gastric ulcers in rats," *Saudi Pharmaceutical Journal*, vol. 19, no. 3, pp. 171–176, 2011.
- [38] X. Q. Li, T. B. Andersson, M. Ahlström, and L. Weidolf, "Comparison of inhibitory effects of the proton pump-inhibiting drugs omeprazole, esomeprazole, lansoprazole, pantoprazole, and rabeprazole on human cytochrome P450 activities," *Drug Metabolism and Disposition*, vol. 32, no. 8, pp. 821–827, 2004.
- [39] O. J. Ode and O. V. Asuzu, "Investigation of cassia singueana leaf extract for antiulcer effects using ethanol-induced gastric ulcer model in rats," *International Journal of Plant, Animal and Environmental Sciences*, vol. 1, pp. 1–7, 2011.
- [40] D. A. A. Bardi, M. A. Sarah Khan, S. Z. Sabri et al., "Anti-ulcerogenic activity of typhonium flagelliforme aqueous leaf extract against ethanol-induced gastric mucosal injury in rats," *Scientific Research and Essays*, vol. 6, no. 15, pp. 3232–3239, 2011.
- [41] R. Sathish, A. Sahu, and K. Natarajan, "Antiulcer and antioxidant activity of ethanolic extract of Passiflora foetida L," *Indian Journal of Pharmacology*, vol. 43, no. 3, pp. 336–339, 2011.
- [42] M. Kalaiselvi and K. Kalaivani, "Phytochemical analysis and antilipid peroxidative effect of Jasminum sambac (L.) Ait oleaceae," *Pharmacologyonline*, vol. 1, pp. 38–43, 2011.
- [43] H. Kobayashi, E. Gil-Guzman, A. M. Mahran et al., "Quality control of reactive oxygen species measurement by luminol-dependent chemiluminescence assay," *Journal of Andrology*, vol. 22, no. 4, pp. 568–574, 2001.
- [44] C. L. Cheng and M. W. L. Koo, "Effects of Centella asiatica on ethanol induced gastric mucosal lesions in rats," *Life Sciences*, vol. 67, no. 21, pp. 2647–2653, 2000.
- [45] S. Swarnakar, A. Mishra, K. Ganguly, and A. V. Sharma, "Matrix metalloproteinase-9 activity and expression is reduced by melatonin during prevention of ethanol-induced gastric ulcer in mice," *Journal of Pineal Research*, vol. 43, no. 1, pp. 56–64, 2007.
- [46] H. Dursun, M. Bilici, F. Albayrak et al., "Antiulcer activity of fluvoxamine in rats and its effect on oxidant and antioxidant parameters in stomach tissue," *BMC Gastroenterology*, vol. 9, article no. 36, 2009.
- [47] F. B. Potrich, A. Allemand, L. M. da Silva et al., "Antiulcerogenic activity of hydroalcoholic extract of Achillea millefolium L.: involvement of the antioxidant system," *Journal of Ethnopharmacology*, vol. 130, no. 1, pp. 85–92, 2010.
- [48] B. Halliwell, K. Zhao, and M. Whiteman, "The gastrointestinal tract: a major site of antioxidant action?" *Free Radical Research*, vol. 33, no. 6, pp. 819–830, 2000.
- [49] J. S. Johansen, A. K. Harris, D. J. Rychly, and A. Ergul, "Oxidative stress and the use of antioxidants in diabetes: linking basic science to clinical practice," *Cardiovascular Diabetology*, vol. 4, article no. 5, 2005.
- [50] M. Yasar, S. Yildiz, R. Mas et al., "The effect of hyperbaric oxygen treatment on oxidative stress in experimental acute necrotizing pancreatitis," *Physiological Research*, vol. 52, no. 1, pp. 111–116, 2003.
- [51] D. Bandyopadhyay, K. Biswas, R. J. Reiter, and R. K. Banerjee, "Gastric toxicity and mucosal ulceration induced by oxygen-derived reactive species: protection by melatonin," *Current Molecular Medicine*, vol. 1, no. 4, pp. 501–513, 2001.
- [52] M. Benamira, K. Johnson, A. Chaudhary, K. Bruner, C. Tibbetts, and L. J. Marnett, "Induction of mutations by replication of malondialdehyde-modified M13 DNA in Escherichia coli: determination of the extent of DNA modification, genetic requirements for mutagenesis, and types of mutations induced," *Carcinogenesis*, vol. 16, no. 1, pp. 93–99, 1995.
- [53] R. Pratibha, R. Sameer, P. V. Rataboli, D. A. Bhiwade, and C. Y. Dhume, "Enzymatic studies of cisplatin induced oxidative stress in hepatic tissue of rats," *European Journal of Pharmacology*, vol. 532, no. 3, pp. 290–293, 2006.
- [54] J. L. Wallace, "Prostaglandins, NSAIDs, and cytoprotection," *Gastroenterology Clinics of North America*, vol. 21, no. 3, pp. 631–641, 1992.
- [55] T. Brzozowski, P. C. Konturek, S. J. Konturek, I. Brzozowska, and T. Pawlik, "Role of prostaglandins in gastroprotection and gastric adaptation," *Journal of Physiology and Pharmacology*, vol. 56, supplement 5, pp. 33–55, 2005.
- [56] W. Zhao, F. Zhu, W. Shen et al., "Protective effects of DIDS against ethanol-induced gastric mucosal injury in rats," *Acta Biochimica et Biophysica Sinica*, vol. 41, no. 4, pp. 301–308, 2009.
- [57] C. J. Hawkey and D. S. Rampton, "Prostaglandins and the gastrointestinal mucosa: are they important in its function, disease, or treatment?" *Gastroenterology*, vol. 89, no. 5, pp. 1162–1188, 1985.
- [58] K. Takeuchi, S. Kato, and A. Tanaka, "Gastrointestinal protective action of prostaglandin E₂ and EP receptor subtypes," in *Gastrointestinal Mucosal Repair and Experimental Therapeutics*, pp. 227–242, Karger, Basel, Switzerland, 2002.
- [59] T. A. Miller, "Protective effects of prostaglandins against gastric mucosal damage: current knowledge and proposed mechanisms," *The American Journal of Physiology*, vol. 245, no. 5, pp. G601–G623, 1983.
- [60] K. Ishihara, H. Kuwata, S. Ohara, H. Okabe, and K. Hotta, "Changes of rat gastric mucus glycoproteins in cytoprotection: influences of prostaglandin derivatives," *Digestion*, vol. 39, no. 3, pp. 162–171, 1988.

- [61] K. Shichijo, M. Ihara, M. Matsuu, M. Ito, Y. Okumura, and I. Sekine, "Overexpression of heat shock protein 70 in stomach of stress-induced gastric ulcer-resistant rats," *Digestive Diseases and Sciences*, vol. 48, no. 2, pp. 340–348, 2003.
- [62] M. Oberringer, H. P. Baum, V. Jung et al., "Differential expression of heat shock protein 70 in well healing and chronic human wound tissue," *Biochemical and Biophysical Research Communications*, vol. 214, no. 3, pp. 1009–1014, 1995.
- [63] M. Tytell and P. L. Hooper, "Heat shock proteins: new keys to the development of cytoprotective therapies," *Expert Opinion on Therapeutic Targets*, vol. 5, no. 2, pp. 267–287, 2001.
- [64] K. Rokutan, "Role of heat shock proteins in gastric mucosal protection," *Journal of Gastroenterology and Hepatology*, vol. 15, pp. D12–D19, 2000.
- [65] W. Tomisato, N. Takahashi, C. Komoto, K. Rokutan, T. Tsuchiya, and T. Mizushima, "Geranylgeranylacetone protects cultured guinea pig gastric mucosal cells from indomethacin," *Digestive Diseases and Sciences*, vol. 45, no. 8, pp. 1674–1679, 2000.
- [66] M. Jin, M. Otaka, A. Okuyama et al., "Association of 72-kDa heat shock protein expression with adaptation to aspirin in rat gastric mucosa," *Digestive Diseases and Sciences*, vol. 44, no. 7, pp. 1401–1407, 1999.
- [67] J. Oyake, M. Otaka, T. Matsushashi et al., "Over-expression of 70-kDa heat shock protein confers protection against monochloramine-induced gastric mucosal cell injury," *Life Sciences*, vol. 79, no. 3, pp. 300–305, 2006.
- [68] G. D. Lappas, I. E. Karl, and R. S. Hotchkiss, "Effect of ethanol and sodium arsenite on HSP-72 formation and on survival in a murine endotoxin model," *Shock*, vol. 2, no. 1, pp. 34–40, 1994.
- [69] S. W. Park, T. Y. Oh, Y. S. Kim et al., "Artemisia asiatica extracts protect against ethanol-induced injury in gastric mucosa of rats," *Journal of Gastroenterology and Hepatology*, vol. 23, no. 6, pp. 976–984, 2008.
- [70] J. S. Lee, T. Y. Oh, Y. K. Kim et al., "Protective effects of green tea polyphenol extracts against ethanol-induced gastric mucosal damages in rats: stress-responsive transcription factors and MAP kinases as potential targets," *Mutation Research*, vol. 579, no. 1-2, pp. 214–224, 2005.

Research Article

Biological Effect of Leaf Aqueous Extract of *Caesalpinia pyramidalis* in Goats Naturally Infected with Gastrointestinal Nematodes

Roberto Robson Borges-dos-Santos,¹ Jorge A. López,² Luciano C. Santos,³ Farouk Zacharias,⁴ Jorge Maurício David,⁵ Juceni Pereira David,⁶ and Fernanda Washington de Mendonça Lima⁶

¹ Escola de Medicina Veterinária, Universidade Federal da Bahia, 40170-000 Salvador, BA, Brazil

² Programa de Pós-Graduação em Biotecnologia Industrial, Instituto de Tecnologia e Pesquisa, Universidade Tiradentes, 49032-490 Aracaju, SE, Brazil

³ Centro de Pesquisa Gonçalo Moniz-FIOCRUZ, 40296-710 Salvador, BA, Brazil

⁴ Empresa Baiana de Desenvolvimento Agrícola, 41635-150 Salvador, BA, Brazil

⁵ Instituto de Química, Universidade Federal da Bahia, 40170-290 Salvador, BA, Brazil

⁶ Faculdade de Farmácia, Universidade Federal da Bahia, 41.170-280, Salvador, BA, Brazil

Correspondence should be addressed to Fernanda Washington de Mendonça Lima, ferwlima@terra.com.br

Received 27 October 2011; Revised 19 January 2012; Accepted 20 January 2012

Academic Editor: Vincenzo De Feo

Copyright © 2012 Roberto Robson Borges-dos-Santos et al. This is an open access article distributed under the Creative Commons Attribution License, which permits unrestricted use, distribution, and reproduction in any medium, provided the original work is properly cited.

Forty-eight goats naturally infected with gastrointestinal nematodes were randomly divided into four groups ($n = 12$): negative control (G1) (untreated), positive control (G2) (treated with doramectin, 1 mL/50 Kg b.w.), and G3 and G4 treated with 2.5 and 5 mg/Kg b.w. of a leaf aqueous extract of *Caesalpinia pyramidalis* (CP). Fecal and blood samples were regularly collected for the evaluation of fecal egg count (FEC), hematological and immunological parameters to assess the anthelmintic activity. In treated animals with CP, there was noted a significant reduction of 54.6 and 71.2% in the mean FEC ($P < 0.05$). An increase in IgA levels was observed in G3 and G4 ($P < 0.05$), during the experimental period, suggesting that it was stimulated by the extract administration. In conclusion, the results showed that CP provoked a protective response in infected animals treated with them. This response could be partly explained by the CP chemical composition.

1. Introduction

Goat herding is an attractive source of income for farmers in northeastern Brazil. However, gastrointestinal nematodes (GINs) remain one of the greatest limiting factors to successful and sustainable livestock production worldwide [1]. Therefore, economic losses caused by GIN are related to decreased production, treatment costs, and even animal death in small ruminant production [2]. In semiarid Brazilian region, haemonchosis causes severe economic losses in livestock production (e.g., weight loss, stunted growth, and death) [3]. Its control based on the use of commercial anthelmintics is no longer considered sustainable due to an increased prevalence of GIN resistance as well as chemical residue and toxicity problems [2]. For these various reasons,

interest in the plant screening for their anthelmintic activity remains of great scientific interest despite extensive use of synthetic chemicals in modern clinical practices all over the world as an alternative source of anthelmintics [4–6]. There are several species of plants used by traditional communities in the Brazilian semiarid.

The genus *Caesalpinia* (Fabaceae), composed of tropical or subtropical trees and shrubs, contains more than 150 species, spread throughout the world [7]. *Caesalpinia pyramidalis* Tul. (CP), known regionally as “catingueira” and “pau-de-rato”, is used as fodder in animal feed [8] and in the traditional medicine [9, 10]. Some compounds from *C. pyramidalis* leaves have previously been reported, such 4-*O*- β -glucopyranosyloxy-*Z*-7-hydroxycinnamic acid, lupeol, aghatisflavone, and other phenolics [10–13].

This work aims at evaluating the anthelmintic effect of CP extract *in vivo* against GIN natural infected goats in order to confirm the benefits.

2. Material and Methods

2.1. Plant Material and Aqueous Extract Preparation. *C. pyramidalis* leaves were collected in the caatinga region from Bahia, Brazil. A voucher herbarium specimen (number 0240291), classified systematically by Professor Leticia Scardino (Instituto de Biologia, UFBA), was deposited at Herbarium Alexandre Leal Costa (UFBA).

Leaves were air dried in an oven at 40°C. The powdered material (200 g) was extracted with boiling water for 20 min. The extract was filtered and lyophilized for bioassay analysis.

2.2. *Haemonchus contortus* Antigen Preparation. *H. contortus* adults of either sex, harvested from abomasums of slaughtered goats, were washed in PBS (pH 7.2) to prepare a crude extract by disrupting parasites in PBS pH 7.2 at 4°C by 30 s periods of ultrasonic treatment. After centrifugation (1200 g, 15 min, 4°C), the supernatant was either used immediately or stored at -20°C. The extract was used as the test antigen in ELISA.

2.3. Animals. The study was carried out with a total of 48 mixed bred goats selected from herded animals maintained at the Experimental Station of Bahia Company for Agro-Livestock Development (EBDA) in Jaguarari, Bahia, Brazil. Goats were traditional grazing under extensive management practices in the Brazilian semiarid region and had naturally acquired gastrointestinal nematode infection, being confirmed prior the experiment beginning by faeces egg count (FEC) (average values before starting the trial G: 483,33 ± 440,73; G2: 375,00 ± 344,11; G3: 591,67 ± 802,79; G4: 491,67 ± 454,19). Animals were randomly divided into four equal groups ($n = 12$). The first group (G1) served as the negative control and received no treatment while second group (G2) was the positive control treated with doramectin (1 mL/50 Kg b.w., Dectomax, Pfizer). The third and fourth groups (G3 and G4) were drenched with CP extract (2.5 and 5.0 mg/Kg b.w., resp.). The anthelmintic doramectin and the extract were administered through three consecutive days from the time zero.

Goats were kept under free management and grazed on the harvested crops, remnants of the fodder and vegetables, herbs, weeds, and shrubs along the banks of water channels throughout the experiment and monitored by examination of blood and faecal samples for immunological and parasitological parameters at 30 and 60 days after treatment. Animals were weighed (average weight before starting the trial G1: 14,70 ± 2,86; G2: 13,45 ± 3,09; G3: 15,10 ± 2,96; G4: 17,0 ± 2,09) at stage zero and five days before the collection intervals to minimise the handling stress effects. The monitoring was carried out between March and May, coinciding with the end of the dry season and beginning of the rainy period. The experiment was conducted in accordance with the guidelines

for care and use of experimental animals of the Brazilian College of Experimental Animal (COBEA).

2.4. FEC and Blood Sampling. Faecal and blood samples were recovered at day 0 and at 30 and 60 days after treatment. For FEC determination, faeces (2 g) were collected directly from the rectum and processed using a modified McMaster technique and expressed as eggs per gram [14].

Blood with and without anticoagulant (Na₂EDTA; 1 mg/mL) was individually collected by jugular venipuncture. Blood collected with anticoagulant was used for monitoring red and white blood cell counts, expressed in number of cell/mm³. The packed cell volume (PCV) was measured by the microhaematocrit method. Sera were separated from blood samples without anticoagulant and stored at -20°C until required.

2.5. Antibody Responses. An ELISA was used to detect total IgG and IgA and specific anti-*Haemonchus* IgG in serum. For anti-*Haemonchus* serum IgG levels, plates were coated with an antigen solution (40 µg/well in 50 mM carbonate buffer pH 9.6) by incubating at 4°C for 20 h. Afterwards, 100 µL serum samples (1 : 200 diluted in PBS/0.05% Tween/0.25% defatty powered milk) were added in duplicate and incubated (1 h/37°C). After washing, 100 µL of optimally diluted anti-goat HRP-conjugated IgG (Bethyl Inc. Montgomery, Texas, USA) was added and incubated (1 h/37°C). After washing, 100 µL of *o*-phenylenediamine (6 mg in 15 mL of 0.1 M citrate phosphate buffer pH 5.0) and 10 µL of H₂O₂ were added to wells. After 20 min of incubation, the reaction was stopped with 50 µL of 0.5 M H₂SO₄. Optical Density (OD) at 450 nm was measured in an ELISA plate reader (Stat Fax, USA).

For total IgA and IgG dosages, the same protocol was employed, using a commercial kit (Bethyl Inc. Montgomery, TX, USA). Dosage standard curves were obtained following the protocols provided by the manufacturer.

2.6. Statistical Analysis. Results were expressed as means ± standard deviation (SD), using Kruskal-Wallis nonparametric (ANOVA on ranks) tests and multiple comparison tests, such as Dunn. $P < 0.05$ was considered statistically significant. All of the analyses were performed using the statistical software Graph Pad (San Diego, USA).

3. Results

3.1. Parasitological and Zootechnical Measures. FEC determination was carried out in four regular intervals, initially, two weeks before assay, with the aim at tracing and randomly distributing the animals into four groups at day zero, prior treatment (extract and doramectin), and then at days 30 and 60 after treatment in all groups.

The *in vivo* trials on the anthelmintic activity of CP extract showed significant reduction in the mean faecal egg count throughout experimental period (Figure 1(a)). The egg excretion pattern was similar for the positive control (G2) and treated groups (G3 and G4). However, a significant

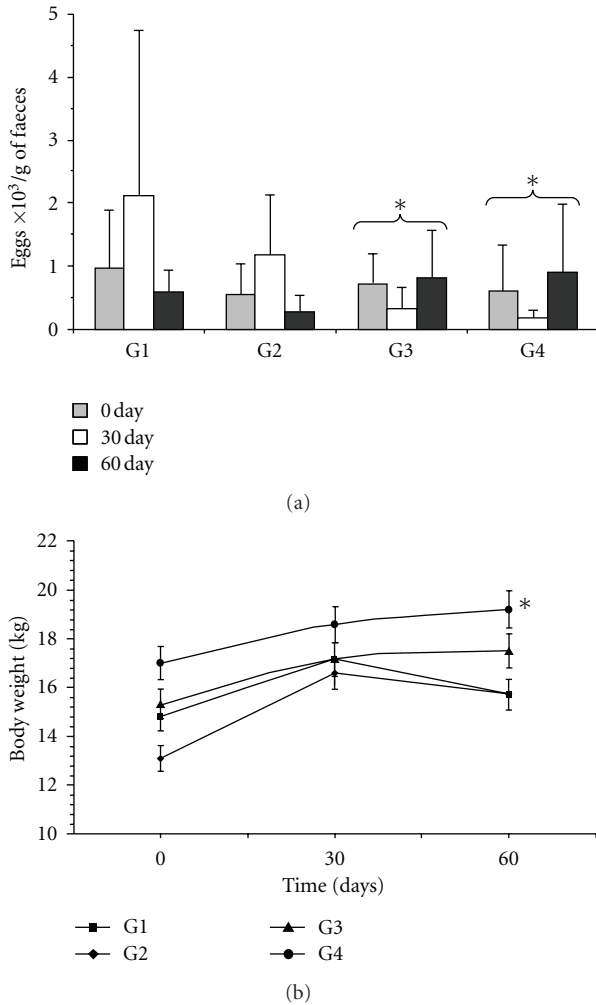


FIGURE 1: Mean number of nematode egg per gram of faeces in naturally infected goats (a) and mean live weight (b) along the experimental period. Values are means \pm standard deviation. An asterisk mark represents significant differences; $P < 0.05$. G1: negative control (untreated); G2: positive control (treated with doramectin, 1 mL/50 Kg b.w.); G3 and G4: animals treated with 2.5 and 5 mg/Kg of CP extract, respectively.

difference ($P < 0.05$) was observed between the negative control (G1), G3 and G4, which received the extract doses of 2.5 and 5.0 mg/Kg b.w., respectively. All groups treated with this extract had a positive FEC reduction of 54.61% for G3 (2.5 mg/Kg b.w.) and 71.21% for G4 (5.0 mg/Kg b.w.). Regarding the change in live body weight, no statistically significant difference was observed among G1, G2, and G3. However, the G4 gained a significant difference in body weight ($P < 0.001$) (Figure 1(b)).

3.2. Haematological Profiles. PCV values did no change during experimental period. The average values were not significantly different between the extract and Doromectin treated groups (G2, G3, G4) and the untreated group (G1). For leukocyte counts, similar results were observed in the posttreatment groups and also no significant differences were

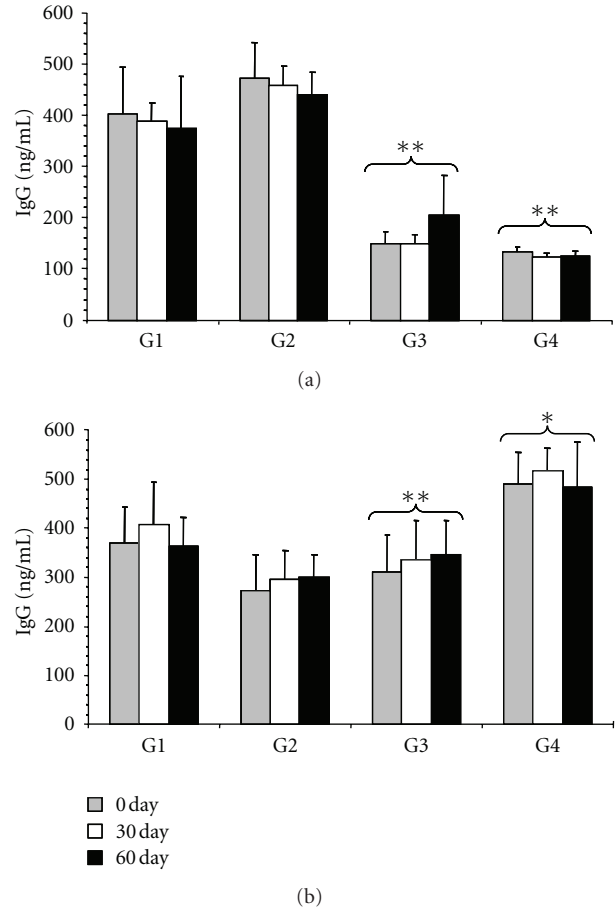


FIGURE 2: Mean concentrations of serum IgG (a) and IgA (b) in goats naturally infected with gastrointestinal nematodes, trated with 2.5 and 5 mg/Kg b.w of CP extract. Values are expressed as means \pm standard deviation. Significant differences are indicated by an asterisk marks; ($*P < 0.05$; $**P < 0.0001$). G1: negative control (untreated); G2: positive control (treated with doramectin, 1 mL/50 Kg b.w.); G3 and G4: animals treated with 2.5 and 5 mg/Kg of CP extract, respectively.

seen in the eosinophil values in blood ($P > 0.05$) when compared to the negative and positive control. Basically, the counts remained stable throughout the experiment without any difference for all groups.

3.3. Serum Antibody Responses. The average values of serum concentration for IgG and IgA are presented in Figure 2. In the positive control (G2), a significant rise in serum IgG ($P < 0.001$) was observed, whereas in the CP extract-treated groups (G3 and G4), IgG levels were low, with a significant decrease ($P < 0.001$) as shown in Figure 2(a). In addition, serum IgA levels had a significant response ($P < 0.05$) in the 5.0 mg CP extract-treated group (G4; Figure 2(b)). The highest concentrations of IgA were detected in samples from G3 and G4. The concentration of G4 was 488.69 ng/mL at the baseline moment, 517.12 ng/mL at 30 days, and 483.51 ng/mL 60 days later. With the exception of the variation observed for G3, which showed the highest IgA

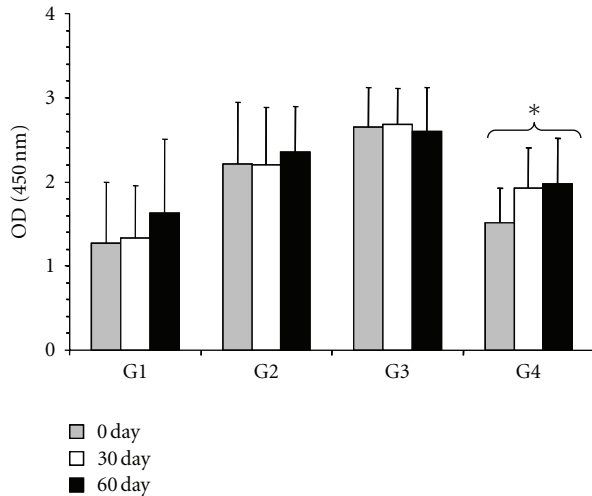


FIGURE 3: Optical density (OD) variations in ELISA Serum-specific IgG response using adult *H. contortus* antigenic extract in naturally infected goats, treated with doramectin and CP extract. Optical densities were measured by ELISA at 450 nm. Significant differences are indicated by an asterisk marks ($P < 0.05$). G1: negative control (untreated); G2: positive control (treated with doramectin, 1 mL/50 Kg b.w.); G3 and G4: animals treated with 2.5 and 5 mg/Kg of CP extract, respectively.

concentration after 60 days of treatment, being 309.04 ng/mL before treatment, 336.18 ng/mL at 30 days, and 345.72 ng/mL at 60 days after treatment, the remaining groups had an increasing concentration values from baseline until 30 days and decreasing concentration at 60 days. Moreover, the serum anti-*Haemonchus* antibody responses presented significant increases in G2 and G3, whereas G4 yielded an average OD of 1.52 ± 0.40 , 1.93 ± 0.48 , and 1.98 ± 0.55 for the three collected sample periods, presenting a decline when compared with those obtained in G3 (Figure 3).

4. Discussion

This work was carried out in order to find a phytotherapeutic to help control GIN in small ruminants. The parasitological analysis indicated that the CP extract exhibited anthelmintic activity in naturally infected goats, whose effectiveness was evidenced by the reduction in FEC as compared to the negative control group. Probably the higher deviations on the determined FEC values were due to the traditional and extensive management practices in the Brazilian semiarid region; therefore, the goats were always exposed to a contaminated environment. In addition, should be considered the differences between animals and their susceptibility to nematode infection [15, 16]. A similar study with a hydroalcoholic extract of *C. crista*, a plant of the same genus, showed *in vivo* a significant FEC reduction [5].

Under the experimental conditions, the results with *C. pyramidalis* extract also provided evidence of a reduction in nematodes of goats compared to controls. A possible

explanation of this reduction may be due to the direct effect of CP extract on parasite leading to drop in FEC in natural infected goats. One of the effects resulting from the extract treatment could be due to the decrease of fecundity of female parasites, which can be explained by the presence of active compounds in this plant extracts.

The active principles for the anthelmintic effect of *C. pyramidalis* have not been exactly identified so far. However, its phytochemical analysis revealed the presence of different chemical compounds, among them polyphenols, like tannins and flavonoids [11, 12], that could be considered as the responsible for this bioactivity [16, 17]. Once some plants have been reported to have anthelmintic properties, attributed to secondary metabolites (e.g., saponins, lignans, tannins, and other polyphenolic compounds), some of them were associated with antiparasitic effect [4]. Thus, the observed FEC reduction in this work is consistent with other studies that have reported that plant extracts rich in polyphenolic compounds induced anthelmintic activity, involving experimental animals that have been used in trials to validate medicinal activities [9, 10, 13, 18].

Despite a significant decline in mean FEC, blood parameters did not change significantly throughout the experiment between any groups. Similarly, the extract does not appear to have influenced the change of weight in animal groups during the experimental period. However, the G4 animals treated with 5.0 mg/Kg b.w. were the only ones to present a significant weight gain. This concentration appears to be the most efficient.

All these parameters are considered to be important element in the response against GIN infection. Although controversial, this is consistent with other experimental findings with helminthes, in which no notable alteration in these parameters was found [19].

In the present experiment, it is likely that another mechanism of the CP extract affects against GIN. The mechanisms whereby the consumption of certain plants and plant extracts can affect parasite cycle both *in vitro* and *in vivo* are unknown. However, their consumption can be associated with an enhanced immune response of the host towards the parasites [20].

In the study of humoral immune response, antibodies of two immunoglobulin classes were investigated: IgA and IgG. A significant increase in IgA levels was observed in G4, while low levels of IgG were observed in groups G3 and G4, corresponding to the animals treated with the CP extract. From the present results and considering the significant reduction in the egg output, this study indicates that IgA may play a role in the parasite control. It appears that the IgA response is involved with the generation of protective immunity against GIN, as parasitological data remained low in animals from G3 and G4 throughout the experiment. Although this was a significant response, no relationship was found between IgA and FEC.

Previous studies in small ruminants suggest that IgA may be the major immunological mechanism of either reduced fecundity and/or eliminate adult worms [21–24]. IgA levels could reflect the degree of sensitisations of the animal.

Therefore, serum IgA might indicate a high level of resistance to reinfection against GIN [25].

The present results also support that *C. pyramidalis*, which showed the presence of phenolic compounds in phytochemical analysis and is involved in anthelmintic activity, as demonstrated by several experiments [13, 17], provoked a protective immune response when the animals were treated with this extract [26]. Phenolic compounds were also evaluated *in vitro* for their antimicrobial activity to control pathogenic bacteria [4, 17, 27].

The role of these substances needs to be better established because plants with anthelmintic properties can be one key factor to the control of nematode infections, whereas a number of medicinal plants have been used to treat parasitic infections in man and animals [4, 17]. According to Siqueira et al. [10], *C. pyramidalis*, a plant with antimicrobial indications, showed a higher content of tannins. Our experimental results suggest a possible relationship between these compounds and the observed activity in goats.

Therefore, further experiments with infected animals are essential to evaluate the best dose of the extract to be administered and still offer subsidies for the development of new drugs for the treatment of livestock against gastrointestinal nematodes.

Acknowledgments

Technical supports of the Empresa Baiana de Desenvolvimento Agrícola are acknowledged. This work was funded by the Banco do Nordeste do Brasil and FAPESB.

References

- [1] R. L. Coop and I. Kyriazakis, "Influence of host nutrition on the development and consequences of nematode parasitism in ruminants," *Trends in Parasitology*, vol. 17, no. 7, pp. 325–330, 2001.
- [2] P. J. Waller, "From discovery to development: current industry perspectives for the development of novel methods of helminth control in livestock," *Veterinary Parasitology*, vol. 139, no. 1–3, pp. 1–14, 2006.
- [3] R. R. Pinheiro, A. M. G. Gouveia, F. S. F. Alves, and J. P. A. Haddad, "Epidemiological aspects of the raising goat in Ceará State, Brazil," *Arquivo Brasileiro de Medicina Veterinária e Zootecnia*, vol. 52, no. 5, pp. 534–543, 2000.
- [4] J. B. Githiori, S. Athanasiadou, and S. M. Thamsborg, "Use of plants in novel approaches for control of gastrointestinal helminths in livestock with emphasis on small ruminants," *Veterinary Parasitology*, vol. 139, no. 4, pp. 308–320, 2006.
- [5] A. Jabbar, M. A. Zaman, Z. Iqbal, M. Yaseen, and A. Shamim, "Anthelmintic activity of *Chenopodium album* (L.) and *Caesalpinia crista* (L.) against trichostrongylid nematodes of sheep," *Journal of Ethnopharmacology*, vol. 114, no. 1, pp. 86–91, 2007.
- [6] T. Eguale, D. Tadesse, and M. Giday, "In vitro anthelmintic activity of crude extracts of five medicinal plants against egg-hatching and larval development of *Haemonchus contortus*," *Journal of Ethnopharmacology*, vol. 137, no. 1, pp. 108–113, 2011.
- [7] A. B. Joly, *Botânica—Introdução à Taxonomia Vegetal*, Companhia Editora Nacional, São Paulo, Brazil, 1998.
- [8] G. R. D. A. Santos, A. M. V. Batista, A. Guim, M. V. F. Dos Santos, M. J. D. A. Silva, and V. L. A. Pereira, "Evaluation of botanical composition of sheep diet in Caatinga pasture," *Revista Brasileira de Zootecnia*, vol. 37, no. 10, pp. 1876–1883, 2008.
- [9] U. P. de Albuquerque, P. M. de Medeiros, A. L. S. de Almeida et al., "Medicinal plants of the caatinga (semi-arid) vegetation of NE Brazil: a quantitative approach," *Journal of Ethnopharmacology*, vol. 114, no. 3, pp. 325–354, 2007.
- [10] C. F. D. Q. Siqueira, D. L.V. Cabral, T. J. D. S. Peixoto Sobrinho et al., "Levels of tannins and flavonoids in medicinal plants: evaluating bioprospecting strategies," *Evidence-based Complementary and Alternative Medicine*, vol. 2012, Article ID 434782, 7 pages, 2012.
- [11] C. C. Mendes, M. V. Bahia, J. M. David, and J. P. David, "Constituents of *Caesalpinia pyramidalis*," *Fitoterapia*, vol. 71, no. 2, pp. 205–207, 2000.
- [12] M. V. Bahia, J. B. Dos Santos, J. P. David, and J. M. David, "Biflavonoids and other phenolics from *Caesalpinia pyramidalis* (Fabaceae)," *Journal of the Brazilian Chemical Society*, vol. 16, no. 6 B, pp. 1402–1405, 2005.
- [13] C. H. T. P. da Silva, T. J. S. P. Sobrinho, V. T. N. A. Castro, D. C. a. Lima, and E. L. C. de Amorim, "Antioxidant capacity and phenolic content of *Caesalpinia pyramidalis* Tul. and *Sapium glandulosum* (L.) morong from northeastern Brazil," *Molecules*, vol. 16, no. 6, pp. 4728–4739, 2011.
- [14] J. H. Whitlock, "The evaluation of pathological growth and parasitic disease," *The Cornell veterinarian*, vol. 45, no. 3, pp. 411–422, 1955.
- [15] W. Pralomkam, V. S. Pandey, W. Ngampongsai et al., "Genetic resistance of three genotypes of goats to experimental infection with *Haemonchus contortus*," *Veterinary Parasitology*, vol. 68, no. 1–2, pp. 79–90, 1997.
- [16] K. M. MacKinnon, J. L. Burton, A. M. Zajac, and D. R. Notter, "Microarray analysis reveals difference in gene expression profiles of hair and wool sheep infected with *Haemonchus contortus*," *Veterinary Immunology and Immunopathology*, vol. 130, no. 3–4, pp. 210–220, 2009.
- [17] H. Hoste, F. Jackson, S. Athanasiadou, S. M. Thamsborg, and S. O. Hoskin, "The effects of tannin-rich plants on parasitic nematodes in ruminants," *Trends in Parasitology*, vol. 22, no. 6, pp. 253–261, 2006.
- [18] A. Novobilský, I. Mueller-Harvey, and S. M. Thamsborg, "Condensed tannins act against cattle nematodes," *Veterinary Parasitology*, vol. 182, no. 2–4, pp. 213–220, 2011.
- [19] M. Cuquerella and J. M. Alunda, "Immunobiological characterization of *Graphidium strigosum* experimental infection in rabbits (*Oryctolagus cuniculus*)," *Parasitology Research*, vol. 104, no. 2, pp. 371–376, 2009.
- [20] P. Hördegen, H. Hertzberg, J. Heilmann, W. Langhans, and V. Maurer, "The anthelmintic efficacy of five plant products against gastrointestinal trichostrongylids in artificially infected lambs," *Veterinary Parasitology*, vol. 117, no. 1–2, pp. 51–60, 2003.
- [21] J. Grønvold, P. Nansen, L. C. Gasbarre et al., "Development of immunity to *Ostertagia ostertagi* (Trichostrongylidae: Nematoda) in pastured young cattle," *Acta veterinaria Scandinavica*, vol. 33, no. 4, pp. 305–316, 1992.
- [22] H. D. F. H. Schallig, M. A. W. Van Leeuwen, and W. M. L. Hendriks, "Isotype-specific serum antibody responses of sheep to *Haemonchus contortus* antigens," *Veterinary Parasitology*, vol. 56, no. 1–3, pp. 149–162, 1995.
- [23] S. A. J. Strain and M. J. Stear, "The recognition of molecules from fourth-stage larvae of *Ostertagia circumcincta* by IgA

- from infected sheep,” *Parasite Immunology*, vol. 21, no. 3, pp. 163–168, 1999.
- [24] J. C. Bambou, C. de la Chevrotière, H. Varo, R. Arquet, F. N. J. Kooyman, and N. Mandonnet, “Serum antibody responses in Creole kids experimentally infected with *Haemonchus contortus*,” *Veterinary Parasitology*, vol. 158, no. 4, pp. 311–318, 2008.
- [25] E. Claerebout and J. Vercruysse, “The immune response and the evaluation of acquired immunity against gastrointestinal nematodes in cattle: a review,” *Parasitology*, vol. 120, pp. S25–S42, 2000.
- [26] L. M. B. Oliveira, C. M. L. Bevilaqua, C. T. C. Costa et al., “Anthelmintic activity of *Cocos nucifera* L. against sheep gastrointestinal nematodes,” *Veterinary Parasitology*, vol. 159, no. 1, pp. 55–59, 2009.
- [27] H. Azaizeh, A. Tafesh, N. Najami, J. Jadoun, F. Halahlih, and H. Riepl, “Synergistic antibacterial effects of polyphenolic compounds from olive mill wastewater,” *Evidence-based Complementary and Alternative Medicine*, vol. 2011, Article ID 431021, 9 pages, 2011.

Research Article

Chemical Composition, Toxicity and Vasodilatation Effect of the Flowers Extract of *Jasminum sambac* (L.) Ait. “G. Duke of Tuscany”

Phanukit Kunhachan,¹ Chuleratana Banchonglikitkul,² Tanwarat Kajsongkram,²
Amonrat Khayungarnawee,² and Wichet Leelamanit¹

¹ Department of Biochemistry, Faculty of Pharmacy, Mahidol University, 447 Sri Ayudhya, Rajathevi, Bangkok 10400, Thailand

² Pharmaceutical and Natural Products Department, Thailand Institute of Scientific and Technological Research (TISTR), Klong 5, Klong Luang, Pathum Thani 12120, Thailand

Correspondence should be addressed to Wichet Leelamanit, pywlt@mahidol.ac.th

Received 11 October 2011; Accepted 1 January 2012

Academic Editor: Vincenzo De Feo

Copyright © 2012 Phanukit Kunhachan et al. This is an open access article distributed under the Creative Commons Attribution License, which permits unrestricted use, distribution, and reproduction in any medium, provided the original work is properly cited.

Phytochemical analysis of the ethanolic Jasmine flower extract of *Jasminum sambac* (L.) Ait. “G. Duke of Tuscany” revealed the mixtures of coumarins, cardiac glycosides, essential oils, flavonoids, phenolics, saponins, and steroids. However, alkaloids, anthraquinones, and tannins were not detected. By intravenous injection at a single dose of 0.5 mL/mouse (15 mg) of the flower extract, no systemic biological toxicity demonstrated in ICR mice was observed. In Wistar rats, the LD₅₀ of the extract was higher than 5,000 mg/kg BW by oral administration. Vasodilatation effect of the 95% ethanolic extract on isolated aortic rats was also investigated. Compared with the control group, the Jasmine flowers extract in 0.05% DMSO clearly reduced tonus of isolated endothelium thoracic aortic rings precontracted with phenylephrine (10⁻⁶ M), as a dose-dependent manner. Nevertheless, this pharmacological effect disappeared after the preincubation of the rings with atropine (10⁻⁶ M) or with N^ω-nitro-L-arginine (10⁻⁴ M). These are possibly due to the actions of the active components on the vessel muscarinic receptors or by causing the release of nitric oxide.

1. Introduction

Jasmine (*Jasminum*) is a genus containing approximately 600 species of small trees and vines in the Family Oleaceae. These glabrous twining shrubs are widely cultivated in gardens and easily found in forests throughout tropical Asia and warm temperate regions in Europe and Africa. Their flowers and leaves have been well recognized for multipurpose uses. For instance, the flowers have been utilized as traditional medicines in Asia to treat many diseases including diarrhea, fever, conjunctivitis, abdominal pain, dermatitis, asthma, abscess, breast cancer, uterine bleeding, and toothache. In China, the leaf parts are used for the treatment of quadriplegia gall, dysentery, and bellyache. According to its high medicinal value, *Jasminum sambac* is one of the most

cultivated species in many countries in Asia including Thailand. Its phytoconstituents contain iridoidal glycosides [1], linalyl 6-O-malonyl-β-D-glucopyranoside, benzyl 6-O-β-D-xylopyranosyl-β-D-glucopyranoside (β-primeveroside), 2-phenylethyl β-primeveroside, 2-phenylethyl 6-O-α-L-rhamnopyranosyl-β-D-glucopyranoside (β-rutinoside) [2], dotriacontanoic acid, dotriacontanol, oleanolic acid, daucosterol, and hesperidin [3]. The volatile constituents consist of benzyl acetate, indole, E-E-α-farnesene, Z-3-hexenyl benzoate, benzyl alcohol, linalool, and methyl anthranilate [4]. Although the whole parts of the plant are employed and prescribed in folk medicines, only two pharmacological studies of *J. sambac* have been reported. The flower displayed the efficacy to suppress puerperal lactation [5] and the essential oil was determined to possess antibacterial activity [6]. The objective

of the present study was to examine the toxicity and vasodilatation activities of *J. sambac* (L.) Ait. "G. Duke of Tuscany" (locally called Ma-li-son), a local variety commonly found in Thailand. The vasodilation effect of the ethanolic extract was first reported using isolated thoracic aortic rings. The phytochemical composition and the toxicity were also assessed.

2. Materials and Methods

2.1. Chemicals. Phenylephrine chloride (PE), N^ω-nitro-L-arginine (L-NA), atropine sulfate, acetylcholine chloride (Ach), rutin hydrate, oleuropein, kaempferol disaccharides, and quercetin were purchased from Sigma-Aldrich Chemical, USA. All other chemicals used were of analytical grade.

2.2. Animals. Wistar rats (*Rattus norvegicus*) and ICR mice (*Mus musculus*) used were obtained from the National Laboratory Animal Center, Salaya, Mahidol University, Nakhon Pathom, Thailand. All animals were acclimatized for 1 week before starting of the experiments in controlled environmental conditions (25 ± 1°C) with a 12 h light/dark cycle and allowed access to standard food and tap water *ad libitum*. Animal welfare was under control by IACUC of the Thailand Institute of Scientific and Technological Research (TISTR).

2.3. Plant Material and Extraction. The flowers of *J. sambac* (L.) Ait. "G. Duke of Tuscany" were collected from Nakhon Pathom province, Thailand, in March 2009. The specimen voucher was TISTR no. 160309, and the samples were deposited at TISTR. Approximately 3.1 grams of the flowers were dried at 50°C for 42 h, powdered, and macerated in 18 mL of 95% ethanol at room temperature overnight. After elution, the flower residues were repeatedly macerated with equal volume of ethanol overnight and eluted again. The ethanol elutes were combined, filtered through Whatmann filter paper no. 42, and evaporated under reduced pressure at 50°C. The semisolid light yellow materials were stored in desiccators until used. Percentage yield of the extract was 17.68% yield (w/w). The extract was dissolved in 0.05% dimethyl sulfoxide (DMSO) for *in vitro* experiments and in 1% Tween or 1% gum tragacanth for *in vivo* studies.

2.4. Thin Layer Chromatography (TLC) Analysis. The ethanolic flower extract was screened for the different classes of compounds by thin layer chromatography using silica gel 60 F254 (Merck, Darmstadt, Germany) plates of 0.25 mm thickness. Briefly, the extract was dissolved in methanol while the development of plates was carried out with different mobile phase systems using appropriate reagents as standard makers (Table 1). After development, the plates were sprayed with the following solvents and reagents for detection of the respective classes of compounds: 0.5% anisaldehyde in sulfuric acid, glacial acetic acid, and methanol 5 : 10 : 85 v/v and heating at 105°C for 5–10 min; 10% solution of antimony trichloride in chloroform and heating at 105°C for 5–6 min (for phenolics/tannins); 1% methanolic diphenylboryloxyethylamine, followed by 5% ethanolic polyethylene

glycol 4000 (PEG) (for flavonoids), 5% ethanolic potassium hydroxide (for anthraquinones/coumarins), Dragendorff's reagent (for alkaloids), DPPH reagent (for antioxidants), the Liebermann-Burchard reagent (for steroids), and the Kedde reagent (for cardiac glycosides). Reagents were prepared according to Wagner and Bladt, 1996 [7]. Saponins were detected by observing froth formation by the extract in a test tube after regular shaking. The colored, double-banded, and fluorescent compounds were detected on the silica gel plates under day light, UV light 254 nm, and UV light 365 nm, respectively.

2.5. HPLC Analysis. For HPLC analysis, the flower extract (1.0 g) was dissolved in 100 mL of water in an ultrasonic bath for 15 min. The solution was partitioned three times with 20 mL of hexane. The aqueous layer was also partitioned three times with 20 mL of ethyl acetate and then three times with 20 mL of butanol. After the partitioned samples were dried in an evaporator, the obtained solid samples were dissolved in 10 mL of 60% methanol and were used for HPLC analysis. HPLC analysis was performed on a Waters apparatus (Waters 2695 separations Module, Alliance and Waters 2996 Photodiode Array Detector) using a Phenomenex Luna C18, 5 μm, 250 × 4.60 mm column (Waters). The mobile phase was 0.05% phosphoric acid (pH 2.3) and methanol. The flow rate was 0.5 mL/min, the injection volume was 20 μL, and the run times was 45 min. UV-visible spectra were recorded in the range of 190–450 nm, and chromatograms were acquired at 280 and 350 nm. Four standard flavonoids (rutin, kaempferol disaccharide, quercetin, kaempferol) and one cardiac glycoside (oleuropein) were dissolved in methanol [8].

2.6. Systemic Biological Reactivity Test. Ten male ICR mice weighing between 22–25 g were divided into two groups. Group I received no treatment. Group II mice individually received 0.5 mL (15 mg) of the extract via intravenous injection using a 26-gauge needle. The treated animals were investigated immediately after injection and at 4, 24, 48, 72 h after injection. The body weights of all animals were measured at Days 8 and 15. At Day 15, the mice were killed by cervical dislocation, and internal organs were weighed and collected for pathological examination.

2.7. Acute Oral Toxicity Test. Twenty Wistar rats (10 animals per sex) weighing 200–250 g were divided into two groups, and both groups were fed under standard laboratory conditions. All rats were kept overnight fasting prior to Jasmine extract administration. One group as control received 1% gum tragacanth, while the treated group received the flower extract orally at a single dose of 5,000 mg/kg. After 3 h of the administration, food was allowed. The rats were observed individually at least once within the first 24 h (with special attention to the first 4 h) and daily thereafter for a period of 15 days. The body weights of the rats were measured at Days 8 and 15. At Day 15, the rats were terminated and the weights of the internal organs were determined.

TABLE 1: TLC Method.

Test	Standard	Mobile phase	Spraying reagent	Detection	Color
Alkaloids	Atropine	Toluene : ethyl acetate : dimethylamine (70 : 20 : 10)	Dragendorff reagent	Visible	Orange spot on yellow background
Anthraquinones	Rhein	Ethyl acetate : methanol : water (81 : 11 : 8)	KOH reagent	UV 366 nm	Yellow/orange/red
Antioxidants	Vit E	Ethyl acetate : toluene (50 : 50)	DPPH reagent	Visible	White spot on purple background
Coumarins	Coumarin	Toluene : ethyl acetate (90 : 10)	KOH reagent	UV 366 nm	Light blue/green
Essential oils	Eugenol	Toluene : ethyl acetate (93 : 7)	Anisaldehyde sulfuric acid reagent	Heat 100°C Visible	Purple/red
Flavonoids	Rutin	Ethyl acetate : formic acid : acetic acid : water (100 : 11 : 11 : 27)	Natural Product (NP/PEG)	UV 366 nm	Orange/yellow/green/blue
Cardiac glycosides	Ouabain	Ethyl acetate : methanol : water (81 : 11 : 8)	Kedde reagent	Visible	Pink/yellow/purple
Phenolics	Catechol	Toluene : ethyl acetate (97 : 3)	Ferric chloride reagent	Visible	Blue/black
Saponins	Saponin	Butanol : ethyl acetate : acetic acid : water (10.8 : 3.6 : 0.2 : 2.7)	Anisaldehyde sulfuric acid reagent	Visible	Blue
Tannins	Gallic acid	Metanol : ethyl acetate : acetic acid (10 : 90 : 0.1)	Ferric chloride reagent	Visible	Blue/black

2.8. Vasodilatation Effect Test. Each rat was killed by cervical dislocation. Its thorax was opened, and the aortic vessel was removed from fat and connective tissues and kept in a Petri dish containing Krebs' solution. Two adjacent aortic rings of 3-4 mm in length were cut. In only one ring, endothelium was removed mechanically by gently rubbing the intimal surface of the vessel using the method as previously described [9]. The organ bath contained the Krebs-Henseleit solution (NaCl 119, KCl 4.7, CaCl₂ 2.5, MgSO₄·7H₂O 1.0, KH₂PO₄ 1.2, NaHCO₃ 25.0, and glucose 11.1 mM). This solution was maintained at 37°C and continuously bubbled with 95% O₂ and 5% CO₂. The two rings were individually suspended horizontally between two stainless steel hooks in a 20 mL organ bath containing Krebs' solution. One of the hooks was fixed to the bottom, and the other was connected to a force displacement transducer that connected to a MP100 (BIOPAC System, Inc., Model MP100 WSW) for the isometric tension record. The stabilization period was of 45 min under a resting tension of 1.0 g and the solution was changed every 15 min to prevent the accumulation of metabolites. After equilibration, the rings were precontracted with 1 × 10⁻⁶ M phenylephrine (PE) until the responses curve reached plateaus (5-8 min), and dilator responses to 1 × 10⁻⁵ M acetylcholine (Ach) were detected. The absence of the relaxation to acetylcholine was taken as evidence that the vessel segment was functionally denuded of endothelium, and at least 70% vasodilatation to

acetylcholine for the endothelium-intact thoracic aorta rings was observed.

2.8.1. Effect of the Jasmine Flower Extract on PE-Induced Tonus in the Endothelium-Intact or Endothelium-Denuded Thoracic Aorta Rings [10]. After 45 minutes re-equilibration, the rings with and without endothelium intact were pre-contracted with 1 × 10⁻⁶ M PE for 20 minutes. After several washings and re-equilibration for 30 minute, five different concentrations of the flower extracts (50, 100, 200, 300, and 400 µg/mL) were added 5 min and the rings were incubated with PE for another 20 min. The contractions were measured by comparing the developed tension before and after the addition of the extract and expressed as percentage of contraction from induced tonus.

2.8.2. Effect of the Extract on PE-Induced Tonus in the Endothelium-Intact Thoracic Aorta Rings with Atropine and N^ω-Nitro-L-arginine [10]. After 45 min re-equilibration, the endothelium-intact aortic rings were pre-constricted with 1 × 10⁻⁶ M PE for 20 min. After several washings and re-equilibration for 30 minutes, the rings were exposed to atropine (1 × 10⁻⁶ M) or N^ω-nitro-L-arginine (L-NA), a nitric oxide synthase inhibitor (1 × 10⁻⁴ M), for 5 minutes. Then, the same serial concentrations of the extracts were added, and the percentage of the contractions before and

after the addition of the extracts was determined as described above.

2.9. Statistical Analysis. The results are expressed as means \pm standard error means (SEMs). Student's *t*-tests or one-way ANOVA were used for statistical analysis. In all cases, *P* values < 0.05 were considered statistically significant.

3. Results

3.1. Phytochemical Evaluation. Phytochemical analysis of the ethanolic extract displayed that antioxidants, coumarins, cardiac glycosides, essential oils, flavonoids, phenolics, saponins, and steroids were investigated. Other compounds such as alkaloids, anthraquinones, and tannins were not found (Table 2).

3.2. Systemic Biological Reactivity Test. At a dose of 15 mg (0.5 mL/mouse) of the extract by tail vein injection, no toxic signs or mortality was observed. Compared to the control group, there was no statically significant difference ($P < 0.05$) in the body and organ weights of the mice between the two groups (Table 3).

3.3. Acute Oral Toxicity Test. The extract at a single dose of 5,000 mg/kg BW did not cause any sign of toxicity in rats. For both sexes, there was no statically significant difference ($P < 0.05$) in the body and organ weights of rats between the control and treated groups (Tables 4 and 5). In addition, the rats of both groups displayed normal behaviors.

3.4. Vasodilatation Effect Test. PE at 1 μ M produced a steady-state contraction in the aortic rings with or without endothelium. As shown in Figure 1, the extract (50–400 μ g/mL) caused vasodilation of the endothelium-intact thoracic aorta ring pre-constricted with phenylephrine in a dose-response manner. However, this effect disappeared after preincubation of the aortic rings with atropine (1×10^{-6} M), L-NA (1×10^{-4} M) or by removal of the vascular endothelium.

4. Discussion

Jasminum sambac is one of the most well-famous fragrant plants worldwide and has been prescribed in folk medicines in many countries according to its multipurpose actions. In addition, Jasmine tea is the most famous scented tea in many countries including China, Japan, and Thailand. Nevertheless, the chemical constituents and pharmacological activities of *J. sambac* have been rarely reported.

To date, the flower of *J. sambac* was reported to contain the mixtures of dimeric and trimeric iridodial glycosides (molihuasides A–E) and glycosidic aroma precursors [1, 2]. Recently, Edris et al. reported that the main volatile constituents from the flower extract were benzyl acetate, indole, E-E- α -farnesene, Z-3-hexenyl benzoate, benzyl alcohol, linalool, and methyl anthranilate [4]. Our TLC analysis indicated that the ethanolic flower extract contained the mixtures of coumarins, cardiac glycosides, essential oils,

TABLE 2: Phytochemical analysis of the ethanolic Jasmine flowers extract.

Compounds	Results
Alkaloids	–
Anthraquinones	–
Antioxidants	+
Coumarins	+
Cardiac glycosides	+
Essential oils	+
Flavonoids	+
Phenolics	+
saponins	+
steroids	+
tannins	–

flavonoids, phenolics, saponins, and steroids. However, alkaloids, anthraquinones, and tannins were not detected. Data from HPLC analysis also revealed high content of flavonoid mixtures (data not shown). Therefore, the various therapeutic actions used in different traditional medicines are definitely attributed to the mixtures of active ingredients in the Jasmine flower.

Although this Jasmine species is used as a principal ingredient in many traditional medicines or in tea industries, its toxicity has never been documented elsewhere. At a high dose of the flower extract via intravenous injection (15 mg/mouse), no biological reactivity in male ICR mice was observed. For acute toxicity, the LD₅₀ was higher than 5,000 mg/kg in both sexes of Wistar rats. In both toxicity assays, there was no statically significant difference ($P < 0.05$) in the body and organ weights between the control and treated groups. In gross examinations, the individual internal organs of the treated and the control groups displayed no significant difference. Additionally, the rats of both groups had normal behavior. For the liver function test, the activities of aspartate aminotransferase (AST) and alanine aminotransferase (ALT) were determined and there were no enzymatic difference between the control and treated groups (data not shown). As confirmed by traditional use for thousand years in many countries, the flower of *J. sambac* is therefore safe for general utilization in medicines or food industry.

The flower extracts of *J. sambac* displayed suppression of puerperal lactation and antibacterial activity. Here, we first described that the flower extract of *J. sambac* possessed vasodilation activity. As shown in Figure 1(a), the vasodilation effect of the Jasmine flower extract was mediated by endothelial cells in the aortic vessel. The flower extract at a dose of 400 μ g/mL reduced the contraction to lower than 43% of the maximal contraction. This result suggests that the vasorelaxation effect of the ethanolic *J. sambac* flowers extract is endothelium dependent. It has been reported that the vasorelaxant property of most plant extracts was from flavonoids [11]. Thus, the vasodilation activity should be attributed to the high content of flavonoid mixtures found in the Jasmine flower extract.

TABLE 3: Systemic biological reactivity of the ethanolic Jasmine flower extract by intravenous injection.

Treatment	Weight (g)	Liver (g)	Kidney (g)	Spleen (g)	Heart (g)	Stomach (g)	Lung (g)	Pancreas (g)	Testis (g)
Group I: Control group	38.2 ± 0.66	2.882 ± 0.06	0.889 ± 0.01	0.158 ± 0.002	0.183 ± 0.004	0.229 ± 0.002	0.190 ± 0.005	0.290 ± 0.0005	0.287 ± 0.004
Group II: Treated group	37.0 ± 0.70	2.838 ± 0.04	0.890 ± 0.01	0.155 ± 0.002	0.177 ± 0.002	0.228 ± 0.002	0.193 ± 0.006	0.290 ± 0.0007	0.283 ± 0.003

Values are expressed as mean ± SEM (*n* = 5). Treated groups received a single dose of 15 mg of the extract via intravenous injection.

TABLE 4: Acute oral toxicity of the ethanolic Jasmine flower extract in male rats.

Male	Weight (g)	Liver (g)	Kidney (g)	Spleen (g)	Heart (g)	Stomach (g)	Lung (g)	Pancreas (g)	Testis (g)
Control (1% gum tragacanth)	318.4 ± 7.38	15.22 ± 0.43	2.70 ± 0.02	0.74 ± 0.03	1.196 ± 0.03	1.934 ± 0.02	1.580 ± 0.01	2.196 ± 0.02	3.726 ± 0.01
Jasmine flowers extract (5,000 mg/kg)	334.6 ± 10.64	14.47 ± 0.82	2.752 ± 0.02	0.744 ± 0.04	1.216 ± 0.05	1.924 ± 0.04	1.586 ± 0.01	2.226 ± 0.02	3.732 ± 0.02

Values are expressed as mean ± SEM (*n* = 5).

TABLE 5: Acute oral toxicity of the ethanolic Jasmine flower extract in female rats.

Female	Weight (g)	Liver (g)	Kidney (g)	Spleen (g)	Heart (g)	Stomach (g)	Lung (g)	Pancreas (g)	Uterus & Ovary (g)
Control (1% gum tragacanth)	237.6 ± 5.91	12.846 ± 0.76	1.978 ± 0.003	0.732 ± 0.001	0.996 ± 0.010	1.776 ± 0.002	1.472 ± 0.001	1.28 ± 0.004	0.916 ± 0.02
Jasmine flowers extract (5,000 mg/kg)	232 ± 5.11	12.788 ± 0.69	1.972 ± 0.01	0.728 ± 0.03	1.03 ± 0.05	1.716 ± 0.01	1.472 ± 0.003	1.282 ± 0.003	0.886 ± 0.012

Values are expressed as mean ± SEM (*n* = 5).

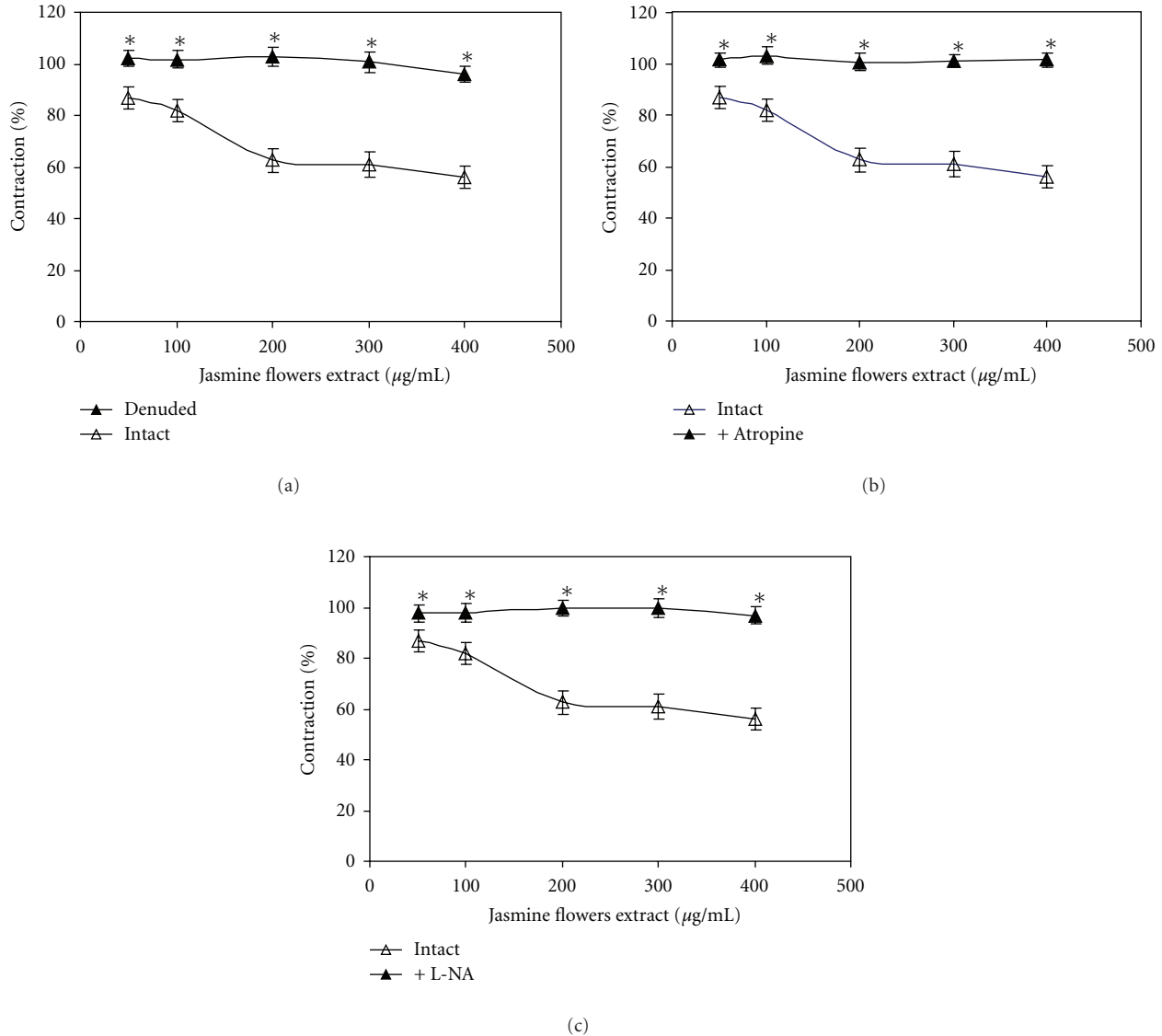


FIGURE 1: Dose-response curves for the vasodilation effects of the ethanolic Jasmine flower extract on the precontracted thoracic aorta rings. Results are presented as means \pm SEM ($n = 6$), (Student's t -test, $*P < 0.05$). (a) Endothelium intact (Δ), endothelium denude (\blacktriangle). (b) Endothelium intact (Δ), with atropine (\blacktriangle). (c) Endothelium intact (Δ), with L-NA (\blacktriangle).

Preincubating the thoracic aortic rings with atropine (10^{-6} M), a muscarinic receptor antagonist completely blocked the relaxant activity of the extract (Figure 1(b)). The pharmacologically relaxant effect of the flower extract was further determined. Pretreatment of endothelium-intact aorta with L-NA (1×10^{-4} M) also reduced the vasodilation effect of the extract to an extent equivalent to the effect in endothelium-denuded aorta (Figure 1(c)). Nowadays, the mechanism of nitric oxide (NO) and the function of endothelial cells in the relaxation of arteries are well described. NO is a potent vasodilator synthesized in the endothelium by NO synthase and causes vascular relaxation [12–14]. The result from the present study suggests that the Jasmine flower extract may exert its endothelium-dependent relaxation activity by stimulating the nitric oxide release from the vascular endothelium via muscarinic receptors.

5. Conclusion

The Jasmine flowers extract at a dose of 0.5 mL/mouse (15 mg) by intravenous injection in male ICR mice showed no biological reactivity, and the LD_{50} was more than 5,000 mg/kg b.w. by oral administration in both sexes of Wistar rats. In the *in vitro* study, the Jasmine flower extract exerted a vasorelaxation activity on the endothelium-intact aorta ring. The mechanisms probably involve the active component acting via the muscarinic receptors at the vascular endothelium and/or by stimulating nitric oxide release. Preliminary phytochemical analysis revealed that the flower of *J. sambac* contains antioxidants, coumarins, cardiac glycosides, essential oils, flavonoids, phenolics, saponins, and steroids, whereas alkaloids, anthraquinones, and tannins were not detected. Since the flower of *J. sambac* is tremendously

employed in traditional medicines and in tea industries, the knowledge of the chemical compositions, toxicity, and pharmacological properties will provide insight information of this plant for its future application.

Conflict of Interests

The authors would like to declare that there is no conflict of interest.

Acknowledgment

The authors are grateful to Institute of Scientific and Technological Research (TISTR) for providing facilities and some financial support.

References

- [1] Y.-J. Zhang, Y.-Q. Liu, X.-Y. Pu, and C.-R. Yang, "Iridoidal glycosides from *Jasminum sambac*," *Phytochemistry*, vol. 38, no. 4, pp. 899–903, 1995.
- [2] J. Inagaki, N. Watanabe, J. H. Moon et al., "Glycosidic aroma precursors of 2-phenylethyl and benzyl alcohols from *Jasminum sambac* flowers," *Bioscience, Biotechnology, and Biochemistry*, vol. 59, no. 4, pp. 738–739, 1995.
- [3] Z. F. Zhang, B. L. Bian, J. Yang, and X. F. Tian, "Studies on chemical constituents in roots of *Jasminum sambac*," *Zhongguo Zhong Yao Za Zhi*, vol. 29, no. 3, pp. 237–239, 2004.
- [4] A. E. Edris, R. Chizzola, and C. Franz, "Isolation and characterization of the volatile aroma compounds from the concrete headspace and the absolute of *Jasminum sambac* (L.) Ait. (Oleaceae) flowers grown in Egypt," *European Food Research and Technology*, vol. 226, no. 3, pp. 621–626, 2008.
- [5] P. Shrivastav, K. George, N. Balasubramaniam, M. P. Jasper, M. Thomas, and A. S. Kanagasabhapathy, "Suppression of puerperal lactation using jasmine flowers (*Jasminum sambac*)," *The Australian and New Zealand Journal of Obstetrics and Gynaecology*, vol. 28, no. 1, pp. 68–71, 1988.
- [6] C. C. Rath, S. Devi, S. K. Dash, and R. Mishra, "Antibacterial potential assessment of Jasmine essential oil against *E. coli*," *Indian Journal of Pharmaceutical Sciences*, vol. 70, no. 2, pp. 238–241, 2008.
- [7] H. Wagner and S. Bladt, *Plant Drug Analysis*, Springer, Berlin, Germany, 2nd edition, 1996.
- [8] A. Romani, P. Pinelli, N. Mulinacci, F. F. Vincieri, E. Gravano, and M. Tattini, "HPLC analysis of flavonoids and secoiridoids in leaves of *Ligustrum vulgare* L. (Oleaceae)," *Journal of Agricultural and Food Chemistry*, vol. 48, no. 9, pp. 4091–4096, 2000.
- [9] R. Khwanchuea, C. Jansakul, and M. J. Mulvany, "Cardiovascular effects of an *n*-butanol extract from fresh fruits of *Randia siamensis*," *Biological and Pharmaceutical Bulletin*, vol. 30, no. 1, pp. 96–104, 2007.
- [10] N. Kitjaroennirut, C. Jansakul, and P. Sawangchote, "Cardiovascular effects of *Tacca integrifolia* Ker-Gawl extract in rats," *Songklanakarinn Journal of Science and Technology*, vol. 27, no. 2, pp. 281–289, 2005.
- [11] C. Heiss, C. L. Keen, and M. Kelm, "Flavanols and cardiovascular disease prevention," *European Heart Journal*, vol. 31, no. 21, pp. 2583–2592, 2010.
- [12] L. J. Ignarro, G. M. Buga, K. S. Wood, R. E. Byrns, and G. Chaudhuri, "Endothelium-derived relaxing factor produced and released from artery and vein is nitric oxide," *Proceedings of the National Academy of Sciences of the United States of America*, vol. 84, no. 24, pp. 9265–9269, 1987.
- [13] R. M. Palmer, A. G. Ferrige, and S. Moncada, "Nitric oxide release accounts for the biological activity of endothelium-derived relaxing factor," *Nature*, vol. 327, no. 6122, pp. 524–526, 1987.
- [14] S. Moncada, R. M. Palmer, and E. A. Higgs, "Nitric oxide: physiology, pathophysiology, and pharmacology," *Pharmacological Reviews*, vol. 43, no. 2, pp. 109–142, 1991.